
Feedback Systems

An Introduction for Scientists and Engineers

Karl Johan Åström
Automatic Control LTH
Lund University

Control, Dynamical Systems and Computation
University of California Santa Barbara

Richard M. Murray
Control and Dynamical Systems
California Institute of Technology

DRAFT v2.7c (14 September 2007)
© 2007 Karl Johan Åström and Richard M. Murray
All rights reserved.

This manuscript is for use in CDS 101/110a at the California Institute of Technology and may not be reproduced, in whole or in part, without written consent from the authors.

Contents

Preface	vii
Chapter 1. Introduction	1
1.1 What is Feedback?	1
1.2 What is Control?	3
1.3 Feedback Examples	5
1.4 Feedback Properties	17
1.5 Simple Forms of Feedback	23
1.6 Further Reading	25
Exercises	26
Chapter 2. System Modeling	27
2.1 Modeling Concepts	27
2.2 State Space Models	34
2.3 Modeling Methodology	44
2.4 Modeling Examples	51
2.5 Further Reading	60
Exercises	61
Chapter 3. Examples	65
3.1 Cruise Control	65
3.2 Bicycle Dynamics	69
3.3 Operational Amplifier Circuits	71
3.4 Computing Systems and Networks	75
3.5 Atomic Force Microscopy	81
3.6 Drug Administration	85
3.7 Population Dynamics	89
Exercises	91
Chapter 4. Dynamic Behavior	95
4.1 Solving Differential Equations	95
4.2 Qualitative Analysis	99
4.3 Stability	102
4.4 Lyapunov Stability	111

4.5	Parametric and Non-Local Behavior	119
4.6	Further Reading	125
	Exercises	126
Chapter 5. Linear Systems		131
5.1	Basic Definitions	131
5.2	The Matrix Exponential	136
5.3	Input/Output Response	145
5.4	Linearization	158
5.5	Further Reading	164
	Exercises	164
Chapter 6. State Feedback		167
6.1	Reachability	167
6.2	Stabilization by State Feedback	175
6.3	State Feedback Design	183
6.4	Integral Action	196
6.5	Further Reading	198
	Exercises	198
Chapter 7. Output Feedback		201
7.1	Observability	201
7.2	State Estimation	206
7.3	Control using Estimated State	211
7.4	Kalman Filtering	214
7.5	Feedforward and Implementation	219
7.6	Further Reading	226
	Exercises	226
Chapter 8. Transfer Functions		229
8.1	Frequency Domain Modeling	229
8.2	Derivation of the Transfer Function	231
8.3	Block Diagrams and Transfer Functions	242
8.4	The Bode Plot	250
8.5	Laplace Transforms	259
8.6	Further Reading	261
	Exercises	262
Chapter 9. Frequency Domain Analysis		265
9.1	The Loop Transfer Function	265
9.2	The Nyquist Criterion	268
9.3	Stability Margins	276
9.4	Bode's Relations and Minimum Phase Systems	280
9.5	The Notions of Gain and Phase	283

9.6	Further Reading	287
	Exercises	288
Chapter 10.	PID Control	291
10.1	Basic Control Functions	291
10.2	Simple Controllers for Complex Systems	296
10.3	PID Tuning	300
10.4	Integrator Windup	304
10.5	Implementation	306
10.6	Further Reading	310
	Exercises	311
Chapter 11.	Frequency Domain Design	313
11.1	Sensitivity Functions	313
11.2	Feedforward Design	317
11.3	Performance Specifications	320
11.4	Feedback Design via Loop Shaping	324
11.5	Fundamental Limitations	329
11.6	Design Example	339
11.7	Further Reading	342
	Exercises	342
Chapter 12.	Robust Performance	345
12.1	Modeling Uncertainty	345
12.2	Stability in the Presence of Uncertainty	350
12.3	Performance in the Presence of Uncertainty	356
12.4	Robust Pole Placement	360
12.5	Design for Robust Performance	367
12.6	Further Reading	372
	Exercises	372
Bibliography		375
Index		385

Preface

This book provides an introduction to the basic principles and tools for design and analysis of feedback systems. It is intended to serve a diverse audience of scientists and engineers who are interested in understanding and utilizing feedback in physical, biological, information and social systems. We have attempted to keep the mathematical prerequisites to a minimum while being careful not to sacrifice rigor in the process. We have also attempted to make use of examples from a variety of disciplines, illustrating the generality of many of the tools while at the same time showing how they can be applied in specific application domains.

This book was originally developed for use in an experimental course at Caltech involving students from a wide set of backgrounds. The course consisted of undergraduates at the junior and senior level in traditional engineering disciplines, as well as first and second year graduate students in engineering and science. This latter group included graduate students in biology, computer science and physics, requiring a broad approach that emphasized basic principles and did not focus on applications in any one given area. Over the course of several years, the text has been classroom tested at Caltech and at Lund University and the feedback from many students and colleagues has been incorporated to help improve the readability and accessibility of the material.

Because of its intended audience, this book is organized in a slightly unusual fashion compared to many other books on feedback and control. In particular, we introduce a number of concepts in the text that are normally reserved for second year courses on control and hence often not available to students who are not control systems majors. This has been done at the expense of certain traditional topics, which we felt that the astute student could learn independently and are often explored through the exercises. Examples of topics that we have included are nonlinear dynamics, Lyapunov stability, reachability and observability, and fundamental limits of performance and robustness. Topics that we have de-emphasized include root locus techniques, lead/lag compensation and detailed rules for generating Bode and Nyquist plots by hand.

Several features of the book are designed to facilitate its dual function as a basic engineering text and as an introduction for researchers in natural, information and social sciences. The bulk of the material is intended to be used regardless of the audience and covers the core principles and tools in the analysis and design of feedback systems. Advanced sections, marked by the “dangerous bend” symbol shown to the right, contain material that requires a slightly more technical background, of the sort that would be expected of senior undergraduates in engineering.



A few sections are marked by two dangerous bend symbols and are intended for readers with more specialized backgrounds, identified at the beginning of the section. To keep the length of the text down, several standard results and extensions are given in the exercises, with appropriate hints toward their solutions. Finally, we have included a glossary and a notation section at the end of the book in which we define some of the terminology and notation that may not be familiar to all readers.

To further augment the printed material contained here, a companion web site has been developed:

<http://www.cds.caltech.edu/~murray/amwiki>

The web site contains a database of frequently asked questions, supplemental examples and exercises, and lecture materials for courses based on this text. The material is organized by chapter and includes a summary of the major points in the text as well as links to external resources. The web site also contains the source code for many examples in the book, as well as utilities to implement the techniques described in the text. Most of the code was originally written using MATLAB M-files, but was also tested with LabVIEW MathScript to ensure compatibility with both packages. Many files can also be run using other scripting languages such as Octave, SciLab, SysQuake and Xmath. [Author's note: the web site is under construction as of this writing and some features described in the text may not yet be available.]

The first half of the book focuses almost exclusively on so-called “state-space” control systems. We begin in Chapter 2 with a description of modeling of physical, biological and information systems using ordinary differential equations and difference equations. Chapter 3 presents a number of examples in some detail, primarily as a reference for problems that will be used throughout the text. Following this, Chapter 4 looks at the dynamic behavior of models, including definitions of stability and more complicated nonlinear behavior. We provide advanced sections in this chapter on Lyapunov stability, because we find that it is useful in a broad array of applications (and is frequently a topic that is not introduced until later in ones studies).

The remaining three chapters of the first half of the book focus on linear systems, beginning with a description of input/output behavior in Chapter 5. In Chapter 6, we formally introduce feedback systems by demonstrating how state space control laws can be designed. This is followed in Chapter 7 by material on output feedback and estimators. Chapters 6 and 7 introduce the key concepts of reachability and observability, which give tremendous insight into the choice of actuators and sensors, whether for engineered or natural systems.

The second half of the book presents material that is often considered to be from the field of “classical control.” This includes the transfer function, introduced in Chapter 8, which is a fundamental tool for understanding feedback systems. Using transfer functions, one can begin to analyze the stability of feedback systems using frequency domain analysis, including the ability to reason about the closed

loop behavior of a system from its open loop characteristics. This is the subject of Chapter 9, which revolves around the Nyquist stability criterion.

In Chapters 10 and 11, we again look at the design problem, focusing first on proportional-integral-derivative (PID) controllers and then on the more general process of loop shaping. PID control is by far the most common design technique in control systems and a useful tool for any student. The chapter on frequency domain design introduces many of the ideas of modern control theory, including the sensitivity function. In Chapter 12, we pull together the results from the second half of the book to analyze some of the fundamental tradeoffs between robustness and performance. This is also a key chapter illustrating the power of the techniques that have been developed and serving as an introduction for more advanced studies.

The book is designed for use in a 10–15 week course in feedback systems that provides many of the key concepts needed in a variety of disciplines. For a 10 week course, Chapters 1–2, 4–6 and 8–11 can each be covered in a week’s time, with some dropping of topics from the final chapters. A more leisurely course, spread out over 14–15 weeks, could cover the entire book, with two weeks on modeling (Chapters 2 and 3)—particularly for students without much background in ordinary differential equations—and two weeks on robust performance (Chapter 12).

The mathematical pre-requisites for the book are modest and in keeping with our goal of providing an introduction that serves a broad audience. We assume familiarity with the basic tools of linear algebra, including matrices, vectors and eigenvalues. These are typically covered in a sophomore level course in the subject and the textbooks by Apostol [10], Arnold [13] or Strang [178] serve as good references. Similarly, we assume basic knowledge of differential equations, including the concepts of homogeneous and particular solutions for linear ordinary differential equations in one variable. Apostol [10] or Boyce and DiPrima [42] cover this material well. Finally, we also make use of complex numbers and functions and, in some of the advanced sections, more detailed concepts in complex variables that are typically covered in a junior level engineering or physics course in mathematical methods. Apostol [9] or Stewart [177] can be used for the basic material, with Ahlfors [6], Marsden and Hoffman [138] or Saff and Snider [163] being good references for the more advanced material. We have chosen not to include appendices summarizing these various topics since there are a number of good books available and we believe that most readers will be familiar with material at this level.

One additional choice that we felt was important was the decision not to rely on knowledge of Laplace transforms in the book. While their use is by far the most common approach to teaching feedback systems in engineering, many students in the natural and information sciences may lack the necessary mathematical background. Since Laplace transforms are not required in any essential way, we have only included them in an advanced section intended to tie things together for students with that background. Of course, we make tremendous use of *transfer functions*, which we introduce through the notion of response to exponential inputs, an approach we feel is more accessible to a broad array of scientists and

engineers. For courses in which students have already had Laplace transforms, it should be quite natural to build on this background in the appropriate sections of the text.

Acknowledgments

The authors would like to thank the many people who helped during the preparation of this book. The idea for writing this book came in part from a report on future directions in control [147] to which Stephen Boyd, Roger Brockett, John Doyle and Gunter Stein were major contributors. Kristi Morgansen and Hideo Mabuchi helped teach early versions of the course at Caltech on which much of the text is based and Steve Waydo served as the head TA for the course taught at Caltech in 2003–04 and provide numerous comments and corrections. Charlotta Johnsson and Anton Cervin taught from early versions of the manuscript in Lund in 2003–2007 and gave very useful feedback. Other colleagues and students who provided feedback and advice include John Carson, K. Mani Chandy, Michel Charpentier, Kate Galloway, Per Hagander, Cole Lepine, Joseph Hellerstein, George Hines, Tore Hägglund, Dawn Tilbury and Francisco Zabala. The reviewers for Princeton University Press and Tom Robbins at NI Press also provided valuable comments that significantly improved the organization, layout and focus of the book. Our editor, Vickie Kearn, was a great source of encouragement and help throughout the publishing process. Finally, we would like to thank Caltech, Lund University and the University of California at Santa Barbara for providing many resources, stimulating colleagues and students, and a pleasant working environment that greatly aided in the writing of this book.

Karl Johan Åström
Lund, Sweden
Santa Barbara, California

Richard M. Murray
Pasadena, California

Chapter One

Introduction

Feedback is a central feature of life. The process of feedback governs how we grow, respond to stress and challenge, and regulate factors such as body temperature, blood pressure and cholesterol level. The mechanisms operate at every level, from the interaction of proteins in cells to the interaction of organisms in complex ecologies.

Mahlon B. Hoagland and B. Dodson, *The Way Life Works*, 1995 [94].

In this chapter we provide an introduction to the basic concept of *feedback* and the related engineering discipline of *control*. We focus on both historical and current examples, with the intention of providing the context for current tools in feedback and control. Much of the material in this chapter is adopted from [147] and the authors gratefully acknowledge the contributions of Roger Brockett and Gunter Stein for portions of this chapter.

1.1 WHAT IS FEEDBACK?

The term *feedback* is used to refer to a situation in which two (or more) dynamical systems are connected together such that each system influences the other and their dynamics are thus strongly coupled. By dynamical system, we refer to a system whose behavior changes over time, often in response to external stimulation or forcing. Simple causal reasoning about a feedback system is difficult because the first system influences the second and the second system influences the first, leading to a circular argument. This makes reasoning based on cause and effect tricky and it is necessary to analyze the system as a whole. A consequence of this is that the behavior of feedback systems is often counter-intuitive and it is therefore necessary to resort to formal methods to understand them.

Figure 1.1 illustrates in block diagram form the idea of feedback. We often use

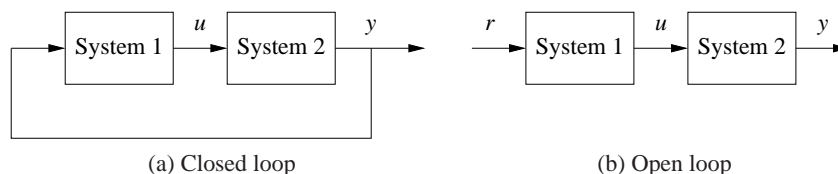


Figure 1.1: Open and closed loop systems. (a) The output of system 1 is used as the input of system 2 and the output of system 2 becomes the input of system 1, creating a “closed loop” system. (b) The interconnection between system 2 and system 1 is removed and the system is said to be “open loop”.

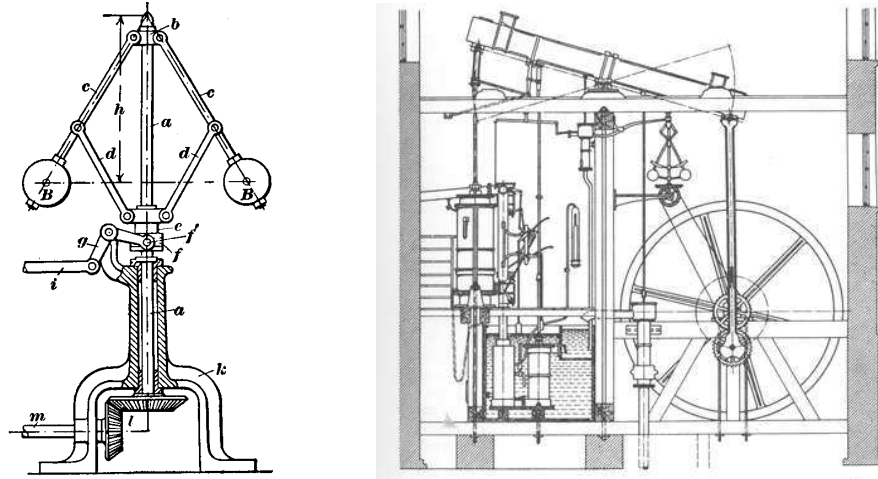


Figure 1.2: The centrifugal governor and the Watt steam engine. The centrifugal governor on the left consists of a set of “flyballs” that spread apart as the speed of the engine increases. The Watt engine on the right uses a centrifugal governor (above and to the left of the fly wheel) to regulate its speed. Figures courtesy Richard Adamek (copyright 1999) and Cambridge University.

the terms *open loop* and *closed loop* when referring to such systems. A system is said to be a closed loop system if the systems are interconnected in a cycle, as shown in Figure 1.1a. If we break the interconnection, we refer to the configuration as an open loop system, as shown in Figure 1.1b.

As the quote at the beginning of this chapter illustrates, a major source of examples for feedback systems is from biology. Biological systems make use of feedback in an extraordinary number of ways, on scales ranging from molecules to cells to organisms to ecosystems. One example is the regulation of glucose in the bloodstream through the production of insulin and glucagon by the pancreas. The body attempts to maintain a constant concentration of glucose, which is used by the body’s cells to produce energy. When glucose levels rise (after eating a meal, for example), the hormone insulin is released and causes the body to store excess glucose in the liver. When glucose levels are low, the pancreas secretes the hormone glucagon, which has the opposite effect. Referring to Figure 1.1, we can view the liver as system 1 and the pancreas as system 2. The “output” from the liver is the glucose concentration in the blood and the “output” from the pancreas is the amount of insulin or glucagon produced. The interplay between insulin and glucagon secretions throughout the day helps to keep the blood-glucose concentration constant, at about 90 mg per 100 mL of blood.

An early engineering example of a feedback system is the centrifugal governor, in which the shaft of a steam engine is connected to a flyball mechanism that is itself connected to the throttle of the steam engine, as illustrated in Figure 1.2. The system is designed so that as the speed of the engine increases (perhaps due to a lessening of the load on the engine), the flyballs spread apart and a linkage causes

the throttle on the steam engine to be closed. This in turn slows down the engine, which causes the flyballs to come back together. We can model this system as a closed loop system by taking system 1 as the steam engine and system 2 as the governor. When properly designed, the flyball governor maintains a constant speed of the engine, roughly independent of the loading conditions. The centrifugal governor was an enabler of the successful Watt steam engine, which fueled the industrial revolution.

Feedback has many interesting properties that can be exploited in designing systems. As in the case of glucose regulation or the flyball governor, feedback can make a system resilient towards external influences. It can also be used to create linear behavior out of nonlinear components, a common approach in electronics. More generally, feedback allows a system to be insensitive both to external disturbances and to variations in its individual elements.

Feedback has potential disadvantages as well. It can create dynamic instabilities in a system, causing oscillations or even runaway behavior. Another drawback, especially in engineering systems, is that feedback can introduce unwanted sensor noise into the system, requiring careful filtering of signals. It is for these reasons that a substantial portion of the study of feedback systems is devoted to developing an understanding of dynamics and mastery of techniques in dynamical systems.

Feedback systems are ubiquitous in both natural and engineered systems. Control systems maintain the environment, lighting and power in our buildings and factories; they regulate the operation of our cars, consumer electronics and manufacturing processes; they enable our transportation and communications systems; and they are critical elements in our military and space systems. For the most part they are hidden from view, buried within the code of embedded microprocessors, executing their functions accurately and reliably. Feedback has also made it possible to increase dramatically the precision of instruments such as atomic force microscopes and telescopes.

In nature, homeostasis in biological systems maintains thermal, chemical and biological conditions through feedback. At the other end of the size scale, global climate dynamics depend on the feedback interactions between the atmosphere, oceans, land and the sun. Ecosystems are filled with examples of feedback due to the complex interactions between animal and plant life. Even the dynamics of economies are based on the feedback between individuals and corporations through markets and the exchange of goods and services.

1.2 WHAT IS CONTROL?

The term “control” has many meanings and often varies between communities. In this book, we define control to be the use of algorithms and feedback in engineered systems. Thus, control includes such examples as feedback loops in electronic amplifiers, setpoint controllers in chemical and materials processing, “fly-by-wire” systems on aircraft and even router protocols that control traffic flow on the Inter-

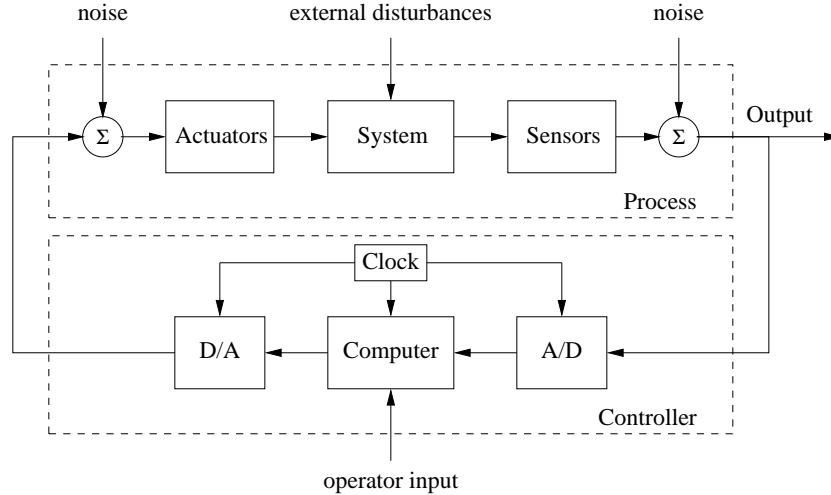


Figure 1.3: Components of a computer-controlled system. The upper dashed box represents the process dynamics, which includes the sensors and actuators in addition to the dynamical system being controlled. Noise and external disturbances can perturb the dynamics of the process. The controller is shown in the lower dashed box. It consists of analog-to-digital (A/D) and digital-to-analog (D/A) converters, as well as a computer that implements the control algorithm. A system clock controls the operation of the controller, synchronizing the A/D, D/A and computing processes. The operator input is also fed to the computer as an external input.

net. Emerging applications include high confidence software systems, autonomous vehicles and robots, real-time resource management systems and biologically engineered systems. At its core, control is an *information science*, and includes the use of information in both analog and digital representations.

A modern controller senses the operation of a system, compares that against the desired behavior, computes corrective actions based on a model of the system's response to external inputs and actuates the system to effect the desired change. This basic *feedback loop* of sensing, computation and actuation is the central concept in control. The key issues in designing control logic are ensuring that the dynamics of the closed loop system are stable (bounded disturbances give bounded errors) and that they have additional desired behavior (good disturbance rejection, fast responsiveness to changes in operating point, etc). These properties are established using a variety of modeling and analysis techniques that capture the essential dynamics of the system and permit the exploration of possible behaviors in the presence of uncertainty, noise and component failures.

A typical example of a modern control system is shown in Figure 1.3. The basic elements of sensing, computation and actuation are clearly seen. In modern control systems, computation is typically implemented on a digital computer, requiring the use of analog-to-digital (A/D) and digital-to-analog (D/A) converters. Uncertainty enters the system through noise in sensing and actuation subsystems, external disturbances that affect the underlying system operation and uncertain dy-

namics in the system (parameter errors, unmodeled effects, etc). The algorithm that computes the control action as a function of the sensor values is often called a *control law*. The system can be influenced externally by an operator who introduces *command signals* to the system.

Control engineering relies on and shares tools from physics (dynamics and modeling), computer science (information and software) and operations research (optimization, probability theory and game theory), but it is also different from these subjects in both insights and approach.

Perhaps the strongest area of overlap between control and other disciplines is in modeling of physical systems, which is common across all areas of engineering and science. One of the fundamental differences between control-oriented modeling and modeling in other disciplines is the way in which interactions between subsystems are represented. Control relies on a type of input/output modeling that allows many new insights into the behavior of systems, such as disturbance rejection and stable interconnection. Model reduction, where a simpler (lower-fidelity) description of the dynamics is derived from a high fidelity model, is also naturally described in an input/output framework. Perhaps most importantly, modeling in a control context allows the design of *robust* interconnections between subsystems, a feature that is crucial in the operation of all large engineered systems.

Control is also closely associated with computer science, since virtually all modern control algorithms for engineering systems are implemented in software. However, control algorithms and software can be very different from traditional computer software due to the central role of the dynamics of the system and the real-time nature of the implementation.

1.3 FEEDBACK EXAMPLES

Feedback has many interesting and useful properties. It makes it possible to design precise systems from imprecise components and to make relevant quantities in a system change in a prescribed fashion. An unstable system can be stabilized using feedback and the effects of external disturbances can be reduced. Feedback also offers new degrees of freedom to a designer by exploiting sensing, actuation and computation. In this section we survey some of the important applications and trends for feedback in the world around us.

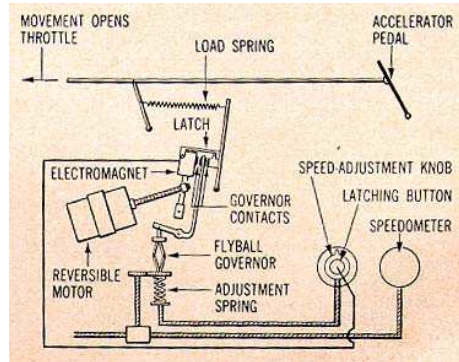
Early Technological Examples

The proliferation of control in engineered systems has occurred primarily in the latter half of the 20th century. There are some important exceptions, such as the centrifugal governor described earlier and the thermostat (Figure 1.4a), designed at the turn of the century to regulate temperature of buildings.

The thermostat, in particular, is a simple example of feedback control that everyone is familiar with. The device measures the temperature in a building, compares that temperature to a desired setpoint, and uses the “feedback error” between



(a) Honeywell thermostat, 1953



(b) Chrysler cruise control, 1958

Figure 1.4: Early control devices. (a) Honeywell T86 thermostat, originally introduced in 1953. The thermostat controls whether a heater is turned on by comparing the current temperature in a room to a desired value that is set using a dial. (b) Chrysler cruise control system, introduced in the 1958 Chrysler Imperial [161]. A centrifugal governor is used to detect the speed of the vehicle and actuate the throttle. The reference speed is specified through an adjustment spring.

these two to operate the heating plant, e.g. to turn heating on when the temperature is too low and to turn it off when the temperature is too high. This explanation captures the essence of feedback, but it is a bit too simple even for a basic device such as the thermostat. Actually, because lags and delays exist in the heating plant and sensor, a good thermostat does a bit of anticipation, turning the heater off before the error actually changes sign. This avoids excessive temperature swings and cycling of the heating plant. This interplay between the dynamics of the process and the operation of the controller is a key element in modern control systems design.

There are many other control system examples that have developed over the years with progressively increasing levels of sophistication. An early system with broad public exposure was the “cruise control” option introduced on automobiles in 1958 (see Figure 1.4b). Cruise control illustrates the dynamic behavior of closed loop feedback systems in action—the slowdown error as the system climbs a grade, the gradual reduction of that error due to integral action in the controller, the small overshoot at the top of the climb, etc. Later control systems on automobiles such as emission controls and fuel metering systems have achieved major reductions of pollutants and increases in fuel economy.

Power Generation and Transmission

Access to electrical power has been one of the major drivers of technological progress in modern society. Much of the early development of control was driven by generation and distribution of electric power. Control is mission critical for power systems and there are many control loops in individual power stations. Control is also important for the operation of the whole power network since it

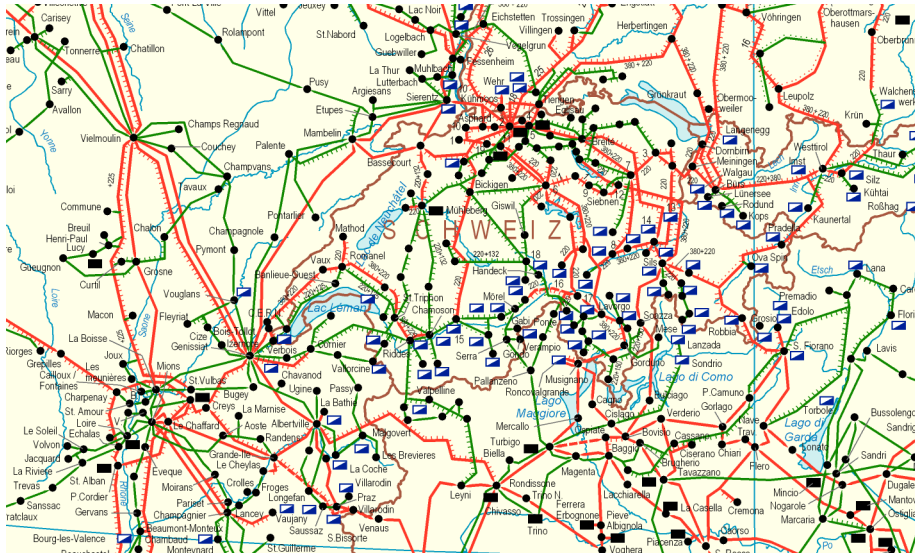


Figure 1.5: The European Power Network. By 2007 the European power suppliers will operate a single interconnected network covering a region from the Arctic to the Mediterranean and from the Atlantic to the Ural. In 2004 the installed power was more than 700 GW (7×10^{11} W).

is difficult to store energy and is thus necessary to match production to consumption. Power management is a straightforward regulation problem for a system with one generator and one power consumer, but it is more difficult in a highly distributed system with many generators and long distances between consumption and generation. Power demand can change rapidly in an unpredictable manner and combining generators and consumers into large networks makes it possible to share loads among many suppliers and to average consumption among many customers. Large transcontinental and transnational power systems have therefore been built, such as the one shown in Figure 1.5.

Most electricity is distributed by alternating current (AC) because the transmission voltage can be changed with small power losses using transformers. Alternating current generators can only deliver power if the generators are synchronized to the voltage variations in the network. This means that the rotors of all generators in a network must be synchronized. To achieve this with local decentralized controllers and a small amount of interaction is a challenging problem. Sporadic low frequency oscillations between distant regions have been observed when regional power grids have been interconnected [126].

Safety and reliability are major concerns in power systems. There may be disturbances due to trees falling down on power lines, lightning or equipment failures. There are sophisticated control systems that attempt to keep the system operating even when there are large disturbances. The control actions can be to reduce voltage, to break up the net into subnets or to switch off lines and power users. These safety systems are an essential element of power distribution systems, but in spite



(a) F/A-18 “Hornet”



(b) X-45 UCAV

Figure 1.6: Military aerospace systems. (a) The F/A-18 aircraft is one of the first production military fighters to use “fly-by-wire” technology. (b) The X-45 (UCAV) unmanned aerial vehicle is capable of autonomous flight, using inertial measurement sensors and the global positioning system (GPS) to monitor its position relative to a desired trajectory. Photographs courtesy of NASA Dryden Flight Research Center.

of all precautions there are occasionally failures in large power systems. The power system is thus a nice example of a complicated distributed system where control is executed on many levels and in many different ways.

Aerospace and Transportation

In aerospace, control has been a key technological capability tracing back to the beginning of the 20th century. Indeed, the Wright brothers are correctly famous not simply for demonstrating powered flight but *controlled* powered flight. Their early Wright Flyer incorporated moving control surfaces (vertical fins and canards) and warpable wings that allowed the pilot to regulate the aircraft’s flight. In fact, the aircraft itself was not stable, so continuous pilot corrections were mandatory. This early example of controlled flight is followed by a fascinating success story of continuous improvements in flight control technology, culminating in the high performance, highly reliable automatic flight control systems we see on modern commercial and military aircraft today.

Similar success stories for control technology have occurred in many other application areas. Early World War II bombsights and fire control servo systems have evolved into today’s highly accurate radar-guided guns and precision-guided weapons. Early failure-prone space missions have evolved into routine launch operations, manned landings on the moon, permanently manned space stations, robotic vehicles roving Mars, orbiting vehicles at the outer planets and a host of commercial and military satellites serving various surveillance, communication, navigation and earth observation needs. Cars have advanced from manually-tuned mechanical/pneumatic technology to computer-controlled operation of all major functions, including fuel injection, emission control, cruise control, braking and cabin comfort.

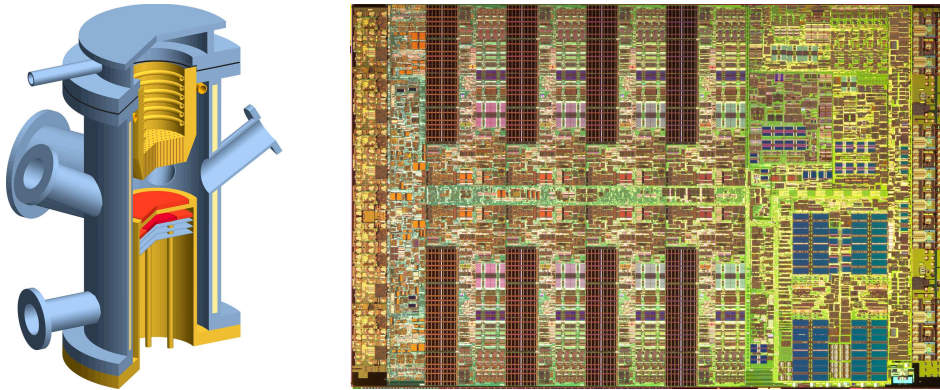


Figure 1.7: Materials processing. Modern materials are processed at carefully controlled conditions, using reactors such as the metal organic chemical vapor deposition (MOCVD) reactor shown on the left, which was for manufacturing superconducting thin films. Using lithography, chemical etching, vapor deposition and other techniques, complex devices can be built, such as the IBM cell processor shown on the right. Photographs courtesy of Caltech and IBM.

Current research in aerospace and transportation systems is investigating the application of feedback to higher levels of decision making, including logical regulation of operating modes, vehicle configurations, payload configurations and health status. These have historically been performed by human operators, but today that boundary is moving and control systems are increasingly taking on these functions. Another dramatic trend on the horizon is the use of large collections of distributed entities with local computation, global communication connections, little regularity imposed by the laws of physics and no possibility of imposing centralized control actions. Examples of this trend include the national airspace management problem, automated highway and traffic management, and command and control for future battlefields.

Materials and Processing

The chemical industry is responsible for the remarkable progress in developing new materials that are key to our modern society. In addition to the continuing need to improve product quality, several other factors in the process control industry are drivers for the use of control. Environmental statutes continue to place stricter limitations on the production of pollutants, forcing the use of sophisticated pollution control devices. Environmental safety considerations have led to the design of smaller storage capacities to diminish the risk of major chemical leakage, requiring tighter control on upstream processes and, in some cases, supply chains. And large increases in energy costs have encouraged engineers to design plants that are highly integrated, coupling many processes that used to operate independently. All of these trends increase the complexity of these processes and the performance requirements for the control systems, making the control system

design increasingly challenging.

As in many other application areas, new sensor technology is creating new opportunities for control. Online sensors—including laser backscattering, video microscopy, and ultraviolet, infrared and Raman spectroscopy—are becoming more robust and less expensive and are appearing in more manufacturing processes. Many of these sensors are already being used by current process control systems, but more sophisticated signal processing and control techniques are needed to use more effectively the real-time information provided by these sensors. Control engineers can also contribute to the design of even better sensors, which are still needed, for example, in the microelectronics industry. As elsewhere, the challenge is making use of the large amounts of data provided by these new sensors in an effective manner. In addition, a control-oriented approach to modeling the essential physics of the underlying processes is required to understand fundamental limits on observability of the internal state through sensor data.

Instrumentation

Measurement of physical variables is of prime interest in science and engineering. Consider for example an accelerometer, where early instruments consisted of a mass suspended on a spring with a deflection sensor. The precision of such an instrument depends critically on accurate calibration of the spring and the sensor. There is also a design compromise because a weak spring gives high sensitivity but also low bandwidth.

A different way of measuring acceleration is to use *force feedback*. The spring is then replaced by a voice coil that is controlled so that the mass remains at a constant position. The acceleration is proportional to the current through the voice coil. In such an instrument, the precision depends entirely on the calibration of the voice coil and does not depend on the sensor, which is only used as the feedback signal. The sensitivity/bandwidth compromise is also avoided. This way of using feedback has been applied to many different engineering fields and has resulted in instruments with dramatically improved performance. Force feedback is also used in haptic devices for manual control.

Feedback is widely used to measure ion currents in cells using a device called the *voltage clamp*, which is illustrated in Figure 1.8. Hodgkin and Huxley used the voltage clamp to investigate propagation of action potentials in the axon of the giant squid. In 1963 they shared the Nobel Prize in Medicine with Eccles for “their discoveries concerning the ionic mechanisms involved in excitation and inhibition in the peripheral and central portions of the nerve cell membrane”. A refinement of the voltage clamp called the *patch clamp* later made it possible to measure exactly when a single ion channel is opened or closed. This was developed by Neher and Sakmann, who received the 1991 Nobel Prize in Medicine “for their discoveries concerning the function of a single ion channels in cells”.

There are many other interesting and useful applications of feedback in scientific instruments. The development of the mass spectrometer is an early example.

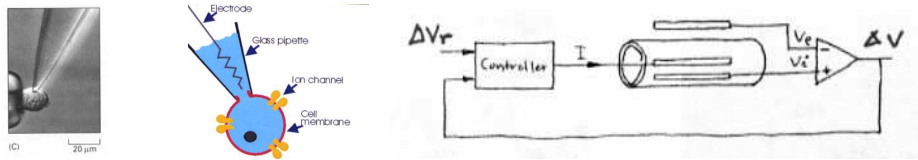


Figure 1.8: The voltage clamp method for measuring ion currents in cells. A pipet is used to place an electrode in a cell (left and middle) and maintain the potential of the cell at a fixed level. The internal voltage in the cell is v_i and the voltage of the external fluid is v_e . The feedback system (right) controls the current I into the cell so that the voltage drop across the cell membrane $\Delta v = v_i - v_e$ is equal to its reference value Δv_r . The current I is then equal to the ion current.

In a 1935 paper, Nier observed that the deflection of the ions depends on both the magnetic and the electric fields [149]. Instead of keeping both fields constant, Nier let the magnetic field fluctuate and the electric field was controlled to keep the ratio of the fields constant. The feedback was implemented using vacuum tube amplifiers. The scheme was crucial for the development of mass spectroscopy.

The Dutch Engineer van der Meer invented a clever way to use feedback to maintain a good quality, high density beam in a particle accelerator [144]. The idea is to sense particle displacement at one point in the accelerator and apply a correcting signal at another point. The scheme, called stochastic cooling, was awarded the Nobel Prize in Physics in 1984. The method was essential for the successful experiments at CERN where the existence of the particles W and Z associated with the weak force was first demonstrated.

The 1986 Nobel Prize in Physics—awarded to Binnig and Rohrer for their design of the scanning tunneling microscope—is another example of an innovative use of feedback. The key idea is to move a narrow tip on a cantilever beam across the surface and to register the forces on the tip [34]. The deflection of the tip is measured using tunneling. The tunneling current is used by a feedback system to control the position cantilever base so that the tunneling current is constant, an example of force feedback. The accuracy is so high that individual atoms can be registered. A map of the atoms is obtained by moving the base of the cantilever horizontally. The performance of the control system is directly reflected in the image quality and scanning speed. This example is described in additional detail in Chapter 3.

Robotics and Intelligent Machines

The goal of cybernetic engineering, already articulated in the 1940s and even before, has been to implement systems capable of exhibiting highly flexible or “intelligent” responses to changing circumstances. In 1948, the MIT mathematician Norbert Wiener gave a widely read account of cybernetics [191]. A more mathematical treatment of the elements of engineering cybernetics was presented by H.S. Tsien in 1954, driven by problems related to control of missiles [186]. Together, these works and others of that time form much of the intellectual basis for

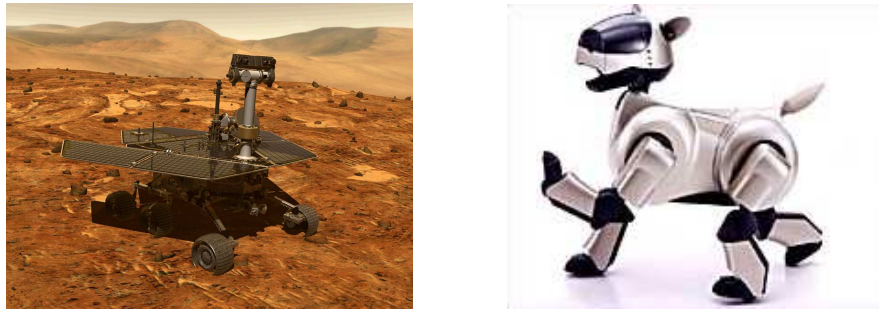


Figure 1.9: Robotic systems. (a) “Spirit”, one of the two Mars Exploratory Rovers that landed on the Mars in January 2004. (b) The Sony AIBO Entertainment Robot, one of the first entertainment robots to be mass marketed. Both robots make use of feedback between sensors, actuators and computation to function in unknown environments. Photographs courtesy of Jet Propulsion Laboratory and Sony.

modern work in robotics and control.

Two accomplishments that demonstrate the successes of the field are the Mars Exploratory Rovers and entertainment robots such as the Sony AIBO, shown in Fig. 1.9. The two Mars Exploratory Rovers, launched by the Jet Propulsion Laboratory (JPL), maneuvered on the surface of Mars for over three years starting in January 2004 and sent back pictures and measurements of their environment. The Sony AIBO robot debuted in June of 1999 and was the first “entertainment” robot to be mass marketed by a major international corporation. It was particularly noteworthy because of its use of AI technologies that allowed it to act in response to external stimulation and its own judgment. This “higher level” of feedback is a key element in robotics, where issues such as obstacle avoidance, goal seeking, learning and autonomy are prevalent.

Despite the enormous progress in robotics over the last half century, in many ways the field is still in its infancy. Today’s robots still exhibit simple behaviors compared with humans, and their ability to locomote, interpret complex sensory inputs, perform higher level reasoning and cooperate together in teams is limited. Indeed, much of Wiener’s vision for robotics and intelligent machines remains unrealized. While advances are needed in many fields to achieve this vision—including advances in sensing, actuation and energy storage—the opportunity to combine the advances of the AI community in planning, adaptation and learning with the techniques in the control community for modeling, analysis and design of feedback systems presents a renewed path for progress.

Networks and Computing Systems

Control of networks is a large research area spanning many topics, including congestion control, routing, data caching and power management. Several features of these control problems make them very challenging. The dominant feature is the extremely large scale of the system; the Internet is probably the largest feedback

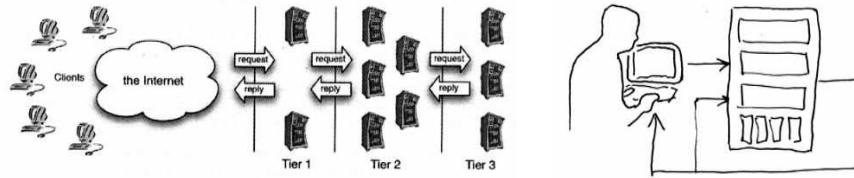


Figure 1.10: A multi-tier system for services on the Internet. In the complete system is shown schematically on the left, users request information from a set of computers (tier 1), which in turn collect information from other computers (tiers 2 and 3). The individual server shown on the right has a set of reference parameters set by a (human) system operator, with feedback used to maintain the operation of the system in the presence of uncertainty (based on Hellerstein *et al.* [92]).

control system humans have ever built. Another is the decentralized nature of the control problem: decisions must be made quickly and based only on local information. Stability is complicated by the presence of varying time lags, as information about the network state can only be observed or relayed to controllers after a delay, and the effect of a local control action can be felt throughout the network only after substantial delay. Uncertainty and variation in the network, through network topology, transmission channel characteristics, traffic demand and available resources, may change constantly and unpredictably. Other complicating issues are the diverse traffic characteristics—in terms of arrival statistics at both the packet and flow time scales—and the different requirements for quality of service that the network must support.

Related to control of networks is control of the servers that sit on these networks. Computers are key components of the systems of routers, web servers and database servers that are used for communication, electronic commerce, advertisement and information storage. While hardware costs for computing have decreased dramatically, the cost of operating these systems has increased due to the difficulty in managing and maintaining these complex, interconnected systems. The situation is similar to the early phases of process control when feedback was first introduced to control industrial processes. As in process control, there are interesting possibilities for increasing performance and decreasing costs by applying feedback. Several promising uses of feedback in operation of computer systems are described in the book by Hellerstein *et al.* [92].

A typical example of a multi-layer system for e-commerce is shown in Figure 1.10a. The system has several tiers of servers. The edge server accepts incoming requests and routes them to the HTTP server tier where they are parsed and distributed to the application servers. The processing for different requests can vary widely and the application servers may also access external servers managed by other organizations.

Control of an individual server in a layer is illustrated in Figure 1.10b. A quantity representing the quality of service or cost of operation such as response time, throughput, service rate or memory usage is measured in the computer. The con-

trol variables might represent incoming messages accepted, priorities in the operating system or memory allocation. The feedback loop then attempts to maintain quality-of-service variables within a target range of values.

Economics

The economy is a large dynamical system with many actors: governments, organizations, companies and individuals. Governments control the economy through laws and taxes, the central banks by setting interest rates and companies by setting prices and making investments. Individuals control the economy through purchases, savings and investments. Many efforts have been made to model the system both at the macro level and at the micro level, but this modeling is difficult because the system is strongly influenced by the behaviors of the different actors in the system.

Keynes [115] developed a simple model to understand relations between gross national product, investment, consumption and government spending. One of Keynes' observations was that under certain conditions, like during the 1930s depression, an increase of investment of government spending could lead to a larger increase in the gross national product. This idea was used by several governments to try to alleviate the depression. Keynes' ideas can be captured by a simple model that is discussed in Exercise 2.4.

A perspective on modeling and control of economic systems can be obtained from the work of some economists who received the “the Sveriges Riksbank Prize in Economics in Memory of Alfred Nobel”, popularly called the Nobel Prize in Economics. Paul A. Samuelson received the prize in 1970 for “the scientific work through which he has developed static and dynamic economic theory and actively contributed to rising the level of analysis in economic science”. Lawrence Klein received the prize in 1980 for development of large dynamical models with many parameters that were fitted to historical data [119], for example a model of the US economy in the period 1929-1952. Other researchers have modeled other countries and other periods. In 1997 Myron Scholes shared the prize with Robert Merton for a new method to determine the value of derivatives. A key ingredient was a dynamic model for variation of stock prices that is widely used by banks and investment companies. In 2004 Finn E. Kydland and Edward C. Prescott shared the economics prize “for their contributions to dynamic macroeconomics: the time consistency of economic policy and the driving forces behind business cycles”, a topic that is clearly related to dynamics and control.

One of the reasons why it is difficult to model economic systems is that there are no conservation laws. A typical example is that the value of a company as expressed by its stock can change rapidly and erratically. There are, however, some areas with conservation laws that permit accurate modeling. One example is the flow of products from a manufacturer to a retailer as illustrated in Figure 1.11. The products are physical quantities that obey a conservation law and the system can be modeled simply by accounting for the number of products in the different inven-

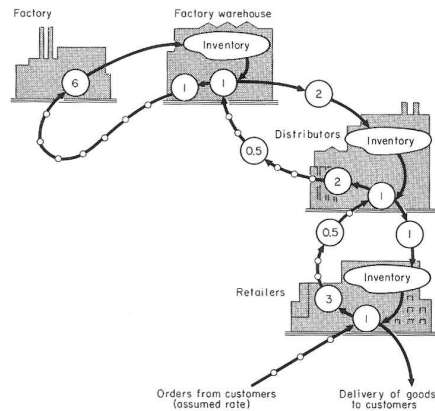


Figure 1.11: Supply chain dynamics (after Forrester [72]). Products flow from the producer to the customer through distributors and retailers as indicated by the solid lines. The dashed lines show the upward flow of orders. The numbers in the circles represent the delays in the flow of information or materials. Multiple feedback loops are present as each agent tries to maintain the proper inventory levels.

tories. There are considerable economic benefits in controlling supply chains so that products are available to the customers while minimizing the products that are in storage. The real problems are more complicated than indicated in the figure because there may be many different products, different factories that are geographically distributed and the factories require raw material or sub-assemblies.

Control of supply chains was proposed by Forrester in 1961 [72]. Considerable economic benefits can be obtained by using models to minimize inventories. Their use accelerated dramatically when information technology was applied to predict sales, keep track of products and enable just-in-time manufacturing. Supply chain management has contributed significantly to the growing success of global distributors.

Advertising on the Internet is an emerging application of control. With network-based advertising it is easy to measure the effect of different marketing strategies quickly. The response of customers can then be modeled and feedback strategies can be developed.

Feedback in Nature

Many problems in the natural sciences involve understanding aggregate behavior in complex large-scale systems. This behavior “emerges” from the interaction of a multitude of simpler systems, with intricate patterns of information flow. Representative examples can be found in fields ranging from embryology to seismology. Researchers who specialize in the study of specific complex systems often develop an intuitive emphasis on analyzing the role of feedback (or interconnection) in facilitating and stabilizing aggregate behavior.

While sophisticated theories have been developed by domain experts for the

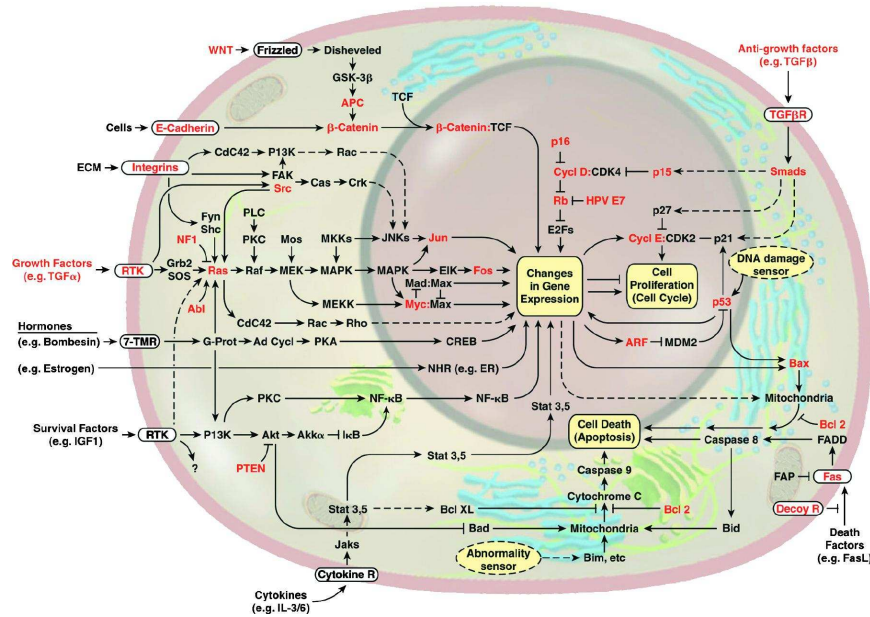


Figure 1.12: The wiring diagram of the growth signaling circuitry of the mammalian cell [91]. The major pathways that are thought to play a role in cancer are indicated in the diagram. Lines represent interaction between genes and proteins in the cell. Lines ending in arrow heads indicated activation of the given gene or pathway; lines ending in a T-shaped head indicate repression.

analysis of various complex systems, the development of rigorous methodology that can discover and exploit common features and essential mathematical structure is just beginning to emerge. Advances in science and technology are creating new understanding of the underlying dynamics and the importance of feedback in a wide variety of natural and technological systems. We briefly highlight three application areas here.

Biological Systems. A major theme currently underway in the biology community is the science of reverse (and eventually forward) engineering of biological control networks such as the one shown in Figure 1.12. There are a wide variety of biological phenomena that provide a rich source of examples for control, including gene regulation and signal transduction; hormonal, immunological and cardiovascular feedback mechanisms; muscular control and locomotion; active sensing, vision and proprioception; attention and consciousness; and population dynamics and epidemics. Each of these (and many more) provide opportunities to figure out what works, how it works, and what we can do to affect it.

One interesting feature of biological systems is the frequent use of positive feedback to shape the dynamics of the system. Positive feedback can be used to create switch-like behavior through auto-regulation of a gene, and to create oscillations such as those present in the cell cycle, central pattern generators or circadian rhythm.

Ecosystems. In contrast to individual cells and organisms, emergent properties of aggregations and ecosystems inherently reflect selection mechanisms that act on multiple levels, and primarily on scales well below that of the system as a whole. Because ecosystems are complex, multiscale dynamical systems, they provide a broad range of new challenges for modeling and analysis of feedback systems. Recent experience in applying tools from control and dynamical systems to bacterial networks suggests that much of the complexity of these networks is due to the presence of multiple layers of feedback loops that provide robust functionality to the individual cell. Yet in other instances, events at the cell level benefit the colony at the expense of the individual. Systems level analysis can be applied to ecosystems with the goal of understanding the robustness of such systems and the extent to which decisions and events affecting individual species contribute to the robustness and/or fragility of the ecosystem as a whole.

Environmental Science. It is now indisputable that human activities have altered the environment on a global scale. Problems of enormous complexity challenge researchers in this area and first among these is to understand the feedback systems that operate on the global scale. One of the challenges in developing such an understanding is the multiscale nature of the problem, with detailed understanding of the dynamics of microscale phenomena such as microbiological organisms being a necessary component of understanding global phenomena, such as the carbon cycle.

1.4 FEEDBACK PROPERTIES

Feedback is a powerful idea which, as we have seen, is used extensively in natural and technological systems. The principle of feedback is simple: base correcting actions on the difference between desired and actual performance. In engineering, feedback has been rediscovered and patented many times in many different contexts. The use of feedback has often resulted in vast improvements in system capability and these improvements have sometimes been revolutionary, as discussed above. The reason for this is that feedback has some truly remarkable properties. In this section we will discuss some of the properties of feedback that can be understood intuitively. This intuition will be formalized in the subsequent chapters.

Robustness to Uncertainty

One of the key uses of feedback is to provide robustness to uncertainty. By measuring the difference between the sensed value of a regulated signal and its desired value, we can supply a corrective action. If the system undergoes some change that affects the regulated signal, then we sense this change and try to force the system back to the desired operating point. This is precisely the effect that Watt exploited in his use of the centrifugal governor on steam engines.

As an example of this principle, consider the simple feedback system shown in Figure 1.13. In this system, the speed of a vehicle is controlled by adjusting

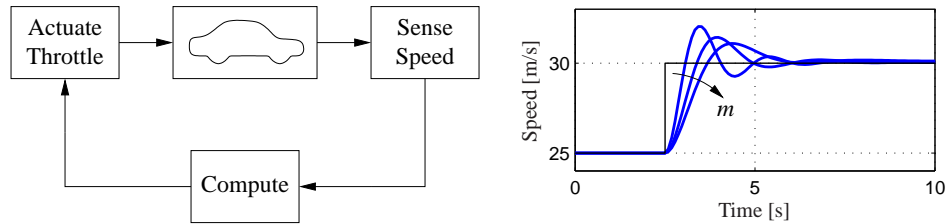


Figure 1.13: A feedback system for controlling the speed of a vehicle. In the block diagram on the left, the speed of the vehicle is measured and compared to the desired speed within the “compute” block. Based on the difference in the actual and desired speed, the throttle (or brake) is used to modify the force applied to the vehicle by the engine, drivetrain and wheels. The figure on the right shows the response of the control system to a commanded change in speed from 25 m/s to 30 m/s. The three different curves correspond to differing masses of the vehicle, between 1000 and 3000 kg, demonstrating the robustness of the closed loop system to a very large change in the vehicle characteristics.

the amount of gas flowing to the engine. A simple “proportional plus integral” feedback is used to make the amount of gas depend on both the error between the current and desired speed, and the integral of that error. The plot on the right shows the results of this feedback for a step change in the desired speed and a variety of different masses for the car, which might result from having a different number of passengers or towing a trailer. Notice that independent of the mass (which varies by a factor of 3!), the steady state speed of the vehicle always approaches the desired speed and achieves that speed within approximately 5 seconds. Thus the performance of the system is robust with respect to this uncertainty.

Another early example of the use of feedback to provide robustness is the negative feedback amplifier. When telephone communications were developed, amplifiers were used to compensate for signal attenuation in long lines. The vacuum tube was a component that could be used to build amplifiers. Distortion caused by the nonlinear characteristics of the tube amplifier together with amplifier drift were obstacles that prevented development of line amplifiers for a long time. A major breakthrough was the invention of the feedback amplifier in 1927 by Harold S. Black, an electrical engineer at the Bell Telephone Laboratories. Black used *negative feedback*, which reduces the gain but makes the amplifier insensitive to variations in tube characteristics. This invention made it possible to build stable amplifiers with linear characteristics despite nonlinearities of the vacuum tube amplifier.

Design of Dynamics

Another use of feedback is to change the dynamics of a system. Through feedback, we can alter the behavior of a system to meet the needs of an application: systems that are unstable can be stabilized, systems that are sluggish can be made responsive and systems that have drifting operating points can be held constant.

Control theory provides a rich collection of techniques to analyze the stability and dynamic response of complex systems and to place bounds on the behavior of such systems by analyzing the gains of linear and nonlinear operators that describe their components.

An example of the use of control in the design of dynamics comes from the area of flight control. The following quote, from a lecture by Wilbur Wright to the Western Society of Engineers in 1901 [141], illustrates the role of control in the development of the airplane:

“Men already know how to construct wings or airplanes, which when driven through the air at sufficient speed, will not only sustain the weight of the wings themselves, but also that of the engine, and of the engineer as well. Men also know how to build engines and screws of sufficient lightness and power to drive these planes at sustaining speed ... Inability to balance and steer still confronts students of the flying problem. ... When this one feature has been worked out, the age of flying will have arrived, for all other difficulties are of minor importance.”

The Wright brothers thus realized that control was a key issue to enable flight. They resolved the compromise between stability and maneuverability by building an airplane, the Wright Flyer, that was unstable but maneuverable. The Flyer had a rudder in the front of the airplane, which made the plane very maneuverable. A disadvantage was the necessity for the pilot to keep adjusting the rudder to fly the plane: if the pilot let go of the stick the plane would crash. Other early aviators tried to build stable airplanes. These would have been easier to fly, but because of their poor maneuverability they could not be brought up into the air. By using their insight and skillful experiments the Wright brothers made the first successful flight at Kitty Hawk in 1905.

Since it was quite tiresome to fly an unstable aircraft, there was strong motivation to find a mechanism that would stabilize an aircraft. Such a device, invented by Sperry, was based on the concept of feedback. Sperry used a gyro-stabilized pendulum to provide an indication of the vertical. He then arranged a feedback mechanism that would pull the stick to make the plane go up if it was pointing down and vice versa. The Sperry autopilot is the first use of feedback in aeronautical engineering and Sperry won a prize in a competition for the safest airplane in Paris in 1914. Figure 1.14 shows the Curtiss seaplane and the Sperry autopilot. The autopilot is a good example of how feedback can be used to stabilize an unstable system and hence “design the dynamics” of the aircraft.

One of the other advantages of designing the dynamics of a device is that it allows for increased modularity in the overall system design. By using feedback to create a system whose response matches a desired profile, we can hide the complexity and variability that may be present inside a subsystem. This allows us to create more complex systems by not having to simultaneously tune the response of a large number of interacting components. This was one of the advantages of



Figure 1.14: Aircraft autopilot system. The 1912 Curtiss (left) used an autopilot to stabilize the pitch of the aircraft. The Sperry Autopilot (right) contained a set of four gyros coupled to a set of air valves that controlled the wing surfaces. The Sperry Autopilot was able to correct for errors in roll, pitch and yaw [99].

Black’s use of negative feedback in vacuum tube amplifiers: the resulting device had a well-defined linear input/output response that did not depend on the individual characteristics of the vacuum tubes being used.

Higher Levels of Automation

A major trend in the use of feedback is its application to higher levels of situational awareness and decision making. This includes not only traditional logical branching based on system conditions, but optimization, adaptation, learning and even higher levels of abstract reasoning. These problems are in the domain of the artificial intelligence (AI) community, with an increasing role of dynamics, robustness and interconnection in many applications.

An example of this trend is the DARPA Grand Challenge, a series of competitions sponsored by the US government to build vehicles that can autonomously drive themselves in desert and urban environments. Caltech competed in the 2005 and 2007 Grand Challenges using a modified Ford E-350 offroad van, nicknamed “Alice.” It was fully automated, including electronically-controlled steering, throttle, brakes, transmission and ignition. Its sensing systems included multiple video cameras scanning at 10–30 Hz, several laser ranging units scanning at 10 Hz, and an inertial navigation package capable of providing position and orientation estimates at 2.5 ms temporal resolution. Computational resources included 7 high speed servers connected together through a 1 Gb/s Ethernet switch. A picture of the vehicle is shown in Figure 1.15, along with a block diagram of its control architecture.

The software and hardware infrastructure that was developed enabled the vehicle to traverse long distances at substantial speeds. In testing, Alice drove itself over 500 kilometers in the Mojave Desert of California, with the ability to follow dirt roads and trails (if present) and avoid obstacles along the path. Speeds

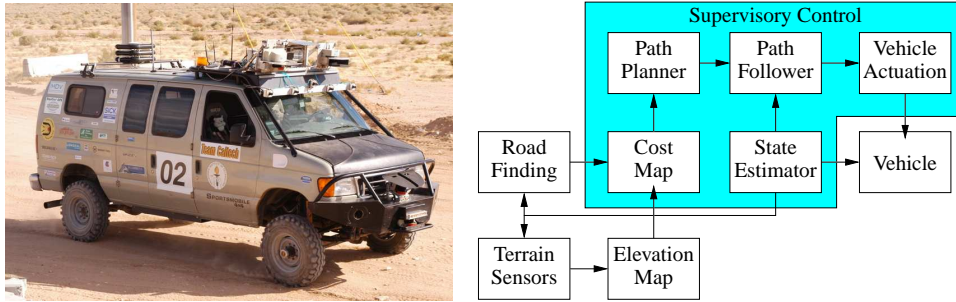


Figure 1.15: DARPA Grand Challenge. “Alice”, Team Caltech’s entry in the 2005 and 2007 competitions and its networked control architecture [52]. The feedback system fuses data from terrain sensors (cameras and laser range finders) to determine a digital elevation map. This map is used to compute the vehicle’s potential speed over the terrain and an optimization-based path planner then commands a trajectory for the vehicle to follow. A supervisory control module performs higher level tasks such as handling sensor and actuator failures.

of over 50 km/hr were obtained in fully autonomous mode. Substantial tuning of the algorithms was done during desert testing, in part due to the lack of systems-level design tools for systems of this level of complexity. Other competitors in the race (including Stanford, which won the competition) used algorithms for adaptive control and learning, increasing the capabilities of their systems in unknown environments. Together, the competitors in the Grand Challenge demonstrated some of the capabilities for the next generation of control systems and highlighted many research directions in control at higher levels of decision making.

Drawbacks of Feedback

While feedback has many advantages, it also has some drawbacks. Chief among these is the possibility for instability if the system is not designed properly. We are all familiar with the effects of “positive feedback” when the amplification on a microphone is turned up too high in a room. This is an example of a feedback instability, something that we obviously want to avoid. This is tricky because we must not only design the system to be stable under nominal conditions, but to remain stable under all possible perturbations of the dynamics.

In addition to the potential for instability, feedback inherently couples different parts of a system. One common problem is that feedback often injects measurement noise into the system. Measurements must be carefully filtered so that the actuation and process dynamics do not respond to them, while at the same time ensuring that the measurement signal from the sensor is properly coupled into the closed loop dynamics (so that the proper levels of performance are achieved).

Another potential drawback of control is the complexity of embedding a control system into a product. While the cost of sensing, computation and actuation has decreased dramatically in the past few decades, the fact remains that control systems are often complicated and hence one must carefully balance the costs and

benefits. An early engineering example of this is the use of microprocessor-based feedback systems in automobiles. The use of microprocessors in automotive applications began in the early 1970s and was driven by increasingly strict emissions standards, which could only be met through electronic controls. Early systems were expensive and failed more often than desired, leading to frequent customer dissatisfaction. It was only through aggressive improvements in technology that the performance, reliability and cost of these systems allowed them to be used in a transparent fashion. Even today, the complexity of these systems is such that it is difficult for an individual car owner to fix problems.

Feedforward

Feedback is reactive: there must be an error before corrective actions are taken. However, in some circumstances it is possible to measure a disturbance before it enters the system and this information can be used to take corrective action before the disturbance has influenced the system. The effect of the disturbance is thus reduced by measuring it and generating a control signal that counteracts it. This way of controlling a system is called *feedforward*. Feedforward is particularly useful to shape the response to command signals because command signals are always available. Since feedforward attempts to match two signals, it requires good process models; otherwise the corrections may have the wrong size or may be badly timed.

The ideas of feedback and feedforward are very general and appear in many different fields. In economics, feedback and feedforward are analogous to a market-based economy versus a planned economy. In business a feedforward strategy corresponds to running a company based on extensive strategic planning while a feedback strategy corresponds to a reactive approach. Experience indicates that it is often advantageous to combine feedback and feedforward. Feedforward is particularly useful when disturbances can be measured or predicted. A typical example is in chemical process control where disturbances in one process may be due to other processes upstream. The correct balance of the approaches requires insight and understanding of their properties.

Positive Feedback

In most of this text, we will consider the role of negative feedback, in which we attempt to regulate the system by reacting to disturbances in a way that decreases the effect of those disturbances. In some systems, particularly biological systems, *positive feedback* can play an important role. In a system with positive feedback, the increase in some variable or signal leads to a situation in which that quantity is further increased through its dynamics. This has a destabilizing effect and is usually accompanied by a saturation that limits the growth of the quantity. Although often considered undesirable, this behavior is used in biological (and engineering) systems to obtain a very fast response to a condition or signal.

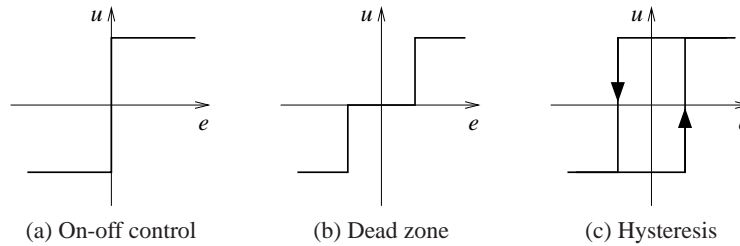


Figure 1.16: Input-output characteristics of on-off controllers. Each plot shows the input on the horizontal axis and the corresponding output on the vertical axis. Ideal on-off control is shown in (a), with modifications for a dead zone (b) or hysteresis (c). Note that for on-off control with hysteresis, the output depends on the value of past inputs.

One example of the use of positive feedback is to create switching behavior, in which a system maintains a given state until some input has crossed a threshold. Hysteresis is often present so that noisy inputs near the threshold do not cause the system to jitter. This type of behavior is called *bistability* and is often associated with memory devices.

1.5 SIMPLE FORMS OF FEEDBACK

The idea of feedback to make corrective actions based on the difference between the desired and actual values of a quantity can be implemented in many different ways. The benefits of feedback can be obtained by very simple feedback laws such as on-off control, proportional control and PID control. In this section we provide a brief preview of some of the topics that will be studied more formally in the remainder of the text.

On-off Control

A simple feedback mechanism can be described as follows:

$$u = \begin{cases} u_{\max} & \text{if } e > 0 \\ u_{\min} & \text{if } e < 0 \end{cases} \quad (1.1)$$

where $e = r - y$ is the difference between the reference signal r and the output of the system y , and u is the actuation command. Figure 1.16a shows the relation between error and control. This control law implies that maximum corrective action is always used.

The feedback in equation (1.1) is called *on-off control*. One of its chief advantages is that it is simple and there are no parameters to choose. On-off control often succeeds in keeping the process variable close to the reference, such as the use of a simple thermostat to maintain the temperature of a room. It typically results in a system where the controlled variables oscillate, which is often acceptable if the oscillation is sufficiently small.

Notice that in equation (1.1) the control variable is not defined when the error is zero. It is common to make modifications either by introducing hysteresis or a dead zone (see Figure 1.16b and 1.16c).

PID Control

The reason why on-off control often gives rise to oscillations is that the system overreacts since a small change in the error will make the actuated variable change over the full range. This effect is avoided in *proportional control*, where the characteristic of the controller is proportional to the control error for small errors. This can be achieved with the control law

$$u = \begin{cases} u_{\max} & \text{if } e \geq e_{\max} \\ k_p e & \text{if } e_{\min} < e < e_{\max} \\ u_{\min} & \text{if } e \leq e_{\min}, \end{cases} \quad (1.2)$$

where where k_p is the controller gain, $e_{\min} = u_{\min}/k_p$, and $e_{\max} = u_{\max}/k_p$. The interval (e_{\min}, e_{\max}) is called the *proportional band* because the behavior of the controller is linear when the error is in this interval:

$$u = k_p(r - y) = k_p e \quad \text{if } e_{\min} \leq e \leq e_{\max}. \quad (1.3)$$

While a vast improvement over on-off control, proportional control has the drawback that the process variable often deviates from its reference value. In particular, if some level of control signal is required for the system to maintain a desired value, then we must have $e \neq 0$ in order to generate the requisite input.

This can be avoided by making the control action proportional to the integral of the error:

$$u(t) = k_i \int_0^t e(\tau) d\tau. \quad (1.4)$$

This control form is called *integral control* and k_i is the integral gain. It can be shown through simple arguments that a controller with integral action will have zero “steady state” error (Exercise 1.5). The catch is that there may not always be a steady state because the system may be oscillating.

An additional refinement is to provide the controller with an anticipative ability by using a prediction of the error. A simple prediction is given by the linear extrapolation

$$e(t + T_d) \approx e(t) + T_d \frac{de(t)}{dt},$$

which predicts the error T_d time units ahead. Combining proportional, integral and derivative control we obtain a controller that can be expressed mathematically as follows:

$$u(t) = k_p e(t) + k_i \int_0^t e(\tau) d\tau + k_d \frac{de(t)}{dt} \quad (1.5)$$

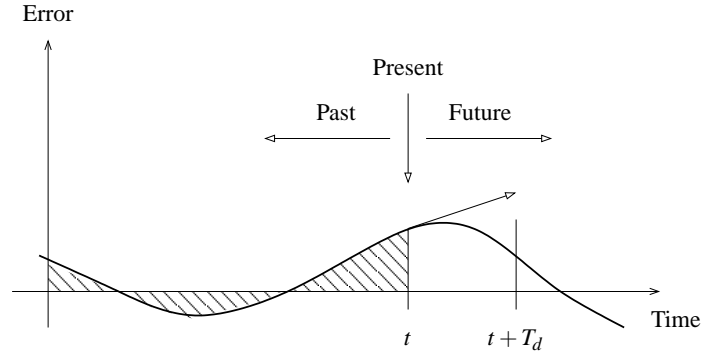


Figure 1.17: Action of a PID controller. At time t , the proportional term depends on the instantaneous value of the error. The integral portion of the feedback is based on the integral of the error up to time t (shaded portion). The derivative term provides an estimate of the growth or decay of the error over time by looking at the rate of change of the error. T_d represents the approximate amount of time in which the error is projected forward (see text).

The control action is thus a sum of three terms: the past as represented by the integral of the error, the present as represented by the proportional term and the future as represented by a linear extrapolation of the error (the derivative term). This form of feedback is called a *proportional-integral-derivative (PID) controller* and its action is illustrated in Figure 1.17.

The PID controller is very useful and is capable of solving a wide range of control problems. Over 95% of all industrial control problems are solved by PID control, although many of these controllers are actually PI controllers because derivative action is often not included [54]. There are also more advanced controllers, which differ from the PID controller by using more sophisticated methods for prediction.

1.6 FURTHER READING

The material in this section draws heavily from the report of the Panel on Future Directions on Control, Dynamics and Systems [147]. Several additional papers and reports have highlighted successes of control [150] and new vistas in control [44, 123]. The early development of control is described by Mayr [140] and the books by Bennett [27, 28], which cover the period 1800-1955. A fascinating examination of some of the early history of control in the United States has been written by Mindell [143]. A popular book that describes many control concepts across a wide range of disciplines is “Out of Control” by Kelly [114]. There are many textbooks available that describe control systems in the context of specific disciplines. For engineers, the textbooks by Franklin, Powell and Emami-Naeini [76], Dorf and Bishop [56], Kuo and Golnaraghi [125], and Seborg, Edgar and Mellichamp [169] are widely used. More mathematically oriented treatments of control theory include Sontag [173] and Lewis [128]. The book by Hellerstein

et al. [92] provides a description of the use of feedback control in computing systems. A number of books look at the role of dynamics and feedback in biological systems, including Milhorn [142] (now out of print), J. D. Murray [146] and Ellner and Guckenheimer [67]. The book by Fradkov [74] and tutorial article by Bechhoefer [24] cover many specific topics of interest to the physics community.

EXERCISES

1.1 (Eye motion) Perform the following experiment and explain your results: Holding your head still, move your right or left hand back and forth in front of your face, following it with your eyes. Record how quickly you can move your hand before you begin to lose track of your hand. Now hold your hand still and move your head back and forth, once again recording how quickly you can move before losing track.

1.2 Identify 5 feedback systems that you encounter in your everyday environment. For each system, identify the sensing mechanism, actuation mechanism and control law. Describe the uncertainty with respect to which the feedback system provides robustness and/or the dynamics that are changed through the use of feedback.

1.3 Balance yourself on one foot with your eyes closed for 15 seconds. Using Figure 1.3 as a guide, describe the control system responsible for keeping you from falling down. Note that the “controller” will differ from the diagram (unless you are an android reading this in the far future).

1.4 Download the MATLAB code used to produce the simulations for the cruise control system in Figure 1.13 from the companion web site. Using trial and error, change the parameters of the control law so that the overshoot in the speed is not more than 1 m/s for a vehicle with mass $m = 1000$ kg.

1.5 We say that a system with a constant input reaches “steady state” if the output of the system approaches a constant value as time increases. Show that a controller with integral action, such as those given in equations (1.4) and (1.5), gives zero error if the closed loop system reaches steady state.

Chapter Two

System Modeling

... I asked Fermi whether he was not impressed by the agreement between our calculated numbers and his measured numbers. He replied, "How many arbitrary parameters did you use for your calculations?" I thought for a moment about our cut-off procedures and said, "Four." He said, "I remember my friend Johnny von Neumann used to say, with four parameters I can fit an elephant, and with five I can make him wiggle his trunk."

Freeman Dyson on describing the predictions of his model for meson-proton scattering to Enrico Fermi in 1953 [62].

A model is a precise representation of a system's dynamics used to answer questions via analysis and simulation. The model we choose depends on the questions we wish to answer, and so there may be multiple models for a single dynamical system, with different levels of fidelity depending on the phenomena of interest. In this chapter we provide an introduction to the concept of modeling, and provide some basic material on two specific methods that are commonly used in feedback and control systems: differential equations and difference equations.

2.1 MODELING CONCEPTS

A model is a mathematical representation of a physical, biological or information system. Models allow us to reason about a system and make predictions about how a system will behave. In this text, we will mainly be interested in models of dynamical systems describing the input/output behavior of systems and we will often work in so-called "state space" form.

Roughly speaking, a dynamical system is one in which the effects of actions do not occur immediately. For example, the velocity of a car does not change immediately when the gas pedal is pushed nor does the temperature in a room rise instantaneously when a heater is switched on. Similarly, a headache does not vanish right after an aspirin is taken, requiring time to take effect. In business systems, increased funding for a development project does not increase revenues in the short term, although it may do so in the long term (if it was a good investment). All of these are examples of dynamical systems, in which the behavior of the system evolves with time.

In the remainder of this section we provide an overview of some of the key concepts in modeling. The mathematical details introduced here are explored more fully in the remainder of the chapter.

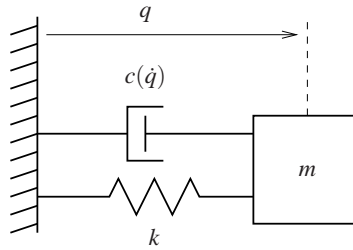


Figure 2.1: Spring-mass system, with nonlinear damping. The position of the mass is denoted by q , with $q = 0$ corresponding to the rest position of the spring. The forces on the mass are generated by a linear spring with spring constant k and a damper with force dependent on the velocity \dot{q} .

The Heritage of Mechanics

The study of dynamics originated in the attempts to describe planetary motion. The basis was detailed observations of the planets by Tycho Brahe and the results of Kepler, who found empirically that the orbits of the planets could be well described by ellipses. Newton embarked on an ambitious program to try to explain why the planets move in ellipses and he found that the motion could be explained by his law of gravitation and the formula that force equals mass times acceleration. In the process he also invented calculus and differential equations.

One of the triumphs of Newton's mechanics was the observation that the motion of the planets could be predicted based on the current positions and velocities of all planets. It was not necessary to know the past motion. The *state* of a dynamical system is a collection of variables that characterizes the motion of a system completely for the purpose of predicting future motion. For a system of planets the state is simply the positions and the velocities of the planets. We call the set of all possible states the *state space*.

A common class of mathematical models for dynamical systems is ordinary differential equations (ODEs). In mechanics, one of the simplest such differential equation is that of a spring-mass system, with damping:

$$m\ddot{q} + c(\dot{q}) + kq = 0. \quad (2.1)$$

This system is illustrated in Figure 2.1. The variable $q \in \mathbb{R}$ represents the position of the mass m with respect to its rest position. We use the notation \dot{q} to denote the derivative of q with respect to time (i.e., the velocity of the mass) and \ddot{q} to represent the second derivative (acceleration). The spring is assumed to satisfy Hooke's law, which says that the force is proportional to the displacement. The friction element (damper) is taken as a nonlinear function, $c(\dot{q})$, which can model effects such as stiction and viscous drag. The position q and velocity \dot{q} represent the instantaneous "state" of the system. We say that this system is a *second order system* since the dynamics depend on the second derivative of q .

The evolution of the position and velocity can be described using either a time plot or a phase plot, both of which are shown in Figure 2.2. The time plot, on the

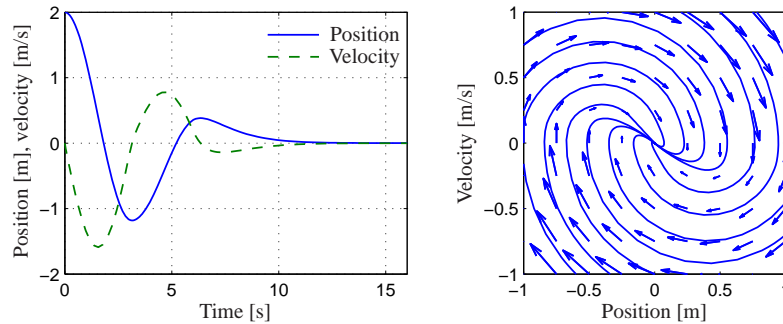


Figure 2.2: Illustration of a state model. A state model gives the rate of change of the state as a function of the state. The plot on the left shows the evolution of the state as a function of time. The plot on the right shows the evolution of the states relative to each other, with the velocity of the state denoted by arrows.

left, shows the values of the individual states as a function of time. The phase plot, on the right, shows the *vector field* for the system, which gives the state velocity (represented as an arrow) at every point in the state space. In addition, we have superimposed the traces of some of the states from different conditions. The phase plot gives a strong intuitive representation of the equation as a vector field or a flow. While systems of second order (two states) can be represented in this way, it is unfortunately difficult to visualize equations of higher order using this approach.

The differential equation (2.1) is called an *autonomous* system because there are no external influences. Such a model is natural to use for celestial mechanics, because it is difficult to influence the motion of the planets. In many examples, it is useful to model the effects of external disturbances or controlled forces on the system. One way to capture this is to replace equation (2.1) by

$$m\ddot{q} + c(\dot{q}) + kq = u \quad (2.2)$$

where u represents the effect of external inputs. The model (2.2) is called a *forced* or *controlled* differential equation. The model implies that the rate of change of the state can be influenced by the input, $u(t)$. Adding the input makes the model richer and allows new questions to be posed. For example, we can examine what influence external disturbances have on the trajectories of a system. Or, in the case when the input variable is something that can be modulated in a controlled way, we can analyze whether it is possible to “steer” the system from one point in the state space to another through proper choice of the input.

The Heritage of Electrical Engineering

A different view of dynamics emerged from electrical engineering, where the design of electronic amplifiers led to a focus on input/output behavior. A system was considered as a device that transformed inputs to outputs, as illustrated in Figure 2.3. Conceptually an input/output model can be viewed as a giant table

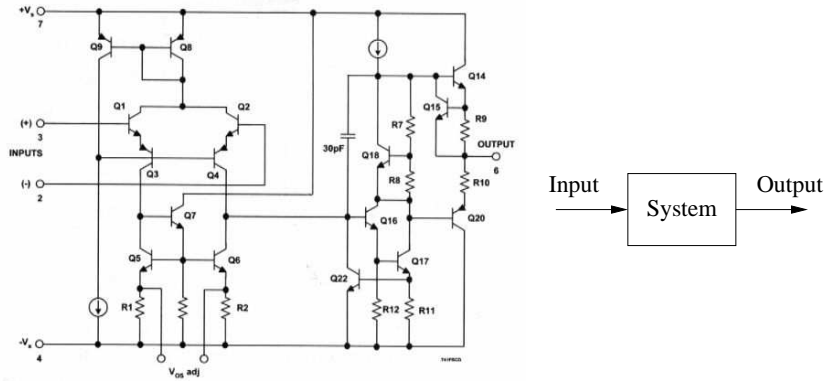


Figure 2.3: Illustration of the input/output view of a dynamical system. The figure on the left shows a detailed circuit diagram for an electronic amplifier; the one of the right its representation as a block diagram.

of inputs and outputs. Given an input signal $u(t)$ over some interval of time, the model should produce the resulting output $y(t)$.

The input/output framework is used in many engineering systems since it allows us to decompose a problem into individual components, connected through their inputs and outputs. Thus, we can take a complicated system such as a radio or a television and break it down into manageable pieces, such as the receiver, demodulator, amplifier and speakers. Each of these pieces has a set of inputs and outputs and, through proper design, these components can be interconnected to form the entire system.

The input/output view is particularly useful for the special class of *linear time-invariant* systems. This term will be defined more carefully later in this chapter, but roughly speaking a system is linear if the superposition (addition) of two inputs yields an output which is the sum of the outputs that would correspond to individual inputs being applied separately. A system is time-invariant if the output response for a given input does not depend on when that input is applied.

Many electrical engineering systems can be modeled by linear, time-invariant systems and hence a large number of tools have been developed to analyze them. One such tool is the *step response*, which describes the relationship between an input that changes from zero to a constant value abruptly (a “step” input) and the corresponding output. As we shall see in the latter part of the text, the step response is very useful in characterizing the performance of a dynamical system and it is often used to specify the desired dynamics. A sample step response is shown in Figure 2.4a.

Another possibility to describe a linear, time-invariant system is to represent the system by its response to sinusoidal input signals. This is called the *frequency response* and a rich, powerful theory with many concepts and strong, useful results has emerged. The results are based on the theory of complex variables and Laplace transforms. The basic idea behind frequency response is that we can completely

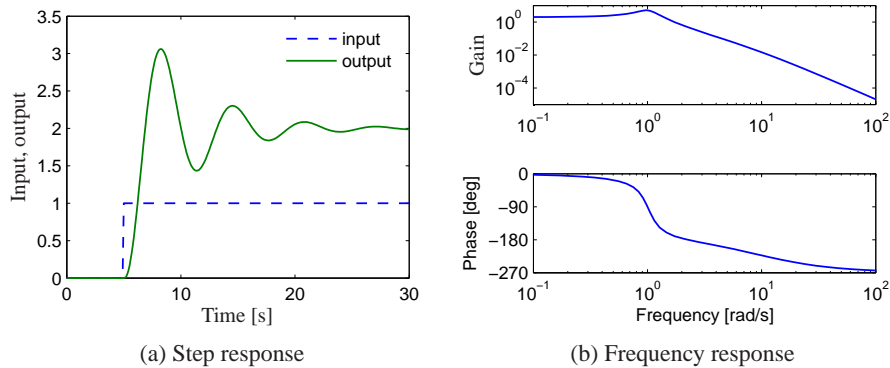


Figure 2.4: Input/output response of a linear system. The step response (a) shows the output of the system due to an input that changes from 0 to 1 at time $t = 5$ s. The frequency response (b) shows the amplitude gain and phase change due to a sinusoidal input at different frequencies.

characterize the behavior of a system by its steady state response to sinusoidal inputs. Roughly speaking, this is done by decomposing any arbitrary signal into a linear combination of sinusoids (e.g., by using the Fourier transform) and then using linearity to compute the output by combining the response to the individual frequencies. A sample frequency response is shown in Figure 2.4b.

The input/output view lends itself naturally to experimental determination of system dynamics, where a system is characterized by recording its response to a particular input, e.g. a step or a sweep across a range of frequencies.

The Control View

When control theory emerged as a discipline in the 1940s, the approach to dynamics was strongly influenced by the electrical engineering (input/output) view. A second wave of developments in control, starting in the late 1950s, was inspired by mechanics, where the state space perspective was used. The emergence of space flight is a typical example, where precise control of the orbit of a spacecraft is essential. These two points of view gradually merged into what is today the state space representation of input/output systems.

The development of state space models involved modifying the models from mechanics to include external actuators and sensors, and utilizing more general forms of equations. In control, the model given by equation (2.2) was replaced by

$$\frac{dx}{dt} = f(x, u), \quad y = h(x, u), \quad (2.3)$$

where x is a vector of state variables, u is a vector of control signals, and y a vector of measurements. The term dx/dt represents the derivative of x with respect to time, now considered as a vector, and f and h are mappings of their arguments to vectors of the appropriate dimension. For mechanical systems, the state consists of

the position and velocity of the system, so that $x = (q, \dot{q})$ in the case of a damped spring-mass system. Note that in the control formulation we model dynamics as first order differential equations, but we will see that this can capture the dynamics of higher order differential equations by appropriate definition of the state and the maps f and h .

Adding inputs and outputs has added to the richness of the classical problems and led to many new concepts. For example it is natural to ask if possible states x can be reached with the proper choice of u (reachability) and if the measurement y contains enough information to reconstruct the state (observability). These topics will be addressed in greater detail in Chapters 6 and 7.

A final development in building the control point of view was the emergence of disturbance and model uncertainty as critical elements in the theory. The simple way of modeling disturbances as deterministic signals like steps and sinusoids has the drawback that such signals can be predicted precisely. A more realistic approach is to model disturbances as random signals. This viewpoint gives a natural connection between prediction and control. The dual views of input/output representations and state space representations are particularly useful when modeling uncertainty, since state models are convenient to describe a nominal model but uncertainties are easier to describe using input/output models (often via a frequency response description). Uncertainty will be a constant theme throughout the text and will be studied in particular detail in Chapter 12.

An interesting experience in design of control systems is that feedback systems can often be analyzed and designed based on comparatively simple models. The reason for this is the inherent robustness of feedback systems. However, other uses of models may require more complexity and more accuracy. One example is feed-forward control strategies, where one uses a model to precompute the inputs that will cause the system to respond in a certain way. Another area is in system validation, where one wishes to verify that the detailed response of the system performs as it was designed. Because of these different uses of models, it is common to use a hierarchy of models having different complexity and fidelity.



Multi-Domain Modeling

Modeling is an essential element of many disciplines, but traditions and methods from individual disciplines can be different from each other, as illustrated by the previous discussion of mechanical and electrical engineering. A difficulty in systems engineering is that it is frequently necessary to deal with heterogeneous systems from many different domains, including chemical, electrical, mechanical and information systems.

To model such multi-domain systems, we start by partitioning a system into smaller subsystems. Each subsystem is represented by balance equations for mass, energy and momentum, or by appropriate descriptions of the information processing in the subsystem. The behavior at the interfaces is captured by describing how the variables of the subsystem behave when the subsystems are interconnected.

These interfaces act by constraining variables within the individual subsystems to be equal (such as mass, energy or momentum fluxes). The complete model is then obtained by combining the descriptions of the subsystems and the interfaces.

Using this methodology it is possible to build up libraries of subsystems that correspond to physical, chemical and informational components. The procedure mimics the engineering approach where systems are built from subsystems that are themselves built from smaller components. As experience is gained, the components and their interfaces can be standardized and collected in model libraries. In practice, it takes several iterations to obtain a good library that can be reused for many applications.

State models or ordinary differential equations are not suitable for component based modeling of this form because states may disappear when components are connected. This implies that the internal description of a component may change when it is connected to other components. As an illustration we consider two capacitors in an electrical circuit. Each capacitor has a state corresponding to the voltage across the capacitors, but one of the states will disappear if the capacitors are connected in parallel. A similar situation happens with two rotating inertias, each of which are individually modeled using the angle of rotation and the angular velocity. Two states will disappear when the inertias are joined by a rigid shaft.

This difficulty can be avoided by replacing differential equations by *differential algebraic equations*, which have the form

$$F(z, \dot{z}) = 0,$$

where $z \in \mathbb{R}^n$. A simple special case is

$$\dot{x} = f(x, y) \quad g(x, y) = 0, \quad (2.4)$$

where $z = (x, y)$ and $F = (\dot{x} - f(x, y), g(x, y))$. The key property is that the derivative \dot{z} is not given explicitly and there may be pure algebraic relations between the components of the vector z .

The model (2.4) captures the examples of the parallel capacitors and the linked rotating inertias. For example, when two capacitors are connected we simply add the algebraic equation expressing that the voltages across the capacitors are the same.

Modelica is a language that has been developed to support component-based modeling. Differential algebraic equations are used as the basic description and object-oriented programming is used to structure the models. Modelica is used to model the dynamics of technical systems in domains such as mechanical, electrical, thermal, hydraulic, thermo-fluid and control subsystems. Modelica is intended to serve as a standard format so that models arising in different domains can be exchanged between tools and users. A large set of free and commercial *Modelica* component libraries are available and are used by a growing number of people in industry, research and academia. For further information about *Modelica*, see <http://www.modelica.org>.

2.2 STATE SPACE MODELS

In this section we introduce the two primary forms of models that we use in this text: differential equations and difference equations. Both make use of the notions of state, inputs, outputs and dynamics to describe the behavior of a system.

Ordinary Differential Equations

The state of a system is a collection of variables that summarize the past of a system for the purpose of predicting the future. For a physical system the state is composed of the variables required to account for storage of mass, momentum and energy. A key issue in modeling is to decide how accurately this storage has to be represented. The state variables are gathered in a vector, $x \in \mathbb{R}^n$, called the *state vector*. The control variables are represented by another vector $u \in \mathbb{R}^p$ and the measured signal by the vector $y \in \mathbb{R}^q$. A system can then be represented by the differential equation

$$\frac{dx}{dt} = f(x, u), \quad y = h(x, u), \quad (2.5)$$

where $f : \mathbb{R}^n \times \mathbb{R}^p \rightarrow \mathbb{R}^n$ and $h : \mathbb{R}^n \times \mathbb{R}^p \rightarrow \mathbb{R}^q$ are smooth mappings. We call a model of this form a *state space model*.

The dimension of the state vector is called the *order* of the system. The system (2.5) is called *time-invariant* because the functions f and g do not depend explicitly on time t ; there are more general time-varying systems where the functions do depend on time. The model consists of two functions: the function f gives the rate of change of the state vector as a function of state x and control u , and the function g gives the measured values as functions of state x and control u .

A system is called a *linear* state space system if the functions f and g are linear in x and u . A linear state space system can thus be represented by

$$\frac{dx}{dt} = Ax + Bu, \quad y = Cx + Du, \quad (2.6)$$

where A , B , C and D are constant matrices. Such a system is said to be *linear and time-invariant*, or LTI for short. The matrix A is called the *dynamics matrix*, the matrix B is called the *control matrix*, the matrix C is called the *sensor matrix* and the matrix D is called the *direct term*. Frequently systems will not have a direct term, indicating that the control signal does not influence the output directly.

A different form of linear differential equations, generalizing the second order dynamics from mechanics, is an equation of the form

$$\frac{d^n y}{dt^n} + a_1 \frac{d^{n-1} y}{dt^{n-1}} + \cdots + a_n y = u, \quad (2.7)$$

where t is the independent (time) variable, $y(t)$ is the dependent (output) variable, and $u(t)$ is the input. The notation $d^k y / dt^k$ is used to denote the k th derivative of y with respect to t , sometimes also written as $y^{(k)}$. The system (2.7) is said to be an

n th order system. This system can be converted into state space form by defining

$$x = \begin{pmatrix} x_1 \\ x_2 \\ \vdots \\ x_{n-1} \\ x_n \end{pmatrix} = \begin{pmatrix} d^{n-1}y/dt^{n-1} \\ d^{n-2}y/dt^{n-2} \\ \vdots \\ dy/dt \\ y \end{pmatrix}$$

and the state space equations become

$$\frac{d}{dt} \begin{pmatrix} x_1 \\ x_2 \\ \vdots \\ x_{n-1} \\ x_n \end{pmatrix} = \begin{pmatrix} -a_1x_1 - \cdots - a_nx_n \\ x_2 \\ \vdots \\ x_{n-2} \\ x_{n-1} \end{pmatrix} + \begin{pmatrix} u \\ 0 \\ \vdots \\ 0 \\ 0 \end{pmatrix}, \quad y = x_n.$$

With the appropriate definition of A , B , C and D , this equation is in linear state space form.

An even more general system is obtained by letting the output be a linear combination of the states of the system, i.e.

$$y = b_1x_1 + b_2x_2 + \cdots + b_nx_n + du$$

This system can be modeled in state space as

$$\frac{d}{dt} \begin{pmatrix} x_1 \\ x_2 \\ x_3 \\ \vdots \\ x_n \end{pmatrix} = \begin{pmatrix} -a_1 & -a_2 & \cdots & -a_{n-1} & -a_n \\ 1 & 0 & \cdots & 0 & 0 \\ 0 & 1 & & 0 & 0 \\ \vdots & & \ddots & & \vdots \\ 0 & 0 & & 1 & 0 \end{pmatrix} x + \begin{pmatrix} 1 \\ 0 \\ 0 \\ \vdots \\ 0 \end{pmatrix} u \quad (2.8)$$

$$y = \begin{pmatrix} b_1 & b_2 & \cdots & b_n \end{pmatrix} x + du.$$

This particular form of a linear state space system is called *reachable canonical form* and will be studied in more detail in later chapters.

Example 2.1 Balance systems

An example of a class of systems that can be modeled using ordinary differential equations is the class of “balance systems.” A balance system is a mechanical system in which the center of mass is balanced above a pivot point. Some common examples of balance systems are shown in Figure 2.5. The Segway human transportation system (Figure 2.5a) uses a motorized platform to stabilize a person standing on top of it. When the rider leans forward, the vehicle propels itself along the ground, but maintains its upright position. Another example is a rocket (Figure 2.5b), in which a gimbaled nozzle at the bottom of the rocket is used to stabilize the body of the rocket above it. Other examples of balance systems include humans or other animals standing upright or a person balancing a stick on

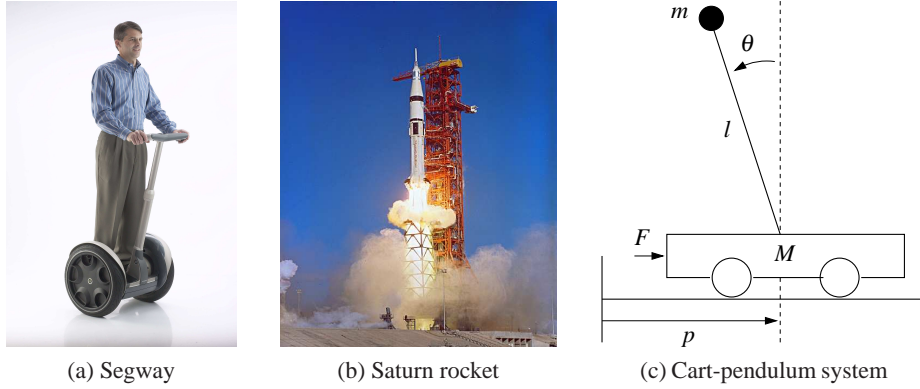


Figure 2.5: Balance systems. (a) Segway human transportation system, (b) Saturn rocket and (c) inverted pendulum on a cart. Each of these examples uses forces at the bottom of the system to keep it upright.

their hand.

Balance systems are a generalization of the spring-mass system we saw earlier. We can write the dynamics for a mechanical system in the general form

$$M(q)\ddot{q} + C(q, \dot{q}) + K(q) = B(q)u,$$

where $M(q)$ is the inertia matrix for the system, $C(q, \dot{q})$ represents the Coriolis forces as well as the damping, $K(q)$ gives the forces due to potential energy and $B(q)$ describes how the external applied forces couple into the dynamics. The specific form of the equations can be derived using Newtonian mechanics. Note that each of the terms depends on the configuration of the system q and these terms are often nonlinear in the configuration variables.

Figure 2.5c shows a simplified diagram for a balance system. To model this system, we choose state variables that represent the position and velocity of the base of the system, p and \dot{p} , and the angle and angular rate of the structure above the base, θ and $\dot{\theta}$. We let F represent the force applied at the base of the system, assumed to be in the horizontal direction (aligned with p), and choose the position and angle of the system as outputs. With this set of definitions, the dynamics of the system can be computed using Newtonian mechanics and has the form

$$\begin{pmatrix} (M+m) & -ml \cos \theta \\ -ml \cos \theta & (J+ml^2) \end{pmatrix} \begin{pmatrix} \ddot{p} \\ \ddot{\theta} \end{pmatrix} + \begin{pmatrix} c\dot{p} + ml \sin \theta \dot{\theta}^2 \\ \gamma\dot{\theta} - mgl \sin \theta \end{pmatrix} = \begin{pmatrix} F \\ 0 \end{pmatrix}, \quad (2.9)$$

where M is the mass of the base, m and J are the mass and moment of inertia of the system to be balanced, l is the distance from the base to the center of mass of the balanced body, c and γ are coefficients of viscous friction, and g is the acceleration due to gravity.

We can rewrite the dynamics of the system in state space form by defining the state as $x = (p, \theta, \dot{p}, \dot{\theta})$, the input as $u = F$ and the output as $y = (p, \theta)$. If we

define the total mass and total inertia as

$$M_t = M + m \quad J_t = J + ml^2,$$

the equations of motion then become

$$\frac{d}{dt} \begin{pmatrix} p \\ \theta \\ \dot{\theta} \end{pmatrix} = \begin{pmatrix} \dot{p} \\ \dot{\theta} \\ \frac{-mls_\theta \dot{\theta}^2 + mg(ml^2/J_t)s_\theta c_\theta - c\dot{p} - \gamma l m c_\theta \dot{\theta} + u}{M_t - m(ml^2/J_t)c_\theta^2} \\ \frac{-ml^2 s_\theta c_\theta \dot{\theta}^2 + M_t g l s_\theta - cl c_\theta \dot{p} - \gamma(M_t/m)\dot{\theta} + lc_\theta u}{J_t(M_t/m) - m(lc_\theta)^2} \end{pmatrix}$$

$$y = \begin{pmatrix} p \\ \theta \end{pmatrix},$$

where we have used the shorthand $c_\theta = \cos \theta$ and $s_\theta = \sin \theta$.

In many cases, the angle θ will be very close to 0 and hence we can use the approximations $\sin \theta \approx \theta$ and $\cos \theta \approx 1$. Furthermore, if $\dot{\theta}$ is small, we can ignore quadratic and higher terms in $\dot{\theta}$. Substituting these approximations into our equations, we see that we are left with a *linear* state space equation

$$\frac{d}{dt} \begin{pmatrix} p \\ \theta \\ \dot{p} \\ \dot{\theta} \end{pmatrix} = \begin{pmatrix} 0 & 0 & 1 & 0 \\ 0 & 0 & 0 & 1 \\ 0 & m^2 l^2 g / \mu & -c J_t / \mu & -\gamma J_t l m / \mu \\ 0 & M_t m g l / \mu & -c l m / \mu & -\gamma M_t / \mu \end{pmatrix} \begin{pmatrix} p \\ \theta \\ \dot{p} \\ \dot{\theta} \end{pmatrix} + \begin{pmatrix} 0 \\ 0 \\ J_t / \mu \\ l m / \mu \end{pmatrix} u$$

$$y = \begin{pmatrix} 1 & 0 & 0 & 0 \\ 0 & 1 & 0 & 0 \end{pmatrix} x,$$

where $\mu = M_t J_t - m^2 l^2$. ∇

Example 2.2 Inverted pendulum

A variation of this example is one in which the location of the base, p , does not need to be controlled. This happens, for example, if we are only interested in stabilizing a rocket's upright orientation, without worrying about the location of base of the rocket. The dynamics of this simplified system are given by

$$\frac{d}{dt} \begin{pmatrix} \theta \\ \dot{\theta} \end{pmatrix} = \begin{pmatrix} \dot{\theta} \\ \frac{mgl}{J_t} \sin \theta - \frac{\gamma}{J_t} \dot{\theta} + \frac{l}{J_t} \cos \theta u \end{pmatrix}, \quad y = \theta, \quad (2.10)$$

where γ is the coefficient of rotational friction, $J_t = J + ml^2$ and u is the force applied at the base. This system is referred to as an *inverted pendulum*. ∇

Difference Equations

In some circumstances, it is more natural to describe the evolution of a system at discrete instants of time rather than continuously in time. If we refer to each

of these times by an integer $k = 0, 1, 2, \dots$, then we can ask how the state of the system changes for each k . Just as in the case of differential equations, we define the state to be those sets of variables that summarize the past of the system for the purpose of predicting its future. Systems described in this manner are referred to as *discrete time systems*.

The evolution of a discrete time system can be written in the form

$$x[k+1] = f(x[k], u[k]), \quad y[k] = h(x[k], u[k]) \quad (2.11)$$

where $x[k] \in \mathbb{R}^n$ is the state of the system at “time” k (an integer), $u[k] \in \mathbb{R}^p$ is the input and $y[k] \in \mathbb{R}^q$ is the output. As before, f and h are smooth mappings of the appropriate dimension. We call equation (2.11) a *difference equation* since it tells us how $x[k+1]$ differs from $x[k]$. The state $x[k]$ can either be a scalar or a vector valued quantity; in the case of the latter we write $x_j[k]$ for the value of the j th state at time k .

Just as in the case of differential equations, it will often be the case that the equations are linear in the state and input, in which case we can write the system as

$$x[k+1] = Ax[k] + Bu[k], \quad y[k] = Cx[k] + Du[k].$$

As before, we refer to the matrices A , B , C and D as the dynamics matrix, the control matrix, the sensor matrix and the direct term. The solution of a linear difference equation with initial condition $x[0]$ and input $u[0], \dots, u[T]$ is given by

$$\begin{aligned} x[k] &= A^k x_0 + \sum_{j=0}^{k-1} A^{k-j-1} Bu[j] \\ y[k] &= CA^k x_0 + \sum_{j=0}^{k-1} CA^{k-j-1} Bu[j] + Du[k] \end{aligned} \quad k > 0. \quad (2.12)$$

Difference equations are also useful as an approximation of differential equations, as we will show later.

Example 2.3 Predator-prey

As an example of a discrete time system, consider a simple model for a predator-prey system. The predator-prey problem refers to an ecological system in which we have two species, one of which feeds on the other. This type of system has been studied for decades and is known to exhibit interesting dynamics. Figure 2.6 shows a historical record taken over 50 years in a population of lynxes versus hares [134]. As can be seen from the graph, the annual records of the populations of each species are oscillatory in nature.

A simple model for this situation can be constructed using a discrete time model by keeping track of the rate of births and deaths of each species. Letting H represent the population of hares and L represent the population of lynxes, we can describe the state in terms of the populations at discrete periods of time. Letting k

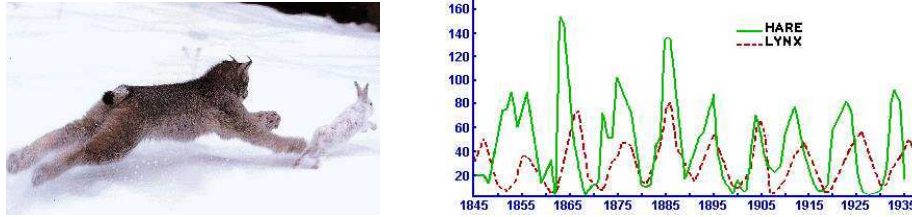


Figure 2.6: Predator versus prey. The photograph on the left shows a Canadian lynx and a snowshoe hare, the lynx’s primary prey. The graph on the right shows the populations of hares and lynxes between 1845 and 1935 in a section of the Canadian Rockies [134, 145]. The data were collected on an annual basis over a period of 90 years. Photograph courtesy Rudolfo’s Usenet Animal Pictures Gallery.

be the discrete time index (e.g., the day number), we can write

$$\begin{aligned} H[k+1] &= H[k] + b_r(u)H[k] - aL[k]H[k] \\ L[k+1] &= L[k] - d_fL[k] + cL[k]H[k], \end{aligned} \quad (2.13)$$

where $b_r(u)$ is the hare birth rate per unit period and as a function of the food supply u , d_f is the lynx death rate, and a and c are the interaction coefficients. The interaction term $aL[k]H[k]$ models the rate of predation, which is assumed to be proportional to the rate at which predators and prey meet and is hence given by the product of the population sizes. The interaction term $cL[k]H[k]$ in the lynx dynamics has a similar form and represents the rate of growth of the lynx population. This model makes many simplifying assumptions—such as the fact that hares only decrease in numbers through predation by lynxes—but it often is sufficient to answer basic questions about the system.

To illustrate the usage of this system, we can compute the number of lynxes and hares at each time point from some initial population. This is done by starting with $x[0] = (H_0, L_0)$ and then using equation (2.13) to compute the populations in the following period. By iterating this procedure, we can generate the population over time. The output of this process for a specific choice of parameters and initial conditions is shown in Figure 2.7. While the details of the simulation are different from the experimental data (to be expected given the simplicity of our assumptions), we see qualitatively similar trends and hence we can use the model to help explore the dynamics of the system. ∇

Example 2.4 Email Server

The IBM Lotus server is a collaborative software system that administers users’ e-mail, documents and notes. Client machines interact with end users to provide access to data and applications. The server also handles other administrative tasks. In the early development of the system it was observed that the performance was poor when the CPU was overloaded because of too many service requests and mechanisms to control the load were therefore introduced.

The interaction between the client and the server is in the form of remote procedure calls (RPCs). The server maintains a log of statistics of completed requests.

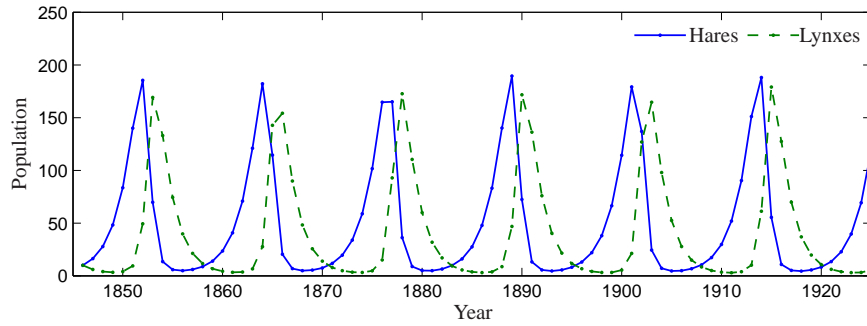


Figure 2.7: Discrete time simulation of the predator-prey model (2.13). Using the parameters $a = c = 0.014$, $b_r(u) = 0.6$ and $d = 0.7$ in equation (2.13), the period and magnitude of the lynx and hare population cycles approximately match the data in Figure 2.6.

The total number of requests being served, called `RIS` (RPCs in server), is also measured. The load on the server is controlled by a parameter called `MaxUsers`, which sets the total number of client connections to the server. This parameter is controlled by the system administrator. The server can be regarded as a dynamical system with `MaxUsers` as input and `RIS` as the output. The relationship between input and output was first investigated by exploring the steady state performance and was found to be linear.

In [92] a dynamic model in the form of a first order difference equation is used to capture the dynamic behavior of this system. Using system identification techniques they construct a model of the form

$$y[k + 1] = ay[k] + bu[k],$$

where $u = \text{MaxUsers} - \overline{\text{MaxUsers}}$ and $y = \text{RIS} - \overline{\text{RIS}}$. The parameters $a = 0.43$ and $b = 0.47$ are parameters that describe the dynamics of the system around the operating point and $\overline{\text{MaxUsers}} = 165$ and $\overline{\text{RIS}} = 135$ represent the nominal operating point of the system. The number of requests was averaged of the sampling period which was 60 s. ∇

Simulation and Analysis

State space models can be used to answer many questions. One of the most common, as we have seen in the previous examples, is to predict the evolution of the system state from a given initial condition. While for simple models this can be done in closed form, more often it is accomplished through computer simulation. One can also use state space models to analyze the overall behavior of the system, without making direct use of simulation.

Consider again the damped spring-mass system from Section 2.1, but this time with an external force applied, as shown in Figure 2.8. We wish to predict the motion of the system for a periodic forcing function, with a given initial condition, and determine the amplitude, frequency and decay rate of the resulting motion.

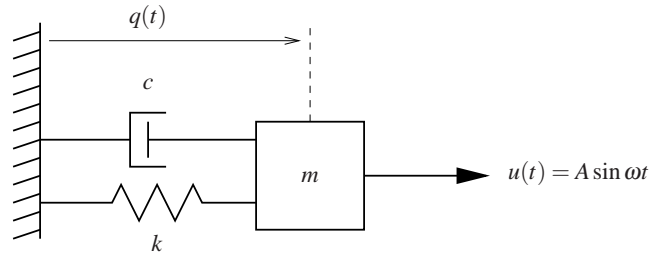


Figure 2.8: A driven spring-mass system, with damping. Here we use a linear damping element with coefficient of viscous friction c . The mass is driven with a sinusoidal force of amplitude A .

We choose to model the system with a linear ordinary differential equation. Using Hooke's law to model the spring and assuming that the damper exerts a force that is proportional to the velocity of the system, we have

$$m\ddot{q} + c\dot{q} + kq = u, \quad (2.14)$$

where m is the mass, q is the displacement of the mass, c is the coefficient of viscous friction, k is the spring constant and u is the applied force. In state space form, using $x = (q, \dot{q})$ as the state and choosing $y = q$ as the output, we have

$$\frac{dx}{dt} = \begin{pmatrix} x_2 \\ -\frac{c}{m}x_2 - \frac{k}{m}x_1 + \frac{u}{m} \end{pmatrix}, \quad y = x_1.$$

We see that this is a linear, second order differential equation with one input and one output.

We now wish to compute the response of the system to an input of the form $u = A \sin \omega t$. Although it is possible to solve for the response analytically, we instead make use of a computational approach that does not rely on the specific form of this system. Consider the general state space system

$$\frac{dx}{dt} = f(x, u).$$

Given the state x at time t , we can approximate the value of the state at a short time $h > 0$ later by assuming that the rate of change of $f(x, u)$ is constant over the interval t to $t + h$. This gives

$$x(t+h) = x(t) + hf(x(t), u(t)). \quad (2.15)$$

Iterating this equation, we can thus solve for x as a function of time. This approximation is known as Euler integration, and is in fact a difference equation if we let h represent the time increment and write $x[k] = x(kh)$. Although modern simulation tools such as MATLAB and Mathematica use more accurate methods than Euler integration, it still illustrates some of the basic tradeoffs.

Returning to our specific example, Figure 2.9 shows the results of computing $x(t)$ using equation (2.15), along with the analytical computation. We see that as

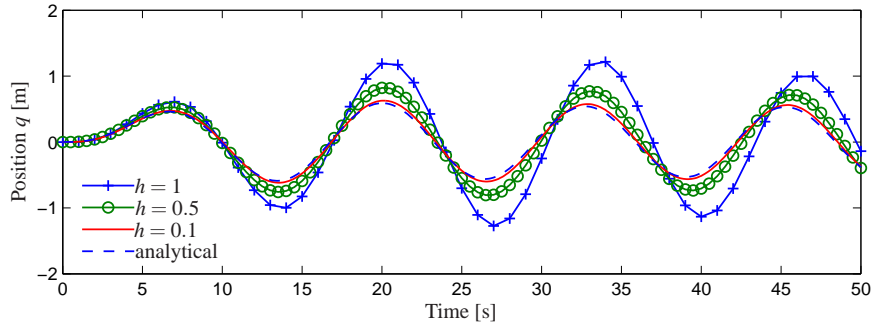


Figure 2.9: Simulation of the forced spring-mass system with different simulation time constants. The darker dashed line represents that analytical solution. The solid lines represent the approximate solution via the method of Euler integration, using decreasing step sizes.

h gets smaller, the computed solution converges to the exact solution. The form of the solution is also worth noticing: after an initial transient, the system settles into a periodic motion. The portion of the response after the transient is called the *steady state response* to the input.

In addition to generating simulations, models can also be used to answer other types of questions. Two that are central to the methods described in this text are stability of an equilibrium point and the input/output frequency response. We illustrate these two computations through the examples below, and return to the general computations in later chapters.

Returning to the damped spring-mass system, the equations of motion with no input forcing are given by

$$\frac{dx}{dt} = \begin{pmatrix} x_2 \\ -\frac{c}{m}x_2 - \frac{k}{m}x_1 \end{pmatrix}, \quad (2.16)$$

where x_1 is the position of the mass (relative to the rest position) and x_2 its velocity. We wish to show that if the initial state of the system is away from the rest position, the system will return to the rest position eventually (we will later define this situation to mean that the rest position is *asymptotically stable*). While we could heuristically show this by simulating many, many initial conditions, we seek instead to prove that this is true for *any* initial condition.

To do so, we construct a function $V : \mathbb{R}^n \rightarrow \mathbb{R}$ that maps the system state to a positive real number. For mechanical systems, a convenient choice is the energy of the system,

$$V(x) = \frac{1}{2}kx_1^2 + \frac{1}{2}mx_2^2. \quad (2.17)$$

If we look at the time derivative of the energy function, we see that

$$\frac{dV}{dt} = kx_1\dot{x}_1 + mx_2\dot{x}_2 = kx_1x_2 + mx_2\left(-\frac{c}{m}x_2 - \frac{k}{m}x_1\right) = -cx_2^2,$$

which is always either negative or zero. Hence $V(x(t))$ is never increasing and, using a bit of analysis that we will see formally later, the individual states must remain bounded.

If we wish to show that the states eventually return to the origin, we must use a more slightly more detailed analysis. Intuitively, we can reason as follows: suppose that for some period of time, $V(x(t))$ stops decreasing. Then it must be true that $\dot{V}(x(t)) = 0$, which in turn implies that $x_2(t) = 0$ for that same period. In that case, $\dot{x}_2(t) = 0$ and we can substitute into the second line of equation (2.16) to obtain:

$$0 = \dot{x}_2 = -\frac{c}{m}x_2 - \frac{k}{m}x_1 = \frac{k}{m}x_1.$$

Thus we must have that x_1 also equals zero and so the only time that $V(x(t))$ can stop decreasing is if the state is at the origin (and hence this system is at its rest position). Since we know that $V(x(t))$ is never increasing (since $\dot{V} \leq 0$), we therefore conclude that the origin is stable (for *any* initial condition).

This type of analysis, called Lyapunov analysis, is considered in detail in Chapter 4 but shows some of the power of using models for analysis of system properties.

Another type of analysis that we can perform with models is to compute the output of a system to a sinusoidal input. We again consider the spring-mass system, but this time keeping the input and leaving the system in its original form:

$$m\ddot{q} + c\dot{q} + kq = u. \quad (2.18)$$

We wish to understand what the response of the system is to a sinusoidal input of the form

$$u(t) = A \sin \omega t.$$

We will see how to do this analytically in Chapter 6, but for now we make use of simulations to compute the answer.

We first begin with the observation that if $q(t)$ is the solution to equation (2.18) with input $u(t)$, then applying an input $2u(t)$ will give a solution $2q(t)$ (this is easily verified by substitution). Hence it suffices to look at an input with unit magnitude, $A = 1$. A second observation, which we will prove in Chapter 5, is that the long term response of the system to a sinusoidal input is itself a sinusoid at the same frequency and so the output has the form

$$q(t) = g(\omega) \sin(\omega t + \varphi(\omega)),$$

where $g(\omega)$ is called the *gain* of the system and $\varphi(\omega)$ is called the *phase* (or phase offset).

To compute the frequency response numerically, we can simply simulate the system at a set of frequencies $\omega_1, \dots, \omega_N$ and plot the gain and phase at each of these frequencies. An example of this type of computation is shown in Figure 2.10.

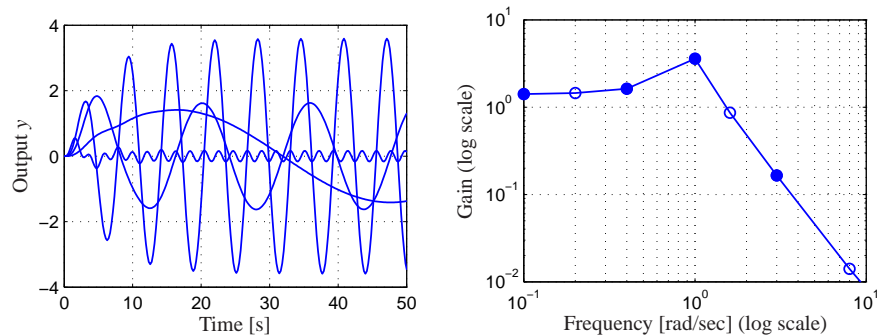


Figure 2.10: A frequency response (magnitude only) computed by measuring the response of individual sinusoids. The figure on the left shows the response of the system as a function of time to a number of different unit magnitude inputs (at different frequencies). The figure on the right shows this same data in a different way, with the magnitude of the response plotted as a function of the input frequency. The filled circles correspond to the particular frequencies shown in the time responses.

2.3 MODELING METHODOLOGY

To deal with large complex systems, it is useful to have different representations of the system that capture the essential features and hide irrelevant details. In all branches of science and engineering it is common practice to use some graphical description of systems. They can range from stylistic pictures to drastically simplified standard symbols. These pictures make it possible to get an overall view of the system and to identify the individual components. Examples of such diagrams are shown in Figure 2.11. Schematic diagrams are useful because they give an overall picture of a system, showing different subprocesses and their interconnection, and indicating variables that can be manipulated and signals that can be measured.

Block Diagrams

A special graphical representation called a *block diagram* has been developed in control engineering. The purpose of a block diagram is to emphasize the information flow and to hide details of the system. In a block diagram, different process elements are shown as boxes and each box has inputs denoted by lines with arrows pointing toward the box and outputs denoted by lines with arrows going out of the box. The inputs denote the variables that influence a process and the outputs denote signals that we are interested in or signals that influence other subsystems. Block diagrams can also be organized in hierarchies, where individual blocks may themselves contain more detailed block diagrams.

Figure 2.12 shows some of the notation that we use for block diagrams. Signals are represented as lines, with arrows to indicate inputs and outputs. The first diagram is the representation for a summation of two signals. An input/output response is represented as a rectangle with the system name (or mathematical description) in the block. Two special cases are a proportional gain, which scales the

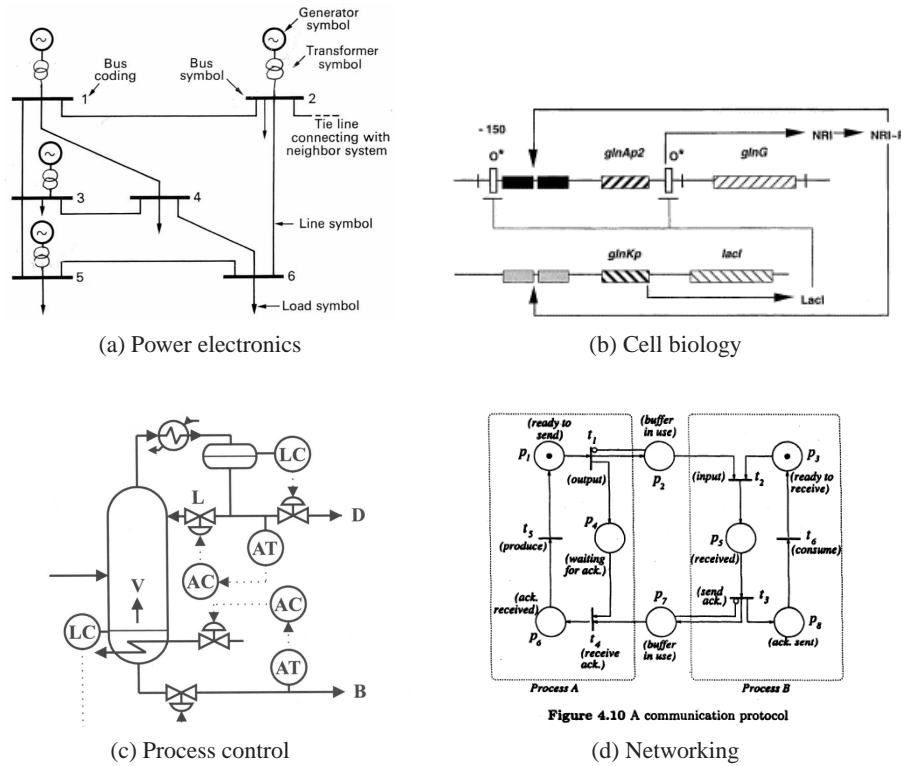


Figure 2.11: Schematic diagrams in different disciplines. Each diagram is used to illustrate the dynamics of a feedback system: (a) electrical schematics for a power system, (b) a biological circuit diagram for a synthetic clock circuit [21], (c) process diagram for a distillation column and (d) Petri net description of a communication protocol [?].

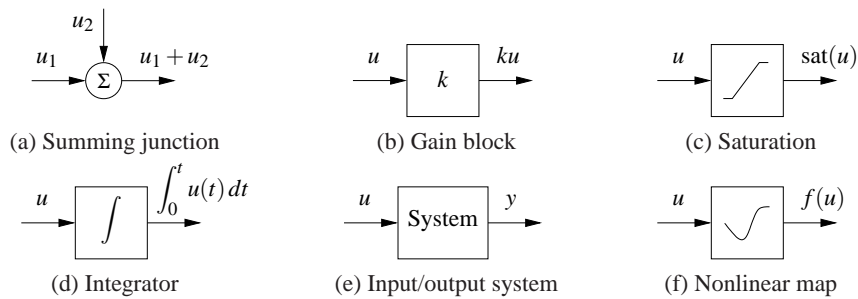


Figure 2.12: Standard block diagram elements. The arrows indicate the the inputs and outputs of each element, with the mathematical operation corresponding to the blocked labeled at the output. The system block (e) represents the full input/output response of a dynamical system.

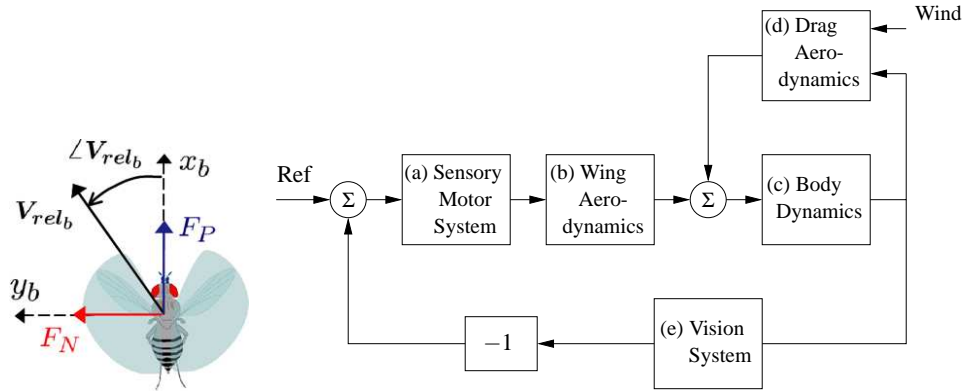


Figure 2.13: A block diagram representation of the flight control system for an insect flying against the wind. The mechanical portion of the model consists of the rigid body dynamics of the fly, the drag due to flying through the air and the forces generated by the wings. The motion of the body causes the visual environment of the fly to change, and this information is then used to control the motion of the wings (through the sensory motor system), closing the loop.

input by a multiplicative factor, and an integrator, which outputs the integral of the input signal.

Figure 2.13 illustrates the use of a block diagram, in this case for modeling the flight response of a fly. The flight dynamics of an insect are incredibly intricate, involving a careful coordination of the muscles within the fly to maintain stable flight in response to external stimuli. One known characteristic of flies is their ability to fly upwind by making use of the optical flow in their compound eyes as a feedback mechanism. Roughly speaking, the fly controls its orientation so that the point of contraction of the visual field is centered in its visual field.

To understand this complex behavior, we can decompose the overall dynamics of the system into a series of interconnected subsystems (or “blocks”). Referring to Figure 2.13, we can model the insect navigation system through an interconnection of five blocks. The sensory motor system (a) takes the information from the visual system (e) and generates muscle commands that attempt to steer the fly so that the point of contraction is centered. These muscle commands are converted into forces through the flapping of the wings (b) and the resulting aerodynamic forces that are produced. The forces from the wings are combined with the drag on the fly (d) to produce a net force on the body of the fly. The wind velocity enters through the drag aerodynamics. Finally, the body dynamics (c) describe how the fly translates and rotates as a function of the net forces that are applied to it. The insect position, speed and orientation is fed back to the drag aerodynamics and vision system blocks as inputs.

Each of the blocks in the diagram can itself be a complicated subsystem. For example, the fly visual system of a fruit fly consists of two complicated compound eyes (with about 700 elements per eye) and the sensory motor system has about 200,000 neurons that are used to process that information. A more detailed block

diagram of the insect flight control system would show the interconnections between these elements, but here we have used one block to represent how the motion of the fly affects the output of the visual system and a second block to represent how the visual field is processed by the fly's brain to generate muscle commands. The choice of the level of detail of the blocks and what elements to separate into different blocks often depends on experience and the questions that one wants to answer using the model. One of the powerful features of block diagrams is their ability to hide information about the details of a system that may not be needed to gain an understanding of the essential dynamics of the system.

Modeling from Experiments

Since control systems are provided with sensors and actuators it is also possible to obtain models of system dynamics from experiments on the process. The models are restricted to input/output models since only these signals are accessible to experiments, but modeling from experiments can also be combined with modeling from physics through the use of feedback and interconnection.

A simple way to determine a system's dynamics is to observe the response to a step change in the control signal. Such an experiment begins by setting the control signal to a constant value, then when steady state is established the control signal is changed quickly to a new level and the output is observed. The experiment will give the step response of the system and the shape of the response gives useful information about the dynamics. It immediately gives an indication of the response time and it tells if the system is oscillatory or if the response is monotone. By repeating the experiment for different steady state values and different amplitudes of the change of the control signal we can also determine ranges where the process can be approximated by a linear system.

Example 2.5 Identification of a spring-mass system

Consider the spring-mass system from Section 2.1, whose dynamics are given by

$$m\ddot{q} + c\dot{q} + kq = u. \quad (2.19)$$

We wish to determine the constants m , c and k by measuring the response of the system to a step input of magnitude F_0 .

We will show in Chapter 5 that when $c^2 < 4km$, the step response for this system from the rest configuration is given by

$$q(t) = \frac{F_0}{k} \left(1 - \exp\left(-\frac{ct}{2m}\right) \sin(\omega_d t + \varphi) \right)$$

$$\omega_d = \frac{\sqrt{4km - c^2}}{2m}$$

$$\varphi = \tan^{-1} \left(\frac{\sqrt{4km - c^2}}{c} \right).$$

From the form of the solution, we see that the form of the response is determined by the parameters of the system. Hence, by measuring certain features of the step response we can determine the parameter values.

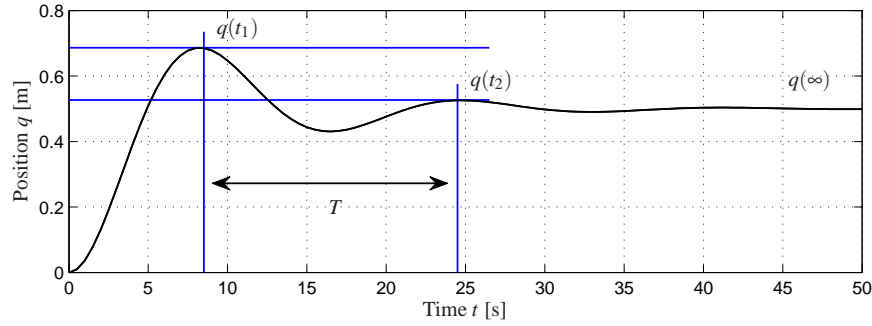


Figure 2.14: Step response for a spring-mass system. The magnitude of the step input is $F_0 = 20$ N. The period of oscillation, T is determined by looking at the time between two subsequent local maxima in the response. The period combined with the steady state value $q(\infty)$ and the relative decrease between local maxima can be used to estimate the parameters in a model of the system.

Figure 2.14 shows the response of the system to a step of magnitude $F_0 = 20$ N, along with some measurements. We start by noting that the steady state position of the mass (after the oscillations die down) is a function of the spring constant, k :

$$q(\infty) = \frac{F_0}{k}, \quad (2.20)$$

where F_0 is the magnitude of the applied force ($F_0 = 1$ for a unit step input). The parameter $1/k$ is called the *gain* of the system. The period of the oscillation can be measured between two peaks and must satisfy

$$\frac{2\pi}{T} = \frac{\sqrt{4km - c^2}}{2m}. \quad (2.21)$$

Finally, the rate of decay of the oscillations is given by the exponential factor in the solution. Measuring the amount of decay between two peaks, we have (using Exercise 2.5)

$$\log(q(t_1) - F_0/k) - \log(q(t_2) - F_0/k) = \frac{c}{2m}(t_2 - t_1). \quad (2.22)$$

Using this set of three equations, we can solve for the parameters and determine that for the step response in Figure 2.14 we have $m \approx 250$ kg, $c \approx 60$ N s/m and $k \approx 40$ N/m. ∇

Modeling from experiments can also be done using many other signals. Sinusoidal signals are commonly used (particularly for systems with fast dynamics) and precise measurements can be obtained by exploiting correlation techniques. An indication of nonlinearities can be obtained by repeating experiments with input signals having different amplitudes.

Normalization and Scaling

Having obtained a model, it is often useful to scale the variables by introducing dimension free variables. Such a procedure can often simplify the equations for a system by reducing the number of parameters and reveal interesting properties of the model. Scaling can also improve the numerical conditioning of the model to allow faster and more accurate simulations.

The procedure of scaling is straightforward: simply choose units for each independent variable and introduce new variables by dividing the variables with the chosen normalization unit. We illustrate the procedure with two examples.

Example 2.6 Spring-mass system

Consider again the spring-mass system introduced earlier. Neglecting the damping, the system is described by

$$m\ddot{q} + kq = u.$$

The model has two parameters m and k . To normalize the model we introduce dimension free variables $x = q/l$ and $\tau = \omega_0 t$, where $\omega_0 = \sqrt{k/m}$ and l is the chosen length scale. We scale force by $ml\omega_0^2$ and introduce $v = u(ml\omega_0^2)$. The scaled equation then becomes

$$\frac{d^2x}{d\tau^2} = \frac{d^2q/l}{d(\omega_0 t)^2} = \frac{1}{\omega_0^2 l m} (-kq + u) = -x + v,$$

which is the normalized undamped spring-mass system. Notice that the normalized model has no parameters while the original model had two parameters m and k . Introducing the scaled, dimension-free state variables $z_1 = x = q/l$ and $z_2 = dx/d\tau = \dot{q}/(l\omega_0)$ the model can be written as

$$\frac{d}{dt} \begin{pmatrix} z_1 \\ z_2 \end{pmatrix} = \begin{pmatrix} 0 & 1 \\ -1 & 0 \end{pmatrix} \begin{pmatrix} z_1 \\ z_2 \end{pmatrix} + \begin{pmatrix} 0 \\ v \end{pmatrix}.$$

This simple linear equation describes the dynamics of any spring-mass system, independent of the particular parameters, and hence gives us insight into the fundamental dynamics of this oscillatory system. To recover the physical frequency of oscillation or its magnitude, we must invert the scaling we have applied. ∇

Example 2.7 Balance system

Consider the balance system described in Section 2.1. Neglecting damping by putting $c = 0$ and $\gamma = 0$ in equation (2.9) the model can be written as

$$\begin{aligned} (M + m) \frac{d^2q}{dt^2} - ml \cos \theta \frac{d^2\theta}{dt^2} + ml \sin \theta \left(\frac{dq}{dt} \right)^2 &= F \\ -ml \cos \theta \frac{d^2q}{dt^2} + (J + ml^2) \frac{d^2\theta}{dt^2} - mgl \sin \theta &= 0 \end{aligned}$$

Let $\omega_0 = \sqrt{mgl/(J + ml^2)}$, choose the length scale as l , the time scale as $1/\omega_0$, the force scale as $(M + m)l\omega_0^2$ and introduce the scaled variables $\tau = \omega_0 t$, $x = q/l$

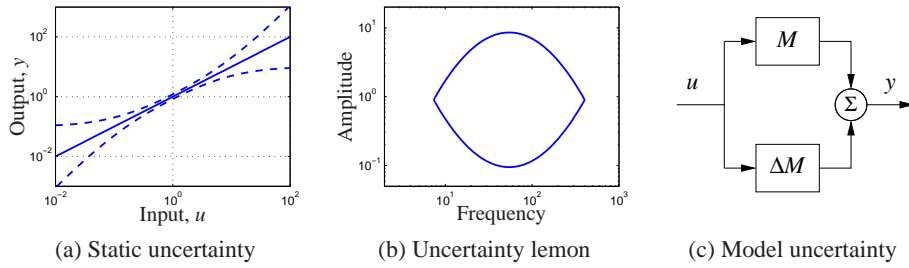


Figure 2.15: Characterization of model uncertainty. Uncertainty of a static system is illustrated in (a). The uncertainty lemon in (b) is one way to capture uncertainty in dynamical systems emphasizing that a model is only valid in some amplitude and frequency ranges. In (c) a model is represented by a nominal model (M) and another model ΔM representing the uncertainty analogous to representation of parameter uncertainty.

and $u = F / ((M + m)l\omega_0^2)$. The equations then become

$$\frac{d^2x}{d\tau^2} - \alpha \cos \theta \frac{d^2\theta}{d\tau^2} + \alpha \left(\frac{d\theta}{d\tau} \right)^2 = u, \quad -\beta \cos \theta \frac{d^2x}{d\tau^2} + \frac{d^2\theta}{d\tau^2} - \sin \theta = 0,$$

where $\alpha = m / (M + m)$ and $\beta = ml^2 / (J + ml^2)$. Notice that the original model has five parameters m, M, J, l and g but the normalized model has only two parameters α and β . If $M \gg m$ and $ml^2 \gg J$ we get $\alpha \approx 0$ and $\beta \approx 1$ and the model can be approximated by

$$\frac{d^2x}{d\tau^2} = u, \quad \frac{d^2\theta}{d\tau^2} - \sin \theta = u \cos \theta.$$

The model can be interpreted as a mass combined with an inverted pendulum driven by the same input. ∇

Model Uncertainty

Reducing uncertainty is one of the main reasons for using feedback and it is therefore important to characterize uncertainty. When making measurements there is a good tradition to assign both a nominal value and a measure of uncertainty. It is useful to apply same principle to modeling, but unfortunately it is often difficult to express the uncertainty of a model quantitatively.

For a static system whose input-output relation can be characterized by a function, uncertainty can be expressed by an uncertainty band as illustrated in In Figure 2.15a. At low signal levels there are uncertainties due to sensor resolution, friction and quantization. Some models for queuing systems or cells are based on averages that exhibit significant variations for small populations. At large signal levels there are saturations or even system failures. The signal ranges where a model is reasonably accurate varies dramatically between applications but it is rare to find models that are accurate for signal ranges larger than 10^4 .

Characterization of uncertainty of dynamic model is much more difficult. We can try to capture uncertainties by assigning uncertainties to parameters of the

model but this is often not sufficient. There may be errors due to phenomena that have been neglected, for example small time delays. In control the ultimate test is how well a control system based on the model performs and time delays can be important. There is also a frequency aspect. There are slow phenomena, such as aging, that can cause changes or drift in the systems. There are also high frequency effects: a resistor will no longer be a pure resistance at very high frequencies and a beam has stiffness and will exhibit additional dynamics when subject to high frequency excitation. The *uncertainty lemon* shown in Figure 2.15b is one way to conceptualize the uncertainty of a system. It illustrates that a model is only valid in certain amplitude and frequency ranges.

We will introduce some formal tools for representing uncertainty in Chapter 12 using figures such as the one shown in Figure 2.15c. These tools make use of the concept of a transfer function, which describes the frequency response of an input/output system. For now, we simply note that one should always be careful to recognize the limits of a model and not to make use of models outside their range of applicability. For example, one can describe the uncertainty lemon and then check to make sure that signals remain in this region.

2.4 MODELING EXAMPLES

In this section we introduce additional examples that illustrate some of the different types of systems for which one can develop differential equation and difference equation models. These examples are specifically chosen from a range of different fields to highlight the broad variety of systems to which feedback and control concepts can be applied. A more detailed set of applications that serve as running examples throughout the text are given in the next chapter.

Motion Control Systems

Motion control systems involve the use of computation and feedback to control the movement of a mechanical system. Motion control systems range from nanopositioning systems (atomic force microscopes, adaptive optics), to control systems for the read/write heads in a disk drive or CD player, to manufacturing systems (transfer machines and industrial robots), to automotive control systems (anti-lock brakes, suspension control, traction control), to air and space flight control systems (airplanes, satellites, rockets and planetary rovers).

Example 2.8 Vehicle steering—the bicycle model

A common problem in motion control is to control the trajectory of a vehicle through an actuator that causes a change in the orientation. A steering wheel on an automobile or the front wheel of a bicycle are two examples, but similar dynamics occur in steering of ships or control of the pitch dynamics of an aircraft. In many cases, we can understand the basic behavior of these systems through the use of a simple model that captures the basic geometry of the system.

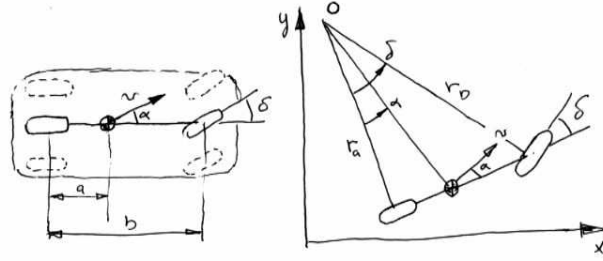


Figure 2.16: Vehicle steering dynamics. The left figure shows an overhead view of a vehicle with four wheels. By approximating the motion of the front and rear pairs of wheels by a single front and rear wheel, we obtain an abstraction called the “bicycle model”, shown on the right. The wheel base is b and the center of mass at a distance a forward of the rear wheels. The steering angle is δ and the velocity at the center of mass has the angle α relative the length axis of the vehicle. The position of the vehicle is given by (x, y) and the orientation (heading) by θ .

Consider a vehicle with two wheels as shown in Figure 2.16. For the purpose of steering we are interested in a model that describes how the velocity of the vehicle depends on the steering angle δ . To be specific, consider the velocity v at the center of mass, a distance a from the rear wheel, and let b be the wheel base, as shown in Figure 2.16. Let x and y be the coordinates of the center of mass, θ the heading angle and α the angle between the velocity vector v and the centerline of the vehicle. Since $b = r_a \tan \delta$ and $a = r_a \tan \alpha$ it follows that $\tan \alpha = (a/b) \tan \delta$ and we get the following relation between α and the steering angle δ :

$$\alpha(\delta) = \arctan\left(\frac{a \tan \delta}{b}\right). \quad (2.23)$$

Assume that the wheels are rolling without slip and that the velocity of the rear wheel is v_0 . The vehicle speed at its center of mass is $v = v_0 / \cos \alpha$ and we find that the motion of this point is given by

$$\begin{aligned} \frac{dx}{dt} &= v \cos(\alpha + \theta) = v_0 \frac{\cos(\alpha + \theta)}{\cos \alpha} \\ \frac{dy}{dt} &= v \sin(\alpha + \theta) = v_0 \frac{\sin(\alpha + \theta)}{\cos \alpha}. \end{aligned} \quad (2.24)$$

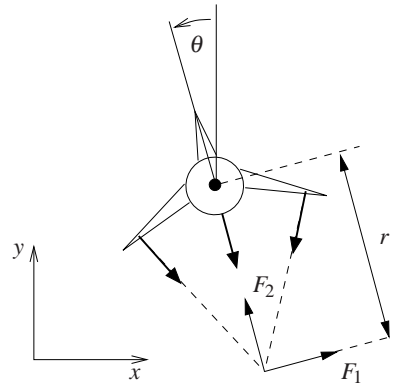
To see how the angle θ is influenced by the steering angle we observe from Figure 2.16 that the vehicle rotates with the angular velocity v_0/r_a around the point O . Hence

$$\frac{d\theta}{dt} = \frac{v_0}{r_a} = \frac{v_0}{b} \tan \delta. \quad (2.25)$$

Equations (2.23)–(2.25) can be used to model an automobile under the assumptions that there is no slip between the wheels and the road and that the two front wheels can be approximated by a single wheel at the center of the car. The assumption of no slip can be relaxed by adding an extra state variable, giving a more



(a) Harrier “jump jet”



(b) Simplified model

Figure 2.17: Vectored thrust aircraft. The Harrier AV-8B military aircraft (a) redirects its engine thrust downward so that it can “hover” above the ground. Some air from the engine is diverted to the wing tips to be used for maneuvering. As shown in (b), the net thrust on the aircraft can be decomposed into a horizontal force F_1 and a vertical force F_2 acting at a distance r from the center of mass.

realistic model. Such a model also describes the steering dynamics of ships as well as the pitch dynamics of aircraft and missiles. It is also possible to place the coordinates of the car at the rear wheels (corresponding to setting $\alpha = 0$), a model which is often referred to as the *Dubins car* [61].

The situation in Figure 2.16 represents the situation when the vehicle moves forward and has front-wheel steering. The case when the vehicle reverses is obtained simply by changing the sign of the velocity, which is equivalent to a vehicle with rear-wheel steering. ∇

Example 2.9 Vectored thrust aircraft

Consider the motion of vectored thrust aircraft, such as the Harrier “jump jet” shown Figure 2.17a. The Harrier is capable of vertical takeoff by redirecting its thrust downward and through the use of smaller maneuvering thrusters located on its wings. A simplified model of the Harrier is shown in Figure 2.17b, where we focus on the motion of the vehicle in a vertical plane through the wings of the aircraft. We resolve the forces generated by the main downward thruster and the maneuvering thrusters as a pair of forces F_1 and F_2 acting at a distance r below the aircraft (determined by the geometry of the thrusters).

Let (x, y, θ) denote the position and orientation of the center of mass of aircraft. Let m be the mass of the vehicle, J the moment of inertia, g the gravitational constant, and c the damping coefficient. Then the equations of motion for the vehicle are given by

$$\begin{aligned} m\ddot{x} &= F_1 \cos \theta - F_2 \sin \theta - c\dot{x} \\ m\ddot{y} &= F_1 \sin \theta + F_2 \cos \theta - mg - c\dot{y} \\ J\ddot{\theta} &= rF_1. \end{aligned} \quad (2.26)$$

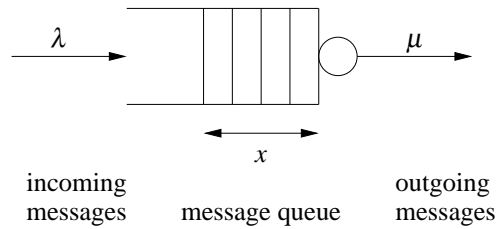


Figure 2.18: Schematic diagram of a queuing system. Messages arrive at rate λ and are stored in a queue. Messages are processed and removed from the queue at rate μ . The average size of the queue is given by $x \in \mathbb{R}$.

It is convenient to redefine the inputs so that the origin is an equilibrium point of the system with zero input. Letting $u_1 = F_1$ and $u_2 = F_2 - mg$, the equations become

$$\begin{aligned}
 m\ddot{x} &= -mg \sin \theta - c\dot{x} + u_1 \cos \theta - u_2 \sin \theta \\
 m\ddot{y} &= mg(\cos \theta - 1) - c\dot{y} + u_1 \sin \theta + u_2 \cos \theta \\
 J\ddot{\theta} &= ru_1.
 \end{aligned} \tag{2.27}$$

These equations described the motion of the vehicle as a set of three coupled second order differential equations. ▽

Information Systems

Information systems range from communication systems like the Internet to software systems that manipulate data or manage enterprise wide resources. Feedback is present in all these systems, and design of strategies for routing, flow control and buffer management are typical problems. Many results in queuing theory emerged from design of telecommunication systems and later from development of the Internet and computer communication systems [32, 120, 168]. Management of queues to avoid congestion is a central problem and we will therefore start by discussing modeling of queuing systems.

Example 2.10 Queuing systems

A schematic picture of a simple queue is shown in Figure 2.18. Requests arrive and are then queued and processed. There can be large variations in arrival rates and service rates and the queue length builds up when the arrival rate is larger than the service rate. When the queue becomes too large, service is denied using an admission control policy.

The system can be modeled in many different ways. One way is to model each incoming request, which leads to an event-based model where the state is an integer that represents the queue length. The queue changes when a request arrives or a request is serviced. The statistics of arrival and servicing are typically modeled as random processes. In many cases it is possible to determine statistics of quantities like queue length and service time but the computations can be quite complicated.

A significant simplification can be obtained by using a *flow model*. Instead of keeping track of each request we instead view service and requests as flows, similar to what is done when replacing molecules by a continuum when analyzing fluids. Assuming that the average queue length x is a continuous variable and that arrivals and services are flows with rates λ and μ , the system can be modeled by the first order differential equation

$$\frac{dx}{dt} = \lambda - \mu = \lambda - \mu_{\max} f(x), \quad x \geq 0, \quad (2.28)$$

where μ_{\max} is the maximum service rate and $f(x)$ is a number between 0 and 1 that describes the effective service rate as a function of the queue length.

It is natural to assume that the effective service rate depends on the queue length because larger queues require more resources. In steady state we have $f(x) = \lambda/\mu_{\max}$ and we assume that the queue length goes to zero when λ/μ_{\max} goes to zero and that it goes to infinity when λ/μ_{\max} goes to 1. This implies that $f(0) = 0$ and that $f(\infty) = 1$. In addition if we assume that the effective service rate deteriorates monotonically with queue length then the function $f(x)$ is monotone and concave. A simple function that satisfies the basic requirements is $f(x) = x/(1+x)$, which gives the model

$$\frac{dx}{dt} = \lambda - \mu_{\max} \frac{x}{x+1}. \quad (2.29)$$

This model was proposed by Agnew [5]. It can be shown that if arrival and service processes are Poisson processes the average queue length is given by equation (2.29) and that equation (2.29) is a good approximation even for short queue lengths; see Tipper [184].

To explore the properties of the model (2.29) we will first investigate the equilibrium value of the queue length when the arrival rate λ is constant. Setting the derivative dx/dt to zero in equation (2.29) and solving for x we find that the queue length x approaches the steady state value

$$x_e = \frac{\lambda}{\mu_{\max} - \lambda}. \quad (2.30)$$

Figure 2.19a shows the steady state queue length as a function of λ/μ_{\max} , the effective service rate excess. Notice that the queue length increases rapidly as λ approaches μ_{\max} . To have a queue length less than 20 requires $\lambda/\mu_{\max} < 0.95$. The average time to service a request is $T_s = (x+1)/\mu_{\max}$ and it also increases dramatically as λ approaches μ_{\max} .

Figure 2.19b illustrates the behavior of the server in a typical overload situation. The maximum service rate is $\mu_{\max} = 1$, and the arrival rate starts at $\lambda = 0.5$. The arrival rate is increased to $\lambda = 4$ at time 20, and it returns to $\lambda = 0.5$ at time 25. The figure shows that the queue builds up quickly and clears very slowly. Since the response time is proportional to queue length, it means that the quality of service is poor for a long period after an overload. This behavior is called the *rush-hour effect* and has been observed in web servers and many other queuing systems such

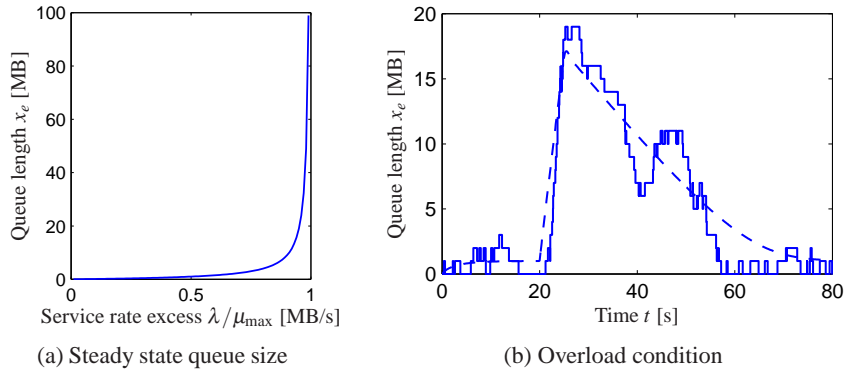


Figure 2.19: Queuing dynamics. The figure on the left shows steady state queue length as a function of λ/μ_{\max} , and the figure on the right shows the behavior of the queue length when there is a temporary overload in the system. The full line shows a realization of an event based simulation and the dashed line shows the behavior of the flow model (2.29).

as automobile traffic.

The dashed line in Figure 2.19b shows the behavior of the flow model, which describes the average queue length. The simple model captures behavior qualitatively, but there are significant variations from sample to sample when the queue length is short. ∇

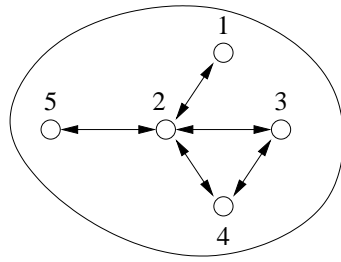
Queuing problems of the type illustrated in Example 2.10 have been observed in many different situations. The following example illustrates an early example of the difficulty and it also describes how it can be avoided by using a simple feedback scheme.

Example 2.11 Consensus protocols in sensor networks

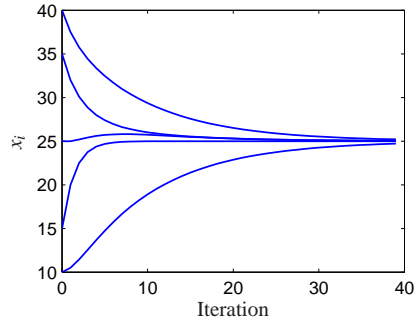
Sensor networks are used in a variety of applications where we want to collect and aggregate information over a region of space using multiple sensors that are connected together via a communications network. Examples include monitoring environmental conditions in a geographical area (or inside a building), monitoring movement of animals or vehicles, or monitoring the resource loading across a group of computers. In many sensor networks the computational resources for the system are distributed along with the sensors and it can be important for the set of distributed agents to reach a consensus about a certain property, such as the average temperature in a region or the average computational load amongst a set of computers.

We model the connectivity of the sensor network using a graph, with nodes corresponding to the sensors and edges corresponding to the existence of a direct communications link between two nodes. We use the notation \mathcal{N}_i to represent the set of neighbors of a node i . For example, in the network shown in Figure 2.20a $\mathcal{N}_2 = \{1, 3, 4, 5\}$ and $\mathcal{N}_3 = \{2, 4\}$.

To solve the consensus problem, we let x_i be the state of the i th sensor, corresponding to that sensor's estimate of the average value that we are trying to com-



(a) Sensor network



(b) Consensus convergence

Figure 2.20: Consensus protocols for sensor networks. A simple sensor network with five nodes is shown on the left. In this network, node 1 communicates with node 2, node 2 communicates with nodes 1, 3, 4 and 5, etc. A simulation demonstrating the convergence of the consensus protocol (2.31) to the average value of the initial conditions is shown on the right.

pute. We initialize the state to the value of the quantity measured by the individual sensor. Our consensus protocol can now be realized as a local update law of the form

$$x_i[k+1] = x_i[k] + \gamma \sum_{j \in \mathcal{N}_i} (x_j[k] - x_i[k]). \quad (2.31)$$

This protocol attempts to compute the average by updating the local state of each agent based on the value of its neighbors. The combined dynamics of all agents can be written in the form

$$\dot{x}[k+1] = x[k] - \gamma(D-A)x[k] \quad (2.32)$$

where A is the adjacency matrix and D is a diagonal matrix whose entries correspond to the number of neighbors of the corresponding node. The constant γ describes the rate at which we update our own estimate of the average based on the information from our neighbors. The matrix $L := D - A$ is called the *Laplacian* of the graph.

The equilibrium points of equation (2.32) are the set of states such that $x_e[k+1] = x_e[k]$. It is easy to show that $x_e = (\alpha, \alpha, \dots, \alpha)$ is an equilibrium state for the system, corresponding to each sensor having an identical estimate α for the average. Furthermore, we can show that α is precisely the average value of the initial states. Since there can be cycles in the graph, it is possible that the state of the system could get into an “infinite loop” and never converge to the desired consensus state. A formal analysis requires tools that will be introduced later in the text, but it can be shown that for any connected graph, we can always find a γ such that the states of the individual agents converge to the average. A simulation demonstrating this property is shown in Figure 2.20b.

Although we have focused here on consensus to the average value of a set of measurements, other consensus states can be achieved through choice of appropri-

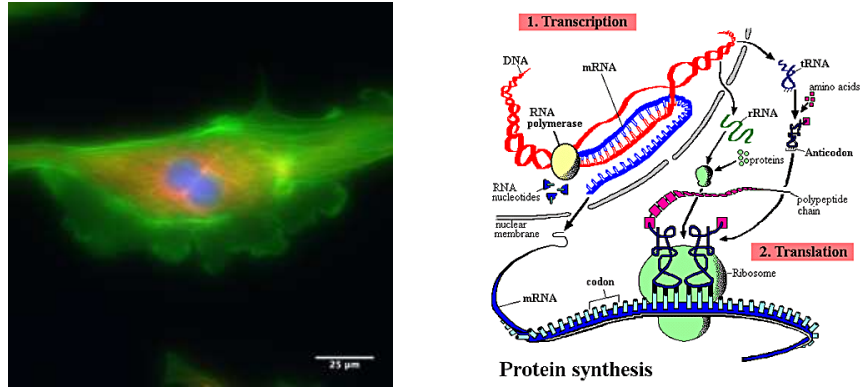


Figure 2.21: Biological circuitry. The cell on the left is a bovine pulmonary cell, stained so that the nucleus, actin and chromatin are visible. The figure on the right gives an overview of the process by which proteins in the cell are made. RNA is transcribed from DNA by an RNA polymerase enzyme. The RNA is then translated into a protein by an organelle called the ribosome.

ate feedback laws. Examples include finding the maximum or minimum value in a network, counting the number of nodes in a network or computing higher order statistical moments of a distributed quantity [154]. ∇

Biological Systems

Biological systems provide perhaps the richest source of feedback and control examples. The basic problem of homeostasis, in which a quantity such as temperature or blood sugar level is regulated to a fixed value, is but one of the many types of complex feedback interactions that can occur in molecular machines, cells, organisms and ecosystems.

Example 2.12 Transcriptional regulation

Transcription is the process by which mRNA is generated from a segment of DNA. The promoter region of a gene allows transcription to be controlled by the presence of other proteins, which bind to the promoter region and either repress or activate RNA polymerase (RNAP), the enzyme that produces an mRNA transcript from DNA. The mRNA is then translated into a protein according to its nucleotide sequence. This process is illustrated in Figure 2.21.

A simple model of the transcriptional regulation process is through the use of a Hill function [53, 146]. Consider the regulation of a protein A with concentration given by p_A and corresponding mRNA concentration m_A . Let B be a second protein with concentration p_B that represses the production of protein A through transcriptional regulation. The resulting dynamics of p_A and m_A can be written as

$$\frac{dm_A}{dt} = -\gamma m_A + \frac{\alpha}{1 + k_B p_B^n} + \alpha_0, \quad \frac{dp_A}{dt} = \beta m_A - \delta p_A, \quad (2.33)$$

where $\alpha + \alpha_0$ is the unregulated transcription rate, γ represents the rate of degra-

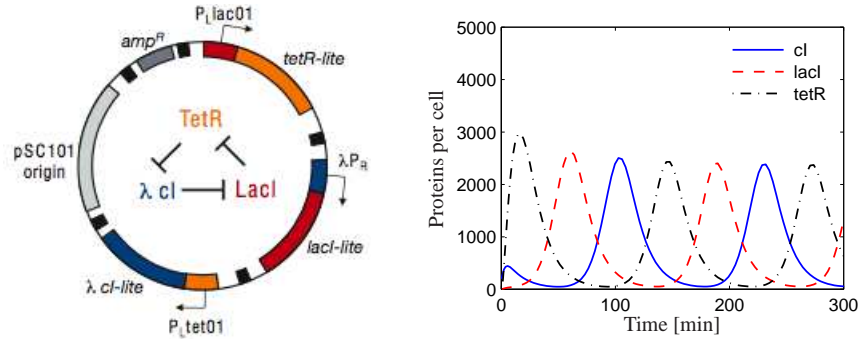


Figure 2.22: The repressilator genetic regulatory network. A schematic diagram of the repressilator is given on the left, showing the layout of the genes in the plasmid that holds the circuit as well as the circuit diagram (center). A simulation of a simple model for the repressilator is shown on the right, showing the oscillation of the individual protein concentrations. Parameter values taken from [68].

dation of mRNA, α and n are parameters that describe how B represses A, β represents the rate of production of the protein from its corresponding mRNA and δ represents the rate of degradation of the protein A. The parameter α_0 describes the “leakiness” of the promoter and n is called the Hill coefficient and relates to the cooperativity of the promoter.

A similar model can be used when a protein activates the production of another protein, rather than repressing it. In this case, the equations have the form

$$\frac{dm_A}{dt} = \frac{\alpha k_B p_B^n}{1 + k_B p_B^n} + \alpha_0 - \gamma m_A, \quad \frac{dp_A}{dt} = \beta m_A - \delta p_A, \quad (2.34)$$

where the variables are the same as described previously. Note that in the case of the activator, if p_B is zero then the production rate is α_0 (versus $\alpha + \alpha_0$ for the repressor). As p_B gets large, the first term in the expression for \dot{m}_A approaches 1 and the transcription rate becomes $\alpha + \alpha_0$ (versus α_0 for the repressor). Thus we see that the activator and repressor act in opposite fashion from each other.

As an example of how these models can be used, we consider the model of a “repressilator”, originally due to Elowitz and Leibler [68]. The repressilator is a synthetic circuit in which three proteins each repress another in a cycle. This is shown schematically in Figure 2.22a, where the three proteins are TetR, λ cI and LacI. The basic idea of the repressilator is that if TetR is present then it represses the production of λ cI. If λ cI is absent, then LacI is produced (at the unregulated transcription rate), which in turn represses TetR. Once TetR is repressed then λ cI is no longer repressed and so on. If the dynamics of the circuit are designed properly, the resulting protein concentrations will oscillate.

We can model this system using three copies of equation (2.33), with A and B replaced by the appropriate combination of TetR, cI and LacI. The state of the system is then given by $x = (m_{TetR}, p_{TetR}, m_{cI}, p_{cI}, m_{LacI}, p_{LacI})$. Figure 2.22b shows the traces of the three protein concentrations for parameters $n = 2$, $\alpha = 0.5$, $k =$

6.25×10^{-4} , $\alpha_0 = 5 \times 10^{-4}$, $\gamma = 5.8 \times 10^{-3}$, $\beta = 0.12$ and $\delta = 1.2 \times 10^{-3}$ with initial conditions $x(0) = (1, 0, 0, 200, 0, 0)$ (following [68]). ∇

Example 2.13 Wave propagation in neuronal networks

The dynamics of the membrane potential in a cell are a fundamental mechanism in understanding signaling in cells, particularly in neurons and muscle cells. The Hodgkin-Huxley equations give a simple model for studying propagation waves in networks of neurons. The model for a single neuron has the form

$$C \frac{dV}{dt} = -I_{\text{Na}} - I_{\text{K}} - I_{\text{leak}} + I_{\text{input}},$$

where V is the membrane potential, C the capacitance, I_{Na} and I_{K} the current caused by transport of sodium and potassium across the cell membrane, I_{leak} a leakage current and I_{input} the external stimulation of the cell. Each current obeys Ohm's law, i.e.

$$I = g(V - E),$$

where g is the conductance and E the equilibrium voltage. The equilibrium voltage is given by Nernst's law

$$E = \frac{RT}{nF} \log(c_e/c_i),$$

where R is Boltzmann's constant, T the absolute temperature, F Faraday's constant, n is the charge (or valence) of the ion, and c_i and c_e are the ion concentrations inside the cell and in the external fluid. At 20°C we have $RT/F = 20 \text{ mV}$.

The Hodgkin-Huxley model was originally developed as a means to predict the quantitative behavior of the squid giant axon [95]. Hodgkin and Huxley shared the 1963 Nobel Prize in Physiology (along with J. C. Eccles) for analysis of the electrical and chemical events in nerve cell discharge. The voltage clamp described in Section 1.3 (see Figure 1.8) was a key element in Hodgkin and Huxley's experiments. ∇

2.5 FURTHER READING

Modeling is ubiquitous in engineering and science and has a long history in applied mathematics. For example, the Fourier series was introduced by Fourier when he modeled heat conduction in solids [73]. Models of dynamics have been developed in many different fields, including mechanics [12, 82], heat conduction [48], fluids [37], vehicles [1, 38, 66], circuit theory [88], acoustics [29] and micromechanical systems [170]. Control theory requires modeling from many different domains and most control theory texts contain several chapters on modeling using ordinary differential equations and difference equations (see, for example, [76]). A classic book on modeling of physical systems, especially mechanical, electrical and thermo-fluid systems, is Cannon [47]. The book by Aris [11] is highly original and has a detailed discussion of the use of dimension free variables. Two of the authors' favorite books on modeling of biological systems are J. D. Murray [146]

and Wilson [194]. For readers interested in learning more about object oriented modeling and Modelica, Tiller [183] provides an excellent introduction.

EXERCISES

2.1 Consider the linear ordinary differential equation (2.7). Show that by choosing a state space representation with $x_1 = y$, the dynamics can be written as

$$A = \begin{pmatrix} 0 & 1 & & 0 \\ 0 & \ddots & \ddots & 0 \\ 0 & \cdots & 0 & 1 \\ -a_n & -a_{n-1} & & -a_1 \end{pmatrix} \quad B = \begin{pmatrix} 0 \\ 0 \\ \vdots \\ 1 \end{pmatrix}$$

$$C = \begin{pmatrix} 1 & \cdots & 0 & 0 \end{pmatrix}.$$

This canonical form is called *chain of integrators* form.

2.2 Use the equations of motion for a balance system to derive a dynamic model for the inverted pendulum described in Example 2.2 and verify that for small θ the dynamics are approximated by equation (2.10).

2.3 Consider the following discrete time system

$$\begin{aligned} x[k+1] &= Ax[k] + Bu[k] \\ y[k] &= Cx[k] \end{aligned}$$

where

$$x = \begin{pmatrix} x_1 \\ x_2 \end{pmatrix} \quad A = \begin{pmatrix} a_{11} & a_{12} \\ 0 & a_{22} \end{pmatrix} \quad B = \begin{pmatrix} 0 \\ 1 \end{pmatrix} \quad C = \begin{pmatrix} 1 & 0 \end{pmatrix}$$

In this problem, we will explore some of the properties of this discrete time system as a function of the parameters, the initial conditions, and the inputs.

- For the case when $a_{12} = 0$ and $u = 0$, give a closed form expression for the output of the system.
- A discrete system is in *equilibrium* when $x[k+1] = x[k]$ for all k . Let $u = r$ be a constant input and compute the resulting equilibrium point for the system. Show that if $|a_{ii}| < 1$ for all i , all initial conditions give solutions that converge to the equilibrium point.
- Write a computer program to plot the output of the system in response to a unit step input, $u[k] = 1$, $k \geq 0$. Plot the response of your system with $x[0] = 0$ and A given by

$$A = \begin{pmatrix} 0.5 & 1 \\ 0 & 0.25 \end{pmatrix}.$$

2.4 Keynes' simple model for an economy is given by

$$Y[k] = C[k] + I[k] + G[k],$$

where Y , C , I and G are gross national product (GNP), consumption, investment and government expenditure for year k . Consumption and investment are modeled by difference equations of the form

$$C[k+1] = aY[k], \quad I[k+1] = b(C[k+1] - C[k]),$$

where a and b are parameters. The first equation implies that consumption increases with GNP but that the effect is delayed. The second equation implies that investment is proportional to the rate of change of consumption.

Show that the equilibrium value of the GNP is given by

$$Y_e = \frac{1}{1-a}(I_e + G_e),$$

where the parameter $1/(1-a)$ is the Keynes multiplier (the gain from I or G to Y). With $a = 0.25$ an increase of government expenditure will result in a fourfold increase of GNP. Also show that the model can be written as the following discrete time state model

$$\begin{pmatrix} C[k+1] \\ I[k+1] \end{pmatrix} = \begin{pmatrix} a & a \\ ab-a & ab \end{pmatrix} \begin{pmatrix} C[k] \\ I[k] \end{pmatrix} + \begin{pmatrix} a \\ ab \end{pmatrix} G[k]$$

$$Y[k] = C[k] + I[k] + G[k].$$

2.5 (Second order system identification) Verify that equation (2.22) in Example 2.5 is correct and use this formula and the others in the example to compute the parameters corresponding to the step response in Figure 2.14.



2.6 (Least squares system identification) Consider a nonlinear differential equation that can be written in the form

$$\frac{dx}{dt} = \sum_{i=1}^M \alpha_i f_i(x),$$

where $f_i(x)$ are known nonlinear functions and α_i are unknown, but constant, parameters. Suppose that we have measurements (or estimates) of the state x at time instants t_1, t_2, \dots, t_N , with $N > M$. Show that the parameters α_i can be determined by finding the least squares solution to a linear equation of the form

$$H\alpha = b,$$

where $\alpha \in \mathbb{R}^M$ is the vector of all parameters and $H \in \mathbb{R}^{N \times M}$ and $b \in \mathbb{R}^N$ are appropriately defined.

2.7 (Normalized oscillator dynamics) Consider a damped spring-mass system with dynamics

$$m\ddot{q} + c\dot{q} + kq = F.$$

Let $\omega_0 = \sqrt{k/m}$ be the undamped natural frequency and $\zeta = c/(2\sqrt{km})$ be the relative damping.

- (a) Show that by rescaling the equations, we can write the system dynamics in the form

$$\ddot{q} + 2\zeta\omega_0\dot{q} + \omega_0^2q = \omega_0^2u \quad (2.35)$$

where $u = F/k$. This form of the dynamics is that of a linear oscillator with natural frequency ω_0 and damping coefficient ζ .

- (b) Show that the system can be further normalized and written in the form

$$\frac{dz_1}{d\tau} = z_2, \quad \frac{dz_2}{d\tau} = -z_1 - 2\zeta z_2 + v. \quad (2.36)$$

We thus see that the essential dynamics of the system are governed by a single damping parameter, ζ . The em Q -value defined as $Q = 1/2\zeta$ is sometimes used instead of ζ .

2.8 Show that the dynamics for a balance system using normalized coordinates can be written in state space form as

$$\frac{dx}{dt} = \begin{pmatrix} x_3 \\ x_4 \\ \frac{-\alpha x_4^2 - \alpha \sin x_2 \cos x_2 + u}{1 - \alpha\beta \cos^2 x_2} \\ \frac{-\alpha\beta \cos x_2 x_4^2 - \sin x_2 + \beta \cos x_2 u}{1 - \alpha\beta \cos^2 x_2} \end{pmatrix},$$

where $x = (q/l, \theta, \dot{q}/l, \dot{\theta})$.

2.9 An electric generator connected to a strong power grid can be modeled by a momentum balance for the rotor of the generator:

$$J \frac{d^2\varphi}{dt^2} = P_m - P_e = P_m - \frac{EV}{X} \sin \varphi,$$

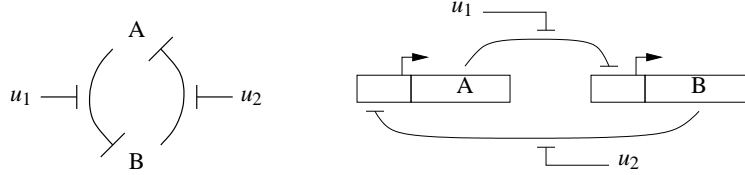
where J is the effective moment of inertia of the generator, φ the angle of rotation, P_m the mechanical power that drives the generator, E is the generator voltage, V the grid voltage and X the reactance of the line. P_e is the active electrical power and, assuming that the line dynamics are much faster than the rotor dynamics, it is given by $P_e = VI = (EV/X) \sin \varphi$, where I is the current component in phase with the voltage E and φ is the phase angle between voltages E and V . Show that the dynamics of the electric generator have a normalized form that is similar to the inverted pendulum in Example 2.2 (note that damping has been neglected in the model above).

2.10 The long delays created by temporary overloads can be reduced by rejecting requests when the queue gets large. This allows requests that are accepted to be serviced quickly and requests that cannot be accommodated to receive a rejection quickly so they can try another server. Consider a simple proportional control with saturation, described by

$$u = \text{sat}_{(0,1)}(k(r - x)), \quad (2.37)$$

where $\text{sat}_{(a,b)}$ is defined in equation (3.9) and r is the desired (reference) queue length. Use a simulation to show that this controller reduces the rush-hour effect and explain how the choice of r effects the system dynamics.

2.11 Consider the dynamics of two repressors connected together in a cycle, as shown below:

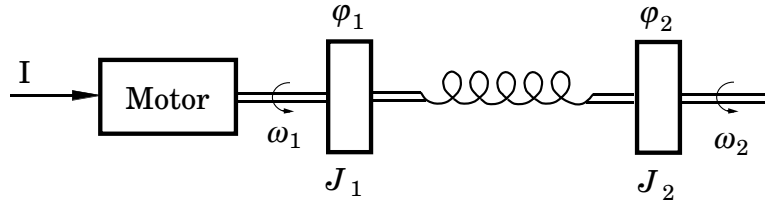


Using the models from Example 2.12, under the assumption that the parameters are the same for both genes, and further assuming that the mRNA concentrations reach steady state quickly, show that the dynamics for this system can be written as

$$\frac{dz_1}{d\tau} = \frac{\mu}{1+z_2^n} - z_1 - v_1, \quad \frac{dz_2}{d\tau} = \frac{\mu}{1+z_1^n} - z_2 - v_2. \quad (2.38)$$

where z_1 and z_2 represent scaled versions of the protein concentrations and the time scale has been changed. Show that $\mu \approx 2.16$ using the parameters in Example 2.12.

2.12 (Motor drive) Consider a system consisting of a motor driving two masses that are connected by a torsional spring, as shown in the diagram below:



This system can represent a motor with a flexible shaft that drives a load. Assuming that the motor delivers a torque that is proportional to the current, the dynamics of the system can be described by the equations

$$\begin{aligned} J_1 \frac{d^2 \phi_1}{dt^2} + c \left(\frac{d\phi_1}{dt} - \frac{d\phi_2}{dt} \right) + k(\phi_1 - \phi_2) &= k_t I \\ J_2 \frac{d^2 \phi_2}{dt^2} + c \left(\frac{d\phi_2}{dt} - \frac{d\phi_1}{dt} \right) + k(\phi_2 - \phi_1) &= T_d \end{aligned} \quad (2.39)$$

Similar equations are obtained for a robot with flexible arms and for the arms of DVDs and optical memories.

Derive a state space model for the system by introducing the (normalized) state variables $x_1 = \phi_1$, $x_2 = \phi_2$, $x_3 = \omega_1/\omega_0$, and $x_4 = \omega_2/\omega_0$, where $\omega_0 = \sqrt{k(J_1 + J_2)/(J_1 J_2)}$ is the undamped natural frequency of the system when the control signal is zero.

Chapter Three

Examples

... Don't apply any model until you understand the simplifying assumptions on which it is based, and you can test their validity. Catch phrase: use only as directed. Don't limit yourself to a single model: More than one model may be useful for understanding different aspects of the same phenomenon. Catch phrase: legalize polygamy."

Saul Golomb in his 1970 paper "Mathematical Models—Uses and Limitations" [83].

In this chapter we present a collection of examples spanning many different fields of science and engineering. These examples will be used throughout the text and in exercises to illustrate different concepts. First time readers may wish to focus only on a few examples with which they have the most prior experience or insight to understand the concepts of state, input, output and dynamics in a familiar setting.

3.1 CRUISE CONTROL

The cruise control system of a car is a common feedback system encountered in everyday life. The system attempts to maintain a constant velocity in the presence of disturbances primarily caused by changes in the slope of a road. The controller compensates for these unknowns by measuring the speed of the car and adjusting the throttle appropriately.

To model the system we start with the block diagram in Figure 3.1. Let v be the speed of the car and v_r the desired (reference) speed. The controller, which typically is of the proportional-integral (PI) type described briefly in Chapter 1, receives the signals v and v_r and generates a control signal u that is sent to an actuator that controls throttle position. The throttle in turn controls the torque T delivered by the engine, which is transmitted through gears and the wheels, generating a force F that moves the car. There are disturbance forces F_d due to variations in the slope of the road, the rolling resistance and aerodynamic forces. The cruise controller also has a human-machine interface that allows the driver to set and modify the desired speed. There are also functions that disconnect the cruise control when the brake is touched.

The system has many individual components—actuator, engine, transmission, wheels and car body—and a detailed model can be very complicated. In spite of this, the model required to design the cruise controller can be quite simple.

To develop a mathematical model we start with a force balance for the car body. Let v be the speed of the car, m the total mass (including passengers), F the force

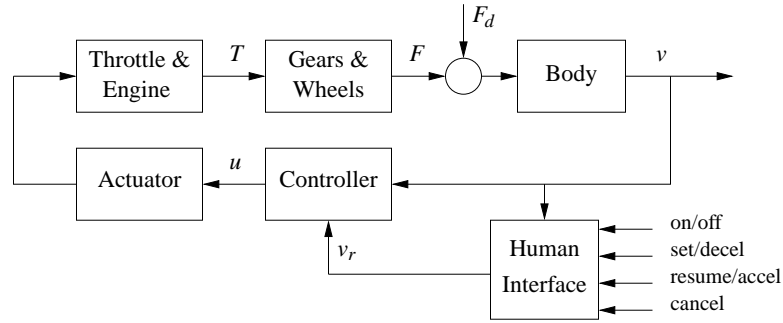


Figure 3.1: Block diagram of a cruise control system for an automobile. The throttle-controlled engine generates a torque T that is transmitted to the ground through the gearbox and wheels. Combined with the external forces from the environment, such as aerodynamic drag and gravitational forces on hills, the net force causes the car to move. The velocity of the car v is measured by a control system that adjusts the throttle through an actuation mechanism. A human interface allows the system to be turned on an off and the reference speed v_r to be established.

generated by the contact of the wheels with the road, and F_d the disturbance force due to gravity and friction. The equation of motion of the car is simply

$$m \frac{dv}{dt} = F - F_d. \quad (3.1)$$

The force F is generated by the engine, whose torque is proportional to the rate of fuel injection, which is itself proportional to a control signal $0 \leq u \leq 1$ that controls throttle position. The torque also depends on engine speed ω . A simple representation of the torque at full throttle is given by the torque curve

$$T(\omega) = T_m \left(1 - \beta \left(\frac{\omega}{\omega_m} - 1 \right)^2 \right), \quad (3.2)$$

where the maximum torque T_m is obtained at engine speed ω_m . Typical parameters are $T_m = 190$ Nm, $\omega_m = 420$ rad/s (about 4000 RPM) and $\beta = 0.4$. Let n be the gear ratio and r the wheel radius. The engine speed is related to the velocity through the expression

$$\omega = \frac{n}{r} v =: \alpha_n v,$$

and the driving force can be written as

$$F = \frac{nu}{r} T(\omega) = \alpha_n u T(\alpha_n v).$$

Typical values of α_n for gears 1 through 5 are $\alpha_1 = 40$, $\alpha_2 = 25$, $\alpha_3 = 16$, $\alpha_4 = 12$ and $\alpha_5 = 10$. The inverse of α_n has a physical interpretation as the *effective wheel radius*. Figure 3.2 shows the torque as a function of engine speed and vehicle speed. The figure shows that the effect of the gear is to “flatten” the torque curve so that a almost full torque can be obtained almost over the whole speed range.

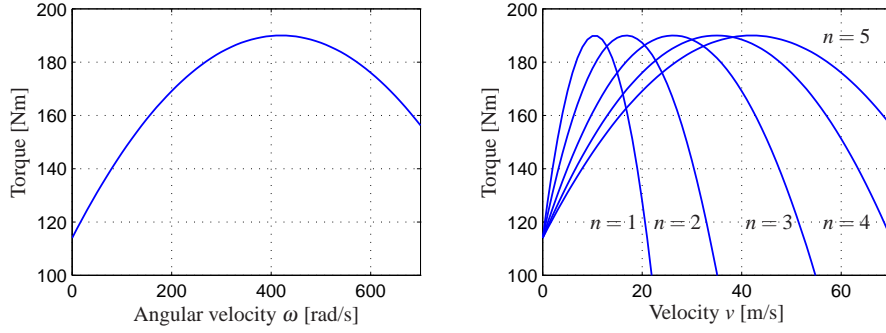


Figure 3.2: Torque curves for typical car engine. The graph on the left shows the torque generated by the engine as a function of the angular velocity of the engine, while the curve on the right shows torque as a function of car speed for different gears.

The disturbance force F_d has three major components: F_g , the forces due to gravity; F_r , the forces due to rolling friction; and F_a , the aerodynamic drag. Letting the slope of the road be θ , gravity gives the force $F_g = mg \sin \theta$, as illustrated in Figure 3.3a, where $g = 9.8 \text{ m/s}^2$ is the gravitational constant. A simple model of rolling friction is

$$F_r = -mgC_r \text{sgn}(v),$$

where C_r is the coefficient of rolling friction and $\text{sgn}(v)$ is the sign of v (± 1) or zero if $v = 0$. A typical value for the coefficient of rolling friction is $C_r = 0.01$. Finally, the aerodynamic drag is proportional to the square of the speed:

$$F_a = \frac{1}{2} \rho C_d A v^2,$$

where ρ is the density of air, C_d is the shape-dependent aerodynamic drag coefficient and A is the frontal area of the car. Typical parameters are $\rho = 1.3 \text{ kg/m}^3$, $C_d = 0.32$ and $A = 2.4 \text{ m}^2$.

Summarizing, we find that the car can be modeled by

$$m \frac{dv}{dt} = \alpha_n u T(\alpha_n v) - mgC_r \text{sgn}(v) - \frac{1}{2} \rho C_d A v^2 - mg \sin \theta, \quad (3.3)$$

where the function T is given by equation (3.2). The model (3.3) is a dynamical system of first order. The state is the car velocity v , which is also the output. The input is the signal u that controls the throttle position, and the disturbance is the force F_d , which depends on the slope of the road. The system is nonlinear because of the torque curve and the nonlinear character of the aerodynamic drag. There can also be variations in the parameters, e.g. the mass of the car depends on the number of passengers and the load being carried in the car.

We add to this model a feedback controller that attempts to regulate the speed of the car in the presence of disturbances. We shall use a PI (proportional-integral)

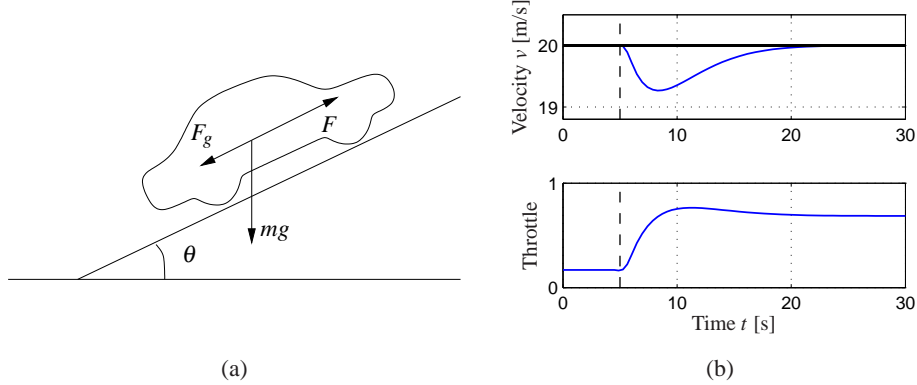


Figure 3.3: Car with cruise control encountering a sloping road: a schematic diagram is shown in (a) and (b) shows the response in speed and throttle when a slope of 4° is encountered. The hill is modeled as a net change in hill angle, θ , of 4° , with a linear change in the angle between $t = 5$ and $t = 6$. The PI controller has proportional gain is $k_p = 0.5$ and the integral gain is $k_i = 0.1$.

controller, which has the form

$$u(t) = k_p e(t) + k_i \int_0^t e(\tau) d\tau.$$

This controller can itself be realized as an input/output dynamical system by defining a controller state z and implementing the differential equation

$$\frac{dz}{dt} = v_r - v \quad u = k_p(v_r - v) + k_i z, \quad (3.4)$$

where v_r is the desired (reference) speed. As discussed briefly in the introduction, the integrator (represented by the state z) ensures that in steady state the error will be driven to zero, even when there are disturbances or modeling errors. (The design of PI controllers is the subject of Chapter 10.) Figure 3.3b shows the response of the closed loop system, consisting of equations (3.3) and (3.4), when it encounters a hill. The figure shows that even if the hill is so steep that the throttle changes from 0.17 to almost full throttle, the largest speed error is less than 1 m/s, and the desired velocity is recovered after 20 s.

Many approximations were made when deriving the model (3.3). It may seem surprising that such a seemingly complicated system can be described by the simple model (3.3). It is important to make sure that we restrict our use of the model to the uncertainty lemon conceptualized in Figure 2.15b. The model is not valid for very rapid changes of the throttle because since we have ignored the details of the engine dynamics, neither is it valid for very slow changes because the properties of the engine will change over the years. Nevertheless the model is very useful for the design of a cruise control system. As we shall see in later chapters, the reason for this is the inherent robustness of feedback systems: even if the model is not perfectly accurate, we can use it to design a controller and make use of the feedback in the controller to manage the uncertainty in the system.

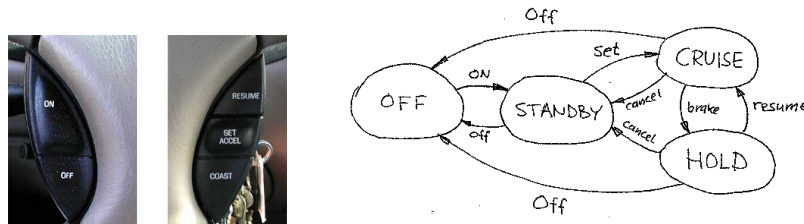


Figure 3.4: Finite state machine for cruise control system. The figure on the left shows some typical buttons used to control the system. The controller can be in one of four modes, corresponding to the nodes in the diagram on the right. Transition between the modes is controlled by pressing one of five buttons on the cruise control interface: on, off, set/accel, resume or cancel.

The cruise control system also has a human-machine interface that allows the driver to communicate with the system. There are many different ways to implement this system; one version is illustrated in Figure 3.4. The system has four buttons: on-off, set/decelerate, resume/accelerate and cancel. The operation of the system is governed by a finite state machine that controls the modes of the PI controller and the reference generator. Implementation of controllers and reference generators will be discussed more fully in Chapter 10.

The use of control in automotive systems goes well beyond the simple cruise control system described here. Modern applications include emissions control, traction control and power control (especially in hybrid vehicles). Many automotive applications are discussed in detail in and the book by Kiencke and Nielsen [117] and the survey papers by Powers *et al.* [22, 157].

3.2 BICYCLE DYNAMICS

The bicycle is an interesting dynamical system with the feature that one of its key properties is due to a feedback mechanism that is created by the design of the front fork. A detailed model of a bicycle is complex because the system has many degrees of freedom and the geometry is complicated. However, a great deal of insight can be obtained from simple models.

To derive the equations of motion we assume that the bicycle rolls on the horizontal xy plane. Introduce a coordinate system that is fixed to the bicycle with the ξ -axis through the contact points of the wheels with the ground, the η -axis horizontal and the ζ -axis vertical, as shown in Figure 3.5. Let v_0 be the velocity of the bicycle at the rear wheel, b the wheel base, φ the tilt angle and δ the steering angle. The coordinate system rotates around the point O with the angular velocity $\omega = v_0\delta/b$, and an observer fixed to the bicycle experiences forces due to the motion of the coordinate system.

The tilting motion of the bicycle is similar to an inverted pendulum, as shown in the rear view in Figure 3.5b. To model the tilt, consider the rigid body obtained

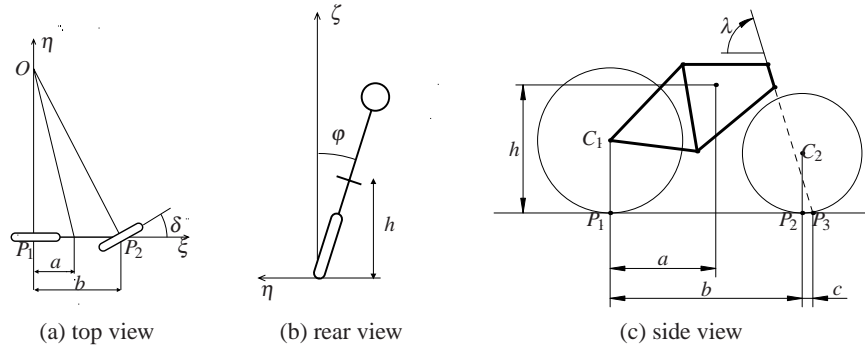


Figure 3.5: Schematic views of a bicycle. The steering angle is δ , the roll angle is φ . The center of mass has height h and distance a from a vertical through the contact point P_1 of the rear wheel. The wheel base is b and the trail is c .

when the wheels, the rider and the front fork assembly are fixed to the bicycle frame. Let m be the total mass of the system, J the moment of inertia of this body with respect to the ξ -axis, and D the product of inertia with respect to the $\xi\zeta$ axes. Furthermore, let the ξ and ζ coordinates of the center of mass with respect to the rear wheel contact point, P_1 , be a and h , respectively. We have $J \approx mh^2$ and $D = mah$. The torques acting on the system are due to gravity and centripetal action. Assuming that the steering angle δ is small, the equation of motion becomes

$$J \frac{d^2 \varphi}{dt^2} - \frac{Dv_0}{b} \frac{d\delta}{dt} = mgh \sin \varphi + \frac{mv_0^2 h}{b} \delta, \quad (3.5)$$

The term $mgh \sin \varphi$ is the torque generated by gravity. The terms containing δ and its derivative are the torques generated by steering, with the term $(Dv_0/b) d\delta/dt$ due to inertial forces and the term $(mv_0^2 h/b) \delta$ due to centripetal forces.

The steering angle is influenced by the torque the rider applies to the handle bar. Because of the tilt of the steering axis and the shape of the front fork, the contact point of the front wheel with the road P_2 is behind the axis of rotation of the front wheel assembly, as shown in Figure 3.5c. The distance c between the contact point of the front wheel P_2 and the projection of the axis of rotation of the front fork assembly P_3 is called the *trail*. The steering properties of a bicycle depend critically on the trail. A large trail increases stability but makes the steering less agile.

A consequence of the design of the front fork is that the steering angle δ is influenced both by steering torque T and by the tilt of the frame φ . This means that the bicycle with a front fork is a *feedback system* as illustrated by the block diagram in Figure 3.6. The steering angle δ influences the tilt angle φ and the tilt angle influences the steering angle giving rise to the circular causality that is characteristic for reasoning about feedback. For a front fork with positive trail, the bicycle will steer into the lean creating a centrifugal force that attempts to diminish the lean. Under certain conditions, the feedback can actually stabilize the bicycle.

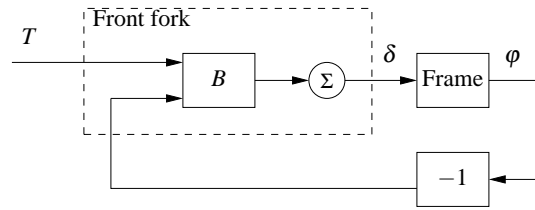


Figure 3.6: Block diagram of the bicycle with a front fork. The steering torque applied to the handlebars is T , the roll angle is ϕ , and the steering angle δ . Notice that the front fork creates a feedback from the roll angle ϕ to the steering angle δ that under certain conditions can stabilize the system.

A crude empirical model is obtained by assuming that the blocks A and B are static gains k_1 and k_2 respectively:

$$\delta = k_1 T - k_2 \phi. \quad (3.6)$$

This model neglects the dynamics of the front fork, the tire-road interaction and the fact that the parameters depend on the velocity. A more accurate model, called the *Whipple model*, is obtained by the rigid body dynamics of the front fork and the frame. Assuming small angles this model becomes

$$M \begin{pmatrix} \ddot{\phi} \\ \ddot{\delta} \end{pmatrix} + C v_0 \begin{pmatrix} \dot{\phi} \\ \dot{\delta} \end{pmatrix} + (K_0 + K_2 v_0^2) \begin{pmatrix} \phi \\ \delta \end{pmatrix} = \begin{pmatrix} 0 \\ T \end{pmatrix}, \quad (3.7)$$

where the elements of the 2×2 matrices M , C , K_0 and K_2 depend on the geometry and the mass distribution of the bicycle. Note that this has a form somewhat similar to the spring-mass system introduced in Chapter 2 and the balance system in Example 2.1. Even this more complex model is inaccurate because the interaction between tire and road is neglected; taking this into account requires two additional state variables. Again, the uncertainty lemon in Figure 2.15b provides a framework for understanding the validity of the model under these assumptions

Interesting presentations on the development of the bicycle are given in the books by D. Wilson [193] and Herlihy [93]. The model (3.7) was presented in a paper by Whipple in 1899 [188]. More details on bicycle modeling is given in the paper [18], which has many references.

3.3 OPERATIONAL AMPLIFIER CIRCUITS

The operational amplifier (op amp) is a modern implementation of Black's feedback amplifier. It is a universal component that is widely used for instrumentation, control and communication. It is also a key element in analog computing.

Schematic diagrams of the operational amplifier are shown in Figure 3.7. The amplifier has one inverting input (v_-), one non-inverting input (v_+), and one output (v_{out}). There are also connections for the supply voltages, e_- and e_+ , and a zero adjustment (offset null). A simple model is obtained by assuming that the input

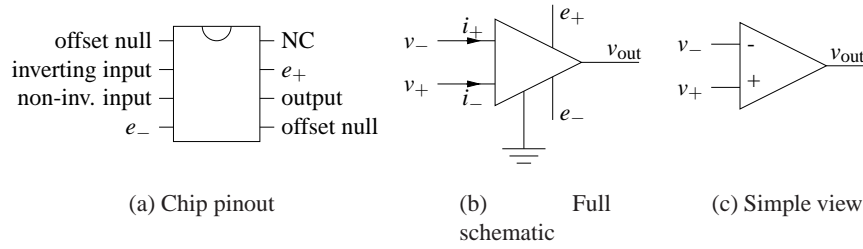


Figure 3.7: An operational amplifier and two schematic diagrams. The figure on the left shows the amplifier pin connections on an integrated circuit chip, the middle figure shows a schematic with all connections, and the diagram on the right shows only the signal connections.

currents i_- and i_+ are zero and that the output is given by the static relation

$$v_{\text{out}} = \text{sat}_{(v_{\min}, v_{\max})}(k(v_+ - v_-)), \quad (3.8)$$

where sat denotes the saturation function

$$\text{sat}_{(a,b)}(x) = \begin{cases} a & \text{if } x < a \\ x & \text{if } a \leq x \leq b \\ b & \text{if } x > b. \end{cases} \quad (3.9)$$

We assume that the gain k is large, in the range of 10^6 – 10^8 , and the voltages v_{\min} and v_{\max} satisfy

$$e_- \leq v_{\min} < v_{\max} \leq e_+$$

and hence are in the range of the supply voltages. More accurate models are obtained by replacing the saturation function with a smooth function as shown in Figure 3.8. For small input signals the amplifier characteristic (3.8) is linear:

$$v_{\text{out}} = k(v_+ - v_-) =: -kv. \quad (3.10)$$

Since the open loop gain k is very large, the range of input signals where the system

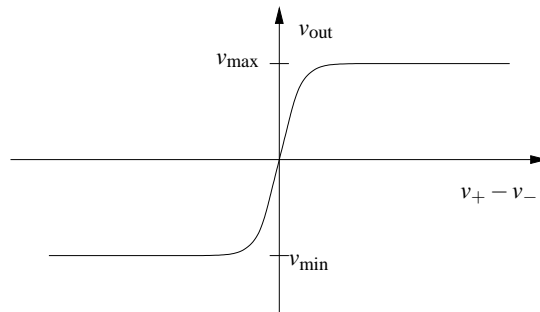


Figure 3.8: Input/output characteristics of an operational amplifier. The differential input is given by $v_+ - v_-$. The output voltage is a linear function of the input in a small range around 0, with saturation at v_{\min} and v_{\max} . In the linear regime the op amp has high gain.

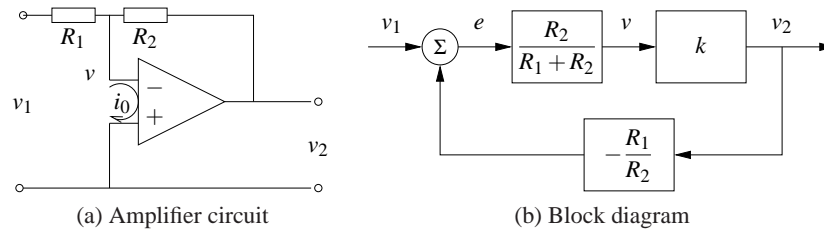


Figure 3.9: Stable amplifier using an op amp. The circuit (a) uses negative feedback around an operational amplifier and has a corresponding block diagram (b). The resistors R_1 and R_2 determine the gain of the amplifier.

is linear is very small.

A simple amplifier is obtained by arranging feedback around the basic operational amplifier as shown in Figure 3.9a. To model the feedback amplifier in the linear range, we assume that the current $i_0 = i_- + i_+$ is zero, and that the gain of the amplifier is so large that the voltage $v = v_- - v_+$ is also zero. It follows from Ohm's law that the currents through resistors R_1 and R_2 are given by

$$\frac{v_1}{R_1} = -\frac{v_2}{R_2}$$

and hence the closed loop gain of the amplifier is

$$\frac{v_2}{v_1} = -k_{cl} \quad \text{where} \quad k_{cl} = \frac{R_2}{R_1}. \quad (3.11)$$

A more accurate model is obtained by continuing to neglect the current i_0 but assuming that the voltage v is small but not negligible. The current balance is then

$$\frac{v_1 - v}{R_1} = \frac{v - v_2}{R_2}. \quad (3.12)$$

Assuming that the amplifier operates in the linear range and using equation (3.10) the gain of the closed loop system becomes

$$k_{cl} = -\frac{v_2}{v_1} = \frac{R_2}{R_1} \frac{1}{1 + \frac{1}{k} \left(1 + \frac{R_2}{R_1}\right)} \quad (3.13)$$

If the open loop gain k of the operational amplifier is large, the closed loop gain k_{cl} is the same as in the simple model given by equation (3.11). Notice that the closed loop gain only depends on the passive components and that variations in k only have a marginal effect on the closed loop gain. For example if $k = 10^6$ and $R_2/R_1 = 100$, a variation of k by 100% only gives a variation of 0.01% in the closed loop gain. The drastic reduction in sensitivity is a nice illustration of how feedback can be used to make precise systems from uncertain components. In this particular case, feedback is used to trade high gain and low robustness for low gain and high robustness. Equation (3.13) was the formula that inspired Black when he invented the feedback amplifier [35] (see the quote at the beginning of Chapter 12).

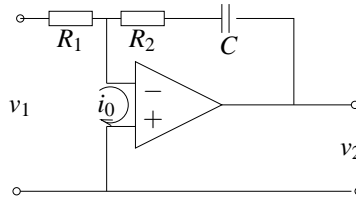


Figure 3.10: Circuit diagram of a PI controller obtained by feedback around an operational amplifier. The capacitor C is used to store charge and represents the integral of the input.

It is instructive to develop a block diagram for the feedback amplifier in Figure 3.9a. To do this we will represent the pure amplifier with input v and output v_2 as one block. To complete the block diagram we must describe how v depends on v_1 and v_2 . Solving equation (3.12) for v gives

$$v = \frac{R_2}{R_1 + R_2} v_1 + \frac{R_1}{R_1 + R_2} v_2 = \frac{R_2}{R_1 + R_2} \left(v_1 + \frac{R_1}{R_2} v_2 \right),$$

and we obtain the block diagram shown in Figure 3.9b. The diagram clearly shows that the system has feedback and that the gain from v_2 to v is $R_1/(R_1 + R_2)$, which can also be read from the circuit diagram in Figure 3.9a. If the loop is stable and the gain of the amplifier is large it follows that the error e is small and then we find that $v_2 = -(R_2/R_1)v_1$. Notice that the resistor R_1 appears in two blocks in the block diagram. This situation is typical in electrical circuits and it is one reason why block diagrams are not always well suited for some types of physical modeling.

The simple model of the amplifier given by equation (3.10) gives qualitative insight but it neglects the fact that the amplifier is a dynamical system. A more realistic model is

$$\frac{dv_{\text{out}}}{dt} = -av_{\text{out}} - bv. \quad (3.14)$$

The parameter b that has dimensions of frequency and is called the gain-bandwidth product of the amplifier. Whether a more complicated model is used depends on the questions to be answered and the required size of the uncertainty margin. The model (3.14) is still not valid for very high or very low frequencies, since drift causes deviations at low frequencies and there are additional dynamics that appear at frequencies close to b . The model is also not valid for large signals—an upper limit is given by the voltage of the power supply, typically in the range of 5-10 V—neither is it valid for very low signals because of electrical noise. These effects can be added, if needed, but increase the complexity of the analysis.

The operational amplifier is very versatile and many different systems can be built by combining it with resistors and capacitors. In fact, any linear system can be implemented by combining operational amplifiers with resistors and capacitors. Exercise 3.5 shows how a second order oscillator is implemented and Figure 3.10 shows the circuit diagram for an analog PI (proportional-integral) controller. To develop a simple model for the circuit we assume that the current i_0 is zero and that

the open loop gain k is so large that the input voltage v is negligible. The current i through the capacitor is $i = Cdv_c/dt$, where v_c is the voltage across the capacitor. Since the same current goes through the resistor R_1 we get

$$i = \frac{v_1}{R_1} = C \frac{dv_c}{dt},$$

which implies that

$$v_c(t) = \frac{1}{C} \int i(t) dt = \frac{1}{R_1 C} \int_0^t v_1(\tau) d\tau.$$

The output voltage is thus given by

$$v_2(t) = -R_2 i - v_c = -\frac{R_2}{R_1} v_1(t) - \frac{1}{R_1 C} \int_0^t v_1(\tau) d\tau,$$

which is the input/output relation for a PI controller.

The development of operational amplifiers was pioneered by Philbrick [130, 156] and their usage is described in many textbooks (e.g. [51]). Good information is also available from suppliers [105, 137].

3.4 COMPUTING SYSTEMS AND NETWORKS

The application of feedback to computing systems follows the same principles as control of physical systems, but the types of measurements and control inputs that can be used are somewhat different. Measurements (sensors) are typically related to resource utilization in the computing system or network, and can include quantities such as the processor load, memory usage or network bandwidth. Control variables (actuators) typically involve setting limits on the resources available to a process. This might be done by controlling the amount of memory, disk space or time that a process can consume, turning on or off processing, delaying availability of a resource, or rejecting incoming requests to a server process. Process modeling for networked computing systems is also challenging, and empirical models based on measurements are often used when a first principles model is not available.

Web Server Control

Web servers respond to requests from the Internet and provide information in the form of web pages. Modern web servers will start multiple processes to respond to requests, with each process assigned to a single source until no further requests are received from that source for a predefined period of time. Processes that are idle become part of a pool that can be used to respond to new requests. To provide fast response to web requests, it is important that the web server processes do not overload the server's computational capabilities nor exhaust its memory. Since other processes may be running on the server, the amount of available processing power

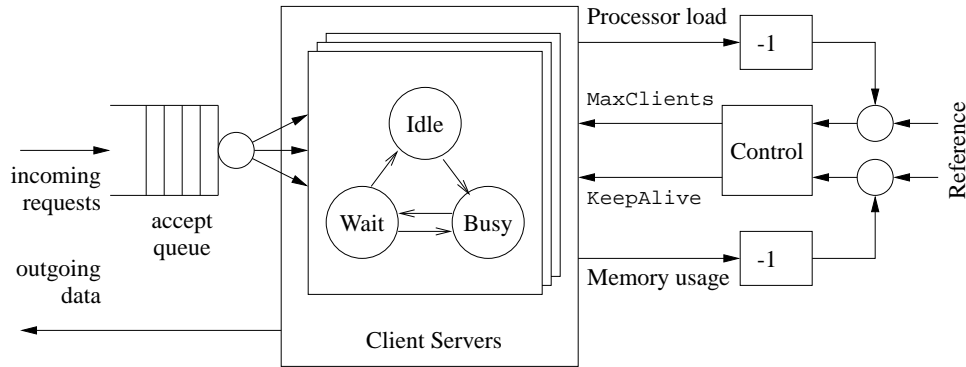


Figure 3.11: Feedback control of a web server. Connection requests arrive on an input queue, where they are sent to a server process. A finite state machine keeps track of the state of the individual server processes and responds to requests. A control algorithm can modify the server’s operation by controlling parameters that affect its behavior, such as the maximum number of requests that can be serviced at a single time (`MaxClients`) or the amount of time that a connection can remain idle before it is dropped (`KeepAlive`).

and memory is uncertain and feedback can be used to provide good performance in the presence of this uncertainty.

Figure 3.11 illustrates the use of feedback to modulate the operation of the Apache web server. The web server operates by placing incoming connection requests on a queue and then starting a subprocess to handle requests for each accepted connection. This subprocess responds to requests from a given connection as they come in, alternating between a `Busy` state and a `Wait` state. (Keeping the subprocess active between requests is known as “persistence” of the connection and provides substantial reduction in latency to requests for multiple pieces of information from a single site.) If no requests are received for a sufficiently long period of time, controlled by the `KeepAlive` parameter, then the connection is dropped and the subprocess enters an `Idle` state, where it can be assigned another connection. A maximum of `MaxClients` simultaneous requests will be served, with the remainder remaining on the incoming request queue.

The parameters that control represent a tradeoff between performance (how quickly requests receive a response) and resource usage (the amount of processing power and memory utilized on the server). Increasing the `MaxClients` parameter allows connection requests to be pulled off of the queue more quickly, but increases the amount of processing power and memory usage that is required. Increasing the `KeepAlive` timeout means that individual connections can remain idle for a longer period of time, which decreases the processing load on the machine but increases the size of the queue (and hence the amount of time required for a user to initiate a connection). Successful operation of a busy server requires proper choice of these parameters, often based on trial and error.

To model the dynamics of this system in more detail, we create a discrete time model with states given by the average processor load x_{cpu} and the percentage

memory usage x_{mem} . The inputs to the system are taken as the maximum number of clients u_{mc} and the keep-alive time u_{ka} . If we assume a linear model around the equilibrium point, the dynamics can be written as

$$\begin{pmatrix} x_{\text{cpu}}[k+1] \\ x_{\text{mem}}[k+1] \end{pmatrix} = \begin{pmatrix} A_{11} & A_{12} \\ A_{21} & A_{22} \end{pmatrix} \begin{pmatrix} x_{\text{cpu}}[k] \\ x_{\text{mem}}[k] \end{pmatrix} + \begin{pmatrix} B_{11} & B_{12} \\ B_{21} & B_{22} \end{pmatrix} \begin{pmatrix} u_{\text{ka}}[k] \\ u_{\text{mc}}[k] \end{pmatrix}, \quad (3.15)$$

where the coefficients of the A and B matrices must be determined based on empirical measurements or detailed modeling of the web server's processing and memory usage. Using system identification, Diao et al. [55, 92] identified the linearized dynamics as

$$A = \begin{pmatrix} 0.54 & -0.11 \\ -0.026 & 0.63 \end{pmatrix}, \quad B = \begin{pmatrix} -85 & 4.4 \\ -2.5 & 2.8 \end{pmatrix} \times 10^{-4},$$

where the system was linearized about the equilibrium point

$$x_{\text{cpu}}^* = 0.58, \quad u_{\text{ka}}^* = 11 \text{ sec}, \quad x_{\text{mem}}^* = 0.55, \quad u_{\text{mc}}^* = 600.$$

This model shows the basic characteristics that were described above. Looking first at the B matrix, we see that increasing the `KeepAlive` timeout (first column of the B matrix) decreases both the processor usage and the memory usage, since there is more persistence in connections and hence the server spends a longer time waiting for a connection to close rather than taking on a new active connection. The `MaxClients` connection increases both the processing and memory requirements. Note that the largest effect on the processor load is the `KeepAlive` timeout. The A matrix tells us about how the processor and memory usage evolve in a region of the state space near the equilibrium point. The diagonal terms describe how the individual resources return to equilibrium after a transient increase or decrease. The off-diagonal terms show that there is coupling between the two resources, so that a change in one could cause a later change in the other.

Although this model is very simple, we will see in later examples that it can be used to modify the parameters controlling the server in real time and provide robustness with respect to uncertainties in the load on the machine. Similar types of mechanisms have been used for other types of servers. It is important to remember the assumptions on the model and their role in determining when the model is valid. In particular, since we have chosen to use average quantities over a given sample time, the model will not provide an accurate representation for high frequency phenomena.

Congestion Control

The Internet was created to obtain a large, highly decentralized, efficient and expandable communication system. The system consists of a large number of interconnected gateways. A message is split into several packets that are transmitted over different paths in the network and the packages are rejoined to recover the message at the receiver. An acknowledgment (“ack”) message is sent back to the

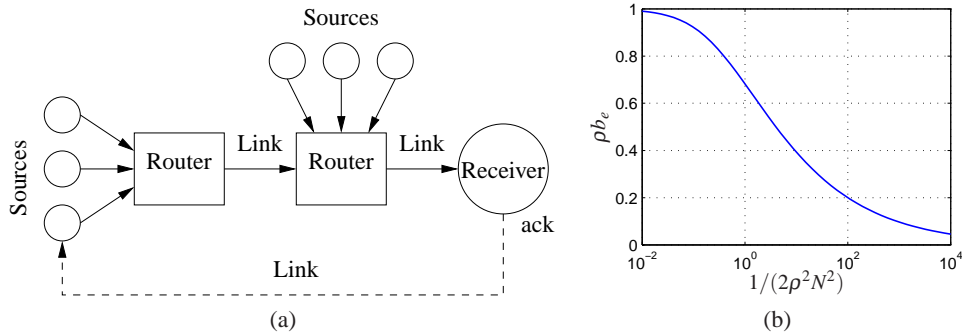


Figure 3.12: Internet congestion control. Source computers send information to routers, which forward the information to other routers that eventually connect to the receiving computer. When a packet is received, an acknowledgment packet is sent back through the routers (not shown). The routers buffer information received from the sources and send the data across the outgoing link. The plot on the right shows the equilibrium buffer size b_e for a set of N identical computers sending packets through a single router with drop probability ρ .

sender when a packet is received. The operation of the system is governed a simple but powerful decentralized control structure that evolved over time.

The system has two control mechanisms, called *protocols*: the Transmission Control Protocol (TCP) for end-to-end network communication and the Internet Protocol (IP) for routing packets and for host-to-gateway or gateway-to-gateway communication. The current protocols evolved after some spectacular congestion collapses occurred in the mid 1980s, when throughput unexpectedly could drop by a factor of 1000 [101]. The control mechanism in TCP is based on conserving the number of packets in the loop from sender to receiver and back to the sender. The sending rate is increased exponentially when there is no congestion and it is dropped to a low level when there is congestion.

To derive a model for congestion control, we model three separate elements of the system: the rate at which packets are sent by individual sources (computers), the dynamics of the queues in the links (routers), and the admission control mechanism for the queues. Figure 3.12a shows a block diagram for the system.

The current source control mechanism on the Internet is a protocol known as TCP/Reno [129]. This protocol operates by sending packets to a receive and waiting to receive an acknowledgment from the receiver that the packet has arrived. If no acknowledgment is sent within a certain timeout period, the packet is retransmitted. To avoid waiting for the acknowledgment before sending the next packet, Reno transmits multiple packets up to a fixed “window” around the latest packet that has been acknowledged. If the window length is chosen properly, packets at the beginning of the window will be acknowledge before the source transmits packets at the end of the window, allowing the computer to continuously stream packets at a high rate.

To determine the size of the window to use, TCP/Reno uses a feedback mechanism in which (roughly speaking) the window size is increased by one every time

a packet is acknowledged and the window size is cut in half when packets are lost. This mechanism allows a dynamic adjustment of the window size in which each computer acts in a greedy fashion as long as packets are being delivered but backs off quickly when congestion occurs.

A model for the behavior of the source can be developed by describing the dynamics of the window size. Suppose we have N computers and let w_i be the current window size (measured in number of packets) for the i th computer. Let q_i represent the end-to-end probability that a packet is dropped someplace between the source and the receiver. We can model the dynamics of the window size by the differential equation

$$\frac{dw_i}{dt} = (1 - q_i) \frac{r_i(t - \tau_i)}{w_i} + q_i \left(-\frac{w_i}{2} r_i(t - \tau_i)\right), \quad r_i = \frac{w_i}{\tau_i}, \quad (3.16)$$

where τ_i is the end-to-end transmission time for a packet to reach its destination and the acknowledgment to be sent back and r_i is the resulting rate at which packets are cleared from the list of packets that have been received. The first term in the dynamics represents the increase in the window size when a packet is received and the second term represents the decrease in window size when a packet is lost. Notice that r_i is evaluated at time $t - \tau_i$, representing the time required to receive additional acknowledgments.

The link dynamics are controlled by the dynamics of the router queue and the admission control mechanism for the queue. Assume that we have L links in the network and use l to index the individual links. We model the queue in terms of the current number of packets in the router's buffer, b_l , and assume that the router can contain a maximum of $b_{l,\max}$ packets and transmits packets at a rate c_l , equal to the capacity of the link. The buffer dynamics can then be written as

$$\frac{db_l}{dt} = s_l - c_l, \quad s_l = \sum_{\{i: l \in L_i\}} r_i(t - \tau_{li}^f), \quad (3.17)$$

where L_i is the set of links that are being used by source i , τ_{li}^f is the time that it takes a packet from source i to reach link l and s_l is the total rate at which packets arrive on link l .

The admission control mechanism determines whether a given packet is accepted by a router. Since our model is based on the average quantities in the network and not the individual packets, one simple model is to assume that the probability that a packet is dropped depends on how full the buffer is: $p_l = m_l(b_l, b_{l,\max})$. For simplicity, we will assume for now that $p_l = \rho_l b_l$ (see Exercise 3.6 for a more detailed model). The probability that a packet is dropped at a given link can be used to determine the end-to-end probability that a packet is lost in transmission:

$$q_i = 1 - \prod_{l \in L_i} (1 - p_l) \approx \sum_{l \in L_i} p_l(t - \tau_{li}^b), \quad (3.18)$$

where τ_{li}^b is the backward delay from link l to source i and the approximation is valid as long as the individual drop probabilities are small. We use the backward

delay since this represents the time required for the acknowledgment packet to be received by the source.

Together, equations (3.16), (3.17) and (3.18) represent a model of the congestion control dynamics. We can obtain substantial insight by considering a special case in which we have N identical sources and 1 link. In addition, we assume for the moment that the forward and backward time delays can be ignored, in which case the dynamics can be reduced to the form

$$\frac{dw_i}{dt} = \frac{1}{\tau} - \frac{\rho b(2 + w_i^2)}{2}, \quad \frac{db}{dt} = \sum_{i=1}^N \frac{w_i}{\tau} - c, \quad \tau = \frac{b}{c}, \quad (3.19)$$

where $w_i \in \mathbb{R}$, $i = 1, \dots, N$ are the window sizes for the sources of data, $b \in \mathbb{R}$ is the current buffer size of the router, ρ controls the rate at which packets are dropped and c is the capacity of the link connecting the router to the computers. The variable τ represents the amount of time required for a packet to be processed by a router, based on the size of the buffer and the capacity of the link. Substituting τ into the equations, we write the state space dynamics as

$$\frac{dw_i}{dt} = \frac{c}{b} - \rho c \left(1 + \frac{w_i^2}{2} \right), \quad \frac{db}{dt} = \sum_{i=1}^N \frac{cw_i}{b} - c, \quad (3.20)$$

More sophisticated models can be found in [96, 129].

The nominal operating point for the system can be found by setting $\dot{w}_i = \dot{b} = 0$:

$$0 = \frac{c}{b} - \rho c \left(1 + \frac{w_i^2}{2} \right), \quad 0 = \sum_{i=1}^N \frac{cw_i}{b} - c, \quad \tau = \frac{b}{c}.$$

Exploiting the fact that each of the source dynamics are identical, it follows that all of the w_i should be the same and it can be shown that there is a unique equilibrium satisfying the equations:

$$w_{i,e} = \frac{b_e}{N} = \frac{c\tau_e}{N}, \quad \frac{1}{2\rho^2 N^2} (\rho b_e)^3 + (\rho b_e) - 1 = 0. \quad (3.21)$$

The solution for the second equation is a bit messy, but can easily be determined numerically. A plot of its solution as a function of $1/(2\rho^2 N^2)$ is shown in Figure 3.12b. We also note that at equilibrium we have the following additional equalities:

$$\tau_e = \frac{b_e}{c} = \frac{Nw_e}{c} \quad q_e = Np_e = N\rho b_e \quad r_e = \frac{w_e}{\tau_e}$$

Figure 3.13 shows a simulation of 60 sources communicating across a single link, with 20 sources dropping out at $T = 20$ s and the remaining sources increasing their rates (window sizes) to compensate. Note that the buffer size and window sizes automatically adjust to match the capacity of the link.

A comprehensive treatment of computer networks is given in Tannenbaum [180]. A good presentation of the ideas behind the control principles for the Internet are given by one of its designers, Van Jacobson, in [101]. Kelly [113] presents an

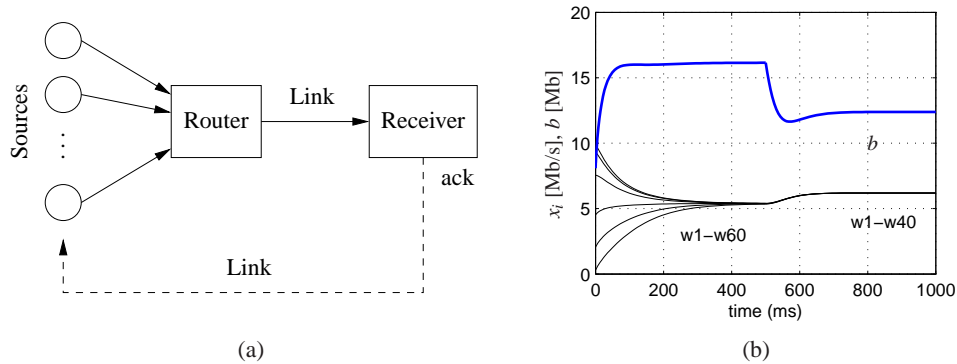


Figure 3.13: Internet congestion control for N identical sources across a single link. As shown on the right, multiple sources attempt to communicate through a router across a single link. An “ack” packet sent by the receiver acknowledges that the message was received; otherwise the message packet is resent and the sending rate is slowed down at the source. The simulation on the left is for 60 sources starting random rates, with 20 sources dropping out at $t = 20$ s. The buffer size is shown on the top and the individual source rates for 6 of the sources are shown on the bottom.

early effort of analysis of the system. The book by Hellerstein et al. [92] gives many examples of use of feedback in computer systems.

3.5 ATOMIC FORCE MICROSCOPY

The 1986 Nobel Prize in Physics was shared by Gerd Binnig and Heinrich Rohrer for their design of the scanning tunneling microscope. The idea of the instrument is to bring an atomically sharp tip so close to a conducting surface that tunneling occurs. An image is obtained by traversing the tip across the sample and measuring the tunneling current as a function of tip position. This invention has stimulated the development of a family of instruments that permit visualization of surface structure at the nanometer scale, including the atomic force microscope (AFM), where a sample is probed by a tip on a cantilever. An AFM can operate in two mode. In tapping mode the cantilever is vibrated and the amplitude of vibration is controlled by feedback. In contact mode the cantilever is in contact with the sample and its bending is control by feedback. In both cases control is actuated by a piezo element that controls the vertical position of the cantilever base. The control system has a direct influence on picture quality and scanning rate.

A schematic picture of an atomic force microscope is shown in Figure 3.14a. A micro-cantilever with a tip having a radius of the order of 10 nm is placed close to the sample. The tip can be moved vertically and horizontally using a piezoelectric scanner. It is clamped to the sample surface by attractive van der Waals forces and repulsive Pauli forces. The cantilever tilt depends on the topography of the surface and the position of the cantilever base which is controlled by the piezo element. The tilt is measured by sensing the deflection of the laser beam using a photo diode.

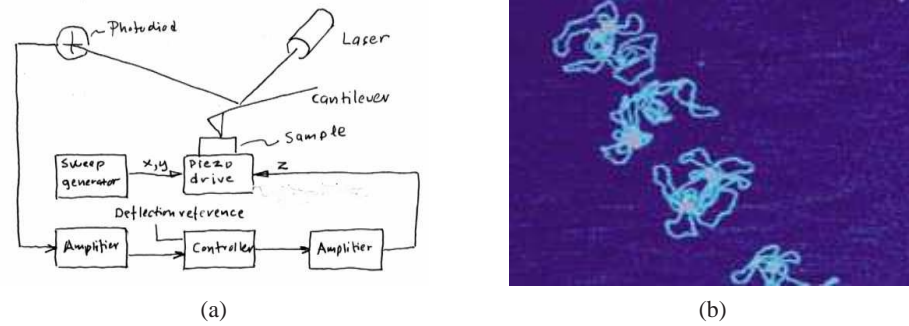


Figure 3.14: Atomic force microscope. A schematic diagram of an atomic force microscope is shown on the left, consisting of a piezo drive that scans the sample under the AFM tip. A laser reflects off of the cantilever and is used to measure the deflection of the tip through a feedback controller. An AFM image of DNA is shown on the right.

The signal from the photo diode is amplified and sent to a controller that drives the amplifier for the vertical deflection of the cantilever. By controlling the piezo element so that the deflection of the cantilever is constant, the signal driving the vertical deflection of the piezo element is a measure of the atomic forces between the cantilever tip and the atoms of the sample. An image of the surface is obtained by scanning the cantilever along the sample. The resolution makes it possible to see the structure of the sample on the atomic scale, as illustrated in Figure 3.14b, which shows an AFM image of a DNA molecule.

The horizontal motion is typically modeled as a spring-mass system with low damping. The vertical motion is more complicated. To model the system, we start with the block diagram shown in Figure 3.15. Signals that are easily accessible are the input voltage u to the power amplifier that drives the piezo element, the voltage v applied to the piezo element and the output voltage y of the signal amplifier for the photo diode. The controller is a PI controller implemented by a computer, which is connected to the system by A/D and D/A converters. The deflection of the cantilever, ϕ , is also shown in the figure. The desired reference value for the deflection is an input to the computer.

There are several different configurations that have different dynamics. Here we will discuss a high performance system from [167] where the cantilever base is positioned vertically using a piezo stack. We begin the modeling by a simple experiment on the system. Figure 3.16a shows a step response of a scanner from the input voltage u to the power amplifier to the output voltage y of the signal amplifier for the photo diode. This experiment captures the dynamics of the chain of blocks from u to y in the block diagram in Figure 3.15. Figure 3.16a shows that the system responds quickly but that there is a poorly damped oscillatory mode with a period of about $35 \mu\text{s}$. A primary task of the modeling is to understand the origin of the oscillatory behavior. To do so we will explore the system in more detail.

The natural frequency of the clamped cantilever is typically several hundred

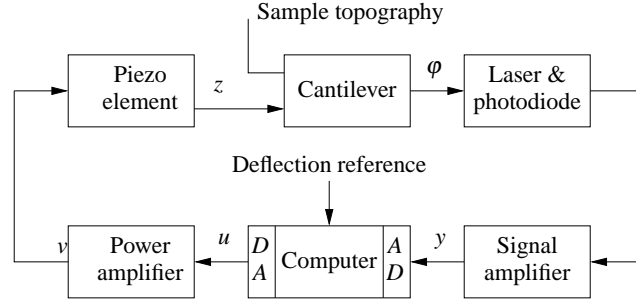


Figure 3.15: Block diagram of the system for vertical positioning of the cantilever for an atomic force microscope (AFM) in scanning mode. The control system attempts to keep the cantilever deflection equal to its reference value. Cantilever deflection is measured, amplified and converted to a digital signal, then compared with its reference value. A correcting signal is generated by the computer, converted to analog form, amplified and sent to the piezo element.

kHz, which is much higher than the observed oscillation of about 30 kHz. As a first approximation we will therefore model the cantilever as a static system. Since the deflections are small we can assume that the bending ϕ of the cantilever is proportional to the difference in heights between the cantilever tip at the probe and the piezo scanner. A more accurate model can be obtained by modeling the cantilever as a spring-mass system of the type discussed in Chapter 2.

Figure 3.16a also shows that the response of the power amplifier is fast. As a first approximation we will model it as a static system. The photo diode and the signal amplifier also have fast responses and can thus be modeled as static systems. The remaining block is a piezo system with suspension. A schematic mechanical representation of the vertical motion of the scanner is shown in Figure 3.16b. We will model the system as two masses separated by an ideal piezo element. The mass m_1 is half of the piezo system plus the mass m_2 is the other half of the piezo system and the mass of the support.

A simple model is obtained by assuming that the piezo crystal generates a force F between the masses and that there is a damping c in the spring. Let the positions of the center of the masses be z_1 and z_2 . A momentum balance gives the following model for the system:

$$m_1 \frac{d^2 z_1}{dt^2} = F, \quad m_2 \frac{d^2 z_2}{dt^2} = -c_2 \frac{dz_2}{dt} - k_2 z_2 - F.$$

Let the elongation of the piezo element $l = z_1 - z_2$ be the control variable and the height z_1 of the cantilever base be the output. Eliminating the variable F in equations (3.22) and substituting $z_1 - l$ for z_2 gives the model

$$(m_1 + m_2) \frac{d^2 z_1}{dt^2} + c_2 \frac{dz_1}{dt} + k_2 z_1 = m_2 \frac{d^2 l}{dt^2} + c_2 \frac{dl}{dt} + k_2 l. \quad (3.22)$$

Summarizing, we find that a simple model of the system is obtained by modeling the piezo by (3.22) and all the other blocks by static models. Introducing

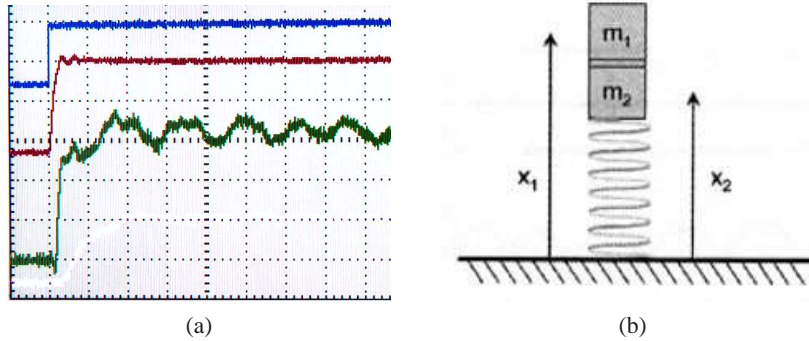


Figure 3.16: Measured step response and model of piezo scanner. The left figure shows a measured step response. The top curve shows the voltage u applied to the drive amplifier (50 mV/div), the middle curve is the output V_p of the power amplifier (500 mV/div) and the bottom curve is the output y of the signal amplifier (500 mV/div). The time scale is 25 μ s/div. Data has been supplied by Georg Schitter. The right figure is a simple mechanical model for the vertical positioner and the piezo crystal.

the linear equations $l = k_3 u$, and $y = k_4 z_1$ we now have a complete model relating the output y to the control signal u . A more accurate model can be obtained by introducing the dynamics of the cantilever and the power amplifier. As in the previous examples, the concept of the uncertainty lemon in Figure 2.15b provides a framework for describing the uncertainty: the model will be accurate up to the frequencies of the fastest modeled modes and over a range of motion in which the linearized stiffness models can be used.

The experimental results in Figure 3.16a can be explained qualitatively as follows. When a voltage is applied to the piezo it expands by l_0 , the mass m_1 is moves up and the mass m_2 moves down instantaneously. The system settles after a poorly damped oscillation.

It is highly desirable to have design a control system for the vertical motion so that it responds quickly with little oscillation. The instrument designer has several choices: to accept the oscillation and have a slow response time, to design a control system that can damp the oscillations, or to redesign the mechanics to give resonances of higher frequency. The last two alternatives give a faster response and faster imaging.

Since the dynamic behavior of the system changes with the properties of the sample, it is necessary to tune the feedback loop. In simple systems this is currently done manually by adjusting parameters of a PI controller. There are interesting possibilities to make AFM systems easier to use by introducing automatic tuning and adaptation.

The book by Sarid [164] gives a broad coverage of atomic force microscopes. The interaction of atoms close to surfaces is fundamental to solid state physics, see Kittel [118]. The model discussed in this section is based on Schitter [166].

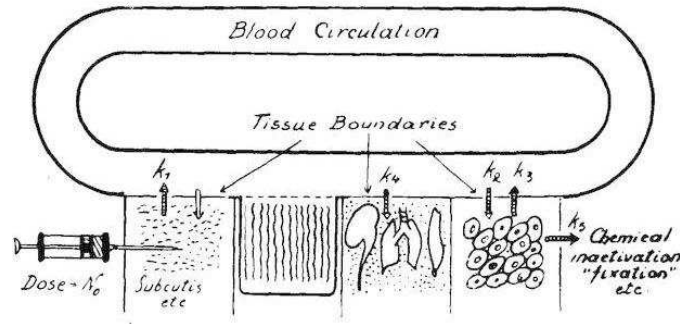


Figure 3.17: The abstraction used to compartmentalize the body for the purpose of describing drug distribution (based on Teorell [181]). The body is abstracted by a number of compartments with perfect mixing and the complex transport processes are approximated by assuming that the flow is proportional to the concentration differences in the compartments. The constants k_i parameterize the rates of flow between different compartments.

3.6 DRUG ADMINISTRATION

The phrase “take two pills three times a day” is a recommendation with which we are all familiar. Behind this recommendation is a solution of an open loop control problem. The key issue is to make sure that the concentration of a medicine in a part of the body is sufficiently high to be effective but not so high that it will cause undesirable side effects. The control action is quantized, *take two pills*, and sampled, *every 8 hours*. The prescriptions are based on simple models captured in empirical tables, and dosage is based on the age and weight of the patient.

Drug administration is a control problem. To solve it we must understand how a drug spreads in the body after it is administered. This topic, called *pharmacokinetics*, is now a discipline of its own and the models used are called *compartment models*. They go back to the 1920s when Widmark modeled propagation of alcohol in the body [190]. Compartment models are now important for screening of all drugs used by humans. The schematic diagram in Figure 3.17 illustrates the idea of a compartment model. The body is viewed as a number of compartments like blood plasma, kidney, liver, and tissues which are separated by membranes. It is assumed that there is perfect mixing so that the drug concentration is constant in each compartment. The complex transport processes are approximated by assuming that the flow rates between the compartments are proportional to the concentration differences in the compartments.

To describe the effect of a drug it is necessary to know both its concentration and how it influences the body. The relation between concentration c and its effect e is typically nonlinear. A simple model is

$$e = \frac{c_0}{c_0 + c} e_{max}. \quad (3.23)$$

The effect is linear for low concentrations and it saturates at high concentrations. The relation can also be dynamic and it is then called *pharmacodynamics*.

Compartment Models

The simplest dynamic model for drug administration is obtained by assuming that the drug is evenly distributed in a single compartment after it has been administered and that the drug is removed at a rate proportional to the concentration. The compartments behave like stirred tanks with perfect mixing. Let c be the concentration, V the volume and q the outflow rate. Converting the description of the system into differential equations gives the model

$$V \frac{dc}{dt} = -qc, \quad c \geq 0. \quad (3.24)$$

This equation has the solution $c(t) = c_0 e^{-qt/V} = c_0 e^{-kt}$, which shows that the concentration decays exponentially with the time constant $T = V/q$ after an injection. The input is introduced implicitly as an initial condition in the model (3.24). More generally, the way the input enters the model depends on how the drug is administered. For example, the input can be represented as a mass flow into the compartment where the drug is injected. A pill that is dissolved can also be interpreted as an input in terms of a mass flow rate.

The model (3.24) is called a *one-compartment model* or a *single pool model*. The parameter q/V is called the elimination rate constant. This simple model is often used to model the concentration in the blood plasma. By measuring the concentration at a few times, the initial concentration can be obtained by extrapolation. If the total amount of injected substance is known, the volume V can then be determined as $V = m/c_0$; this volume is called *the apparent volume of distribution*. This volume is larger than the real volume if the concentration in the plasma is lower than in other parts of the body. The model (3.24) is very simple and there are large individual variations in the parameters. The parameters V and q are often normalized by dividing by the weight of the person. Typical parameters for aspirin are $V = 0.2 \text{ L/kg}$ and $q = 0.01 \text{ (L/h)/kg}$. These numbers can be compared with a blood volume of 0.07 L/kg , a plasma volume of 0.05 L/kg , intracellular fluid volume of 0.4 L/kg and an outflow of 0.0015 L/min/kg .

The simple one-compartment model captures the gross behavior of drug distribution but it is based on many simplifications. Improved models can be obtained by considering the body as composed of several compartments. Examples of such systems are shown in Figure 3.18, where the compartments are represented as circles and the flows by arrows.

Modeling will be illustrated using the two-compartment model in Figure 3.18a. We assume that there is perfect mixing in each compartment and that the transport between the compartments are driven by concentration differences. We further assume that a drug with concentration c_0 is injected in compartment 1 at a volume flow rate of u and that the concentration in compartment 2 is the output. Let c_1 and c_2 be the concentrations of the drug in the compartments and let V_1 and V_2 be the

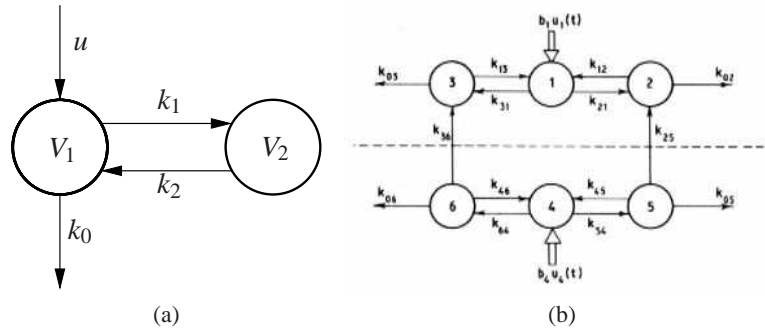


Figure 3.18: Schematic diagrams of compartment models. A simple two-compartment model is shown on the left. Each compartment is labeled by its volume and arrows indicate the flow of chemical into, out of and between compartments. The compartment model on the right shows a system with six compartments used to study metabolism of thyroid hormone [81]. The notation k_{ij} denotes the transport from compartment j to compartment i .

volumes of the compartments. The mass balances for the compartments are

$$\begin{aligned} V_1 \frac{dc_1}{dt} &= q(c_2 - c_1) - q_0 c_1 + c_0 u & c_1 &\geq 0 \\ V_2 \frac{dc_2}{dt} &= q(c_1 - c_2) & c_2 &\geq 0 \end{aligned} \quad (3.25)$$

$$y = c_2.$$

Introducing the variables $k_0 = q_0/V_1$, $k_1 = q/V_1$, $k_2 = q/V_2$ and $b_0 = c_0/V_1$ and using matrix notation, the model can be written as

$$\begin{aligned} \frac{dc}{dt} &= \begin{pmatrix} -k_0 - k_1 & k_1 \\ k_2 & -k_2 \end{pmatrix} c + \begin{pmatrix} b_0 \\ 0 \end{pmatrix} u \\ y &= \begin{pmatrix} 0 & 1 \end{pmatrix} x. \end{aligned} \quad (3.26)$$

Comparing this model with its graphical representation in Figure 3.18a we find that the the mathematical representation (3.26) can be written by inspection.

It should also be emphasized that simple compartment models such as the one in equation (3.26) have a limited range of validity. Low frequency limits exist because the human body changes with time and since the compartment model uses average concentrations they will not accurately represent rapid changes. There are also nonlinear effects that influence transportation between the compartments.

Compartment models are widely used in medicine, engineering and environmental science. An interesting property of these systems is that variables like concentration and mass are always positive. An essential difficulty in compartment modeling is deciding how to divide a complex system into compartments. Compartment models can also be nonlinear, as illustrated in the next section.

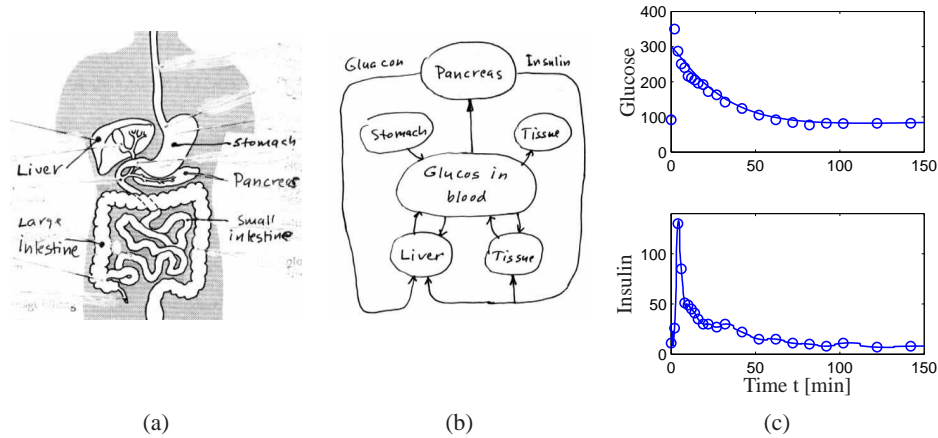


Figure 3.19: Insulin-glucose dynamics. (a) Sketch of body parts involved in control of glucose, (b) schematic diagram of the system, and (c) responses in insulin and glucose when glucose is injected intravenously. From [155].

Insulin-Glucose Dynamics

It is essential that the blood glucose concentration in the body is kept in a narrow range (0.7–1.1 g/L). Glucose concentration is influenced by many factors like food intake, digestion and exercise. A schematic picture of the relevant parts of the body is shown in Figure 3.19.

There is a sophisticated mechanism that regulates glucose concentration. Glucose concentration is maintained by the pancreas that secretes the hormones insulin and glucagon. Glucagon is released into the blood stream when the glucose level is low. It acts on cells in the liver that release glucose. Insulin is secreted when the glucose level is high and the glucose level is lowered by causing the liver and other cells to take up more glucose. In diseases, like juvenile diabetes, the pancreas is unable to produce insulin and the patient must inject insulin into the body to maintain a proper glucose level.

The mechanisms that regulate glucose and insulin are complicated, dynamics with time scales that range from seconds to hours have been observed. Models of different complexity have been developed. The models are typically tested with data from experiments where glucose is injected intravenously and insulin and glucose concentrations are measured at regular time intervals.

A relatively simple model called the *minimal model* was developed by Bergman and coworkers [30]. This model uses two compartments, one representing the concentration of glucose in the blood stream and the other representing the concentration of insulin in the interstitial fluid. Insulin in the blood stream is considered as an input. The reaction of glucose to insulin can be modeled by the equations

$$\frac{dx_1}{dt} = -(p_1 + x_2)x_1 + p_1 g_e, \quad \frac{dx_2}{dt} = -p_2 x_2 + p_3(u - i_e), \quad (3.27)$$

where g_e and i_e represent the equilibrium values of glucose and insulin, x_1 is the concentration of glucose and x_2 is proportional to the concentration of interstitial insulin. Notice the presence of the term x_1x_2 in the first equation. Also notice that the model does not capture the complete feedback loop because it does not describe how the pancreas reacts to the glucose. Figure 3.19c shows a fit of the model to a test on a normal person where glucose was injected intravenously at time $t = 0$. Glucose concentration rises rapidly and the pancreas responds with a rapid spike-like injection of insulin. The glucose and insulin levels then gradually approach the equilibrium values.

Models of the type (3.27) and more complicated models having many compartments have been developed and fitted to experimental data. A difficulty in modeling is that there are significant variations in model parameters over time and for different patients. For example the parameter p_1 in (3.27) has been reported to vary with an order of magnitude for normal persons. The models have been used for diagnosis and to develop schemes for treatment of persons with diseases. Attempts to develop a fully automatic artificial pancreas has been hampered by the lack of reliable sensors.

The papers by Widmark and Tandberg [190] and Teorell [181] are classics in pharmacokinetics which is now an established discipline with many textbooks [57, 102, 80]. Because of its medical importance pharmacokinetics is now an essential component of drug development. The book by Riggs [159] is a good source for modeling of physiological systems and a more mathematical treatment is given in [112]. Compartment models are discussed in [81]. The problem of determining rate coefficients from experimental data is discussed in [25] and [81]. There are many publications on the insulin-glucose model. The minimal model is discussed in [50, 30, 31] more recent references are [135, 69].

3.7 POPULATION DYNAMICS

Population growth is a complex dynamic process that involves the interaction of one or more species with their environment and the larger ecosystem. The dynamics of population groups are interesting and important in many different areas of social and environmental policy. There are examples where new species have been introduced into new habitats, sometimes with disastrous results. There are also been attempts to control population growth both through incentives and through legislation. In this section we describe some of the models that can be used to understand how populations evolve with time and as a function of their environment.

Logistic Growth Model

Let x the population of a species at time t . A simple model is to assume that the birth and death rates are proportional to the total population. This gives the linear

model

$$\frac{dx}{dt} = bx - dx = (b - d)x = rx, \quad x \geq 0, \quad (3.28)$$

where birth rate b and death rate d are parameters. The model gives an exponential increase if $b > d$ or an exponential decrease if $b < d$. A more realistic model is to assume that the birth rate decreases when the population is large. The following modification of the model (3.28) has this property:

$$\frac{dx}{dt} = rx\left(1 - \frac{x}{x_c}\right), \quad x \geq 0, \quad (3.29)$$

where x_c is the *carrying capacity* of the environment. The model (3.29) is called the *logistic growth* model.

Predator-Prey Models

A more sophisticated model of population dynamics includes the effects of competing populations, where one species may feed on another. This situation, referred to as the *predator-prey problem*, was already introduced in Example 2.3, where we developed a discrete time model that captured some of the features of historical records of lynx and hare populations.

In this section, we replace the difference equation model used there with a more sophisticated differential equation model. Let $H(t)$ represent the number of hares (prey) and $L(t)$ represent the number of lynxes (predator). The dynamics of the system are modeled as

$$\begin{aligned} \frac{dH}{dt} &= r_h H \left(1 - \frac{H}{K}\right) - \frac{aHL}{1 + aHT_h} & H \geq 0 \\ \frac{dL}{dt} &= r_l L \left(1 - \frac{L}{kH}\right) & L \geq 0. \end{aligned} \quad (3.30)$$

In the first equation, r_h represents the growth rate of the hares, K represents the maximum population of hares (in the absence of lynxes), a represents the interaction term that describes how the hares are diminished as a function of the lynx population, and T_h depends is a time constant for prey consumption. In the second equation, r_l represents the growth rate of the lynxes and k represents the fraction of hares versus lynxes at equilibrium. Note that both the hare and lynx dynamics include terms that resemble the logistic growth model (3.29).

Of particular interest are the values at which the population values remain constant, called *equilibrium points*. The equilibrium points for this system can be determined by setting the right hand side of the above equations to zero. Letting H_e and L_e represent the equilibrium state, from the second equation we have

$$L_e = kH_e.$$

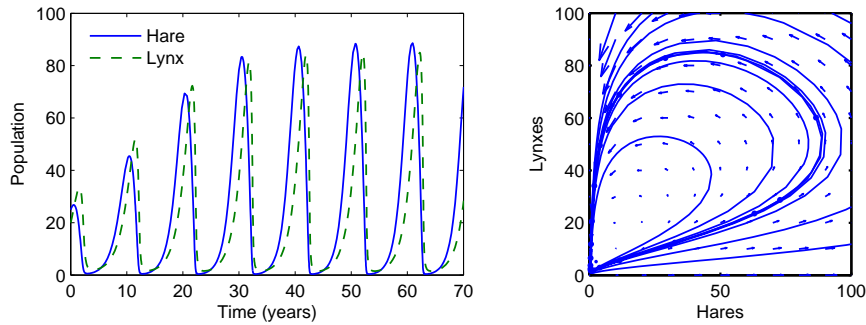


Figure 3.20: Simulation of the predator-prey system. The figure on the left shows a simulation of the two populations as a function of time. The figure on the right shows the populations plotted against each other, starting from different values of the population. The oscillation seen in both figures is an example of a “limit cycle”. The parameter values used for the simulations were $r_h = 0.02$, $K = 500$, $a = 0.03$, $T_h = 5$, $r_l = 0.01$, $k = 0.2$.

Substituting this into the first equation, we must solve

$$r_h H_e \left(1 - \frac{H_e}{K} \right) - \frac{akH_e^2}{1 + aH_e T_h} = 0.$$

Multiplying through by the denominator, we get

$$\begin{aligned} 0 &= H_e \cdot \left(r_h \left(1 - \frac{H_e}{K} \right) (1 + aH_e T_h) - akH_e \right) \\ &= H_e \cdot \left(\frac{r_h a T_h}{K} H_e^2 + (ak + r_h/K - r_h a T_h) H_e - r_h \right). \end{aligned}$$

This gives one solution at $H_e = 0$ and a second that can be solved analytically or numerically.

Figure 3.20 shows a simulation of the dynamics starting from a set of population values near the nonzero equilibrium values. We see that for this choice of parameters, the simulation predicts an oscillatory population count for each species, reminiscent of the data shown in Figure 2.6 (page 39).

Volume I of the two volume set by J. D. Murray [146] give a broad coverage of population dynamics.

EXERCISES

3.1 Consider the cruise control example described in Section 3.1. Build a simulation that recreates the response to a hill shown in Figure 3.3b and show the effects of increasing and decreasing the mass of the car by 25%. Redesign the controller (using trial and error is fine) so that it returns to within 10% of the desired speed within 3 seconds of encountering the beginning of the hill.

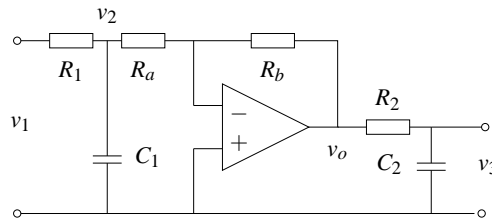
3.2 Show that the dynamics of a bicycle frame given by equation (3.5) can be written in state space form as

$$\begin{aligned} \frac{d}{dt} \begin{pmatrix} x_1 \\ x_2 \end{pmatrix} &= \begin{pmatrix} 0 & mgh/J \\ 1 & 0 \end{pmatrix} \begin{pmatrix} x_1 \\ x_2 \end{pmatrix} + \begin{pmatrix} 1 \\ 0 \end{pmatrix} u \\ y &= \begin{pmatrix} Dv_0 & mv_0^2h \\ bJ & bJ \end{pmatrix} x, \end{aligned} \quad (3.31)$$

where the input u is the torque applied to the handle bars and the output y is the title angle φ . What do the states x_1 and x_2 represent?

3.3 Combine the bicycle model given by equation (3.5) and the model for steering kinematics in Example 2.8 to obtain a model that describes the path of the center of mass of the bicycle.

3.4 Consider the op amp circuit shown below:

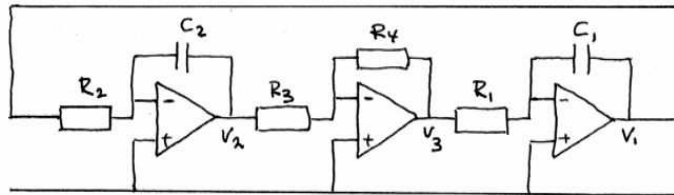


Show that the dynamics can be written in state space form as

$$\begin{aligned} \frac{dx}{dt} &= \begin{pmatrix} -\frac{1}{R_1 C_1} - \frac{1}{R_a C_1} & 0 \\ \frac{R_b}{R_a} \frac{1}{R_2 C_2} & -\frac{1}{R_2 C_2} \end{pmatrix} x + \begin{pmatrix} \frac{1}{R_1 C_1} \\ 0 \end{pmatrix} u \\ y &= \begin{pmatrix} 0 & 1 \end{pmatrix} x \end{aligned}$$

where $u = v_1$ and $y = v_3$. (Hint: Use v_2 and v_3 as your state variables.)

3.5 The op amp circuit shown below is an implementation of an oscillator. Show



that the dynamics can be written in state space form as

$$\frac{dx}{dt} = \begin{pmatrix} 0 & \frac{R_4}{R_1 R_3 C_1} \\ -\frac{1}{R_1 C_1} & 0 \end{pmatrix} x,$$

where the state variables represents the voltages across the capacitors $x_1 = v_1$ and $x_2 = v_2$.

3.6 A number of improvements can be made to the model for Internet congestion control presented in Section 3.4 [?]. To insure that the router's buffer size remains positive, we can modify the buffer dynamics to satisfy

$$\dot{b}_l = \begin{cases} s_l - c_l & b_l > 0 \\ \text{sat}_{(0,\infty)}(s_l - c_l) & b_l = 0 \end{cases}$$

In addition, we can model the drop probability of a packet based on how close we are to the buffer limits, a mechanism known as random early detection (RED):

$$p_l = m_l(a_l) = \begin{cases} 0 & a_l(t) \leq b_l^{\text{lower}} \\ \rho_l r_i(t) - \rho_l b_l^{\text{lower}} & b_l^{\text{lower}} < a_l(t) < b_l^{\text{upper}} \\ \eta_l r_i(t) - (1 - 2b_l^{\text{upper}}) & b_l^{\text{upper}} < a_l(t) < 2b_l^{\text{upper}} \\ 1 & a_l(t) \geq 2b_l^{\text{upper}} \end{cases}$$

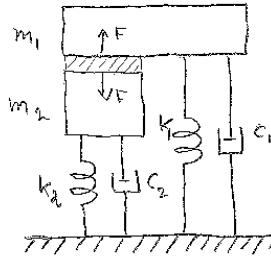
$$\dot{a}_l = -\alpha_l c_l (a_l - b_l),$$

where α_l , b_l^{upper} , b_l^{lower} and p_l^{upper} are parameters for the RED protocol.

Using the model above, write a simulation for the system and find a set of parameter values for which there is a stable equilibrium point and a set for which the system exhibits oscillatory solutions. The following sets of parameters should be explored:

$$\begin{array}{lll} N = 20, 30, \dots, 60 & b_l^{\text{lower}} = 40 \text{ pkts} & \rho_l = 0.1 \\ c = 8, 9, \dots, 15 \text{ pkts/ms} & b_l^{\text{upper}} = 540 \text{ pkts} & \alpha_l = 10^{-4} \\ \tau = 55, 60, \dots, 100 \text{ ms} & & \end{array}$$

3.7 A schematic diagram an AFM where the vertical scanner is a piezo tube with preloading is shown below



Show that the dynamics can be written as

$$(m_1 + m_2) \frac{d^2 z_1}{dt^2} + (c_1 + c_2) \frac{dz_1}{dt} + (k_1 + k_2) z_1 = m_2 \frac{d^2 l}{dt^2} + c_2 \frac{dl}{dt} + k_2 l.$$

Are there parameters values which makes the dynamics particularly simple?

3.8 (Drug administration) The metabolism of alcohol in the body can be modeled by the nonlinear compartment model

$$\begin{aligned} V_b \frac{dc_b}{dt} &= q(c_l - c_b) + q_{iv} \\ V_l \frac{dc_l}{dt} &= q(c_b - c_l) - q_{max} \frac{c_l}{c_0 + c_l} + q_{gi} \end{aligned}$$

where $V_b = 48$ l and $V_l = 0.6$ l are the effective distribution volumes of body water and liver water, c_b and c_l are the concentrations of alcohol in the compartments, q_{iv} and q_{gi} are the injection rates for intravenously and gastrointestinal intake, $q = 1.5$ L/min is the total hepatic blood flow, $q_{max} = 2.75$ mmol/min and $c_0 = 0.1$ mmol. Simulate the system and compute the concentration in the blood for oral and intravenous doses of 12 g and 40 g of alcohol.

3.9 (State variables in compartment models) Consider the compartment model described by equation (3.26). Let x_1 and x_2 be the total mass of the drug in the compartments. Show that the system can be described by the equation

$$\begin{aligned} \frac{dx}{dt} &= \begin{pmatrix} -k_0 - k_1 & k_2 \\ k_1 & -k_2 \end{pmatrix} x + \begin{pmatrix} c_0 \\ 0 \end{pmatrix} u \\ y &= \begin{pmatrix} 0 & 1/V_2 \end{pmatrix} x. \end{aligned} \tag{3.32}$$

Compare this equation with the (3.26) where the state variables were concentrations. Mass is called an *extensive variable* and concentration is called an *intensive variable*.

3.10 (Population dynamics) Consider the model for logistic growth given by equation (3.29). Show that the maximum growth rate occurs when the size of the population is half of the steady state value.

Chapter Four

Dynamic Behavior

It Don't Mean a Thing If It Ain't Got That Swing.

Duke Ellington (1899-1974)

In this chapter we give a broad discussion of the behavior of dynamical systems, focused on systems modeled by nonlinear differential equations. This allows us to discuss equilibrium points, stability, limit cycles and other key concepts for understanding dynamic behavior. We also introduce some methods for analyzing global behavior of solutions.

4.1 SOLVING DIFFERENTIAL EQUATIONS

In the last two chapters we saw that one of the methods of modeling dynamical systems is through the use of ordinary differential equations (ODEs). A state space, input/output system has the form

$$\frac{dx}{dt} = f(x, u), \quad y = h(x, u), \quad (4.1)$$

where $x = (x_1, \dots, x_n) \in \mathbb{R}^n$ is the state, $u \in \mathbb{R}^p$ is the input and $y \in \mathbb{R}^q$ is the output. The smooth maps $f: \mathbb{R}^n \times \mathbb{R}^p \rightarrow \mathbb{R}^n$ and $h: \mathbb{R}^n \times \mathbb{R}^p \rightarrow \mathbb{R}^q$ represent the dynamics and measurements for the system. We will sometimes focus on single input, single output (SISO) systems, for which $p = q = 1$.

We begin by investigating systems in which the input has been set to a function of the state, $u = \alpha(x)$. This is one of the simplest types of feedback, in which the system regulates its own behavior. The differential equations in this case become

$$\frac{dx}{dt} = f(x, \alpha(x)) =: F(x). \quad (4.2)$$

To understand the dynamic behavior of this system, we need to analyze the features of the solutions of equation (4.2). While in some simple situations we can write down the solutions in analytical form, often we must rely on computational approaches. We begin by describing the class of solutions for this problem.

Initial Value Problems

We say that $x(t)$ is a *solution* of the differential equation (4.2) on the time interval $t_0 \in \mathbb{R}$ to $t_f \in \mathbb{R}$ if

$$\frac{dx(t)}{dt} = F(x(t)) \quad \text{for all } t_0 < t < t_f.$$

A given differential equation may have many solutions. We will most often be interested in the *initial value problem*, where $x(t)$ is prescribed at a given time $t_0 \in \mathbb{R}$ and we wish to find a solution valid for all *future* time, $t > t_0$.

We say that $x(t)$ is a solution of the differential equation (4.2) with initial value $x_0 \in \mathbb{R}^n$ at $t_0 \in \mathbb{R}$ if

$$x(t_0) = x_0 \quad \text{and} \quad \frac{dx(t)}{dt} = F(x(t)) \quad \text{for all } t_0 < t < t_f.$$

For most differential equations we will encounter, there is a *unique* solution that is defined for $t_0 < t < t_f$. The solution may be defined for all time $t > t_0$, in which case we take $t_f = \infty$. Because we will primarily be interested in solutions of the initial value problem for ODEs, we will usually refer to this simply as the solution of an ODE.

We will typically assume that t_0 is equal to 0. In the case when F is independent of time (as in equation (4.2)), we can do so without loss of generality by choosing a new independent (time) variable, $\tau = t - t_0$ (Exercise 4.1).

Example 4.1 Damped oscillator

Consider a damped linear oscillator with dynamics of the form

$$\ddot{q} + 2\zeta\omega_0\dot{q} + \omega_0^2q = 0,$$

where q is the displacement of the oscillator from its rest position. These dynamics are equivalent to those of a spring-mass system, as shown in Exercise 2.7. We assume that $\zeta < 1$, corresponding to a lightly damped system (the reason for this particular choice will become clear later). We can rewrite this in state space form by setting $x_1 = q$ and $x_2 = \dot{q}/\omega_0$, giving

$$\frac{dx_1}{dt} = \omega_0 x_2, \quad \frac{dx_2}{dt} = -\omega_0 x_1 - 2\zeta\omega_0 x_2.$$

In vector form, the right hand side can be written as

$$F(x) = \begin{pmatrix} \omega_0 x_2 \\ -\omega_0 x_1 - 2\zeta\omega_0 x_2 \end{pmatrix}.$$

The solution to the initial value problem can be written in a number of different ways and will be explored in more detail in Chapter 5. Here we simply assert that

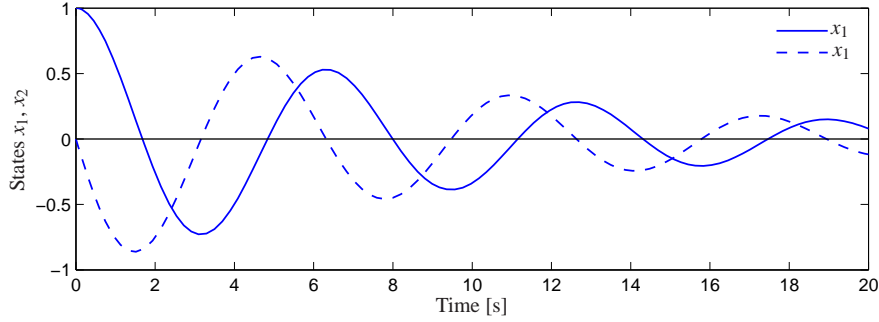


Figure 4.1: Response of the damped oscillator to the initial condition $x_0 = (1, 0)$. The solution is unique for the given initial conditions and consists of an oscillatory solution for each state, with an exponentially decaying magnitude.

the solution can be written as

$$\begin{aligned} x_1(t) &= e^{-\zeta\omega_0 t} \left(x_{10} \cos \omega_d t + \frac{1}{\omega_d} (\omega_0 \zeta x_{10} + x_{20}) \sin \omega_d t \right) \\ x_2(t) &= e^{-\zeta\omega_0 t} \left(x_{20} \cos \omega_d t - \frac{1}{\omega_d} (\omega_0^2 x_{10} + \omega_0 \zeta x_{20}) \sin \omega_d t \right) \end{aligned}$$

where $x_0 = (x_{10}, x_{20})$ is the initial condition and $\omega_d = \omega_0 \sqrt{1 - \zeta^2}$. This solution can be verified by substituting it into the differential equation. We see that the solution is explicitly dependent on the initial condition and it can be shown that this solution is unique. A plot of the initial condition response is shown in Figure 4.1. We note that this form of the solution only holds for $0 < \zeta < 1$, corresponding to an “underdamped” oscillator. ∇

Existence and Uniqueness



Without imposing some mathematical conditions on the function F , the differential equation (4.2) may not have a solution for all t , and there is no guarantee that the solution is unique. We illustrate these possibilities with two examples.

Example 4.2 Finite escape time

Let $x \in \mathbb{R}$ and consider the differential equation

$$\frac{dx}{dt} = x^2 \quad (4.3)$$

with initial condition $x(0) = 1$. By differentiation we can verify that the function

$$x(t) = \frac{1}{1-t} \quad (4.4)$$

satisfies the differential equation and it also satisfies the initial condition. A graph of the solution is given in Figure 4.2a; notice that the solution goes to infinity as t goes to 1. We say that this system has *finite escape time*. Thus the solution only

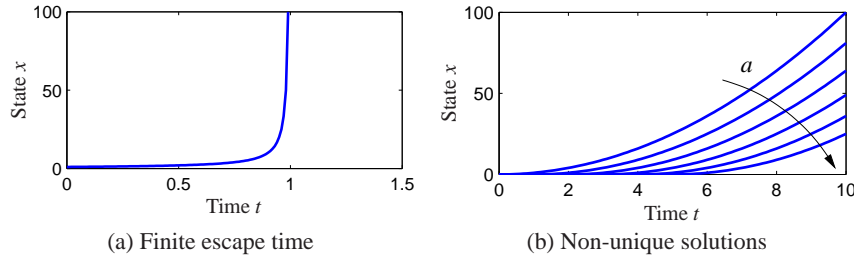


Figure 4.2: Existence and uniqueness of solutions. Equation (4.3) only has a solution for time $t < 1$, at which point the solution goes to ∞ , as shown in (a). Equation (4.4) is an example of a system with many solutions, as shown in (b). For each value of a , we get a different solution starting from the same initial condition.

exists in the time interval $0 \leq t < 1$. ▽

Example 4.3 No unique solution

Let $x \in \mathbb{R}$ and consider the differential equation

$$\frac{dx}{dt} = 2\sqrt{x}$$

with initial condition $x(0) = 0$. We can show that the function

$$x(t) = \begin{cases} 0 & \text{if } 0 \leq t \leq a \\ (t-a)^2 & \text{if } t > a \end{cases}$$

satisfies the differential equation for all values of the parameter $a \geq 0$. To see this, we differentiate $x(t)$ to obtain

$$\frac{dx}{dt} = \begin{cases} 0 & \text{if } 0 \leq t \leq a \\ 2(t-a) & \text{if } t > a \end{cases}$$

and hence $\dot{x} = 2\sqrt{x}$ for all $t \geq 0$ with $x(0) = 0$. A graph of some of the possible solutions is given in Figure 4.2b. Notice that in this case there are many solutions to the differential equation. ▽

These simple examples show that there may be difficulties even with simple differential equations. Existence and uniqueness can be guaranteed by requiring that the function F has the property that for some fixed $c \in \mathbb{R}$

$$\|F(x) - F(y)\| < c\|x - y\| \quad \text{for all } x, y,$$

which is called *Lipschitz continuity*. A sufficient condition for a function to be Lipschitz is that the Jacobian, $\partial F/\partial x$, is uniformly bounded for all x . The difficulty in Example 4.2 is that the derivative $\partial F/\partial x$ becomes large for large x and the difficulty in Example 4.3 is that the derivative $\partial F/\partial x$ is infinite at the origin.

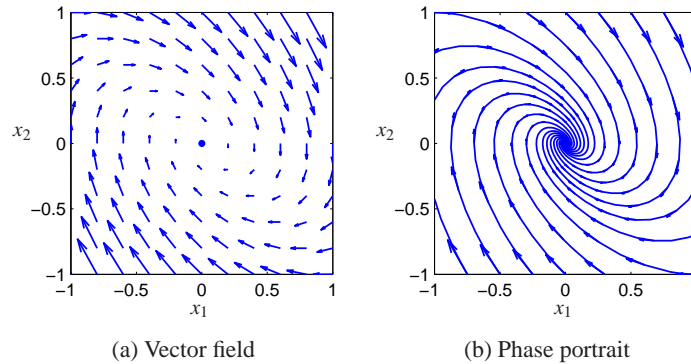


Figure 4.3: Phase portraits. The plot on the left shows the vector field for a planar dynamical system. Each arrow shows the velocity at that point in the state space. The plot on the right includes the solutions (sometimes called streamlines) from different initial conditions, with the vector field superimposed.

4.2 QUALITATIVE ANALYSIS

The qualitative behavior of nonlinear systems is important for understanding some of the key concepts of stability in nonlinear dynamics. We will focus on an important class of systems known as planar dynamical systems. These systems have two state variables $x \in \mathbb{R}^2$, allowing their solutions to be plotted in the (x_1, x_2) plane. The basic concepts that we describe hold more generally and can be used to understand dynamical behavior in higher dimensions.

Phase Portraits

A convenient way to understand the behavior of dynamical systems with state $x \in \mathbb{R}^2$ is to plot the *phase portrait* of the system, briefly introduced in Chapter 2. We start by introducing the concept of a vector field. For a system of ordinary differential equations

$$\frac{dx}{dt} = F(x),$$

the right hand side of the differential equation defines at every $x \in \mathbb{R}^n$ a velocity $F(x) \in \mathbb{R}^n$. This velocity tells us how x changes and can be represented as a vector $F(x) \in \mathbb{R}^n$.

For planar dynamical systems, each state corresponds to a point in the plane and $F(x)$ is a vector representing the velocity of that state. We can plot these vectors on a grid of points in the plane and obtain a visual image of the dynamics of the system, as shown in Figure 4.3a. The points where the velocities are zero are of particular interest, since they define stationary points of the flow: if we start at such a state, we stay at that state.

A phase portrait is constructed by plotting the flow of the vector field corresponding to the planar dynamical system. That is, for a set of initial conditions,

we plot the solution of the differential equation in the plane \mathbb{R}^2 . This corresponds to following the arrows at each point in the phase plane and drawing the resulting trajectory. By plotting the resulting trajectories for several different initial conditions, we obtain a phase portrait, as shown in Figure 4.3b.

Phase portraits give us insight into the dynamics of the system by showing us the trajectories plotted in the (two dimensional) state space of the system. For example, we can see whether all trajectories tend to a single point as time increases or whether there are more complicated behaviors as the system evolves. In the example in Figure 4.3, corresponding to a damped oscillator, the system approaches the origin for all initial conditions. This is consistent with our simulation in Figure 4.1 but it allows us to infer the behavior for all initial conditions rather than a single initial condition. However, the phase portrait does not readily tell us the rate of change of the states (although this can be inferred from the length of the arrows in the vector field plot).

Equilibrium Points and Limit Cycles

An *equilibrium point* of a dynamical system represents a stationary condition for the dynamics. We say that a state x_e is an equilibrium point for a dynamical system

$$\frac{dx}{dt} = F(x)$$

if $F(x_e) = 0$. If a dynamical system has an initial condition $x(0) = x_e$ then it will stay at the equilibrium point: $x(t) = x_e$ for all $t \geq 0$, where we have taken $t_0 = 0$.

Equilibrium points are one of the most important features of a dynamical system since they define the states corresponding to constant operating conditions. A dynamical system can have zero, one or more equilibrium points.

Example 4.4 Inverted pendulum

Consider the inverted pendulum in Figure 4.4, which is a part of the balance system we considered in Chapter 2. The inverted pendulum is a simplified version of the problem of stabilizing a rocket: by applying forces at the base of the rocket, we seek to keep the rocket stabilized in the upright position. The state variables are the angle $\theta = x_1$ and the angular velocity $d\theta/dt = x_2$, the control variable is the acceleration u of the pivot, and the output is the angle θ .

For simplicity we assume that $mgL/J_t = 1$ and $ml/J_t = 1$, where $J_t = J + ml^2$, so that the dynamics (equation (2.10)) become

$$\frac{dx}{dt} = \begin{pmatrix} x_2 \\ \sin x_1 - \gamma x_2 + u \cos x_1 \end{pmatrix} \quad (4.5)$$

This is a nonlinear time-invariant system of second order. This same set of equations can also be obtained by appropriate normalization of the system dynamics as illustrated in Example 2.7.

We consider the open loop dynamics by setting $u = 0$. The equilibrium points

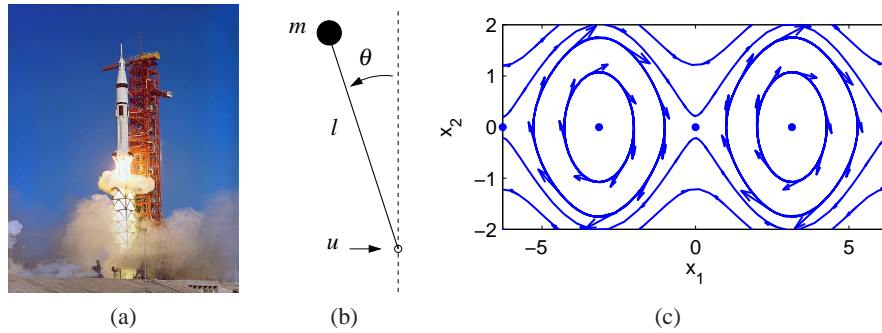


Figure 4.4: Equilibrium points for an inverted pendulum. An inverted pendulum is a model for a class of balance systems in which we wish to keep a system upright, such as a rocket (a). Using a simplified model of an inverted pendulum (b), we can develop a phase plane diagram that shows the dynamics of the system (c). The system has multiple equilibrium points, marked by the solid dots along the $x_2 = 0$ line.

for the system are given by

$$x_e = \begin{pmatrix} 0 \\ \pm n\pi \end{pmatrix},$$

where $n = 0, 1, 2, \dots$. The equilibrium points for n even correspond to the pendulum pointing up and those for n odd correspond to the pendulum hanging down. A phase portrait for this system (without corrective inputs) is shown in Figure 4.4c. The phase portrait shows $-2\pi \leq x_1 \leq 2\pi$, so 5 of the equilibrium points are shown. ∇

Nonlinear systems can exhibit rich behavior. Apart from equilibria they can also exhibit stationary periodic solutions. This is of great practical value to generate sinusoidally varying voltages in power systems or to generate periodic signals for animal locomotion. A simple example is given in Exercise 4.11, which shows the circuit diagram for an electronic oscillator. A normalized model of the oscillator is given by the equation

$$\begin{aligned} \frac{dx_1}{dt} &= x_2 + x_1(1 - x_1^2 - x_2^2) \\ \frac{dx_2}{dt} &= -x_1 + x_2(1 - x_1^2 - x_2^2). \end{aligned} \quad (4.6)$$

The phase portrait and time domain solutions are given in Figure 4.5. The figure shows that the solutions in the phase plane converge to a circular trajectory. In the time domain this corresponds to an oscillatory solution. Mathematically the circle is called a *limit cycle*. More formally, we call an isolated solution $x(t)$ a limit cycle of period $T > 0$ if $x(t+T) = x(t)$ for all $t \in \mathbb{R}$.

There are methods for determining limit cycles for second order systems, but for general higher order systems we have to resort to computational analysis. Computer algorithms find limit cycles by searching for periodic trajectories in state space that satisfy the dynamics of the system. In many situations, stable limit

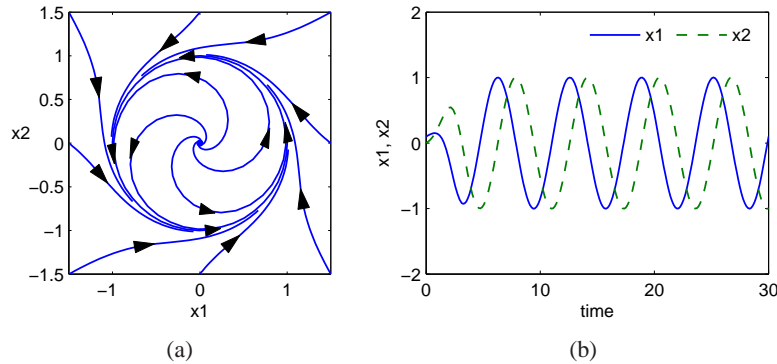


Figure 4.5: Phase portrait and time domain simulation for a system with a limit cycle. The phase portrait (a) shows the states of the solution plotted for different initial conditions. The limit cycle corresponds to a closed loop trajectory. The simulation (b) shows a single solution plotted as a function of time, with the limit cycle corresponding to a steady oscillation of fixed amplitude.

cycles can be found by simulating the system with different initial conditions.

4.3 STABILITY

The stability of a solution determines whether or not solutions nearby the solution remain nearby, get closer or move further away.

Definitions

Let $x(t; a)$ be a solution to the differential equation with initial condition a . A solution is stable if other solutions that start near a stay close to $x(t; a)$. Formally, we say that the solution $x(t; a)$ is stable if for all $\varepsilon > 0$, there exists a $\delta > 0$ such that

$$\|b - a\| < \delta \implies \|x(t; b) - x(t; a)\| < \varepsilon \quad \text{for all } t > 0.$$

Note that this definition does not imply that $x(t; b)$ approaches $x(t; a)$ as time increases, but just that it stays nearby. Furthermore, the value of δ may depend on ε , so that if we wish to stay very close to the solution, we may have to start very, very close ($\delta \ll \varepsilon$). This type of stability which is illustrated in Figure 4.6 is sometimes called stability “in the sense of Lyapunov”. If a solution is stable in this sense and the trajectories do not converge, we say that the solution is *neutrally stable*.

An important special case is when the solution $x(t; a) = x_e$ is an equilibrium solution. Instead of saying that the solution is stable we simply say that the equilibrium point is stable. An example of a neutrally stable equilibrium point is shown in Figure 4.7. From the phase portrait, we see that if we start near the equilibrium point then we stay near the equilibrium point. Indeed, for this example, given any ε that defines the range of possible initial conditions, we can simply choose $\delta = \varepsilon$

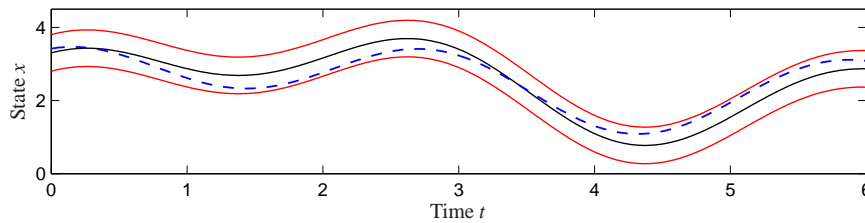


Figure 4.6: Illustration of Lyapunov's concept of a stable solution. The solution represented by the full line is stable if we can guarantee that all solutions remain within a tube of diameter ε by choosing initial conditions sufficiently close the solution.

to satisfy the definition of stability since the trajectories are perfect circles.

A solution $x(t; a)$ is *asymptotically stable* if it is stable in the sense of Lyapunov and also $x(t; b) \rightarrow x(t; a)$ as $t \rightarrow \infty$ for b sufficiently close to a . This corresponds to the case where all nearby trajectories converge to the stable solution for large time. Figure 4.8 shows an example of an asymptotically stable equilibrium point. Note from the phase portraits that not only do all trajectories stay near the equilibrium point at the origin, but they all approach the origin as t gets large (the directions of the arrows on the phase plot show the direction in which the trajectories move).

A solution $x(t; a)$ is *unstable* if it is not stable. More specifically, we say that a solution $x(t; a)$ is unstable if given some $\varepsilon > 0$, there does *not* exist a $\delta > 0$ such that if $\|b - a\| < \delta$ then $\|x(t; b) - x(t; a)\| < \varepsilon$ for all t . An example of an unstable equilibrium point is shown in Figure 4.9.

The definitions above are given without careful description of their domain of applicability. More formally, we define a solution to be *locally stable* (or asymptotically stable) if it is stable for all initial conditions $x \in B_r(a)$ where

$$B_r(a) = \{x : \|x - a\| < r\}$$

is a ball of radius r around a and $r > 0$. A system is globally stable if it is stable for all $r > 0$. Systems whose equilibrium points are only locally stable can

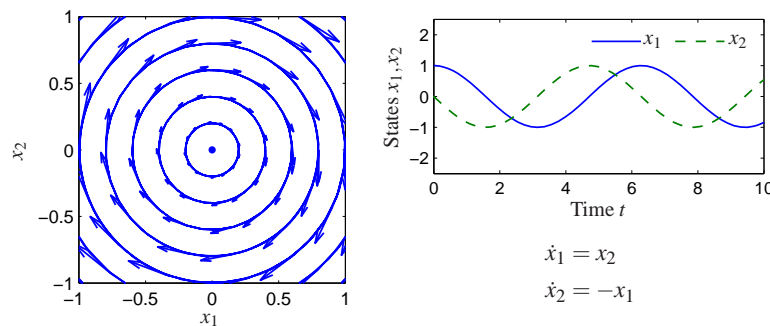


Figure 4.7: Phase portrait and time domain simulation for a system with a single stable equilibrium point. The equilibrium point x_e at the origin is stable since all trajectories that start near x_e stay near x_e .

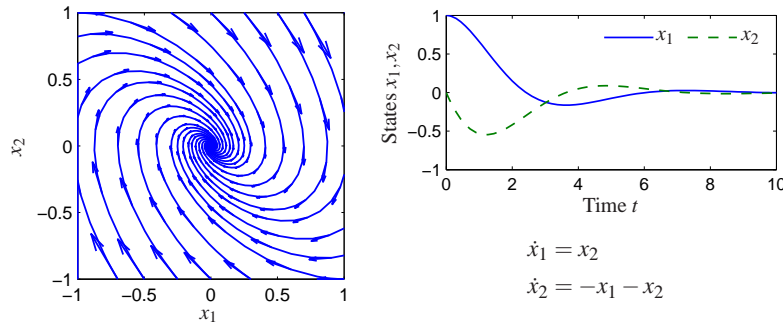


Figure 4.8: Phase portrait and time domain simulation for a system with a single asymptotically stable equilibrium point. The equilibrium point x_e at the origin is asymptotically stable since the trajectories converge to this point as $t \rightarrow \infty$.

have interesting behavior away from equilibrium points, as we explore in the next section.

For planar dynamical systems, equilibrium points have been assigned names based on their stability type. An asymptotically stable equilibrium point is called a *sink* or sometimes an *attractor*. An unstable equilibrium point can either be a *source*, if all trajectories lead away from the equilibrium point, or a *saddle*, if some trajectories lead to the equilibrium point and others move away (this is the situation pictured in Figure 4.9). Finally, an equilibrium point that is stable but not asymptotically stable (i.e. neutrally stable, such as the one in Figure 4.7) is called a *center*.

Example 4.5 Congestion control

The model for congestion control in a network consisting of N identical computers connected to a single router, introduced in Section 3.4, is given by

$$\frac{dw}{dt} = \frac{c}{b} - \rho c \left(1 + \frac{w^2}{2}\right), \quad \frac{db}{dt} = N \frac{wc}{b} - c,$$

where w is the window size and b is the buffer size of the router. Phase portraits are shown in Figure 4.10 for two different sets of parameter values. In each case we see that the system converges to an equilibrium point in which the buffers are below their full capacity of 500 packets. The equilibrium size of the buffer represents a balance between the transmission rates for the sources and the capacity of the link. We see from the phase portraits that the equilibrium points are stable since all initial conditions result in trajectories that converge to these points. ∇

Stability of Linear Systems

A linear dynamical system has the form

$$\frac{dx}{dt} = Ax \quad x(0) = x_0, \quad (4.7)$$

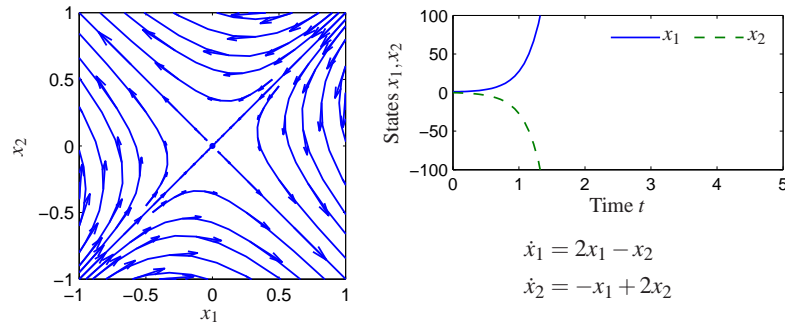


Figure 4.9: Phase portrait and time domain simulation for a system with a single unstable equilibrium point. The equilibrium point x_e at the origin is unstable since not all trajectories that start near x_e stay near x_e . The sample trajectory on the right shows that the trajectories very quickly depart from zero.

where $A \in \mathbb{R}^{n \times n}$ is a square matrix, corresponding to the dynamics matrix of a linear control system (2.6). For a linear system, the stability of the equilibrium at the origin can be determined from the eigenvalues of the matrix A :

$$\lambda(A) = \{s \in \mathbb{C} : \det(sI - A) = 0\}.$$

We use the notation λ_i for the i th eigenvalue of A , so that $\lambda_i \in \lambda(A)$. In general λ can be complex valued, although if A is real-valued then for any eigenvalue λ , its complex conjugate λ^* will also be an eigenvalue.

The easiest class of linear systems to analyze are those whose system matrices are in diagonal form. In this case, the dynamics have the form

$$\frac{dx}{dt} = \begin{pmatrix} \lambda_1 & & 0 \\ & \lambda_2 & \\ 0 & & \ddots \\ & & & \lambda_n \end{pmatrix} x. \quad (4.8)$$

It is easy to see that the state trajectories for this system are independent of each other, so that we can write the solution in terms of n individual systems

$$\dot{x}_i = \lambda_i x_i.$$

Each of these scalar solutions is of the form

$$x_i(t) = e^{\lambda_i t} x_i(0).$$

We see that the equilibrium point $x_e = 0$ is stable if $\lambda_i \leq 0$ and asymptotically stable if $\lambda_i < 0$. The origin is always an equilibrium for a linear system. Since the stability of a linear system only depends on the matrix A we find that stability is a property of the system. For linear system we can therefore talk about the stability of the system rather than the stability of a particular solution or equilibrium point.

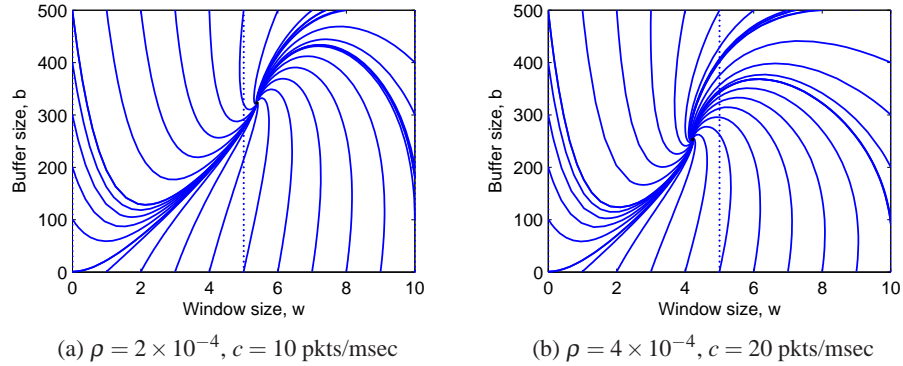


Figure 4.10: Phase portraits for a congestion control protocol running with $N = 60$ identical source computers. The equilibrium values correspond to a fixed window at the source, which results in a steady state buffer size and corresponding transmission rate. A faster link (b) uses a smaller buffer size since it can handle packets at a higher rate.

Another simple case is when the dynamics are in the block diagonal form

$$\frac{dx}{dt} = \begin{pmatrix} \sigma_1 & \omega_1 & & 0 & 0 \\ -\omega_1 & \sigma_1 & & 0 & 0 \\ & & \ddots & \vdots & \vdots \\ 0 & 0 & & \sigma_m & \omega_m \\ 0 & 0 & & -\omega_m & \sigma_m \end{pmatrix} x.$$

In this case, the eigenvalues can be shown to be $\lambda_j = \sigma_j \pm i\omega_j$. We once again can separate the state trajectories into independent solutions for each pair of states and the solutions are of the form

$$\begin{aligned} x_{2j-1}(t) &= e^{\sigma_j t} (x_i(0) \cos \omega_j t + x_{i+1}(0) \sin \omega_j t) \\ x_{2j}(t) &= e^{\sigma_j t} (x_i(0) \sin \omega_j t - x_{i+1}(0) \cos \omega_j t) \end{aligned}$$

where $j = 1, 2, \dots, m$. We see that this system is asymptotically stable if and only if $\sigma_j = \text{Re } \lambda_j < 0$. It is also possible to combine real and complex eigenvalues in (block) diagonal form, resulting in a mixture of solutions of the two types.

Very few systems are in one of the diagonal forms above, but some systems can be transformed into these forms via coordinate transformations. One such class of systems is those for which the dynamics matrix has distinct (non-repeating) eigenvalues. In this case there is a matrix $T \in \mathbb{R}^{n \times n}$ such that the matrix TAT^{-1} is in (block) diagonal form, with the block diagonal elements corresponding to the eigenvalues of the original matrix A (see Exercise 4.13). If we choose new coordinates $z = Tx$ then

$$\dot{z} = T\dot{x} = TAx = TAT^{-1}z$$

and the linear system has a (block) diagonal dynamics matrix. Furthermore, the eigenvalues of the transformed system are the same as the original system since

if v is an eigenvector of A then $w = Tv$ can be shown to be an eigenvector of TAT^{-1} . We can reason about the stability of the original system by noting that $x(t) = T^{-1}z(t)$ and so if the transformed system is stable (or asymptotically stable) then the original system has the same type of stability.

This analysis shows that for linear systems with distinct eigenvalues, the stability of the system can be completely determined by examining the real part of the eigenvalues of the dynamics matrix. For more general systems, we make use of the following theorem, proved in the next chapter:

Theorem 4.1. *The system*

$$\frac{dx}{dt} = Ax$$

is asymptotically stable if and only if all eigenvalues of A all have strictly negative real part and is unstable if any eigenvalue of A has strictly positive real part.

Example 4.6 Compartment model

Consider the two-compartment module for drug delivery introduced in Section 3.6. Using concentrations as state variables and denoting the state vector by x , the system dynamics are given by

$$\frac{dx}{dt} = \begin{pmatrix} -k_0 - k_1 & k_1 \\ k_2 & -k_2 \end{pmatrix} x + \begin{pmatrix} b_0 \\ 0 \end{pmatrix} u, \quad y = \begin{pmatrix} 0 & 1 \end{pmatrix} x,$$

where the input u is the rate of injection of a drug into compartment 1 and the concentration of the drug in compartment 2 is the measured output y . We wish to design a feedback control law that maintains a constant output given by $y = y_d$.

We choose an output feedback control law of the form

$$u = -k(y - y_d) + u_d$$

where u_d is the rate of injection required to maintain the desired concentration and k is a feedback gain that should be chosen such that the closed loop system is stable. Substituting the control law into the system, we obtain

$$\begin{aligned} \frac{dx}{dt} &= \begin{pmatrix} -k_0 - k_1 & -k_1 b_0 k \\ k_2 & -k_2 \end{pmatrix} x + \begin{pmatrix} b_0 \\ 0 \end{pmatrix} u_d =: Ax + Bu_d \\ y &= \begin{pmatrix} 0 & 1 \end{pmatrix} x =: Cx. \end{aligned}$$

The equilibrium concentration $x_e \in \mathbb{R}^2$ is given by $x_e = -A^{-1}Bu_d$ and

$$y_e = -CA^{-1}Bu_d = \frac{b_0 k_2}{k_0 k_2 + k_1 k_2 + k k_1 k_2 b_0} u_d.$$

Choosing u_d such that $y_e = y_d$ provides the constant rate of injection required to maintain the desired output. We can now shift coordinates to place the equilibrium point at the origin, which yields

$$\frac{dz}{dt} = \begin{pmatrix} -k_0 - k_1 & -k_1 b_0 k \\ k_2 & -k_2 \end{pmatrix} z,$$

where $z = x - x_e$. We can now apply the results of Theorem 4.1 to determine the stability of the system. The eigenvalues of the system are given by the roots of the characteristic polynomial

$$\lambda(s) = s^2 + (k_0 + k_1 + k_2)s + (k_0 + k_1 + k_1 k_2 b_0 k).$$

While the specific form of the roots is messy, it can be shown that the roots are positive as long as the linear term and the constant term are both positive. Hence the system is stable for any $k > 0$. ∇

Stability Analysis via Linear Approximation

An important feature of differential equations is that it is often possible to determine the local stability of an equilibrium point by approximating the system by a linear system. The following example illustrates the basic idea.

Example 4.7 Inverted pendulum

Consider again the inverted pendulum, whose open loop dynamics are given by

$$\frac{dx}{dt} = \begin{pmatrix} x_2 \\ \sin x_1 - \gamma x_2 \end{pmatrix},$$

where we have defined the state as $x = (\theta, \dot{\theta})$. We first consider the equilibrium point at $x = (0, 0)$, corresponding to the straight up position. If we assume that the angle $\theta = x_1$ remains small, then we can replace $\sin x_1$ with x_1 and $\cos x_1$ with 1, which gives the approximate system

$$\frac{dx}{dt} = \begin{pmatrix} x_2 \\ x_1 - x_2 \end{pmatrix} = \begin{pmatrix} 0 & 1 \\ 1 & -\gamma \end{pmatrix} x. \quad (4.9)$$

Intuitively, this system should behave similarly to the more complicated model as long as x_1 is small. In particular, it can be verified that the equilibrium point $(0, 0)$ is unstable by plotting the phase portrait or computing the eigenvalues of the dynamics matrix in equation (4.9)

We can also approximate the system around the stable equilibrium point at $x = (\pi, 0)$. In this case we have to expand $\sin x_1$ and $\cos x_1$ around $x_1 = \pi$, according to the expansions

$$\sin(\pi + \theta) = -\sin \theta \approx -\theta \quad \cos(\pi + \theta) = \cos(\theta) \approx 1.$$

If we define $z_1 = x_1 - \pi$ and $z_2 = x_2$, the resulting approximate dynamics are given by

$$\frac{dz}{dt} = \begin{pmatrix} z_2 \\ -z_1 - \gamma z_2 \end{pmatrix} = \begin{pmatrix} 0 & 1 \\ -1 & -\gamma \end{pmatrix} z. \quad (4.10)$$

Note that $z = (0, 0)$ is the equilibrium point for this system and that it has the same basic form as the dynamics shown in Figure 4.8. Figure 4.11 shows the phase portraits for the original system and the approximate system around the corresponding equilibrium points. Note that they are very similar, although not exactly the same. It can be shown that if a linear approximation has either asymptotically stable or

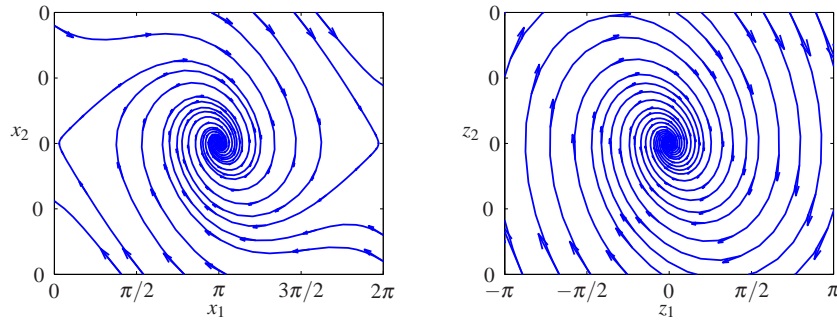


Figure 4.11: Comparison between the phase portraits for the full nonlinear systems (left) and its linear approximation around the origin (right). Notice that near the equilibrium point at the center of the plots, the phase portraits (and hence the dynamics) are almost identical.

unstable equilibrium points, then the local stability of the original system must be the same (Theorem 4.3, page 118). ∇

More generally, suppose that we have a nonlinear system

$$\dot{x} = F(x)$$

that has an equilibrium point at x_e . Computing the Taylor series expansion of the vector field, we can write

$$\dot{x} = F(x_e) + \left. \frac{\partial F}{\partial x} \right|_{x_e} (x - x_e) + \text{higher order terms in } (x - x_e).$$

Since $F(x_e) = 0$, we can approximate the system by choosing a new state variable $z = x - x_e$ and writing

$$\dot{z} = Az \quad \text{where} \quad A = \left. \frac{\partial F}{\partial x} \right|_{x_e}. \quad (4.11)$$

We call the system (4.11) the *linear approximation* of the original nonlinear system.

The fact that a linear model can be used to study the behavior of a nonlinear system near an equilibrium point is a powerful one. Indeed, we can take this even further and use a local linear approximations of a nonlinear system to design a feedback law that keeps the system near its equilibrium point (design of dynamics). Thus, feedback can be used to make sure that solutions remain close to the equilibrium point, which in turn ensures that the linear approximation used to stabilize it is valid.

Linear approximations can also used to understand stability of non-equilibrium solutions, as illustrated by the following example.

Example 4.8 Stable limit cycle

Consider the system given by equation (4.6),

$$\begin{aligned}\frac{dx_1}{dt} &= x_2 + x_1(1 - x_1^2 - x_2^2) \\ \frac{dx_2}{dt} &= -x_1 + x_2(1 - x_1^2 - x_2^2),\end{aligned}$$

whose phase portrait is shown in Figure 4.5. The differential equation has a periodic solution

$$x_1(t) = x_1(0) \cos t + x_2(0) \sin t, \quad (4.12)$$

with $x_1^2(0) + x_2^2(0) = 1$.

To explore the stability of this solution, we introduce polar coordinates r and φ that are related to the state variables x_1 and x_2 by

$$x_1 = r \cos \varphi, \quad x_2 = r \sin \varphi.$$

Differentiation gives the following linear equations for \dot{r} and $\dot{\varphi}$

$$\dot{x}_1 = \dot{r} \cos \varphi - r \dot{\varphi} \sin \varphi, \quad \dot{x}_2 = \dot{r} \sin \varphi + r \dot{\varphi} \cos \varphi$$

Solving this linear system for \dot{r} and $\dot{\varphi}$ gives, after some calculation,

$$\dot{r} = r(1 - r^2), \quad \dot{\varphi} = -1.$$

Notice that the equations are decoupled, hence we can analyze the stability of each state separately.

The equation for r has three equilibria: $r = 0$, $r = 1$ and $r = -1$ (not realizable since r must be positive). We can analyze the stability of these equilibria by linearizing the radial dynamics with $F(r) = r(1 - r^2)$. The corresponding linear dynamics are given by

$$\dot{r} = \left. \frac{\partial F}{\partial r} \right|_{r_e} r = (1 - 2r_e^2)r \quad r_e = 0, 1,$$

where we have abused notation and used r to represent the deviation from the equilibrium point. It follows from the sign of $(1 - 2r_e^2)$ that the equilibrium $r = 0$ is unstable and the equilibrium $r = 1$ is asymptotically stable. Thus for any initial condition $r > 0$ the solution goes to $r = 1$ as time goes to infinity, but if the system starts with $r = 0$ it will remain at the equilibrium for all times. This implies that all solutions to the original system that do not start at $x_1 = x_2 = 0$ will approach the circle $x_1^2 + x_2^2 = 1$ as time increases.

To show stability of the full solution (4.12), we must investigate the behavior of neighboring solutions with different initial conditions. We have already shown that the radius r will approach that of the solution 4.12 as long as $r(0) > 0$. The equation for the angle φ can be integrated analytically to give $\varphi(t) = -t + \varphi(0)$, which shows that solutions starting at different angles φ will neither converge nor diverge. Thus, the unit circle is *attracting* but the solution (4.12) is only stable, not asymptotically stable. The behavior of the system is illustrated by the simulation

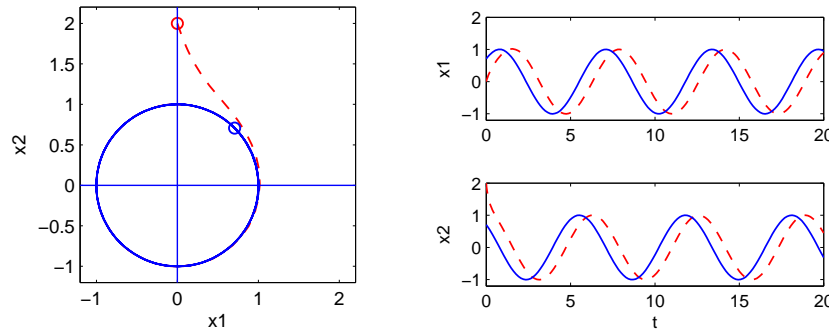


Figure 4.12: Solution curves for a stable limit cycle. The phase plane plot on the left shows that the trajectory for the system rapidly converges to the stable limit cycle. The starting points for the trajectories are marked by circles in the phase portrait. The time domain plots on the right show that the states do not convert to the solution but instead maintain a constant phase error.

in Figure 4.12. Notice that the solutions approach the circle rapidly but that there is a constant phase shift between the solutions. ∇

4.4 LYAPUNOV STABILITY



We now return to the study of the full nonlinear system

$$\frac{dx}{dt} = F(x) \quad x \in \mathbb{R}^n. \quad (4.13)$$

Having defined when a solution for a nonlinear dynamical system is stable, we can now ask how to prove that a given solution is stable, asymptotically stable or unstable. For physical systems, one can often argue about stability based on dissipation of energy. The generalization of that technique to arbitrary dynamical systems is based on the use of Lyapunov functions in place of energy.

In this section we will describe techniques for determining the stability of solutions for a nonlinear system (4.13). We will generally be interested in stability of equilibrium points and it will be convenient to assume that $x_e = 0$ is the equilibrium point of interest. (If not, rewrite the equations in a new set of coordinates $z = x - x_e$.)

Lyapunov Functions

A *Lyapunov function* $V : \mathbb{R}^n \rightarrow \mathbb{R}$ is an energy-like function that can be used to determine stability of a system. Roughly speaking, if we can find a non-negative function that always decreases along trajectories of the system, we can conclude that the minimum of the function is a stable equilibrium point (locally).

To describe this more formally, we start with a few definitions. We say that a continuous function V is *positive definite* if $V(x) > 0$ for all $x \neq 0$ and $V(0) = 0$.

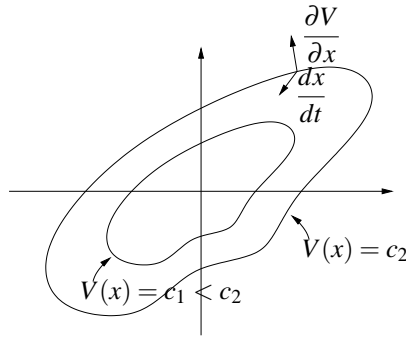


Figure 4.13: Geometric illustration of Lyapunov's stability theorem. The closed contours represent the level sets of the Lyapunov function, $V(x) = c$. If dx/dt points inward to these sets at all points along the contour, then the trajectories of the system will always cause $V(x)$ to decrease along the trajectory.

Similarly, a function is *negative definite* if $V(x) < 0$ for all $x \neq 0$ and $V(0) = 0$. We say that a function V is *positive semidefinite* if $V(x) \geq 0$ for all x but $V(x)$ can be zero at points other than just $x = 0$.

To illustrate the difference between a positive definite function and a positive semi-definite function, suppose that $x \in \mathbb{R}^2$ and let

$$V_1(x) = x_1^2, \quad V_2(x) = x_1^2 + x_2^2.$$

Both V_1 and V_2 are always non-negative. However, it is possible for V_1 to be zero even if $x \neq 0$. Specifically, if we set $x = (0, c)$ where $c \in \mathbb{R}$ is any nonzero number, then $V_1(x) = 0$. On the other hand, $V_2(x) = 0$ if and only if $x = (0, 0)$. Thus V_1 is positive semi-definite and V_2 is positive definite.

We can now characterize the stability of an equilibrium point $x_e = 0$ for the system (4.13).

Theorem 4.2 (Lyapunov stability). *Let V be a non-negative function on \mathbb{R}^n and let \dot{V} represent the time derivative of V along trajectories of the system dynamics (4.13):*

$$\dot{V} = \frac{\partial V}{\partial x} \frac{dx}{dt} = \frac{\partial V}{\partial x} F(x).$$

Let $B_r = B_r(0)$ be a ball of radius r around the origin. If there exists $r > 0$ such that V is positive definite and \dot{V} is negative semi-definite for all $x \in B_r$, then $x = 0$ is locally stable in the sense of Lyapunov. If V is positive definite and \dot{V} is negative definite in B_r , then $x = 0$ is locally asymptotically stable.

If V satisfies one of the conditions above, we say that V is a (local) *Lyapunov function* for the system. These results have a nice geometric interpretation. The level curves for a positive definite function are the curves defined by $V(x) = c$, $c > 0$ and for each c this gives a closed contour, as shown in Figure 4.13. The condition that $\dot{V}(x)$ is negative simply means that the vector field points towards lower level contours. This means that the trajectories move to smaller and smaller values of V and if \dot{V} is negative definite then x must approach 0.

Example 4.9 Stability of a simple nonlinear system

Consider the scalar nonlinear system

$$\dot{x} = \frac{2}{1+x} - x.$$

This system has equilibrium points at $x = 1$ and $x = -2$. We consider the equilibrium point at $x = 1$ and rewrite the dynamics using $z = x - 1$:

$$\dot{z} = \frac{2}{2+z} - z - 1,$$

which has an equilibrium point at $z = 0$. Now consider the candidate Lyapunov function

$$V(x) = \frac{1}{2}z^2$$

which is globally positive definite. The derivative of V along trajectories of the system is given by

$$\dot{V}(z) = z\dot{z} = \frac{2z}{2+z} - z^2 - z.$$

If we restrict our analysis to a ball B_r where $r < 2$, then $2 + z > 0$ and we can multiply through by $2 + z$ to obtain

$$2z - (z^2 + z)(2 + z) = -z^3 - 3z^2 = -z^2(z + 3) < 0 \quad z \in B_r, r < 2.$$

It follows that $\dot{V}(z) < 0$ for all $z \in B_r, z \neq 0$ and hence the equilibrium point $x_e = 1$ is locally asymptotically stable. ∇

A slightly more complicated situation occurs if \dot{V} is negative semi-definite. In this case it is possible that $\dot{V}(x) = 0$ when $x \neq 0$ and hence x could stop decreasing in value. The following example illustrates this case.

Example 4.10 Hanging pendulum

A normalized model for a hanging pendulum is

$$\frac{dx_1}{dt} = x_2, \quad \frac{dx_2}{dt} = -\sin x_1,$$

where x_1 is the angle between the pendulum and the vertical, with positive x_1 corresponding to counter-clockwise rotation. The equation has an equilibrium $x_1 = x_2 = 0$, which corresponds to the pendulum hanging straight down. To explore the stability of this equilibrium we choose the total energy as a Lyapunov function:

$$V(x) = 1 - \cos x_1 + \frac{1}{2}x_2^2 \approx \frac{1}{2}x_1^2 + \frac{1}{2}x_2^2.$$

The Taylor series approximation shows that the function is positive definite for small x . The time derivative of $V(x)$ is

$$\dot{V} = \dot{x}_1 \sin x_1 + \dot{x}_2 x_2 = x_2 \sin x_1 - x_2 \sin x_1 = 0.$$

Since this function is positive semi-definite it follows from Lyapunov's theorem that the equilibrium is stable but not necessarily asymptotically stable. When per-

turbed the pendulum actually moves in a trajectory which corresponds to constant energy. ∇

Lyapunov functions are not always easy to find and they are not unique. In many cases energy functions can be used as a starting point as was done in Example 4.10. It turns out that Lyapunov functions can always be found for any stable system (under certain conditions) and hence one knows that if a system is stable, a Lyapunov function exists (and vice versa). Recent results using “sum of squares” methods have provided systematic approaches for finding Lyapunov systems [158]. Sum of squares techniques can be applied to a broad variety of systems, including systems whose dynamics are described by polynomial equations as well as “hybrid” systems, which can have different models for different regions of state space.

For a linear dynamical system of the form

$$\dot{x} = Ax$$

it is possible to construct Lyapunov functions in a systematic manner. To do so, we consider quadratic functions of the form

$$V(x) = x^T Px,$$

where $P \in \mathbb{R}^{n \times n}$ is a symmetric matrix ($P = P^T$). The condition that V be positive definite is equivalent to the condition that P is a *positive definite matrix*:

$$x^T Px > 0 \quad \text{for all } x \neq 0,$$

which we write as $P > 0$. It can be shown that if P is symmetric then P is positive definite if and only if all of its eigenvalues are real and positive.

Given a candidate Lyapunov function $V(x) = x^T Px$, we can now compute its derivative along flows of the system:

$$\dot{V} = \frac{\partial V}{\partial x} \frac{dx}{dt} = x^T (A^T P + PA)x =: -x^T Qx.$$

The requirement that \dot{V} be negative definite (for asymptotic stability) becomes a condition that the matrix Q be positive definite. Thus, to find a Lyapunov function for a linear system it is sufficient to choose a $Q > 0$ and solve the *Lyapunov equation*:

$$A^T P + PA = -Q. \tag{4.14}$$

This is a linear equation in the entries of P , and hence it can be solved using linear algebra. It can be shown that the equation always has a solution if all of the eigenvalues of the matrix A are in the left half plane (see Exercise 4.7). Moreover the solution P is positive definite if Q is positive definite. It is thus always possible to find a quadratic Lyapunov function for a stable linear system. We will defer a proof of this until Chapter 5 where more tools for analysis of linear systems will be developed.

Knowing that we have a direct method to find Lyapunov functions for linear systems we can now investigate stability of nonlinear systems. Consider the sys-

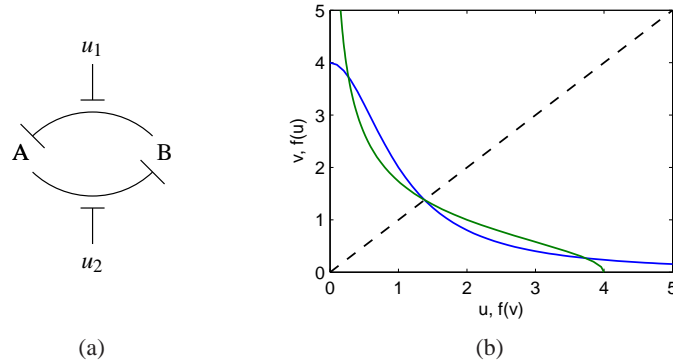


Figure 4.14: Stability of a genetic switch. The circuit diagram on the left represents two proteins that are each repressing the production of the other. The inputs u_1 and u_2 interfere with this repression, allowing the circuit dynamics to be modified. The equilibrium points for this circuit can be determined by the intersection of the two curves shown on the right.

tem

$$\frac{dx}{dt} = F(x) =: Ax + \tilde{F}(x), \quad (4.15)$$

where $F(0) = 0$, and $\tilde{F}(x)$ contains terms that are second order and higher in the elements of x . The function Ax is an approximation of $F(x)$ near the origin and we can determine the Lyapunov function for the linear approximation and investigate if it also is a Lyapunov function for the full nonlinear system. The following example illustrates the approach.

Example 4.11 Stability of a Genetic Switch

Consider the dynamics of a set of repressors connected together in a cycle, as shown in Figure 4.14a. The normalized dynamics for this system were given in Exercise 2.11:

$$\frac{dz_1}{d\tau} = \frac{\mu}{1+z_2^n} - z_1, \quad \frac{dz_2}{d\tau} = \frac{\mu}{1+z_1^n} - z_2, \quad (4.16)$$

where z_1 and z_2 are scaled versions of the protein concentrations, n and μ are parameters that describe the interconnection between the genes, and we have set the external inputs u_1 and u_2 to zero.

The equilibrium points for the system are found by equating the time derivatives to zero. We define

$$f(u) = \frac{\mu}{1+u^n} \quad f'(u) = \frac{df}{du} = \frac{-\mu n u^{n-1}}{(1+u^n)^2}$$

and the equilibrium point are defined as the solutions of the equations

$$z_1 = f(z_2) \quad z_2 = f(z_1).$$

If we plot the curves $(z_1, f(z_1))$ and $(f(z_2), z_2)$ on a graph, then these equations will have a solution when the curves intersect, as shown in Figure 4.14b. Because of the shape of the curves, it can be shown that there will always be three solutions:

one at $z_{1e} = z_{2e}$, one with $z_{1e} < z_{2e}$ and one with $z_{1e} > z_{2e}$. If $\mu \gg 1$, then we can show that the solutions are given approximately by

$$z_{1e} \approx \mu, \quad z_{2e} \approx \frac{1}{\mu^{n-1}}, \quad z_{1e} = z_{2e}, \quad z_{1e} \approx \frac{1}{\mu^{n-1}}, \quad z_{2e} \approx \mu. \quad (4.17)$$

To check the stability of the system, we write $f(u)$ in terms of its Taylor series expansion about u_e

$$f(u) = f(u_e) + f'(u_e) \cdot (u - u_e) + f''(u_e) \cdot (u - u_e)^2 + \text{higher order terms},$$

where f' represents the first derivative of the function and f'' the second. Using these approximations, the dynamics can then be written as

$$\frac{dw}{dt} = \begin{pmatrix} -1 & f'(z_{2e}) \\ f'(z_{1e}) & -1 \end{pmatrix} w + \tilde{F}(w),$$

where $w = z - z_e$ is the shifted state and $\tilde{F}(w)$ represents quadratic and higher order terms.

We now use equation (4.14) to search for a Lyapunov function. Choosing $Q = I$ and letting $P \in \mathbb{R}^{2 \times 2}$ have elements p_{ij} , we search for a solution of the equation

$$\begin{pmatrix} -1 & f'_2 \\ f'_1 & -1 \end{pmatrix} \begin{pmatrix} p_{11} & p_{12} \\ p_{12} & p_{22} \end{pmatrix} + \begin{pmatrix} p_{11} & p_{12} \\ p_{12} & p_{22} \end{pmatrix} \begin{pmatrix} -1 & f'_1 \\ f'_2 & -1 \end{pmatrix} = \begin{pmatrix} -1 & 0 \\ 0 & -1 \end{pmatrix},$$

where $f'_1 = f'(z_{1e})$ and $f'_2 = f'(z_{2e})$. Note that we have set $p_{21} = p_{12}$ to force P to be symmetric. Multiplying out the matrices, we obtain

$$\begin{pmatrix} -2p_{11} + 2f'_2 p_{12} & p_{11} f'_1 - 2p_{12} + p_{22} f'_2 \\ p_{11} f'_1 - 2p_{12} + p_{22} f'_2 & -2p_{22} + 2f'_1 p_{12} \end{pmatrix} = \begin{pmatrix} -1 & 0 \\ 0 & -1 \end{pmatrix},$$

which is a set of *linear* equations for the unknowns p_{ij} . We can solve these linear equations to obtain

$$p_{11} = -\frac{f_1'^2 - f_2' f_1' + 2}{4(f_1' f_2' - 1)}, \quad p_{12} = -\frac{f_1' + f_2'}{4(f_1' f_2' - 1)}, \quad p_{22} = -\frac{f_2'^2 - f_1' f_2' + 2}{4(f_1' f_2' - 1)}.$$

To check that $V(w) = w^T P w$ is a Lyapunov function, we must verify that $V(w)$ is positive definite function or equivalently that $P > 0$. Since P is a 2×2 symmetric matrix, it has two real eigenvalues λ_1 and λ_2 that satisfy

$$\lambda_1 + \lambda_2 = \text{trace}(P), \quad \lambda_1 \cdot \lambda_2 = \det(P).$$

In order for P to be positive definite we must have that λ_1 and λ_2 are positive and we thus require that

$$\text{trace}(P) = \frac{f_1'^2 - 2f_2' f_1' + f_2'^2 + 4}{4 - 4f_1' f_2'} > 0, \quad \det(P) = \frac{f_1'^2 - 2f_2' f_1' + f_2'^2 + 4}{16 - 16f_1' f_2'} > 0.$$

We see that $\text{trace}(P) = 4 \det(P)$ and the numerator of the expressions is just $(f_1 - f_2)^2 + 4 > 0$, so it suffices to check the sign of $1 - f_1' f_2'$. In particular, for P to be

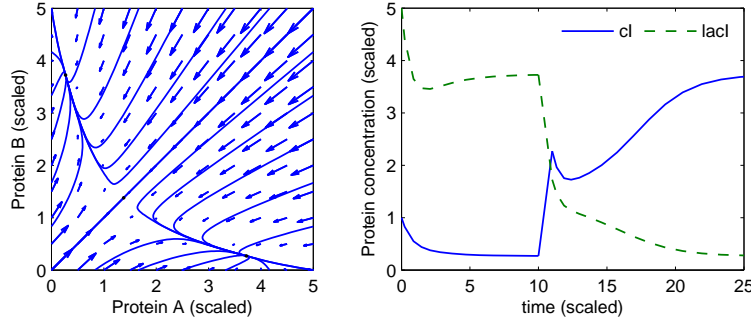


Figure 4.15: Dynamics of a genetic switch. The phase portrait on the left shows that the switch has three equilibrium points, corresponding to protein 1 having concentration greater than, equal to or less than protein 2. The concentration with equal protein concentrations is unstable, but the other equilibrium points are stable. The simulation on the right shows the time response of the system starting from two different initial conditions.

positive definite, we require that

$$f'(z_{1e})f'(z_{2e}) < 1.$$

We can now make use of the expressions for f' defined earlier and evaluate at the approximate locations of the equilibrium points derived in equation (4.17). For the equilibrium points where $z_{1e} \neq z_{2e}$, we can show that

$$f'(z_{1e})f'(z_{2e}) \approx f'(\mu)f'\left(\frac{1}{\mu^{n-1}}\right) = \frac{-\mu n \mu^{n-1}}{(1+\mu^n)^2} \cdot \frac{-\mu n \mu^{-(n-1)^2}}{1+\mu^{-n(n-1)}} \approx n^2 \mu^{-n^2+n}.$$

Using $n = 2$ and $\mu \approx 200$ from Exercise 2.11 we see that $f'(z_{1e})f'(z_{2e}) \ll 1$ and hence P is a positive definite. This implies that V is a positive definite function and hence a potential Lyapunov function for the system.

To determine if the system (4.16) is stable, we now compute \dot{V} at the equilibrium point. By construction

$$\dot{V} = w^T(PA + A^T P)w + \tilde{F}^T(w)Pw + w^T P \tilde{F}(w) = -w^T w + \tilde{F}^T(w)Pw + w^T P \tilde{F}(w).$$

Since all terms in \tilde{F} are quadratic or higher order in w , it follows that $\tilde{F}^T(w)Pw$ and $w^T P \tilde{F}(w)$ consist of terms that are at least third order in w . Therefore if w is sufficiently close to zero then the cubic and higher order terms will be smaller than the quadratic terms. Hence, sufficiently close to $w = 0$, \dot{V} is negative definite allowing us to conclude that these equilibrium points are both stable.

Figure 4.15 shows the phase portrait and time traces for a system with $\mu = 4$, illustrating the bistable nature of the system. When the initial condition starts with a concentration of protein B greater than protein A, the solution converges to the equilibrium point at (approximately) $(1/\mu^{n-1}, \mu)$ and if A is greater than B then it goes to $(\mu, 1/\mu^{n-1})$. The equilibrium point with $z_{1e} = z_{2e}$ is seen to be unstable. ∇

More generally, we can investigate what the linear approximation tells about

the stability of a solution to a nonlinear equation. The following theorem gives a partial answer for the case of stability of an equilibrium point.

Theorem 4.3. *Consider the dynamical system (4.15) with $F(0) = 0$ and \tilde{F} such that $\lim_{\|x\| \rightarrow 0} \|\tilde{F}(x)\|/\|x\| \rightarrow 0$. If the real parts of all eigenvalues of A are strictly less than zero, then $x_e = 0$ is a locally asymptotically stable equilibrium point of equation (4.15).*

This theorem implies that asymptotic stability of the linear approximation implies *local* asymptotic stability of the original nonlinear system. The theorem is very important for control because it implies that stabilization of a linear approximation of a nonlinear system results in a stable equilibrium for the nonlinear system. The proof of this theorem follows the technique used in Example 4.11. A formal proof can be found in [116].



Krasovskii-Lasalle Invariance Principle

For general nonlinear systems, especially those in symbolic form, it can be difficult to find a positive definite function V whose derivative is strictly negative definite. The Krasovskii-Lasalle theorem enables us to conclude asymptotic stability of an equilibrium point under less restrictive conditions, namely in the case that \dot{V} is negative semi-definite, which is often easier to construct. However, it applies only to time-invariant or periodic systems.

We will deal with the time-invariant case and begin by introducing a few more definitions. We denote the solution trajectories of the time-invariant system

$$\frac{dx}{dt} = F(x) \quad (4.18)$$

as $x(t; a)$, which is the solution of equation (4.18) at time t starting from a at $t_0 = 0$. The ω limit set of a trajectory $x(t; a)$ is the set of all points $z \in \mathbb{R}^n$ such that there exists a strictly increasing sequence of times t_n such that $x(t_n; a) \rightarrow z$ as $n \rightarrow \infty$. A set $M \subset \mathbb{R}^n$ is said to be an *invariant set* if for all $b \in M$, we have $x(t; b) \in M$ for all $t \geq 0$. It can be proved that the ω limit set of every trajectory is closed and invariant. We may now state the Krasovskii-Lasalle principle.

Theorem 4.4 (Krasovskii-Lasalle principle). *Let $V : \mathbb{R}^n \rightarrow \mathbb{R}$ be a locally positive definite function such that on the compact set $\Omega_r = \{x \in \mathbb{R}^n : V(x) \leq r\}$ we have $\dot{V}(x) \leq 0$. Define*

$$S = \{x \in \Omega_r : \dot{V}(x) = 0\}.$$

As $t \rightarrow \infty$, the trajectory tends to the largest invariant set inside S ; i.e., its ω limit set is contained inside the largest invariant set in S . In particular, if S contains no invariant sets other than $x = 0$, then 0 is asymptotically stable.

Proofs are given in [121] and [127].

Lyapunov functions can often be used to design stabilizing controllers as is illustrated by the following example, which also illustrates how the Krasovskii-Lasalle principle can be applied.

Example 4.12 Stabilization of an inverted pendulum

Following the analysis in Example 2.7, an inverted pendulum can be described by the following normalized model:

$$\frac{dx_1}{dt} = x_2, \quad \frac{dx_2}{dt} = \sin x_1 + u \cos x_1, \quad (4.19)$$

where x_1 is the angular deviation from the upright position and u is the (scaled) acceleration of the pivot. The system has an equilibrium at $x_1 = x_2 = 0$, which corresponds to the pendulum standing upright. This equilibrium is unstable.

To find a stabilizing controller we consider the following candidate for a Lyapunov function

$$V(x) = (\cos x_1 - 1) + a(1 - \cos^2 x_1) + \frac{1}{2}x_2^2 \approx \left(a - \frac{1}{2}\right)x_1^2 + \frac{1}{2}x_2^2.$$

The Taylor series expansion shows that the function is positive definite near the origin if $a > 0.5$. The time derivative of $V(x)$ is

$$\dot{V} = -\dot{x}_1 \sin x_1 + 2a\dot{x}_1 \sin x_1 \cos x_1 + \dot{x}_2 x_2 = x_2(u + 2a \sin x_1) \cos x_1.$$

Choosing the feedback law

$$u = -2a \sin x_1 - x_2 \cos x_1,$$

gives

$$\dot{V} = -x_2^2 \cos^2 x_1,$$

It follows from Lyapunov's theorem that the equilibrium is locally stable. However, since the function is only negative semi-definite we cannot conclude asymptotic stability using Theorem 4.2. However, note that $\dot{V} = 0$ implies that $x_2 = 0$ or $x_1 = \pi/2 \pm n\pi$.

If we restrict our analysis to a small neighborhood of the origin Ω_r , $r \ll \pi/2$ then we can define

$$S = \{(x_1, x_2) \in \Omega_r : x_2 = 0\}$$

and we can compute the largest invariant set inside S . For a trajectory to remain in this set we must have $x_2 = 0$ for all t and hence $\dot{x}_2(t) = 0$ as well. Using the dynamics of the system (4.19), we see that $x_2(t) = 0$ and $\dot{x}_2(t) = 0$ implies $x_1(t) = 0$ as well. Hence the largest invariant set inside S is $(x_1, x_2) = 0$ and we can use the Krasovskii-Lasalle principle to conclude that the origin is locally asymptotically stable. A phase portrait of the closed loop system is shown in Figure 4.16.

▽

4.5 PARAMETRIC AND NON-LOCAL BEHAVIOR



Most of the tools that we have explored are focused on the local behavior of a fixed system near an equilibrium point. In this section we briefly introduce some

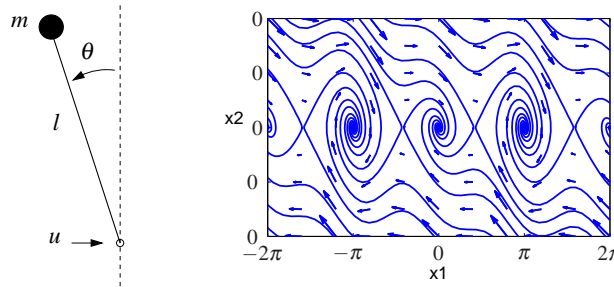


Figure 4.16: Phase portrait for a stabilized inverted pendulum. The shaded region indicates the set of initial conditions that converge to the origin. The ellipse corresponds to a level set of a Lyapunov function $V(x)$ for which $V(x) > 0$ and $\dot{V}(x) < 0$ for all points inside the ellipse. This can be used as an estimate of the region of attraction of the equilibrium point.

concepts regarding the global behavior of nonlinear systems and the dependence of a system's behavior on parameters in the system model.

Regions of attraction

To get some insight into the behavior of a nonlinear system we can start by finding the equilibrium points. We can then proceed to analyze the local behavior around the equilibria. The behavior of a system near an equilibrium point is called the *local* behavior of the system.

The solutions of the system can be very different far away from an equilibrium point. This is seen, for example, in the stabilized pendulum in Example 4.12. The inverted equilibrium point is stable, with small oscillations that eventually converge to the origin. But far away from this equilibrium point there are trajectories that converge to other equilibrium points or even cases in which the pendulum swings around the top multiple times, giving very long oscillations that are topologically different from those near the origin.

To better understand the dynamics of the system, we can examine the set of all initial conditions that converge to a given asymptotically stable equilibrium point. This set is called the *region of attraction* for the equilibrium point. An example is shown by the shaded region in Figure 4.16. In general, computing regions of attraction is difficult. However, even if we cannot determine the region of attraction, we can often obtain patches around the stable equilibria that are attracting. This gives partial information about the behavior of the system.

One method for approximating the region of attraction is through the use of Lyapunov functions. Suppose that V is a local Lyapunov function for a system around an equilibrium point x_0 . Let Ω_r be set on which $V(x)$ has value less than r ,

$$\Omega_r = \{x \in \mathbb{R}^n : V(x) \leq r\},$$

and suppose that $\dot{V}(x) \leq 0$ for all $x \in \Omega_r$, with equality only at the equilibrium point x_0 . Then Ω_r is inside the region of attraction of the equilibrium point. Since this approximation depends on the Lyapunov function and the choice of Lyapunov

function is not unique, it can sometimes be a very conservative estimate.

It is sometimes the case that we can find a Lyapunov function V such that V is positive definite and \dot{V} is negative (semi-) definite for all $x \in \mathbb{R}^n$. In this case it can be shown that the region of attraction for the equilibrium point is the entire state space and the equilibrium point is said to be *globally stable*.

Example 4.13 Stabilized inverted pendulum

Consider again the stabilized inverted pendulum from Example 4.12. The Lyapunov function for the system was

$$V(x) = (\cos x_1 - 1) + a(1 - \cos^2 x_1) + \frac{1}{2}x_2^2$$

and \dot{V} was negative semidefinite for all x and nonzero when $x_1 \neq \pm\pi/2$. Hence any x such that $|x_2| < \pi/2$, $V(x) > 0$ will be inside the invariant set defined by the level curves of $V(x)$. These level sets are shown in Figure 4.16. ∇

Bifurcations

Another important property of nonlinear systems is how their behavior changes as the parameters governing the dynamics change. We can study this in the context of models by exploring how the location of equilibrium points, their stability, their regions of attraction, and other dynamic phenomena such as limit cycles, vary based on the values of the parameters in the model.

Consider a differential equation of the form

$$\frac{dx}{dt} = F(x, \mu), \quad x \in \mathbb{R}^n, \mu \in \mathbb{R}^k, \quad (4.20)$$

where x is the state and μ is a set of parameters that describe the family of equations. The equilibrium solutions satisfy

$$F(x, \mu) = 0$$

and as μ is varied, the corresponding solutions $x_e(\mu)$ can also vary. We say that the system (4.20) has a *bifurcation* at $\mu = \mu^*$ if the behavior of the system changes qualitatively at μ^* . This can occur either due to a change in stability type or a change in the number of solutions at a given value of μ .

Example 4.14 Predator-prey

Consider the predator-prey system described in Section 3.7. The dynamics of the system are given by

$$\begin{aligned} \frac{dH}{dt} &= r_h H \left(1 - \frac{H}{K}\right) - \frac{aHL}{1 + aHT_h} \\ \frac{dL}{dt} &= r_l L \left(1 - \frac{L}{kH}\right), \end{aligned} \quad (4.21)$$

where H and L are the number of hares (prey) and lynxes (predators), and r_h , r_l , K , k , a and T_h are parameters that model a given predator-prey system (described

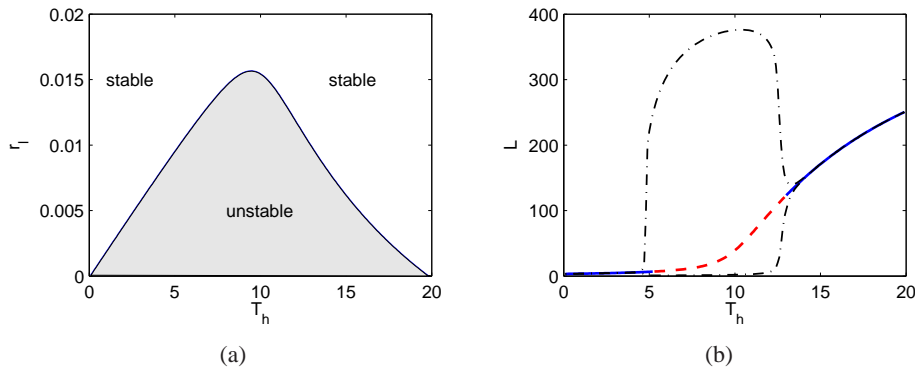


Figure 4.17: Bifurcation analysis of the predator-prey system. (a) Parametric stability diagram showing the regions in parameter space for which the system is stable and (b) bifurcation diagram showing the location and stability of the equilibrium point as a function of T_h . The dotted lines indicate the upper and lower bounds for the limit cycle at that parameter value (computed via simulation). The nominal values of the parameters in the model are $r_h = 0.02$, $K = 500$, $a = 0.03$, $T_h = 5$, $r_l = 0.01$ and $k = 0.2$.

in more detail in Section 3.7). The system has an equilibrium point at $H_e > 0$ and $L_e > 0$ that can be found numerically.

To explore how the parameters of the model affect the behavior of the system, we choose to focus on two specific parameters of interest: r_l , the growth rate of the lynxes, and T_h , the time constant for prey consumption. Figure 4.17a is a numerically computed *parametric stability diagram* showing the regions in the chosen parameter space for which the equilibrium point is stable (leaving the other parameters at their nominal values). We see from this figure that for certain combinations of r_l and T_h we get a stable equilibrium point while at other values this equilibrium point is unstable.

Figure 4.17b shows a numerically computed *bifurcation diagram* for the system. In this plot, we choose one parameter to vary (T_h) and then plot the equilibrium value of one of the states (L) on the vertical axis. The remaining parameters are set to their nominal values. A solid line indicates that the equilibrium point is stable; a dashed line indicates that the equilibrium point is unstable. Note that the stability in the bifurcation diagram matches that in the parametric stability diagram for $r_l = 0.01$ (the nominal value) and T_h varying from 0 to 20. For the predator-prey system, when the equilibrium point is unstable, the solution converges to a stable limit cycle. The amplitude of this limit cycle is shown using the dot-dashed line in Figure 4.17b. ∇

A particular form of bifurcation that is very common when controlling linear systems is that the equilibrium remains fixed, but the stability of the equilibrium changes as the parameters are varied. In such a case it is revealing to plot the eigenvalues of the system as a function of the parameters. Such plots are called *root locus plots* because they give the locus of the eigenvalues when parameters

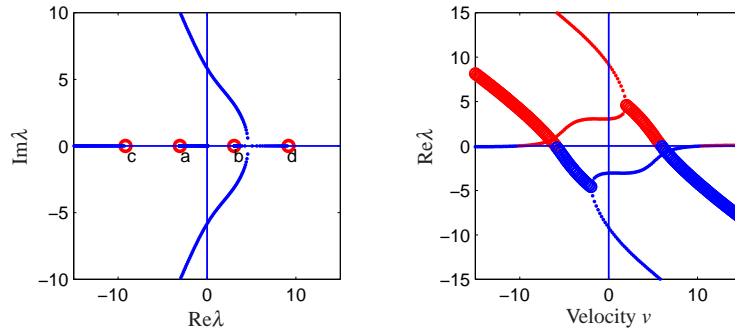


Figure 4.18: Stability plots for balancing a bicycle. The left plot shows the real part of the system eigenvalues as a function of the bicycle velocity v . When one or more eigenvalues have positive real part, the system is unstable. The figure on the right shows the locus of eigenvalues on the complex plane as the velocity v is varied and gives a different view of the stability of the system. This type of plot is called a root locus plot.

change. Bifurcations occur when parameter values are such that there are eigenvalues with zero real part. Computing environments such as LabVIEW, MATLAB and Mathematica have tools for plotting root loci.

Example 4.15 Root locus plot for a bicycle model

Consider the linear bicycle model given by equation (3.7) in Section 3.2. Introducing the state variables $x_1 = \varphi$, $x_2 = \delta$, $x_3 = \dot{\varphi}$ and $x_4 = \dot{\delta}$ and setting the steering torque $T = 0$ the equations can be written as

$$\frac{dx}{dt} = \begin{pmatrix} 0 & I \\ -M^{-1}(K_0 + K_2 v_0^2) & -M_1 C v_0 \end{pmatrix} x = Ax,$$

where I is a 2×2 identity matrix and v_0 is the velocity of the bicycle. Figure 4.18a shows the real parts of the eigenvalues as a function of velocity. Figure 4.18b shows the dependence of the eigenvalues of A on the velocity v_0 . The figures show that the bicycle is unstable for low velocities because two eigenvalues are in the right half plane. As the velocity increases these eigenvalues move into the left half plane indicating that the bicycle becomes self-stabilizing. As the velocity is increased further there is an eigenvalue close to the origin that moves into the right half plane making the bicycle unstable again. However, this eigenvalue is small so it can easily be stabilized by a rider. Figure 4.18b shows that the bicycle is self-stabilizing for velocities between 6 and 10 m/s. ∇

Parametric stability diagrams and bifurcation diagrams can provide valuable insights into the dynamics of a nonlinear system. It is usually necessary to carefully choose the parameters that one plots, including combining the natural parameters of the system to eliminate extra parameters when possible. Computer programs such as AUTO, LOCBIFF and XPPAUT provide numerical algorithms for producing stability and bifurcation diagrams.

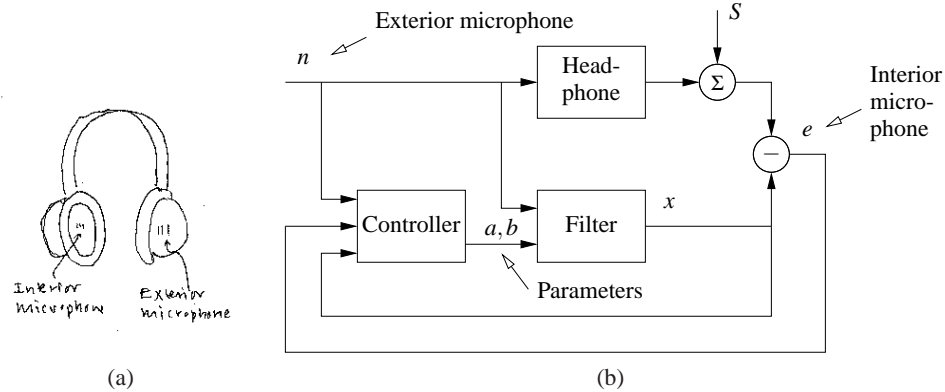


Figure 4.19: Headphones with noise cancellation. Noise is sensed by the exterior microphone (a) and sent to a filter in such a way that it cancels the noise that penetrates the headphone (b). The parameters of the filter are adjusted by the controller.

Design of Nonlinear Dynamics Using Feedback

In most of the text we will rely on linear approximations to design feedback laws that stabilize an equilibrium point and provide a desired level of performance. However, for some classes of problems the feedback controller must be nonlinear to accomplish its function. By making use of Lyapunov functions we can often design a nonlinear control law that provides stable behavior, as we saw already in Example 4.12.

One way to systematically design a nonlinear controller is to begin with a candidate Lyapunov function $V(x)$ and a control system $\dot{x} = f(x, u)$. We say that $V(x)$ is a *control Lyapunov function* if for every x there exists a u such that $\dot{V}(x) = \frac{\partial V}{\partial x} f(x, u) < 0$. In this case, it may be possible to find a function $\alpha(x)$ such that $u = \alpha(x)$ stabilizes the system. The following example illustrates the approach.

Example 4.16 Noise cancellation

Noise cancellation is used in consumer electronics and in industrial systems to reduce the effects of noise and vibrations. The idea is to locally reduce the effect of noise by generating opposing signals. A pair of headphones with noise cancellation such as those shown in Figure 4.19a is a typical example. A schematic diagram of the system is shown in Figure 4.19b. The system has two microphones, one outside the headphones that picks up exterior noise n and another inside the headphones that picks up the signal e , which is a combination of the desired signal and the external noise that penetrates the headphone. The signal from the exterior microphone is filtered and sent to the headphones in such a way that it cancels the external noise that penetrates into the headphones. The parameters of the filter are adjusted by a feedback mechanism to make the noise signal in the internal microphone as small as possible. The feedback is inherently nonlinear because it acts by changing the parameters of the filter.

To analyze the system we assume for simplicity that the propagation of external noise into the headphones is modeled by a first order dynamical system described by

$$\frac{dz}{dt} = a_0z + b_0n, \quad (4.22)$$

where z is the sound level and the parameters $a_0 < 0$ and b_0 are not known. Assume that the filter is a dynamical system of the same type

$$\frac{dw}{dt} = aw + bn.$$

We wish to find a controller that updates a and b so that they converge to the (unknown) parameters a_0 and b_0 . Introduce $x_1 = e = w - z$, $x_2 = a - a_0$ and $x_3 = b - b_0$, then

$$\frac{dx_1}{dt} = -a_0(x - z) + (a - a_0)w + (b - b_0)n = -a_0x_1 - x_2x + x_3n. \quad (4.23)$$

We will achieve noise cancellation if we can find a feedback law for changing the parameters a and b so that the error e goes to zero. To do this we choose

$$V(x_1, x_2, x_3) = \frac{1}{2}(\alpha x_1^2 + x_2^2 + x_3^2)$$

as a candidate Lyapunov function for (4.23). The derivative of V is

$$\dot{V} = \alpha x_1 \dot{x}_1 + x_2 \dot{x}_2 + x_3 \dot{x}_3 = -\alpha a_0 x_1^2 + x_2(\dot{x}_2 + \alpha x_1 w) + x_3(\dot{x}_3 + x_1 n)$$

Choosing

$$\dot{x}_2 = \alpha x_1 w = \alpha e w, \quad \dot{x}_3 = \alpha x_1 n = \alpha e n, \quad (4.24)$$

we find that $\dot{V} = -\alpha a_0 x_1^2$, and it follows that the quadratic function will decrease as long as $e = x_1 = w - z \neq 0$. The nonlinear feedback (4.24) thus attempts to change the parameters so that the error between the signal and the noise is small. Notice that feedback law (4.24) does not use the model (4.22) explicitly.

A simulation of the system is shown in Figure 4.20. In the simulation we have represented the signal as a pure sinusoid and the noise as broad band noise. The figure shows the dramatic improvement with noise cancellation. The sinusoidal signal is not visible without noise cancellation. The filter parameters change quickly from their initial values $a = b = 0$. Filters of higher order with more coefficients are used in practice. ∇

4.6 FURTHER READING

The field of dynamical systems has a rich literature that characterizes the possible features of dynamical systems and describes how parametric changes in the dynamics can lead to topological changes in behavior. Readable introductions to dynamical systems are given by Strogatz [179] and the highly illustrated text by Abraham and Shaw [2]. More technical treatments include Andronov, Vitt and

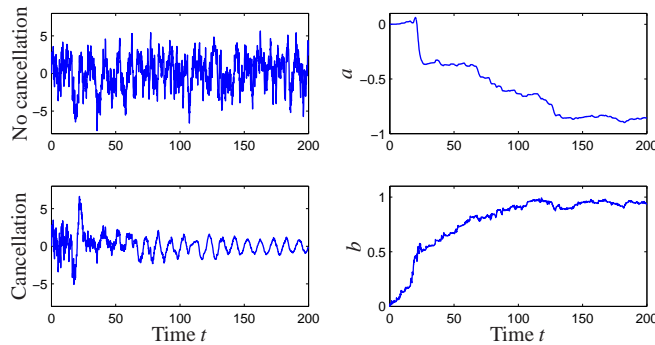


Figure 4.20: Simulation of noise cancellation. The top left figure shows the headphone signal without noise cancellation and the bottom left shows the signal with noise cancellation. The right figures show the parameters a and b of the filter.

Khaikin [8], Guckenheimer and Holmes [87] and Wiggins [192]. For students with a strong interest in mechanics, the texts by Arnold [13] and Marsden and Ratiu [139] provide an elegant approach using tools from differential geometry. Finally, nice treatments of dynamical systems methods in biology are given by Wilson [194] and Ellner and Guckenheimer [67]. There is a large literature on Lyapunov stability theory, including the classic texts by Malkin [136], Hahn [90] and Krasovskii [121]. We highly recommend the comprehensive treatment by Khalil [116].

EXERCISES

4.1 Show that if we have a solution of the differential equation (4.1) given by $x(t)$ with initial condition $x(t_0) = x_0$, then $\tilde{x}(\tau) = x(t - t_0) - x_0$ is a solution of the differential equation

$$\frac{d\tilde{x}}{d\tau} = F(\tilde{x})$$

with initial condition $\tilde{x}(0) = 0$.

4.2 A cylindrical tank has cross section $A \text{ m}^2$, effective outlet area $a \text{ m}^2$ and the inflow $q_{in} \text{ m}^3/\text{s}$. An energy balance shows that the outlet velocity is $v = \sqrt{2gh} \text{ m/s}$, where $g \text{ m/s}^2$ is the acceleration of gravity and $h \text{ m}$ is the distance between the outlet and the water level in the tank. Show that the system can be modeled by

$$\frac{dh}{dt} = -\frac{a}{A}\sqrt{2gh} - \frac{1}{A}q_{in}, \quad q_{out} = a\sqrt{2gh}.$$

Use the parameters $A = 0.2$, $a_e = 0.01$. Simulate the system when the inflow is zero and the initial level is $h = 0.2$. Do you expect some difficulties in the simulation?

4.3 Consider the cruise control system described in Section 3.1. Plot the phase portrait for the combined vehicle dynamics and PI compensator with $k_p = 1$ and $k_i = 0.5$.

4.4 Consider the second order system

$$\begin{aligned}\frac{dx_1}{dt} &= -ax_1 \\ \frac{dx_2}{dt} &= -bx_1 - cx_2.\end{aligned}$$

where $a, b, c > 0$.

(a) Check whether

$$V(x) = \frac{1}{2}x_1^2 + \frac{1}{2}x_2^2.$$

is a Lyapunov function for the system and give any conditions that must hold.

(b) Check whether

$$V(x) = \frac{1}{2}x_1^2 + \frac{1}{2}\left(x_2 - \frac{b}{c-a}x_1\right)^2.$$

is a Lyapunov function for the system and give any conditions that must hold.

(c) Use the Lyapunov equation to find another V which is a Lyapunov function for all values of the parameters.

4.5 (Damped spring-mass system) Consider a damped spring-mass system with dynamics 

$$m\ddot{q} + c\dot{q} + kq = 0.$$

A natural candidate for a Lyapunov function is the total energy of the system, given by

$$V = \frac{1}{2}m\dot{q}^2 + \frac{1}{2}kq^2.$$

Use the Krasovskii-Lasalle theorem to show that the system is asymptotically stable.

4.6 The following simple model for an electric generator connected to a strong power grid was given in Exercise 2.9:

$$J\frac{d^2\varphi}{dt^2} = P_m - P_e = P_m - \frac{EV}{X}\sin\varphi.$$

The parameter

$$a = \frac{P_{max}}{P_m} = \frac{EV}{XP_m} \quad (4.25)$$

is the ratio between the maximum deliverable power $P_{max} = EV/X$, and the mechanical power P_m .

(a) Consider a as a bifurcation parameter and discuss how the equilibria depend on a .

- (b) For the case when $a > 1$, show that there is a center at $\varphi_0 = \arcsin(1/a)$ and a saddle at $\varphi = \pi - \varphi_0$.
- (c) Show that there is a solution through the saddle that satisfies

$$\left(\frac{1}{2} \frac{d\varphi}{dt}\right)^2 - \varphi + \varphi_0 - a \cos \varphi - \sqrt{a^2 - 1} = 0. \quad (4.26)$$

Use simulation to show that the stability region is the interior of the area enclosed by this solution. Investigate what happens if the system is in equilibrium with a value of a that is slightly larger than 1 and a suddenly decreases, corresponding to the reactance of the line suddenly increasing.

4.7 Show that Lyapunov equation (4.14) always has a solution if all of the eigenvalues of A are in the left half plane. (Hint: use the fact that the Lyapunov equation is linear in P and start with the case where A has distinct eigenvalues.)

4.8 (Congestion control) Consider the congestion control problem described in Section 3.4. Confirm that the equilibrium point for the system is given by equation (3.21) and compute the stability of this equilibrium point using a linear approximation.

4.9 (Swinging up a pendulum) Consider the inverted pendulum, discussed in Example 4.4, which is described by

$$\ddot{\theta} = \sin \theta + u \cos \theta,$$

where θ is the angle between the pendulum and the vertical and the control signal u is the acceleration of the pivot. Using the energy function

$$V(\theta, \dot{\theta}) = \cos \theta - 1 + \frac{1}{2} \dot{\theta}^2,$$

show that the state feedback

$$u = k(V_0 - V)\dot{\theta} \cos \theta \quad (4.27)$$

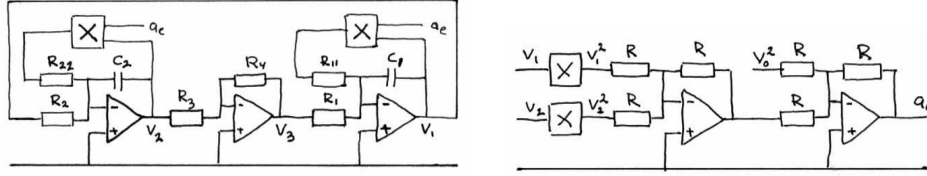
causes the pendulum to “swing up” to upright position.

4.10 (Root locus plot) Consider the linear system

$$\begin{aligned} \frac{dx}{dt} &= \begin{pmatrix} 0 & 1 \\ 0 & -3 \end{pmatrix} x + \begin{pmatrix} -1 \\ 4 \end{pmatrix} u \\ y &= \begin{pmatrix} 1 & 0 \end{pmatrix} x \end{aligned}$$

with the feedback $u = -ky$. Plot the location of the eigenvalues as a function the parameter k .

4.11 An op amp circuit for an oscillator was shown in Exercise 3.5. The oscillatory solution for that linear circuit was stable but not asymptotically stable. A schematic of a modified circuit that has nonlinear elements is shown in the figure below.



The modification is obtained by making a feedback around each operational amplifier which has capacitors using multipliers. The signal $a_e = v_1^2 + v_2^2 - v_0^2$ is the amplitude error. Show that the system is modeled by

$$\begin{aligned}\frac{dv_1}{dt} &= \frac{R_4}{R_1 R_3 C_1} v_2 + \frac{1}{R_{11} C_1} v_1 (v_0^2 - v_1^2 - v_2^2) \\ \frac{dv_2}{dt} &= -\frac{1}{R_2 C_2} v_1 + \frac{1}{R_{22} C_2} v_2 (v_0^2 - v_1^2 - v_2^2).\end{aligned}$$

Show that the circuit gives an oscillation with a stable limit cycle with amplitude v_0 . (Hint: Use the results of Example 4.8.)

4.12 (Self activating genetic circuit) Consider the dynamics of a genetic circuit that implements *self activation*: the protein produced by the gene is an activator for the protein, thus stimulating its own production. Using the models presented in Example 2.12, the dynamics for the system can be written as

$$\frac{dm}{dt} = \frac{\alpha p^2}{1 + k p^2} + \alpha_0 - \gamma m, \quad \frac{dp}{dt} = \beta m - \delta p \quad (4.28)$$

for $p, m \geq 0$. Find the equilibrium points for the system and analyze the local stability of each using Lyapunov analysis.

4.13 Let $A \in \mathbb{R}^{n \times n}$ be a matrix with real eigenvalues $\lambda_1, \dots, \lambda_n$ and corresponding eigenvectors v_1, \dots, v_n .

- Show that if the eigenvalues are distinct ($\lambda_i \neq \lambda_j$ for $i \neq j$) then $v_i \neq v_j$ for $i \neq j$.
- Show that the eigenvectors form a basis for \mathbb{R}^n so that any vector x can be written as $x = \sum \alpha_i v_i$ for $\alpha_i \in \mathbb{R}$.
- Let $T = \begin{pmatrix} v_1 & v_2 & \dots & v_n \end{pmatrix}$ and show that TAT^{-1} is a diagonal matrix of the form (4.8) on page 105.
- Show that if some of the λ_i are complex numbers, then A can be written as

$$A = \begin{pmatrix} \Lambda_1 & & 0 \\ & \ddots & \\ 0 & & \Lambda_k \end{pmatrix} \quad \text{where} \quad \Lambda_i = \lambda \in \mathbb{R} \quad \text{or} \quad \Lambda_i = \begin{pmatrix} \sigma & \omega \\ -\omega & \sigma \end{pmatrix}.$$

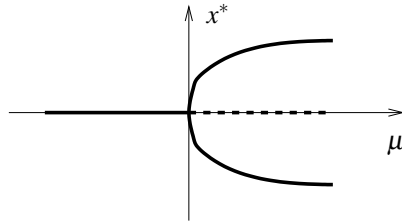
in an appropriate set of coordinates.

This form of the dynamics of a linear system is often referred to as *modal form*.

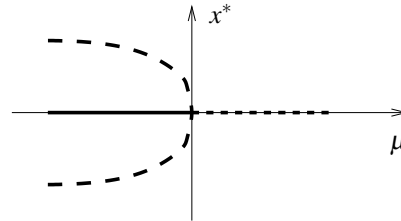
4.14 (Pitchfork bifurcation) Consider the scalar dynamical system

$$\dot{x} = \mu x - \rho x^3.$$

Show that the equilibrium values of x have the form shown below, with solid lines representing stable equilibria and dashed lines representing unstable equilibria:



(a) supercritical pitchfork



(b) subcritical pitchfork

Label each branch according to the signs of μ and ρ that correspond to the equilibrium point.

4.15 (Steering dynamics of a tanker) The normalized steering dynamics of a large tanker can be described by the equations

$$\begin{aligned} \frac{dv}{dt} &= a_1 v + a_2 r + \alpha v |v| + b_1 \delta \\ \frac{dr}{dt} &= a_3 v + a_4 r + b_2 \delta \end{aligned}$$

where v is the normalized sway velocity, i.e. the component of the velocity vector that is orthogonal to the long ship direction, r the turning rate and δ the rudder angle. (The normalization is made by using the ship length l as length unit, the time to travel one ship length as the time unit and the mass is normalized by $\rho l^3/2$, where ρ is the density of water.)

Consider the following parameters $a_1 = -0.6$, $a_2 = -0.3$, $a_3 = -5$, $a_4 = -2$, $\alpha = -2$, $b_1 = 0.1$ and $b_2 = -0.8$. Determine all steady state solutions that are obtained when the rudder is fixed in the mid ship position ($\delta = 0$). For each equilibrium point, linearize the system about the equilibrium point, determine the stability of the equilibrium point and describe how the ship will behave near this equilibrium point.

Chapter Five

Linear Systems

Few physical elements display truly linear characteristics. For example the relation between force on a spring and displacement of the spring is always nonlinear to some degree. The relation between current through a resistor and voltage drop across it also deviates from a straight-line relation. However, if in each case the relation is reasonably linear, then it will be found that the system behavior will be very close to that obtained by assuming an ideal, linear physical element, and the analytical simplification is so enormous that we make linear assumptions wherever we can possibly do so in good conscience.

R. Cannon, *Dynamics of Physical Systems*, 1967 [47].

In Chapters 2–4 we considered the construction and analysis of differential equation models for dynamical systems. In this chapter we specialize our results to the case of linear, time-invariant, input/output systems. Two central concepts are the matrix exponential and the convolution equation, through which we can completely characterize the behavior of a linear system. We also describe some properties of the input/output response and show how to approximate a nonlinear system by a linear one.

5.1 BASIC DEFINITIONS

We have seen several instances of linear differential equations in the examples of the previous chapters, including the spring-mass system (damped oscillator) and the operational amplifier in the presence of small (non-saturating) input signals. More generally, many dynamical systems can be modeled accurately by linear differential equations. Electrical circuits are one example of a broad class of systems for which linear models can be used effectively. Linear models are also broadly applicable in mechanical engineering, for example as models of small deviations from equilibria in solid and fluid mechanics. Signal processing systems, including digital filters of the sort used in CD and MP3 players, are another source of good examples, although often these are best modeled in discrete time (as described in more detail in the exercises).

In many cases, we *create* systems with linear input/output response through the use of feedback. Indeed, it was the desire for linear behavior that led Harold S. Black to the invention of the negative feedback amplifier. Almost all modern single processing systems, whether analog or digital, use feedback to produce linear or near-linear input/output characteristics. For these systems, it is often useful to represent the input/output characteristics as linear, ignoring the internal details required to get that linear response.

For other systems nonlinearities cannot be ignored, especially if one cares about the global behavior of the system. The predator-prey problem is one example of this: to capture the oscillatory behavior of the interdependent populations we must include the nonlinear coupling terms. Other examples include switching behavior and generating periodic motion for locomotion. However, if we care about what happens near an equilibrium point, it often suffices to approximate the nonlinear dynamics by their local *linearization*, as we already explored briefly in Section 4.3. The linearization is essentially an approximation of the nonlinear dynamics around the desired operating point.

Linearity

We now proceed to define linearity of input/output systems more formally. Consider a state space system of the form

$$\frac{dx}{dt} = f(x, u), \quad y = h(x, u), \quad (5.1)$$

where $x \in \mathbb{R}^n$, $u \in \mathbb{R}^p$ and $y \in \mathbb{R}^q$. As in the previous chapters, we will usually restrict ourselves to the single input, single output case by taking $p = q = 1$. We also assume that all functions are smooth and that for a reasonable class of inputs (e.g., piecewise continuous functions of time) that the solutions of equation (5.1) exist for all time.

It will be convenient to assume that the origin $x = 0$, $u = 0$ is an equilibrium point for this system ($\dot{x} = 0$) and that $h(0, 0) = 0$. Indeed, we can do so without loss of generality. To see this, suppose that $(x_e, u_e) \neq (0, 0)$ is an equilibrium point of the system with output $y_e = h(x_e, u_e)$. Then we can define a new set of states, inputs and outputs

$$\tilde{x} = x - x_e \quad \tilde{u} = u - u_e \quad \tilde{y} = y - y_e$$

and rewrite the equations of motion in terms of these variables:

$$\begin{aligned} \frac{d}{dt} \tilde{x} &= f(\tilde{x} + x_e, \tilde{u} + u_e) && =: \tilde{f}(\tilde{x}, \tilde{u}) \\ \tilde{y} &= h(\tilde{x} + x_e, \tilde{u} + u_e) - y_e && =: \tilde{h}(\tilde{x}, \tilde{u}). \end{aligned}$$

In the new set of variables, the origin is an equilibrium point with output 0, and hence we can carry out our analysis in this set of variables. Once we have obtained our answers in this new set of variables, we simply “translate” them back to the original coordinates using $x = x_e + \tilde{x}$, $u = u_e + \tilde{u}$ and $y = y_e + \tilde{y}$.

Returning to the original equations (5.1), now assuming without loss of generality that the origin is the equilibrium point of interest, we write the output $y(t)$ corresponding to initial condition $x(0) = x_0$ and input $u(t)$ as $y(t; x_0, u)$. Using this notation, a system is said to be a *linear input/output system* if the following

conditions are satisfied:

$$\begin{aligned}
 \text{(i)} \quad & y(t; \alpha x_1 + \beta x_2, 0) = \alpha y(t; x_1, 0) + \beta y(t; x_2, 0) \\
 \text{(ii)} \quad & y(t; \alpha x_0, \delta u) = \alpha y(t; x_0, 0) + \delta y(t; 0, u) \\
 \text{(iii)} \quad & y(t; 0, \delta u_1 + \gamma u_2) = \delta y(t; 0, u_1) + \gamma y(t; 0, u_2).
 \end{aligned} \tag{5.2}$$

Thus, we define a system to be linear if the outputs are jointly linear in the initial condition response and the forced response. Property (ii) is the usual decomposition of a system response into the homogeneous response ($u = 0$) and the particular response ($x_0 = 0$). Property (iii) is the formal definition of the *principle of superposition*.

The general form of a linear state space system is

$$\frac{dx}{dt} = Ax + Bu, \quad y = Cx + Du, \tag{5.3}$$

where $A \in \mathbb{R}^{n \times n}$, $B \in \mathbb{R}^{n \times p}$, $C \in \mathbb{R}^{q \times n}$, $D \in \mathbb{R}^{q \times p}$. In the special case of a single-input, single-output systems, B is a column vector, C is a row vector and D is scalar. Equation (5.3) is a system of linear, first order, differential equations with input u , state x and output y . It is easy to show that given solutions $x_1(t)$ and $x_2(t)$ for this set of equations, that they satisfy the linearity conditions.

We define the solution $x_h(t)$ with zero input as the *homogeneous* solution and the solution $x_p(t)$ with zero initial condition as the *particular* solution. Figure 5.1 illustrates how the homogeneous and particular solutions can be superimposed to form the complete solution.

It is also possible to show that if a finite dimensional dynamical system is input/output linear in the sense we have described, that it can always be represented by a state space equation of the form (5.3) through appropriate choice of state variables. In Section 5.2 we will give an explicit solution of equation (5.3) but we illustrate the basic form through a simple example.

Example 5.1 Scalar system

Consider the first order differential equation

$$\frac{dx}{dt} = ax + u, \quad y = x$$

with $x(0) = x_0$. Let $u_1 = A \sin \omega_1 t$ and $u_2 = B \cos \omega_2 t$. The homogeneous solution is $x_h(t) = e^{at} x_0$, and the two particular solutions are

$$\begin{aligned}
 x_{p1}(t) &= -A \frac{-\omega_1 e^{at} + \omega_1 \cos \omega_1 t + a \sin \omega_1 t}{a^2 + \omega_1^2}, \\
 x_{p2}(t) &= B \frac{ae^{at} - a \cos \omega_2 t + \omega_2 \sin \omega_2 t}{a^2 + \omega_2^2}.
 \end{aligned}$$

Suppose that we now choose $x(0) = \alpha x_0$ and $u = u_1 + u_2$. Then the resulting

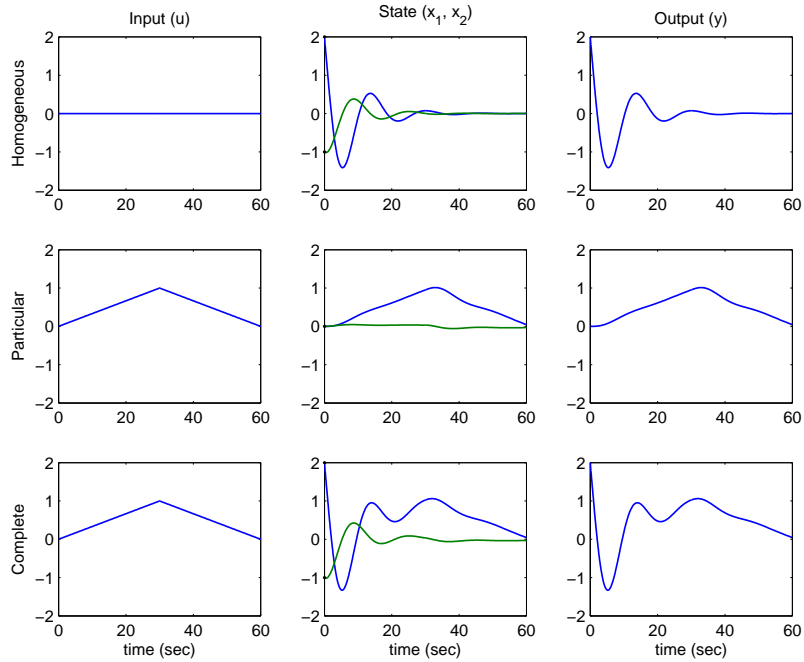


Figure 5.1: Superposition of homogeneous and particular solutions. The first row shows the input, state and output corresponding to the initial condition response. The second row shows the same variables corresponding to zero initial condition, but nonzero input. The third row is the complete solution, which is the sum of the two individual solutions.

solution is

$$x(t) = e^{at} \left(\alpha x_0 + \frac{A\omega_1}{a^2 + \omega_1^2} + \frac{Ba}{a^2 + \omega_2^2} \right) - A \frac{\omega_1 \cos \omega_1 t + a \sin \omega_1 t}{a^2 + \omega_1^2} + B \frac{-a \cos \omega_2 t + \omega_2 \sin \omega_2 t}{a^2 + \omega_2^2}. \quad (5.4)$$

To see this, substitute equation (5.4) into the differential equation. Thus, the properties of a linear system are satisfied. ∇

Time Invariance

Time invariance is an important concept that is used to describe a system whose properties do not change with time. More precisely, for a time invariant system if the input $u(t)$ gives output $y(t)$, then if we shift the time at which the input is applied by a constant amount a , $u(t+a)$ gives the output $y(t+a)$. Systems that are linear and time-invariant, often called *LTI systems*, have the interesting property that their response to an arbitrary input is completely characterized by their response to step inputs or their response to short “impulses”.

To explore the consequences of time-invariance, we first compute the response

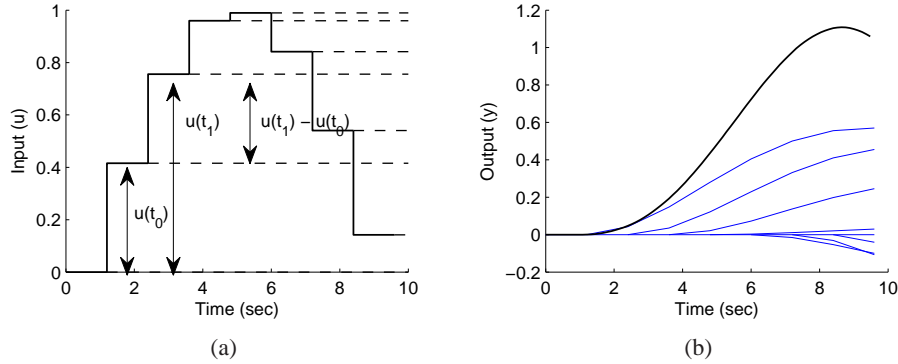


Figure 5.2: Response to piecewise constant inputs. A piecewise constant signal can be represented as a sum of step signals (a) and the resulting output is the sum of the individual outputs (b).

to a piecewise constant input. Assume that the system is initially at rest and consider the piecewise constant input shown in Figure 5.2a. The input has jumps at times t_k and its values after the jumps are $u(t_k)$. The input can be viewed as a combination of steps: the first step at time t_0 has amplitude $u(t_0)$, the second step at time t_1 has amplitude $u(t_1) - u(t_0)$, etc.

Assuming that the system is initially at an equilibrium point (so that the initial condition response is zero), the response to the input can be obtained by superimposing the responses to a combination of step inputs. Let $H(t)$ be the response to a unit step applied at time 0. The response to the first step is then $H(t - t_0)u(t_0)$, the response to the second step is $H(t - t_1)(u(t_1) - u(t_0))$, and we find that the complete response is given by

$$\begin{aligned}
 y(t) &= H(t - t_0)u(t_0) + H(t - t_1)(u(t_1) - u(t_0)) + \cdots \\
 &= (H(t) - H(t - t_1))u(t_0) + (H(t - t_1) - H(t - t_2))u(t_1) + \cdots \\
 &= \sum_{n=0}^{\infty} (H(t - t_n) - H(t - t_{n+1}))u(t_n) \\
 &= \sum_{n=0}^{\infty} \frac{H(t - t_n) - H(t - t_{n+1})}{t_{n+1} - t_n} u(t_n) (t_{n+1} - t_n).
 \end{aligned}$$

An example of this computation is shown in Figure 5.2.

The response to a continuous input signal is obtained by taking the limit as $t_{n+1} - t_n \rightarrow 0$, which gives

$$y(t) = \int_0^{\infty} H'(t - \tau)u(\tau)d\tau, \quad (5.5)$$

where H' is the derivative of the step response, also called the *impulse response*. The response of a linear time-invariant system to any input can thus be computed from the step response. Notice that the output only depends on the input since we

assumed the system was initially at rest, $x(0) = 0$. We will derive equation (5.5) in a slightly different way in the next section.

5.2 THE MATRIX EXPONENTIAL

Equation (5.5) shows that the output of a linear system can be written as an integral over the inputs $u(t)$. In this section and the next we derive a more general version of this formula, which includes nonzero initial conditions. We begin by exploring the initial condition response using the matrix exponential.

Initial Condition Response

Although we have shown that the solution of a linear set of differential equations defines a linear input/output system, we have not fully computed the solution of the system. We begin by considering the homogeneous response corresponding to the system

$$\frac{dx}{dt} = Ax. \quad (5.6)$$

For the *scalar* differential equation

$$\dot{x} = ax \quad x \in \mathbb{R}, a \in \mathbb{R}$$

the solution is given by the exponential

$$x(t) = e^{at}x(0).$$

We wish to generalize this to the vector case, where A becomes a matrix. We define the *matrix exponential* as the infinite series

$$e^X = I + X + \frac{1}{2}X^2 + \frac{1}{3!}X^3 + \cdots = \sum_{k=0}^{\infty} \frac{1}{k!}X^k, \quad (5.7)$$

where $X \in \mathbb{R}^{n \times n}$ is a square matrix and I is the $n \times n$ identity matrix. We make use of the notation

$$X^0 = I \quad X^2 = XX \quad X^n = X^{n-1}X,$$

which defines what we mean by the “power” of a matrix. Equation (5.7) is easy to remember since it is just the Taylor series for the scalar exponential, applied to the matrix X . It can be shown that the series in equation (5.7) converges for any matrix $X \in \mathbb{R}^{n \times n}$ in the same way that the normal exponential is defined for any scalar $a \in \mathbb{R}$.

Replacing X in equation (5.7) by At where $t \in \mathbb{R}$ we find that

$$e^{At} = I + At + \frac{1}{2}A^2t^2 + \frac{1}{3!}A^3t^3 + \cdots = \sum_{k=0}^{\infty} \frac{1}{k!}A^k t^k,$$

and differentiating this expression with respect to t gives

$$\frac{d}{dt}e^{At} = A + A^2t + \frac{1}{2}A^3t^2 + \cdots = A \sum_{k=0}^{\infty} \frac{1}{k!}A^k t^k = Ae^{At}. \quad (5.8)$$

Multiplying by $x(0)$ from the right we find that $x(t) = e^{At}x(0)$ is the solution to the differential equation (5.6) with initial condition $x(0)$. We summarize this important result as a proposition.

Proposition 5.1. *The solution to the homogeneous system of differential equations (5.6) is given by*

$$x(t) = e^{At}x(0).$$

Notice that the form of the solution is exactly the same as for scalar equations, but we must put the vector $x(0)$ on the right of the matrix e^{At} .

The form of the solution immediately allows us to see that the solution is linear in the initial condition. In particular, if $x_{h1}(t)$ is the solution to equation (5.6) with initial condition $x(0) = x_{01}$ and $x_{h2}(t)$ with initial condition $x(0) = x_{02}$, then the solution with initial condition $x(0) = \alpha x_{01} + \beta x_{02}$ is given by

$$x(t) = e^{At}(\alpha x_{01} + \beta x_{02}) = (\alpha e^{At}x_{01} + \beta e^{At}x_{02}) = \alpha x_{h1}(t) + \beta x_{h2}(t).$$

Similarly, we see that the corresponding output is given by

$$y(t) = Cx(t) = \alpha y_{h1}(t) + \beta y_{h2}(t),$$

where $y_{h1}(t)$ and $y_{h2}(t)$ are the outputs corresponding to $x_{h1}(t)$ and $x_{h2}(t)$.

We illustrate computation of the matrix exponential by two examples.

Example 5.2 Double integrator

A very simple linear system that is useful for understanding basic concepts is the second order system given by

$$\begin{aligned} \ddot{q} &= u \\ y &= q. \end{aligned}$$

This system is called a *double integrator* because the input u is integrated twice to determine the output y .

In state space form, we write $x = (q, \dot{q})$ and

$$\frac{dx}{dt} = \begin{pmatrix} 0 & 1 \\ 0 & 0 \end{pmatrix} x + \begin{pmatrix} 0 \\ 1 \end{pmatrix} u.$$

The dynamics matrix of a double integrator is

$$A = \begin{pmatrix} 0 & 1 \\ 0 & 0 \end{pmatrix}$$

and we find by direct calculation that $A^2 = 0$ and hence

$$e^{At} = \begin{pmatrix} 1 & t \\ 0 & 1 \end{pmatrix}.$$

Thus the homogeneous solution ($u = 0$) for the double integrator is given by

$$\begin{aligned} x(t) &= \begin{pmatrix} 1 & t \\ 0 & 1 \end{pmatrix} \begin{pmatrix} x_1(0) \\ x_2(0) \end{pmatrix} = \begin{pmatrix} x_1(0) + tx_2(0) \\ x_2(0) \end{pmatrix} \\ y(t) &= x_1(0) + tx_2(0). \end{aligned}$$

▽

Example 5.3 Undamped oscillator

A simple model for an oscillator, such as the spring-mass system with zero damping, is

$$\ddot{q} + \omega_0^2 q = u.$$

Putting the system into state space form, the dynamics matrix for this system can be written as

$$A = \begin{pmatrix} 0 & \omega_0 \\ -\omega_0 & 0 \end{pmatrix} \quad \text{and} \quad e^{At} = \begin{pmatrix} \cos \omega_0 t & \sin \omega_0 t \\ -\sin \omega_0 t & \cos \omega_0 t \end{pmatrix}.$$

This expression for e^{At} can be verified by differentiation:

$$\begin{aligned} \frac{d}{dt} e^{At} &= \begin{pmatrix} -\omega_0 \sin \omega_0 t & \omega_0 \cos \omega_0 t \\ -\omega_0 \cos \omega_0 t & -\omega_0 \sin \omega_0 t \end{pmatrix} \\ &= \begin{pmatrix} 0 & \omega_0 \\ -\omega_0 & 0 \end{pmatrix} \begin{pmatrix} \cos \omega_0 t & \sin \omega_0 t \\ -\sin \omega_0 t & \cos \omega_0 t \end{pmatrix} = Ax(t). \end{aligned}$$

The solution is then given by

$$x(t) = e^{At} x(0) = \begin{pmatrix} \cos \omega_0 t & \sin \omega_0 t \\ -\sin \omega_0 t & \cos \omega_0 t \end{pmatrix} \begin{pmatrix} x_1(0) \\ x_2(0) \end{pmatrix}.$$

If $\zeta \neq 0$ then the solution is more complicated, but the matrix exponential can be shown to be

$$e^{-\omega_0 \zeta t} \begin{pmatrix} \frac{\zeta e^{i\omega_d t} - \zeta e^{-i\omega_d t}}{2\sqrt{\zeta^2 - 1}} + \frac{e^{i\omega_d t} + e^{-i\omega_d t}}{2} & \frac{e^{i\omega_d t} - e^{-i\omega_d t}}{2\sqrt{\zeta^2 - 1}} \\ \frac{e^{-i\omega_d t} - e^{i\omega_d t}}{2\sqrt{\zeta^2 - 1}} & \frac{\zeta e^{-i\omega_d t} - \zeta e^{i\omega_d t}}{2\sqrt{\zeta^2 - 1}} + \frac{e^{i\omega_d t} + e^{-i\omega_d t}}{2} \end{pmatrix},$$

where $\omega_d = \omega_0 \sqrt{\zeta^2 - 1}$. Note that ω_d and $\sqrt{\zeta^2 - 1}$ can either be real or complex, but the combinations of terms will always yield a real value for the entries in the matrix exponential. ▽

An important class of linear systems are those that can be converted into diagonal form. Suppose that we are given a system

$$\frac{dx}{dt} = Ax$$

such that all of the eigenvalues of A are distinct. It can be shown (Exercise 4.13) that we can find an invertible matrix T such that TAT^{-1} is diagonal. If we choose

a set of coordinates $z = Tx$, then in the new coordinates the dynamics become

$$\frac{dz}{dt} = T \frac{dx}{dt} = TAx = TAT^{-1}z.$$

By construction of T , this system will be diagonal.

Now consider a diagonal matrix A and the corresponding k th power of At , which is also diagonal:

$$A = \begin{pmatrix} \lambda_1 & & & 0 \\ & \lambda_2 & & \\ & & \ddots & \\ 0 & & & \lambda_n \end{pmatrix} \quad (At)^k = \begin{pmatrix} \lambda_1^k t^k & & & 0 \\ & \lambda_2^k t^k & & \\ & & \ddots & \\ 0 & & & \lambda_n^k t^k \end{pmatrix},$$

It follows from the series expansion that the matrix exponential is given by

$$e^{At} = \begin{pmatrix} e^{\lambda_1 t} & & & 0 \\ & e^{\lambda_2 t} & & \\ & & \ddots & \\ 0 & & & e^{\lambda_n t} \end{pmatrix}.$$

A similar expansion can be done in the case that the eigenvalues are complex, using a block diagonal matrix, similar to what was done in Section 4.3.

Jordan Form



Some matrices with equal eigenvalues cannot be transformed to diagonal form. They can however be transformed to a closely related form, called the *Jordan form*, in which the dynamics matrix has the eigenvalues along the diagonal. When there are equal eigenvalues there may be 1s appearing in the super diagonal indicating that there is coupling between the states.

More specifically, we define a matrix to be in Jordan form if it can be written as

$$J = \begin{pmatrix} J_1 & 0 & \dots & 0 \\ 0 & J_2 & & \\ 0 & \dots & \ddots & \\ 0 & \dots & & J_k \end{pmatrix} \quad \text{where} \quad J_i = \begin{pmatrix} \lambda_i & 1 & 0 & \dots & 0 \\ 0 & \lambda_i & 1 & & 0 \\ \vdots & & \ddots & \ddots & \vdots \\ 0 & 0 & \dots & \lambda_i & 1 \\ 0 & 0 & \dots & 0 & \lambda_i \end{pmatrix}. \quad (5.9)$$

Each matrix J_i is called a *Jordan block* and λ_i for that block corresponds to an eigenvalue of J . A first order Jordan block can be represented as a system consisting of an integrator with the feedback λ . Jordan of higher order can be represented as series connections of such systems, as illustrated in Figure 5.3.

Theorem 5.2 (Jordan decomposition). *Any matrix $A \in \mathbb{R}^{n \times n}$ can be transformed into Jordan form with the eigenvalues of A determining λ_i in the Jordan form.*

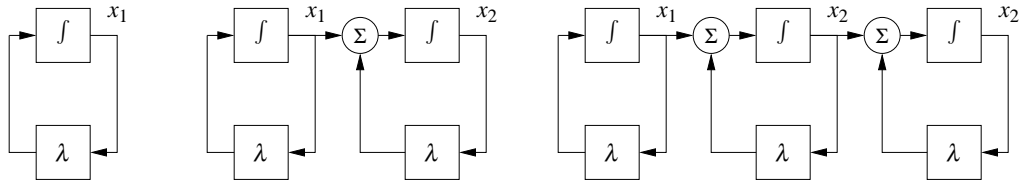


Figure 5.3: Representation of linear system where the dynamics matrix is a Jordan block. A first order Jordan block can be represented as an integrator with feedback λ , as shown on the left. Second and third order Jordan blocks can be represented as series connections of integrators with feedback, as shown on the right.

Proof. See any standard text on linear algebra, such as Strang [178]. The special case where the eigenvalues are distinct is examined in Exercise 4.13. \square

Converting a matrix into Jordan form can be complicated, although MATLAB can do this conversion for numerical matrices using the `jordan` function. The structure of the resulting Jordan form is particularly interesting since there is no requirement that the individual λ_i 's be unique, and hence for a given eigenvalue we can have one or more Jordan blocks of different size.

Once a matrix is in Jordan form, the exponential of the matrix can be computed in terms of the Jordan blocks:

$$e^J = \begin{pmatrix} e^{J_1} & 0 & \dots & 0 \\ 0 & e^{J_2} & & 0 \\ 0 & \dots & \ddots & 0 \\ 0 & \dots & & e^{J_k} \end{pmatrix}. \tag{5.10}$$

This follows from the block diagonal form of J . The exponentials of the Jordan blocks can in turn be written as

$$e^{J_i t} = \begin{pmatrix} e^{\lambda_i t} & t e^{\lambda_i t} & \frac{t^2}{2!} e^{\lambda_i t} & \dots & \frac{t^{n-1}}{(n-1)!} e^{\lambda_i t} \\ 0 & e^{\lambda_i t} & t e^{\lambda_i t} & \dots & \frac{t^{n-2}}{(n-2)!} e^{\lambda_i t} \\ & & e^{\lambda_i t} & \ddots & \vdots \\ & & & \ddots & t e^{\lambda_i t} \\ 0 & & & & e^{\lambda_i t} \end{pmatrix}. \tag{5.11}$$

When there are multiple eigenvalues, the invariant subspaces associated with each eigenvalue correspond to the Jordan blocks of the matrix A . Note that λ may be complex, in which case the transformation T that converts a matrix into Jordan form will also be complex. When λ has a nonzero imaginary component, the solutions will have oscillatory components since

$$e^{\sigma + i\omega t} = e^{\sigma t} (\cos \omega t + i \sin \omega t).$$

We can now use these results to prove Theorem 4.1, which states that the equilibrium point $x_e = 0$ of a linear system is asymptotically stable if and only if $\text{Re } \lambda_i < 0$.

Proof of Theorem 4.1. Let $T \in \mathbb{C}^{n \times n}$ be an invertible matrix that transforms A into Jordan form, $J = TAT^{-1}$. Using coordinates $z = Tx$, we can write the solution $z(t)$ as

$$z(t) = e^{Jt}z(0).$$

Since any solution $x(t)$ can be written in terms of a solution $z(t)$ with $z(0) = Tx(0)$, it follows that it is sufficient to prove the theorem in the transformed coordinates.

The solution $z(t)$ can be written as a combination of the elements of the matrix exponential and from equation (5.11) these elements all decay to zero for arbitrary $z(0)$ if and only if $\operatorname{Re} \lambda_i < 0$. Furthermore, if any λ_i has positive real part, then there exists an initial condition $z(0)$ such that the corresponding solution increases without bound. Since we can scale this initial condition to be arbitrarily small, it follows that the equilibrium point is unstable if any eigenvalue has positive real part. \square

The existence of a canonical form allows us to prove many properties of linear systems by changing to a set of coordinates in which the A matrix is in Jordan form. This will be used in Chapters 6 and 7 to design controllers. We illustrate this in the following proposition, which follows along the same lines as the proof of Theorem 4.1.

Proposition 5.3. *Suppose that the system*

$$\dot{x} = Ax$$

has no eigenvalues with strictly positive real part and one or more eigenvalues with zero real part. Then the system is stable if and only if the Jordan blocks corresponding to each eigenvalue with zero real part are scalar (1×1) blocks.

Proof. See Exercise 5.7. \square

The following example illustrates the use of Jordan form.

Example 5.4 Linear model of a thrust vectored aircraft.

Consider the dynamics of a thrust vectored aircraft such as that described in Example 2.9. Suppose that we choose $u_1 = u_2 = 0$, so that the dynamics of the system become

$$\frac{d\xi}{dt} = \begin{pmatrix} \xi_4 \\ \xi_5 \\ \xi_6 \\ -g \sin \xi_3 - \frac{c}{m} \xi_1 \\ -g(\cos \xi_3 - 1) - \frac{c}{m} \xi_2 \\ 0 \end{pmatrix}, \quad (5.12)$$

where $\xi = (x, y, \theta, \dot{x}, \dot{y}, \dot{\theta})$. The equilibrium points for the system are given by setting the velocities \dot{x}_e, \dot{y}_e and $\dot{\theta}_e$ to zero and choosing the remaining variables to satisfy

$$\begin{aligned} -g \sin \xi_{3,e} &= 0 \\ -g(\cos \xi_{3,e} - 1) &= 0 \end{aligned} \quad \implies \quad \xi_{3,e} = \theta_e = 0.$$

This corresponds to the upright orientation for the aircraft. Note that x_e and y_e are not specified. This is because we can translate the system to a new (upright) position and we still obtain an equilibrium point.

To compute the stability of the equilibrium point, we compute the linearization using equation (4.11):

$$A = \left. \frac{\partial F}{\partial \xi} \right|_{\xi_e} = \begin{pmatrix} 0 & 0 & 0 & 1 & 0 & 0 \\ 0 & 0 & 0 & 0 & 1 & 0 \\ 0 & 0 & 0 & 0 & 0 & 1 \\ 0 & 0 & -g & -c/m & 0 & 0 \\ 0 & 0 & 0 & 0 & -c/m & 0 \\ 0 & 0 & 0 & 0 & 0 & 0 \end{pmatrix}.$$

The eigenvalues of the system can be computed as

$$\lambda(A) = \{0, 0, 0, 0, -c/m, -c/m\}.$$

We see that the linearized system is not asymptotically stable since not all of the eigenvalues have strictly negative real part.

To determine with the system is stable in the sense of Lyapunov, we must make use of the Jordan form. It can be shown that the Jordan form of A is given by

$$J = \left(\begin{array}{cccc|cc} 0 & 0 & 0 & 0 & 0 & 0 \\ 0 & 0 & 1 & 0 & 0 & 0 \\ 0 & 0 & 0 & 1 & 0 & 0 \\ 0 & 0 & 0 & 0 & 0 & 0 \\ \hline 0 & 0 & 0 & 0 & -c/m & 0 \\ \hline 0 & 0 & 0 & 0 & 0 & -c/m \end{array} \right)$$

Since the second Jordan block has eigenvalue 0 and is not a simple eigenvalue, the linearization is unstable. ∇

Eigenvalues and Modes

The eigenvalues and eigenvectors of a system provide a description of the types of behavior the system can exhibit. For oscillatory systems, the term *mode* is often used to describe the vibration patterns that can occur. Figure 5.4 illustrates modes for a system consisting of two masses connected by springs. One pattern is when both masses oscillate left and right in unison, another is when the masses moves towards and from each other.

The initial condition response of a linear system can be written in terms of a matrix exponential involving the dynamics matrix A . The properties of the matrix A therefore determine the resulting behavior of the system. Given a matrix $A \in \mathbb{R}^{n \times n}$, recall that v is an eigenvector of A with eigenvalue λ if

$$Av = \lambda v.$$

In general λ and v may be complex valued, although if A is real-valued then for any eigenvalue λ , its complex conjugate λ^* will also be an eigenvalue (with v^* as

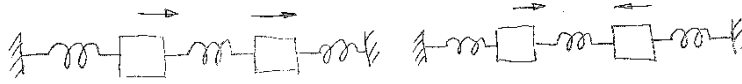


Figure 5.4: Modes of vibration for a system consisting of two masses connected by springs. In (a) the masses move left and right in synchronization in (b) they move towards or against each other.

the corresponding eigenvector).

Suppose first that λ and v are a real-valued eigenvalue/eigenvector pair for A . If we look at the solution of the differential equation for $x(0) = v$, it follows from the definition of the matrix exponential that

$$e^{At}v = \left(I + At + \frac{1}{2}A^2t^2 + \dots\right)v = v + \lambda tv + \frac{\lambda^2 t^2}{2}v + \dots = e^{\lambda t}v.$$

The solution thus lies in the subspace spanned by the eigenvector. The eigenvalue λ describes how the solution varies in time and this solution is often called a *mode* of the system. (In the literature, the term mode is also often used to refer to the eigenvalue, rather than the solution.)

If we look at the individual elements of the vectors x and v , it follows that

$$\frac{x_i(t)}{x_j(t)} = \frac{e^{\lambda t}v_i}{e^{\lambda t}v_j},$$

and hence the ratios of the components of the state x are constants for a (real) mode. The eigenvector thus gives the “shape” of the solution and is also called a *mode shape* of the system. Figure 5.5 illustrates the modes for a second order system consisting of a fast mode and a slow mode. Notice that the state variables have the same sign for the slow mode different signs for the fast mode.

The situation is more complicated when the eigenvalues of A are complex. Since A has real elements, the eigenvalues and the eigenvectors are complex conjugates $\lambda = \sigma \pm i\omega$ and $v = u \pm iw$, which implies that

$$u = \frac{v + v^*}{2} \quad w = \frac{v - v^*}{2i}.$$

Making use of the matrix exponential, we have

$$e^{At}v = e^{\lambda t}(u + iw) = e^{\sigma t}((u \cos \omega t - w \sin \omega t) + i(u \sin \omega t + w \cos \omega t)),$$

which implies

$$\begin{aligned} e^{At}u &= \frac{1}{2} \left(e^{At}v + e^{At}v^* \right) = ue^{\sigma t} \cos \omega t - we^{\sigma t} \sin \omega t \\ e^{At}w &= \frac{1}{2i} \left(e^{At}v - e^{At}v^* \right) = ue^{\sigma t} \sin \omega t + we^{\sigma t} \cos \omega t. \end{aligned}$$

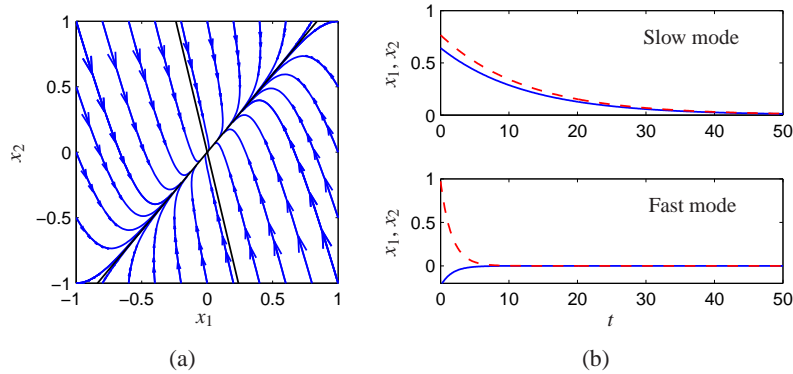


Figure 5.5: Illustration of the notion of modes for a second order system with real eigenvalues. The left figure (a) shows the phase plane and the modes corresponds to solutions that start on the eigenvectors (bold lines). The corresponding time functions are shown in (b).

A solution with initial conditions in the subspace spanned by the real part u and imaginary part w of the eigenvector will thus remain in that subspace. The solution will be a logarithmic spiral characterized by σ and ω . We again call the solution corresponding to λ a mode of the system and v the mode shape.

If a matrix A has n distinct eigenvalues $\lambda_1, \dots, \lambda_n$, then the initial condition response can be written as a linear combination of the modes. To see this, suppose for simplicity that we have all real eigenvalues with corresponding unit eigenvectors v_1, \dots, v_n . From linear algebra, these eigenvectors are linearly independent and we can write the initial condition $x(0)$ as

$$x(0) = \alpha_1 v_1 + \alpha_2 v_2 + \dots + \alpha_n v_n.$$

Using linearity, the initial condition response can be written as

$$x(t) = \alpha_1 e^{\lambda_1 t} v_1 + \alpha_2 e^{\lambda_2 t} v_2 + \dots + \alpha_n e^{\lambda_n t} v_n.$$

Thus, the response is a linear combination the modes of the system, with the amplitude of the individual modes growing or decaying as $e^{\lambda_i t}$. The case for distinct complex eigenvalues follows similarly (the case for non-distinct eigenvalues is more subtle and requires making use of the Jordan form discussed in the previous section).

Example 5.5 Coupled spring-mass system

Consider the spring-mass system shown in Figure 5.4. The equation of motion of the system are

$$\begin{aligned} m_1 \ddot{q}_1 &= -2kq_1 - c\dot{q}_1 + kq_2 \\ m_2 \ddot{q}_2 &= kq_1 - 2kq_2 - c\dot{q}_2 \end{aligned}$$

In state-space form, we define the state to be $x = (q_1, q_2, \dot{q}_1, \dot{q}_2)$ and we can rewrite

the equations as

$$\frac{dx}{dt} = \begin{pmatrix} 0 & 0 & 1 & 0 \\ 0 & 0 & 0 & 1 \\ -\frac{2k}{m} & \frac{k}{m} & -\frac{c}{m} & 0 \\ \frac{k}{m} & -\frac{2k}{m} & 0 & -\frac{c}{m} \end{pmatrix} x.$$

We now define a transformation $z = Tx$ that puts this system into a simpler form. Let $z_1 = \frac{1}{2}(q_1 + q_2)$, $z_2 = \dot{z}_1$, $z_3 = \frac{1}{2}(q_1 - q_2)$ and $z_4 = \dot{z}_3$, so that

$$z = Tx = \frac{1}{2} \begin{pmatrix} 1 & 1 & 0 & 0 \\ 0 & 0 & 1 & 1 \\ 1 & -1 & 0 & 0 \\ 0 & 0 & 1 & -1 \end{pmatrix} x.$$

In the new coordinates, the dynamics become

$$\frac{dz}{dt} = \begin{pmatrix} 0 & 1 & 0 & 0 \\ -\frac{k}{m} & -\frac{c}{m} & 0 & 0 \\ 0 & 0 & 0 & 1 \\ 0 & 0 & -\frac{3k}{m} & -\frac{c}{m} \end{pmatrix} z.$$

and we see that the system is in block diagonal (or *modal*) form.

In the z coordinates, the states z_1 and z_2 parameterize one mode with eigenvalues $\lambda \approx c/(2\sqrt{km}) \pm i\sqrt{k/m}$, and the states z_3 and z_4 another mode with $\lambda \approx c/(2\sqrt{3km}) \pm i\sqrt{3k/m}$. From the form of the transformation T we see that these modes correspond exactly to the modes in Figure 5.4, in which q_1 and q_2 move either toward or against each other. The real and imaginary parts of the eigenvalues give the decay rates σ and frequencies ω for each mode. ∇

5.3 INPUT/OUTPUT RESPONSE

In the previous section we saw how to compute the initial condition response using the matrix exponential. In this section we derive the *convolution equation*, which includes the inputs and outputs as well.

The Convolution Equation

We return to the general input/output case in equation (5.3), repeated here:

$$\begin{aligned} \frac{dx}{dt} &= Ax + Bu \\ y &= Cx + Du. \end{aligned} \tag{5.13}$$

Using the matrix exponential, the solution to equation (5.13) can be written as follows.

Theorem 5.4. *The solution to the linear differential equation (5.13) is given by*

$$x(t) = e^{At}x(0) + \int_0^t e^{A(t-\tau)}Bu(\tau)d\tau. \quad (5.14)$$

Proof. To prove this, we differentiate both sides and use the property (5.8) of the matrix exponential. This gives

$$\frac{dx}{dt} = Ae^{At}x(0) + \int_0^t Ae^{A(t-\tau)}Bu(\tau)d\tau + Bu(t) = Ax + Bu,$$

which proves the result. Notice that the calculation is essentially the same as for proving the result for a first order equation. \square

It follows from equations (5.13) and (5.14) that the input/output relation for a linear system is given by

$$y(t) = Ce^{At}x(0) + \int_0^t Ce^{A(t-\tau)}Bu(\tau)d\tau + Du(t). \quad (5.15)$$

It is easy to see from this equation that the output is jointly linear in both the initial conditions and the state, which follows from the linearity of matrix/vector multiplication and integration.

Equation (5.15) is called the *convolution equation* and it represents the general form of the solution of a system of coupled linear differential equations. We see immediately that the dynamics of the system, as characterized by the matrix A , play a critical role in both the stability and performance of the system. Indeed, the matrix exponential describes *both* what happens when we perturb the initial condition and how the system responds to inputs.



Another interpretation of the convolution equation can be given using the concept of the *impulse response* of a system. Consider the application of an input signal $u(t)$ given by the following equation:

$$u(t) = p_\varepsilon(t) = \begin{cases} 0 & t < 0 \\ 1/\varepsilon & 0 \leq t < \varepsilon \\ 0 & t \geq \varepsilon. \end{cases} \quad (5.16)$$

This signal is a “pulse” of duration ε and amplitude $1/\varepsilon$, as illustrated in Figure 5.6a. We define an *impulse*, $\delta(t)$, to be the limit of this signal as $\varepsilon \rightarrow 0$:

$$\delta(t) = \lim_{\varepsilon \rightarrow 0} p_\varepsilon(t). \quad (5.17)$$

This signal, sometimes called a *delta function*, is not physically achievable but provides a convenient abstraction for understanding the response of a system. Note

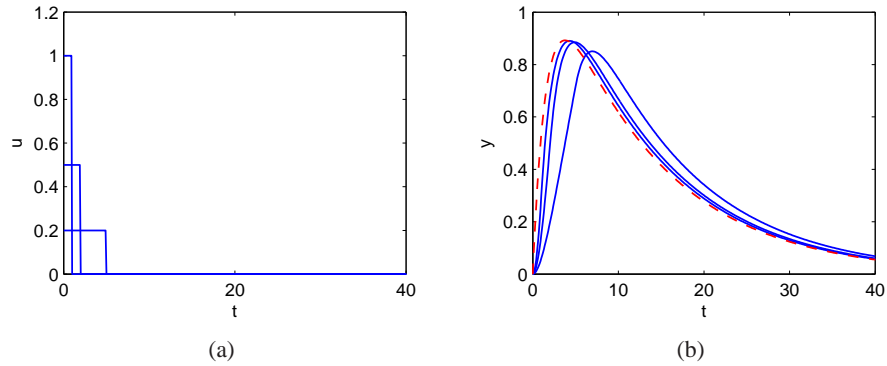


Figure 5.6: Pulse response and impulse response. The figure on the left shows pulses of width 5, 2 and 1, each with total area equal to 1. The corresponding pulse responses for a linear system with eigenvalues $\lambda = \{-0.08, -0.62\}$ are shown on the right as solid lines. The dashed line is the true impulse response, which is well-approximated by a pulse of duration 1.

that the integral of an impulse is one:

$$\begin{aligned} \int_0^t \delta(\tau) d\tau &= \int_0^t \lim_{\varepsilon \rightarrow 0} p_\varepsilon(t) d\tau = \lim_{\varepsilon \rightarrow 0} \int_0^t p_\varepsilon(t) d\tau \\ &= \lim_{\varepsilon \rightarrow 0} \int_0^\varepsilon 1/\varepsilon d\tau = 1 \quad t > 0. \end{aligned}$$

In particular, the integral of an impulse over an arbitrarily short period of time is identically 1.

We define the *impulse response* of a system, $h(t)$, to be the output corresponding to having an impulse as its input:

$$h(t) = \int_0^t C e^{A(t-\tau)} B \delta(\tau) d\tau = C e^{At} B, \quad (5.18)$$

where the second equality follows from the fact that $\delta(t)$ is zero everywhere except the origin and its integral is identically one. We can now write the convolution equation in terms of the initial condition response, the convolution of the impulse response and the input signal, and the direct term:

$$y(t) = C e^{At} x(0) + \int_0^t h(t-\tau) u(\tau) d\tau + D u(t). \quad (5.19)$$

One interpretation of this equation, explored in Exercise 5.2, is that the response of the linear system is the superposition of the response to an infinite set of shifted impulses whose magnitude is given by the input, $u(t)$. This is essentially the argument used in analyzing Figure 5.2 and deriving equation (5.5). Note that the second term in equation (5.19) is identical to equation (5.5) and it can be shown that the impulse response is formally equivalent to the derivative of the step response.

The use of pulses as an approximation of the impulse response also provides a mechanism for identifying the dynamics of a system from data. Figure 5.6b shows the pulse responses of a system for different pulse widths. Notice that the pulse responses approaches the impulse response as the pulse width goes to zero. As a general rule, if the fastest eigenvalue of a stable system has real part $-\sigma_{\max}$, then a pulse of length ε will provide a good estimate of the impulse response if $\varepsilon\sigma_{\max} \ll 1$. Note that for Figure 5.6, a pulse width of $\varepsilon = 1$ s gives $\varepsilon\sigma_{\max} = 0.62$ and the pulse response is already close to the impulse response.

Coordinate Invariance

The components of the input vector u and the output vector y are given by the chosen inputs and outputs of a model, but the state variables depend on the coordinate frame chosen to represent the state. This choice of coordinates affects the values of the matrices A , B and C that are used in the model. (The direct term D is not affected since it maps inputs to outputs.) We now investigate some of the consequences of changing coordinate systems.

Introduce new coordinates z by the transformation $z = Tx$, where T is an invertible matrix. It follows from equation (5.3) that

$$\begin{aligned}\frac{dz}{dt} &= T(Ax + Bu) = TAT^{-1}z + TBu = \tilde{A}z + \tilde{B}u \\ y &= Cx + Du = CT^{-1}z + Du = \tilde{C}z + Du.\end{aligned}$$

The transformed system has the same form as equation (5.3) but the matrices A , B and C are different:

$$\tilde{A} = TAT^{-1} \quad \tilde{B} = TB \quad \tilde{C} = CT^{-1}. \quad (5.20)$$

There are often special choices of coordinate systems that allow us to see a particular property of the system, hence coordinate transformations can be used to gain new insight into the dynamics.

We can also compare the solution of the system in transformed coordinates to that in the original state coordinates. We make use of an important property of the exponential map,

$$e^{TST^{-1}} = Te^ST^{-1},$$

which can be verified by substitution in the definition of the exponential map. Using this property, it is easy to show that

$$x(t) = T^{-1}z(t) = T^{-1}e^{\tilde{A}t}Tx(0) + T^{-1}\int_0^t e^{\tilde{A}(t-\tau)}\tilde{B}u(\tau)d\tau.$$

From this form of the equation, we see that if it is possible to transform A into a form \tilde{A} for which the matrix exponential is easy to compute, we can use that computation to solve the general convolution equation for the untransformed state x by simple matrix multiplications. This technique is illustrated in the following examples.

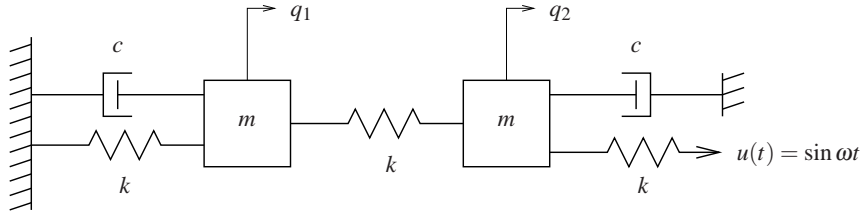


Figure 5.7: Coupled spring mass system. Each mass is connected to two springs with stiffness k and a viscous damper with damping coefficient c . The mass on the right is driven through a spring connected to a sinusoidally varying attachment.

Example 5.6 Coupled spring-mass system

Consider the coupled spring-mass system shown in Figure 5.7. The input to this system is the sinusoidal motion of the end of rightmost spring and the output is the position of each mass, q_1 and q_2 . The equations of motion are given by

$$\begin{aligned} m_1 \ddot{q}_1 &= -2kq_1 - c\dot{q}_1 + kq_2 \\ m_2 \ddot{q}_2 &= kq_1 - 2kq_2 - c\dot{q}_2 + ku. \end{aligned}$$

In state-space form, we define the state to be $x = (q_1, q_2, \dot{q}_1, \dot{q}_2)$ and we can rewrite the equations as

$$\frac{dx}{dt} = \begin{pmatrix} 0 & 0 & 1 & 0 \\ 0 & 0 & 0 & 1 \\ -\frac{2k}{m} & \frac{k}{m} & -\frac{c}{m} & 0 \\ \frac{k}{m} & -\frac{2k}{m} & 0 & -\frac{c}{m} \end{pmatrix} x + \begin{pmatrix} 0 \\ 0 \\ 0 \\ \frac{k}{m} \end{pmatrix} u.$$

This is a coupled set of four differential equations and quite complicated to solve in analytical form.

The dynamics matrix is the same as in Example 5.5 and we can use the coordinate transformation defined there to put the system in modal form:

$$\frac{dz}{dt} = \begin{pmatrix} 0 & 1 & 0 & 0 \\ -\frac{k}{m} & -\frac{c}{m} & 0 & 0 \\ 0 & 0 & 0 & 1 \\ 0 & 0 & -\frac{3k}{m} & -\frac{c}{m} \end{pmatrix} z + \begin{pmatrix} 0 \\ \frac{k}{2m} \\ 0 \\ -\frac{k}{2m} \end{pmatrix} u.$$

Note that the resulting matrix equations are block diagonal and hence decoupled. We can thus solve for the solutions by computing the solutions of two sets of second order systems represented by the states (z_1, z_2) and (z_3, z_4) . Indeed, the functional form of each set of equations is identical to that of a single spring-mass system.

Once we have solved the two sets of independent second order equations, we

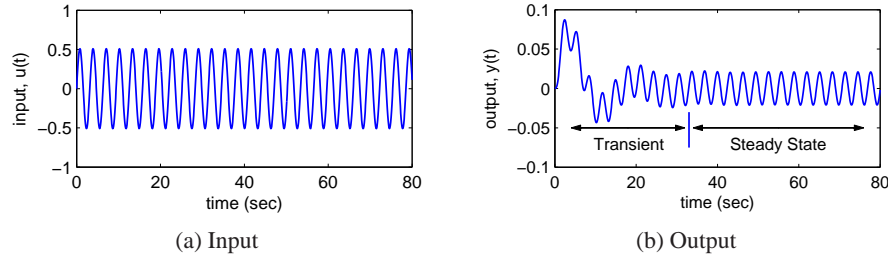


Figure 5.8: Transient versus steady state response. The left plot shows the input to a linear system and the right plot the corresponding output. The output signal initially undergoes a transient before settling into its steady state behavior.

can recover the dynamics in the original coordinates by inverting the state transformation and writing $x = T^{-1}z$. We can also determine the stability of the system by looking at the stability of the independent second order systems. ∇

Steady State Response

Given a linear input/output system

$$\frac{dx}{dt} = Ax + Bu, \quad y = Cx + Du, \quad (5.21)$$

the general form of the solution to equation (5.21) is given by the convolution equation:

$$y(t) = Ce^{At}x(0) + \int_0^t Ce^{A(t-\tau)}Bu(\tau)d\tau + Du(t).$$

We see from the form of this equation that the solution consists of an initial condition response and an input response.

The input response, corresponding to the last two terms in the equation above, itself consists of two components—the *transient response* and *steady state response*. The transient response occurs in the first period of time after the input is applied and reflects the mismatch between the initial condition and the steady state solution. The steady state response is the portion of the output response that reflects the long term behavior of the system under the given inputs. For inputs that are periodic the steady state response will often be periodic and for constant inputs the response will often be constant. An example of the transient and steady state response for a periodic input is shown in Figure 5.8.

A particularly common form of input is a *step input*, which represents an abrupt change in input from one value to another. A *unit step* (sometimes called the Heaviside step function) is defined as

$$u = S(t) = \begin{cases} 0 & t = 0 \\ 1 & t > 0. \end{cases}$$

The *step response* of the system (5.21) is defined as the output $y(t)$ starting from

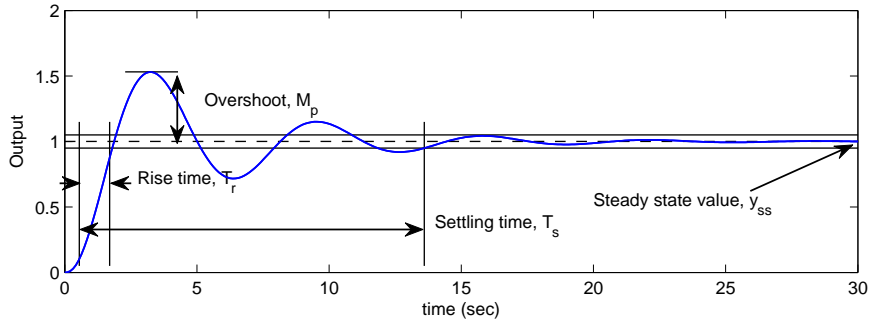


Figure 5.9: Sample step response. The rise time, overshoot, settling time and steady state value give the key performance properties of the signal.

zero initial condition (or the appropriate equilibrium point) and given a step input. We note that the step input is discontinuous and hence is not practically implementable. However, it is a convenient abstraction that is widely used in studying input/output systems.

We can compute the step response to a linear system using the convolution equation. Setting $x(0) = 0$ and using the definition of the step input above, we have

$$\begin{aligned} y(t) &= \int_0^t C e^{A(t-\tau)} B u(\tau) d\tau + D u(t) = C \int_0^t C e^{A(t-\tau)} B d\tau + D \\ &= C \int_0^t e^{A\sigma} B d\sigma + D = C (A^{-1} e^{A\sigma} B) \Big|_{\sigma=0}^{\sigma=t} + D \\ &= C A^{-1} e^{At} B - C A^{-1} B + D. \end{aligned}$$

If A has eigenvalues with negative real part (implying that the origin is a stable equilibrium point in the absence of any input), then we can rewrite the solution as

$$y(t) = \underbrace{C A^{-1} e^{At} B}_{\text{transient}} + \underbrace{D - C A^{-1} B}_{\text{steady state}} \quad t > 0. \quad (5.22)$$

The first term is the transient response and decays to zero as $t \rightarrow \infty$. The second term is the steady state response and represents the value of the output for large time.

A sample step response is shown in Figure 5.9. Several terms are used when referring to a step response. The *steady state value*, y_{ss} , of a step response is the final level of the output, assuming it converges. The *rise time*, T_r , is the amount of time required for the signal to go from 10% of its final value to 90% of its final value. It is possible to define other limits as well, but in this book we shall use these percentages unless otherwise indicated. The *overshoot*, M_p , is the percentage of the final value by which the signal initially rises above the final value. This usually assumes that future values of the signal do not overshoot the final value by more than this initial transient, otherwise the term can be ambiguous. Finally, the *settling time*, T_s , is the amount of time required for the signal to stay within 5% of its final

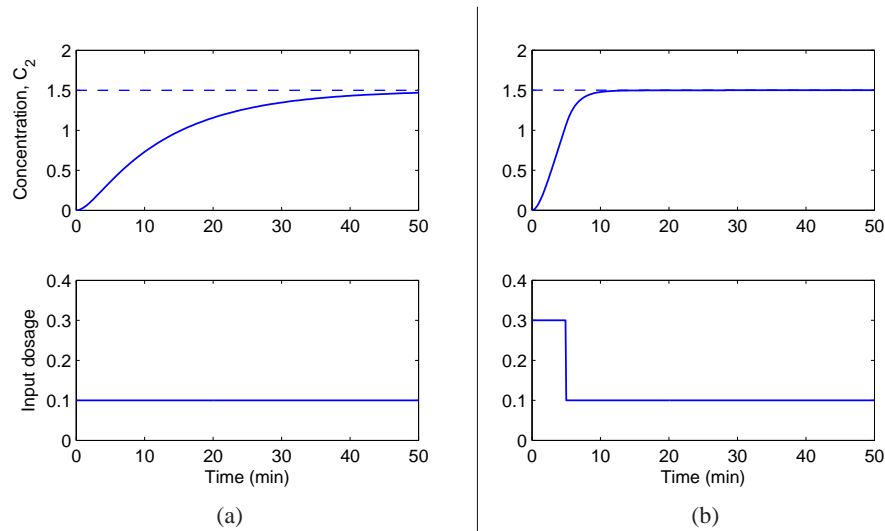


Figure 5.10: Response of a compartment model to a constant drug infusion. The step response (b) shows the rate of concentration buildup in compartment 2. In (c) a pulse of initial concentration is used to speed up the response.

value for all future times. The settling time is also sometimes defined as reaching 1% or 2% of the final value (see Exercise 5.9). In general these performance measures can depend on the amplitude of the input step, but for linear systems it can be shown that the last three quantities defined above are independent of the size of the step.

Example 5.7 Compartment Model

Consider the compartment model illustrated in Figure 5.10 and described in more detail in Section 3.6. Assume that a drug is administered by constant infusion in compartment V_1 and that the drug has its effect in compartment V_2 . To assess how the quickly the concentration in the compartment reaches steady state we compute the step response which is shown in Figure 5.10b. The step response is quite slow with a settling time of 39 minutes. It is possible to obtain the steady state concentration much faster by having a faster injection rate initially, as is shown in Figure 5.10c. The response of the system in this case can be computed by combining two step responses (Exercise ??). ▽

Another common input signal to a linear system is a sinusoid (or combination of sinusoids). The *frequency response* of an input/output system measures the way in which the system responds to a sinusoidal excitation on one of its inputs. As we have already seen for scalar systems, the particular solution associated with a sinusoidal excitation is itself a sinusoid at the same frequency. Hence we can compare the magnitude and phase of the output sinusoid to the input. More generally, if a system has a sinusoidal output response at the same frequency as the input forcing, we can speak of the frequency response of the system.

To see this in more detail, we must evaluate the convolution equation (5.15) for

$u = \cos \omega t$. This turns out to be a very messy calculation, but we can make use of the fact that the system is linear to simplify the derivation. In particular, we note that

$$\cos \omega t = \frac{1}{2} \left(e^{i\omega t} + e^{-i\omega t} \right).$$

Since the system is linear, it suffices to compute the response of the system to the complex input $u(t) = e^{st}$ and we can then reconstruct the input to a sinusoid by averaging the responses corresponding to $s = i\omega$ and $s = -i\omega$.

Applying the convolution equation to the input $u = e^{st}$ we have

$$\begin{aligned} y(t) &= Ce^{At}x(0) + \int_0^t Ce^{A(t-\tau)}Be^{s\tau}d\tau + De^{st} \\ &= Ce^{At}x(0) + Ce^{At} \int_0^t Ce^{(sI-A)\tau}Bd\tau + De^{st}. \end{aligned}$$

If we assume that none of the eigenvalues of A are equal to $s = \pm i\omega$, then the matrix $sI - A$ is invertible and we can write

$$\begin{aligned} y(t) &= Ce^{At}x(0) + Ce^{At} \left((sI - A)^{-1} e^{(sI-A)\tau} B \right) \Big|_0^t + De^{st} \\ &= Ce^{At}x(0) + Ce^{At} (sI - A)^{-1} \left(e^{(sI-A)t} - I \right) B + De^{st} \\ &= Ce^{At}x(0) + C(sI - A)^{-1} e^{st} B - Ce^{At} (sI - A) B, \end{aligned}$$

and we obtain

$$y(t) = \underbrace{Ce^{At} \left(x(0) - (sI - A)^{-1} B \right)}_{\text{transient}} + \underbrace{\left(C(sI - A)^{-1} B + D \right) e^{st}}_{\text{steady state}}.$$

Notice that once again the solution consists of both a transient component and a steady state component. The transient component decays to zero if the system is asymptotically stable and the steady state component is proportional to the (complex) input $u = e^{st}$.

We can simplify the form of the solution slightly further by rewriting the steady state response as

$$y_{\text{ss}}(t) = Me^{i\theta} e^{st} = Me^{(st+i\theta)}$$

where

$$Me^{j\theta} = C(sI - A)^{-1} B + D \quad (5.23)$$

and M and θ represent the magnitude and phase of the complex number $C(sI - A)^{-1} B + D$. When $s = i\omega$, we say that M is the *gain* and θ is the *phase* of the system at a given forcing frequency ω . Using linearity and combining the solutions for $s = +i\omega$ and $s = -i\omega$, we can show that if we have an input $u = A_u \sin(\omega t + \psi)$ and output $y = A_y \sin(\omega t + \phi)$, then

$$\text{gain}(\omega) = \frac{A_y}{A_u} = M \quad \text{phase}(\omega) = \phi - \psi = \theta.$$

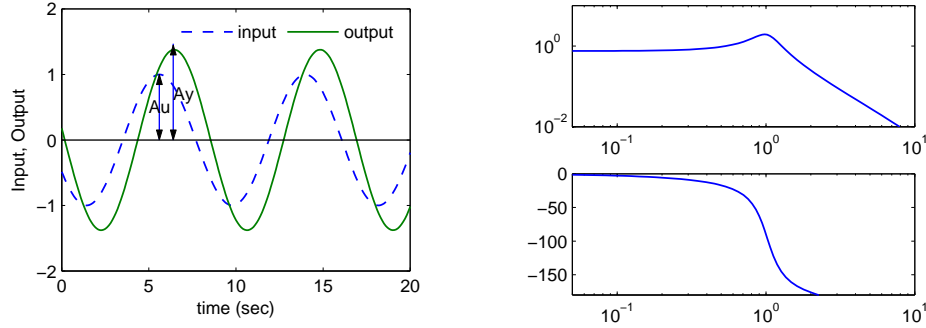


Figure 5.11: Frequency response, showing gain and phase. The gain is given by the ratio of the output amplitude to the input amplitude, $M = A_y/A_u$. The phase lag is given by $\theta = -2\pi(t_1 - t_2)/T$; it is negative for the case shown because the output lags the input.

The steady state solution for a sinusoid $u = \cos \omega t$ is now given by

$$y_{ss}(t) = M \cos(\omega t + \theta).$$

If the phase θ is positive, we say that the output “leads” the input, otherwise we say it “lags” the input.

A sample frequency response is illustrated in Figure 5.11. The solid line shows the input sinusoid, which has amplitude 1. The output sinusoid is shown as a dashed line, and has a different amplitude plus a shifted phase. The gain is the ratio of the amplitudes of the sinusoids, which can be determined by measuring the height of the peaks. The phase is determined by comparing the ratio of the time between zero crossings of the input and output to the overall period of the sinusoid:

$$\theta = -2\pi \cdot \frac{\Delta T}{T}.$$

Another way to view the frequency response is to plot how the gain and phase in equation (5.23) depend on ω (through $s = i\omega$). Figure 5.11 shows an example of this type of representation.

Example 5.8 Active band pass filter

Consider the op amp circuit shown in Figure 5.12a. We can derive dynamics of the system by writing the “nodal equations”, which state that the sum of the currents at any node must be zero. Assuming that $v_- = v_+ = 0$, as we did in Section 3.3, we have

$$0 = \frac{v_1 - v_2}{R_1} - C_1 \frac{dv_2}{dt}, \quad 0 = C_1 \frac{dv_2}{dt} + \frac{v_3}{R_2} + C_2 \frac{dv_3}{dt}, \quad 0 = C_2 \frac{dv_3}{dt} + \frac{v_3}{R_2} - C_1 \frac{dv_2}{dt}.$$

Choosing v_2 and v_3 as our states and using the first and last equations, we obtain

$$\frac{dv_2}{dt} = \frac{v_1 - v_2}{R_1 C_1}, \quad \frac{dv_3}{dt} = \frac{-v_3}{R_2 C_2} - \frac{v_1 - v_2}{R_1 C_2}.$$

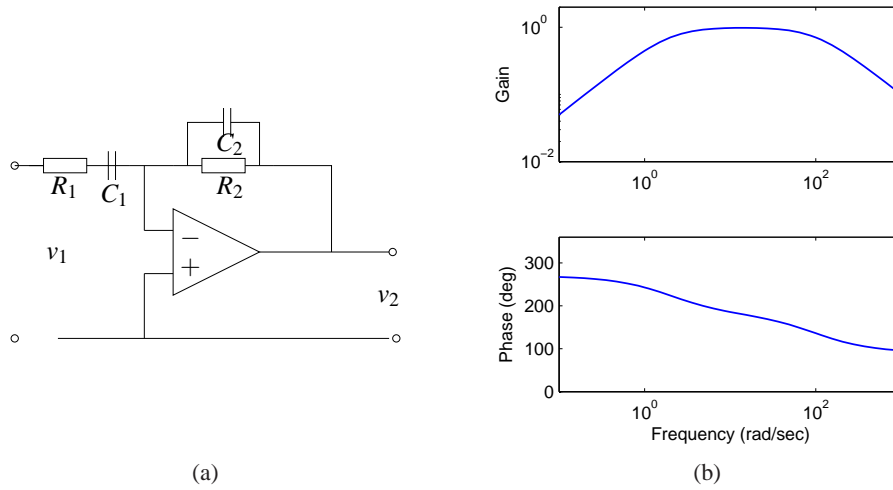


Figure 5.12: Active band pass filter. The circuit diagram shows an op amp with two RC filters arranged to provide a band pass filter. The plot on the right shows the gain and phase of the filter as a function of frequency.

Rewriting these in linear state space form we obtain

$$\frac{dx}{dt} = \begin{pmatrix} -\frac{1}{R_1 C_1} & 0 \\ \frac{1}{R_1 C_2} & -\frac{1}{R_2 C_2} \end{pmatrix} x + \begin{pmatrix} \frac{1}{R_1 C_1} \\ -\frac{1}{R_1 C_2} \end{pmatrix} u \quad (5.24)$$

$$y = \begin{pmatrix} 0 & 1 \end{pmatrix} x$$

where $x = (v_2, v_3)$, $u = v_1$ and $y = v_3$.

The frequency response for the system can be computed using equation (5.23):

$$M e^{j\theta} = C(sI - A)^{-1} B + D = -\frac{R_2}{R_1} \frac{R_1 C_1 s}{(1 + R_1 C_1 s)(1 + R_2 C_2 s)} \quad s = i\omega.$$

The magnitude and phase are plotted in Figure 5.12b for $R_1 = 100 \Omega$, $R_2 = 5 \text{ k}\Omega$ and $C_1 = C_2 = 100 \mu\text{F}$. We see that the circuit passes through signals with frequencies around 10 rad/s, but attenuates frequencies below 5 rad/s and above 50 rad/s. At 0.1 rad/s the input signal is attenuated by 20x (0.05). This type of circuit is called a *band pass filter* since it pass through signals in the band of frequencies between 5 and 50 rad/s.

▽

As in the case of the step response, a number of standard properties are defined for frequency responses. The gain of the system at $\omega = 0$ is called the *zero frequency gain* and corresponds to the ratio between a constant input and the steady output:

$$M_0 = -CA^{-1}B + D.$$

The zero frequency gain is only well defined if A is invertible (and, in particular, if it does has not eigenvalues at 0). It is also important to note that the zero frequency gain is only a relevant quantity when a system is stable about the corresponding equilibrium point. So, if we apply a constant input $u = r$ then the corresponding equilibrium point $x_e = -A^{-1}Br$ must be stable in order to talk about the zero frequency gain. (In electrical engineering, the zero frequency gain is often called the “DC gain”. DC stands for “direct current” and reflects the common separation of signals in electrical engineering into a direct current (zero frequency) term and an alternating current (AC) term.)

The *bandwidth* ω_b of a system is the frequency where the gain has decreased by a factor of $1/\sqrt{2}$ from its zero frequency gain. This definition assumes that we have nonzero, finite zero frequency gain. For systems that attenuate low frequencies but pass through high frequencies, the reference gain is taken as the high frequency gain. For a system such as the band-pass filter in Example 5.8, bandwidth is defined as the range of frequencies where the gain is larger than $1/\sqrt{2}$ of the gain at the center of the band. (For Example 5.8 this would give a bandwidth of approximately 50 rad/s.)

Another important property of the frequency response is the *resonance peak* M_r , the largest value of the frequency response, and the *peak frequency* ω_{mr} , the frequency where the maximum occurs. These two properties describe the frequency of the sinusoidal input that produces the largest possible output and the gain at the frequency.

Example 5.9 AFM Dynamics

Consider the model for the vertical dynamics of the atomic force microscope in contact mode, discussed in Section 3.5. The basic dynamics are given by equation (3.22). The piezo stack can be modeled by a second order system with undamped natural frequency ω_3 and relative damping ζ_3 . The dynamics are then described by the linear system

$$\frac{dx}{dt} = \begin{pmatrix} 0 & 1 & 0 & 0 \\ -k/(m_1+m_2) & -c/(m_1+m_2) & 1/m_2 & 0 \\ 0 & 0 & 0 & 1 \\ 0 & 0 & -\omega_3^2 & -2\zeta_3\omega_3 \end{pmatrix} x + \begin{pmatrix} 0 \\ 0 \\ 0 \\ \omega_3^2 \end{pmatrix} u$$

$$y = \frac{m_2}{m_1+m_2} \begin{pmatrix} \frac{m_1 k}{m_1+m_2} & \frac{m_1 c}{m_1+m_2} & 1 & 0 \end{pmatrix} x,$$

where the input signal is the drive signal to the amplifier driving the piezo stack and the output is the elongation of the piezo. The frequency response of the system is shown in Figure 5.13. The zero frequency gain of the system is $M_0 = 1$. There are two resonant poles with peaks $M_{r1} = 2.12$ at $\omega_{mr1} = 238$ krad/s and $M_{r2} = 4.29$ at $\omega_{mr2} = 746$ krad/s. The bandwidth of the system, defined as the lowest frequency where the gain is $\sqrt{2}$ less than the zero frequency gain, is $\omega_b = 292$ krad/s. There is also a dip in the gain $M_d = 0.556$ for $\omega_{md} = 268$ krad/s. This dip (sometimes called an *anti-resonance*) is associated with a dip in the phase and will limit the performance when the system is controlled by simple controllers, as will see

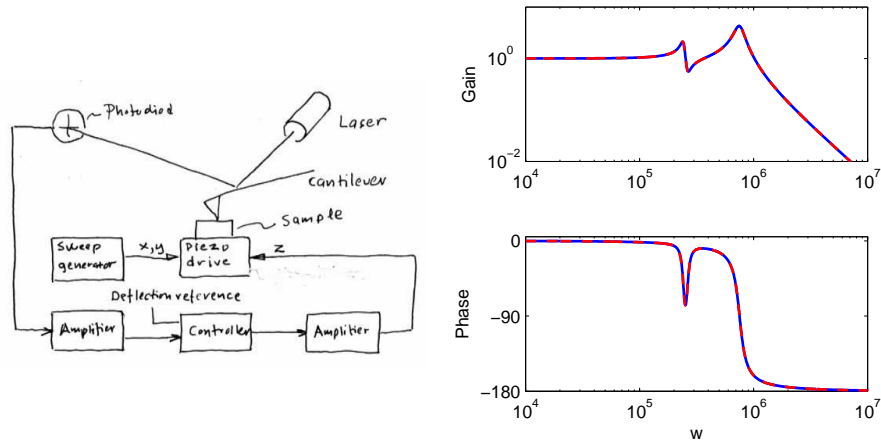


Figure 5.13: AFM frequency response. The plot on the right shows the gain and phase for the piezo stack of an atomic force microscope. The response contains two frequency peaks at resonances of the system, along with an antiresonance at $\omega = 268$ krad/s. The combination of a resonant peak followed by an antiresonance is common for systems with multiple lightly damped modes.

in Chapter 10.

▽

Sampling

It is often convenient to use both differential and difference equations in modeling and control. For linear systems it is straightforward to transform from one to the other. Consider the general linear system described by equation (5.13) and assume that the control signal is constant over sampling interval of constant length h . It follows from equation (5.14) of Theorem 5.4 that

$$x(t+h) = e^{Ah}x(t) + \int_t^{t+h} e^{t+h-\tau}Bu(k)d\tau = \Phi x(t) + \Gamma u(t), \quad (5.25)$$

where we have assumed that the discontinuous control signal is continuous from the right. The behavior of the system at the sampling times $t = kh$ is described by the difference equation

$$x[k+1] = \Phi x[k] + \Gamma u[k], \quad y[k] = Cx[k] + Du[k]. \quad (5.26)$$

Notice that the difference equation (5.26) is an exact representation of the behavior of the system at the sampling instants. Similar expressions can also be obtained if the control signal is linear over the sampling interval.

The transformation from (5.25) to (5.26) is called sampling. The relations between the system matrices in the continuous and sampled representations is

$$\Phi = e^{Ah}, \quad \Gamma = \left(\int_0^h e^{As} ds \right) B; \quad A = \frac{1}{h} \log \Phi, \quad B = \left(\int_0^h e^{At} dt \right)^{-1} \Gamma. \quad (5.27)$$

Notice that if A is invertible we have

$$\Gamma = A^{-1}(e^{Ah} - I).$$

All continuous time systems have a discrete time version but there are discrete time systems which do not have a continuous time equivalent. The precise condition is that the matrix Φ cannot have real eigenvalues on the negative real axis.

Example 5.10 Differential equation for IBM Lotus server

In Example 2.4 we described how the dynamics of an IBM Lotus server were obtained as the discrete time system

$$y[k+1] = ay[k] + bu[k]$$

where $a = 0.43$, $b = 0.47$ and the sampling period is $h = 60$ s. A differential equation model is needed if we would like to design control systems based on continuous time theory. Such a model is obtained by applying equation (5.27), hence

$$A = \frac{\log a}{h} = -0.0141, \quad B = \left(\int_0^h e^{At} dt \right)^{-1} b = 0.0141.$$

and we find that the difference equation can be interpreted as a sampled version of the ordinary differential equation

$$\frac{dx}{dt} = -0.141x + 0.141u$$

▽

5.4 LINEARIZATION

As described in the beginning of the chapter, a common source of linear system models is through the *approximation* of a nonlinear system by a linear one. These approximations are aimed at studying the local behavior of a system, where the nonlinear effects are expected to be small. In this section we discuss how to locally approximate a system by its linearization and what can be said about the approximation in terms of stability. We begin with an illustration of the basic concept using the cruise control example from Chapter 3.

Example 5.11 Cruise control

The dynamics for the cruise control system are derived in Section 3.1 and have the form

$$m \frac{dv}{dt} = \alpha_n u T(\alpha_n v) - mg C_r \operatorname{sgn}(v) - \frac{1}{2} \rho C_v A v^2 - mg \sin \theta, \quad (5.28)$$

where the first term on the right hand side of the equation is the force generated by the engine and the remaining three terms are the rolling friction, aerodynamic drag and gravitational disturbance force. There is an equilibrium (v_e, u_e) when the force applied by the engine balances the disturbance forces.

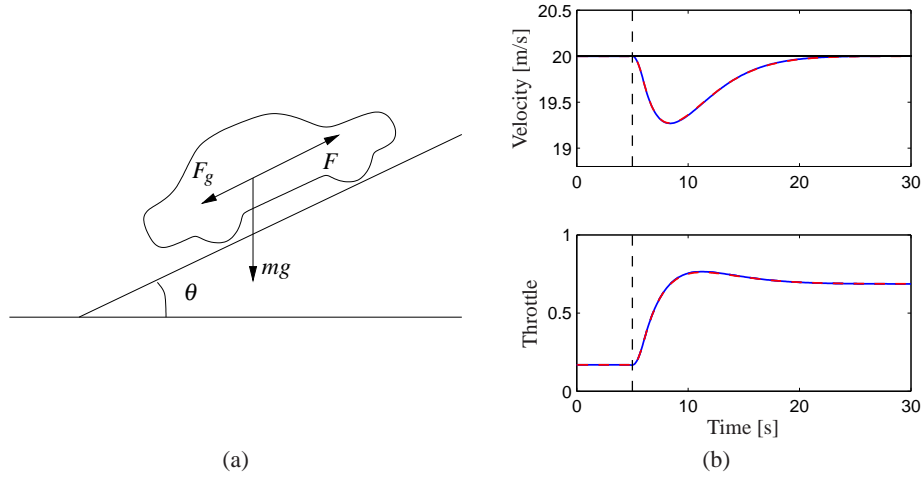


Figure 5.14: Simulated response of a vehicle with PI cruise control as it climbs a hill with a slope of 4° . The full lines is the simulation based on a nonlinear model and the dashed line shows the corresponding simulation using a linear model. The controller gains are $k_p = 0.5$ and $k_i = 0.1$.

To explore the behavior of the system near the equilibrium we will linearize the system. A Taylor series expansion of equation (5.28) around the equilibrium gives

$$\frac{d(v - v_e)}{dt} = a(v - v_e) - b_g(\theta - \theta_e) + b(u - u_e) \quad (5.29)$$

where

$$a = \frac{u_e \alpha_n^2 T'(\alpha_n v_e) - \rho C_v A v_e}{m} \quad b_g = g \cos \theta_e \quad b = \frac{\alpha_n T(\alpha_n v_e)}{m}. \quad (5.30)$$

Notice that the term corresponding to rolling friction disappears if $v \neq 0$. For a car in fourth gear with $v_e = 25$ m/s, $\theta_e = 0$ and the numerical values for the car from Section 3.1, the equilibrium value for the throttle is $u_e = 0.1687$ and the parameters are $a = -0.0101$, $b = 1.32$ and $c = 9.8$. This linear model describes how small perturbations in the velocity about the nominal speed evolve in time.

Figure 5.14 shows a simulation of a cruise controller with linear and nonlinear models; the differences between the linear and nonlinear models are small and hence the linearized model provides a reasonable approximation. ∇

Jacobian Linearization around an Equilibrium Point

To proceed more formally, consider a single input, single output nonlinear system

$$\begin{aligned} \frac{dx}{dt} &= f(x, u) & x &\in \mathbb{R}^n, u \in \mathbb{R} \\ y &= h(x, u) & y &\in \mathbb{R} \end{aligned} \quad (5.31)$$

with an equilibrium point at $x = x_e$, $u = u_e$. Without loss of generality we can assume that $x_e = 0$ and $u_e = 0$, although initially we will consider the general case to make the shift of coordinates explicit.

To study the *local* behavior of the system around the equilibrium point (x_e, u_e) , we suppose that $x - x_e$ and $u - u_e$ are both small, so that nonlinear perturbations around this equilibrium point can be ignored compared with the (lower order) linear terms. This is roughly the same type of argument that is used when we do small angle approximations, replacing $\sin \theta$ with θ and $\cos \theta$ with 1 for θ near zero.

As we did in Chapter 4, we define a new set of state variables z , as well as inputs v and outputs w :

$$z = x - x_e \quad v = u - u_e \quad w = y - h(x_e, u_e).$$

These variables are all close to zero when we are near the equilibrium point, and so in these variables the nonlinear terms can be thought of as the higher order terms in a Taylor series expansion of the relevant vector fields (assuming for now that these exist).

Formally, the *Jacobian linearization* of the nonlinear system (5.31) is

$$\begin{aligned} \dot{z} &= Az + Bv \\ w &= Cz + Dv, \end{aligned} \tag{5.32}$$

where

$$A = \left. \frac{\partial f}{\partial x} \right|_{(x_e, u_e)} \quad B = \left. \frac{\partial f}{\partial u} \right|_{(x_e, u_e)} \quad C = \left. \frac{\partial h}{\partial x} \right|_{(x_e, u_e)} \quad D = \left. \frac{\partial h}{\partial u} \right|_{(x_e, u_e)} \tag{5.33}$$

The system (5.32) approximates the original system (5.31) when we are near the equilibrium point about which the system was linearized.

It is important to note that we can only define the linearization of a system about an equilibrium point. To see this, consider a polynomial system

$$\dot{x} = a_0 + a_1x + a_2x^2 + a_3x^3 + u,$$

where $a_0 \neq 0$. There are a family of equilibrium points for this system given by $(x_e, u_e) = (x_e, -a_0 - a_1x_e - a_2x_e^2 - a_3x_e^3)$ and we can linearize around any of these. Suppose that we try to linearize around the origin of the system, $x = 0$, $u = 0$. If we drop the higher order terms in x , then we get

$$\dot{x} = a_0 + a_1x + u,$$

which is *not* the Jacobian linearization if $a_0 \neq 0$. The constant term must be kept and this is not present in (5.32). Furthermore, even if we kept the constant term in the approximate model, the system would quickly move away from this point (since it is “driven” by the constant term a_0) and hence the approximation could soon fail to hold.

Software for modeling and simulation frequently has facilities for performing linearization symbolically or numerically. The MATLAB command `trim` finds

the equilibrium and `linmod` extracts linear state-space models from a SIMULINK system around an operating point.

Example 5.12 Vehicle steering

Consider the vehicle steering system introduced in Example 2.8. The nonlinear equations of motion for the system are given by equations (2.23)–(2.25) and can be written as

$$\frac{d}{dt} \begin{pmatrix} x \\ y \\ \theta \end{pmatrix} = \begin{pmatrix} v \cos(\alpha(\delta) + \theta) \\ v \sin(\alpha(\delta) + \theta) \\ \frac{v_0}{b} \tan \delta \end{pmatrix}, \quad \alpha(\delta) = \arctan\left(\frac{a \tan \delta}{b}\right),$$

where x , y and θ are the position and orientation of the center of mass of the vehicle, v_0 is the velocity of the rear wheel, b is the distance between the front and rear wheels and δ is the angle of the front wheel. The function $\alpha(\delta)$ is the angle between the velocity vector and the vehicle's length axis.

We are interested in the motion of the vehicle about a straight line path ($\theta = \theta_0$) with fixed velocity $v_0 \neq 0$. To find the relevant equilibrium point, we first set $\dot{\theta} = 0$ and we see that we must have $\delta = 0$, corresponding to the steering wheel being straight. This also yields $\alpha = 0$. Looking at the first two equations in the dynamics, we see that the motion in the xy direction is by definition *not* at equilibrium since $\dot{x}^2 + \dot{y}^2 = v_0^2 \neq 0$. Therefore we cannot formally linearize the full model.

Suppose instead that we are concerned with the lateral deviation of the vehicle from a straight line. For simplicity, we let $\theta_0 = 0$, which corresponds to driving along the x axis. We can then focus on the equations of motion in the y and θ directions. With some abuse of notation we introduce the state $x = (y, \theta)$ and $u = \delta$. The system is then in standard form with

$$f(x, u) = \begin{pmatrix} v \sin(\alpha(u) + x_2) \\ \frac{v_0}{b} \tan u \end{pmatrix}, \quad \alpha(u) = \arctan\left(\frac{a \tan u}{b}\right), \quad h(x, u) = x_1.$$

The equilibrium point of interest is given by $x = (0, 0)$ and $u = 0$. To compute the linearization the model around this equilibrium point, we make use of the formulas (5.33). A straightforward calculation yields

$$\begin{aligned} A &= \left. \frac{\partial f}{\partial x} \right|_{\substack{x=0 \\ u=0}} = \begin{pmatrix} 0 & v_0 \\ 0 & 0 \end{pmatrix} & B &= \left. \frac{\partial f}{\partial u} \right|_{\substack{x=0 \\ u=0}} = \begin{pmatrix} av_0/b \\ v_0/b \end{pmatrix} \\ C &= \left. \frac{\partial h}{\partial x} \right|_{\substack{x=0 \\ u=0}} = \begin{pmatrix} 1 & 0 \end{pmatrix} & D &= \left. \frac{\partial h}{\partial u} \right|_{\substack{x=0 \\ u=0}} = 0 \end{aligned}$$

and the linearized system

$$\dot{x} = Ax + Bu, \quad y = Cx + Du \quad (5.34)$$

thus provides an approximation to the original nonlinear dynamics.

The linearized model can be simplified further by introducing normalized variables, as discussed in Section 2.3. For this system, we choose the wheel base b

as the length unit and the unit as the time required to travel a wheel base. The normalized state is thus $z = (x_1/b, x_2)$ and the new time variable is $\tau = v_0 t/b$. The model (5.34) then becomes

$$\frac{dz}{d\tau} = \begin{pmatrix} z_2 + \gamma u \\ u \end{pmatrix} = \begin{pmatrix} 0 & 1 \\ 0 & 0 \end{pmatrix} z + \begin{pmatrix} \gamma \\ 1 \end{pmatrix} u, \quad y = \begin{pmatrix} 1 & 0 \end{pmatrix} z, \quad (5.35)$$

where $\gamma = a/b$. The normalized linear model for vehicle steering with non-slipping wheels is thus a linear system with only one parameter. ∇

Feedback Linearization

Another type of linearization is the use of feedback to convert the dynamics of a nonlinear system into a linear one. We illustrate the basic idea with an example.

Example 5.13 Cruise control

Consider again the cruise control system from Example 5.11, whose dynamics are given in equation (5.28):

$$m \frac{dv}{dt} = \alpha_n u T(\alpha_n v) - mg C_r \operatorname{sgn}(v) - \frac{1}{2} \rho C_d A v^2 - mg \sin \theta.$$

If we choose u as a feedback law of the form

$$u = \frac{1}{\alpha_n T(\alpha_n v)} \left(u' + mg C_r + \frac{1}{2} \rho C_d A v^2 \right) \quad (5.36)$$

then the resulting dynamics become

$$m \frac{dv}{dt} = u' + d \quad (5.37)$$

where $d = mg \sin \theta$ is the disturbance force due the slope of the road. If we now define a feedback law for u' (such as a proportional-integral-derivative [PID] controller), we can use equation (5.36) to compute the final input that should be commanded.

Equation (5.37) is a linear differential equation. We have essentially “inverted” the nonlinearity through the use of the feedback law (5.36). This requires that we have an accurate measurement of the vehicle velocity v as well as an accurate model of the torque characteristics of the engine, gear ratios, drag and friction characteristics and mass of the car. While such a model is not generally available (remembering that the parameter values can change), if we design a good feedback law for u' , then we can achieve robustness to these uncertainties. ∇

More generally, we say that a system of the form

$$\frac{dx}{dt} = f(x, u), \quad y = h(x)$$

is *feedback linearizable* if we can find a control law $u = \alpha(x, v)$ such that the resulting closed loop system is input/output linear with input v and output y , as shown in Figure 5.15. To fully characterize such systems is beyond the scope of

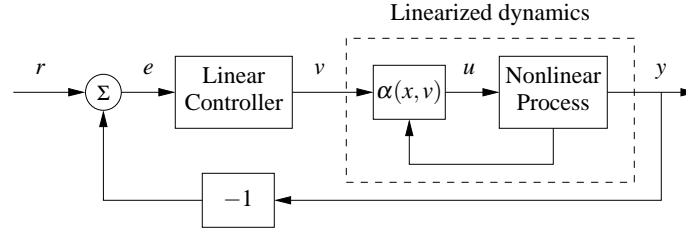


Figure 5.15: Feedback linearization using feedback. A nonlinear feedback of the form $u = \alpha(x, v)$ is used to modify the dynamics of a nonlinear process so that the response from the input v to the output y is linear. A linear controller can then be used to regulate the system's dynamics.

this text, but we note that in addition to changes in the input, the general theory also allows for (nonlinear) changes in the states that are used to describe the system, keeping only the input and output variables fixed. More details of this process can be found in the textbooks by Isidori [100] and Khalil [116].

One case that comes up relatively frequently, and is hence worth special mention, is the set of mechanical systems of the form ◇

$$M(q)\ddot{q} + C(q, \dot{q}) = B(q)u.$$

Here $q \in \mathbb{R}^n$ is the configuration of the mechanical system, $M(q) \in \mathbb{R}^{n \times n}$ is the configuration-dependent inertia matrix, $C(q, \dot{q}) \in \mathbb{R}^n$ represents the Coriolis forces and additional nonlinear forces (such as stiffness and friction) and $B(q) \in \mathbb{R}^{n \times p}$ is the input matrix. If $p = n$ then we have the same number of inputs and configuration variables and if we further have that $B(q)$ is an invertible matrix for all configurations q , then we can choose

$$u = B^{-1}(q)(M(q)v - C(q, \dot{q})). \quad (5.38)$$

The resulting dynamics become

$$M(q)\ddot{q} = M(q)v \quad \implies \quad \ddot{q} = v,$$

which is a linear system. We can now use the tools of linear system theory to analyze and design control laws for the linearized system, remembering to apply equation (5.38) to obtain the actual input that will be applied to the system.

This type of control is common in robotics, where it goes by the name of *computed torque*, and aircraft flight control, where it is called *dynamic inversion*. Some modeling tools like Modelica can generate the code for the inverse model automatically. One caution is that feedback linearization can often cancel out beneficial terms in the natural dynamics, and hence it must be used with care. Extensions that do not require complete cancellation of nonlinearities are discussed in Khalil [116] and Krstić *et al.* [122].

5.5 FURTHER READING

The idea to characterize dynamics by considering the responses to step inputs is due to Heaviside. The unit step is therefore also called the *Heaviside step function*. The majority of the material in this chapter is very classical and can be found in most books on dynamics and control theory, including early works on control such as James, Nichols and Phillips [103], and more recent textbooks such as Franklin, Powell and Emami-Naeini [76] and Ogata [153]. A delightful presentation of linear systems is given in the book by Brockett [43], a more comprehensive treatment is given by Rugh [162] and an elegant mathematical treatment is given in Sonntag [173]. The material on feedback linearization is found in books on nonlinear control theory, such as Isidori [100] and Khalil [116].

EXERCISES

5.1 Show that if $y(t)$ is the output of a linear system corresponding to input $u(t)$, then the output corresponding to an input $\dot{u}(t)$ is given by $\dot{y}(t)$. (Hint: use the definition of the derivative: $\dot{y}(t) = \lim_{\varepsilon \rightarrow 0} (y(t + \varepsilon) - y(t)) / \varepsilon$.)



5.2 Show that a signal $u(t)$ can be decomposed in terms of the impulse function $\delta(t)$ as

$$u(t) = \int_0^t \delta(t - \tau) u(\tau) d\tau$$

and use this decomposition plus the principle of superposition to show that the response of a linear system to an input $u(t)$ (assuming zero initial condition) can be written as

$$y(t) = \int_0^t h(t - \tau) u(\tau) d\tau,$$

where $h(t)$ is the impulse response of the system.

5.3 Assume that $\zeta < 1$ and let $\omega_d = \omega_0 \sqrt{1 - \zeta^2}$. Show that

$$\exp \begin{pmatrix} \zeta \omega_0 & \omega_d \\ -\omega_d & \zeta \omega_0 \end{pmatrix} t = \begin{pmatrix} e^{\zeta \omega_0 t} \cos \omega_d t & e^{\zeta \omega_0 t} \sin \omega_d t \\ -e^{\zeta \omega_0 t} \sin \omega_d t & e^{\zeta \omega_0 t} \cos \omega_d t \end{pmatrix}$$

5.4 Assume that $\zeta < 1$ and let $\omega_d = \omega_0 \sqrt{1 - \zeta^2}$. Show that the systems

$$\frac{dx}{dt} = \begin{pmatrix} \zeta \omega_0 & \omega_d \\ -\omega_d & -\zeta \omega_0 \end{pmatrix} x, \quad \frac{dz}{dt} = \begin{pmatrix} 0 & \omega_0 \\ -\omega_0 & -2\zeta \omega_0 \end{pmatrix} z$$

are related through $z = Tx$ where

$$T = \begin{pmatrix} \zeta + \sqrt{1 - \zeta^2} & \zeta + \sqrt{1 - \zeta^2} \\ 1 & 1 \end{pmatrix}.$$

5.5 Consider a linear system $\dot{x} = Ax$ with $\operatorname{Re} \lambda_j < 0$ for all eigenvalues λ_j of the matrix A . Show that the matrix


$$P = \int_0^{\infty} e^{A^T \tau} Q e^{A \tau} d\tau$$

defines a Lyapunov function of the form $V(x) = x^T P x$.

5.6 Using the computation for the matrix exponential, show that equation (5.11) holds for the case of a 3×3 Jordan block. (Hint: decompose the matrix into the form $S + N$ where S is a diagonal matrix.)

5.7 Consider a linear system with a Jordan form that is non-diagonal.

(a) Show that there exists a periodic input does not produce a periodic output.

(b) Prove Proposition 5.3 by showing that if the system contains a real eigenvalue $\lambda = 0$ with nontrivial Jordan block, then there exists an initial condition which has a solution that grows in time. Extend this argument to the case of complex eigenvalues with $\operatorname{Re} \lambda = 0$ by using the block Jordan form 

$$J_i = \begin{pmatrix} 0 & \omega & 1 & 0 \\ -\omega & 0 & 0 & 1 \\ 0 & 0 & 0 & \omega \\ 0 & 0 & -\omega & 0 \end{pmatrix}$$

5.8 Using the convolution equation, write down the complete solution for a second order linear system with sinusoidal input:

$$\ddot{x} + 2\zeta \omega_0 \dot{x} + \omega_0^2 x = A \sin \omega t.$$

Make sure to describe any cases in which the form of the solution changes.

5.9 Consider a first order system of the form

$$\tau \dot{x} = -x + u$$

$$y = x.$$

We say that the parameter τ is the *time constant* for the system since the zero input system approaches the origin as $e^{-t/\tau}$. For a first order system of this form, show that the rise time of the system is approximately 2τ , a 5% settling time corresponds to approximately 3τ and a 2% settling time corresponds to approximately 4τ .

5.10 Consider a linear discrete time system of the form

$$x[k+1] = Ax[k] + Bu[k]$$

$$y[k] = Cx[k] + Du[k].$$

(a) Show that the general form of the output of a discrete time linear system is given by the discrete time convolution equation:

$$y[k] = CA^k x_0 + \sum_{i=0}^{k-1} CA^{k-i-1} Bu[i] + Du[k]$$

- (b) Show that a discrete time linear system is asymptotically stable if and only if all eigenvalues of A have magnitude strictly less than 1.
- (c) Let $u[k] = A \sin(\omega k)$ represent an oscillatory input with frequency $\omega < \pi$ (to avoid “aliasing”). Show that the steady state component of the response has gain M and phase θ where

$$M e^{j\theta} = C(e^{i\omega} I - A)^{-1} B + D.$$

- (d) Show that if we have a nonlinear discrete time system

$$\begin{aligned} x[k] &= f(x[k], u[k]) & x[k] \in \mathbb{R}^n, u \in \mathbb{R} \\ y[k] &= h(x[k], u[k]) & y \in \mathbb{R} \end{aligned}$$

then we can linearize the system around an equilibrium point (x_e, u_e) by defining the matrices A , B , C and D as in equation (5.33).

5.11 Consider the following simple Keynesian macro-economic model in the form of a linear discrete time system discussed in Exercise 5.10

$$\begin{aligned} \begin{pmatrix} C[t+1] \\ I[t+1] \end{pmatrix} &= \begin{pmatrix} a & a \\ ab - a & ab \end{pmatrix} \begin{pmatrix} C[t] \\ I[t] \end{pmatrix} + \begin{pmatrix} a \\ ab \end{pmatrix} G[t] \\ Y[t] &= C[t] + I[t] + G[t] \end{aligned}$$

Determine the eigenvalues of the dynamics matrix. When are the magnitudes of the eigenvalues less than 1? Assume that the system is in equilibrium with constant values capital spending C , investment I and government expenditure G . Explore what happens when government expenditure increases by 10%. Use the values $a = 0.25$ and $b = 0.5$.

5.12 Consider a scalar system,

$$\dot{x} = 1 - x^3 + u.$$

Compute the equilibrium points for the unforced system ($u = 0$) and use a Taylor series expansion around the equilibrium point to compute the linearization. Verify that this agrees with the linearization in equation (5.32).

5.13 Consider the dynamics of a genetic circuit that implements *self-repression*: the protein produced by the gene is a repressor for the protein, thus restricting its own production. Using the models presented in Example 2.12, the dynamics for the system can be written as

$$\begin{aligned} \frac{dm}{dt} &= \frac{\alpha}{1 + kp^2} + \alpha_0 - \gamma m \\ \frac{dp}{dt} &= \beta m - \delta p \end{aligned} \tag{5.39}$$

for $p, m \geq 0$. Find the equilibrium points for the system and use the linearized dynamics around each equilibrium point to determine the local stability of the system.

Chapter Six

State Feedback

Intuitively, the state may be regarded as a kind of information storage or memory or accumulation of past causes. We must, of course, demand that the set of internal states Σ be sufficiently rich to carry all information about the past history of Σ to predict the effect of the past upon the future. We do not insist, however, that the state is the least such information although this is often a convenient assumption.

R. E. Kalman, P. L. Falb and M. A. Arbib, 1969 [110].

This chapter describes how feedback of a system's state can be used to shape the local behavior of a system. The concept of reachability is introduced and used to investigate how to "design" the dynamics of a system through assignment of its eigenvalues. In particular, it will be shown that under certain conditions it is possible to assign the system eigenvalues arbitrarily by appropriate feedback of the system state.

6.1 REACHABILITY

One of the fundamental properties of a control system is what set of points in the state space can be reached through the choice of a control input. It turns out that the property of "reachability" is also fundamental in understanding the extent to which feedback can be used to design the dynamics of a system.

Definition of Reachability

We begin by disregarding the output measurements of the system and focusing on the evolution of the state, given by

$$\frac{dx}{dt} = Ax + Bu, \quad (6.1)$$

where $x \in \mathbb{R}^n$, $u \in \mathbb{R}$, A is an $n \times n$ matrix and B a column vector. A fundamental question is whether it is possible to find control signals so that any point in the state space can be reached through some choice of input. To study this, we define the reachable set $\mathcal{R}(x_0, \leq T)$ as the set of all points x_f such that there exists an input $u(t)$, $0 \leq t \leq T$ that steers the system from $x(0) = x_0$ to $x(T) = x_f$, as illustrated in Figure 6.1a.

Definition 6.1 (Reachability). A linear system is *reachable* if for any $x_0, x_f \in \mathbb{R}^n$ there exists a $T > 0$ and $u: [0, T] \rightarrow \mathbb{R}$ such that the corresponding solution satisfies $x(0) = x_0$ and $x(T) = x_f$.

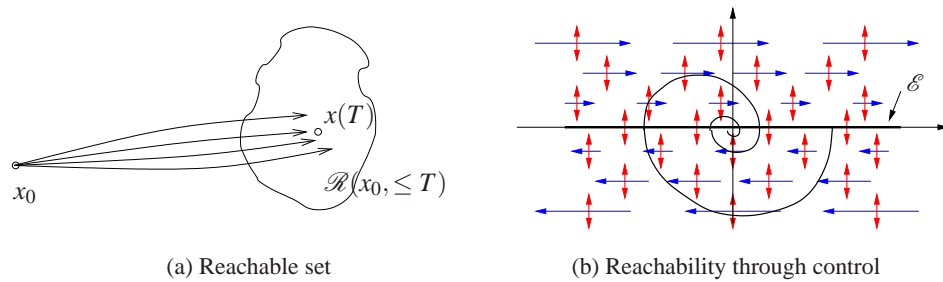


Figure 6.1: The reachable set for a control system. The set $\mathcal{R}(x_0, \leq T)$ shown on the left is the set of points reachable from x_0 in time less than T . The phase portrait on the right shows the dynamics for a double integrator, with the natural dynamics drawn as horizontal arrows and the control inputs drawn as vertical arrows. The set of achievable equilibrium points is the x axis. By setting the control inputs as a function of the state, it is possible to steer the system to the origin, as shown on the sample path.

The definition of reachability addresses whether it is possible to reach all points in the state space in a *transient* fashion. In many applications, the set of points that we are most interested in reaching is the set of equilibrium points of the system (since we can remain at those points once we get there). The set of all possible equilibria for constant controls is given by

$$\mathcal{E} = \{x_e : Ax_e + bu_e = 0 \text{ for some } u_e \in \mathbb{R}\}.$$

This means that possible equilibria lie in a one (or possibly higher) dimensional subspace. If the matrix A is invertible this subspace is spanned by $A^{-1}B$.

The following example provides some insight into the possibilities.

Example 6.1 Double integrator

Consider a linear system consisting of a double integrator, whose dynamics are given by

$$\begin{aligned}\dot{x}_1 &= x_2 \\ \dot{x}_2 &= u.\end{aligned}$$

Figure 6.1b shows a phase portrait of the system. The open loop dynamics ($u = 0$) are shown as horizontal arrows pointed to the right for $x_2 > 0$ and to the left for $x_2 < 0$. The control input is represented by a double-headed arrow in the vertical direction, corresponding to our ability to set the value of \dot{x}_2 . The set of equilibrium points \mathcal{E} corresponds to the x_1 axis, with $u_e = 0$.

Suppose first that we wish to reach the origin from an initial condition $(a, 0)$. We can directly move the state up and down in the phase plane, but we must rely on the natural dynamics to control the motion to the left and right. If $a > 0$, we can move the origin by first setting $u < 0$, which will cause x_2 to become negative. Once $x_2 < 0$, the value of x_1 will begin to decrease and we will move to the left. After a while, we can set u_2 to be positive, moving x_2 back toward zero and slowing the motion in the x_1 direction. If we bring $x_2 > 0$, we can move the system state in the

opposite direction.

Figure 6.1b shows a sample trajectory bringing the system to the origin. Note that if we steer the system to an equilibrium point, it is possible to remain there indefinitely (since $\dot{x}_1 = 0$ when $x_2 = 0$), but if we go to any other point in the state space, we can only pass through the point in a transient fashion. ∇

To find general conditions under which a linear system is reachable, we will first give a heuristic argument based on formal calculations with impulse functions. We note that if we can reach all points in the state space through some choice of input, then we can also reach all equilibrium points.

Testing for Reachability

When the initial state is zero, the response of the state to a unit step in the input is given by

$$x(t) = \int_0^t e^{A(t-\tau)} B d\tau = A^{-1}(e^{At} - I)B \quad (6.2)$$

(see equation (5.22)). The derivative of a unit step function is the impulse function, $\delta(t)$, defined in Section 5.3. Since derivatives are linear operations, it follows (see Exercise 5.1) that the response of the system to an impulse function is the derivative of equation (6.2):

$$\frac{dx}{dt} = e^{At} B.$$

Similarly we find that the response to the derivative of a impulse function is

$$\frac{d^2x}{dt^2} = A e^{At} B.$$

Continuing this process and using the linearity of the system, the input

$$u(t) = \alpha_1 \delta(t) + \alpha_2 \dot{\delta}(t) + \alpha_3 \ddot{\delta}(t) + \cdots + \alpha_n \delta^{(n-1)}(t)$$

gives the state

$$x(t) = \alpha_1 e^{At} B + \alpha_2 A e^{At} B + \alpha_3 A^2 e^{At} B + \cdots + \alpha_n A^{n-1} e^{At} B.$$

Taking the limit as t goes to zero through positive values we get

$$x(0+) = \alpha_1 B + \alpha_2 AB + \alpha_3 A^2 B + \cdots + \alpha_n A^{n-1} B.$$

The right hand is a linear combination of the columns of the matrix

$$W_r = \begin{pmatrix} B & AB & \cdots & A^{n-1}B \end{pmatrix}. \quad (6.3)$$

To reach an arbitrary point in the state space we thus require that there are n linear independent columns of the matrix W_r . The matrix W_r is called the *reachability matrix*.

An input consisting of a sum of impulse functions and their derivatives is a very violent signal. To see that an arbitrary point can be reached with smoother signals

we can make use of the convolution equation. Assuming that the initial condition is zero, the state of a linear system is given by

$$x(t) = \int_0^t e^{A(t-\tau)} Bu(\tau) d\tau = \int_0^t e^{A\tau} Bu(t-\tau) d\tau.$$

It follows from the theory of matrix functions, specifically the Cayley-Hamilton theorem (see Exercise 6.10) that

$$e^{A\tau} = I\alpha_0(\tau) + A\alpha_1(\tau) + \cdots + A^{n-1}\alpha_{n-1}(\tau),$$

where $\alpha_i(\tau)$ are scalar functions, and we find that

$$\begin{aligned} x(t) = B \int_0^t \alpha_0(\tau) u(t-\tau) d\tau + AB \int_0^t \alpha_1(\tau) u(t-\tau) d\tau + \\ \cdots + A^{n-1}B \int_0^t \alpha_{n-1}(\tau) u(t-\tau) d\tau. \end{aligned}$$

Again we observe that the right hand side is a linear combination of the columns of the reachability matrix W_r given by equation (6.3). This basic approach leads to the following theorem.

Theorem 6.1. *A linear system is reachable if and only if the reachability matrix W_r is invertible.*

The formal proof of this theorem is beyond the scope of this text, but follows along the lines of the sketch above and can be found in most books on linear control theory, such as [46, 128]. We illustrate the concept of reachability with the following example.

Example 6.2 Reachability of balance systems

Consider the balance system introduced in Example 2.1 and shown in Figure 6.2. Recall that this system is a model for a class of examples in which the center of mass is balanced above a pivot point. One example is the Segway transportation system shown in the left portion of the figure, for which a natural question to ask is whether we can move from one stationary point to another by appropriate application of forces through the wheels.

The nonlinear equations of motion for the system are given in equation (2.9) and repeated here:

$$\begin{aligned} (M+m)\ddot{p} - ml \cos \theta \ddot{\theta} &= -c\dot{p} - ml \sin \theta \dot{\theta}^2 + F \\ (J+ml^2)\ddot{\theta} - ml \cos \theta \ddot{p} &= -\gamma\dot{\theta} + mgl \sin \theta, \end{aligned} \tag{6.4}$$

For simplicity, we take $c = \gamma = 0$. Linearizing around the equilibrium point $x_e =$

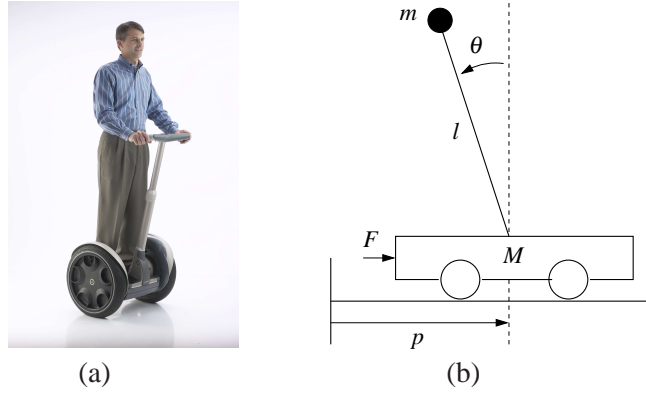


Figure 6.2: Balance system. The Segway human transportation system shown on the left is an example of a balance system which uses torque applied to the wheels to keep the rider upright. A simplified diagram for a balance system is shown on the right. The system consists of a mass m on a rod of length l connected by a pivot to a cart with mass M .

$(p, 0, 0, 0)$, the dynamics matrix and the control matrix are

$$A = \begin{pmatrix} 0 & 0 & 1 & 0 \\ 0 & 0 & 0 & 1 \\ 0 & \frac{m^2 l^2 g}{M_t J_t - m^2 l^2} & 0 & 0 \\ 0 & \frac{M_t m g l}{M_t J_t - m^2 l^2} & 0 & 0 \end{pmatrix} \quad B = \begin{pmatrix} 0 \\ 0 \\ \frac{J_t}{M_t J_t - m^2 l^2} \\ \frac{lm}{M_t J_t - m^2 l^2} \end{pmatrix},$$

where $M_t = M + m$ and $J_t = J + ml^2$. The reachability matrix is

$$W_r = \begin{pmatrix} 0 & \frac{J_t}{M_t J_t - m^2 l^2} & 0 & \frac{gl^3 m^3}{(M_t J_t - m^2 l^2)^2} \\ 0 & \frac{lm}{M_t J_t - m^2 l^2} & 0 & \frac{gl^2 m^2 (m+M)}{(M_t J_t - m^2 l^2)^2} \\ \frac{J_t}{M_t J_t - m^2 l^2} & 0 & \frac{gl^3 m^3}{(M_t J_t - m^2 l^2)^2} & 0 \\ \frac{lm}{M_t J_t - m^2 l^2} & 0 & \frac{g^2 l^2 m^2 (m+M)}{(M_t J_t - m^2 l^2)^2} & 0 \end{pmatrix}. \quad (6.5)$$

This matrix has determinant

$$\det(W_r) = \frac{g^2 l^4 m^4}{(M_t J_t - m^2 l^2)^4} \neq 0$$

and we can conclude that the system is reachable. This implies that we can move the system from any initial state to any final state and, in particular, that we can always find an input to bring the system from an initial state to an equilibrium point. ∇

It is useful to have an intuitive understanding of the mechanisms that make a system unreachable. An example of such a system is given in Figure 6.3. The system consists of two identical systems with the same input. Clearly, we can not

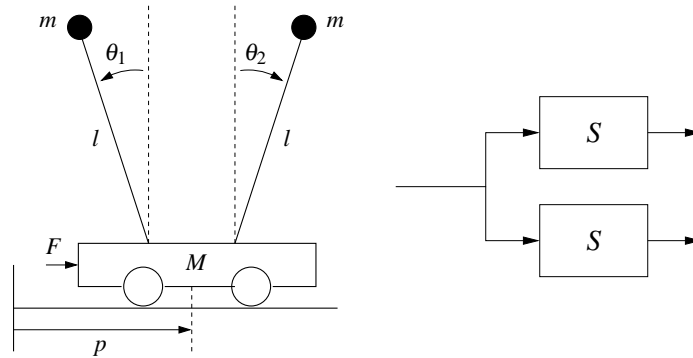


Figure 6.3: A unreachable system. The cart-pendulum system shown on the left has a single input that affects two pendula of equal length and mass. Since the forces affecting the two pendula are the same and their dynamics are identical, it is not arbitrarily control the state of the system. The figure on the right gives a block diagram representation of this situation.

separately cause the first and second system to do something different since they have the same input. Hence we cannot reach arbitrary states and so the system is not reachable (Exercise 6.3).

More subtle mechanisms for non-reachability can also occur. For example, if there is a linear combination of states that always remains constant, then the system is not reachable. To see this, suppose that there exists a row vector H such that

$$0 = \frac{d}{dt} Hx = H(Ax + Bu) \quad \text{for all } u.$$

Then H is in the left null space of both A and B and it follows that

$$HW_r = H \begin{pmatrix} B & AB & \cdots & A^{n-1}B \end{pmatrix} = 0.$$

Hence the reachability matrix is not full rank. In this case, if we have an initial condition x_0 and we wish to reach a state x_f for which $Hx_0 \neq Hx_f$, then since $Hx(t)$ is constant, no input u can move from x_0 to x_f .

Reachable Canonical Form

As we have already seen in previous chapters, it is often convenient to change coordinates and write the dynamics of the system in the transformed coordinates $z = Tx$. One application of a change of coordinates is to convert a system into a canonical form in which it is easy to perform certain types of analysis.

A linear state space system is in *reachable canonical form* if its dynamics are

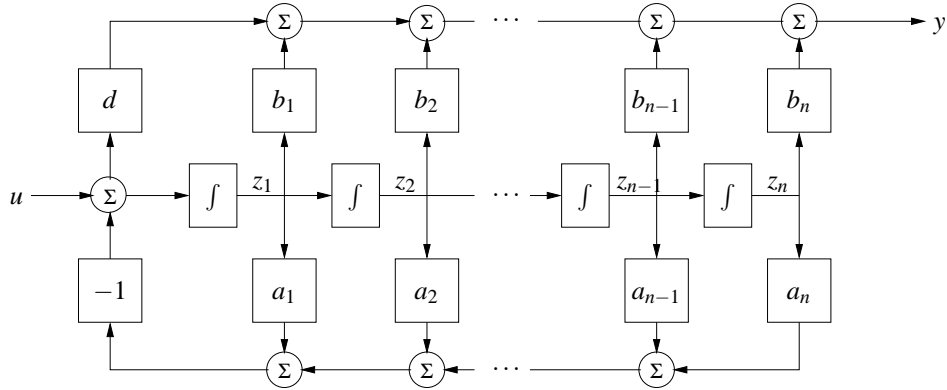


Figure 6.4: Block diagram for a system in reachable canonical form. The individual states of the system are represented by a chain of integrators whose input depends on the weighted values of the states. The output is given by an appropriate combination of the system input and other states.

given by

$$\frac{dz}{dt} = \begin{pmatrix} -a_1 & -a_2 & -a_3 & \dots & -a_n \\ 1 & 0 & 0 & \dots & 0 \\ 0 & 1 & 0 & \dots & 0 \\ \vdots & & \ddots & \ddots & \vdots \\ 0 & & & 1 & 0 \end{pmatrix} z + \begin{pmatrix} 1 \\ 0 \\ 0 \\ \vdots \\ 0 \end{pmatrix} u \quad (6.6)$$

$$y = \begin{pmatrix} b_1 & b_2 & b_3 & \dots & b_n \end{pmatrix} z + du.$$

A block diagram for a system in reachable canonical form is shown in Figure 6.4. We see that the coefficients that appear in the A and B matrices show up directly in the block diagram. Furthermore, the output of the system is a simple linear combination of the outputs of the integration blocks.

The characteristic polynomial for a system in reachable canonical form is given by

$$\lambda(s) = s^n + a_1 s^{n-1} + \dots + a_{n-1} s + a_n. \quad (6.7)$$

The reachability matrix also has a relatively simple structure:

$$W_r = \begin{pmatrix} B & AB & \dots & A^{n-1}B \end{pmatrix} = \begin{pmatrix} 1 & -a_1 & a_1^2 - a_2 & \dots & * \\ 0 & 1 & -a_1 & \dots & * \\ \vdots & \vdots & \ddots & \ddots & \vdots \\ 0 & 0 & 0 & 1 & * \\ 0 & 0 & 0 & \dots & 1 \end{pmatrix},$$

where $*$ indicates a possibly nonzero term. This matrix is full rank since no column can be written as a linear combination of the others due to the triangular structure of the matrix.

We now consider the problem of changing coordinates such that the dynamics of a

system can be written in reachable canonical form. Let A, B represent the dynamics of a given system and \tilde{A}, \tilde{B} be the dynamics in reachable canonical form. Suppose that we wish to transform the original system into reachable canonical form using a coordinate transformation $z = Tx$. As shown in the last chapter, the dynamics matrix and the control matrix for the transformed system are

$$\tilde{A} = TAT^{-1}, \quad \tilde{B} = TB.$$

The reachability matrix for the transformed system then becomes

$$\tilde{W}_r = \begin{pmatrix} \tilde{B} & \tilde{A}\tilde{B} & \cdots & \tilde{A}^{n-1}\tilde{B} \end{pmatrix}.$$

Transforming each element individually, we have

$$\begin{aligned} \tilde{A}\tilde{B} &= TAT^{-1}TB = TAB \\ \tilde{A}^2\tilde{B} &= (TAT^{-1})^2TB = TAT^{-1}TAT^{-1}TB = TA^2B \\ &\vdots \\ \tilde{A}^n\tilde{B} &= TA^nB. \end{aligned}$$

and hence the reachability matrix for the transformed system is

$$\tilde{W}_r = T \begin{pmatrix} B & AB & \cdots & A^{n-1}B \end{pmatrix} = TW_r. \quad (6.8)$$

Since W_r is invertible, we can thus solve for the transformation T that takes the system into reachable canonical form:

$$T = \tilde{W}_r W_r^{-1}.$$

The following example illustrates the approach.

Example 6.3 Transformation to reachable form

Consider a simple two dimensional system of the form

$$\dot{x} = \begin{pmatrix} \alpha & \omega \\ -\omega & \alpha \end{pmatrix} x + \begin{pmatrix} 0 \\ 1 \end{pmatrix} u.$$

We wish to find the transformation that converts the system into reachable canonical form:

$$\tilde{A} = \begin{pmatrix} -a_1 & -a_2 \\ 1 & 0 \end{pmatrix} \quad \tilde{B} = \begin{pmatrix} 1 \\ 0 \end{pmatrix}.$$

The coefficients a_1 and a_2 can be determined from the characteristic equation for the original system:

$$\lambda(s) = \det(sI - A) = s^2 - 2\alpha s + (\alpha^2 + \omega^2) \quad \implies \begin{aligned} a_1 &= -2\alpha \\ a_2 &= \alpha^2 + \omega^2. \end{aligned}$$

The reachability matrix for each system is

$$W_r = \begin{pmatrix} 0 & \omega \\ 1 & \alpha \end{pmatrix} \quad \tilde{W}_r = \begin{pmatrix} 1 & -a_1 \\ 0 & 1 \end{pmatrix}.$$

The transformation T becomes

$$T = \tilde{W}_r W_r^{-1} = \begin{pmatrix} -d \frac{a_1 + \alpha}{\omega} & 1 \\ \frac{1}{\omega} & 0 \end{pmatrix} = \begin{pmatrix} \frac{\alpha}{\omega} & 1 \\ \frac{1}{\omega} & 0 \end{pmatrix}$$

and hence the coordinates

$$\begin{pmatrix} z_1 \\ z_2 \end{pmatrix} = Tx = \begin{pmatrix} \frac{\alpha}{\omega} x_1 + x_2 \\ x_2 \end{pmatrix}$$

put the system in reachable canonical form. ∇

We summarize the results of this section in the following theorem.

Theorem 6.2. *Let A and B be the dynamics and control matrices for a reachable system. Then there exists a transformation $z = Tx$ such that in the transformed coordinates the dynamics and control matrices are in reachable canonical form (6.6) and the characteristic polynomial for A is given by*

$$\det(sI - A) = s^n + a_1 s^{n-1} + \cdots + a_{n-1} s + a_n.$$

One important implication of this theorem is that for any reachable system, we can always assume without loss of generality that the coordinates are chosen such that the system is in reachable canonical form. This is particularly useful for proofs, as we shall see later in this chapter. However, for high order systems, small changes in the coefficients a_i can give large changes of the eigenvalues. Hence, the reachable canonical form is not always well conditioned and must be used with some care.

6.2 STABILIZATION BY STATE FEEDBACK

The state of a dynamical system is a collection of variables that permits prediction of the future development of a system. We now explore the idea of designing the dynamics a system through feedback of the state. We will assume that the system to be controlled is described by a linear state model and has a single input (for simplicity). The feedback control will be developed step by step using one single idea: the positioning of closed loop eigenvalues in desired locations.

State Space Controller Structure

Figure 6.5 shows a diagram of a typical control system using state feedback. The full system consists of the process dynamics, which we take to be linear, the controller elements, K and k_r , the reference input, r , and processes disturbances, d . The goal of the feedback controller is to regulate the output of the system, y , such that it tracks the reference input in the presence of disturbances and also uncertainty in the process dynamics.

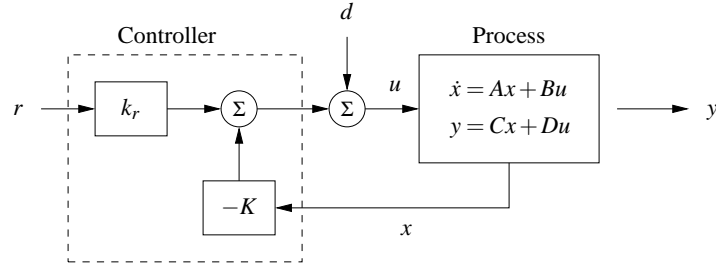


Figure 6.5: A feedback control system with state feedback. The controller uses the system state x and the reference input r to command the process through its input u . We model disturbances via the additive input d .

An important element of the control design is the performance specification. The simplest performance specification is that of stability: in the absence of any disturbances, we would like the equilibrium point of the system to be asymptotically stable. More sophisticated performance specifications typically involve giving desired properties of the step or frequency response of the system, such as specifying the desired rise time, overshoot and settling time of the step response. Finally, we are often concerned with the disturbance rejection properties of the system: to what extent can we tolerate disturbance inputs d and still hold the output y near the desired value?

Consider a system described by the linear differential equation

$$\frac{dx}{dt} = Ax + Bu, \quad y = Cx + Du, \quad (6.9)$$

where we have ignored the disturbance signal d for now. Our goal is to drive the output y to a given reference value, r , and hold it there.

We begin by assuming that all components of the state vector are measured. Since the state at time t contains all information necessary to predict the future behavior of the system, the most general time invariant control law is a function of the state and the reference input:

$$u = \alpha(x, r).$$

If the feedback is restricted to be a linear, it can be written as

$$u = -Kx + k_r r, \quad (6.10)$$

where r is the reference value, assumed for now to be a constant.

This control law corresponds to the structure shown in Figure 6.5. The negative sign is a convention to indicate that negative feedback is the normal situation. The closed loop system obtained when the feedback (6.10) is applied to the system (6.9) is given by

$$\frac{dx}{dt} = (A - BK)x + Bk_r r. \quad (6.11)$$

We attempt to determine the feedback gain K so that the closed loop system has

the characteristic polynomial

$$p(s) = s^n + p_1s^{n-1} + \cdots + p_{n-1}s + p_n. \quad (6.12)$$

This control problem is called the eigenvalue assignment problem or “pole placement” problem (we will define “poles” more formally in a later chapter).

Note that the k_r does not affect the stability of the system (which is determined by the eigenvalues of $A - BK$), but does affect the steady state solution. In particular, the equilibrium point and steady state output for the closed loop system are given by

$$x_e = -(A - BK)^{-1}Bk_r r \quad y_e = Cx_e + Du_e,$$

hence k_r should be chosen such that $y_e = r$ (the desired output value). Since k_r is a scalar, we can easily solve to show that if $D = 0$ (the most common case).

$$k_r = -1/(C(A - BK)^{-1}B). \quad (6.13)$$

Notice that k_r is exactly the inverse of the zero frequency gain of the closed loop system. The solution for $D \neq 0$ is left as an exercise.

Using the gains K and k_r , we are thus able to design the dynamics of the closed loop system to satisfy our goal. To illustrate how to construct such a state feedback control law, we begin with a few examples that provide some basic intuition and insights.

Example 6.4 Vehicle steering

In Example 5.12 we derived a normalized linear model for vehicle steering. The dynamics describing the lateral deviation where given by

$$\begin{aligned} A &= \begin{pmatrix} 0 & 1 \\ 0 & 0 \end{pmatrix} & B &= \begin{pmatrix} \gamma \\ 1 \end{pmatrix} \\ C &= \begin{pmatrix} 1 & 0 \end{pmatrix} & D &= 0. \end{aligned}$$

The reachability matrix for the system is thus

$$W_r = \begin{pmatrix} B & AB \end{pmatrix} = \begin{pmatrix} \gamma & 1 \\ 1 & 0 \end{pmatrix}.$$

The system is reachable since $\det W_r = -1 \neq 0$.

We now want to design a controller that stabilizes the dynamics and tracks a given reference value r of the lateral position of the vehicle. To do this we introduce the feedback

$$u = -Kx + k_r r = -k_1x_1 - k_2x_2 + k_r r,$$

and the closed loop system becomes

$$\begin{aligned} \frac{dx}{dt} &= (A - BK)x + Bk_r r = \begin{pmatrix} -\gamma k_1 & 1 - \gamma k_2 \\ -k_1 & -k_2 \end{pmatrix} x + \begin{pmatrix} \gamma k_r \\ k_r \end{pmatrix} r \\ y &= Cx + Du = \begin{pmatrix} 1 & 0 \end{pmatrix} x. \end{aligned} \quad (6.14)$$

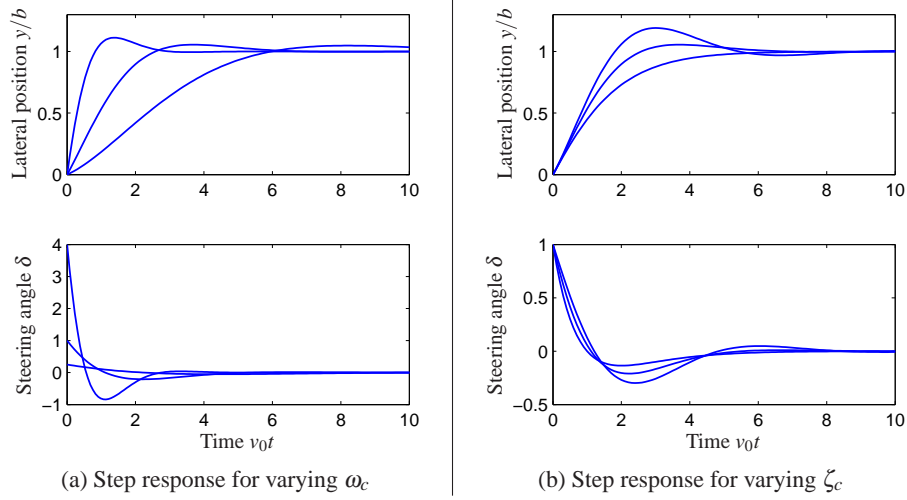


Figure 6.6: State feedback control of a steering system. Step responses obtained with controllers designed with $\zeta_c = 0.7$ and $\omega_c = 0.5, 1$ and 2 [rad/s] are shown in (a). Notice that response speed increases with increasing ω_c , but that large ω_c also give large initial control actions. Step responses obtained with controller designed with $\omega_c = 1$ and $\zeta_c = 0.5, 0.7$ and 1 are shown in (b).

The closed loop system has the characteristic polynomial

$$\det(sI - A + BK) = \det \begin{pmatrix} s + \gamma k_1 & \gamma k_2 - 1 \\ k_1 & s + k_2 \end{pmatrix} = s^2 + (\gamma k_1 + k_2)s + k_1.$$

Suppose that we would like to use feedback to design the dynamics of the system to have the characteristic polynomial

$$p(s) = s^2 + 2\zeta_c \omega_c s + \omega_c^2.$$

Comparing this polynomial with the characteristic polynomial of the closed loop system we see that the feedback gains should be chosen as

$$k_1 = \omega_c^2 \quad k_2 = 2\zeta_c \omega_c - \gamma \omega_c^2.$$

Equation (6.13) gives $k_r = k_1 = \omega_c^2$, and the control law can be written as

$$u = k_1(r - x_1) - k_2 x_2 = \omega_c^2(r - x_1) - (2\zeta_c \omega_c - \gamma \omega_c^2)x_2.$$

The step responses for the closed loop system for different values of the design parameters are shown in Figure 6.6. The effect of ω_c is shown in Figure 6.6a, which shows that the response speed increases with increasing ω_c . The responses for $\omega_c = 0.5$ and 1 have reasonable overshoot. The settling time is about 15 car lengths for $\omega_c = 0.5$ (beyond the end of the plot) and decreases to about 6 car lengths for $\omega_c = 1$. The control signal δ is large initially and goes to zero as time increases because the controller has an integrator. The initial value of the control signal is $k_r = \omega_c^2 r$ and thus the achievable response time is limited by the available

actuator signal. Notice in particular the dramatic increase in control signal when ω_c changes from 1 to 2. The effect of ζ_c is shown in Figure 6.6b. The response speed and the overshoot increase with decreasing damping. Using these plots, we conclude that reasonable values of the design parameters are to have ω_c in the range of 0.5 to 1 and $\zeta_c \approx 0.7$. ∇

The example of the vehicle steering system illustrates how state feedback can be used to set the eigenvalues of the closed loop system to arbitrary values.

State Feedback for Systems in Reachable Canonical Form

The reachable canonical form has the property that the parameters of the system are the coefficients of the characteristic equation. It is therefore natural to consider systems in this form when solving the eigenvalue assignment problem.

Consider a system in reachable canonical form, i.e.,

$$\frac{dz}{dt} = \tilde{A}z + \tilde{B}u = \begin{pmatrix} -a_1 & -a_2 & -a_3 & \cdots & -a_n \\ 1 & 0 & 0 & \cdots & 0 \\ 0 & 1 & 0 & \cdots & 0 \\ \vdots & & \ddots & \ddots & \vdots \\ 0 & & & 1 & 0 \end{pmatrix} z + \begin{pmatrix} 1 \\ 0 \\ \vdots \\ 0 \\ 0 \end{pmatrix} u \quad (6.15)$$

$$y = \tilde{C}z = \begin{pmatrix} b_1 & b_2 & \cdots & b_n \end{pmatrix} z.$$

It follows from(6.7) that the open loop system has the characteristic polynomial

$$\det(sI - A) = s^n + a_1s^{n-1} + \cdots + a_{n-1}s + a_n.$$

Before making a formal analysis we can gain some insight by investigating the block diagram of the system shown in Figure 6.4 on page 173. The characteristic polynomial is given by the parameters a_k in the figure. Notice that the parameter a_k can be changed by feedback from state x_k to the input u . It is thus straightforward to change the coefficients of the characteristic polynomial by state feedback.

Returning to equations, introducing the control law

$$u = -\tilde{K}z + k_r r = -\tilde{k}_1 z_1 - \tilde{k}_2 z_2 - \cdots - \tilde{k}_n z_n + k_r r, \quad (6.16)$$

the closed loop system becomes

$$\frac{dz}{dt} = \begin{pmatrix} -a_1 - \tilde{k}_1 & -a_2 - \tilde{k}_2 & -a_3 - \tilde{k}_3 & \cdots & -a_n - \tilde{k}_n \\ 1 & 0 & 0 & \cdots & 0 \\ 0 & 1 & 0 & \cdots & 0 \\ \vdots & & \ddots & \ddots & \vdots \\ 0 & & & 1 & 0 \end{pmatrix} z + \begin{pmatrix} k_r \\ 0 \\ 0 \\ \vdots \\ 0 \end{pmatrix} r \quad (6.17)$$

$$y = \begin{pmatrix} b_n & \cdots & b_2 & b_1 \end{pmatrix} z.$$

The feedback changes the elements of the first row of the A matrix, which corresponds to the parameters of the characteristic equation. The closed loop system

thus has the characteristic polynomial

$$s^n + (a_1 + \tilde{k}_1)s^{n-1} + (a_2 + \tilde{k}_2)s^{n-2} + \cdots + (a_{n-1} + \tilde{k}_{n-1})s + a_n + \tilde{k}_n.$$

Requiring this polynomial to be equal to the desired closed loop polynomial

$$p(s) = s^n + p_1s^{n-1} + \cdots + p_{n-1}s + p_n$$

we find that the controller gains should be chosen as

$$\tilde{k}_1 = p_1 - a_1, \quad \tilde{k}_2 = p_2 - a_2, \quad \cdots \quad \tilde{k}_n = p_n - a_n.$$

This feedback simply replaces the parameters a_i in the system (6.17) by p_i . The feedback gain for a system in reachable canonical form is thus

$$\tilde{K} = \begin{pmatrix} p_1 - a_1 & p_2 - a_2 & \cdots & p_n - a_n \end{pmatrix}. \quad (6.18)$$

To have zero frequency gain equal to unity, the parameter k_r should be chosen as

$$k_r = \frac{a_n + \tilde{k}_n}{b_n} = \frac{p_n}{b_n}. \quad (6.19)$$

Notice that it is essential to know the precise values of parameters a_n and b_n in order to obtain the correct zero frequency gain. The zero frequency gain is thus obtained by precise calibration. This is very different from obtaining the correct steady state value by integral action, which we shall see in later sections.

Eigenvalue Placement

We have seen through the examples how feedback can be used to design the dynamics of a system through assignment of its eigenvalues. To solve the problem in the general case, we simply change coordinates so that the system is in reachable canonical form. Consider the system

$$\begin{aligned} \frac{dx}{dt} &= Ax + Bu \\ y &= Cx + Du. \end{aligned} \quad (6.20)$$

We can change the coordinates by a linear transformation $z = Tx$ so that the transformed system is in reachable canonical form (6.15). For such a system the feedback is given by equation (6.16), where the coefficients are given by equation (6.18). Transforming back to the original coordinates gives the feedback

$$u = -\tilde{K}z + k_r r = -\tilde{K}Tx + k_r r.$$

The results obtained can be summarized as follows.

Theorem 6.3 (Eigenvalue assignment by state feedback). *Consider the system given by equation (6.20), with one input and one output. Let $\lambda(s) = s^n + a_1s^{n-1} + \cdots + a_{n-1}s + a_n$ be the characteristic polynomial of A . If the system is reachable then there exists a feedback*

$$u = -Kx + k_r r$$

that gives a closed loop system with the characteristic polynomial

$$p(s) = s^n + p_1s^{n-1} + \cdots + p_{n-1}s + p_n$$

and unity zero frequency gain between r and y . The feedback gain is given by

$$K = \tilde{K}T = \begin{pmatrix} p_1 - a_1 & p_2 - a_2 & \cdots & p_n - a_n \end{pmatrix} \tilde{W}_r W_r^{-1} \quad k_r = \frac{p_n}{a_n}, \quad (6.21)$$

where a_i are the coefficients of the characteristic polynomial of the matrix A and the matrices W_r and \tilde{W}_r are given by

$$W_r = \begin{pmatrix} B & AB & \cdots & A^{n-1}B \end{pmatrix}, \quad \tilde{W}_r = \begin{pmatrix} 1 & a_1 & a_2 & \cdots & a_{n-1} \\ 0 & 1 & a_1 & \cdots & a_{n-2} \\ \vdots & & \ddots & \ddots & \vdots \\ 0 & 0 & \cdots & 1 & a_1 \\ 0 & 0 & 0 & \cdots & 1 \end{pmatrix}^{-1}.$$

For simple problems, the eigenvalue assignment problem can be solved by introducing the elements k_i of K as unknown variables. We then compute the characteristic polynomial

$$\lambda(s) = \det(sI - A + BK)$$

and equate coefficients of equal powers of s to the coefficients of the desired characteristic polynomial

$$p(s) = s^n + p_1s^{n-1} + \cdots + p_{n-1} + p_n.$$

This gives a system of linear equations to determine k_i . The equations can always be solved if the system is reachable, exactly as we did in Example 6.4.

Equation (6.21), which is called Ackermann's formula [3, 4], can be used for numeric computations. It is implemented in the MATLAB function `acker`. The MATLAB function `place` is preferable for systems of high order because it is better conditioned numerically.

Example 6.5 Predator-prey

Consider the problem of regulating the population of an ecosystem by modulating the food supply. We use the predator-prey model introduced in Section 3.7. The dynamics for the system are given by

$$\begin{aligned} \frac{dH}{dt} &= (r_h + u)H \left(1 - \frac{H}{K}\right) - \frac{aHL}{1 + aHT_h} & H \geq 0 \\ \frac{dL}{dt} &= r_l L \left(1 - \frac{L}{kH}\right) & L \geq 0. \end{aligned}$$

We choose the following nominal parameters for the system, which correspond to the values used in previous simulations:

$$\begin{aligned} r_h &= 0.02 & K &= 500 & a &= 0.03 \\ r_l &= 0.01 & k &= 0.2 & T_h &= 5. \end{aligned}$$

We take the parameter r_h , corresponding to the growth rate for hares, as the input to the system, which we might modulate by controlling a food source for the hares. This is reflected in our model by the term $(r_h + u)$ in the first equation.

To control this system, we first linearize the system around the equilibrium point of the system, (H_e, L_e) , which can be determined numerically to be $H \approx (6.5, 1.3)$. This yields a linear dynamical system

$$\frac{d}{dt} \begin{pmatrix} z_1 \\ z_2 \end{pmatrix} = \begin{pmatrix} 0.001 & -0.01 \\ 0.002 & -0.01 \end{pmatrix} \begin{pmatrix} z_1 \\ z_2 \end{pmatrix} + \begin{pmatrix} 6.4 \\ 0 \end{pmatrix} v$$

where $z_1 = L - L_e$, $z_2 = H - H_e$ and $v = u$. It is easy to check that the system is reachable around the equilibrium $(z, v) = (0, 0)$ and hence we can assign the eigenvalues of the system using state feedback.

Determining the eigenvalues of the closed loop system requires balancing the ability to modulate the input against the natural dynamics of the system. This can be done by the process of trial and error or by using some of the more systematic techniques discussed in the remainder of the text. For now, we simply choose the desired closed loop poles to be at $\lambda = \{-0.01, -0.02\}$. We can then solve for the feedback gains using the techniques described earlier, which results in

$$K = \begin{pmatrix} 0.005 & -0.15 \end{pmatrix}.$$

Finally, we solve for the reference gain, k_r , using equation (6.13) to obtain $k_r = 0.003$.

Putting these steps together, our control law becomes

$$v = -Kz + k_r r.$$

In order to implement the control law, we must rewrite it using the original coordinates for the system, yielding

$$\begin{aligned} u &= u_e - K(x - x_e) + k_r(r - y_e) \\ &= \begin{pmatrix} 0.005 & -0.015 \end{pmatrix} \begin{pmatrix} H - 6.5 \\ L - 1.3 \end{pmatrix} + 0.003(r - 6.5). \end{aligned}$$

This rule tells us how much we should modulate r_h as a function of the current number of lynxes and hares in the ecosystem. Figure 6.7a shows a simulation of the resulting closed loop system using the parameters defined above and starting an initial population of 15 hares and 5 lynxes. Note that the system quickly stabilizes the population of lynxes at the reference value ($H = 20$). A phase portrait of the system is given in Figure 6.7b, showing how other initial conditions converge to the stabilized equilibrium population. Notice that the dynamics are very different than the natural dynamics (shown in Figure 3.20 on page 91). ∇

The results of this section show that we can use state feedback to design the dynamics of a system, under the strong assumption that we can measure all of the states. We shall address the availability of the states in the next chapter, when we consider output feedback and state estimation. In addition, Theorem 6.3 states that

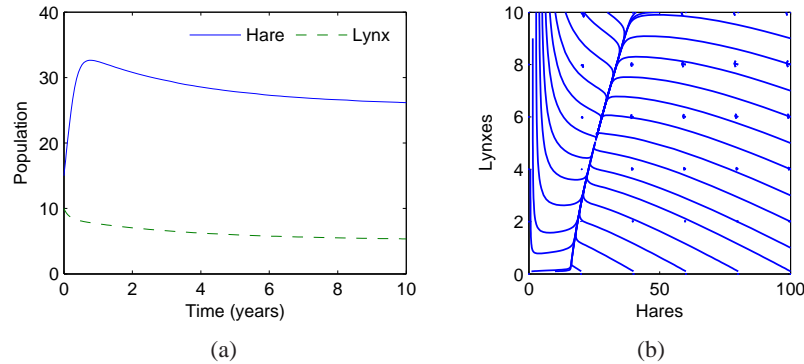


Figure 6.7: Simulation results for the controlled predator-prey system. The population of lynxes and hares as a function of time is shown in (a) and a phase portrait for the controlled system is shown in (b). Feedback is used to make the population stable at $H_e = \text{missing}$ and $L_e = \text{missing}$.

the eigenvalues can be assigned to arbitrary locations is also highly idealized and assumes that the dynamics of the process are known to high precision. The robustness of state feedback combined with state estimators is considered in Chapter 12, after we have developed the requisite tools.

6.3 STATE FEEDBACK DESIGN

The location of the eigenvalues determines the behavior of the closed loop dynamics and hence where we place the eigenvalues is the main design decision to be made. As with all other feedback design problems, there are tradeoffs between the magnitude of the control inputs, the robustness of the system to perturbations and the closed loop performance of the system. In this section we examine some of these tradeoffs, starting with the special case of second order systems.

Second Order Systems

One class of systems that occurs frequently in the analysis and design of feedback systems is second order, linear differential equations. Because of their ubiquitous nature, it is useful to apply the concepts of this chapter to that specific class of systems and build more intuition about the relationship between stability and performance.

The canonical second order system is a differential equation of the form

$$\begin{aligned} \ddot{q} + 2\zeta\omega_0\dot{q} + \omega_0^2q &= ku \\ y &= q. \end{aligned} \tag{6.22}$$

In state space form, this system can be represented as

$$\begin{aligned} \dot{x} &= \begin{pmatrix} 0 & \omega_0 \\ -\omega_0 & -2\zeta\omega_0 \end{pmatrix} x + \begin{pmatrix} 0 \\ k/\omega_0 \end{pmatrix} u \\ y &= \begin{pmatrix} 1 & 0 \end{pmatrix} x. \end{aligned} \quad (6.23)$$

The eigenvalues of this system are given by

$$\lambda = -\zeta\omega_0 \pm \sqrt{\omega_0^2(\zeta^2 - 1)}$$

and we see that the origin is a stable equilibrium point if $\omega_0 > 0$ and $\zeta > 0$. Note that the eigenvalues are complex if $\zeta < 1$ and real otherwise. Equations (6.22) and (6.23) can be used to describe many second order systems, including damped oscillators, active filters and flexible structures, as shown in the examples below.

The form of the solution depends on the value of ζ , which is referred to as the *damping factor* for the system. If $\zeta > 1$, we say that the system is *overdamped* and the natural response ($u = 0$) of the system is given by

$$y(t) = \frac{\beta x_{10} + x_{20}}{\beta - \alpha} e^{-\alpha t} - \frac{\alpha x_{10} + x_{20}}{\beta - \alpha} e^{-\beta t}$$

where $\alpha = \omega_0(\zeta + \sqrt{\zeta^2 - 1})$ and $\beta = \omega_0(\zeta - \sqrt{\zeta^2 - 1})$. We see that the response consists of the sum of two exponentially decaying signals. If $\zeta = 1$ then the system is *critically damped* and solution becomes

$$y(t) = e^{-\zeta\omega_0 t} (x_{10} + (x_{20} + \zeta\omega_0 x_{10})t).$$

Note that this is still asymptotically stable as long as $\omega_0 > 0$, although the second term in the solution is increasing with time (but more slowly than the decaying exponential that is multiplying it).

Finally, if $0 < \zeta < 1$, then the solution is oscillatory and equation (6.22) is said to be *underdamped*. The parameter ω_0 is referred to as the natural frequency of the system, stemming from the fact that for small ζ , the eigenvalues of the system are approximately $\lambda = -\zeta \pm j\omega_0$. The natural response of the system is given by

$$y(t) = e^{-\zeta\omega_0 t} \left(x_{10} \cos \omega_d t + \left(\frac{\zeta\omega_0}{\omega_d} x_{10} + \frac{1}{\omega_d} x_{20} \right) \sin \omega_d t \right),$$

where $\omega_d = \omega_0 \sqrt{1 - \zeta^2}$ is called the *damped frequency*. For $\zeta \ll 1$, $\omega_d \approx \omega_0$ defines the oscillation frequency of the solution and ζ gives the damping rate relative to ω_0 .

Because of the simple form of a second order system, it is possible to solve for the step and frequency responses in analytical form. The solution for the step

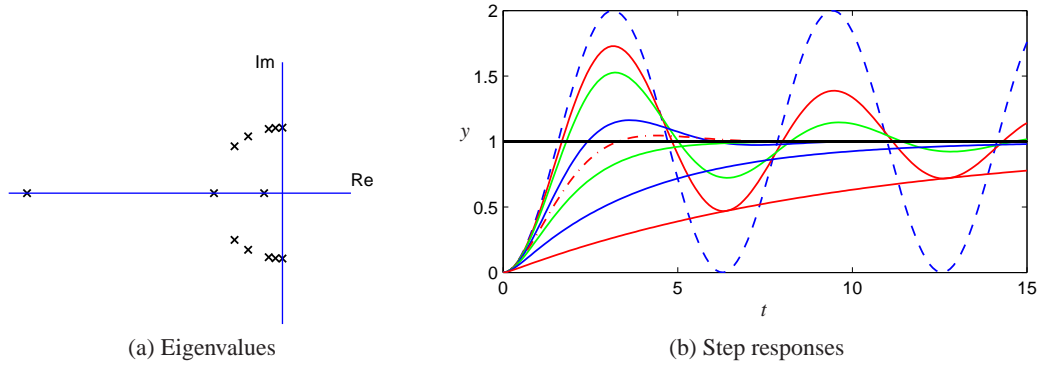


Figure 6.8: Step response for a second order system. Normalized step responses h for the system (6.23) for $\zeta = 0$ (dashed), 0.1, 0.2, 0.5, 0.707 (dash dotted), 1, 2, 5 and 10 (dotted). As the damping ratio is increased, the rise time of the system gets longer, but there is less overshoot. The horizontal axis is in scaled units $\omega_0 t$; higher values of ω_0 results in faster response (rise time and settling time).

response depends on the magnitude of ζ :

$$\begin{aligned}
 y(t) &= \frac{k}{\omega_0^2} \left(1 - e^{-\zeta\omega_0 t} \cos \omega_d t + \frac{\zeta}{\sqrt{1-\zeta^2}} e^{-\zeta\omega_0 t} \sin \omega_d t \right) & \zeta < 1 \\
 y(t) &= \frac{k}{\omega_0^2} (1 - e^{-\omega_0 t} (1 + \omega_0 t)) & \zeta = 1 \\
 y(t) &= \frac{k}{\omega_0^2} \left(1 - e^{-\omega_0 t} - \frac{1}{2(1+\zeta)} e^{\omega_0(1-2\zeta)t} \right) & \zeta > 1,
 \end{aligned} \tag{6.24}$$

where we have taken $x(0) = 0$. Note that for the lightly damped case ($\zeta < 1$) we have an oscillatory solution at frequency ω_d .

Step responses of systems with $k = \omega_0^2$ and different values of ζ are shown in Figure 6.8. The shape of the response is determined by ζ and the speed of the response is determined by ω_0 (included in the time axis scaling): the response is faster if ω_0 is larger.

In addition to the explicit form of the solution, we can also compute the properties of the step response that were defined in Section 5.3. For example, to compute the maximum overshoot for an underdamped system, we rewrite the output as

$$y(t) = \frac{k}{\omega_0^2} \left(1 - \frac{1}{\sqrt{1-\zeta^2}} e^{-\zeta\omega_0 t} \sin(\omega_d t + \varphi) \right) \tag{6.25}$$

where $\varphi = \arccos \zeta$. The maximum overshoot will occur at the first time in which

Table 6.1: Properties of the response to reference values of a second order system for $|\zeta| < 1$. The parameter $\varphi = \arccos \zeta$.

Property	Value	$\zeta = 0.5$	$\zeta = 1/\sqrt{2}$	$\zeta = 1$
Steady state value	k/ω_0^2	k/ω_0^2	k/ω_0^2	k/ω_0^2
Rise time	$T_r = 1/\omega_0 \cdot e^{\varphi/\tan \varphi}$	$1.8/\omega_0$	$2.2/\omega_0$	$2.7/\omega_0$
Overshoot	$M_p = e^{-\pi\zeta/\sqrt{1-\zeta^2}}$	16%	4%	0%
Settling time (2%)	$T_s \approx 4/\zeta\omega_0$	$8.0/\omega_0$	$5.9/\omega_0$	$5.8/\omega_0$

the derivative of y is zero, and hence we look for the time t_p at which

$$0 = \frac{k}{\omega_0^2} \left(\frac{\zeta \omega_0}{\sqrt{1-\zeta^2}} e^{-\zeta \omega_0 t} \sin(\omega_d t + \varphi) - \frac{\omega_d}{\sqrt{1-\zeta^2}} e^{-\zeta \omega_0 t} \cos(\omega_d t + \varphi) \right). \quad (6.26)$$

Eliminating the common factors, we are left with

$$\tan(\omega_d t_p + \varphi) = \frac{\sqrt{1-\zeta^2}}{\zeta}.$$

Since $\varphi = \arccos \zeta$, it follows that we must have $\omega_d t_p = \pi$ (for the first non-trivial extremum) and hence $t_p = \pi/\omega_d$. Substituting this back into equation (6.25), subtracting off the steady state value and normalizing, we have

$$M_p = e^{-\pi\zeta/\sqrt{1-\zeta^2}}.$$

Similar computations can be done for the other characteristics of a step response. Table 6.1 summarizes the calculations.

The frequency response for a second order system can also be computed explicitly and is given by

$$M e^{j\theta} = \frac{k}{(i\omega)^2 + 2\zeta\omega_0(i\omega) + \omega_0^2} = \frac{k}{\omega_0^2 - \omega^2 + 2i\zeta\omega_0\omega}.$$

A graphical illustration of the frequency response is given in Figure 6.9. Notice the resonance peak that increases with decreasing ζ . The peak is often characterized by its Q -value, defined as $Q = 1/2\zeta$. The properties of the frequency response for a second order system are summarized in Table 6.2.

Example 6.6 Drug administration

To illustrate the usage of these formulas, consider the two-compartment model for

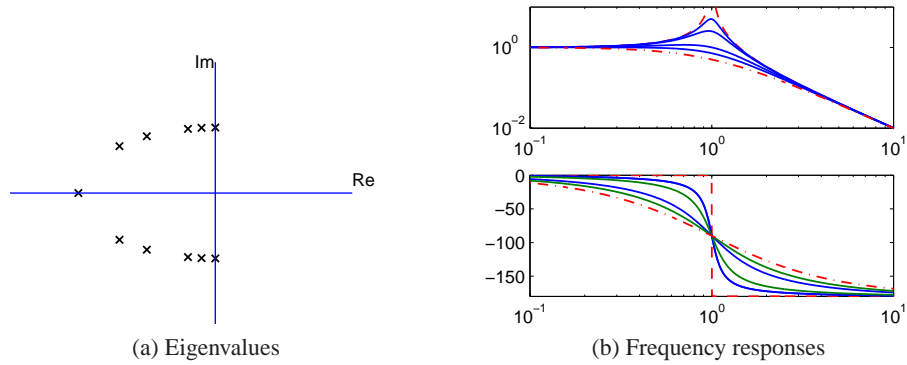


Figure 6.9: Frequency response of a second order system (6.23). The upper curve shows the gain ratio, M , and the lower curve shows the phase shift, θ . The parameters is Bode plot of the system with $\zeta = 0$ (dashed), 0.1, 0.2, 0.5, 0.7 and 1.0 (dashed-dot).

drug administration, described in Section 3.6. The dynamics of the system are

$$\begin{aligned} \frac{dc}{dt} &= \begin{pmatrix} -k_0 - k_1 & k_1 \\ k_2 & -k_2 \end{pmatrix} c + \begin{pmatrix} b_0 \\ 0 \end{pmatrix} u \\ y &= \begin{pmatrix} 0 & 1 \end{pmatrix} x, \end{aligned}$$

where c_1 and c_2 are the concentrations of the drug in each compartment, $k_i, i = 0, \dots, 2$ and b are parameters of the system, u is the flow rate of the drug into compartment 1 and y is the concentration of the drug in compartment 2. We assume that we can measure the concentrations of the drug in each compartment and we would like to design a feedback law to maintain the output at a given reference value r .

We choose $\zeta = 0.9$ to minimize the overshoot and choose the rise time to be $T_r = 10$ min. Using the formulas in Table 6.1 this gives a value for $\omega_0 = 0.22$. We can now compute the gain to place the eigenvalues at this location. Setting $u = -Kx + k_r r$, the closed loop eigenvalues for the system satisfy

$$\lambda(s) = -0.198 \pm 0.0959i$$

Table 6.2: Properties of the frequency response for a second order system with $|\zeta| < 1$.

Property	Value	$\zeta = 0.1$	$\zeta = 0.5$	$\zeta = 1/\sqrt{2}$
Zero frequency gain	M_0	k/ω_0^2	k/ω_0^2	k/ω_0^2
Bandwidth	ω_b	$1.54\omega_0$	$1.27\omega_0$	ω_0
Resonant peak gain	M_r	$1.54k/\omega_0^2$	$1.27k/\omega_0^2$	k/ω_0^2
Resonant frequency	ω_{mr}	ω_0	$0.707\omega_0$	0

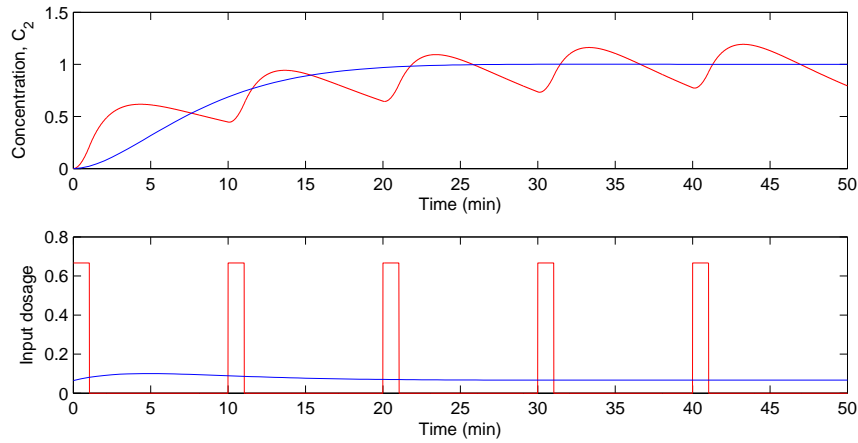


Figure 6.10: Open loop versus closed loop drug administration. Comparison between drug administration using a sequence of doses versus continuously monitoring the concentrations and adjusting the dosage continuously. In each case, the concentration is (approximately) maintained at the desired level, but the closed loop system has substantially less variability in the drug concentration.

Choose $k_1 = -0.2027$ and $k_2 = 0.2005$ gives the desired closed loop behavior. Equation 6.13 gives the reference gain $k_r = 0.0645$. The response of the controller is shown in Figure 6.10 and compared with an “open loop” strategy involving administering periodic doses of the drug. ∇

Higher Order Systems

Our emphasis so far has only considered second order systems. For higher order systems, eigenvalue assignment is considerably more difficult, especially when trying to account for the many tradeoffs that are present in a feedback design.

One of the other reasons why second order systems play such an important role in feedback systems is that even for more complicated systems the response is often characterized by the “dominant eigenvalues”. To define these more precisely, consider a system with eigenvalues λ_i , $i = 1, \dots, n$. We define the damping factor for a complex eigenvalue λ to be

$$\zeta = \frac{-\operatorname{Re} \lambda}{|\lambda|}.$$

We say that a complex conjugate pair of eigenvalues λ, λ^* is a *dominant pair* if it has the lowest damping factor compared with all other eigenvalues of the system.

Assuming that a system is stable, the dominant pair of eigenvalues tends to be the most important element of the response. To see this, assume that we have a system in Jordan form with a simple Jordan block corresponding to the dominant

pair of eigenvalues:

$$\dot{z} = \begin{pmatrix} \lambda & & & & \\ & \lambda^* & & & \\ & & J_2 & & \\ & & & \ddots & \\ & & & & J_k \end{pmatrix} z + Bu$$

$$y = Cz.$$

(Note that the state z may be complex due to the Jordan transformation.) The response of the system will be a linear combination of the responses from each of the individual Jordan subsystems. As we see from Figure 6.8, for $\zeta < 1$ the subsystem with the slowest response is precisely the one with the smallest damping factor. Hence when we add the responses from each of the individual subsystems, it is the dominant pair of eigenvalues that will be the primary factor after the initial transients due to the other terms in the solution die out. While this simple analysis does not always hold (for example, if some non-dominant terms have larger coefficients due to the particular form of the system), it is often the case that the dominant eigenvalues determine the (step) response of the system.

The only formal requirement for eigenvalue placement is that the system is reachable. In practice there are many other constraints because the selection of eigenvalues has strong effect on the magnitude and rate of change of the control signal. Large eigenvalues will in general require large control signals as well as fast changes of the signals. The capability of the actuators will therefore impose constraints on the possible location of closed loop eigenvalues. These issues will be discussed in depth in Chapters 11 and 12.

We illustrate some of the main ideas using the balance system as an example.

Example 6.7 Balance system

Consider the problem of stabilizing a balance system, whose dynamics were given in Example 6.2. The dynamics are given by

$$A = \begin{pmatrix} 0 & 0 & 1 & 0 \\ 0 & 0 & 0 & 1 \\ 0 & \frac{m^2 l^2 g}{M_t J_t - m^2 l^2} & \frac{-c J_t}{M_t J_t - m^2 l^2} & \frac{-\gamma l m}{M_t J_t - m^2 l^2} \\ 0 & \frac{M_t m g l}{M_t J_t - m^2 l^2} & \frac{-c l m}{M_t J_t - m^2 l^2} & \frac{-\gamma J_t}{M_t J_t - m^2 l^2} \end{pmatrix} \quad B = \begin{pmatrix} 0 \\ 0 \\ \frac{J_t}{M_t J_t - m^2 l^2} \\ \frac{l m}{M_t J_t - m^2 l^2} \end{pmatrix},$$

where $M_t = M + m$, $J_t = J + m l^2$ and we have left c and γ non-zero. We use the following parameters for the system (corresponding roughly to a human being balanced on a stabilizing cart):

$$\begin{array}{llll} M = 10 \text{ kg} & m = 80 \text{ kg} & c = 0.1 \text{ N s/m} & g = 9.8 \text{ m/s}^2 \\ J = 100 \text{ kg m}^2/\text{s}^2 & l = 1 \text{ m} & \gamma = 0.01 \text{ N m s} & \end{array}$$

The eigenvalues of the open loop dynamics are given by $\lambda \approx 0, 4.7, -1.9 \pm 2.7$.

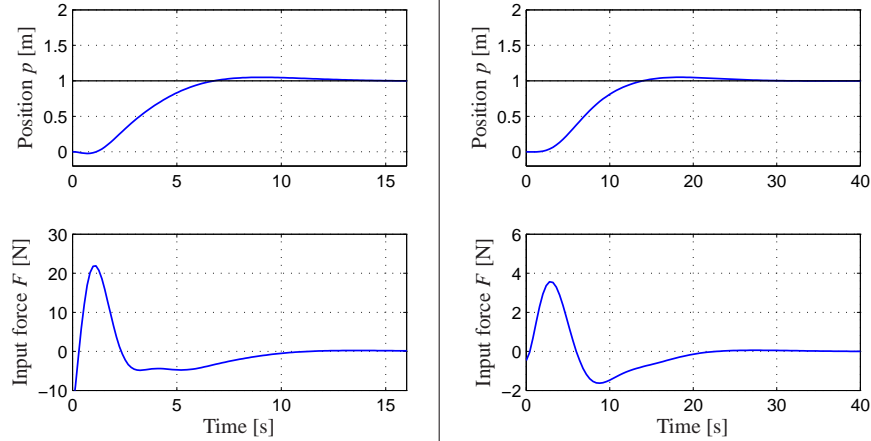


Figure 6.11: State feedback control of a balance system. The step response of a controller designed to give fast performance is shown in (a). Although the response characteristics (top left) look very good, the input magnitude (bottom left) is very large. A less aggressive controller is shown in (b). Here the response time is slowed down, but the input magnitude is much more reasonable. Both step responses are applied to the linearized dynamics.

We have verified already in Example 6.2 that the system is reachable and hence we can use state feedback to stabilize the system and provide a desired level of performance.

To decide where to place the closed loop eigenvalues, we note that the closed loop dynamics will roughly consist of two components: a set of fast dynamics that stabilize the pendulum in the inverted position and a set of slower dynamics that will control the position of the cart. For the fast dynamics, we look to the natural period of the pendulum (in the hanging down position), which is given by $\omega_0 = \sqrt{mgl/(J + ml^2)} \approx 2.1$ rad/s. To provide a fast response we choose a damping ratio of $\zeta = 0.5$ and try to place the first pair of poles at $\lambda_{1,2} \approx -\zeta\omega_0 \pm \omega_0 \approx -1 \pm 2i$, where we have used the approximation that $\sqrt{1 - \zeta^2} \approx 1$. For the slow dynamics, we choose the damping ratio to be 0.7 to provide small overshoot and choose the natural frequency to be 0.5 to give a rise time of approximately 5 seconds. This gives eigenvalues $\lambda_{3,4} = -0.35 \pm 0.35i$.

The controller consists of a feedback on the state and a feedforward gain for the reference input. The feedback gain is given by

$$K = \begin{pmatrix} -18.8 & 4500 & 597 & -876 \end{pmatrix},$$

which can be computed using Theorem 6.3 or using the MATLAB `place` command. The feedforward gain is $k_r = -1/(C(A - BK)^{-1}B) = -15.5$. The step response for the resulting controller (applied to the linearized system) is given in Figure 6.11a. While the step response gives the desired characteristics, the input required (bottom left) is excessively large, almost three times the force of gravity

at its peak.

To provide a more realistic response, we can redesign the controller to have slower dynamics. We see that the peak of the input force occurs at the fast time scale and hence we choose to slow this down by a factor of 3, leaving the damping ratio unchanged. We also slow down second set of eigenvalues, with the intuition that we should move the position of the cart more slowly than we stabilize the pendulum dynamics. Leaving the damping ratio for the slow dynamics unchanged at 0.7 and changing the frequency to 1 (corresponding to a rise time of approximately 10 seconds), the desired eigenvalues become

$$\lambda = \{-0.33 \pm 0.66i, -0.175 \pm 0.18i\}$$

The performance of the resulting controller is shown in Figure 6.11b. ∇

As we see from this example, it can be difficult to reason about where to place the eigenvalues using state feedback. This is one of the principle limitations of this approach, especially for systems of higher dimension. Optimal control techniques, such as the linear quadratic regular problem discussed next, are one approach that is available. One can also focus on the frequency response for performing the design, which is the subject of Chapters 8–12.

Linear Quadratic Regulators

In addition to selecting the closed loop eigenvalue locations to accomplish a certain objective, another way that the gains for a state feedback controller can be chosen is by attempting to optimize a cost function. This can be particularly useful in helping balance the performance of the system with the magnitude of the inputs required to achieve that level of performance.

The infinite horizon, linear quadratic regulator (LQR) problem is one of the most common optimal control problems. Given a multi-input linear system

$$\dot{x} = Ax + Bu \quad x \in \mathbb{R}^n, u \in \mathbb{R}^p,$$

we attempt to minimize the quadratic cost function

$$\tilde{J} = \int_0^{\infty} (x^T Q_x x + u^T Q_u u) dt$$

where $Q_x \geq 0$ and $Q_u > 0$ are symmetric, positive (semi-) definite matrices of the appropriate dimension. This cost function represents a tradeoff between the distance of the state from the origin and the cost of the control input. By choosing the matrices Q_x and Q_u , we can balance the rate of convergence of the solutions with the cost of the control.

The solution to the LQR problem is given by a linear control law of the form

$$u = -Q_u^{-1} B^T P x$$

where $P \in \mathbb{R}^{n \times n}$ is a positive definite, symmetric matrix that satisfies the equation

$$PA + A^T P - PBQ_u^{-1} B^T P + Q_x = 0. \quad (6.27)$$

Equation (6.27) is called the *algebraic Riccati equation* and can be solved numerically (for example, using the `lqr` command in MATLAB).

One of the key questions in LQR design is how to choose the weights Q_x and Q_u . To guarantee that a solution exists, we must have $Q_x \geq 0$ and $Q_u > 0$. In addition, there are certain “observability” conditions on Q_x that limit its choice. We assume here $Q_x > 0$ to ensure that solutions to the algebraic Riccati equation always exist.

To choose specific values for the cost function weights Q_x and Q_u , we must use our knowledge of the system we are trying to control. A particularly simple choice is to use diagonal weights

$$Q_x = \begin{pmatrix} q_1 & & 0 \\ & \ddots & \\ 0 & & q_n \end{pmatrix} \quad Q_u = \rho \begin{pmatrix} r_1 & & 0 \\ & \ddots & \\ 0 & & r_n \end{pmatrix}.$$

For this choice of Q_x and Q_u , the individual diagonal elements describe how much each state and input (squared) should contribute to the overall cost. Hence, we can take states that should remain small and attach higher weight values to them. Similarly, we can penalize an input versus the states and other inputs through choice of the corresponding input weight ρ .

Example 6.8 Vectored thrust aircraft

Consider the original dynamics of the system (2.26), written in state space form as

$$\frac{d\xi}{dt} = \begin{pmatrix} \ddot{\xi}_4 \\ \ddot{\xi}_5 \\ \ddot{\xi}_6 \\ -g \sin \theta - \frac{c}{m} \dot{\xi}_1 \\ -g \cos \theta - \frac{c}{m} \dot{\xi}_2 \\ 0 \end{pmatrix} + \begin{pmatrix} 0 \\ 0 \\ 0 \\ \frac{1}{m} \cos \theta F_1 - \frac{1}{m} \sin \theta F_2 \\ \frac{1}{m} \sin \theta F_1 + \frac{1}{m} \cos \theta F_2 \\ \frac{r}{J} F_1 \end{pmatrix}.$$

The system parameters are $m = 4$ kg, $J = 0.0475$ kg m², $r = 0.25$ m, $g = 9.8$ m/s², $c = 0.05$ N s/m, which corresponds to a scaled model of the system. The equilibrium point for the system is given by $F_1 = 0$, $F_2 = mg$ and $\xi_e = (x_e, y_e, 0, 0, 0, 0)$. To derive the linearized model near an equilibrium point, we compute the linearization according to equation (5.33):

$$A = \begin{pmatrix} 0 & 0 & 0 & 1 & 0 & 0 \\ 0 & 0 & 0 & 0 & 1 & 0 \\ 0 & 0 & 0 & 0 & 0 & 1 \\ 0 & 0 & -g & -c/m & 0 & 0 \\ 0 & 0 & 0 & 0 & -c/m & 0 \\ 0 & 0 & 0 & 0 & 0 & 0 \end{pmatrix} \quad B = \begin{pmatrix} 0 & 0 \\ 0 & 0 \\ 0 & 0 \\ 1/m & 0 \\ 0 & 1/m \\ r/J & 0 \end{pmatrix}$$

$$C = \begin{pmatrix} 1 & 0 & 0 & 0 & 0 & 0 \\ 0 & 1 & 0 & 0 & 0 & 0 \end{pmatrix} \quad D = \begin{pmatrix} 0 & 0 \\ 0 & 0 \end{pmatrix}$$

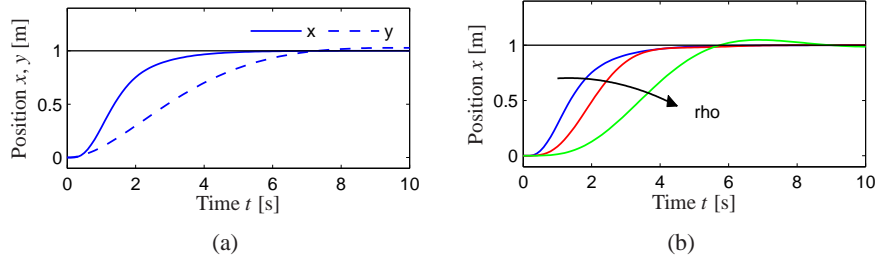


Figure 6.12: Step response for vectored thrust aircraft. The plot on the left shows the x and y positions of the aircraft when it is commanded to move 1 m in each direction. In the right figure the x motion is shown for control weights $\rho = 1, 10^2, 10^4$. A higher weight of the input term in the cost function causes a more sluggish response.

Letting $z = \xi - \xi_e$ and $v = u - u_e$, the linearized system is given by

$$\begin{aligned}\dot{z} &= Az + Bv \\ y &= Cx.\end{aligned}$$

It can be verified that the system is reachable.

To compute a linear quadratic regulator for the system, write the cost function as

$$J = \int_0^{\infty} (z^T Q_z z + \rho v^T Q_v v) dt$$


where $z = \xi - \xi_e$ and $v = u - u_e$ represent the local coordinates around the desired equilibrium point (ξ_e, u_e) . We begin with diagonal matrices for the state and input costs:

$$Q_z = \begin{pmatrix} 1 & 0 & 0 & 0 & 0 & 0 \\ 0 & 1 & 0 & 0 & 0 & 0 \\ 0 & 0 & 1 & 0 & 0 & 0 \\ 0 & 0 & 0 & 1 & 0 & 0 \\ 0 & 0 & 0 & 0 & 1 & 0 \\ 0 & 0 & 0 & 0 & 0 & 1 \end{pmatrix} \quad Q_v = \begin{pmatrix} 1 & 0 \\ 0 & 1 \end{pmatrix} \quad \rho = 1.$$

This gives a control law of the form $v = -Kz$, which can then be used to derive the control law in terms of the original variables:

$$u = v + u_e = -K(\xi - \xi_e) + u_e.$$

As computed in Example 5.4, the equilibrium points have $u_e = (0, mg)$ and $\xi_e = (x_e, y_e, 0, 0, 0, 0)$. The response of the controller to a step change in the desired position is shown in Figure 6.12a. The response can be tuned by adjusted the weights in the LQR cost. Figure 6.12b shows the response in the x direction for different choices of the weight ρ . ∇

Linear quadratic regulators can also be designed for discrete time systems, as illustrated by the following example. 

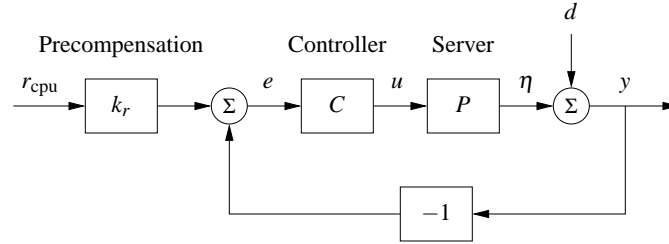


Figure 6.13: Feedback control of a web server. The controller sets the values of the web server parameters based on the difference between the nominal parameters (determined by $k_r r$) and the current load y_{cpu} . The disturbance d represents the load due to other processes running on the server. Note that the measurement is taken after the disturbance, so that we measure the total load on the server.

Example 6.9 Web server control

Consider the web server example given in Section 3.4, where a discrete time model for the system was given. We wish to design a control law that sets the server parameters so that average processor load of the server is maintained at a desired level. Since other processes may be running on the server, the web server must adjust its parameters in response to changes in the load.

A block diagram for the control system is shown in Figure 6.13. We focus on the special case where we wish to control only the processor load using both the `KeepAlive` and `MaxClients` parameters. We also include a “disturbance” on the measured load that represents the usage of the processing cycles by other processes running on the server. The system has the same basic structure as the generic control system in Figure 6.5, with the variation that the disturbance enters after the process dynamics.

The dynamics of the system are given by a set of difference equations of the form

$$x[k+1] = Ax[k] + Bu[k], \quad y_{\text{cpu}}[k] = C_{\text{cpu}}x[k] + d_{\text{cpu}}[k],$$

where $x = (x_{\text{cpu}}, x_{\text{mem}})$, $u = (u_{\text{ka}}, u_{\text{mc}})$, d_{cpu} is the processing load from other processes on the computer and y_{cpu} is the total processor load.

We choose our controller to be a state feedback controller of the form

$$u = -K \begin{pmatrix} y_{\text{cpu}} \\ x_{\text{mem}} \end{pmatrix} + k_r r_{\text{cpu}},$$

where r_{cpu} is the desired processor load. Note that we have used the measured processor load y_{cpu} instead of the state to ensure that we adjust the system operation based on the measured load. (This modification is necessary because of the non-standard way in which the disturbance enters the process dynamics.)

The feedback gain matrix K can be chosen by any of the methods described in this chapter. Here we use a linear quadratic regulator, with cost function given by

$$Q_x = \begin{pmatrix} 5 & 0 \\ 0 & 1 \end{pmatrix}, \quad Q_u = \begin{pmatrix} 1/50^2 & 0 \\ 0 & 1/1000^2 \end{pmatrix}.$$

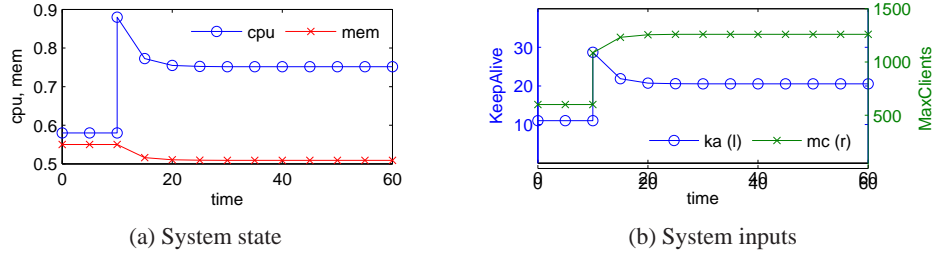


Figure 6.14: Web server with LQR control. The plot on the left shows the state of the system under a change in external load applied at $t = 10$ s. The corresponding web server parameters (system inputs) are shown on the right. The controller is able to reduce the effect of the disturbance by approximately 40%.

The cost function for the state Q_x is chosen so that we place more emphasis on the processor load versus the memory usage. The cost function for the inputs Q_u is chosen so as to normalize the two inputs, with a `KeepAlive` timeout of 50 seconds having the same weight as a `MaxClients` value of 1000. These values are squared since the cost associated with the inputs is given by $u^T Q_u u$. Using the dynamics in Section 3.4, the resulting gains become

$$K = \begin{pmatrix} -22.3 & 10.1 \\ 382.7 & 77.7 \end{pmatrix}.$$

As in the case of a continuous time control system, the reference gain k_r is chosen to yield the desired equilibrium point for the system. Setting $x[k+1] = x[k] = x_e$, the steady state equilibrium point and output for a given reference input r is given by

$$x_e = (A - BK)x_e + Bk_r r, \quad y_e = Cx_e.$$

This is a matrix differential equation in which k_r is a column vector that sets the two inputs values based on the desired reference. If we take the desired output to be of the form $y_e = (r, 0)$, then we must solve

$$\begin{pmatrix} 1 \\ 0 \end{pmatrix} = C(A - BK - I)^{-1} Bk_r$$

Solving this equation for k_r , we obtain

$$k_r = \left((C(A - BK - I)^{-1} B) \right)^{-1} \begin{pmatrix} 1 \\ 0 \end{pmatrix} = \begin{pmatrix} 49.3 \\ 539.5 \end{pmatrix}.$$

The dynamics of the closed loop system are illustrated in Figure 6.14. We apply a change in load of $d_{\text{cpu}} = 0.3$ at time $t = 10$ s, forcing the controller to adjust the operation of the server to attempt to maintain the desired load at 0.57. Note that both the `KeepAlive` and `MaxClients` parameters are adjusted. Although the load is decreased, it remains approximately 0.2 above the desired steady state. (Better results can be obtained using the techniques of the next section.) ∇

6.4 INTEGRAL ACTION

Controllers based on state feedback achieve the correct steady state response to reference signals by careful calibration of the gain k_r . However, one of the primary uses of feedback is to allow good performance in the presence of uncertainty, and hence requiring that we have an *exact* model of the process is undesirable. An alternative to calibration is to make use of integral feedback, in which the controller uses an integrator to provide zero steady state error. The basic concept of integral feedback was already given in Section 1.5 and in Section 3.1; here we provide a more complete description and analysis.

The basic approach in integral feedback is to create a state within the controller that computes the integral of the error signal, which is then used as a feedback term. We do this by augmenting the description of the system with a new state z :

$$\frac{d}{dt} \begin{pmatrix} x \\ z \end{pmatrix} = \begin{pmatrix} Ax + Bu \\ y - r \end{pmatrix} = \begin{pmatrix} Ax + Bu \\ Cx - r \end{pmatrix}.$$

The state z is seen to be the integral of the error between the desired output r and the actual output y . Note that if we find a compensator that stabilizes the system then we will necessarily have $\dot{z} = 0$ in steady state and hence $y = r$ in steady state.

Given the augmented system, we design a state space controller in the usual fashion, with a control law of the form

$$u = -Kx - k_i z + k_r r,$$

where K is the usual state feedback term, k_i is the integral term and k_r is used to set the nominal input for the desired steady state. The resulting equilibrium point for the system is given as

$$x_e = -(A - BK)^{-1} B(k_r r - k_i z_e)$$

Note that the value of z_e is not specified, but rather will automatically settle to the value that makes $\dot{z} = y - r = 0$, which implies that at equilibrium the output will equal the reference value. This holds independently of the specific values of A , B and K , as long as the system is stable (which can be done through appropriate choice of K and k_i).

The final compensator is given by

$$\begin{aligned} u &= -Kx - k_i z + k_r r \\ \dot{z} &= y - r, \end{aligned}$$

where we have now included the dynamics of the integrator as part of the specification of the controller. This type of compensator is known as a *dynamic compensator* since it has its own internal dynamics. The following example illustrates the basic approach.

Example 6.10 Cruise control

Consider the cruise control example introduced in Section 3.1 and considered further in Example 5.11. The linearized dynamics of the process around an equilib-

rium point v_e , u_e are given by

$$\begin{aligned}\dot{x} &= ax - b_g\theta + bw \\ y &= v = x + v_e,\end{aligned}$$

where $x = v - v_e$, $w = u - u_e$, m is the mass of the car and θ is the angle of the road. The constant a depends on the throttle characteristic and is given in Example 5.11.

If we augment the system with an integrator, the process dynamics become

$$\begin{aligned}\dot{x} &= ax - b_g\theta + bw \\ \dot{z} &= y - v_r = v_e + x - v_r,\end{aligned}$$

or, in state space form,

$$\frac{d}{dt} \begin{pmatrix} x \\ z \end{pmatrix} = \begin{pmatrix} a & 0 \\ 1 & 0 \end{pmatrix} \begin{pmatrix} x \\ z \end{pmatrix} + \begin{pmatrix} b \\ 0 \end{pmatrix} u + \begin{pmatrix} -b_g \\ 0 \end{pmatrix} \theta + \begin{pmatrix} 0 \\ v_e - v_r \end{pmatrix}.$$

Note that when the system is at equilibrium we have that $\dot{z} = 0$, which implies that the vehicle speed, $v = v_e + x$, should be equal to the desired reference speed, v_r . Our controller will be of the form

$$\begin{aligned}\dot{z} &= y - v_r \\ u &= -k_p x - k_i z + k_r v_r\end{aligned}$$

and the gains k_p , k_i and k_r will be chosen to stabilize the system and provide the correct input for the reference speed.

Assume that we wish to design the closed loop system to have characteristic polynomial

$$\lambda(s) = s^2 + a_1 s + a_2.$$

Setting the disturbance $\theta = 0$, the characteristic polynomial of the closed loop system is given by

$$\det(sI - (A - BK)) = s^2 + (bk_p - a)s + bk_i$$

and hence we set

$$k_p = \frac{a_1 + a}{b} \quad k_i = \frac{a_2}{b} \quad k_r = \frac{a_2}{b}.$$

The resulting controller stabilizes the system and hence brings $\dot{z} = y - v_r$ to zero, resulting in perfect tracking. Notice that even if we have a small error in the values of the parameters defining the system, as long as the closed loop poles are still stable then the tracking error will approach zero. Thus the exact calibration required in our previous approach (using k_r) is not needed here. Indeed, we can even choose $k_r = 0$ and let the feedback controller do all of the work.

Integral feedback can also be used to compensate for constant disturbances. Figure 6.15 shows the results of a simulation in which the car encounters a hill with angle $\theta = 4^\circ$ at $t = 8$ s. The stability of the system is not affected by this external disturbance and so we once again see that the car's velocity converges

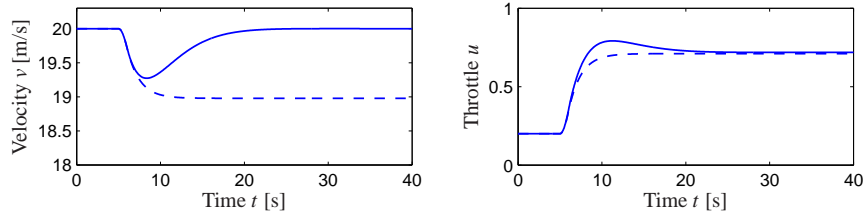


Figure 6.15: Velocity and throttle for car with cruise control based on proportional (dashed) and PI control (full). The PI controller is able to adjust the throttle to compensate for the effect of the hill and maintain the speed at the reference value of $v_r = 25$ m/s.

to the reference speed. This ability to handle constant disturbances is a general property of controllers with integral feedback (see Exercise 1.5). ∇

6.5 FURTHER READING

The importance of state models and state feedback was discussed in the seminal paper by Kalman [106], where the state feedback gain was obtained by solving an optimization problem that minimized a quadratic loss function. The notions of reachability and observability (next chapter) are also due to Kalman [108] (see also [79, 111]). Kalman defines controllability and reachability as the ability to reach the origin and an arbitrary state, respectively [110]. We note that in most textbooks the term “controllability” is used instead of “reachability”, but we prefer the latter term because it is more descriptive of the fundamental property of being able to reach arbitrary states. Most undergraduate textbooks on control will contain material on state space systems, including, for example, Franklin, Powell and Emami-Naeini [76] and Ogata [153]. Friedland’s textbook [77] covers the material in the previous, current and next chapter in considerable detail, including the topic of optimal control.

EXERCISES

6.1 Consider the double integrator. Find a piece-wise constant control strategy which drives the system from the origin to the state $x = \begin{pmatrix} 1 \\ 1 \end{pmatrix}$.

6.2 Extend the argument in Section 6.1 to show that if a system is reachable from an initial state of zero, it is reachable from a nonzero initial state.

6.3 Consider the system shown in Figure 6.3. Write the dynamics of the two systems as

$$\frac{dx}{dt} = Ax + Bu, \quad \frac{dz}{dt} = Az + Bu.$$

Observe that if x and z have the same initial condition, they will always have the

same state, regardless of the input that is applied. Show that this violates the definition of reachability and further show that the reachability matrix W_r is not full rank.

6.4 Show that integral feedback can be used to compensate for a constant disturbance by giving zero steady state error even when $d \neq 0$.

6.5 (Rear steered bicycle) A simple model for a bicycle was given by (3.5) in Section 3.2. A model for a bicycle with rear-wheel steering is obtained simply by reversing the sign of the velocity in the model. Determine the conditions under which this systems is reachable and explain any situations in which the system is not reachable.

6.6 Show that the characteristic polynomial for a system in reachable canonical form is given by equation (6.7) and that

$$\frac{d^n z_k}{dt^n} + a_1 \frac{d^{n-1} z_k}{dt^{n-1}} + \cdots + a_{n-1} \frac{dz_k}{dt} + a_n z_k = \frac{d^{n-k} u}{dt^{n-k}}.$$

6.7 Consider a system in reachable canonical form. Show that the inverse of the reachability matrix is given by

$$\tilde{W}_r^{-1} = \begin{pmatrix} 1 & a_1 & a_2 & \cdots & a_n \\ 0 & 1 & a_1 & \cdots & a_{n-1} \\ \vdots & & & & \\ 0 & 0 & 0 & \cdots & 1 \end{pmatrix}. \quad (6.28)$$

6.8 Equation (6.13) gives the gain required to maintain a given reference value for a system with no direct term. Compute the reference gain in the case where $D \neq 0$.

6.9 (An unreachable system) Consider the system

$$\begin{aligned} \frac{dx}{dt} &= \begin{pmatrix} 0 & 1 \\ 0 & 0 \end{pmatrix} x + \begin{pmatrix} 1 \\ 0 \end{pmatrix} u \\ y &= \begin{pmatrix} 1 & 0 \end{pmatrix} x \end{aligned}$$

with the control law

$$u = -k_1 x_1 - k_2 x_2 + k_r r.$$

Show that eigenvalues of the system cannot be assigned to arbitrary values.

6.10 Prove the Cayley-Hamilton theorem

6.11 Consider the normalized model of the motor drive in Exercise 2.12. Verify that the eigenvalues of the open loop system are $0, 0, -0.05 \pm i$. Design a state feedback that gives a closed loop system with eigenvalues in $-2, -1$ and $-1 \pm i$. This choice implies that the oscillatory eigenvalues will be well damped and that the eigenvalues at the origin are replaced by eigenvalues on the negative real axis. Simulate the responses of the closed loop system to step changes in the command signal and a step change in a disturbance torque on the second rotor. Try to write your design and simulation programs in such a way that they are generic.

6.12 (The Whipple bicycle model) Consider the Whipple bicycle model given by equation (3.7) in Section 3.2. The model is unstable at the velocity $v = 5$ m/s and the open loop eigenvalues are -1.84 , -14.29 and $1.30 \pm 4.60i$. Find the gains of a controller that stabilizes the bicycle and give closed loop eigenvalues at -2 , -10 and $-1 \pm i$. Simulate the response of the system when the for a step reference of 0.01 rad/s in the steering command.

6.13 Consider the model of an AFM in contact mode

$$\frac{dx}{dt} = \begin{pmatrix} 0 & 1 & 0 & 0 \\ -k/(m_1+m_2) & -c/(m_1+m_2) & 1/m_2 & 0 \\ 0 & 0 & 0 & \omega_3 \\ 0 & 0 & -\omega_3 & -2\zeta_3\omega_3 \end{pmatrix} x + \begin{pmatrix} 0 \\ 0 \\ 0 \\ \omega_3^2 \end{pmatrix} u$$

$$y = \frac{m_2}{m_1+m_2} \begin{pmatrix} \frac{m_1 k}{m_1+m_2} & \frac{m_1 c}{m_1+m_2} & 1 & 0 \end{pmatrix} x,$$

given in Example 5.9. Pick up the program `afm ata` from the web to generate the system matrices.

- Compute the controllability matrix of the system and determine its rank. Scale the model by using `ms` instead of `s` as time units. Repeat the calculation of the controllability matrix and its rank.
- Find a state feedback that increases the gives a closed loop system where the complex poles have damping 0.707 . Use the scaled model for the computations.
- Compute state feedback gains using linear quadratic control theory. Experiment by using different weights. Compute the gains for $q_1 = q_2 = 0, q_3 = q_4 = 1, R = 1$ and $\rho = 0.1$ and explain the result. Choose $q_1 = q_2 = q_3 = q_4 = r_1 = 1$ and explore what happens to the feedback gains and closed loop eigenvalues when you change ρ . Use the scaled system for this computation.

Chapter Seven

Output Feedback

One may separate the problem of physical realization into two stages: computation of the “best approximation” $\hat{x}(t_1)$ of the state from knowledge of $y(t)$ for $t \leq t_1$ and computation of $u(t_1)$ given $\hat{x}(t_1)$.

From R. E. Kalman “Contributions to the theory of optimal control” [106]

In this chapter we show how to use output feedback to modify the dynamics of the system, through the use of observers. We introduce the concept of observability and show that if a system is observable, it is possible to recover the state from measurements of the inputs and outputs to the system. It is then shown how to design a controller with feedback from the observer state. An important concept is the separation principle quoted above, which is also proved. The structure of the controllers derived in this chapter is quite general and is obtained by many other design methods.

7.1 OBSERVABILITY

In Section 6.2 of the previous chapter it was shown that it is possible to find a feedback that gives desired closed loop eigenvalues provided that the system is reachable and that all states are measured. For many situations, it is highly unrealistic to assume that all states are measured. In this section we investigate how the state can be estimated by using a mathematical model and a few measurements. It will be shown that the computation of the states can be carried out by a dynamical system called an *observer*.

Definition of Observability

Consider a system described by a set of differential equations

$$\frac{dx}{dt} = Ax + Bu, \quad y = Cx + Du, \quad (7.1)$$

where $x \in \mathbb{R}^n$ is the state, $u \in \mathbb{R}^p$ the input, and $y \in \mathbb{R}^q$ the measured output. We wish to estimate the state of the system from its inputs and outputs, as illustrated in Figure 7.1. In some situations we will assume that there is only one measured signal, i.e. that the signal y is a scalar and that C is a (row) vector. This signal may be corrupted by noise, n , although we shall start by considering the noise-free case. We write \hat{x} for the state estimate given by the observer.

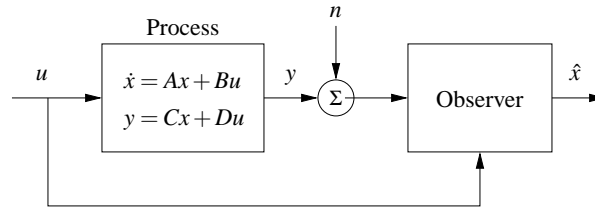


Figure 7.1: Block diagram for an observer. The observer uses the process measurement y (possibly corrupted by noise n) and the input u to estimate the current state of the process, denoted \hat{x} .

Definition 7.1 (Observability). A linear system is *observable* if for any $T > 0$ it is possible to determine the state of the system $x(T)$ through measurements of $y(t)$ and $u(t)$ on the interval $[0, T]$.

The definition above holds for nonlinear systems as well, and the results discussed here have extensions to the nonlinear case.

The problem of observability is one that has many important applications, even outside of feedback systems. If a system is observable, then there are no “hidden” dynamics inside it; we can understand everything that is going on through observation (over time) of the inputs and outputs. As we shall see, the problem of observability is of significant practical interest because it will determine if a set of sensors is sufficient for controlling a system. Sensors combined with a mathematical model can also be viewed as a “virtual sensor” that gives information about variables that are not measured directly. The process of reconciling signals from many sensors with mathematical models is also called *sensor fusion*.

Testing for Observability

When discussing reachability in the last chapter we neglected the output and focused on the state. Similarly, it is convenient here to initially neglect the input and focus on the autonomous system

$$\frac{dx}{dt} = Ax, \quad y = Cx. \quad (7.2)$$

We wish to understand when it is possible to determine the state from observations of the output.

The output itself gives the projection of the state on vectors that are rows of the matrix C . The observability problem can immediately be solved if the matrix C is invertible. If the matrix is not invertible we can take derivatives of the output to obtain

$$\frac{dy}{dt} = C \frac{dx}{dt} = CAx.$$

From the derivative of the output we thus get the projection of the state on vectors

that are rows of the matrix CA . Proceeding in this way we get

$$\begin{pmatrix} y \\ \dot{y} \\ \ddot{y} \\ \vdots \\ y^{(n-1)} \end{pmatrix} = \begin{pmatrix} C \\ CA \\ CA^2 \\ \vdots \\ CA^{n-1} \end{pmatrix} x. \quad (7.3)$$

We thus find that the state can be determined if the matrix

$$W_o = \begin{pmatrix} C \\ CA \\ CA^2 \\ \vdots \\ CA^{n-1} \end{pmatrix} \quad (7.4)$$

has n independent rows. It turns out that we need not consider any derivatives higher than $n - 1$ (this is an application of the Cayley-Hamilton theorem (Exercise 6.10)).

The calculation can easily be extended to systems with inputs. The state is then given by a linear combination of inputs and outputs and their higher derivatives. The observability criterion is unchanged. We leave this case as an exercise for the reader.

In practice, differentiation of the output can give large errors when there is measurement noise and therefore the method sketched above is not particularly practical. We will address this issue in more detail in the next section, but for now we have the following basic result:

Theorem 7.1. *A linear system of the form (7.1) is observable if and only if the observability matrix W_o is full rank.*

Proof. The sufficiency of the observability rank condition follows from the analysis above. To prove necessity, suppose that the system is observable but W_o is not full rank. Let $v \in \mathbb{R}^n$, $v \neq 0$ be a vector in the null space of W_o , so that $W_o v = 0$. If we let $x(0) = v$ be the initial condition for the system and choose $u = 0$, then the output is given by $y(t) = C e^{At} v$. Since e^{At} can be written as a power series in A and since A^n and higher powers can be rewritten in terms of lower powers of A (by the Cayley-Hamilton theorem), it follows that the output will be identically zero (the reader should fill in the missing steps if this is not clear). However, if both the input and output of the system are 0, then a valid estimate of the state is $\hat{x} = 0$ for all time, which is clearly incorrect since $x(0) = v \neq 0$. Hence by contradiction we must have that W_o is full rank if the system is observable. \square



Example 7.1 Compartment model

Consider the two compartment model in Figure 3.18a on page 87 but assume that

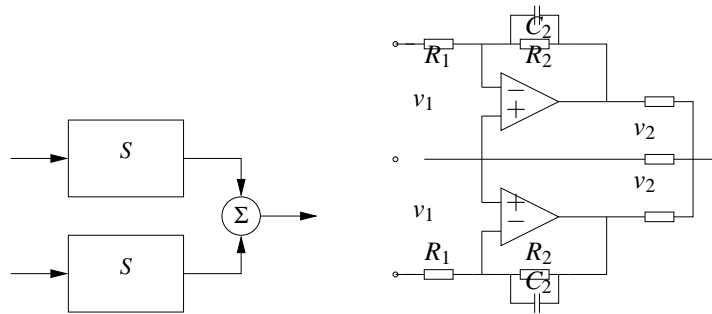


Figure 7.2: An unobservable system. Two identical subsystems have outputs that add together to form the overall system output. The individual states of the subsystem cannot be determined since the contributions of each to the output are not distinguishable. The circuit diagram on the right is an example of such a system.

the the concentration in the first compartment can be measured. The system is described by the linear system

$$\frac{dc}{dt} = \begin{pmatrix} -k_0 - k_1 & k_1 \\ k_2 & -k_2 \end{pmatrix} c + \begin{pmatrix} b_0 \\ 0 \end{pmatrix} u, \quad y = \begin{pmatrix} 1 & 0 \end{pmatrix} x.$$

The first compartment represents the concentration in the blood plasma and the second compartment the drug concentration in the tissue where it is active. To determine if it is possible to find the concentration in the tissue compartment from measurement of blood plasma we investigate the observability of the system by forming the observability matrix

$$W_o = \begin{pmatrix} C \\ CA \end{pmatrix} = \begin{pmatrix} 1 & 0 \\ -k_0 - k_1 & k_1 \end{pmatrix}.$$

The rows are linearly independent if $k_1 \neq 0$ and under this condition it is thus possible to determine the concentration of the drug in the active compartment from measurements of the drug concentration in the blood. ∇

It is useful to have an understanding of the mechanisms that make a system unobservable. Such a system is shown in Figure 7.2. The system is composed of two identical systems whose outputs are added. It seems intuitively clear that it is not possible to deduce the states from the output since we cannot deduce the individual output contributions from the sum. This can also be seen formally (Exercise 7.2).

Observable Canonical Form

As in the case of reachability, certain canonical forms will be useful in studying observability. We define the observable canonical form to be the dual of the reachable canonical form.

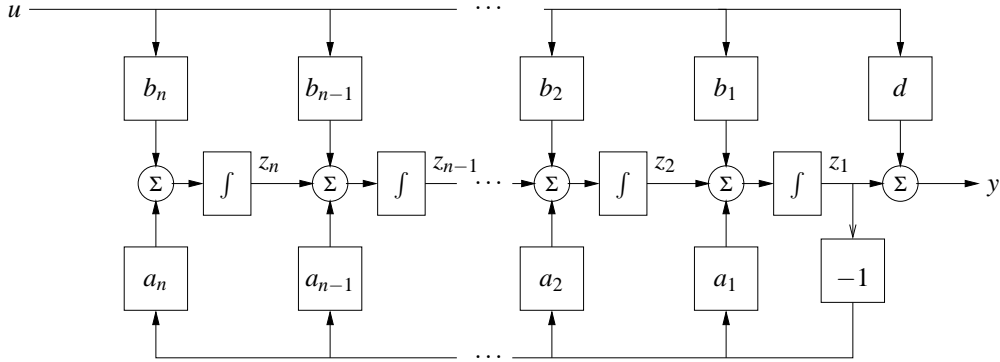


Figure 7.3: Block diagram of a system on observable canonical form. The states of the system are represented by individual integrators whose inputs are a weighted combination of the next integrator in the chain, the first state (rightmost integrator) and the system input. The output is a combination of the first state and the input.

Definition 7.2 (Observable canonical form). A linear single input, single output (SISO) state space system is in *observable canonical form* if its dynamics are given by

$$\frac{dz}{dt} = \begin{pmatrix} -a_1 & 1 & 0 & \cdots & 0 \\ -a_2 & 0 & 1 & & 0 \\ \vdots & & & \ddots & \\ -a_{n-1} & 0 & 0 & & 1 \\ -a_n & 0 & 0 & \cdots & 0 \end{pmatrix} z + \begin{pmatrix} b_1 \\ b_2 \\ \vdots \\ b_{n-1} \\ b_n \end{pmatrix} u$$

$$y = \begin{pmatrix} 1 & 0 & 0 & \cdots & 0 \end{pmatrix} z + Du.$$

The definition can be extended to systems with many inputs the only difference is that the vector multiplying u is replaced by a matrix.

Figure 7.3 shows a block diagram for a system in observable canonical form. As in the case of reachable canonical form, we see that the coefficients in the system description appear directly in the block diagram. The characteristic equation for a system in observable canonical form is given by

$$\lambda(s) = s^n + a_1 s^{n-1} + \cdots + a_{n-1} s + a_n. \quad (7.5)$$

It is possible to reason about the observability of a system in observable canonical form by studying the block diagram. If the input u and the output y are available the state z_1 can clearly be computed. Differentiating z_1 we also obtain the input to the integrator that generates z_1 and we can now obtain $z_2 = \dot{z}_1 + a_1 z_1 - b_1 u$. Proceeding in this way we can compute all states. The computation will however require that the signals are differentiated.

To check observability more formally, we compute the observability matrix for

a system in observable canonical form, which is given by

$$W_o = \begin{pmatrix} 1 & 0 & 0 & \dots & 0 \\ -a_1 & 1 & 0 & \dots & 0 \\ -a_1^2 - a_1 a_2 & -a_1 & 1 & & 0 \\ \vdots & \vdots & & \ddots & \vdots \\ * & * & & \dots & 1 \end{pmatrix},$$

where * represents an entry whose exact value is not important. The rows of this matrix are linearly independent (since it is lower triangular) and hence W_o is full rank. A straightforward but tedious calculation shows that the inverse of the observability matrix has a simple form, given by

$$W_o^{-1} = \begin{pmatrix} 1 & 0 & 0 & \dots & 0 \\ a_1 & 1 & 0 & \dots & 0 \\ a_2 & a_1 & 1 & \dots & 0 \\ \vdots & \vdots & & \ddots & \vdots \\ a_{n-1} & a_{n-2} & a_{n-3} & \dots & 1 \end{pmatrix}.$$

As in the case of reachability, it turns out that if a system is observable then there always exists a transformation T that converts the system into observable canonical form. This is useful for proofs, since it lets us assume that a system is in reachable canonical form without any loss of generality. The reachable canonical form may be poorly conditioned numerically.

7.2 STATE ESTIMATION

Having defined the concept of observability, we now return to the question of how to construct an observer for a system. We will look for observers that can be represented as a linear dynamical system that takes the inputs and outputs of the system we are observing and produces an estimate of the system's state. That is, we wish to construct a dynamical system of the form

$$\frac{d\hat{x}}{dt} = F\hat{x} + Gu + Hy,$$

where u and y are the input and output of the original system and $\hat{x} \in \mathbb{R}^n$ is an estimate of the state with the property that $\hat{x}(t) \rightarrow x(t)$ as $t \rightarrow \infty$.

The Observer

We consider the system in equation (7.1) with D set to zero to simplify the exposition:

$$\frac{dx}{dt} = Ax + Bu, \quad y = Cx, \quad (7.6)$$

We can attempt to determine the state simply by simulating the equations with the correct input. An estimate of the state is then given by

$$\frac{d\hat{x}}{dt} = A\hat{x} + Bu. \quad (7.7)$$

To find the properties of this estimate, introduce the estimation error $\tilde{x} = x - \hat{x}$. It follows from equations (7.6) and (7.7) that

$$\frac{d\tilde{x}}{dt} = A\tilde{x}.$$

If matrix A has all its eigenvalues in the left half plane, the error \tilde{x} will go to zero and hence equation (7.7) is a dynamical system whose output converges to the state of the system (7.6).

The observer given by equation (7.7) uses only the process input u ; the measured signal does not appear in the equation. We must also require that the system is stable, and essentially our estimator converges because the state of both the observer and the estimator are going zero. This is not very useful in a control design context since we want to have our estimate converge quickly to a nonzero state, so that we can make use of it in our controller. We will therefore attempt to modify the observer so that the output is used and its convergence properties can be designed to be fast relative to the system's dynamics. This version will also work for unstable systems.

Consider the observer

$$\frac{d\hat{x}}{dt} = A\hat{x} + Bu + L(y - C\hat{x}). \quad (7.8)$$

This can be considered as a generalization of equation (7.7). Feedback from the measured output is provided by adding the term $L(y - C\hat{x})$, which is proportional to the difference between the observed output and the output that is predicted by the observer. It follows from equations (7.6) and (7.8) that

$$\frac{d\tilde{x}}{dt} = (A - LC)\tilde{x}.$$

If the matrix L can be chosen in such a way that the matrix $A - LC$ has eigenvalues with negative real parts, the error \tilde{x} will go to zero. The convergence rate is determined by an appropriate selection of the eigenvalues.

Notice the similarity between the problems of finding a state feedback and finding the observer. State feedback design by eigenvalue assignment is equivalent to finding a matrix K so that $A - BK$ has given eigenvalues. Design of an observer with prescribed eigenvalues is equivalent to finding a matrix L so that $A - LC$ has given eigenvalues. Since the eigenvalues of a matrix and its transpose are the same we can establish the following equivalence:

$$A \leftrightarrow A^T, \quad B \leftrightarrow C^T, \quad K \leftrightarrow L^T, \quad W_r \leftrightarrow W_o^T$$

The observer design problem is the *dual* of the state feedback design problem. Using the results of Theorem 6.3, we get the following theorem on observer design:

Theorem 7.2 (Observer design by eigenvalue assignment). *Consider the system given by*

$$\frac{dx}{dt} = Ax + Bu \quad y = Cx \quad (7.9)$$

with one input and one output. Let $\lambda(s) = s^n + a_1s^{n-1} + \dots + a_{n-1}s + a_n$ be the characteristic polynomial for A . If the system is observable then the dynamical system

$$\frac{d\hat{x}}{dt} = A\hat{x} + Bu + L(y - C\hat{x}) \quad (7.10)$$

is an observer for the system, with L chosen as

$$L = W_o^{-1} \tilde{W}_o \begin{pmatrix} p_1 - a_1 \\ p_2 - a_2 \\ \vdots \\ p_n - a_n \end{pmatrix}, \quad (7.11)$$

and the matrices W_o and \tilde{W}_o given by

$$W_o = \begin{pmatrix} C \\ CA \\ \vdots \\ CA^{n-1} \end{pmatrix} \quad \tilde{W}_o = \begin{pmatrix} 1 & 0 & 0 & \dots & 0 \\ a_1 & 1 & 0 & \dots & 0 \\ a_2 & a_1 & 1 & & 0 \\ \vdots & \vdots & & \ddots & \\ a_{n-1} & a_{n-2} & a_{n-3} & & 1 \end{pmatrix}^{-1}.$$

The resulting observer error $\tilde{x} = x - \hat{x}$ is governed by a differential equation having the characteristic polynomial

$$p(s) = s^n + p_1s^{n-1} + \dots + p_n.$$

The dynamical system (7.10) is called an observer for (the states of) the system (7.9) because it will generate an approximation of the states of the system from its inputs and outputs. This form of an observer is a much more useful form than the one given by pure differentiation in equation (7.3).

Example 7.2 Compartment model

Consider the compartment model in Example 7.1 which is characterized by the matrices

$$A = \begin{pmatrix} -k_0 - k_1 & k_1 \\ k_2 & -k_2 \end{pmatrix} \quad B = \begin{pmatrix} b_0 \\ 0 \end{pmatrix}, \quad C = \begin{pmatrix} 1 & 0 \end{pmatrix}.$$

The observability matrix was computed in Example 7.1 where we concluded that the system was observable if $k_1 \neq 0$. The dynamics matrix has the characteristic polynomial

$$\lambda(s) = \det \begin{pmatrix} s + k_0 + k_1 & -k_1 \\ -k_2 & s + k_2 \end{pmatrix} = s^2 + (k_0 + k_1 + k_2)s + k_0k_2.$$

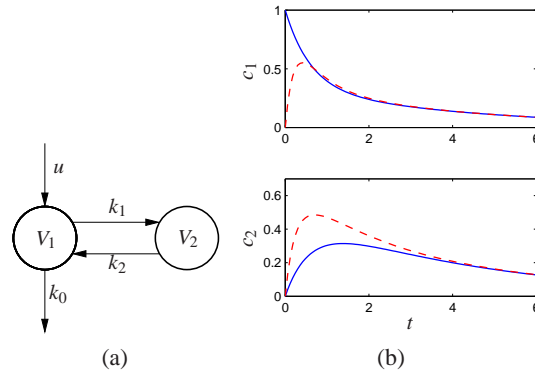


Figure 7.4: Observer for a two compartment system. The observer measures the input concentration u and output concentration y to determine the compartment concentrations, shown on the right. The true concentrations are shown in full lines and the estimates generated by the observer in dashed lines.

Let the desired characteristic polynomial of the observer be $s^2 + p_1s + p_2$. and equation 7.1 gives the observer gain

$$L = \begin{pmatrix} 1 & 0 \\ -k_0 - k_1 & k_1 \end{pmatrix}^{-1} \begin{pmatrix} 1 & 0 \\ k_0 + k_1 + k_2 & 1 \end{pmatrix}^{-1} \begin{pmatrix} p_1 - k_0 - k_1 - k_2 \\ p_2 - k_0k_2 \end{pmatrix} \\ = \begin{pmatrix} p_1 - k_0 - k_1 - k_2 \\ (p_2 - p_1k_2 + k_1k_2 + k_2^2)/k_1 \end{pmatrix}$$

Notice that the observability condition $k_1 \neq 0$ is essential. The behavior of the observer is illustrated by the simulation in Figure 7.4b. Notice how the observed concentrations approaches the true concentrations. ∇

The observer is a dynamical system whose inputs are the process input u and process output y . The rate of change of the estimate is composed of two terms. One term, $A\hat{x} + Bu$, is the rate of change computed from the model with \hat{x} substituted for x . The other term, $L(y - \hat{y})$, is proportional to the difference $e = y - \hat{y}$ between measured output y and its estimate $\hat{y} = C\hat{x}$. The estimator gain L is a matrix that tells how the error e is weighted and distributed among the states. The observer thus combines measurements with a dynamical model of the system. A block diagram of the observer is shown in Figure 7.5.

Computing the Observer Gain

For simple low order problems it is convenient to introduce the elements of the observer gain L as unknown parameters and solve for the values required to give the desired characteristic polynomial, as illustrated in the following example.

Example 7.3 Vehicle steering

The normalized, linear model for vehicle steering derived in Examples 5.12 and 6.4 gives the following state space model dynamics relating lateral path deviation y to

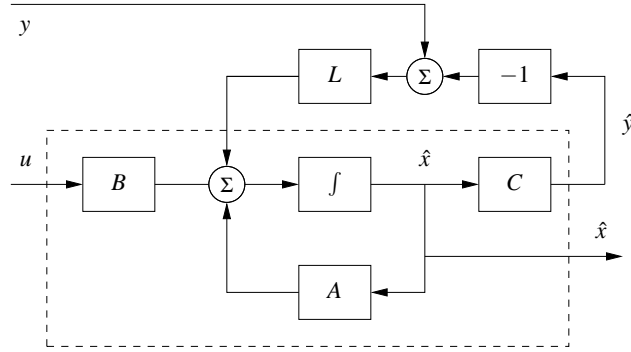


Figure 7.5: Block diagram of the observer. The observer takes the signals y and u as inputs and produces an estimate \hat{x} . Notice that the observer contains a copy of the process model that is driven by $y - \hat{y}$ through the observer gain L .

steering angle u

$$\begin{aligned} \frac{dx}{dt} &= \begin{pmatrix} 0 & 1 \\ 0 & 0 \end{pmatrix} x + \begin{pmatrix} \gamma \\ 1 \end{pmatrix} u \\ y &= \begin{pmatrix} 1 & 0 \end{pmatrix} x \end{aligned} \quad (7.12)$$

Recall that the state x_1 represents the lateral path deviation and that x_2 represents turning rate. We will now derive an observer that uses the system model to determine turning rate from the measured path deviation.

The observability matrix is

$$W_o = \begin{pmatrix} 1 & 0 \\ 0 & 1 \end{pmatrix},$$

i.e., the identity matrix. The system is thus observable and the eigenvalue assignment problem can be solved. We have

$$A - LC = \begin{pmatrix} -l_1 & 1 \\ -l_2 & 0 \end{pmatrix},$$

which has the characteristic polynomial

$$\det(sI - A + LC) = \det \begin{pmatrix} s + l_1 & -1 \\ l_2 & s \end{pmatrix} = s^2 + l_1 s + l_2.$$

Assuming that we want to have an observer with the characteristic polynomial

$$s^2 + p_1 s + p_2 = s^2 + 2\zeta_o \omega_o s + \omega_o^2,$$

the observer gains should be chosen as

$$l_1 = p_1 = 2\zeta_o \omega_o, \quad l_2 = p_2 = \omega_o^2.$$

The observer is then

$$\frac{d\hat{x}}{dt} = A\hat{x} + Bu + L(y - C\hat{x}) = \begin{pmatrix} 0 & 1 \\ 0 & 0 \end{pmatrix} \hat{x} + \begin{pmatrix} \gamma \\ 1 \end{pmatrix} u + \begin{pmatrix} l_1 \\ l_2 \end{pmatrix} (y - \hat{x}_1).$$

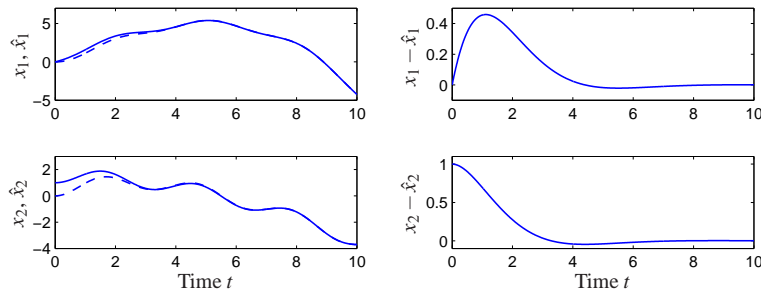


Figure 7.6: Simulation of an observer for a vehicle driving on a curvy road. The observer has an initial velocity error. The plots on the left show the lateral deviation x_1 , the lateral velocity x_2 in full lines and their estimates \hat{x}_1 and \hat{x}_2 in dashed lines. The plots on the right show the estimation errors.

A simulation of the observer for a vehicle driving on a curvy road is simulated in Figure 7.6. The vehicle length is the length unit in the normalized model. The figure shows that the observer error settles in about 8 vehicle lengths. ∇

For systems of high order we have to use numerical calculations. The duality between design of a state feedback and design of an observer means that means that the computer algorithms for state feedback can be used also for the observer design; we simply use the transpose of the dynamics matrix and the output matrix. The MATLAB command `acker`, which essentially is a direct implementation of the calculations given in Theorem 7.2, can be used for systems with one output. The MATLAB command `place` can be used for systems with many outputs. It is also better conditioned numerically.

7.3 CONTROL USING ESTIMATED STATE

In this section we will consider a state space system with no direct term (the most common case):

$$\frac{dx}{dt} = Ax + Bu, \quad y = Cx. \quad (7.13)$$

Notice that we have assumed that there is no direct term in the system ($D = 0$). This is often a realistic assumption. The presence of a direct term in combination with a controller having proportional action creates a so called algebraic loop which will be discussed in Section 8.3. The problem can be solved even if there is a direct term but the calculations are more complicated.

We wish to design a feedback controller for the system where only the output is measured. As before, we will assume that u and y are scalars. We also assume that the system is reachable and observable. In Chapter 6 we found a feedback of the form

$$u = -Kx + k_r r$$

for the case that all states could be measured and in Section 7.2 we developed an

observer that can generate estimates of the state \hat{x} based on inputs and outputs. In this section we will combine the ideas of these sections to find a feedback that gives desired closed loop eigenvalues for systems where only outputs are available for feedback.

If all states are not measurable, it seems reasonable to try the feedback

$$u = -K\hat{x} + k_r r, \quad (7.14)$$

where \hat{x} is the output of an observer of the state, i.e.

$$\frac{d\hat{x}}{dt} = A\hat{x} + Bu + L(y - C\hat{x}). \quad (7.15)$$

Since the system (7.13) and the observer (7.15) are both of state dimension n , the closed loop system has state dimension $2n$ with state (x, \hat{x}) . The evolution of the states is described by equations (7.13), (7.14) and (7.15). To analyze the closed loop system, the state variable \hat{x} is replaced by

$$\tilde{x} = x - \hat{x}. \quad (7.16)$$

Subtraction of equation (7.15) from equation (7.13) gives

$$\frac{d\tilde{x}}{dt} = Ax - A\hat{x} - L(Cx - C\hat{x}) = A\tilde{x} - LC\tilde{x} = (A - LC)\tilde{x}.$$

Returning to the process dynamics, introducing u from equation (7.14) into equation (7.13) and using equation (7.16) to eliminate \hat{x} gives

$$\begin{aligned} \frac{dx}{dt} &= Ax + Bu = Ax - BK\hat{x} + Bk_r r = Ax - BK(x - \tilde{x}) + Bk_r r \\ &= (A - BK)x + BK\tilde{x} + Bk_r r. \end{aligned}$$

The closed loop system is thus governed by

$$\frac{d}{dt} \begin{pmatrix} x \\ \tilde{x} \end{pmatrix} = \begin{pmatrix} A - BK & BK \\ 0 & A - LC \end{pmatrix} \begin{pmatrix} x \\ \tilde{x} \end{pmatrix} + \begin{pmatrix} Bk_r \\ 0 \end{pmatrix} r. \quad (7.17)$$

Notice that the state \tilde{x} , representing the observer error, is not affected by the command signal r . This is desirable since we do not want the reference signal to generate observer errors.

Since the dynamics matrix is block diagonal, we find that the characteristic polynomial of the closed loop system is

$$\lambda(s) = \det(sI - A + BK) \det(sI - A + LC).$$

This polynomial is a product of two terms: the characteristic polynomial of the closed loop system obtained with state feedback and the characteristic polynomial of the observer error. The feedback (7.14) that was motivated heuristically thus provides a neat solution to the eigenvalue assignment problem. The result is summarized as follows.

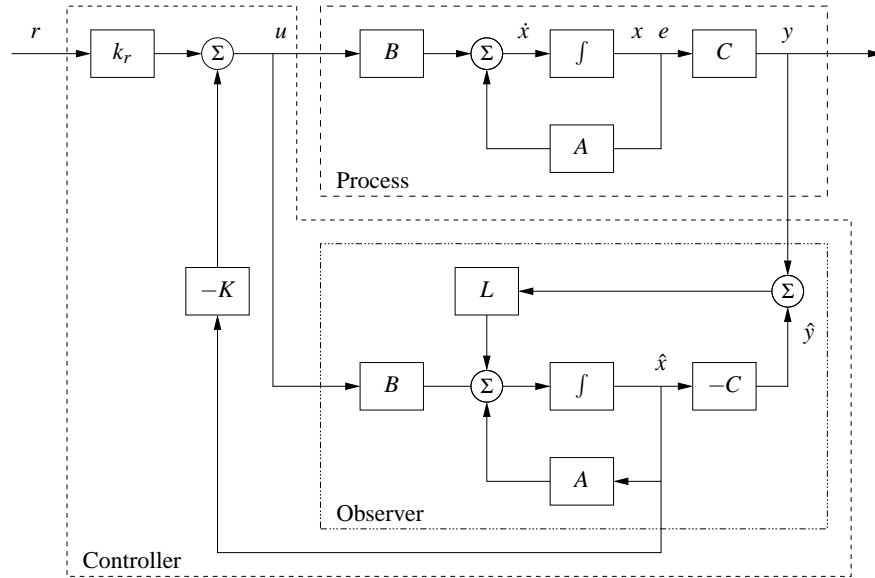


Figure 7.7: Block diagram of an observer-based control system. The observer uses the measured output y and the input u to construct an estimate of the state. This estimate is used by a state feedback controller to generate the corrective input. The controller consists of the observer and the state feedback; the observer is identical to Figure 7.5.

Theorem 7.3 (Eigenvalue assignment by output feedback). *Consider the system*

$$\frac{dx}{dt} = Ax + Bu, \quad y = Cx.$$

The controller described by

$$u = -K\hat{x} + k_r r$$

$$\frac{d\hat{x}}{dt} = A\hat{x} + Bu + L(y - C\hat{x}) = (A - BL - KC)\hat{x} + Ly$$

gives a closed loop system with the characteristic polynomial

$$\lambda(s) = \det(sI - A + BK) \det(sI - A + LC).$$

This polynomial can be assigned arbitrary roots if the system is reachable and observable.

The controller has a strong intuitive appeal: it can be thought of as composed of two parts, one state feedback and one observer. The dynamics of the controller is generated by the observer. The feedback gain K can be computed as if all state variables can be measured and it only depends on A and B . The observer gain L only depends on A and C . The property that the eigenvalue assignment for output feedback can be separated into eigenvalue assignment for a state feedback and an observer is called the *separation principle*.

A block diagram of the controller is shown in Figure 7.7. Notice that the con-

troller contains a dynamical model of the plant. This is called the *internal model principle*: the controller contains a model of the process being controlled. Indeed, the dynamics of the controller are due to the observer and the controller can thus be viewed as a dynamical system with input y and output u :

$$\frac{d\hat{x}}{dt} = (A - BK - LC)\hat{x} + Ly, \quad u = -K\hat{x} + k_r r. \quad (7.18)$$

Example 7.4 Vehicle steering

Consider again the normalized, linear model for vehicle steering in Example 6.4. The dynamics relating steering angle u to lateral path deviation y is given by the state space model (7.12). Combining the state feedback derived in Example 6.4 with the observer determined in Example 7.3 we find that the controller is given by

$$\begin{aligned} \frac{d\hat{x}}{dt} &= A\hat{x} + Bu + L(y - C\hat{x}) = \begin{pmatrix} 0 & 1 \\ 0 & 0 \end{pmatrix} \hat{x} + \begin{pmatrix} \gamma \\ 1 \end{pmatrix} u + \begin{pmatrix} l_1 \\ l_2 \end{pmatrix} (y - \hat{x}_1) \\ u &= -K\hat{x} + k_r r = k_1(r - x_1) - k_2 x_2. \end{aligned}$$

Elimination of the variable u gives

$$\begin{aligned} \frac{d\hat{x}}{dt} &= (A - BK - LC)\hat{x} + Ly + Bk_r r \\ &= \begin{pmatrix} -l_1 - \gamma k_1 & 1 - \gamma k_2 \\ -k_1 - l_2 & -k_2 \end{pmatrix} \hat{x} + \begin{pmatrix} l_1 \\ l_2 \end{pmatrix} y + \begin{pmatrix} \gamma \\ 1 \end{pmatrix} k_1 r. \end{aligned}$$

The controller is a dynamical system of second order, with two inputs y and r and one output u . Figure 7.8 shows a simulation of the the system when the vehicle is driven along a curvy road. Since we are using a normalized model the length unit is the vehicle length and the time unit is the time it takes to travel one vehicle length. The estimator is initialized with all states equal to zero but the real system has an initial velocity 0.5. The figures show that the estimates converge quickly to their true values. The vehicle tracks the desired path which is in the middle of the road, but there are errors because the road is irregular. The tracking error can be improved by introducing feedforward. ∇



7.4 KALMAN FILTERING

One of the principal uses of observers in practice is to estimate the state of a system in the presence of *noisy* measurements. We have not yet treated noise in our analysis and a full treatment of stochastic dynamical systems is beyond the scope of this text. In this section, we present a brief introduction to the use of stochastic systems analysis for constructing observers. We work primarily in discrete time to avoid some of the complications associated with continuous time random processes and to keep the mathematical prerequisites to a minimum. This section assumes basic knowledge of random variables and stochastic processes; see Kumar and Varaiya [124] or Åström [14] for the required material.

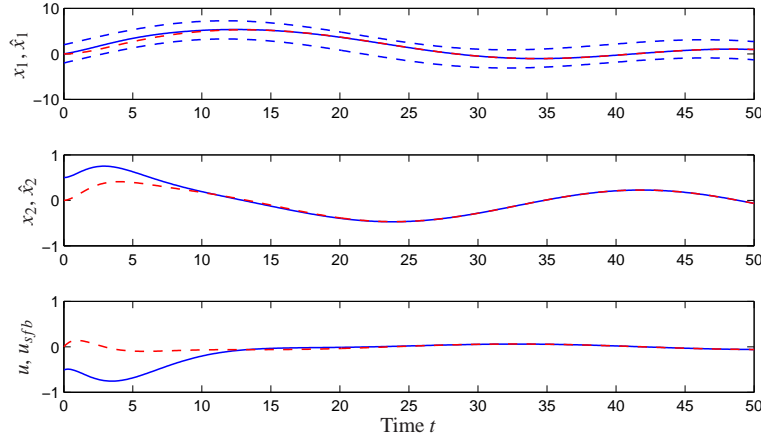


Figure 7.8: Simulation of a vehicle driving on a curvy road with a controller based on state feedback and an observer. The upper curves show the road markings (dotted), the vehicle position (full) and its estimate (dashed), the middle curve shows the velocity (full) and its estimate (dashed) and the bottom curve shows the control signal with a controller based on state feedback (full) and the control signal (dashed).

Consider a discrete time, linear system with dynamics

$$\begin{aligned} x[k+1] &= Ax[k] + Bu[k] + Fv[k] \\ y[k] &= Cx[k] + w[k], \end{aligned} \quad (7.19)$$

where $v[k]$ and $w[k]$ are Gaussian, white noise processes satisfying

$$\begin{aligned} E\{v[k]\} &= 0 & E\{w[k]\} &= 0 \\ E\{v[k]v^T[j]\} &= \begin{cases} 0 & k \neq j \\ R_v & k = j \end{cases} & E\{w[k]w^T[j]\} &= \begin{cases} 0 & k \neq j \\ R_w & k = j \end{cases} \\ E\{v[k]w^T[j]\} &= 0. \end{aligned} \quad (7.20)$$

$E\{v[k]\}$ represents the expected value of $v[k]$ and $E\{v[k]v^T[j]\}$ the correlation matrix. We assume that the initial condition is also modeled as a Gaussian random variable with

$$E\{x[0]\} = x_0 \quad E\{x[0]x^T[0]\} = P_0. \quad (7.21)$$

We wish to find an estimate $\hat{x}[k]$ that minimizes the mean square error $E\{(x[k] - \hat{x}[k])(x[k] - \hat{x}[k])^T\}$ given the measurements $\{y(\tau) : 0 \leq \tau \leq t\}$. We consider an observer in the same basic form as derived previously:

$$\hat{x}[k+1] = A\hat{x}[k] + Bu[k] + L[k](y[k] - C\hat{x}[k]). \quad (7.22)$$

The following theorem summarizes the main result.

Theorem 7.4. Consider a random process $x[k]$ with dynamics (7.19) and noise processes and initial conditions described by equations (7.20) and (7.21). The

observer gain L that minimizes the mean square error is given by

$$L[k] = AP[k]C^T (R_w + CP[k]C^T)^{-1},$$

where

$$\begin{aligned} P[k+1] &= (A - LC)P[k](A - LC)^T + FR_v F^T + LR_w L^T \\ P_0 &= E\{x[0]x^T[0]\}. \end{aligned} \quad (7.23)$$

Before we prove this result, we reflect on its form and function. First, note that the Kalman filter has the form of a *recursive* filter: given $P[k] = E\{E[k]E^T[k]\}$ at time k , can compute how the estimate and covariance *change*. Thus we do not need to keep track of old values of the output. Furthermore, the Kalman filter gives the estimate $\hat{x}[k]$ and the covariance $P[k]$, so we can see how reliable the estimate is. It can also be shown that the Kalman filter extracts the maximum possible information about output data. If we form the residual between the measured output and the estimated output,

$$e[k] = y[k] - C\hat{x}[k],$$

we can show that for the Kalman filter the correlation matrix is

$$R_e(j, k) = E\{e[j]e^T[k]\} = W[k]\delta_{jk}, \quad \delta_{jk} = \begin{cases} 0 & j \neq k \\ 1 & j = k. \end{cases}$$

In other words, the error is a white noise process, so there is no remaining dynamic information content in the error.

The Kalman filter is extremely versatile and can be used even if the process, noise or disturbances are non-stationary. When the system is stationary and if $P[k]$ converges, then the observer gain is constant:

$$L = APC^T (R_w + CPC^T)^{-1},$$

where P satisfies

$$P = APA^T + FR_v F^T - APC^T (R_w + CPC^T)^{-1} CPA^T.$$

We see that the optimal gain depends on both the process noise and the measurement noise, but in a nontrivial way. Like the use of LQR to choose state feedback gains, the Kalman filter permits a systematic derivation of the observer gains given a description of the noise processes. The solution for the constant gain case is solved by the `dlqe` command in MATLAB.

Proof (of theorem). We wish to minimize the mean square of the error, $E\{(x[k] - \hat{x}[k])(x[k] - \hat{x}[k])^T\}$. We will define this quantity as $P[k]$ and then show that it satisfies the recursion given in equation (7.23). By definition,

$$\begin{aligned} P[k+1] &= E\{x[k+1]x^T[k+1]\} \\ &= (A - LC)P[k](A - LC)^T + FR_v F^T + LR_w L^T \\ &= AP[k]A^T - AP[k]C^T L^T - LCA^T + L(R_w + CP[k]C^T)L^T. \end{aligned}$$

Letting $R_\varepsilon = (R_w + CP[k]C^T)$, we have

$$\begin{aligned} P[k+1] &= AP[k]A^T - AP[k]C^T L^T - LCA^T + LR_\varepsilon L^T \\ &= AP[k]A^T + (L - AP[k]C^T R_\varepsilon^{-1})R_\varepsilon(L - AP[k]C^T R_\varepsilon^{-1})^T \\ &\quad - AP[k]C^T R_\varepsilon^{-1}CP^T[k]A^T + R_w. \end{aligned}$$

To minimize this expression, we choose $L = AP[k]C^T R_\varepsilon^{-1}$ and the theorem is proved. \square

The Kalman filter can also be applied to continuous time stochastic processes. The mathematical derivation of this result requires more sophisticated tools, but the final form of the estimator is relatively straightforward.

Consider a continuous stochastic system

$$\begin{aligned} \dot{x} &= Ax + Bu + Fv & E\{v(s)v^T(t)\} &= R_v(t)\delta(t-s) \\ y &= Cx + w & E\{w(s)w^T(t)\} &= R_w(t)\delta(t-s), \end{aligned}$$

where $\delta(\tau)$ is the unit impulse function. Assume that the disturbance v and noise w are zero-mean and Gaussian (but not necessarily stationary):

$$\begin{aligned} \text{pdf}(v) &= \frac{1}{\sqrt[2]{2\pi} \sqrt{\det R_v}} e^{-\frac{1}{2}v^T R_v^{-1}v} \\ \text{pdf}(w) &= \frac{1}{\sqrt[2]{2\pi} \sqrt{\det R_w}} e^{-\frac{1}{2}w^T R_w^{-1}w} \end{aligned}$$

We wish to find the estimate $\hat{x}(t)$ that minimizes the mean square error $E\{(x(t) - \hat{x}(t))(x(t) - \hat{x}(t))^T\}$ given $\{y(\tau) : 0 \leq \tau \leq t\}$.

Theorem 7.5 (Kalman-Bucy, 1961). *The optimal estimator has the form of a linear observer*

$$\dot{\hat{x}} = A\hat{x} + Bu + L(y - C\hat{x})$$

where $L(t) = P(t)C^T R_w^{-1}$ and $P(t) = E\{(x(t) - \hat{x}(t))(x(t) - \hat{x}(t))^T\}$ and satisfies

$$\begin{aligned} \dot{P} &= AP + PA^T - PC^T R_w^{-1}(t)CP + FR_v(t)F^T \\ P[0] &= E\{x[0]x^T[0]\} \end{aligned}$$

Example 7.5 Vectored thrust aircraft

We consider the lateral dynamics of the system, consisting of the subsystems whose states are given by $\xi = (x, \theta, \dot{x}, \dot{\theta})$. To design a Kalman filter for the system, we must include a description of the process disturbances and the sensor noise. We thus augment the system to have the form

$$\begin{aligned} \frac{dz}{dt} &= Az + Bu + Fv \\ y &= Cz + w \end{aligned}$$

where G represents the structure of the disturbances (including the effects of nonlinearities that we have ignored in the linearization), w represents the disturbance

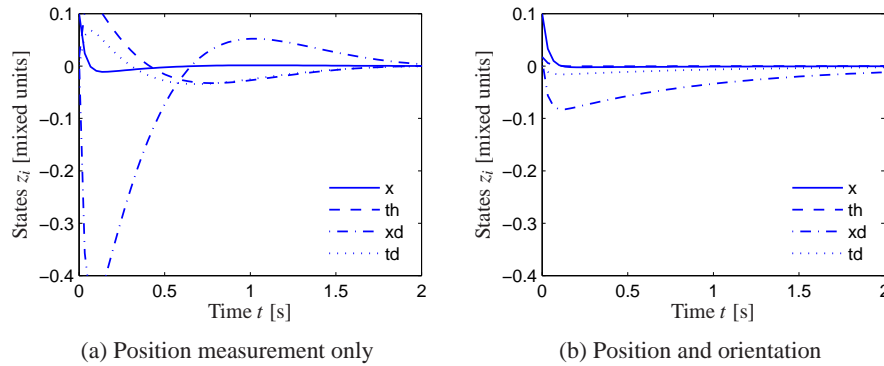


Figure 7.9: Kalman filter design for a vectored thrust aircraft. In the first design (left), only the lateral position of the aircraft is measured. Adding a direct measurement of the roll angle produces a much better observer (right). The initial condition for both simulations is $(0.1, 0.0175, 0.01, 0)$.

source (modeled as zero mean, Gaussian white noise) and v represents that measurement noise (also zero mean, Gaussian and white).

For this example, we choose F as the identity matrix and choose disturbances $v_i, i = 1, \dots, n$ to be independent disturbances with covariance given by $R_{ii} = 0.1, R_{ij} = 0, i \neq j$. The sensor noise is a single random variable which we model as having covariance $R_w = 10^{-4}$. Using the same parameters as before, the resulting Kalman gain is given by

$$L = \begin{pmatrix} 12.3 \\ -22.1 \\ 75.3 \\ -31.6 \end{pmatrix}$$

The performance of the estimator is shown in Figure 7.9a. We see that while the estimator converges to the system state, it contains significant “ringing” in the state estimate, which can lead to poor performance in a closed loop setting.

To improve the performance of the estimator, we explore the impact of adding a new output measurement. Suppose that instead of measuring just the output position x , we also measure the orientation of the aircraft, θ . The output becomes

$$y = \begin{pmatrix} 1 & 0 & 0 & 0 \\ 0 & 1 & 0 & 0 \end{pmatrix} z + \begin{pmatrix} w_1 \\ w_2 \end{pmatrix}$$

and if we assume that v_1 and v_2 are independent noise sources each with covariance $R_{v_i} = 10^{-4}$ then the optimal estimator gain matrix becomes

$$L = \begin{pmatrix} 8.10 & -0.611 \\ -0.611 & 7.93 \\ 33.0 & -9.73 \\ -0.0552 & 31.6 \end{pmatrix}.$$

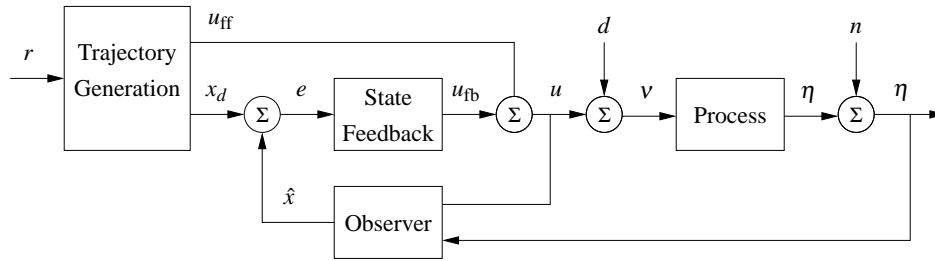


Figure 7.10: Block diagram of a controller based on a structure with two degrees of freedom. The controller consists of a trajectory generator, state feedback and an observer. The trajectory generation subsystem computes a feedforward command u_{ff} along with the desired state x_d . The state feedback controller uses the estimated state and desired state to compute a corrective input u_{fb} .

These gains provide good immunity to noise and high performance, as illustrated in Figure 7.9b.

▽

7.5 FEEDFORWARD AND IMPLEMENTATION

In this section we will discuss improved ways to introduce reference values by using feedforward. This leads to a system structure is one that appears in many places in control theory and is the heart of most modern control systems. We will also briefly discuss how computers can be used to implement a controller based on output feedback.

Feedforward

In this chapter and the previous one we have emphasized feedback as a mechanism for minimizing tracking error; reference values were introduced simply by adding them to the state feedback through a gain k_r . A more sophisticated way of doing this is shown by the block diagram in Figure 7.10, where the controller consists of three parts: an observer that computes estimates of the states based on a model and measured process inputs and outputs, a state feedback, and a trajectory generator that generates the desired behavior of all states x_d and a feedforward signal u_{ff} . Under the ideal conditions of no disturbances and no modeling errors the signal u_{ff} generates the desired behavior x_d when applied to the process.

To get some insight into the behavior of the system, we assume that there are no disturbances and that the system is in equilibrium with constant reference signal and with the observer state \hat{x} equal to the process state x . When the command signal is changed the signals u_{ff} and x_d will change. The observer tracks the state perfectly because the initial state was correct. The estimated state \hat{x} is thus equal to the desired state x_d and the feedback signal $u_{fb} = L(x_d - \hat{x})$ will also be zero. All action is thus created by the signals from the trajectory generator. If there are some

disturbances or some modeling errors the feedback signal will attempt to correct the situation.

This controller is said to have *two degrees of freedom* because the responses to command signals and disturbances are decoupled. Disturbance responses are governed by the observer and the state feedback while the response to command signals is governed by the trajectory generator (feedforward).

For an analytic description we start with the full nonlinear dynamics of the process

$$\dot{x} = f(x, u), \quad y = h(x, u). \quad (7.24)$$

Assume that the trajectory generator is able to generate a desired trajectory (x_d, u_{ff}) that satisfies the dynamics (7.24) and satisfies $r = h(x_d, u_{\text{ff}})$. To design the controller, we construct the error system. Let $e = x - x_d$, $v = u - u_{\text{ff}}$ and compute the dynamics for the error:

$$\begin{aligned} \dot{e} &= \dot{x} - \dot{x}_d = f(x, u) - f(x_d, u_{\text{ff}}) \\ &= f(e + x_d, v + u_{\text{ff}}) - f(x_d, u_{\text{ff}}) \\ &= F(e, v, x_d(t), u_{\text{ff}}(t)). \end{aligned}$$

In general, this system is time varying.

For trajectory tracking, we can assume that e is small (if our controller is doing a good job) and so we can linearize around $e = 0$:

$$\dot{e} \approx A(t)e + B(t)v, \quad A(t) = \left. \frac{\partial F}{\partial e} \right|_{(x_d(t), u_{\text{ff}}(t))} \quad B(t) = \left. \frac{\partial F}{\partial v} \right|_{(x_d(t), u_{\text{ff}}(t))}.$$

It is often the case that $A(t)$ and $B(t)$ depend only on x_d , in which case it is convenient to write $A(t) = A(x_d)$ and $B(t) = B(x_d)$.

Assume now that x_d and u_{ff} are either constant or slowly varying (with respect to the performance criterion). This allows us to consider just the (constant) linear system given by $(A(x_d), B(x_d))$. If we design a state feedback controller $K(x_d)$ for each x_d , then we can regulate the system using the feedback

$$v = K(x_d)e.$$

Substituting back the definitions of e and v , our controller becomes

$$u = -K(x_d)(x - x_d) + u_{\text{ff}}$$

This form of controller is called a *gain scheduled* linear controller with *feedforward* u_{ff} .

Finally, we consider the observer. The full nonlinear dynamics can be used for the prediction portion of the observer and the linearized system for the correction term:

$$\dot{\hat{x}} = f(\hat{x}, u) + L(\hat{x})(y - h(\hat{x}, u))$$

where $L(\hat{x})$ is the observer gain obtained by linearizing the system around the currently estimated state. This form of the observer is known as an *extended Kalman*

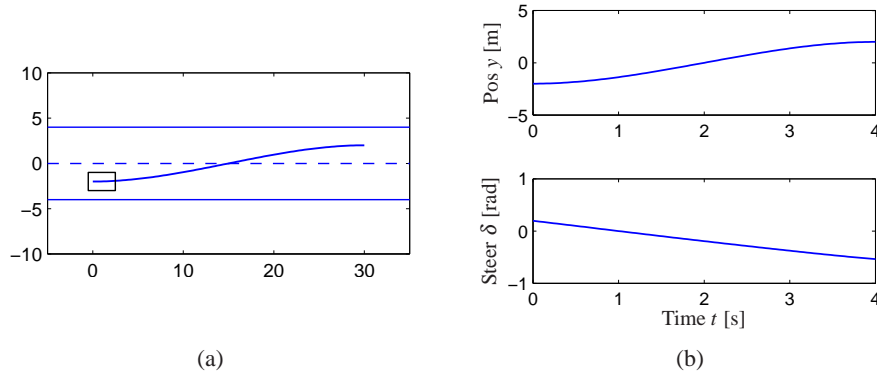


Figure 7.11: Trajectory generation for changing lanes. We wish to change from the left lane to the right lane over a distance of 30 meters in 4 seconds. The left figure shows the planned trajectory in the xy plane and the right figure shows the lateral position y and the steering angle δ over the maneuver time interval.

filter and has proved to be a very effective means of estimating the state of a non-linear system.

There are many ways to generate the feedforward signal and there are also many different ways to compute the feedback gain K and the observer gain L . Note that once again the internal model principle applies: the controller contains a model of the system to be controlled, through the observer.

Example 7.6 Vehicle steering

To illustrate how we can use two degree of freedom design to improve the performance of the system, consider the problem of steering a car to change lanes on a road, as illustrated in Figure 7.11.

The dynamics of the system were derived in Example 2.8. Using the center of the rear wheels as the reference ($\alpha = 0$), the dynamics can be written as

$$\dot{x} = \cos \theta v, \quad \dot{y} = \sin \theta v, \quad \dot{\theta} = 1/b \tan \delta,$$

where v is the forward velocity of the vehicle and δ is the steering angle. To generate a trajectory for the system, we note that we can solve for the states and inputs of the system given x , y by solving the following sets of equations:

$$\begin{aligned} \dot{x} &= v \cos \theta & \ddot{x} &= \dot{v} \cos \theta - v \sin \theta \dot{\theta} \\ \dot{y} &= v \sin \theta & \ddot{y} &= \dot{v} \sin \theta + v \cos \theta \dot{\theta} \\ \dot{\theta} &= v/l \tan \delta \end{aligned} \quad (7.25)$$

This set of five equations has five unknowns (θ , $\dot{\theta}$, v , \dot{v} and δ) that can be solved using trigonometry and linear algebra. It follows that we can compute a feasible trajectory for the system given any path $x(t)$, $y(t)$. (This special property of a system is something that is known as *differential flatness* [70, 71].)

To find a trajectory from an initial state (x_0, y_0, θ_0) to a final state (x_f, y_f, θ_f) at

at time T , we look for a path $x(t), y(t)$ that satisfies

$$\begin{aligned} x(0) &= x_0 & x(T) &= x_f \\ y(0) &= y_0 & y(T) &= y_f \\ \dot{x}(0) \sin \theta_0 + \dot{y}(0) \cos \theta_0 &= 0 & \dot{x}(T) \sin \theta_T + \dot{y}(T) \cos \theta_T &= 0 \\ \dot{y}(0) \sin \theta_0 + \dot{x}(0) \cos \theta_0 &= 0 & \dot{y}(T) \sin \theta_T + \dot{x}(T) \cos \theta_T &= 0 \end{aligned} \quad (7.26)$$

One such trajectory can be found by choosing $x(t)$ and $y(t)$ to have the form

$$x_d(t) = \alpha_0 + \alpha_1 t + \alpha_2 t^2 + \alpha_3 t^3, \quad y_d(t) = \beta_0 + \beta_1 t + \beta_2 t^2 + \beta_3 t^3.$$

Substituting these equations into equation (7.26), we are left with a set of linear equations that can be solved for $\alpha_i, \beta_i, i = 0, 1, 2, 3$. This gives a feasible trajectory for the system by using equation (7.25) to solve for θ_d, v_d and δ_d .

Figure 7.11b shows a sample trajectory generated by solving these equations. Notice that the feedforward input is quite different from 0, allowing the controller to command a steering angle that executes the turn in the absence of errors.

▽



Kalman's Decomposition of a Linear System

In this chapter and the previous one we have seen that two fundamental properties of a linear input/output system are reachability and observability. It turns out that these two properties can be used to classify the dynamics of a system. The key result is Kalman's decomposition theorem, which says that a linear system can be divided into four subsystems: Σ_{ro} which is reachable and observable, $\Sigma_{r\bar{o}}$ which is reachable but not observable, $\Sigma_{\bar{r}o}$ which is not reachable but is observable, and $\Sigma_{\bar{r}\bar{o}}$ which is neither reachable nor observable.

We will first consider this in the special case of systems where the matrix A has distinct eigenvalues. In this case we can find a set of coordinates such that the A matrix is diagonal and, with some additional reordering of the states, the system can be written as

$$\begin{aligned} \frac{dx}{dt} &= \begin{pmatrix} A_{ro} & 0 & 0 & 0 \\ 0 & A_{r\bar{o}} & 0 & 0 \\ 0 & 0 & A_{\bar{r}o} & 0 \\ 0 & 0 & 0 & A_{\bar{r}\bar{o}} \end{pmatrix} x + \begin{pmatrix} B_{ro} \\ B_{r\bar{o}} \\ 0 \\ 0 \end{pmatrix} u \\ y &= \begin{pmatrix} C_{ro} & 0 & C_{\bar{r}o} & 0 \end{pmatrix} x + Du. \end{aligned} \quad (7.27)$$

All states x_k such that $B_k \neq 0$ are reachable and all states such that $C_k \neq 0$ are observable. If we set the initial state to zero (or equivalently look at the steady state response if A is stable), the states given by $x_{\bar{r}o}$ and $x_{\bar{r}\bar{o}}$ will be zero and $x_{r\bar{o}}$ does not affect the output. Hence the output y can be determined from the system

$$\dot{x}_{ro} = A_{ro}x_{ro} + B_{ro}u, \quad y = C_{ro}x_{ro} + Du.$$

Thus from the input/output point of view, it is only the reachable and observable

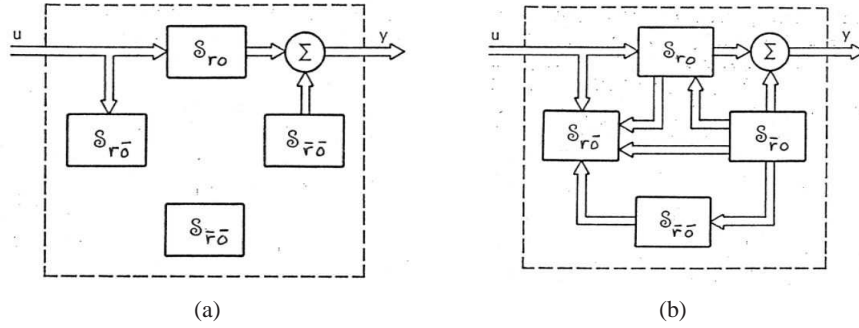


Figure 7.12: Kalman's decomposition of a linear system. The decomposition on the left is for a system with distinct eigenvalues, the one on the right is the general case. The system is broken into four subsystems, representing the various combinations of reachable and observable states. The input/output relationship only depends on the subset of states that are both reachable and observable.

dynamics that matter. A block diagram of the system illustrating this property is given in Figure 7.12a.

The general case of the Kalman decomposition is more complicated and requires some additional linear algebra. Introduce the reachable subspace \mathcal{X}_r which is the linear subspace spanned by the columns of the reachability matrix W_r . The state space is the direct sum of \mathcal{X}_r and another linear subspace $\mathcal{X}_{\bar{r}}$. Notice that \mathcal{X}_r is unique but that $\mathcal{X}_{\bar{r}}$ can be chosen in many different ways. Choosing coordinates with $x_r \in \mathcal{X}_r$ and $x_{\bar{r}} \in \mathcal{X}_{\bar{r}}$ the system equations can be written as

$$\frac{d}{dt} \begin{pmatrix} x_r \\ x_{\bar{r}} \end{pmatrix} = \begin{pmatrix} A_r^{11} & A_r^{12} \\ 0 & A_r^{22} \end{pmatrix} \begin{pmatrix} x_r \\ x_{\bar{r}} \end{pmatrix} + \begin{pmatrix} B_1 \\ 0 \end{pmatrix} u, \quad (7.28)$$

where the states x_r are reachable and $x_{\bar{r}}$ are non-reachable.

Introduce the unique subspace $\mathcal{X}_{\bar{o}}$ of unobservable states. This is the right null space of the observability matrix W_o . The state space is the direct sum of $\mathcal{X}_{\bar{o}}$ and the non-unique subspace \mathcal{X}_o . Choosing a coordinate system with $x_o \in \mathcal{X}_o$ and $x_{\bar{o}} \in \mathcal{X}_{\bar{o}}$ the system equations can be written as

$$\begin{aligned} \frac{d}{dt} \begin{pmatrix} x_o \\ x_{\bar{o}} \end{pmatrix} &= \begin{pmatrix} A_o^{11} & 0 \\ A_o^{21} & A_o^{22} \end{pmatrix} \begin{pmatrix} x_o \\ x_{\bar{o}} \end{pmatrix} + \begin{pmatrix} B_o^1 \\ B_o^2 \end{pmatrix} u \\ y &= \begin{pmatrix} C^1 & 0 \end{pmatrix} \begin{pmatrix} x_o \\ x_{\bar{o}} \end{pmatrix}, \end{aligned} \quad (7.29)$$

where the states x_o are observable and $x_{\bar{o}}$ are not observable.

The intersection of two linear subspaces is also a linear subspace. Introduce $\mathcal{X}_{r\bar{o}}$ as the intersection of \mathcal{X}_r and $\mathcal{X}_{\bar{o}}$ and the complementary linear subspace $\mathcal{X}_{r\bar{o}}$, which together with $\mathcal{X}_{r\bar{o}}$ spans \mathcal{X}_r . Finally, we introduce the linear subspace $\mathcal{X}_{\bar{r}\bar{o}}$ which together with $\mathcal{X}_{r\bar{o}}$, $\mathcal{X}_{r\bar{o}}$ and $\mathcal{X}_{\bar{r}\bar{o}}$ spans the full state space. Notice that the decomposition is not unique because only the subspace $\mathcal{X}_{r\bar{o}}$ is unique. Combining the representations (7.28) and (7.29) we find that a linear system can

be transformed to the form

$$\begin{aligned} \frac{dx}{dt} &= \begin{pmatrix} A^{11} & 0 & A^{13} & 0 \\ A^{21} & A^{22} & A^{23} & A^{24} \\ 0 & 0 & A^{33} & 0 \\ 0 & 0 & A^{43} & A^{44} \end{pmatrix} x + \begin{pmatrix} B^1 \\ B^2 \\ 0 \\ 0 \end{pmatrix} u \\ y &= \begin{pmatrix} C^1 & 0 & C^2 & 0 \end{pmatrix} x, \end{aligned} \quad (7.30)$$

where the state vector has been partitioned as

$$x = \begin{pmatrix} x_{ro} \\ x_{r\bar{o}} \\ x_{\bar{r}o} \\ x_{\bar{r}\bar{o}} \end{pmatrix}$$

A block diagram of the system is shown in Figure 7.12b. By tracing the arrows in the diagram we find that the input influences the systems Σ_{ro} and $\Sigma_{\bar{r}o}$ and that the output is influenced by Σ_{ro} and $\Sigma_{\bar{r}o}$. The system $\Sigma_{\bar{r}\bar{o}}$ is neither connected to the input nor the output. The input/output response of the system is thus given by

$$\dot{x}_{ro} = A^{11}x_{ro} + B^1u, \quad y = C^1x_{ro} + Du, \quad (7.31)$$

which is the dynamics of the reachable and observable subsystem Σ_{ro} .

Example 7.7 System and controller with feedback from observer states

Consider the system

$$\frac{dx}{dt} = Ax + Bu, \quad y = Cx,$$

The following controller based on feedback from the observer state was given in Theorem 7.3

$$u = -K\hat{x} + k_r r, \quad \frac{d\hat{x}}{dt} = A\hat{x} + Bu + L(y - C\hat{x})$$

Introducing the states x and $\tilde{x} = x - \hat{x}$ the closed loop system can be written as

$$\frac{d}{dt} \begin{pmatrix} x \\ \tilde{x} \end{pmatrix} = \begin{pmatrix} A - BK & 0 \\ BK & A - LC \end{pmatrix} \begin{pmatrix} x \\ \tilde{x} \end{pmatrix} + \begin{pmatrix} Bk_r \\ 0 \end{pmatrix} r, \quad y = Cx.$$

The state \tilde{x} is clearly not reachable from the command signal r and the relation between the reference r and the output y is the same as for a system with full state feedback.

▽

Computer Implementation

The controllers obtained so far have been described by ordinary differential equations. They can be implemented directly using analog components, whether electronic circuits, hydraulic valves or other physical devices. Since in modern en-

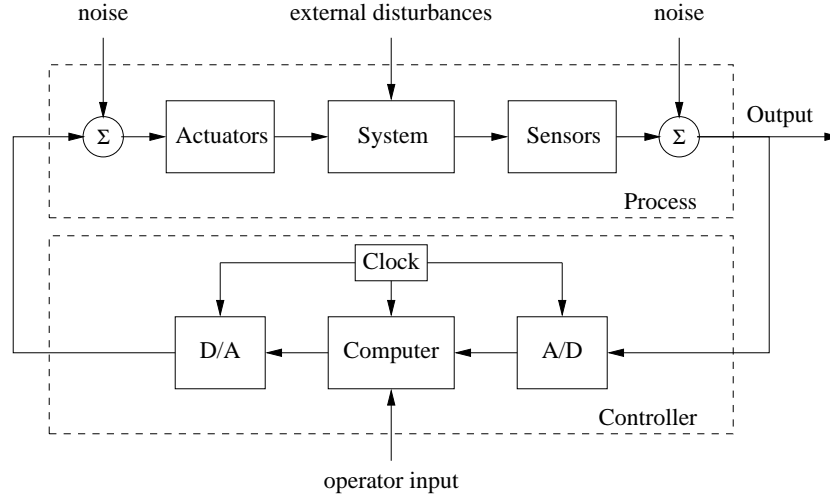


Figure 7.13: Components of a computer-controlled system. The controller consists of analog-to-digital (A/D) and digital-to-analog (D/A) converters, as well as a computer that implements the control algorithm. A system clock controls the operation of the controller, synchronizing the A/D, D/A and computing processes. The operator input is also fed to the computer as an external input.

engineering applications most controllers are implemented using computers we will briefly discuss how this can be done.

A computer-controlled system typically operates periodically: every cycle, signals from the sensors are sampled and converted to digital form by the A/D converter, the control signal is computed and the resulting output is converted to analog form for the actuators, as shown in Figure 7.13. To illustrate the main principles of how to implement feedback in this environment, we consider the controller described by equations (7.14) and (7.15), i.e.,

$$u = -K\hat{x} + k_r r, \quad \frac{d\hat{x}}{dt} = A\hat{x} + Bu + L(y - C\hat{x}).$$

The first equation consists only of additions and multiplications and can thus be implemented directly on a computer. The second equation can be implemented by approximating the derivative by a difference

$$\frac{dx}{dt} \approx \frac{\hat{x}(t_{k+1}) - \hat{x}(t_k)}{h} = A\hat{x}(t_k) + Bu(t_k) + L(y(t_k) - C\hat{x}(t_k)),$$

where t_k are the sampling instants and $h = t_{k+1} - t_k$ is the sampling period. Rewriting the equation to isolate $\hat{x}(t_{k+1})$, we get

$$\hat{x}(t_{k+1}) = \hat{x}(t_k) + h(A\hat{x}(t_k) + Bu(t_k) + L(y(t_k) - C\hat{x}(t_k))). \quad (7.32)$$

The calculation of the estimated state at time t_{k+1} only requires addition and multiplication and can easily be done by a computer. A section of pseudo code for the program that performs this calculation is

```
% Control algorithm - main loop
```

```

r = adin(ch1)           % read reference
y = adin(ch2)           % get process output
u = -K*xhat + Kr*r      % compute control variable
daout(ch1, u)           % set analog output
xhat = xhat + h*(A*x+B*u+L*(y-C*x)) % update state estimate

```

The program runs periodically at a fixed rate h . Notice that the number of computations between reading the analog input and setting the analog output has been minimized by updating the state after the analog output has been set. The program has an array of states, `xhat`, that represents the state estimate. The choice of sampling period requires some care.

There are more sophisticated ways of approximating a differential equation by a difference equation. If the control signal is constant between the sampling instants it is possible to obtain exact equations; see [19].

There are several practical issues that also must be dealt with. For example, it is necessary to filter a signal before it is sampled so that the filtered signal has little frequency content above $f_s/2$ where f_s is the sampling frequency. If controllers with integral action are used, it is also necessary to provide protection so that the integral does not become too large when the actuator saturates. This issue, called *integrator windup*, is studied in more detail in Chapter 10. Care must also be taken so that parameter changes do not cause disturbances.

7.6 FURTHER READING

The notion of observability is due to Kalman [108] and, combined with the dual notion of reachability, it was a major stepping stone toward establishing state space control theory beginning in the 1960s. The observer first appeared as the Kalman filter, in the paper by Kalman [107] for the discrete time case and Kalman and Bucy [109] for the the continuous time case. Kalman also conjectured that the controller for output feedback could be obtained by combining a state feedback with an observer; see the quote in the beginning of this chapter. This result was formally proved by Josep and Tou [104] and Gunckel and Franklin [89]. The combined result is known as the linear quadratic Gaussian control theory; a compact treatment is given in the books by Anderson and Moore [7] and Åström [14]. Much later it was shown that solutions to robust control problems also had a similar structure but with different ways of computing observer and state feedback gains [60].

EXERCISES

7.1 (Coordinate transformations) Consider a system under a coordinate transformation $z = Tx$, where $T \in \mathbb{R}^{n \times n}$ is an invertible matrix. Show that the observability matrix for the transformed system is given by $\tilde{W}_o = W_o T^{-1}$ and hence observability is independent of the choice of coordinates.

7.2 Show that the system depicted in Figure 7.2 is not observable.

7.3 (Coordinate transformations) Show that if a system is observable, then there exists a change of coordinates $z = Tx$ that puts the transformed system into observable canonical form.

7.4 (Bicycle dynamics) The linearized model for a bicycle are given in equation (3.5), which has the form


$$J \frac{d^2 \varphi}{dt^2} - \frac{Dv_0}{b} \frac{d\delta}{dt} = mgh\varphi + \frac{mv_0^2 h}{b} \delta,$$

where φ is the tilt of the bicycle and δ is the steering angle. Given conditions under which the system is observable and explain any special situations where it loses observability.

7.5 (State space control of balance system) A normalized model of the pendulum on a cart is described by the equations

$$\ddot{x} = u, \quad \ddot{\theta} = \theta + u,$$

where it has been assumed that the cart is very heavy; see Example 2.7. Assume that cart position x and the pendulum angle θ are measured, but that there is a bias in the measurement of the angle, which is modeled by $y_2 = \theta + \theta_0$, where θ_0 is a constant bias, hence $\dot{\theta}_0 = 0$. Introduce state variables $x_1 = x$, $x_2 = \theta$, $x_3 = \dot{x}$, $x_4 = \dot{\theta}$ and $x_5 = \theta_0$. Show that the system is observable. What is the engineering implication of the result?

7.6 (Vectored thrust aircraft) The lateral dynamics of the vectored thrust aircraft example considered in Example 6.8 can be obtained by considering the motion described by the states $\xi = (x, \theta, \dot{x}, \dot{\theta})$. Construct an estimator for these dynamics by setting the eigenvalues of the observer into a “Butterworth” pattern with $\lambda_{bw} = -3.83 \pm 9.24i, -9.24 \pm 3.83i$. Using this estimator combined with the state space controller computed in Example 6.8, plot the step response of the closed loop system. 

7.7 (Uniqueness) Show that design of an observer by eigenvalue placement is unique for single output systems. Construct examples that show that the problem is not necessarily unique for systems with many outputs. Suggest how the lack of uniqueness can be exploited.

7.8 (Observer for Teorell’s compartment model) Teorell’s compartment model shown in Figure 3.17 has the following state space representation

$$\frac{dx}{dt} = \begin{pmatrix} -k_1 & 0 & 0 & 0 & 0 \\ k_1 & -k_2 - k_4 & 0 & k_3 & 0 \\ 0 & k_4 & 0 & 0 & 0 \\ 0 & k_2 & 0 & -k_3 - k_5 & 0 \\ 0 & 0 & 0 & k_5 & 0 \end{pmatrix} x + \begin{pmatrix} 1 \\ 0 \\ 0 \\ 0 \\ 0 \end{pmatrix} u$$

where representative parameters are $k_1 = 0.02$, $k_2 = 0.1$, $k_3 = 0.05$, $k_4 = k_5 = 0.005$. The concentration of a drug which is active in compartment 5 is measured in the blood stream (compartment 2). Determine the compartments that are observable from measurement of concentration in the blood stream and design an estimator for these concentrations base on eigenvalue placement. Choose the closed loop eigenvalues -0.03 -0.05 and -0.1 . Simulate the system when the input is a pulse injection and illustrate the effect of modeling errors.

7.9 (Feedforward design for motor drive) Consider the normalized model of the motor drive in Exercise 2.12. Design the dynamics of the block labeled trajectory generation in Figure 7.10 so that the dynamics relating the output η to the reference signal r has the dynamics

$$\frac{d^3 y_m}{dt^3} + a_{m1} \frac{d^2 y_m}{dt^2} + a_{m2} \frac{dy_m}{dt} + a_{m3} y_m = a_{m3} r, \quad (7.33)$$

with parameters $a_{m1} = 2.5\omega_m$, $a_{m2} = 2.5\omega_m^2$ and $a_{m3} = \omega_m^3$. Discuss how the largest value of the command signal for a unit step in the command signal depends on ω_m .

7.10 (Whipple's bicycle model) Consider the Whipple bicycle model given by equation (3.7) in Section 3.2. A state feedback for the system was designed in Exercise 6.12. We will now design an observer and an output feedback for the system.

Chapter Eight

Transfer Functions

The typical regulator system can frequently be described, in essentials, by differential equations of no more than perhaps the second, third or fourth order. . . . In contrast, the order of the set of differential equations describing the typical negative feedback amplifier used in telephony is likely to be very much greater. As a matter of idle curiosity, I once counted to find out what the order of the set of equations in an amplifier I had just designed would have been, if I had worked with the differential equations directly. It turned out to be 55.

Henrik Bode, 1960 [41].

This chapter introduces the concept of the *transfer function*, which is a compact description of the input/output relation for a linear system. Combining transfer functions with block diagrams gives a powerful method for dealing with complex linear systems. The relationship between transfer functions and other system descriptions of system dynamics is also discussed.

8.1 FREQUENCY DOMAIN MODELING

Figure 8.1 shows a block diagram for a typical control system, consisting of a process to be controlled and a (dynamic) compensator, connected in a feedback loop. We saw in the previous two chapters how to analyze and design such systems using state space descriptions of the blocks. As was mentioned in Chapter 2, an alternative approach is to focus on the input/output characteristics of the system. Since it is the inputs and outputs that are used to connect the systems, one could expect that this point of view would allow an understanding of the overall behavior

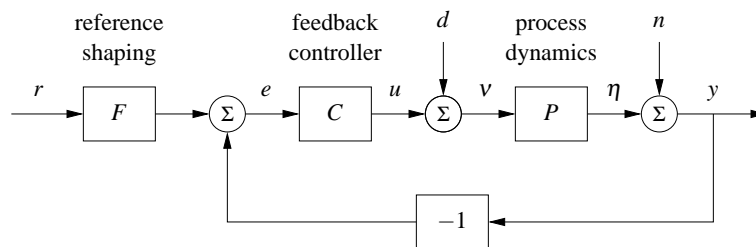


Figure 8.1: A block diagram for a feedback control system. The reference signal r is fed through a reference shaping block, which produces the signal that will be tracked. The error between this signal and the output is fed to a controller, which produces the input to the process. Disturbances and noise are included at the input and output of the process dynamics, as external signals.

of the system. Transfer functions are the main tool in implementing this point of view for linear systems.

The basic idea of the transfer function comes from looking at the frequency response of a system. Suppose that we have an input signal that is periodic. Then we can decompose this signal into the sum of a set of sines and cosines,

$$u(t) = \sum_{k=0}^{\infty} a_k \sin(k\omega t) + b_k \cos(k\omega t),$$

where ω is the fundamental frequency of the periodic input. Each of the terms in this input generates a corresponding sinusoidal output (in steady state), with possibly shifted magnitude and phase. The gain and phase at each frequency is determined by the frequency response, given in equation (5.23):

$$G(s) = C(sI - A)^{-1}B + D, \quad (8.1)$$

where we set $s = i(k\omega)$ for each $k = 1, \dots, \infty$ and $i = \sqrt{-1}$. If we know the steady state frequency response $G(s)$, we can thus compute the response to any (periodic) signal using superposition.

The transfer function generalizes this notion to allow a broader class of input signals besides periodic ones. As we shall see in the next section, the transfer function represents the response of the system to an “exponential input”, $u = e^{st}$. It turns out that the form of the transfer function is precisely the same as equation (8.1). This should not be surprising since we derived equation (8.1) by writing sinusoids as sums of complex exponentials. Formally, the transfer function corresponds to the Laplace transform of the steady state response of a system, although one does not have to understand the details of Laplace transforms in order to make use of transfer functions.

Modeling a system through its response to sinusoidal and exponential signals is known as *frequency domain modeling*. This terminology stems from the fact that we represent the dynamics of the system in terms of the generalized frequency s rather than the time domain variable t . The transfer function provides a complete representation of a linear system in the frequency domain.

The power of transfer functions is that they provide a particularly convenient representation for manipulating and analyzing complex feedback systems. As we shall see, there are many graphical representations of transfer functions that capture interesting properties of dynamics. Transfer functions also make it possible to express the changes in a system because of modeling error, which is essential when discussing sensitivity to process variations of the sort discussed in Chapter 12. More specifically, using transfer functions it is possible to analyze what happens when dynamic models are approximated by static models or when high order models are approximated by low order models. One consequence is that we can introduce concepts that express the degree of stability of a system.

While many of the concepts for state space modeling and analysis directly apply to nonlinear systems, frequency domain analysis applies primarily to linear systems. The notions of gain and phase can be generalized to nonlinear systems

and, in particular, propagation of sinusoidal signals through a nonlinear system can approximately be captured by an analog of the frequency response called the describing function. These extensions of frequency response will be discussed in Section 9.5.

8.2 DERIVATION OF THE TRANSFER FUNCTION

As we have seen in previous chapters, the input/output dynamics of a linear system has two components: the initial condition response and the forced response. In addition, we can speak of the transient properties of the system and its steady state response to an input. The transfer function focuses on the steady state response due to a given input, and provides a mapping between inputs and their corresponding outputs. In this section, we will derive the transfer function in terms of the “exponential response” of a linear system.

Transmission of Exponential Signals

To formally compute the transfer function of a system, we will make use of a special type of signal, called an *exponential signal*, of the form e^{st} where $s = \sigma + i\omega$ is a complex number. Exponential signals play an important role in linear systems. They appear in the solution of differential equations and in the impulse response of linear systems, and many signals can be represented as exponentials or sums of exponentials. For example, a constant signal is simply $e^{\alpha t}$ with $\alpha = 0$. Damped sine and cosine signals can be represented by

$$e^{(\sigma+i\omega)t} = e^{\sigma t} e^{i\omega t} = e^{\sigma t} (\cos \omega t + i \sin \omega t),$$

where $\sigma < 0$ determines the decay rate. Figure 8.2 give examples of signals that can be represented by complex exponentials; many other signals can be represented by linear combinations of these signals. As in the case of sinusoidal signals, we will allow complex valued signals in the derivation that follows, although in practice we always add together combinations of signals that result in real-valued functions.

To investigate how a linear system responds to an exponential input $u(t) = e^{st}$ we consider the state space system

$$\frac{dx}{dt} = Ax + Bu, \quad y = Cx + Du. \quad (8.2)$$

Let the input signal be $u(t) = e^{st}$ and assume that $s \neq \lambda_j(A)$, $j = 1, \dots, n$, where $\lambda_j(A)$ is the j th eigenvalue of A . The state is then given by

$$x(t) = e^{At}x(0) + \int_0^t e^{A(t-\tau)} B e^{s\tau} d\tau = e^{At}x(0) + e^{At} \int_0^t e^{(sI-A)\tau} B d\tau.$$

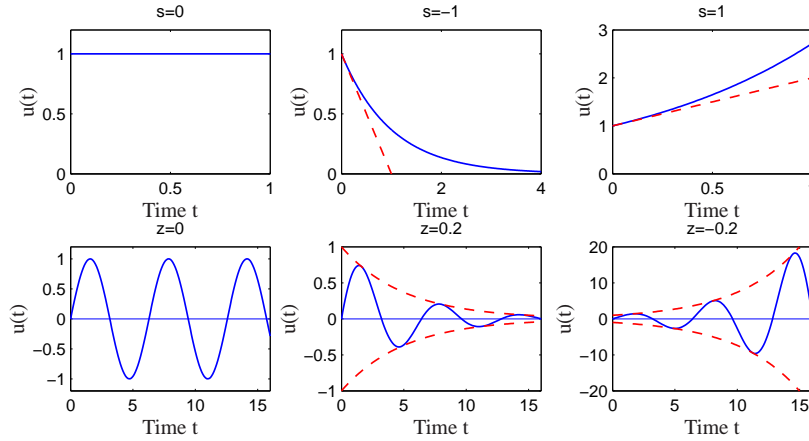


Figure 8.2: Examples of exponential signals. The top row corresponds to exponential signals with a real exponent and the bottom row corresponds to those with complex exponents. In each case, if the real part is negative then the signal decays, while if the real part is positive then it grows.

If $s \neq \lambda(A)$ the integral can be evaluated and we get

$$\begin{aligned} x(t) &= e^{At}x(0) + e^{At}(sI - A)^{-1}\left(e^{(sI - A)t} - I\right)B \\ &= e^{At}\left(x(0) - (sI - A)^{-1}B\right) + (sI - A)^{-1}Be^{st}. \end{aligned}$$

The output of equation (8.2) is thus

$$\begin{aligned} y(t) &= Cx(t) + Du(t) \\ &= Ce^{At}\left(x(0) - (sI - A)^{-1}B\right) + \left(C(sI - A)^{-1}B + D\right)e^{st}, \end{aligned} \quad (8.3)$$

a linear combination of the exponential functions e^{st} and e^{At} . The first term in equation (8.3) is the transient response of the system. Recall that e^{At} can be written in terms of the eigenvalues of A (using the Jordan form in the case of repeated eigenvalues) and hence the transient response is a linear combination of terms of the form $e^{\lambda_j t}$, where λ_j are eigenvalues of A . If the system is stable then $e^{At} \rightarrow 0$ as $t \rightarrow \infty$ and this term dies away.

The second term of the output (8.3) is proportional to the input $u(t) = e^{st}$. This term is called the *pure exponential response*. If the initial state is chosen as

$$x(0) = (sI - A)^{-1}B,$$

then the output only consists of the pure exponential response and both the state and the output are proportional to the input:

$$\begin{aligned} x(t) &= (sI - A)^{-1}Be^{st} = (sI - A)^{-1}Bu(t) \\ y(t) &= \left(C(sI - A)^{-1}B + D\right)e^{st} = \left(C(sI - A)^{-1}B + D\right)u(t). \end{aligned}$$

This is also the output we see in steady state, when the transients represented by the first term in equation (8.3) have died out. The map from the input to output,

$$G_{yu}(s) = C(sI - A)^{-1}B + D, \quad (8.4)$$

is the *transfer function* from u to y for the system (8.2) and we can write $y(t) = G_{yu}(s)u(t)$ for the case that $u(t) = e^{st}$. Compare with the definition of frequency response given by equation (5.23).

An important point in the derivation of the transfer function is the fact that we have restricted s so that $s \neq \lambda_j(A)$, the eigenvalues of A . At those values of s , we see that the response of the system is singular (since $sI - A$ will fail to be invertible). If $s = \lambda_j(A)$, the response of the system to the exponential input $u = e^{\lambda_j t}$ is $y = p(t)e^{\lambda_j t}$, where $p(t)$ is a polynomial of degree less than or equal to the multiplicity of the eigenvalue λ_j (see Exercise 8.3).

Example 8.1 Damped oscillator

Consider the response of a damped linear oscillator, whose state space dynamics were studied in Section 6.3:

$$\begin{aligned} \dot{x} &= \begin{pmatrix} 0 & \omega_0 \\ -\omega_0 & -2\zeta\omega_0 \end{pmatrix} x + \begin{pmatrix} 0 \\ k/\omega_0 \end{pmatrix} u \\ y &= \begin{pmatrix} 1 & 0 \end{pmatrix} x. \end{aligned} \quad (8.5)$$

This system is stable if $\zeta > 0$ and so we can look at the steady state response to an input $u = e^{st}$,

$$\begin{aligned} G_{yu}(s) &= C(sI - A)^{-1}B = \begin{pmatrix} 1 & 0 \end{pmatrix} \begin{pmatrix} s & \omega_0 \\ -\omega_0 & s + 2\zeta\omega_0 \end{pmatrix}^{-1} \begin{pmatrix} 1 \\ k/\omega_0 \end{pmatrix} \\ &= \begin{pmatrix} 1 & 0 \end{pmatrix} \left(\frac{1}{s^2 + 2\zeta\omega_0 s + \omega_0^2} \begin{pmatrix} s & -\omega_0 \\ \omega_0 & s + 2\zeta\omega_0 \end{pmatrix} \right) \begin{pmatrix} 1 \\ k/\omega_0 \end{pmatrix} \\ &= \frac{k}{s^2 + 2\zeta\omega_0 s + \omega_0^2}. \end{aligned} \quad (8.6)$$

To compute the steady state response to a step function, we set $s = 0$ and we see that

$$u = 1 \quad \implies \quad y = G_{yu}(0)u = \frac{k}{\omega_0^2}.$$

If we wish to compute the steady state response to a sinusoid, we write

$$\begin{aligned} u &= \sin \omega t = \frac{1}{2} (ie^{-i\omega t} - ie^{i\omega t}) \\ y &= \frac{1}{2} (iG_{yu}(-i\omega)e^{-i\omega t} - iG_{yu}(i\omega)e^{i\omega t}). \end{aligned}$$

We can now write $G(s)$ in terms of its magnitude and phase,

$$G(i\omega) = \frac{k}{s^2 + 2\zeta\omega_0 s + \omega_0^2} =: M e^{i\theta},$$

where the magnitude M and phase θ satisfy

$$M = \frac{k}{\sqrt{(\omega_0^2 - \omega^2)^2 + (2\zeta\omega_0\omega)^2}}, \quad (\omega_0^2 - \omega^2) \cos \theta - (2\zeta\omega_0\omega) \sin \theta = 0.$$

We can also make use of the fact that $G(-i\omega)$ is given by its complex conjugate $G^*(i\omega)$ and it follows that $G(-i\omega) = Me^{-i\theta}$. Substituting these expressions into our output equation, we obtain

$$\begin{aligned} y &= \frac{1}{2} \left(i(Me^{-i\theta})e^{-i\omega t} - i(Me^{i\theta})e^{i\omega t} \right) \\ &= M \cdot \frac{1}{2} \left(ie^{-i(\omega t + \theta)} - ie^{i(\omega t + \theta)} \right) = M \sin(\omega t + \theta). \end{aligned}$$

The responses to other signals can be computed by writing the input as an appropriate combination of exponential responses and using linearity. ∇

Coordinate Changes

The matrices A , B and C in equation (8.2) depend on the choice of coordinate system for the states. Since the transfer function relates input to outputs, it should be invariant to coordinate changes in the state space. To show this, consider the model (8.2) and introduce new coordinates z by the transformation $z = Tx$, where T is a nonsingular matrix. The system is then described by

$$\begin{aligned} \frac{dz}{dt} &= T(Ax + Bu) = TAT^{-1}z + TBu =: \tilde{A}z + \tilde{B}u \\ y &= Cx + Du = CT^{-1}z + Du =: \tilde{C}z + Du \end{aligned}$$

This system has the same form as equation (8.2) but the matrices A , B and C are different:

$$\tilde{A} = TAT^{-1} \quad \tilde{B} = TB \quad \tilde{C} = CT^{-1}. \quad (8.7)$$

Computing the transfer function of the transformed model we get

$$\begin{aligned} \tilde{G}(s) &= \tilde{C}(sI - \tilde{A})^{-1}\tilde{B} + \tilde{D} = CT^{-1}(sI - TAT^{-1})^{-1}TB + D \\ &= C(T^{-1}(sI - TAT^{-1})T)^{-1}B + D = C(sI - A)^{-1}B + D = G(s), \end{aligned}$$

which is identical to the transfer function (8.4) computed from the system description (8.2). The transfer function is thus invariant to changes of the coordinates in the state space.



Another property of the transfer function is that it corresponds to the portion of the state space dynamics that are both reachable and observable. In particular, if we make use of the Kalman decomposition (Section 7.5), then the transfer function only depends on the dynamics in the reachable and observable subspace, Σ_{ro} (Exercise 8.2).

Transfer Functions for Linear Systems

Consider a linear input/output system described by the differential equation

$$\frac{d^n y}{dt^n} + a_1 \frac{d^{n-1} y}{dt^{n-1}} + \cdots + a_n y = b_0 \frac{d^m u}{dt^m} + b_1 \frac{d^{m-1} u}{dt^{m-1}} + \cdots + b_m u, \quad (8.8)$$

where u is the input and y is the output. This type of description arises in many applications, as described briefly in Section 2.2; bicycle dynamics and AFM modeling are two specific examples. Note that here we have generalized our previous system description to allow both the input and its derivatives to appear.

To determine the transfer function of the system (8.8), let the input be $u(t) = e^{st}$. Since the system is linear, there is an output of the system that is also an exponential function $y(t) = y_0 e^{st}$. Inserting the signals into equation (8.8) we find

$$(s^n + a_1 s^{n-1} + \cdots + a_n) y_0 e^{st} = (b_0 s^m + b_1 s^{m-1} \cdots + b_m) e^{-st}$$

and the response of the system can be completely described by two polynomials

$$\begin{aligned} a(s) &= s^n + a_1 s^{n-1} + \cdots + a_n \\ b(s) &= b_0 s^m + b_1 s^{m-1} + \cdots + b_m. \end{aligned} \quad (8.9)$$

The polynomial $a(s)$ is the characteristic polynomial of the ordinary differential equation. If $a(s) \neq 0$ it follows that

$$y(t) = y_0 e^{st} = \frac{b(s)}{a(s)} e^{st} \quad (8.10)$$

The transfer function of the system (8.8) is thus the rational function

$$G(s) = \frac{b(s)}{a(s)}, \quad (8.11)$$

where the polynomials $a(s)$ and $b(s)$ are given by equation (8.9). Notice that the transfer function for the system (8.8) can be obtained by inspection, since the coefficients of $a(s)$ and $b(s)$ are precisely the coefficients of the derivatives of u and y .

Equations (8.8)–(8.11) can be used to compute the transfer functions of many simple ODEs. Table 8.1 gives some of the more common forms. The first five of these follow directly from the analysis above. For the proportional-integral-derivative (PID) controller, we make use of the fact that the integral of an exponential input is given by $(1/s)e^{st}$. The last entry in Table 8.1 is for a pure time delay, in which the output is identical to the input at an earlier time. Time delays appear in many systems: typical examples are delays in nerve propagation, communication and mass transport. A system with a time delay has the input/output relation

$$y(t) = u(t - \tau). \quad (8.12)$$

As before, let the input be $u(t) = e^{st}$. Assuming that there is an output of the form

Table 8.1: Laplace transforms for some common ordinary differential equations.

Type	ODE	Transfer Function
Integrator	$\dot{y} = u$	$\frac{1}{s}$
Differentiator	$y = \dot{u}$	s
First order system	$\dot{y} + ay = u$	$\frac{1}{s+a}$
Double Integrator	$\ddot{y} = u$	$\frac{1}{s^2}$
Damped oscillator	$\ddot{y} + 2\zeta\omega_n\dot{y} + \omega_n^2y = u$	$\frac{1}{s^2 + 2\zeta\omega_ns + \omega_n^2}$
PID controller	$y = k_p u + k_d \dot{u} + k_i \int u$	$k_p + k_d s + \frac{k_i}{s}$
Time delay	$y(t) = u(t - \tau)$	$e^{-s\tau}$

$y(t) = y_0 e^{st}$ and inserting into equation (8.12) we get

$$y(t) = y_0 e^{st} = e^{s(t-\tau)} = e^{-s\tau} e^{st} = e^{-s\tau} u(t).$$

The transfer function of a time delay is thus $G(s) = e^{-s\tau}$, which is not a rational function but is analytic except at infinity. (A complex function is *analytic* if it has no singularities in the closed left half plane.)

Example 8.2 Electrical circuit elements

Modeling of electrical circuits is a common use of transfer functions. Consider for example a resistor modeled by Ohm's law $V = IR$, where V is the voltage across the resistor, I is the current through the resistor and R is the resistance value. If we consider current to be the input and voltage to be the output the resistor has the transfer function $Z(s) = R$. $Z(s)$ is also called the *impedance* of the circuit element.

Next we consider an inductor whose input/output characteristic is given by

$$L \frac{dI}{dt} = V.$$

Letting the current be $I(t) = e^{st}$, we find that the voltage is $V(t) = Ls e^{st}$ and the transfer function of an inductor is thus $Z(s) = Ls$. A capacitor is characterized by

$$C \frac{dV}{dt} = I$$

and a similar analysis gives a transfer function from current to voltage of $Z(s) = 1/(Cs)$. Using transfer functions, complex electrical circuits can be analyzed algebraically by using the complex impedance $Z(s)$ just as one would use the resistance value in a resistor network. ∇

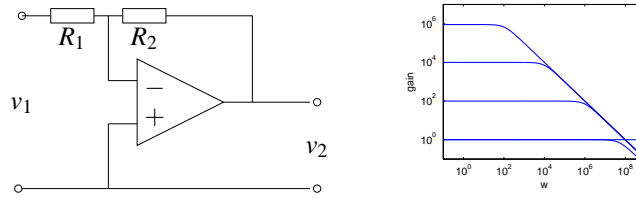


Figure 8.3: Stable amplifier based on negative feedback around an operational amplifier. The block diagram on the left shows a typical amplifier with low frequency gain R_2/R_1 . If we model the dynamic response of the op amp as $G(s) = ak/(s + a)$ then the gain falls off at frequency $\omega = a$, as shown in the gain curves on the right. The frequency response is computed for $k = 10^7$, $a = 100$ rad/s, $R_2 = 106 \Omega$, and $R_1 = 1, 10^2, 10^4$ and 106Ω .

Example 8.3 Operational amplifiers

To further illustrate the use of exponential signals, we consider the operational amplifier circuit introduced in Section 3.3 and reproduced in Figure 8.3a. The model introduced in Section 3.3 is a simplification because the linear behavior of the amplifier was modeled as a constant gain. In reality there are significant dynamics in the amplifier and the static model $v_{\text{out}} = -kv$ (equation (3.10)), should therefore be replaced by a dynamic model. In the linear range the amplifier, we can model the operational amplifier as having a steady state frequency response

$$\frac{v_{\text{out}}}{v} = -\frac{ak}{s + a} =: G(s). \quad (8.13)$$

This response corresponds to a first order system with time constant $1/a$. The parameter k is called the *open loop gain* and the product ak is called the *gain-bandwidth product*; typical values for these parameters are $k = 10^7$ and $ak = 10^7 - 10^9$ rad/s.

Since all of the elements of the circuit are modeled as being linear, if we drive the input v_1 with an exponential signal e^{st} then in steady state all signals will be exponentials of the same form. This allows us to manipulate the equations describing the system in an algebraic fashion. Hence we can write

$$\frac{v_1 - v}{R_1} = \frac{v - v_2}{R_2} \quad \text{and} \quad v_2 = G(s)v, \quad (8.14)$$

using the fact that the current into the amplifier is very small, as we did in Section 3.3. Eliminating v between these equation gives the following transfer function of the system

$$\frac{v_2}{v_1} = \frac{R_2 G(s)}{R_1 + R_2 + R_1 G(s)} = \frac{R_2 ak}{R_1 ak + (R_1 + R_2)(s + a)}.$$

The low frequency gain is obtained by setting $s = 0$, hence

$$G(0) = \frac{v_2}{v_1} = -\frac{kR_2}{(k+1)R_1 + R_2} \approx -\frac{R_2}{R_1},$$

which is the result given by (3.11) in Section 3.3. The bandwidth of the amplifier

circuit is

$$\omega_b = a \frac{R_1(k+1) + R_2}{R_1 + R_2} \approx a \frac{R_1 k}{R_2},$$

where the approximation holds for $R_2/R_1 \gg 1$. The gain of the closed loop system drops off at high frequencies as $R_2/(\omega(R_1 + R_2))$. The frequency response of the transfer function is shown in Figure 8.3 for $k = 10^7$, $a = 100$ rad/s, $R_2 = 106 \Omega$, and $R_1 = 1, 10^2, 10^4$ and $10^6 \Omega$.

Note that in solving this example, we bypassed explicitly writing the signals as $v = v_0 e^{st}$ and instead worked directly with v , assuming it was an exponential. This shortcut is handy in solving problems of this sort. A comparison with Section 3.3, where we made the same calculation when $G(s)$ was a constant, shows analysis of systems using transfer functions is as easy as to deal with as static systems. The calculations are the same if the resistances R_1 and R_2 are replaced by impedances, as discussed in Example 8.2.

▽



Although we have focused thus far on ordinary differential equations, transfer functions can also be used for other types of linear systems. We illustrate this via an example of a transfer function for a partial differential equation.

Example 8.4 Transfer function for heat propagation

Consider the problem of one dimensional heat propagation in a semi-infinite metal rod. Assume that the input is the temperature at one end and that the output is the temperature at a point along the rod. Let $\theta(x, t)$ be the temperature at position x and time t . With proper choice of length scales and units, heat propagation is described by the partial differential equation

$$\frac{\partial \theta}{\partial t} = \frac{\partial^2 \theta}{\partial x^2}, \quad (8.15)$$

and the point of interest can be assumed to have $x = 1$. The boundary condition for the partial differential equation is

$$\theta(0, t) = u(t).$$

To determine the transfer function we choose the input as $u(t) = e^{st}$. Assume that there is a solution to the partial differential equation of the form $\theta(x, t) = \psi(x)e^{st}$, and insert this into equation (8.15) to obtain

$$s\psi(x) = \frac{d^2 \psi}{dx^2},$$

with boundary condition $\psi(0) = e^{st}$. This ordinary differential equation (with independent variable x) has the solution

$$\psi(x) = Ae^{x\sqrt{s}} + Be^{-x\sqrt{s}}.$$

Matching the boundary conditions gives $A = 0$ and $B = e^{st}$, so the solution is

$$y(t) = \theta(1, t) = \psi(1)e^{st} = e^{-\sqrt{s}}e^{st} = e^{-\sqrt{s}}u(t).$$

The system thus has the transfer function $G(s) = e^{-\sqrt{s}}$. As in the case of a time delay, the transfer function is not a rational function but it is an analytic function.

▽

Gains, Poles and Zeros

The transfer function has many useful interpretations and the features of a transfer function are often associated with important system properties. Three of the most important features are the gain and locations of the poles and zeros.

The *zero frequency gain* of a system is given by the magnitude of the transfer function at $s = 0$. It represents the ratio of the steady state value of the output with respect to a step input (which can be represented as $u = e^{st}$ with $s = 0$). For a state space system, we computed the zero frequency gain in equation (5.22):

$$G(0) = D - CA^{-1}B.$$

For a system written as a linear ODE, as in equation (8.8),

$$\frac{d^n y}{dt^n} + a_1 \frac{d^{n-1} y}{dt^{n-1}} + \cdots + a_n y = b_0 \frac{d^m u}{dt^m} + b_1 \frac{d^{m-1} u}{dt^{m-1}} + \cdots + b_m u,$$

if we assume that the input and output of the system are constants y_0 and u_0 , then we find that $a_n y_0 = b_m u_0$. Hence the zero frequency gain is

$$G(0) = \frac{y_0}{u_0} = \frac{b_m}{a_n}. \quad (8.16)$$

Next consider a linear system with the rational transfer function

$$G(s) = \frac{b(s)}{a(s)}.$$

The roots of the polynomial $a(s)$ are called *poles* of the system and the roots of $b(s)$ are called the *zeros* of the system. If p is a pole it follows that $y(t) = e^{pt}$ is a solution of equation (8.8) with $u = 0$ (the homogeneous solution). A pole p corresponds to a *mode* of the system with corresponding modal solution e^{pt} . The unforced motion of the system after an arbitrary excitation is a weighted sum of modes.

Zeros have some what different interpretation. Since the pure exponential output corresponding to the input $u(t) = e^{st}$ with $a(s) \neq 0$ is $G(s)e^{st}$, it follows that the pure exponential output is zero if $b(s) = 0$. Zeros of the transfer function thus block the transmission of the corresponding exponential signals.

For a state space system with transfer function $G(s) = C(sI - A)^{-1}B + D$, the poles of the transfer function are the eigenvalues of the matrix A in the state space model. One easy way to see this is to notice that the value of $G(s)$ is unbounded when s is an eigenvalue of a system, since this is precisely the set of points where the characteristic polynomial $\lambda(s) = \det(sI - A) = 0$ (and hence $sI - A$ is non-invertible). It follows that the poles of a state space system depend only on the

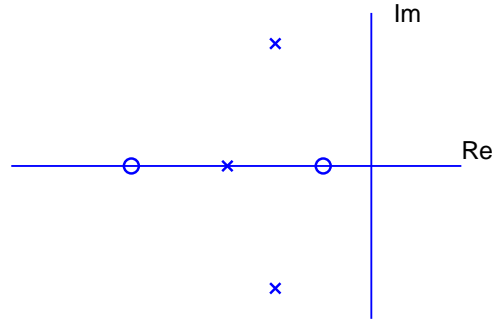


Figure 8.4: A pole zero diagram for a transfer function with zeros at -5 and -1 , and poles at -3 and $-2 \pm 2j$. The circles represent the locations of the zeros and the crosses the locations of the poles. A complete characterization requires we also specify the gain of the system.

matrix A , which represents the intrinsic dynamics of the system. We say that a transfer function is stable if all of its poles have negative real part.

To find the zeros of a state space system, we observe that the zeros are complex numbers s such that the input $u(t) = e^{st}$ gives zero output. Inserting the pure exponential response $x(t) = x_0 e^{st}$ and $y(t) = 0$ in equation (8.2) gives

$$s e^{st} x_0 = A x_0 e^{st} + B u_0 e^{st}, \quad 0 = C e^{st} x_0 + D e^{st} u_0,$$

which can be written as

$$\begin{pmatrix} sI - A & B \\ C & D \end{pmatrix} \begin{pmatrix} x_0 \\ u_0 \end{pmatrix} = 0.$$

This equation has a solution with nonzero x_0, u_0 only if the matrix on the left does not have full rank. The zeros are thus the values s such that

$$\det \begin{pmatrix} sI - A & B \\ C & D \end{pmatrix} = 0. \quad (8.17)$$

Since the zeros depend on A, B, C and D , they therefore depend on how the inputs and outputs are coupled to the states. Notice in particular that if the matrix B has full rank then the matrix in equation (8.17) has n linearly independent rows for all values of s . Similarly there are n linearly independent columns if the matrix C has full rank. This implies that systems where the matrices B or C are of full rank do not have zeros. In particular it means that a system has no zeros if it is fully actuated (each state can be controlled independently) or if the full state is measured.

A convenient way to view the poles and zeros of a transfer function is through a *pole zero diagram*, as shown in Figure 8.4. In this diagram, each pole is marked with a cross and each zero with a circle. If there are multiple poles or zeros at a fixed location, these are often indicated with overlapping crosses or circles (or other annotations). Poles in the left half plane correspond to stable modes of the system and poles in the right half plane correspond to unstable modes. Notice that

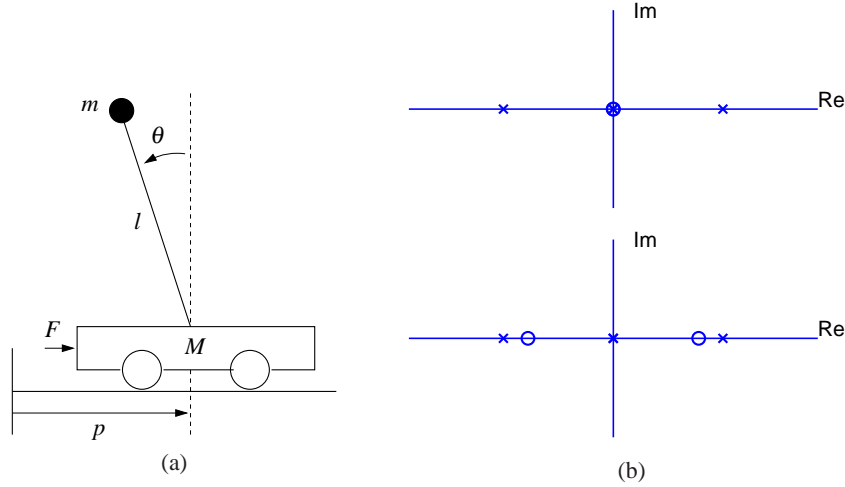


Figure 8.5: Poles and zeros for a balance system. The balance system (a) can be modeled around its vertical equilibrium point by a fourth order linear system. The poles and zeros for the transfer function $H_{\theta,F}$ and $H_{\theta,p}$ are shown on the right top and bottom, respectively.

the gain must also be given to have a complete description of the transfer function.

Example 8.5 Balance system

Consider the dynamics for a balance system, shown in Figure 8.5a. The transfer function for a balance system can be derived directly from the second order equations, given in Example 2.1:

$$M_t \frac{d^2 p}{dt^2} - ml \frac{d^2 \theta}{dt^2} \cos \theta + c \frac{dp}{dt} + ml \sin \theta \left(\frac{dq}{dt} \right)^2 = F$$

$$-ml \cos \theta \frac{d^2 p}{dt^2} + J_t \frac{d^2 \theta}{dt^2} - mgl \sin \theta + \gamma \dot{\theta} = 0.$$

If we assume that θ and \dot{q} are small, we can approximate this nonlinear system by a set of linear second order differential equations,

$$M_t \frac{d^2 p}{dt^2} - ml \frac{d^2 \theta}{dt^2} + c \frac{dp}{dt} = F$$

$$-ml \frac{d^2 p}{dt^2} + J_t \frac{d^2 \theta}{dt^2} + \gamma \frac{d\theta}{dt} - mgl \theta = 0.$$

If we let F be an exponential signal, the resulting response satisfies

$$M_t s^2 p - ml s^2 \theta + cs p = F$$

$$J_t s^2 \theta - ml s^2 p + \gamma s \theta - mgl \theta = 0,$$

where all signals are exponential signals. The resulting transfer functions for the position of the cart and orientation of the pendulum are given by solving for p and

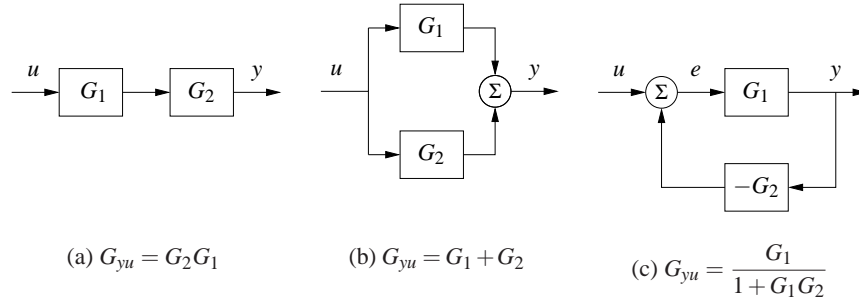


Figure 8.6: Interconnections of linear systems. Series (a), parallel (b) and feedback (c) connections are shown. The transfer functions for the composite systems can be derived by algebraic manipulations assuming exponential functions for all signals.

θ in terms of F to obtain

$$H_{\theta F} = \frac{mIs}{-(M_t J_t - m^2 l^2)s^3 - (\gamma M_t + c J_t)s^2 + (mglM_t - c\gamma)s + mgl}$$

$$H_{pF} = \frac{-J_t s^2 - \gamma s + mgl}{-(M_t J_t - m^2 l^2)s^4 - (\gamma M_t + c J_t)s^3 + (mglM_t - c\gamma)s^2 + mglcs},$$

where each of the coefficients is positive. The pole zero diagrams for these two transfer functions are shown in Figures 8.5 using the parameters from Example 6.7.

If we assume the damping is small and set $c = 0$ and $\gamma = 0$, we obtain

$$H_{\theta F} = \frac{ml}{-(M_t J_t - m^2 l^2)s^2 + mglM_t}$$

$$H_{pF} = \frac{-J_t s^2 + mgl}{s^2(-(M_t J_t - m^2 l^2)s^2 + mglM_t)}.$$

This gives nonzero poles and zeros at

$$p = \pm \sqrt{\frac{mglM_t}{M_t J_t - m^2 l^2}} \approx \pm 2.68, \quad z = \pm \sqrt{\frac{mgl}{J_t}} \approx \pm 2.09.$$

We see that these are quite close to the pole and zero locations in Figure 8.5. ∇

8.3 BLOCK DIAGRAMS AND TRANSFER FUNCTIONS

The combination of block diagrams and transfer functions is a powerful way to represent control systems. Transfer functions relating different signals in the system can be derived by purely algebraic manipulations of the transfer functions of the blocks using *block diagram algebra*. To show how this can be done, we will begin with simple combinations of systems.

Consider a system that is a cascade combination of systems with the transfer functions $G_1(s)$ and $G_2(s)$, as shown in Figure 8.6a. Let the input of the system be $u = e^{st}$. The pure exponential output of the first block is the exponential signal

G_1u , which is also the input to the second system. The pure exponential output of the second system is

$$y = G_2(G_1u) = (G_2G_1)u.$$

The transfer function of the system is thus $G = G_2G_1$, i.e. the product of the transfer functions. The order of the individual transfer functions is due to the fact that we place the input signal on the right hand side of this expression, hence we first multiply by G_1 and then by G_2 . Unfortunately, this has the opposite ordering from the diagrams that we use, where we typically have the signal flow from left to right, so one needs to be careful. The ordering is important if either G_1 or G_2 is a vector-valued transfer function, as we shall see in some examples.

Consider next a parallel connection of systems with the transfer functions G_1 and G_2 , as shown in Figure 8.6b. Letting $u = e^{st}$ be the input to the system, the pure exponential output of the first system is then $y_1 = G_1u$ and the output of the second system is $y_2 = G_2u$. The pure exponential output of the parallel connection is thus

$$y = G_1u + G_2u = (G_1 + G_2)u$$

and the transfer function for a parallel connection is $G = G_1 + G_2$.

Finally, consider a feedback connection of systems with the transfer functions G_1 and G_2 , as shown in Figure 8.6c. Let $u = e^{st}$ be the input to the system, y the pure exponential output, and e be the pure exponential part of the intermediate signal given by the sum of u and the output of the second block. Writing the relations for the different blocks and the summation unit we find

$$y = G_1e \quad e = u - G_2y.$$

Elimination of e gives

$$y = G_1(u - G_2y) \implies (1 + G_1G_2)y = G_1u \implies y = \frac{G_1}{1 + G_1G_2}u.$$

The transfer function of the feedback connection is thus

$$G = \frac{G_1}{1 + G_1G_2}.$$

These three basic interconnections can be used as the basis for computing transfer functions for more complicated systems.

Control System Transfer Functions

Consider the system in Figure 8.7, which was given already at the beginning of the chapter. The system has three blocks representing a process P , a feedback controller C and a feedforward controller F . There are three external signals: the reference r , the load disturbance d and the measurement noise n . A typical problem is to find out how the error e is related to the signals r , d and n .

To derive the relevant transfer functions we assume that all signals are exponential functions, drop the arguments of signals and transfer functions and trace

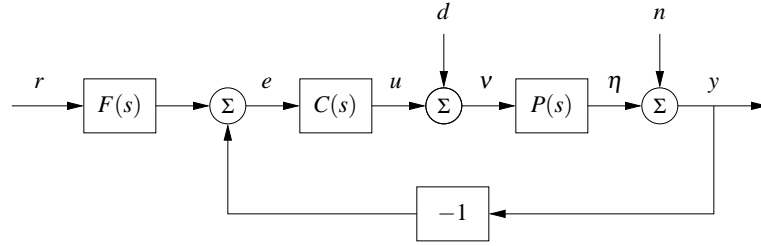


Figure 8.7: Block diagram of a feedback system. The inputs to the system are the reference signal r , the process disturbance d and the process noise n . The remaining signals in the system can all be chosen as possible outputs and transfer functions can be used to relate the system inputs to the other labeled signals.

the signals around the loop. We begin with the signal in which we are interested, in this case the error e , given by

$$e = Fr - y.$$

The signal y is the sum of n and η , where η is the output of the process:

$$y = n + \eta \quad \eta = P(d + u) \quad u = Ce.$$

Combining these equations gives

$$\begin{aligned} e &= Fr - y = Fr - (n + \eta) = Fr - (n + P(d + u)) \\ &= Fr - (n + P(d + Ce)) \end{aligned}$$

and hence

$$e = Fr - n - Pd - PCe.$$

Finally, solving this equation for e gives

$$e = \frac{F}{1+PC}r - \frac{1}{1+PC}n - \frac{P}{1+PC}d = G_{er}r + G_{en}n + G_{ed}d \quad (8.18)$$

and the error is thus the sum of three terms, depending on the reference r , the measurement noise n and the load disturbance d . The functions

$$G_{er} = \frac{F}{1+PC} \quad G_{en} = \frac{-1}{1+PC} \quad G_{ed} = \frac{-P}{1+PC} \quad (8.19)$$

are the transfer functions from reference r , noise n and disturbance d to the error e .

We can also derive transfer functions by manipulating the block diagrams directly, as illustrated in Figure 8.8. Suppose we wish to compute the transfer function between the reference r and the output y . We begin by combining the process and controller blocks in Figure 8.7 to obtain the diagram in Figure 8.8a. We can now eliminate the feedback loop using the algebra for a feedback interconnection (Figure 8.8b) and then use the series interconnection rule to obtain

$$G_{yr} = \frac{PCF}{1+PC}. \quad (8.20)$$

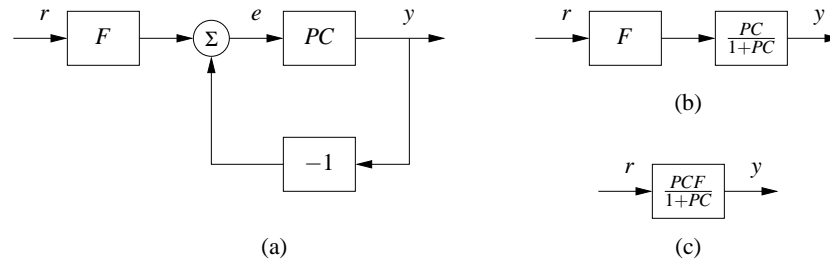


Figure 8.8: Example of block diagram algebra. Figure (a) results from multiplying the process and controller transfer functions (from Figure 8.7). Replacing the feedback loop with its transfer function equivalent yields (b) and finally multiplying the two remaining blocks gives the reference to output representation in (c).

Similar manipulations can be used to obtain the other transfer functions (Exercise 8.8).

The derivation illustrates an effective way to manipulate the equations to obtain the relations between inputs and outputs in a feedback system. The general idea is to start with the signal of interest and to trace signals around the feedback loop until coming back to the signal we started with. With some practice, equations (8.18) and (8.19) can be written directly by inspection of the block diagram. Notice, for example, that all terms in equation (8.19) have the same denominators and that the numerators are the blocks that one passes through when going directly from input to output (ignoring the feedback). This type of rule can be used to compute transfer functions by inspection, although for systems with multiple feedback loops it can be tricky to compute them without writing down the algebra explicitly.

Example 8.6 Vehicle steering

Consider the linearized model for vehicle steering introduced in Example 5.12. In Examples 6.4 and 7.3 we designed a state feedback compensator and state estimator for the system. A block diagram for the resulting control system is given in Figure 8.9. Note that we have split the estimator into two components, $G_{\hat{x}u}(s)$ and $G_{\hat{x}y}(s)$, corresponding to its inputs u and y . The controller can be described as the sum of two (open loop) transfer functions

$$u = G_{uy}(s)y + G_{ur}(s)r.$$

The first transfer function, $G_{uy}(s)$, describes the feedback term and the second, $G_{ur}(s)$, describes the feedforward term. We call these “open loop” transfer functions because they represent the relationships between the signals without considering the dynamics of the process (e.g., removing $P(s)$ from the system description). To derive these functions, we compute the the transfer functions for each block and then use block diagram algebra.

We begin with the estimator, which takes u and y as its inputs and produces an estimate \hat{x} . The dynamics for this process was derived in Example 7.3 and is given

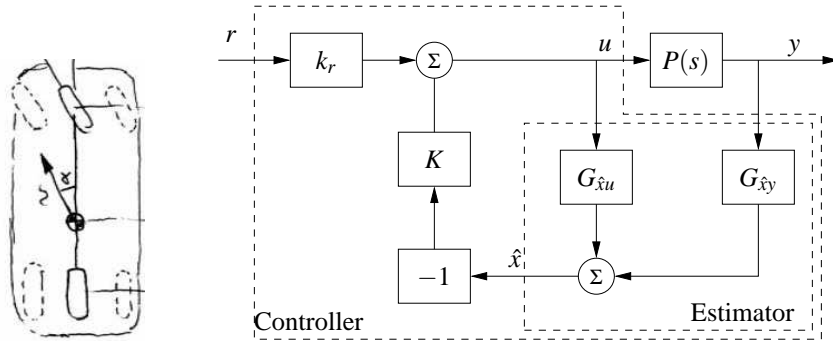


Figure 8.9: Block diagram for the steering control system. The control system is designed to maintain the lateral position of the vehicle along a reference curve (left). The structure of the control system is shown on the right as a block diagram of transfer functions. The estimator consists of two components that compute the estimated state \hat{x} from the combination of the input u and output y of the process. The estimated state is fed through a state feedback controller and combined with a reference gain to obtain the commanded steering angle, u .

by

$$\begin{aligned} \frac{d\hat{x}}{dt} &= (A - LC)\hat{x} + Ly + Bu \\ \hat{x} &= \underbrace{(sI - (A - LC))^{-1}Bu}_{G_{\hat{x}u}} + \underbrace{(sI - (A - LC))^{-1}Ly}_{G_{\hat{x}y}}. \end{aligned}$$

Using the expressions for A , B , C and L from Example 7.3, we obtain

$$G_{\hat{x}u}(s) = \begin{pmatrix} \frac{\gamma s + 1}{s^2 + l_1 s + l_2} \\ \frac{s + l_1 - \gamma l_2}{s^2 + l_1 s + l_2} \end{pmatrix} \quad G_{\hat{x}y}(s) = \begin{pmatrix} \frac{l_1 s + l_2}{s^2 + l_1 s + l_2} \\ \frac{l_2 s}{s^2 + l_1 s + l_2} \end{pmatrix},$$

where l_1 and l_2 are the observer gains and γ is the scaled position of the center of mass from the rear wheels. The controller was a state feedback compensator, which can be viewed as a constant, multi-input, single output transfer function of the form $u = -K\hat{x}$.

We can now proceed to compute the transfer function for the overall control system. Using block diagram algebra, we have

$$G_{wy}(s) = \frac{-KG_{\hat{x}y}(s)}{1 + KG_{\hat{x}u}(s)} = -\frac{s(k_1 l_1 + k_2 l_2) + k_1 l_2}{s^2 + s(\gamma k_1 + k_2 + l_1) + k_1 + l_2 + k_2 l_1 - \gamma k_2 l_2}$$

and

$$G_{ur}(s) = \frac{k_r}{1 + KG_{\hat{x}u}(s)} = \frac{k_1(s^2 + l_1 s + l_2)}{s^2 + s(\gamma k_1 + k_2 + l_1) + k_1 + l_2 + k_2 l_1 - \gamma k_2 l_2},$$

where k_1 and k_2 are the controller gains.

Finally, we compute the full closed loop dynamics. We begin by deriving the

transfer function for the process, $P(s)$. We can compute this directly from the state space description of the dynamics, which was given in Example 6.4. Using that description, we have

$$P(s) = G_{yu}(s) = C(sI - A)^{-1}B + D = \begin{pmatrix} 1 & 0 \end{pmatrix} \begin{pmatrix} s & -1 \\ 0 & s \end{pmatrix}^{-1} \begin{pmatrix} \gamma \\ 1 \end{pmatrix} = \frac{\gamma s + 1}{s^2}.$$

The transfer function for the full closed loop system between the input r and the output y is then given by

$$G_{yr} = \frac{k_r P(s)}{1 + P(s)G_{uy}(s)} = \frac{k_1(\gamma s + 1)}{s^2 + (k_1\gamma + k_2)s + k_1}.$$

Note that the observer gains l_1 and l_2 do not appear in this equation. This is because we are considering steady state analysis and, in steady state, the estimated state exactly tracks the state of the system assuming perfect models. We will return to this example in Chapter 12 to study the robustness of this particular approach. ∇

Pole/Zero Cancellations

Because transfer functions are often polynomials in s , it can sometimes happen that the numerator and denominator have a common factor, which can be canceled. Sometimes these cancellations are simply algebraic simplifications, but in other situations these cancellations can mask potential fragilities in the model. In particular, if a pole/zero cancellation occurs due to terms in separate blocks that just happen to coincide, the cancellation may not occur if one of the systems is slightly perturbed. In some situations this can result in severe differences between the expected behavior and the actual behavior, as illustrated in this section.

To illustrate when we can have pole/zero cancellations, consider the block diagram shown in Figure 8.7 with $F = 1$ (no feedforward compensation) and C and P given by

$$C(s) = \frac{n_c(s)}{d_c(s)} \quad P(s) = \frac{n_p(s)}{d_p(s)}.$$

The transfer function from r to e is then given by

$$G_{er}(s) = \frac{1}{1 + PC} = \frac{d_c(s)d_p(s)}{d_c(s)d_p(s) + n_c(s)n_p(s)}.$$

If there are common factors in the numerator and denominator polynomials, then these terms can be factored out and eliminated from both the numerator and denominator. For example, if the controller has a zero at $s = a$ and the process has a pole at $s = a$, then we will have

$$G_{er}(s) = \frac{(s+a)d'_c(s)d_p(s)}{(s+a)d_c(s)d'_p(s) + (s+a)n'_c(s)n_p(s)} = \frac{d'_c(s)d_p(s)}{d_c(s)d'_p(s) + n'_c(s)n_p(s)},$$

where $n'_c(s)$ and $d'_p(s)$ represent the relevant polynomials with the term $s + a$ factored out. In the case when $a < 0$ (so that the zero or pole is in the right half plane),

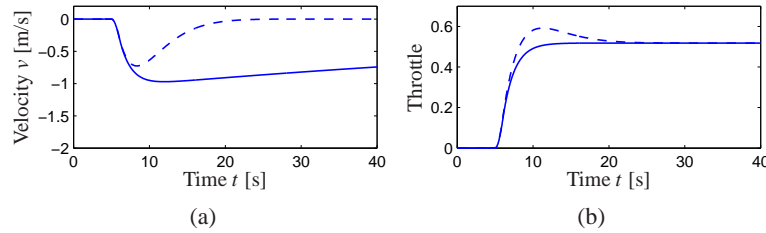


Figure 8.10: Car with PI cruise control encountering a sloping road. Figure 8.10a shows the velocity error and Figure 8.10b shows the throttle. Results with a PI controller with $k_p = 0.5$ and $k_i = 0.0051$, where the process pole $s = -0.101$ is shown in full lines and a controller with $k_p = 0.5$ and $k_i = 0.5$ are shown in dashed lines. Compare with Figure 3.3b on page 68.

we see that there is no impact on the transfer function G_{er} .

Suppose instead that we compute the transfer function from d to e , which represents the effect of a disturbance on the error between the reference and the output. This transfer function is given by

$$G_{ed}(s) = \frac{d'_c(s)n_p(s)}{(s+a)d_c(s)d'_p(s) + (s+a)n'_c(s)n_p(s)}.$$

Notice that if $a < 0$ then the pole is in the right half plane and the transfer function G_{ed} is *unstable*. Hence, even though the transfer function from r to e appears to be OK (assuming a perfect pole/zero cancellation), the transfer function from d to e can exhibit unbounded behavior. This unwanted behavior is typical of an *unstable pole/zero cancellation*.

It turns out that the cancellation of a pole with a zero can also be understood in terms of the state space representation of the systems. Reachability or observability is lost when there are cancellations of poles and zeros (Exercise 8.10). A consequence is that the transfer function only represents the dynamics in the reachable and observable subspace of a system (see Section 7.5).

Example 8.7 Cruise control with pole-zero cancellation

The linearized model from throttle to velocity for the linearized model for a car has the transfer function $G(s) = b/(s-a)$. A simple way (but not necessarily good way) to design a PI controller is to choose the parameters of the PI controller so that the controller zero at $s = -k_i/k_p$ cancels the process pole at $s = a$. The transfer function from reference to velocity is $G_{vr}(s) = bk_p/(s + bk_p)$ and control design is simply a matter of choosing the gain k_p . The closed loop system dynamics are of first order with the time constant $1/bk_p$.

Figure 8.10 shows the velocity error when the car encounters an increase in the road slope. A comparison with the controller used in Figure 3.3b (reproduced in dashed curves) show that the controller based on pole-zero cancellation has very poor performance. The velocity error is larger and it takes a long time to settle. Notice that the control signal remains practically constant after $t = 15$ even if the error is large after that time. To understand what happens we will analyze the system. The parameters of the system are $a = -0.0101$, $b = 1.32$ and the

controller parameters are $k_p = 0.5$ and $k_i = 0.0051$. The closed loop time constant is $1/(bk_p) = 2.5$ s and we would expect that the error would settle in about 10 s (4 time constants). The transfer functions from road slope to velocity and control signals are

$$G_{v\theta}(s) = \frac{b_g k_p s}{(s-a)(s+bk_p)} \quad G_{u\theta}(s) = \frac{bk_p}{s+bk_p}.$$

Notice that the canceled mode $s = a = -0.0101$ appears in $G_{v\theta}$ but not in $G_{u\theta}$, which explains why v settles very slowly. The reason why the control signal remains constant is that the controller has a zero at $s = -0.0101$ which cancels the slowly decaying process mode. Notice that the error would diverge if the canceled pole is unstable. ∇

The lesson we can learn from this example is that it is a bad idea to try to cancel unstable or slow process poles. A more detailed discussion of pole/zero cancellations is given in Section 12.4.

Algebraic Loops

When analyzing or simulating a system described by a block diagram it is necessary to form the differential equations that describe the complete system. In many cases the equations can be obtained by combining the differential equations that describe each subsystem and substituting variables. This simple procedure cannot be used when there are closed loops of subsystems that all have a direct connection between inputs and outputs, a so-called *algebraic loop*.

To see what can happen, consider a system with two blocks, a first order non-linear system

$$\frac{dx}{dt} = f(x, u), \quad y = g(x), \quad (8.21)$$

and a proportional controller described by $u = -ky$. There is no direct term since the function g does not depend on u . In that case we can obtain the equation for the closed loop system simply by substituting u by $-ky$ in (8.21) to give

$$\frac{dx}{dt} = f(x, -ky), \quad y = g(x).$$

Such a procedure can easily be automated using simple formula manipulation.

The situation is more complicated if there is a direct term. If $y = g(x, u)$ then substituting u by $-ky$ gives

$$\frac{dx}{dt} = f(x, -ky), \quad y = g(x, -ky),$$

To obtain a differential equation for x , the algebraic equation $y = g(x, -ky)$ must be solved to give $y = h(x)$, which in general is a complicated task.

When algebraic loops are present it is necessary to solve algebraic equations to obtain the differential equations for the complete system. Resolving algebraic loops is a non-trivial problem because it requires symbolic solution of algebraic

equations. Most block-diagram oriented modeling languages cannot handle algebraic loops and they simply give a diagnosis that such loops are present. In the era of analog computing, algebraic loops were eliminated by introducing fast dynamics between the loops. This created differential equations with fast and slow modes that are difficult to solve numerically. Advanced modeling languages like Modelica use several sophisticated methods so resolve algebraic loops.

8.4 THE BODE PLOT

The frequency response of a linear system can be computed from its transfer function by setting $s = i\omega$, corresponding to a complex exponential

$$u(t) = e^{i\omega t} = \cos(\omega t) + i \sin(\omega t).$$

The resulting output has the form

$$y(t) = G(i\omega)e^{i\omega t} = Me^{i\omega t + \varphi} = M \cos(\omega t + \varphi) + iM \sin(\omega t + \varphi)$$

where M and φ are the gain and phase of G :

$$M = |G(i\omega)| \quad \varphi = \arctan \frac{\operatorname{Im} G(i\omega)}{\operatorname{Re} G(i\omega)}.$$

The phase of G is also called the *argument* of G , a term that comes from the theory of complex variables.

It follows from linearity that the response to a single sinusoid (sin or cos) is amplified by M and phase shifted by φ . Note that $-\pi < \varphi \leq \pi$, so the arctangent must be taken respecting the signs of the numerator and denominator. It will often be convenient to represent the phase in degrees rather than radians. We will use the notation $\angle G(i\omega)$ for the phase in degrees and $\arg G(i\omega)$ for the phase in radians. In addition, while we always take $\arg G(i\omega)$ to be in the range $(-\pi, \pi]$, we will take $\angle G(i\omega)$ to be continuous, so that it can take on values outside of the range of -180° to 180° .

The frequency response $G(i\omega)$ can thus be represented by two curves: the gain curve and the phase curve. The gain curve gives $|G(i\omega)|$ as a function of frequency ω and the phase curve gives $\angle G(i\omega)$ as a function of frequency ω . One particularly useful way of drawing these curves is to use a log/log scale for the magnitude plot and a log/linear scale for the phase plot. This type of plot is called a *Bode plot* and is shown in Figure 8.11.

Sketching and Interpreting Bode Plots

Part of the popularity of Bode plots is that they are easy to sketch and interpret. Since the frequency scale is logarithmic they cover the behavior of a linear system over a wide frequency range.

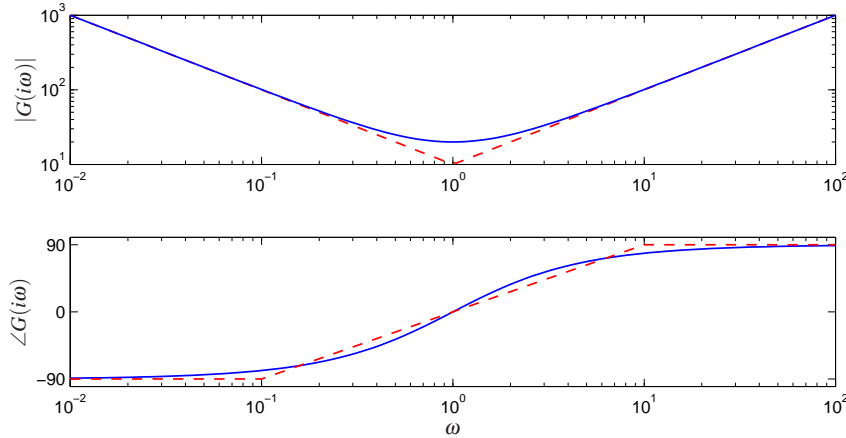


Figure 8.11: Bode plot of the transfer function $C(s) = 20 + 10/s + 10s$ of an ideal PID controller. The top plot is the gain curve and bottom plot is the phase curve. The dashed lines show straight line approximations of the gain curve and the corresponding phase curve.

Consider a transfer function that is a rational function of the form

$$G(s) = \frac{b_1(s)b_2(s)}{a_1(s)a_2(s)}.$$

We have

$$\log |G(s)| = \log |b_1(s)| + \log |b_2(s)| - \log |a_1(s)| - \log |a_2(s)|$$

and hence we can compute the gain curve by simply adding and subtracting gains corresponding to terms in the numerator and denominator. Similarly

$$\angle G(s) = \angle b_1(s) + \angle b_2(s) - \angle a_1(s) - \angle a_2(s)$$

and so the phase curve can be determined in an analogous fashion. Since a polynomial can be written as a product of terms of the type

$$k, \quad s, \quad s + a, \quad s^2 + 2\zeta as + a^2,$$

it suffices to be able to sketch Bode diagrams for these terms. The Bode plot of a complex system is then obtained by adding the gains and phases of the terms.

The simplest term in a transfer function is one of the form s^k , where $k > 0$ if the term appears in the numerator and $k < 0$ if the term is in the denominator. The magnitude and phase of the term are given by

$$\log |G(i\omega)| = k \log \omega, \quad \angle G(i\omega) = 90k.$$

The gain curve is thus a straight line with slope k and the phase curve is a constant at $90^\circ \times k$. The case when $k = 1$ corresponds to a differentiator and has slope 1 with phase 90° . The case when $k = -1$ corresponds to an integrator and has slope -1 with phase -90° . Bode plots of the various powers of k are shown in Figure 8.12.

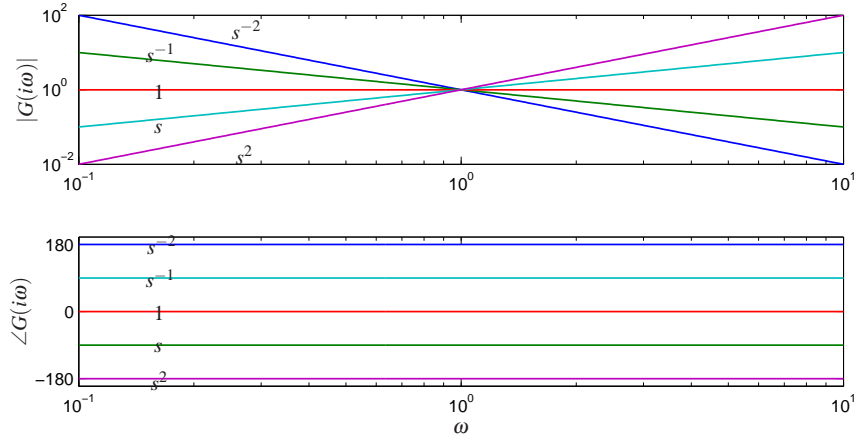


Figure 8.12: Bode plot of the transfer functions $G(s) = s^k$ for $k = -2, -1, 0, 1, 2$. On a log-log scale, the gain curve is a straight line with slope k . Using a log-linear scale, the phase curves the transfer functions are constants, with phase equal to $k \cdot 90^\circ$

Consider next the transfer function of a first order system, given by

$$G(s) = \frac{a}{s+a}.$$

We have

$$|G(s)| = \frac{|a|}{|s+a|} \quad \angle G(s) = \angle(a) - \angle(s+a)$$

and hence

$$\log |G(i\omega)| = \log a - \frac{1}{2} \log(\omega^2 + a^2) \quad \angle G(i\omega) = -\frac{180}{\pi} \arctan \omega/a.$$

The Bode plot is shown in Figure 8.13a, with the magnitude normalized by the zero frequency gain. Both the gain curve and the phase curve can be approximated by the following straight lines

$$\log |G(i\omega)| \approx \begin{cases} \log a & \text{if } \omega < a \\ -\log \omega & \text{if } \omega > a \end{cases}$$

$$\angle G(i\omega) \approx \begin{cases} 0 & \text{if } \omega < a/10 \\ -45 - 45(\log \omega - \log a) & a/10 < \omega < 10a \\ -90 & \text{if } \omega > 10a. \end{cases}$$

The approximate gain curve consists of a horizontal line up to frequency $\omega = a$, called the *breakpoint*, at which point the curve is a line of slope -1 (on a log-log scale). The phase curve is zero up to frequency $a/10$ and then decreases linearly by $45^\circ/\text{decade}$ up to frequency $10a$, at which point it remains constant at 90° . Notice that a first order system behaves like a constant for low frequencies and like an integrator for high frequencies; compare with the Bode plot in Figure 8.12.

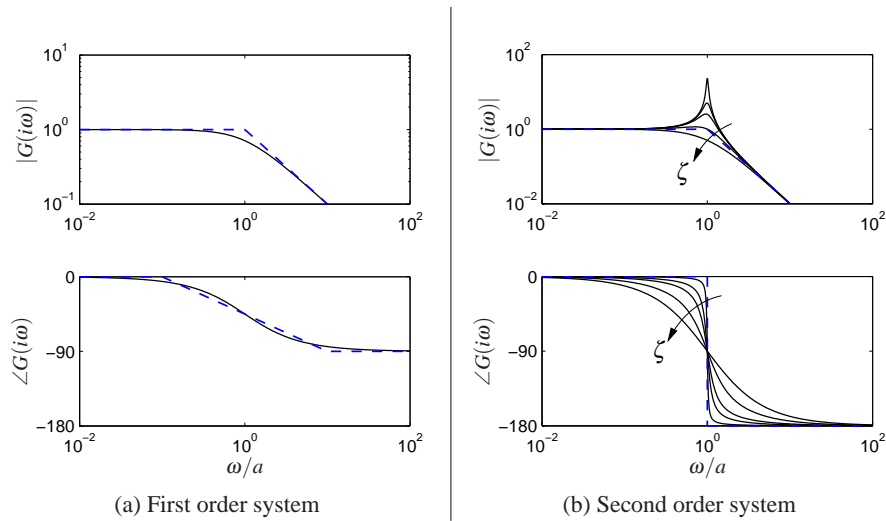


Figure 8.13: Bode plots for first and second order systems. The first order system $G(s) = a/(s + a)$ (left) can be approximated by asymptotic curves (dashed) in both the gain and frequency, with the breakpoint in the gain curve at $\omega = a$ and the phase decreasing by 90° over a factor of 100 in frequency. The second order system $G(s) = \omega_0^2/(s^2 + 2\zeta\omega_0s + \omega_0^2)$ (right) has a peak at frequency a and then a slope of -2 beyond the peak; the phase decreases from 0° to 180° . The height of the peak and rate of change of phase depending on the damping factor ζ ($\zeta = 0.02, 0.1, 0.2, 0.5$ and 1.0 shown).

Finally, consider the transfer function for a second order system

$$G(s) = \frac{\omega_0^2}{s^2 + 2a\zeta s + \omega_0^2}.$$

for which we have

$$\begin{aligned} \log |G(i\omega)| &= 2 \log \omega_0 - \frac{1}{2} \log (\omega^4 + 2\omega_0^2\omega^2(2\zeta^2 - 1) + \omega_0^4) \\ \angle G(i\omega) &= -\frac{180}{\pi} \arctan \frac{2\zeta\omega_0\omega}{\omega_0^2 - \omega^2}. \end{aligned}$$

The gain curve has an asymptote with zero slope for $\omega \ll \omega_0$. For large values of ω the gain curve has an asymptote with slope -2 . The largest gain $Q = \max_{\omega} |G(i\omega)| \approx 1/(2\zeta)$, called the *Q-value*, is obtained for $\omega \approx \omega_0$. The phase is zero for low frequencies and approaches 180° for large frequencies. The curves can be approximated with the following piecewise linear expressions

$$\log |G(i\omega)| \approx \begin{cases} 0 & \text{if } \omega \ll \omega_0, \\ -2 \log \omega & \text{if } \omega \gg \omega_0 \end{cases}, \quad \angle G(i\omega) \approx \begin{cases} 0 & \text{if } \omega \ll \omega_0, \\ -180 & \text{if } \omega \gg \omega_0 \end{cases}.$$

The Bode plot is shown in Figure 8.13b. Note that the asymptotic approximation is poor near $\omega = a$ and the Bode plot depends strongly on ζ near this frequency.

Given the Bode plots of the basic functions, we can now sketch the frequency

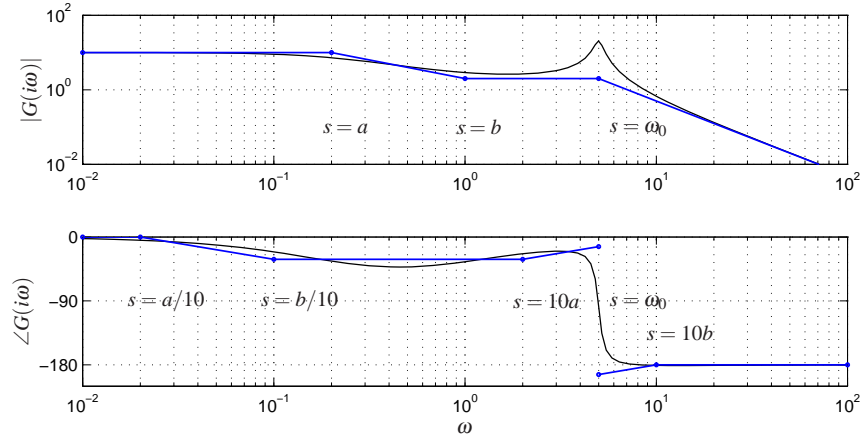


Figure 8.14: Asymptotic approximation to a Bode plot. The thin line is the Bode plot for the transfer function $G(s) = k(s+b)/(s+a)(s^2 + 2\zeta\omega_0s + \omega_0^2)$, where $a \ll b \ll \omega_0$. Each segment in the gain and phase curves represents a separate portion of the approximation, where either a pole or a zero begins to have effect. Each segment of the approximation is a straight line between these points at a slope given by the rules for computing the effects of poles and zeros.

response for a more general system. The following example illustrates the basic idea.

Example 8.8 Asymptotic approximation for a transfer function

Consider the transfer function given by

$$G(s) = \frac{k(s+b)}{(s+a)(s^2 + 2\zeta\omega_0s + \omega_0^2)} \quad a \ll b \ll \omega_0.$$

The Bode plot for this transfer function is shown in Figure 8.14, with the complete transfer function shown in as a solid line and a sketch of the Bode plot shown as a dashed line.

We begin with the magnitude curve. At low frequency, the magnitude is given by

$$G(0) = \frac{kb}{a\omega^2}.$$

When we reach the pole at $s = a$, the magnitude begins to decrease with slope -1 until it reaches the zero at $s = b$. At that point, we increase the slope by 1, leaving the asymptote with net slope 0. This slope is used until we reach the second order pole at $s = \omega_c$, at which point the asymptote changes to slope -2 . We see that the magnitude curve is fairly accurate except in the region of the peak of the second order pole (since for this case ζ is reasonably small).

The phase curve is more complicated, since the effect of the phase stretches out much further. The effect of the pole begins at $s = a/10$, at which point we change from phase 0 to a slope of $-45^\circ/\text{decade}$. The zero begins to affect the phase at $s = b/10$, giving us a flat section in the phase. At $s = 10a$ the phase contributions

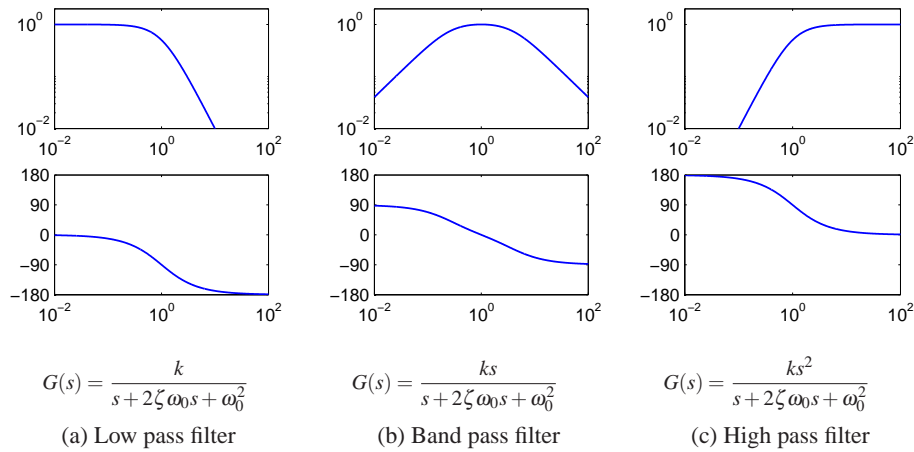


Figure 8.15: Bode plots for low pass, band pass and high pass filters. The top plots are the gain curves and the bottom plots are the phase curves. Each system passes frequencies in a different range and attenuates frequencies outside of that range.

from the pole end and we are left with a slope of $+45^\circ/\text{decade}$ (from the zero). At the location of the second order pole, $s \approx i\omega_c$, we get a jump in phase of -180° . Finally, at $s = 10b$ the phase contributions of the zero end and we are left with phase -180 degrees. We see that the straight line approximation for the phase is not as accurate as it was for the gain curve, but it does capture the basic features of the phase changes as a function of frequency. ∇

The Bode plot gives a quick overview of a system. Since any signal can be decomposed into a sum of sinusoids it is possible to visualize the behavior of a system for different frequency ranges. The system can be viewed as a filter that can change the amplitude (and phase) of the input signals according to the frequency response. For example if there are frequency ranges where the gain curve has constant slope and the phase is close to zero, the action of the system for signals with these frequencies can be interpreted as a pure gain. Similarly for frequencies where the slope is $+1$ and the phase close to 90° , the action of the system can be interpreted as a differentiator, as shown in Figure 8.12.

Three common types of frequency responses are shown in Figure 8.15. The system in Figure 8.15a is called a *low pass filter* because the gain is constant for low frequencies and it drops for high frequencies. Notice that the phase is zero for low frequencies and -180° for high frequencies. The systems in Figure 8.15b and c are called a *band pass filter* and *high pass filter* for similar reasons.

To illustrate how different system behaviors can be read from the Bode plots we consider the band pass filter in Figure 8.15b. For frequencies around $\omega = \omega_0$, the signal is passed through with no change in gain. However, for frequencies well below or well above ω_0 , the signal is attenuated. The phase of the signal is also affected by the filter, as shown in the phase curve. For frequencies below $a/100$ there is a phase lead of 90° and for frequencies above $100a$ there is a phase lag

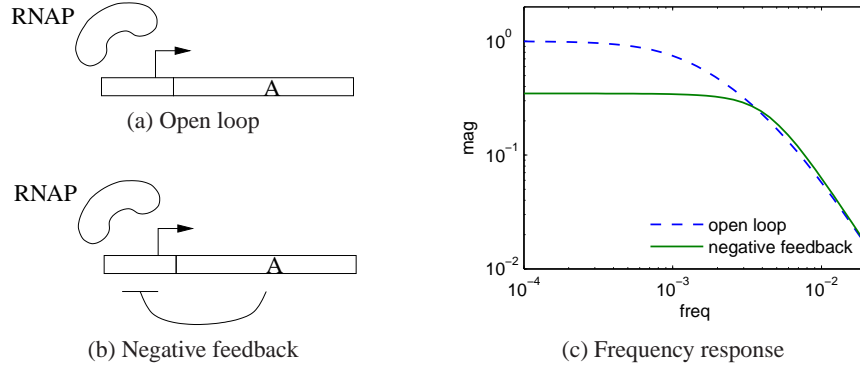


Figure 8.16: Noise attenuation in a genetic circuit. The open loop system (a) consists of a constitutive promoter, while the closed loop circuit (b) is self-regulated with negative feedback (repressor). The frequency response for each circuit is shown on the right.

of 90° . These actions correspond to differentiation and integration of the signal in these frequency ranges.

Example 8.9 Transcriptional regulation in a biological circuit

Consider a genetic circuit consisting of a single gene. We wish to study the response of the protein concentration to fluctuations in the mRNA dynamics. We consider two cases: a *constitutive promoter* (no regulation) and self-repression (negative feedback), illustrated in Figure 8.16. The dynamics of the system are given by

$$\frac{dm}{dt} = \alpha(p) - \gamma m - u, \quad \frac{dp}{dt} = \beta m - \delta p,$$

where u is a disturbance term that affects mRNA transcription.

For the case of no feedback we have $\alpha(p) = \alpha_0$ and the system has an equilibrium point at $m_e = \alpha_0/\gamma$, $p_e = \beta/\delta \cdot \alpha_0/\gamma$. The transfer function from v to p is given by

$$G_{pv}^{\text{ol}}(s) = \frac{-\beta}{(s + \gamma)(s + \delta)}.$$

For the case of negative regulation, we have

$$\alpha(p) = \frac{\alpha_1}{1 + kp^n} + \alpha_0$$

and the equilibrium points satisfy

$$m_e = \frac{\delta}{\beta} p_e, \quad \frac{\alpha}{1 + kp_e^n} + \alpha_0 = \gamma m_e = \frac{\gamma \delta}{\beta} p_e.$$

The resulting transfer function is given by

$$G_{pv}^{\text{cl}}(s) = \frac{\beta}{(s + \gamma)(s + \delta) + \beta \sigma}, \quad \sigma = \frac{2\beta \alpha k p_e}{(1 + kp_e^n)^2}.$$

Figure 8.16c shows the frequency response for the two circuits. We see that the feedback circuit attenuates the response of the system to disturbances with low frequency content, but slightly amplifies disturbances at high frequency (compared to the open loop system). Notice that these curves are very similar to the frequency response curves for the op amp, shown in Figure 8.3 on page 237.

▽

Transfer Functions from Experiments

The transfer function of a system provides a summary of the input/output response and is very useful for analysis and design. However, modeling from first principles can be difficult and time consuming. Fortunately, we can often build an input/output model for a given application by directly measuring the frequency response and fitting a transfer function to it. To do so, we perturb the input to the system using a sinusoidal signal at a fixed frequency. When steady state is reached, the amplitude ratio and the phase lag give the frequency response for the excitation frequency. The complete frequency response is obtained by sweeping over a range of frequencies.

By using correlation techniques it is possible to determine the frequency response very accurately and an analytic transfer function can be obtained from the frequency response by curve fitting. The success of this approach has led to instruments and software that automate this process, called *spectrum analyzers*. We illustrate the basic concept through two examples.

Example 8.10 Atomic force microscope

To illustrate the utility of spectrum analysis, we consider the dynamics of the atomic force microscope, introduced in Section 3.5. Experimental determination of the frequency response is particularly attractive for this system because its dynamics are very fast and hence experiments can be done quickly. A typical example is given in Figure 8.17, which shows an experimentally determined frequency response (solid line). In this case the frequency response was obtained in less than a second. The transfer function

$$G(s) = \frac{k\omega_2^2\omega_3^2\omega_5^2(s^2 + 2\zeta_1\omega_1s + \omega_1^2)(s^2 + 2\zeta_4\omega_4s + \omega_4^2)e^{-sT}}{\omega_1^2\omega_4^2(s^2 + 2\zeta_2\omega_2s + \omega_2^2)(s^2 + 2\zeta_3\omega_3s + \omega_3^2)(s^2 + 2\zeta_5\omega_5s + \omega_5^2)},$$

with $\omega_1 = 2420$, $\zeta_1 = 0.03$, $\omega_2 = 2550$, $\zeta_2 = 0.03$, $\omega_3 = 6450$, $\zeta_3 = 0.042$, $\omega_4 = 8250$, $\zeta_4 = 0.025$, $\omega_5 = 9300$, $\zeta_5 = 0.032$, $T = 10^{-4}$ and $k = 5$, was fit to the data (dashed line). The frequencies associated with the zeros are located where the gain curve has minima and the frequencies associated with the poles are located where the gain curve has local maxima. The relative damping ratios are adjusted to give a good fit to maxima and minima. When a good fit to the gain curve is obtained the time delay is adjusted to give a good fit to the phase curve. The piezo drive is preloaded and a simple model of its dynamics is derived in Exercise 3.7. The pole at 2500 kHz corresponds to the trampoline mode derived in the exercise; the other resonances are higher modes.

▽

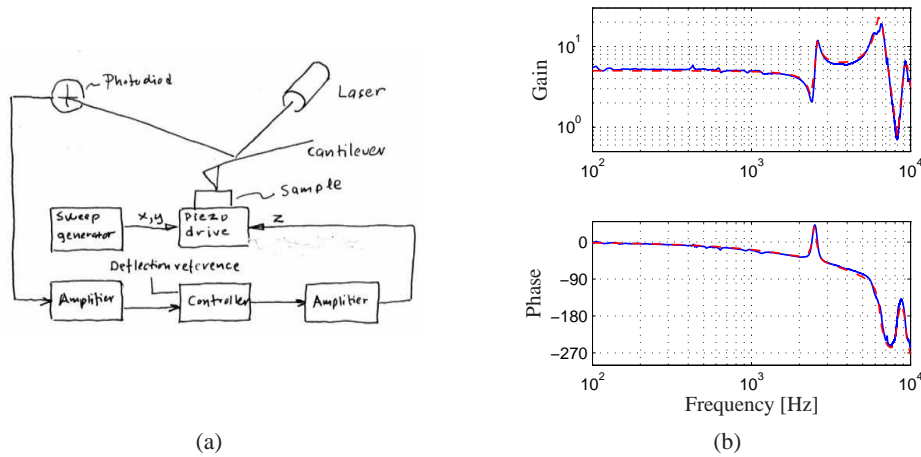


Figure 8.17: Frequency response of a preloaded piezoelectric drive for an atomic force microscope. Figure 8.17a is a schematic which indicates the measured input (the voltage to the drive amplifier) and output (the output of the amplifier measuring beam deflection). Figure 8.17b is a Bode plot of the measured transfer function (full lines) and the fitted transfer function (dashed lines).

Example 8.11 Pupillary light reflex dynamics

The human eye is an organ that is easily accessible for experiments. It has a control system that adjusts the pupil opening to regulate the light intensity at the retina.

This control system was explored extensively by Stark in the late 1960s [175]. To determine the dynamics, light intensity on the eye was varied sinusoidally and the pupil opening was measured. A fundamental difficulty is that the closed loop system is insensitive to internal system parameters, so analysis of a closed loop system thus gives little information about the internal properties of the system. Stark used a clever experimental technique that allowed him to investigate both open and closed loop dynamics. He excited the system by varying the intensity of a light beam focused on the eye and he measured pupil area, as illustrated in Figure 8.18. By using a wide light beam that covers the whole pupil the mea-

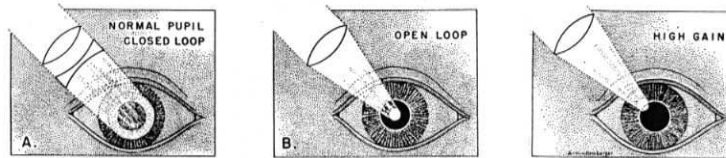


Figure 8.18: Light stimulation of the eye. In (a) the light beam is so large that it always covers the whole pupil, giving the closed loop dynamics. In (b) the light is focused into a beam which is so narrow that it is not influenced by the pupil opening, giving the open loop dynamics. In (c) the light beam is focused on the edge of the pupil opening, which has the effect of increasing the gain of the system since small changes in the pupil opening have a large effect on the amount of light entering the eye. From [174].

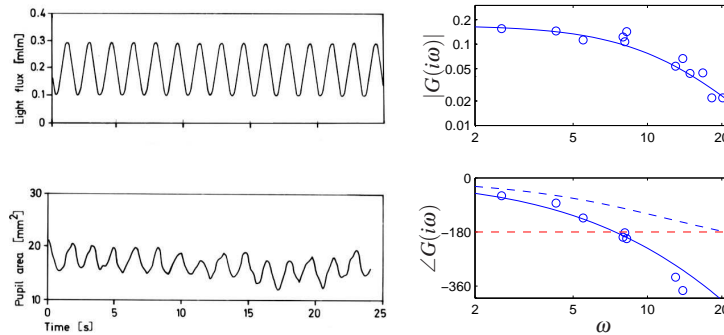


Figure 8.19: Sample curves from open loop frequency response of the eye (left) and Bode plot for the open loop dynamics (right). The solid curve shows a fit of the data using a third order transfer function with time delay. The dashed curve in the Bode plot is the phase of the system without time delay, showing that the delay is needed to properly capture the phase. Figure redrawn from the data of Stark [174].

surement gives the closed loop dynamics. The open loop dynamics were obtained by using a narrow beam, which is small enough that it is not influenced by the pupil opening. The result of one experiment for determining open loop dynamics is given in Figure 8.19. Fitting a transfer function to the gain curves gives a good fit for $G(s) = 0.17/(1 + 0.08s)^3$. This curve gives a poor fit to the phase curve as shown by the dashed curve in Figure 8.19. The fit to the phase curve is improved by adding a time delay, which leaves the gain curve unchanged while substantially modifying the phase curve. The final fit gives the model

$$G(s) = \frac{0.17}{(1 + 0.08s)^3} e^{-0.2s}.$$

The Bode plot of this is shown with solid curves in Figure 8.19. Modeling of the pupillary reflex from first principles is discussed in detail in [112]. ▽

Notice that for both the AFM drive and the pupillary dynamics it is not easy to derive appropriate models from first principles. In practice, it is often fruitful to use a combination of analytical modeling and experimental identification of parameters. Experimental determination of frequency response is less attractive for systems with slow dynamics because the experiment takes a long time.

8.5 LAPLACE TRANSFORMS



Transfer functions are typically introduced using Laplace transforms and in this section we derive the transfer function using this formalism. We assume basic familiarity with Laplace transforms; students who are not familiar with them can safely skip this section. A good reference for the mathematical material in this section is the classic book by Widder [189].

Traditionally, Laplace transforms were also used to compute responses of lin-

ear systems to different stimuli. Today we can easily generate the responses using computers. Only a few elementary properties are needed for basic control applications. There is, however, a beautiful theory for Laplace transforms that makes it possible to use many powerful tools from the theory of functions of a complex variable to get deep insights into the behavior of systems.

Consider a function $f(t)$, $f: \mathbb{R}^+ \rightarrow \mathbb{R}$ that is integrable and grows no faster than $e^{s_0 t}$ for some finite $s_0 \in \mathbb{R}$ and large t . The Laplace transform maps f to a function $F = \mathcal{L}f: \mathbb{C} \rightarrow \mathbb{C}$ of a complex variable. It is defined by

$$F(s) = \int_0^{\infty} e^{-st} f(t) dt, \quad \operatorname{Re} s > s_0. \quad (8.22)$$

The transform has some properties that makes it well suited to deal with linear systems.

First we observe that the transform is linear because

$$\begin{aligned} \mathcal{L}(af + bg) &= \int_0^{\infty} e^{-st} (af(t) + bg(t)) dt \\ &= a \int_0^{\infty} e^{-st} f(t) dt + b \int_0^{\infty} e^{-st} g(t) dt = a\mathcal{L}f + b\mathcal{L}g. \end{aligned} \quad (8.23)$$

Next we calculate the Laplace transform of the derivative of a function. We have

$$\mathcal{L} \frac{df}{dt} = \int_0^{\infty} e^{-st} f'(t) dt = e^{-st} f(t) \Big|_0^{\infty} + s \int_0^{\infty} e^{-st} f(t) dt = -f(0) + s\mathcal{L}f,$$

where the second equality is obtained using integration by parts. We thus obtain

$$\mathcal{L} \frac{df}{dt} = s\mathcal{L}f - f(0) = sF(s) - f(0). \quad (8.24)$$

This formula is particularly simple if the initial conditions are zero because it follows that differentiation of a function corresponds to multiplication of the transform by s .

Since differentiation corresponds to multiplication by s we can expect that integration corresponds to division by s . This is true, as can be seen by calculating the Laplace transform of an integral. Using integration by parts we get

$$\begin{aligned} \mathcal{L} \int_0^t f(\tau) d\tau &= \int_0^{\infty} \left(e^{-st} \int_0^t f(\tau) d\tau \right) dt \\ &= -\frac{e^{-st}}{s} \int_0^t e^{-s\tau} f(\tau) d\tau \Big|_0^{\infty} + \int_0^{\infty} \frac{e^{-s\tau}}{s} f(\tau) d\tau = \frac{1}{s} \int_0^{\infty} e^{-s\tau} f(\tau) d\tau, \end{aligned}$$

hence

$$\mathcal{L} \int_0^t f(\tau) d\tau = \frac{1}{s} \mathcal{L}f = \frac{1}{s} F(s). \quad (8.25)$$

Next consider a linear time-invariant system with zero initial state. We saw in Section 5.3 that the relation between the input u and the output y is given by the convolution integral

$$y(t) = \int_0^{\infty} h(t - \tau) u(\tau) d\tau,$$

where $h(t)$ is the impulse response for the system. Taking the Laplace transform of this expression, we have

$$\begin{aligned} Y(s) &= \int_0^{\infty} e^{-st} y(t) dt = \int_0^{\infty} e^{-st} \int_0^{\infty} h(t-\tau) u(\tau) d\tau dt \\ &= \int_0^{\infty} \int_0^t e^{-s(t-\tau)} e^{-s\tau} h(t-\tau) u(\tau) d\tau dt \\ &= \int_0^{\infty} e^{-s\tau} u(\tau) d\tau \int_0^{\infty} e^{-st} h(t) dt = H(s)U(s). \end{aligned}$$

Thus, the input/output response is given by $Y(s) = H(s)U(s)$ where H , U and Y are the Laplace transforms of h , u and y . The system theoretic interpretation is that the Laplace transform of the output of a linear system is a product of two terms, the Laplace transform of the input $U(s)$ and the Laplace transform of the impulse response of the system $H(s)$. A mathematical interpretation is that the Laplace transform of a convolution is the product of the transforms of the functions that are convolved. The fact that the formula $Y(s) = H(s)U(s)$ is much simpler than a convolution is one reason why Laplace transforms have become popular in engineering.

We can also use the Laplace transform to derive the transfer function for a state space system. Consider for example a linear state space system described by

$$\dot{x} = Ax + Bu, \quad y = Cx + Du.$$

Taking Laplace transforms *under the assumption that all initial values are zero* gives

$$sX(s) = AX(s) + BU(s), \quad Y(s) = CX(s) + DU(s).$$

Elimination of $X(s)$ gives

$$Y(s) = \left(C(sI - A)^{-1}B + D \right) U(s). \quad (8.26)$$

The transfer function is $G(s) = C(sI - A)^{-1}B + D$ (compare with equation (8.4)).

8.6 FURTHER READING

Heaviside, who introduced the idea of characterizing dynamics by the response to a unit step function, also introduced a formal operator calculus for analyzing linear systems. This was a significant advance because it gave the possibility to analyze linear systems algebraically. Heaviside and his work is described in the biography [148]. Unfortunately it was difficult to formalize Heaviside's calculus properly and Heaviside's work was therefore heavily criticized. This was not done rigorously until the mathematician Laurent Schwartz developed *distribution theory* in the late 1940s. Schwartz was awarded the Fields Medal for this work in 1950. The idea of characterizing a linear system by its steady state response to sinusoids was introduced by Fourier in his investigation of heat conduction in solids [73]. Much later it was used by Steinmetz when he introduced the $i\omega$ method to develop

a theory for alternating currents. The concept of transfer functions was an important part of classical control theory; see [103]. It was introduced via the Laplace transform by Gardner Barnes [78], who also used it to calculate response of linear systems. The Laplace transform was very important in the early phase of control because it made it possible to find transients via tables. The Laplace transform is of less importance today when responses to linear systems can easily be generated using computers. There are many excellent books on the use of Laplace transforms and transfer functions for modeling and analysis of linear input/output systems. Traditional texts on control such as [56] and [76] are representative examples.

EXERCISES

8.1 Let $G(s)$ be the transfer function for a linear system. Show that if we apply an input $u(t) = A \sin(\omega t)$ then the steady state output is given by $y(t) = |G(i\omega)|A \sin(\omega t + \arg G(i\omega))$. (Hint: start by taking the real part of a complex number is a linear operation and then use this fact.)



8.2 Show that the transfer function of a system only depends on the dynamics in the reachable and observable subspace of the Kalman decomposition. (Hint: Consider the representation given by Equation (7.29).)

8.3 Consider the system

$$\frac{dx}{dt} = ax + u$$

Show that the response to the input $u(t) = e^{at}$ is $x(t) = e^{at}x(0) + te^{at}$.

8.4 The linearized model of the pendulum in the upright position is characterized by the matrices

$$A = \begin{pmatrix} 0 & 1 \\ 1 & 0 \end{pmatrix}, \quad B = \begin{pmatrix} 0 \\ 1 \end{pmatrix}, \quad C = \begin{pmatrix} 1 & 0 \end{pmatrix}, \quad D = 0.$$

Determine the transfer function of the system.

8.5 Consider the differential equation

$$\frac{d^n y}{dt^n} + a_1 \frac{d^{n-1} y}{dt^{n-1}} + \cdots + a_n y = b_1 \frac{d^{n-1} u}{dt^{n-1}} + b_2 \frac{d^{n-2} u}{dt^{n-2}} + \cdots + b_n u,$$

(a) Let λ be a root of the polynomial

$$s^n + a_1 s^{n-1} + \cdots + a_n = 0.$$

Show that if $u(t) = 0$ the differential equation has the solution $y(t) = e^{\lambda t}$.

(b) Let κ be a zero of the polynomial

$$b(s) = b_1 s^{n-1} + b_2 s^{n-2} + \cdots + b_n.$$

Show that if the input is $u(t) = e^{\kappa t}$ then there is a solution to the differential equation that is identically zero.

8.6 Compute the frequency response of a PI controller using an op amp with dynamics given by equation (8.13).

8.7 Consider the linear state space system

$$\dot{x} = Ax + Bu, \quad y = Cx.$$

Show that the transfer function is

$$G(s) = \frac{b_1 s^{n-1} + b_2 s^{n-2} + \cdots + b_n}{s^n + a_1 s^{n-1} + \cdots + a_n}$$

where

$$b_1 = CB$$

$$b_2 = CAB + a_1 CB$$

$$b_3 = CA^2 B + a_1 CAB + a_2 CB$$

\vdots

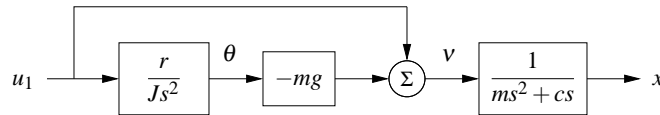
$$b_n = CA^{n-1} B + a_1 CA^{n-2} B + \cdots + a_{n-1} CB$$

and $\lambda(s) = s^n + a_1 s^{n-1} + \cdots + a_n$ is the characteristic polynomial for A .

8.8 Using block diagram algebra, show that the transfer functions from d to y and n to y in Figure 8.8 are given by



8.9 Consider the lateral dynamics of a vectored thrust aircraft, as described in Example 2.9. Show that the dynamics can be described using the following block diagram:



Use this block diagram to compute the transfer functions from u_1 to θ and x and show that they satisfy

$$H_{\theta u_1} = \frac{r}{Js^2}, \quad H_{xu_1} = \frac{Js^2 - mgr}{Js^2(ms^2 + cs)}.$$

8.10 (Pole zero cancellation) Consider a closed loop system of the form of Figure 8.7 with $F = 1$ and P and C having a common pole. Show that if each system is written in state space form, the resulting closed loop system is not reachable and not observable.

8.11 Consider the TCP/AQM model described in Section 3.4. Show that the linearized model can be described by the transfer functions

$$G_{bw}(s) = \frac{Nw^*e^{-\tau^f s}}{\tau^* s + e^{-\tau^f s}}, \quad G_{wq}(s) = -\frac{N}{q^*(\tau^* s + q^* w^*)}, \quad G_{pb}(s) = \rho,$$

where (w^*, b^*) is the equilibrium point for the system, N is the number of sources, τ^* is the steady state round trip time and τ^f is the forward propagation time.

8.12 (Inverted pendulum with PD control) Consider the normalized inverted pendulum system, whose transfer function is given by $P(s) = 1/(s^2 - 1)$ (Exercise 8.4). A proportional-derivative (PD) control law for this system has transfer function $C(s) = k_p + k_d s$ (see Table 8.1). Suppose that we choose $C(s) = \alpha(s - 1)$. Compute the closed loop dynamics and show that the system has good tracking of reference signals but does not have good disturbance rejection properties.

Chapter Nine

Frequency Domain Analysis

Mr. Black proposed a negative feedback repeater and proved by tests that it possessed the advantages which he had predicted for it. In particular, its gain was constant to a high degree, and it was linear enough so that spurious signals caused by the interaction of the various channels could be kept within permissible limits. For best results the feedback factor $\mu\beta$ had to be numerically much larger than unity. The possibility of stability with a feedback factor larger than unity was puzzling.

From “The Regeneration Theory”, Harry Nyquist, 1956 [152].

In this chapter we study how stability and robustness of closed loop systems can be determined by investigating how sinusoidal signals of different frequencies propagate around the feedback loop. This technique allows us to reason about the closed loop behavior of a system through the frequency domain properties of the open loop transfer function. The Nyquist stability theorem is a key result that provides a way to analyze stability and introduce measures of degrees of stability.

9.1 THE LOOP TRANSFER FUNCTION

Determining the stability of systems interconnected by feedback can be tricky because each system influences the other, leading to potentially circular reasoning. Indeed, as the quote from Nyquist above illustrates, the behavior of feedback systems can often be puzzling. However, using the mathematical framework of transfer functions provides an elegant way to reason about such systems, which we call *loop analysis*.

The basic idea of loop analysis is to trace how a sinusoidal signal propagates in the feedback loop and explore the resulting stability by investigating if the propagated signal grows or decays. This is easy to do because the transmission of sinusoidal signals through a linear dynamical system is characterized by the frequency response of the system. The key result is the Nyquist stability theorem, which provides a great deal of insight regarding the stability of a system. Unlike proving stability with Lyapunov functions, studied in Chapter 4, the Nyquist criterion allows us to determine more than just whether a system is stable or unstable. It provides a measure of the degree of stability through the definition of stability margins. The Nyquist theorem also indicates how an unstable system should be changed to make it stable, which we shall study in detail in Chapters 10–12.

Consider the system in Figure 9.1a. The traditional way to determine if the closed loop system is stable is to investigate if the closed loop characteristic polynomial has all its roots in the left half plane. If the process and the controller have

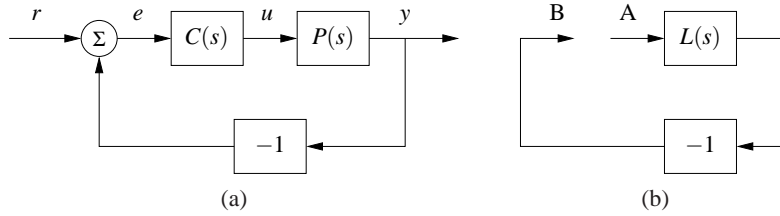


Figure 9.1: The loop transfer function. The stability of the feedback system (a) can be determined by tracing signals around the loop. Letting $L = PC$ represent the loop transfer function, we break the loop in (b) and ask whether a signal injected at the point A has the same magnitude and phase when it reaches B.

rational transfer functions $P(s) = n_p(s)/d_p(s)$ and $C(s) = n_c(s)/d_c(s)$, then the closed loop system has the transfer function

$$G_{yr}(s) = \frac{PC}{1 + PC} = \frac{n_p(s)n_c(s)}{d_p(s)d_c(s) + n_p(s)n_c(s)},$$

and the characteristic polynomial is

$$\lambda(s) = d_p(s)d_c(s) + n_p(s)n_c(s).$$

To check stability, we simply compute the roots of the characteristic polynomial and verify that they each have negative real part. This approach is straightforward but it gives little guidance for design: it is not easy to tell how the controller should be modified to make an unstable system stable.

Nyquist's idea was to investigate conditions under which oscillations can occur in a feedback loop. To study this, we introduce the *loop transfer function*, $L(s) = P(s)C(s)$ which is the transfer function obtained by breaking the feedback loop, as shown in Figure 9.1b. The loop transfer function is simply the transfer function from the input at position A to the output at position B.

We will first determine conditions for having a periodic oscillation in the loop. Assume that a sinusoid of frequency ω_0 is injected at point A. In steady state the signal at point B will also be a sinusoid with the frequency ω_0 . It seems reasonable that an oscillation can be maintained if the signal at B has the same amplitude and phase as the injected signal, because we could then connect A to B. Tracing signals around the loop we find that the signals at A and B are identical if

$$L(i\omega_0) = -1, \tag{9.1}$$

which provides a condition for maintaining an oscillation. The key idea of the Nyquist stability criterion is to understand when this can happen in a general setting. As we shall see, this basic argument becomes more subtle when the loop transfer function has poles in the right half plane.

Example 9.1 Loop transfer function for operational amplifier

Consider the op amp circuit in Figure 9.2a where Z_1 and Z_2 are the transfer functions from voltage to current of the feedback elements. There is feedback because

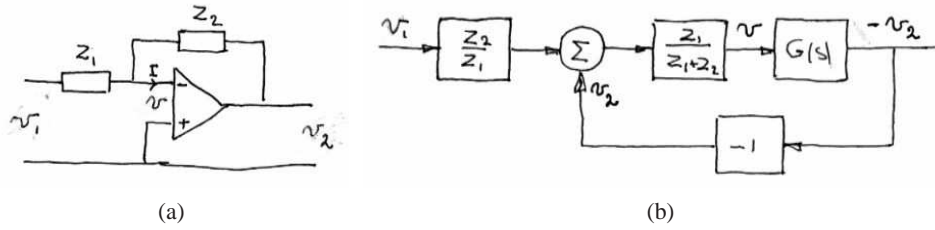


Figure 9.2: Loop transfer function for an op amp. The op amp circuit on the left has a nominal transfer function $v_2/v_1 = Z_2(s)/Z_1(s)$, where Z_1 and Z_2 are the impedances of the circuit elements. The system can be represented by its block diagram on the right, where we now include the op amp dynamics $G(s)$. The loop transfer function is $L = Z_1G/(Z_1 + Z_2)$.

the voltage v_2 is related to the voltage v through the transfer function $-G$ describing the op amp dynamics and the voltage v is related to the voltage v_2 through the transfer function $Z_1/(Z_1 + Z_2)$. The loop transfer function is thus

$$L = \frac{GZ_1}{Z_1 + Z_2}. \quad (9.2)$$

Assuming that the current I is zero, the current through the elements Z_1 and Z_2 is the same which implies

$$\frac{v_1 - v}{Z_1} = \frac{v - v_2}{Z_2}$$

Solving for v gives

$$v = \frac{Z_2v_1 + Z_1v_2}{Z_1 + Z_2} = \frac{Z_2v_1 - Z_1Gv}{Z_1 + Z_2} = \frac{Z_2}{Z_1}Lv_1 - Lv.$$

Since $v_2 = -Gv$ the input-output relation for the circuit becomes

$$Gv_2v_1 = -\frac{Z_2}{Z_1} \frac{L}{1+L}.$$

A block diagram is shown in Figure 9.2b. It follows from (9.1) that the condition for oscillation of the op amp circuit is

$$L(i\omega) = \frac{Z_1(i\omega)G(i\omega)}{Z_1(i\omega) + Z_2(i\omega)} = -1 \quad (9.3)$$

▽

One of the powerful concepts embedded in Nyquist's approach to stability analysis is that it allows us to study the stability of the feedback system by looking at properties of the loop transfer function. The advantage of doing this is that it is easy to see how the controller should be chosen to obtain a desired the loop transfer function. For example if we change the gain of the controller the loop transfer function will be scaled accordingly. A simple way to stabilize an unstable system is then to reduce the gain so that the -1 point is avoided. Another way is to introduce a controller with the property that it bends the loop transfer function away

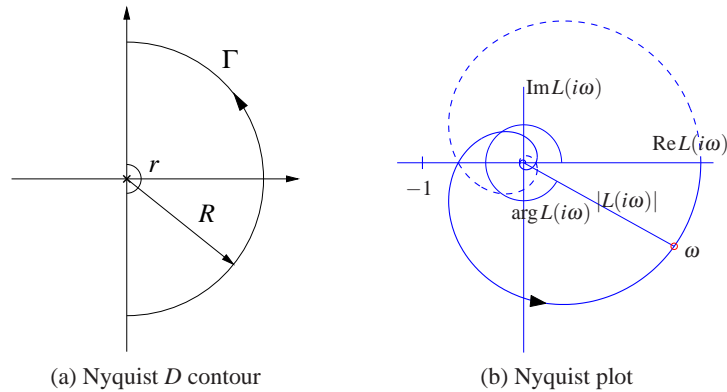


Figure 9.3: The Nyquist contour Γ and the Nyquist plot. The Nyquist contour (a) encloses the right half plane, with a small semicircles around any poles of $L(s)$ on the imaginary axis (illustrated here at the origin) and an arc at infinity, represented by $R \rightarrow \infty$. The Nyquist plot (b) is the image of the loop transfer function $L(s)$ when s traverses Γ in the counter-clockwise direction. The solid line corresponds to $\omega > 0$ and the dashed line to $\omega < 0$. The gain and phase at the frequency ω are $g = |L(i\omega)|$ and $\varphi = \angle L(i\omega)$. The curve is generated for $L(s) = 1.4e^{-s}/(s+1)^2$.

from the critical point, as we shall see in the next section. Different ways to do this, called loop shaping, will be developed as will be discussed in Chapter 11.

9.2 THE NYQUIST CRITERION

In this section we present Nyquist's criterion for determining the stability of a feedback system through analysis of the loop transfer function. We begin by introducing a convenient graphical tool, the Nyquist plot, and show how it can be used to ascertain stability.

The Nyquist Plot

We saw in the last chapter that the dynamics of a linear system can be represented by its frequency response and graphically illustrated by the Bode plot. To study the stability of a system, we will make use of a different representation of the frequency response called a *Nyquist plot*. The Nyquist plot of the loop transfer function $L(s)$ is formed by tracing $s \in \mathbb{C}$ around the Nyquist "D contour", consisting of the imaginary axis combined with an arc at infinity connecting the endpoints of the imaginary axis. The contour, denoted as $\Gamma \in \mathbb{C}$, is illustrated in Figure 9.3a. The image of $L(s)$ when s traverses Γ gives a closed curve in the complex plane and is referred to as the Nyquist plot for $L(s)$, as shown in Figure 9.3b. Note that if the transfer function $L(s)$ goes to zero as s gets large (the usual case), then the portion of the contour "at infinity" maps to the origin. Furthermore, the portion of the plot corresponding to $\omega < 0$ is the mirror image of the portion with $\omega > 0$.

There is a subtlety with the Nyquist plot when the loop transfer function has poles on the imaginary axis because the gain is infinite at the poles. To solve this problem, we modify the contour Γ to include small deviations that avoid any poles on the imaginary axis, as illustrated in Figure 9.3a (assuming a pole of $L(s)$ at the origin). The deviation consists of a small semicircle to the right of the imaginary axis pole location.

The condition for oscillation given in equation (9.1) implies that the Nyquist plot of the loop transfer function goes through the point $L = -1$, which is called the *critical point*. Let ω_c represent a frequency at which $\angle L(i\omega_c) = 180^\circ$, corresponding to the Nyquist curve crossing the negative real axis. Intuitively it seems reasonable that the system is stable if $|L(i\omega_c)| < 1$, which means that the critical point -1 is on the left hand side of the Nyquist curve, as indicated in Figure 9.3b. This means that the signal at point B will have smaller amplitude than the injected signal. This is essentially true, but there are several subtleties that require a proper mathematical analysis to clear up. We defer the details for now and state the Nyquist condition for the special case where $L(s)$ is a stable transfer function.

Theorem 9.1 (Simplified Nyquist criterion). *Let $L(s)$ be the loop transfer function for a negative feedback system (as shown in Figure 9.1a) and assume that L has no poles in the closed right half plane ($\text{Re } s \geq 0$), except for single poles on the imaginary axis. Then the closed loop system is stable if and only if the closed contour given by $\Omega = \{L(i\omega) : -\infty < \omega < \infty\} \subset \mathbb{C}$ has no net encirclements of $s = -1$.*

The following conceptual procedure can be used to determine that there are no encirclements: Fix a pin at the critical point $s = -1$, orthogonal to the plane. Attach a string with one end at the critical point and the other on the Nyquist plot. Let the end of the string attached to the Nyquist curve traverse the whole curve. There are no encirclements if the string does not wind up on the pin when the curve is encircled. The number of encirclements is called the winding number. (In the theory of complex functions it is the customary to encircle the Nyquist contour in the counter-clockwise direction, which means that the imaginary axis is traversed in the direction from ∞ to $-\infty$.)

Example 9.2 Third order system

Consider a third order transfer function

$$L(s) = \frac{1}{(s+a)^3}.$$

To compute the Nyquist plot we start by evaluating points on the imaginary axis $s = i\omega$, which yields

$$L(i\omega) = \frac{1}{(i\omega + a)^3} = \frac{(a - i\omega)^3}{(a^2 + \omega^2)^3} = \frac{a^3 - 3a\omega^2}{(a^2 + \omega^2)^3} + i \frac{\omega^3 - 3a^2\omega}{(a^2 + \omega^2)^3}.$$

This is plotted in the complex plane in Figure 9.4, with the points corresponding to $\omega > 0$ drawn as solid line and $\omega < 0$ as a dashed line. Notice that these curves

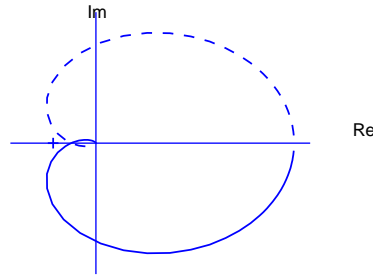


Figure 9.4: Nyquist plot for a third order transfer function. The Nyquist plot consists of a trace of the loop transfer function $L(s) = 1/(s+a)^3$. The solid line represents the portion of the transfer function along the positive imaginary axis and the dashed line the negative imaginary axis. The outer arc of the D contour maps to the origin.

are mirror images of each other.

To complete the Nyquist plot, we compute $L(s)$ for s on the outer arc of the Nyquist D contour. This arc has the form $s = Re^{i\theta}$ for $R \rightarrow \infty$. This gives

$$L(Re^{i\theta}) = \frac{1}{(Re^{i\theta} + a)^3} \rightarrow 0 \quad \text{as } R \rightarrow \infty.$$

Thus the outer arc of the D contour maps to the origin on the Nyquist plot. ∇

An alternative to computing the Nyquist plot explicitly is to determine the plot from the frequency response (Bode plot), which gives the Nyquist curve for $s = i\omega$, $\omega > 0$. We start by plotting $G(i\omega)$ from $\omega = 0$ to $\omega = \infty$, which can be read off from the magnitude and phase of the transfer function. We then plot $G(Re^{i\theta})$ with $\theta \in [0, \pi/2]$ and $R \rightarrow \infty$, which almost always maps to zero. The remaining parts of the plot can be determined by taking the mirror image of the curve thus far (normally plotted using a dashed line style). The plot can then be labeled with arrows corresponding to a counter-clockwise traversal around the D contour (opposite the direction that the first portion of the curve was plotted).

Example 9.3 Third order system with a pole at the origin

Consider the transfer function

$$L(s) = \frac{k}{s(s+1)^2},$$

where the gain has the nominal value $k = 1$. The Bode plot is shown in Figure 9.5a. The system has a single pole at $s = 1$ and a double pole at $s = -1$. The gain curve of the Bode plot thus has the slope -1 for low frequencies and at the double pole $s = 1$ the slope changes to -3 . For small s we have $L \approx k/s$ which means that the low frequency asymptote intersects the unit gain line at $\omega = k$. The phase curve starts at -90° for low frequencies, it is -180° at the break point $\omega = 1$, and it is -270° at high frequencies.

Having obtained the Bode plot we can now sketch the Nyquist plot, shown in Figure 9.5b. It starts with a phase of -90° for low frequencies, intersects the

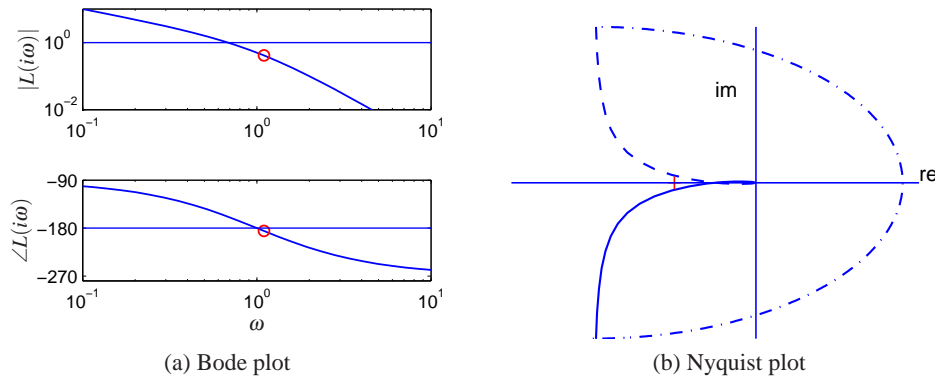


Figure 9.5: Sketching Nyquist and Bode plots. The loop transfer function is $L(s) = 1/(s(s+1)^2)$. The large semi circle is the map of the small semi circle of the Γ contour around the pole at the origin. The closed loop is stable because the Nyquist curve does not encircle the critical point. The point where the phase is -180° is marked with a circle.

negative real axis at the breakpoint $\omega = 1$ where $L(i) = 0.5$ and goes to zero along the imaginary axis for high frequencies. The small half circle of the Γ contour at the origin is mapped on a large circle enclosing the right half plane. The Nyquist curve does not encircle the critical point and it follows from the simplified Nyquist theorem that the closed loop is stable. Since $L(i) = -k/2$ we find the system becomes unstable if the gain is increased to $k = 2$ or beyond. ∇

The Nyquist criterion does not require that $|L(i\omega_c)| < 1$ for all ω_c corresponding to a crossing of the negative real axis. Rather, it says that the number of encirclements must be zero, allowing for the possibility that the Nyquist curve could cross the negative real axis and cross back at magnitudes greater than 1. The fact that it was possible to have high feedback gains surprised the early practitioners of feedback amplifiers, as mentioned in the quote in the beginning of this chapter.

One advantage of the Nyquist criterion is that it tells us how a system is influenced by changes of the controller parameters. For example, it is very easy to visualize what happens when the gain is changed since this just scales the Nyquist curve.

Example 9.4 Congestion control

Consider the Internet congestion control system described in Section 3.4. Suppose we have N identical sources and a disturbance d representing an external data source, as shown in Figure 9.6a. We also include a time delay between the router and the senders, representing the time delays between the sender and receiver.

To analyze the stability of the system, we use the transfer functions computed in Exercise 8.11:

$$G_{bw}(s) = \frac{Nw_e e^{-\tau^f s}}{\tau_e s + e^{-\tau^f s}}, \quad G_{wq}(s) = -\frac{N}{q_e(\tau_e s + q_e w_e)}, \quad G_{pb}(s) = \rho,$$

where (w_e, b_e) is the equilibrium point for the system, N is the number of sources,

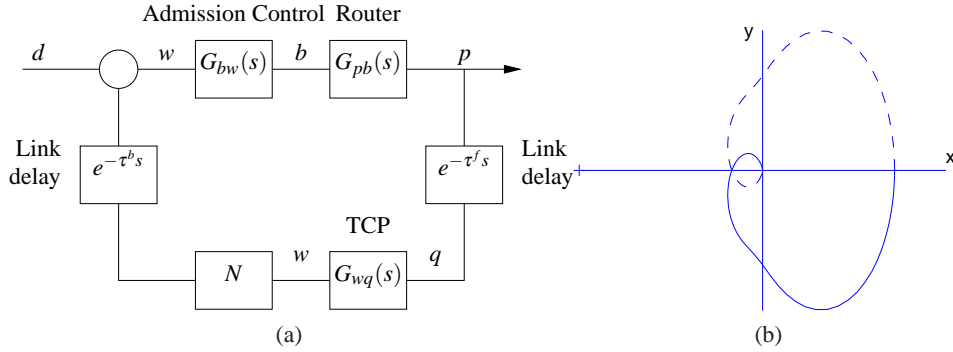


Figure 9.6: Internet congestion control. A set of N sources using TCP/Reno send messages through a single router with admission control. Link delays are included for the forward and backward directions. The Nyquist plot for the loop transfer function is shown to the right.

τ_e is the steady state round trip time and τ^f is the forward propagation time.

The loop transfer function is given by

$$L(s) = \rho \cdot \frac{N}{\tau_e s + e^{-\tau^f s}} \cdot \frac{1}{q_e(\tau_e s + q_e w_e)} e^{-\tau_e s}$$

Using the fact that $q_e \approx 2N/w_e^2 = 2N^3/(\tau_e c)^2$ and $w_e = b_e/N = \tau_e c/N$, we can show that

$$L(s) = \rho \cdot \frac{N}{\tau_e s + e^{-\tau^f s}} \cdot \frac{c^3 \tau_e^3}{2N^3(c\tau_e^2 s + 2N^2)} e^{-\tau_e s}$$

Note that we have chosen the sign of $L(s)$ to use the same sign convention as Figure 9.1b. The exponential term representing the time delay gives significant phase above $\omega = 1/\tau$ and the gain at the crossover frequency will determine stability.

To check stability, we require that the gain be sufficiently small at crossover. If we assume that the pole due to the queue dynamics is sufficiently fast that the TCP dynamics are dominant, the gain at the crossover frequency ω_c is given by

$$|L(i\omega_c)| = \rho \cdot N \cdot \frac{c^3 \tau_e^3}{2N^3 c \tau_e^2 \omega_c} = \frac{\rho c^2 \tau_e}{2N \omega_c}$$

Using the Nyquist criterion, the closed loop system will be unstable if this quantity is greater than 1. In particular, for a fixed time delay, the system will become unstable as the link capacity c is increased. This indicates that the TCP protocol may not be scalable to high capacity networks, as pointed out by Low *et al.* [129]. Exercise 9.7 provides some ideas of how this might be overcome. ∇

Conditional Stability

Normally, we find that unstable systems can be stabilized simply by reducing the loop gain. There are however situations where a system can be stabilized by increasing the gain. This was first encountered by electrical engineers in the design

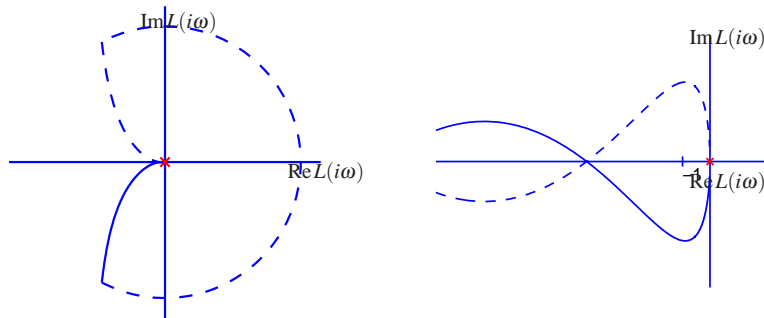


Figure 9.7: Nyquist curve for the loop transfer function $L(s) = \frac{3(s+1)^2}{s(s+6)^2}$. The plot on the right is an enlargement of the area around the origin of the plot on the left. The Nyquist curve intersects the negative real axis twice but has no net encirclements of -1 .

of feedback amplifiers, who coined the term *conditional stability*. The problem was actually a strong motivation for Nyquist to develop his theory. We will illustrate by an example.

Example 9.5 Conditional stability

Consider a feedback system with the loop transfer function

$$L(s) = \frac{3(s+1)^2}{s(s+6)^2}. \quad (9.4)$$

The Nyquist plot of the loop transfer function is shown in Figure 9.7. Notice that the Nyquist curve intersects the negative real axis twice. The first intersection occurs at $L = -12$ for $\omega = 2$ and the second at $L = -4.5$ for $\omega = 3$. The intuitive argument based on signal tracing around the loop in Figure 9.1b is strongly misleading in this case. Injection of a sinusoid with frequency 2 rad/s and amplitude 1 at A gives, in steady state, an oscillation at B that is in phase with the input and has amplitude 12. Intuitively it seems unlikely that closing of the loop will result in a stable system. However, it follows from Nyquist's stability criterion that the system is stable because there are no net encirclements of the critical point. ∇

General Nyquist Criterion

Theorem 9.1 requires that $L(s)$ has no poles in the closed right half plane. In some situations this is not the case and a more general result is required. Nyquist originally considered this general case, which we summarize in the following theorem.

Theorem 9.2 (Nyquist's stability theorem). *Consider a closed loop system with the loop transfer function $L(s)$, that has P poles in the region enclosed by the Nyquist contour. Let w_n be the net number of counter-clockwise encirclements of -1 by $L(s)$ when s encircles the Nyquist contour Γ in the counter-clockwise direction. The closed loop system then has $w_n + P$ poles in the right half plane.*

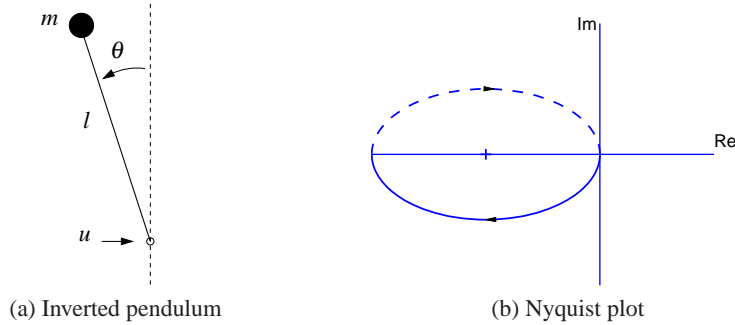


Figure 9.8: PD control of an inverted pendulum. A proportional-derivative controller with transfer function $C(s) = k(s+2)$ is used to command u based on θ . A Nyquist plot of the loop transfer function for gain $k = 2$ is shown in on the right. There is one clockwise encirclement of the critical point, giving a winding number $w_n = -1$.

The full Nyquist criterion states that if $L(s)$ has P poles in the right half plane, then the Nyquist curve for $L(s)$ should have P clockwise encirclements of -1 (so that $w_n = -P$). In particular, this *requires* that $|L(i\omega_c)| > 1$ for some ω_c corresponding to a crossing of the negative real axis. Care has to be taken to get the right sign of the winding number. The Nyquist contour has to be traversed counter-clockwise, which means that ω moves from ∞ to $-\infty$ and w_n is positive if the Nyquist curve winds counter-clockwise.

As in the case of the simplified Nyquist criterion, we use small semicircles of radius r to avoid any poles on the imaginary axis. By letting $r \rightarrow 0$, we can use Theorem 9.2 to reason about stability. Note that the image of the small semicircles generates a section of the Nyquist curve whose magnitude approaches infinity, requiring care in computing the winding number. When plotting Nyquist curves on the computer, one must be careful to see that such poles are properly handled and often one must sketch those portions of the Nyquist plot by hand, being careful to loop the right way around the poles.

Example 9.6 Stabilization of an inverted pendulum

The linearized dynamics of a normalized inverted pendulum can be represented by the transfer function $P(s) = 1/(s^2 - 1)$, where the input is acceleration of the pivot and the output is the pendulum angle θ , as shown in Figure 9.8 (Exercise 8.4). We attempt to stabilize the pendulum with a proportional-derivative (PD) controller having the transfer function $C(s) = k(s+2)$. The loop transfer function is

$$L(s) = \frac{k(s+2)}{s^2 - 1}.$$

The Nyquist plot of the loop transfer function is shown in Figure 9.8b. We have $L(0) = -k$ and $L(\infty) = 0$, the Nyquist curve is actually an ellipse. If $k > 1$ the Nyquist curve encircles the critical point $s = -1$ in the clockwise direction when the Nyquist contour γ is encircled in the counter-clockwise direction. The winding number is thus $w_n = -1$. Since the loop transfer function has one pole in the right

half plane ($P = 1$) we find that $N = P + w_n = 0$ and the system is thus stable for $k > 1$. If $k < 1$ there is no encirclement and the closed loop will have one pole in the right half plane. ∇

Derivation of Nyquist's Stability Theorem



We will now prove the Nyquist stability theorem for a general loop transfer function $L(s)$. This requires some results from the theory of complex variables, for which the reader can consult [6]. Since some precision is needed in stating Nyquist's criterion properly, we will also use a more mathematical style of presentation. The key result is the following theorem about functions of complex variables.

Theorem 9.3 (Principle of variation of the argument). *Let D be a closed region in the complex plane and let Γ be the boundary of the region. Assume the function $f : \mathbb{C} \rightarrow \mathbb{C}$ is analytic in D and on Γ , except at a finite number of poles and zeros. Then the winding number, w_n , is given by*

$$w_n = \frac{1}{2\pi} \Delta_{\Gamma} \arg f(z) = \frac{1}{2\pi i} \int_{\Gamma} \frac{f'(z)}{f(z)} dz = N - P,$$

where Δ_{Γ} is the net variation in the angle along the contour Γ , N is the number of zeros and P the number of poles in D . Poles and zeros of multiplicity m are counted m times.

Proof. Assume that $z = a$ is a zero of multiplicity m . In the neighborhood of $z = a$ we have

$$f(z) = (z - a)^m g(z),$$

where the function g is analytic and different from zero. The ratio of the derivative of f to itself is then given by

$$\frac{f'(z)}{f(z)} = \frac{m}{z - a} + \frac{g'(z)}{g(z)}$$

and the second term is analytic at $z = a$. The function f'/f thus has a single pole at $z = a$ with the residue m . The sum of the residues at the zeros of the function is N . Similarly we find that the sum of the residues of the poles of is $-P$ and hence

$$N - P = \int_{\Gamma} \frac{f'(z)}{f(z)} dz = \int_{\Gamma} \frac{d}{dz} \log f(z) dz = \Delta_{\Gamma} \log f(z),$$

where Δ_{Γ} again denotes the variation along the contour Γ . We have

$$\log f(z) = \log |f(z)| + i \arg f(z)$$

and since the variation of $|f(z)|$ around a closed contour is zero it follows that

$$\Delta_{\Gamma} \log f(z) = i \Delta_{\Gamma} \arg f(z)$$

and the theorem is proved. \square

This theorem is useful for determining the number of poles and zeros of a function of complex variables in a given region. By choosing an appropriate closed region D with boundary Γ , we can determine the difference between the number of poles and zeros through computation of the winding number.

Theorem 9.3 can be used to prove Nyquist's stability theorem by choosing Γ as the Nyquist contour shown in Figure 9.3a, which encloses the right half plane. To construct the contour, we start with part of the imaginary axis $-jR \leq s \leq jR$, and a semicircle to the right with radius R . If the function f has poles on the imaginary axis we introduce small semicircles with radii r to the right of the poles as shown in the figure. The Nyquist contour is obtained by letting $R \rightarrow \infty$ and $r \rightarrow 0$.

To see how we use this to compute stability, consider a closed loop system with the loop transfer function $L(s)$. The closed loop poles of the system are the zeros of the function $f(s) = 1 + L(s)$. To find the number of zeros in the right half plane, we investigate the winding number of the function $f(s) = 1 + L(s)$ as s moves along the Nyquist contour Γ in the counter-clockwise direction. The winding number can conveniently be determined from the Nyquist plot. A direct application of the Theorem 9.3 gives the Nyquist criterion. Since the image of $1 + L(s)$ is a shifted version of $L(s)$, we usually state the Nyquist criterion as net encirclements of the -1 point by the image of $L(s)$.

9.3 STABILITY MARGINS

In practice it is not enough that a system is stable. There must also be some margins of stability that describe how stable the system is and its robustness to perturbations. There are many ways to express this, but one of the most common is the use of gain and phase margins, inspired by Nyquist's stability criterion. The key idea is that it is easy to plot the loop transfer function $L(s)$. An increase of controller gain simply expands the Nyquist plot radially. An increase of the phase of the controller twists the Nyquist plot clockwise. Hence from the Nyquist plot we can easily pick off the amount of gain or phase that can be added without causing the system to go unstable.

Let ω_{pc} be the *phase crossover frequency*, the smallest frequency where the phase of the loop transfer function $L(s)$ is -180° . The *gain margin* is defined as

$$g_m = \frac{1}{|L(i\omega_{pc})|}. \quad (9.5)$$

It tells us how much the controller gain can be increased before reaching the stability limit.

Similarly, let ω_{gc} be the *gain crossover frequency*, the lowest frequency where the loop transfer function $L(s)$ has unit magnitude. The *phase margin* is

$$\phi_m = \pi + \arg L(i\omega_{gc}), \quad (9.6)$$

the amount of phase lag required to reach the stability limit. These margins have simple geometric interpretations in the Nyquist diagram of the loop transfer func-

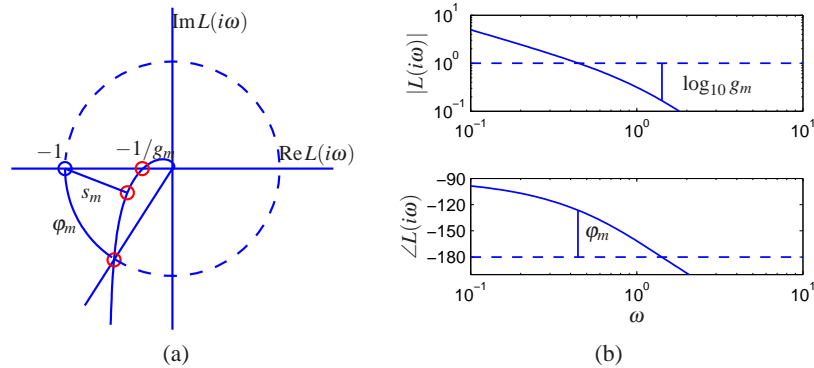


Figure 9.9: Stability margins. The gain margin g_m and phase margins ϕ_m are shown on the Nyquist plot (left) and the Bode plot (right). The Nyquist plot also shows the stability margin s_m , which is the shortest distance to the critical point.

tion, as shown in Figure 9.9a.

A drawback with gain and phase margins is that it is necessary to give both of them in order to guarantee that the Nyquist curve is not close to the critical point. An alternative way to express margins is by a single number, the *stability margin*, s_m , which is the shortest distance from the Nyquist curve to the critical point. This number is related to disturbance attenuation as will be discussed in Section 11.3.

Gain and phase margins can be determined from the Bode plot of the loop transfer function. To find the gain margin we first find the phase crossover frequency ω_{pc} where the phase is -180° . The gain margin is the inverse of the gain at that frequency. To determine the phase margin we first determine the gain crossover frequency ω_{gc} , i.e. the frequency where the gain of the loop transfer function is 1. The phase margin is the phase of the loop transfer function at that frequency plus 180° . Figure 9.9b illustrates how the margins are found in the Bode plot of the loop transfer function. The margins can be computed analytically for simple systems of low order but it is straightforward to compute them numerically.

Example 9.7 Third order transfer function

Consider a loop transfer function $L(s) = 3/(s+1)^3$. The Nyquist and Bode plots are shown in Figure 9.10. To compute the gain, phase and stability margins, we can use the Nyquist plot as described in Figure 9.9a. This yields the following values:

$$g_m = 2.67, \quad \phi_m = 41.7^\circ, \quad s_m = 0.464.$$

The gain and phase margin can also be determined from the Bode plot shown in Figure 9.9b. ▽

The gain and phase margins are classical robustness measures that have been used for a long time in control system design. The gain margin is well defined if the Nyquist curve intersects the negative real axis once. Analogously the phase margin is well defined if the Nyquist curve intersects the unit circle only at one point. Other more general robustness measures will be introduced in Chapter 12.

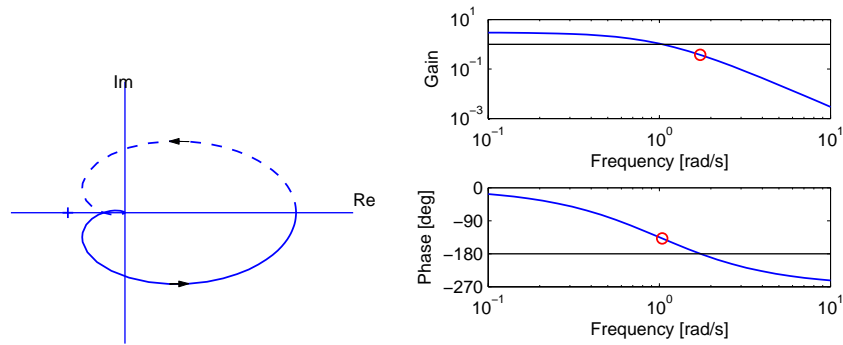


Figure 9.10: Stability margins for a third order transfer function. The Nyquist plot on the left allows the gain, phase and stability margins to be determined by measuring the distances of relevant features. The gain and phase margins can also be read off of the Bode plot on the right.

Even if both gain and phase margins are reasonable the system may still not be robust as is illustrated by the following example.

Example 9.8 Good gain and phase margins but poor stability margins

Consider a system with the loop transfer function

$$L(s) = \frac{0.38(s^2 + 0.1s + 0.55)}{s(s + 1)(s^2 + 0.06s + 0.5)}.$$

A numerical calculation gives the gain margin is $g_m = 266$, the phase margin is 70° . These values indicate that the system is robust but the Nyquist curve is still close to the critical point, as shown in Figure 9.11. The stability margin is $s_m = 0.27$, which is very low. The closed loop system has two resonant modes, one with relative damping $\zeta = 0.81$ and the other with $\zeta = 0.014$. The step response of the system is highly oscillatory, as shown in Figure 9.11c. ∇

The stability margin cannot easily be found from the Bode plot of the loop transfer function. There are however other Bode plots that will give s_m ; these will be discussed in Chapter 12. In general, it is best to use the Nyquist plot to check stability, since this provides more complete information than the Bode plot.

When we are designing feedback systems, it will often be useful to define the robustness of the system using gain, phase and stability margins. These numbers tell us how much the system can vary from our nominal model and still be stable. Reasonable values of the margins are phase margin $\phi_m = 30^\circ - 60^\circ$, gain margin $g_m = 2 - 5$, and stability margin $s_m = 0.5 - 0.8$.

There are also other stability measures, such as the *delay margin*, which is the smallest time delay required to make the system unstable. For loop transfer functions that decay quickly, the delay margin is closely related to the phase margin, but for systems where the amplitude ratio of the loop transfer function has several peaks at high frequencies, the delay margin is a more relevant measure.

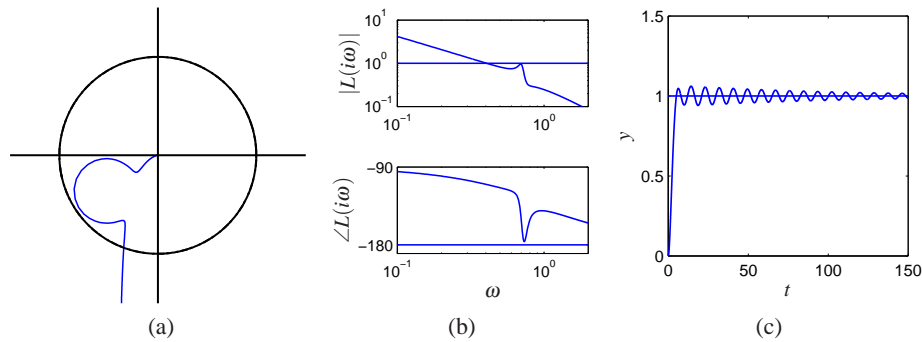


Figure 9.11: System with good gain and phase margin, but poor stability margin. Nyquist (a) and Bode (b) plots of the loop transfer function and step response (c) for a system with good gain and phase margins but with poor stability margin.

Example 9.9 AFM nanopositioning system

Consider the system for horizontal positioning of the sample in an atomic force microscope. The system has oscillatory dynamics and a simple model is a spring-mass system with low damping. The normalized transfer function is given by

$$P(s) = \frac{a^2}{s^2 + 2\zeta as + a^2} \quad (9.7)$$

where the relative damping typically is a very small number, e.g. $\zeta = 0.1$.

We will start with a controller that only has integral action. The resulting loop transfer function is

$$L(s) = \frac{k_i a^2}{s(s^2 + 2\zeta as + a^2)},$$

where k_i is the gain of the controller. Nyquist and Bode plots of the loop transfer function are shown in Figure 9.12. Notice that the part of the Nyquist curve that is close to the critical point -1 is approximately circular.

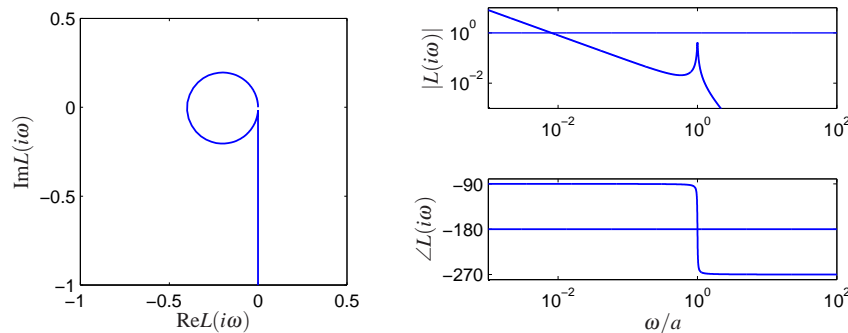


Figure 9.12: Nyquist and Bode plots of the loop transfer function for the AFM system (9.7) with an integral controller. The frequency in the Bode plot is normalized by a . The parameters are $\zeta = 0.01$ and $k_i = 0.008$.

From the Bode plot in Figure 9.12b, we see that the phase crossover frequency is $\omega_{pc} = a$, which will be independent of the gain k_i . Evaluating the loop transfer function at this frequency, we have $L(ia) = -k_i/(2\zeta a)$, which means that the gain margin is $g_m = 1 - k_i/(2\zeta a)$. To have a desired gain margin of g_m the integral gain should be chosen as

$$k_i = 2a\zeta(1 - g_m).$$

Figure 9.12 shows Nyquist and Bode plots for the system with gain margin $g_m = 0.60$ and stability margin $s_m = 0.597$. The gain curve in the Bode plot is almost a straight line for low frequencies and a resonance peak at $\omega = a$. The gain crossover frequency is approximately equal to k_i . The phase decreases monotonically from -90° to -270° : it is equal to -180° at $\omega = a$. The curve can be shifted vertically by changing k_i : increasing k_i shifts the gain curve upwards and increases the gain crossover frequency. Since the phase is -180° at the resonance peak, it is necessary that the peak does not touch the line $|L(i\omega)| = 1$. ∇

9.4 BODE'S RELATIONS AND MINIMUM PHASE SYSTEMS

An analysis of Bode plots reveals that there appears to be a relation between the gain curve and the phase curve. Consider for example the Bode plots for the differentiator and the integrator (shown in Figure 8.12 on page 252). For the differentiator the slope is $+1$ and the phase is constant $\pi/2$ radians. For the integrator the slope is -1 and the phase is $-\pi/2$. For the first order system $G(s) = s + a$, the amplitude curve has the slope 0 for small frequencies and the slope $+1$ for high frequencies and the phase is 0 for low frequencies and $\pi/2$ for high frequencies.

Bode investigated the relations between the curves for systems with no poles and zeros in the right half plane. He found that the phase was uniquely given by the shape of the gain curve and vice versa:

$$\arg G(i\omega_0) = \frac{\pi}{2} \int_0^\infty f(\omega) \frac{d \log |G(i\omega)|}{d \log \omega} d \log \omega \approx \frac{\pi}{2} \frac{d \log |G(i\omega)|}{d \log \omega}, \quad (9.8)$$

where f is the weighting kernel

$$f(\omega) = \frac{2}{\pi^2} \log \left| \frac{\omega + \omega_0}{\omega - \omega_0} \right|.$$

The phase curve is thus a weighted average of the derivative of the gain curve. If the gain curve has constant slope n the phase curve has the constant value $n\pi/2$.

Bode's relations (9.8) hold for systems that do not have poles and zeros in the right half plane. Such systems are called *minimum phase systems* because systems with poles and zeros in the right half plane have larger phase lag. The distinction is important in practice because minimum phase systems are easier to control than systems with larger phase lag. We will now give a few examples of non-minimum phase transfer functions.

The transfer function of a time delay of T_d units is $G(s) = e^{-sT_d}$. This transfer function has unit gain, $|G(i\omega)| = 1$, and the phase is $\arg G(i\omega) = -\omega T_d$. The corre-

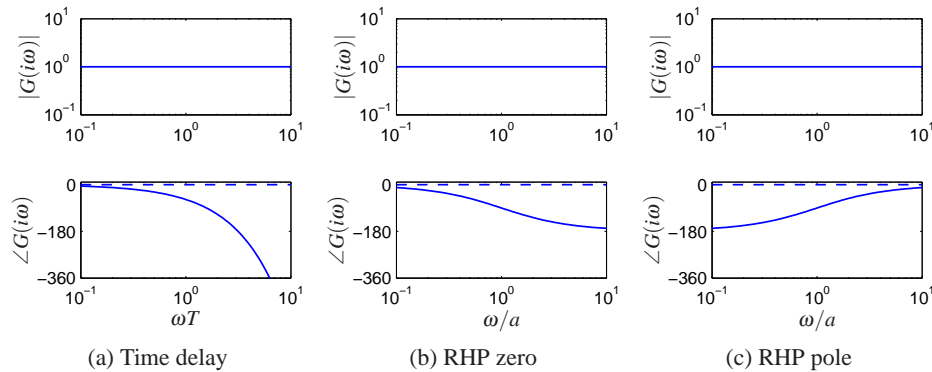


Figure 9.13: Bode plots of systems that are not minimum phase. (a) Time delay $G(s) = e^{-sT}$, (b) system with a right half plane zero $G(s) = (a - s)/(a + s)$ and (c) system with right half plane pole. The corresponding minimum phase systems has the transfer function $G(s) = 1$ in all cases, the phase curves for that system are shown dashed.

spending minimum phase system with unit gain has the transfer function $G(s) = 1$. The time delay thus has an additional phase lag of ωT_d . Notice that the phase lag increases linearly with frequency. Figure 9.13a shows the Bode plot of the transfer function. (Because we use a log scale for frequency, the phase falls off much faster than linearly in the plot.)

Consider a system with the transfer function $G(s) = (a - s)/(a + s)$ with $a > 0$, which has a zero $s = a$ in the right half plane. The transfer function has unit gain, $|G(i\omega)| = 1$, and the phase is $\arg G(i\omega) = -2 \arctan(\omega/a)$. The corresponding minimum phase system with unit gain has the transfer function $G(s) = 1$. Figure 9.13b shows the Bode plot of the transfer function.

A similar analysis of the transfer function $G(s) = (s + a)/s - a$ with $a > 0$, which has a pole in the right half plane, shows that its phase is $\arg G(i\omega) = -2 \arctan(a/\omega)$. The Bode plot is shown in Figure 9.13c

The presence of poles and zeros in the right half plane imposes severe limitations on the achievable performance. Dynamics of this type should be avoided by redesign of the system whenever possible. While the poles are intrinsic properties of the system and they do not depend on sensors and actuators, the zeros depend on how inputs and outputs of a system are coupled to the states. Zeros can thus be changed by moving sensors and actuators or by introducing new sensors and actuators. Non-minimum phase systems are unfortunately quite common in practice.

The following example gives a system theoretic interpretation of the common experience that it is more difficult to drive in reverse gear and illustrates some of the properties of transfer functions in terms of their poles and zeros.

Example 9.10 Vehicle steering

The non-normalized transfer function from steering angle to lateral velocity for the

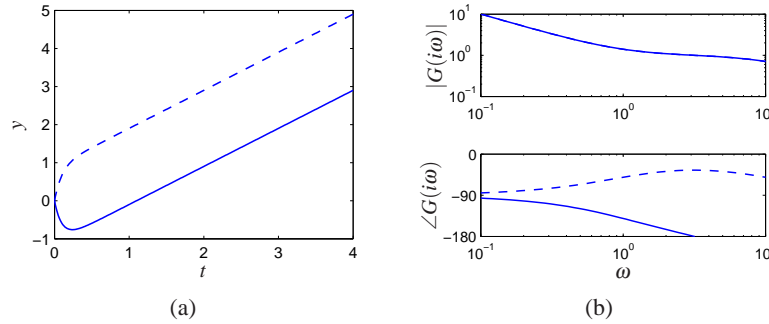


Figure 9.14: Step responses from steering angle to lateral translation for simple kinematics model when driving forward (dashed) and reverse (full). Notice that the with rear wheel steering the center of mass first moves in the wrong direction and that the overall response with rear wheel steering is significantly delayed compared with front wheel steering. The response in rear steering lags the response in forward steering with 4s.

simple vehicle model is

$$G(s) = \frac{av_0s + v_0^2}{bs}.$$

The transfer function has a zero at $s = v_0/a$. In normal driving this zero is in the left half plane but it is in the right half plane when driving in reverse, $v_0 < 0$. The unit step response is

$$y(t) = \frac{av_0}{b} + \frac{av_0^2t}{b}$$

The lateral velocity thus responds immediately to a steering command. For reverse steering γ is negative and the initial response is in the wrong direction, a behavior that is representative for non-minimum phase systems. Figure 9.14 shows the step response for forward and reverse driving. In this simulation we have added an extra pole with the time constant T to approximately account for the dynamics in the steering system. The parameters are $a = b = 1$, $T = 0.1$, $v_0 = 1$ for forward driving and $v_0 = -1$ for reverse driving. Notice that for $t > t_0 = a/v_0$, where t_0 is the time required to drive the distance a the step response for reverse driving is that of forward driving with the time delay t_0 . Notice that the position of the zero v_0/a depends on the location of the sensor. In our calculation we have assumed that the sensor is at the center of mass. The zero in the transfer function disappears if the sensor is located at the rear wheel. The difficulty with zeros in the right half plane can thus be visualized by a thought experiment where we drive a car in forward and reverse and observe the lateral position through a hole in the floor of the car.

▽



9.5 THE NOTIONS OF GAIN AND PHASE

A key idea in frequency domain analysis is to trace the behavior of sinusoidal signals through a system. The concepts of gain and phase represented by the transfer function are strongly intuitive because they describe amplitude and phase relations between input and output. In this section we will see how to extend the concepts of gain and phase to more general systems, including some nonlinear systems. We will also show that there are analogs of Nyquist's stability criterion if signals are approximately sinusoidal.

System Gain

We begin by considering the case of a static linear system $y = Au$, where A is a matrix whose elements are complex numbers. The matrix does not have to be square. Let the inputs and outputs be vectors whose elements are complex numbers and use the Euclidean norm

$$\|u\| = \sqrt{\sum |u_i|^2}. \quad (9.9)$$

The norm of the output is

$$\|y\|^2 = u^* A^* A u,$$

where $*$ denotes the complex conjugate transpose. The matrix $A^* A$ is symmetric and positive semidefinite and the right hand side is a quadratic form. The eigenvalues of the matrix $A^* A$ are all real and we have

$$\|y\|^2 \leq \lambda_{\max}(A^* A) \|u\|^2.$$

The gain of the system can then be defined as the maximum ratio of the output to the input over all possible inputs:

$$\gamma = \max_u \frac{\|y\|}{\|u\|} = \sqrt{\lambda_{\max}(A^* A)}. \quad (9.10)$$

The eigenvalues of the matrix $A^* A$ are called the *singular values* of the matrix A and the largest singular value is denoted $\bar{\sigma}(A)$.

To generalize this to the case of an input/output dynamical system, we need to think of the inputs and outputs not as vectors of real numbers, but as vectors of *signals*. For simplicity, consider first the case of scalar signals and let the signal space L_2 be square integrable functions with the norm

$$\|u\|_2 = \sqrt{\int_0^\infty |u|^2(\tau) d\tau}.$$

This definition can be generalized to vector signals by replacing the absolute value with the vector norm (9.9). We can now formally define the gain of a system taking inputs $u \in L_2$ and producing outputs $y \in L_2$ as

$$\gamma = \sup_{u \in L_2} \frac{\|y\|}{\|u\|}, \quad (9.11)$$

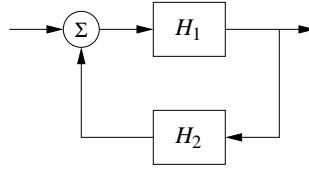


Figure 9.15: A feedback connection of two general nonlinear systems H_1 and H_2 . The stability of the system can be explored using the small gain theorem.

where \sup is the *supremum*, defined as the smallest number that is larger than its argument. The reason for using supremum is that the maximum may not be defined for $u \in L_2$. This definition of the system gain is quite general and can even be used for some classes of nonlinear systems, though one needs to be careful about how initial conditions and global nonlinearities are handled.

It turns out that the norm (9.11) has some very nice properties in the case of linear systems. In particular, given a stable linear system with transfer function $G(s)$ it can be shown that the norm of the system is given by

$$\gamma = \sup_{\omega} |G(i\omega)| =: \|G\|_{\infty}. \quad (9.12)$$

In other words, the gain of the system corresponds to the peak value of the frequency response. This corresponds to our intuition that an input produces the largest output when we are at the resonant frequencies of the system. $\|G\|_{\infty}$ is called the *infinity norm* of the transfer function $G(s)$.

This notion of gain can be generalized to the multi-input, multi-output case as well. For a linear multivariable system with a real rational transfer function matrix $G(s)$ we can define the gain as

$$\gamma = \|G\|_{\infty} = \sup_{\omega} \bar{\sigma}(G(i\omega)). \quad (9.13)$$

Thus we see that combine the ideas of the gain of a matrix with the gain of a linear system by looking at the maximum singular value over all frequencies.

Small Gain and Passivity

For linear systems it follows from Nyquist's theorem that the closed loop is stable if the gain of the loop transfer function is less than one for all frequencies. This result can be extended to a larger class of systems by using the concept of the system gain defined in equation (9.11).

Theorem 9.4 (Small gain theorem). *Consider the closed loop system in Figure 9.15 where H_1 and H_2 are stable systems and the signal spaces are properly defined. Let the gains of the systems H_1 and H_2 be γ_1 and γ_2 . Then the closed loop system is input/output stable if $\gamma_1\gamma_2 < 1$, and the gain of the closed loop system is*

$$\gamma = \frac{\gamma_1}{1 - \gamma_1\gamma_2}.$$

Notice that if systems H_1 and H_2 are linear it follows from the Nyquist stability theorem that the closed loop is stable, because if $\gamma_1 \gamma_2 < 1$ the Nyquist curve is always inside the unit circle. The small gain theorem is thus an extension of the Nyquist stability theorem.

Note that although we have focused on linear systems, the small gain theorem actually holds nonlinear input/output systems as well. The definition of gain in equation (9.11) holds for nonlinear systems as well, with some care needed in handling the initial condition.

The main limitation of the small gain theorem is that it does not consider the phasing of signals around the loop, so it can be very conservative. To define the notion of phase we require that there is a scalar product. For square integrable functions this can be defined as

$$\langle u, y \rangle = \int_0^{\infty} u(\tau)y(\tau) d\tau$$

The phase φ between two signals can now be defined as

$$\langle x, y \rangle = \|u\| \|y\| \cos(\varphi)$$

Systems where the phase between inputs and outputs is 90° or less for all inputs are called *passive systems*. It follows from the Nyquist stability theorem that a closed loop linear system is stable if the phase of the loop transfer function is between $-\pi$ and π . This result can be extended to nonlinear systems as well. It is called the *passivity theorem* and is closely related to the small gain theorem.

Additional applications of the small gain theorem and its application to robust stability are given in Chapter 12.

Describing Functions



For special nonlinear systems like the one shown in Figure 9.16a, which consists of a feedback connection of a linear system and a static nonlinearity, it is possible to obtain a generalization of Nyquist's stability criterion based on the idea of *describing functions*. Following the approach of the Nyquist stability condition, we will investigate the conditions for maintaining an oscillation in the system. If the linear subsystem has low-pass character, its output is approximately sinusoidal even if its input is highly irregular. The condition for oscillation can then be found by exploring the propagation of a sinusoid that corresponds to the first harmonic.

To carry out this analysis, we have to analyze how a sinusoidal signal propagates through a static nonlinear system. In particular we investigate how the first harmonic of the output of the nonlinearity is related to its (sinusoidal) input. Letting F represent the nonlinear function, we expand $F(e^{-i\omega t})$ in terms of its harmonics:

$$F(ae^{-i\omega t}) = \sum_{n=0}^{\infty} M_n(a) e^{in\omega t - \varphi_n(a)},$$

where $M_n(a)$ and $\varphi_n(a)$ represent the gain and phase of n th harmonic, which depend on the input amplitude since the function F is nonlinear. We define the

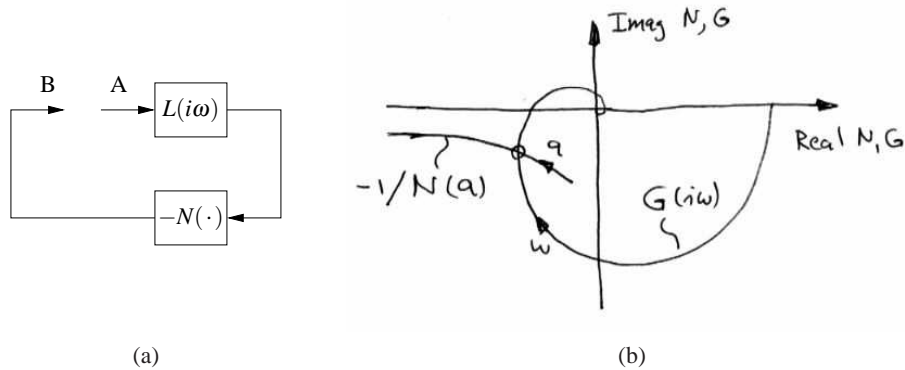


Figure 9.16: Illustration of describing function analysis. A feedback connection of a static nonlinearity and a linear system is shown in (a). The linear system is characterized by its transfer function $L(i\omega)$, which depends on frequency, and the nonlinearity by its describing function $N(a)$ which depends on the amplitude a of its input. (b) shows the Nyquist plot of $G(i\omega)$ and the a plot of the $-1/N(a)$. The intersection of the curves represent a possible limit cycle.

describing function to be the complex gain of the first harmonic:

$$N(a) = M_1(a)e^{i\phi_n(a)}. \quad (9.14)$$

The function can also be computed by assuming that the input is a sinusoid and using the first term in the Fourier series of the resulting output.

Arguing as we did when deriving Nyquist's stability criterion we find that an oscillation can be maintained if

$$L(i\omega)N(a) = -1. \quad (9.15)$$

This equation means that if we inject a sinusoid at A in Figure 9.16 the same signal will appear at B and an oscillation can be maintained by connecting the points. Equation (9.15) gives two conditions for finding the frequency ω of the oscillation and its amplitude a : the phase must be 180° and the magnitude must be unity. A convenient way to solve the equation is to plot $L(i\omega)$ and $-1/N(a)$ on the same diagram as shown in Figure 9.16c. The diagram is similar to the Nyquist plot where the critical point -1 is replaced by the curve $-1/N(a)$ and a ranges from 0 to ∞ .

It is possible to define describing functions for other types of inputs than sinusoids. Describing function analysis is a simple method but it is approximate because it assumes that higher harmonics can be neglected. Excellent treatments of describing function techniques can be found in the texts by Graham and McRuer [85] and Atherton [20].

Example 9.11 Relay with hysteresis

Consider a linear system with a nonlinearity consisting of a relay with hysteresis. The output has amplitude b and the relay switches when the input is $\pm c$, as shown in Figure 9.17a. Assuming that the input is $u = a \sin(\omega t)$ we find that the output is

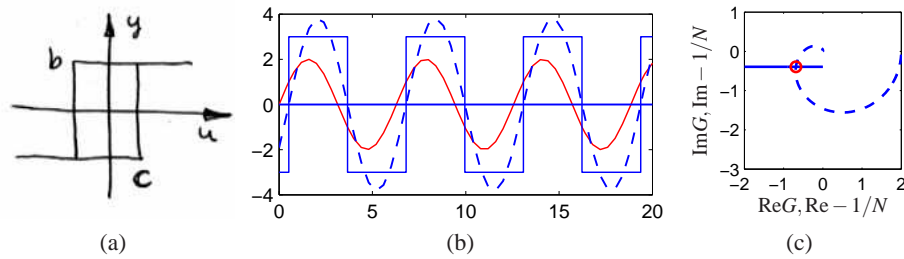


Figure 9.17: Describing function analysis for relay with hysteresis. The input-output relation of the hysteresis is shown in Figure 9.17a and Figure 9.17b shows the input, the output and its first harmonic. Figure 9.17c shows the Nyquist plots of the transfer function $G(s) = (s+1)^{-4}$ and the negative of the inverse describing function for the relay with $b = 1$ and $c = 1$.

zero if $a \leq c$ and if $a > c$ the output is a square wave with amplitude b that switches at times $\omega t = \arcsin(c/a) + n\pi$. The first harmonic is then $y(t) = (4b/\pi) \sin(\omega t - \alpha)$, where $\sin \alpha = c/a$. For $a > c$ the describing function and its inverse are

$$N(a) = \frac{4b}{a\pi} \left(\sqrt{1 - \frac{c^2}{a^2}} - i \frac{c}{a} \right), \quad \frac{1}{N(a)} = \frac{\pi \sqrt{a^2 - c^2}}{4b} + i \frac{\pi c}{4b},$$

where the inverse is obtained after simple calculations. Figure 9.17b shows the response of the relay to a sinusoidal input with the first harmonic of the output shown as a dashed line. Describing function analysis is illustrated in Figure 9.16b which shows the Nyquist plot of the transfer function $G(s) = 2/(s+1)^4$ (dashed) and the negative inverse describing function of a relay with $b = 1$ and $c = 0.5$. The curves intersect for $a = 1$ and $\omega = 0.77$ rad/s indicating the amplitude and frequency for a possible oscillation if the process and the relay are connected in a feedback loop. ∇

9.6 FURTHER READING

Nyquist's original paper giving his now famous stability criterion was published in the Bell Systems Technical Journal in 1932 [151]. More accessible versions are found in the book [26], which also has other interesting early papers on control. Nyquist's paper is also reprinted in an IEEE collection of seminal papers on control [64]. Nyquist used +1 as the critical point but Bode changed it to -1, which is now the standard notation. Interesting perspectives on the early development are given by Black [36], Bode [41] and Bennett [28]. Nyquist did a direct calculation based on his insight of propagation of sinusoidal signals through systems; he did not use results from the theory of complex functions. The idea that a short proof can be given by using the principle of variation of the argument is given in the delightful little book by MacColl [131]. Bode made extensive use of complex function theory in his book [40], which laid the foundation for frequency response analysis where the notion of minimum phase was treated in detail. A good source

for theory of complex functions is the classic by Ahlfors [6]. Frequency response analysis was a key element in the emergence of control theory as described in the early texts by James *et al.* [103], Brown and Campbell [45] and Oldenburger [63], and it became one of the cornerstones of early control theory. Frequency response had a resurgence when robust control emerged in the 1980s, as will be discussed in Chapter 12.

EXERCISES

9.1 The dynamics of the tapping mode of an atomic force microscope is dominated by the damping of the cantilever vibrations and the system that averages the vibrations. Modeling the cantilever as a spring-mass system with low damping we find that the amplitude of the vibrations decay as $\exp(-\zeta\omega t)$ where ζ is the relative damping and ω the undamped natural frequency of the cantilever. The cantilever dynamics can thus be modeled by the transfer function

$$G(s) = \frac{b}{s+a}.$$

where $a = \zeta\omega_0$. The averaging process can be modeled by the input-output relation

$$y(t) = \frac{1}{\tau} \int_{t-\tau}^t u(v)dv,$$

where the averaging time is a multiple n of the period of the oscillation $2\pi/\omega$. The dynamics of the piezo scanner can be neglected in the first approximation because it is typically much faster than a . A simple model for the complete system is thus given by the transfer function

$$P(s) = \frac{a(1 - e^{-s\tau})}{s\tau(s+a)}.$$

Plot the Nyquist curve of the system and determine the gain of a proportional controller which brings the system to the boundary of stability.

9.2 (Loop transfer function with RHP pole) Consider a feedback system with the loop transfer function

$$L(s) = \frac{k}{s(s-1)(s+5)}.$$

This transfer function has a pole at $s = 1$ which is inside the Nyquist contour. Draw the Nyquist plot for this system and determine if the closed loop system is stable.

9.3 A simple model for heat conduction in a solid is given by the transfer function

$$P(s) = ke^{-\sqrt{s}}.$$

Sketch the Nyquist plot of the system. Determine the frequency where the phase of the process is -180° and the gain at that frequency. Show that the gain required to bring the system to the stability boundary is $k = e^\pi$.

9.4 In Example 9.4 we developed a linearize model of the dynamics for a congestion control mechanism on the Internet, following [129] and [96]. A linearized version of the model is represented by the transfer function

$$L(s)\rho \cdot \frac{N}{\tau^*s + e^{-\tau^*s}} \cdot \frac{c^3\tau^{*3}}{2N^3(c\tau^{*2}s + 2N^2)} e^{-\tau^*s}$$

where c is the link capacity in packets/ms, N load factor (number of TCP sessions), ρ is the drop probability factor and τ is the round-trip time in seconds. Consider the situation with the parameters $N = 80$, $c = 4$, $\rho = 10^{-2}$ and $\tau^* = 0.25$. Find the stability margin of the system, also determine the stability margin if the time delay becomes $\tau^* = 0.5$.



9.5 (Vectored thrust aircraft) Consider the state space controller designed for the vectored thrust aircraft in Examples 6.8 and 7.5. The controller consists of two components: an optimal estimator to compute the state of the system from the output and a state feedback compensator that computes the input given the (estimated) state. Compute the loop transfer function for the system and determine the gain, phase and stability margins for the closed loop dynamics.

9.6 Consider the linearized model for vehicle steering with a controller based on state feedback discussed in Example 7.4. The transfer function of the process is

$$P(s) = \frac{\gamma s + 1}{s^2}$$

and the controller has the transfer function

$$C(s) = \frac{s(k_1 l_1 + k_2 l_2) + k_1 l_2}{s^2 + s(\gamma k_1 + k_2 + l_1) + k_1 + l_2 + k_2 l_1 - \gamma k_2 l_2},$$

as computed in Example 8.6. Let the process parameter be $\gamma = 0.5$ and assume that the state feedback gains are $k_1 = 1$ and $k_2 = 0.914$, and the observer gains are $l_1 = 2.828$ and $l_2 = 4$. Compute the stability margins numerically. The phase margin of the system is 44° and the gain margin is infinite since the phase lag is never greater than 180° , indicating that the closed loop system is robust.

9.7 (Congestion control) A strongly simplified flow model of TCP loop in overload conditions is given by the loop transfer function

$$L(s) = \frac{k}{s} e^{-sT_d},$$

where the queuing dynamics are modeled by an integrator, the TCP window control by a time delay T_d is the time delay and the controller is simply a proportional controller. A major difficulty is that the time delay may change significantly during the operation of the system. Show that if we can measure the time delay, it is possible to choose a gain that gives a stability margin of $s_n \geq 0.6$ for all time delays T_d .

9.8 (Stability margins) A process whose dynamics is described by a double integrator is controlled by an ideal PD controller with the transfer function $C(s) = k_d s + k_p$, where the gains are $k_d = 2\zeta_0\omega_0$ and $k_p = \omega_0^2$. Determine phase, gain, and stability margins. Plot the margins as functions of the parameter ζ_0 .

9.9 Consider Bode's formula (9.8) for the relation between gain and phase for a transfer function that has all its singularities in the left half plane. Plot the weighting function and make an assessment of the frequencies where the approximation $\arg G \approx (\pi/2)d \log |G|/d \log \omega$ is valid.

9.10 Consider the transfer functions

$$G_1(s) = e^{-sT_d}, \quad G_2(s) = \frac{a-s}{a+s}.$$

Use the approximation

$$e^{-sT} \approx \frac{1-sT/2}{1+sT/2}.$$

to show that the minimum phase properties of the transfer functions are similar if $T_d = 2/a$. A long time delay T_d is thus equivalent to a small right half plane zero.

9.11 Consider the system

$$G(s) = \frac{6(-s+1)}{s^2+5s+6},$$

which has a zero in the right half plane. Compute the step response for the system and show that the output goes in the wrong direction initially, which is also referred to as an *inverse response*. Compare the response to a minimum phase system obtained by replacing the zero at $s = 1$ with a zero at $s = -1$.

Chapter Ten

PID Control

Based on a survey of over eleven thousand controllers in the refining, chemicals and pulp and paper industries, 97% of regulatory controllers utilize PID feedback.

Desborough Honeywell, 2000 [54].

This chapter treats the basic properties of proportional-integral-derivative (PID) control and the methods for choosing the parameters of the controllers. We also analyze the effects of actuator saturation and time delay, two important features of many feedback systems, and methods for compensating for these effects. Finally, we will discuss the implementation of PID controllers as an example of how to implement feedback control systems using analog or digital computation.

10.1 BASIC CONTROL FUNCTIONS

PID control, which was introduced already in Section 1.5 and has been used in several examples, is by far the most common way of using feedback in engineering systems. It appears in simple devices and in large factories with thousands of controllers. PID controllers appear in many different forms: as a standalone controller, as part of hierarchical, distributed control systems or built into embedded components. Most PID controllers do not use derivative action so they should strictly speaking be called PI controllers; we will however use PID as a generic term for this class of controller. There is also growing evidence that PID control appears in biological systems [196].

Block diagrams of closed loop systems with PID controllers are shown in Figure 10.1. The control signal u for the system in Figure 10.1a is formed entirely from the error e ; there is no feedforward term (which would correspond to $k_r r$ in the state feedback case). A common alternative in which proportional and derivative action do not act on the reference is shown in Figure 10.1b; combinations of the schemes will be discussed in Section 10.5. The command signal r is called the reference value in regulation problems, or the *setpoint* in literature of PID control. The input-output relation for an ideal PID controller with error feedback is

$$u = k_p e + k_i \int_0^t e(\tau) d\tau + k_d \frac{de}{dt} = k_p \left(e + \frac{1}{T_i} \int_0^t e(\tau) d\tau + T_d \frac{de}{dt} \right). \quad (10.1)$$

The control action is thus the sum of three terms: proportional feedback, the integral term, and derivative action. For this reason PID controllers were originally called *three term controllers*. The controller parameters are the proportional gain

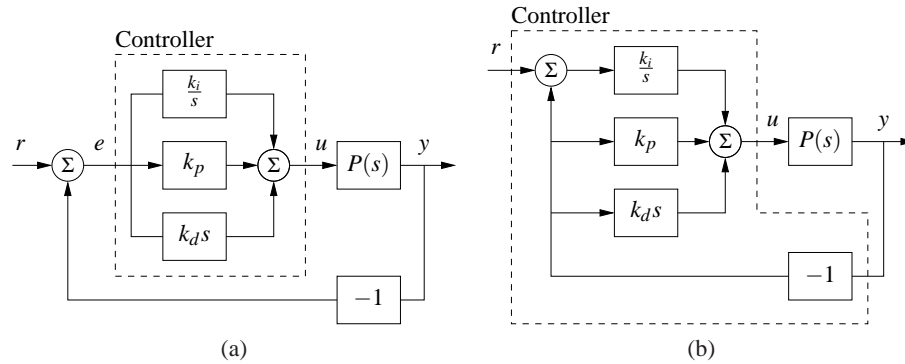


Figure 10.1: Block diagrams of closed loop systems with ideal PID controllers. Both controllers have one output the control signal u . The controller in (a), which is based on error feedback, has one input, the control error $e = r - y$. For this controller proportional, integral and derivative action acts on the error $e = r - y$. The two-degree-of-freedom controller in (b), has two inputs, the reference r and the process output y . Integral action acts on the error, but proportional and derivative action acts on the process output y .

k_p , the integral gain k_i and the derivative gain k_d . The time constants T_i and T_d , called integral time (constant) and derivative time (constant), are sometimes used instead of the integral and derivative gains.

The controller (10.1) represents an idealized controller. It is a useful abstraction for understanding the PID controller, but several modifications must be made in order to obtain a controller that is practically useful. Before discussing these practical issues we will develop some intuition about PID control.

We start by considering pure proportional feedback. Figure 10.2a shows the responses of the process output to a unit step in the reference value for a system with pure proportional control at different gain settings. All of the systems have error feedback. In the absence of a feedforward term, the output never reaches the reference and hence we are left with nonzero steady state error. Letting the process and the controller have transfer functions $P(s)$ and $C(s)$, the transfer function from reference to output is

$$G_{yr} = \frac{PC}{1 + PC}. \quad (10.2)$$

and thus the steady state error for a unit step is

$$1 - G_{yr}(0) = \frac{1}{1 + k_p P(0)}.$$

For the system in Figure 10.2a with gains $k_p = 1, 2$ and 5 , the steady state error is $0.5, 0.33$ and 0.17 . The error decreases with increasing gain, but the system also becomes more oscillatory. Notice in the figure that the initial value of the control signal equals the controller gain.

To avoid having a steady state error, the proportional term can be changed to

$$u(t) = k_p e(t) + u_{\text{ff}}, \quad (10.3)$$

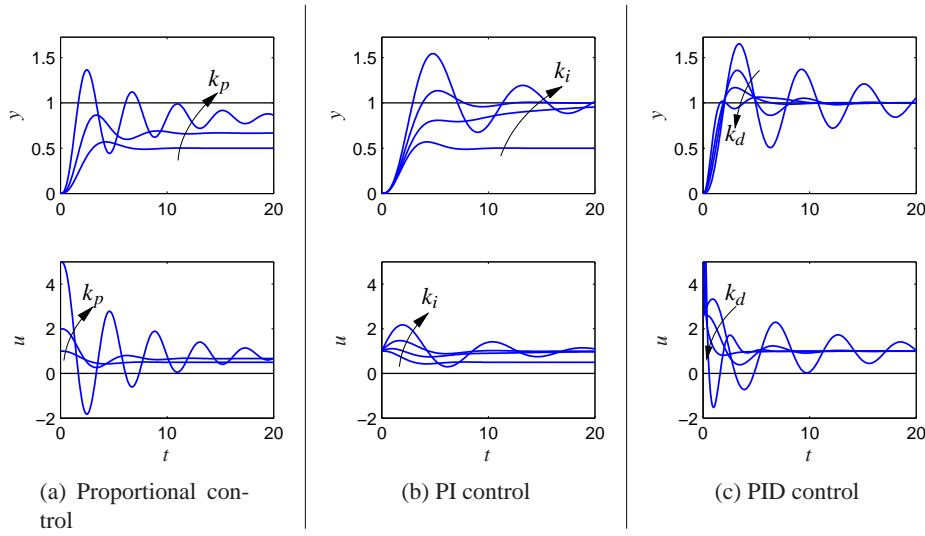


Figure 10.2: Responses to step changes in the reference value for system with a proportional controller (a), PI controller (b) and PID controller (c). The process has the transfer function $P(s) = 1/(s+1)^3$, the proportional controller (left) had parameters $k_p = 1, 2$ and 5 , the PI controller has parameters $k_p = 1, k_i = 0, 0.2, 0.5$ and 1 , and the PID controller has parameters are $k_p = 2.5, k_i = 1.5$ and $k_d = 0, 1, 2$ and 4 .

where u_{ff} is a feedforward term that is adjusted to give the desired steady state value. If we choose $u_{\text{ff}} = r/P(0) = k_r r$, then the output will be exactly equal to the reference value, as it was in the state space case, provided that there are no disturbances. However, this requires exact knowledge of the process dynamics, which is usually not available. The parameter u_{ff} , called *reset* in the PID literature, must therefore be adjusted manually.

As we saw in Sections 6.4, integral action guarantees that the process output agrees with the reference in steady state and provides an alternative to the feedforward term. Since this result is so important we will provide a general proof. Consider the controller given by equation (10.1). Assume that there exist a steady state with $u = u_0$ and $e = e_0$. It then follows from equation (10.1) that

$$u_0 = k_p e_0 + k_i e_0 t,$$

which is a contradiction unless e_0 or k_i are zero. We can thus conclude that with integral action the error will be zero if it reaches a steady state. Notice that we have not made any assumptions about linearity of the process or the disturbances. We have, however assumed that an equilibrium exists. Using integral action to achieve zero steady state error is much better than using feedforward, which requires precise knowledge of process parameters.

The effect of integral action can also be understood from frequency domain analysis. The transfer function of the PID controller is

$$C(s) = k_p + \frac{k_i}{s} + k_d s. \quad (10.4)$$

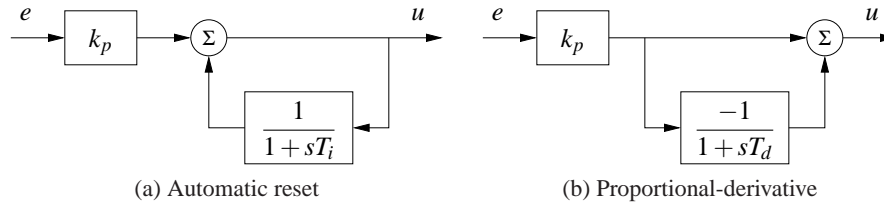


Figure 10.3: Implementation of PI and PD controllers. The block diagram on the left shows how integral action is implemented using *positive feedback* with a first order system, sometimes called *automatic reset*. The block diagram on the right shows how derivative action can be implemented by taking differences between a static system and a first order system.

The controller has infinite gain at zero frequency ($C(0) = \infty$) and it then follows from equation (10.2) that $G_{yr}(0) = 1$, which implies that there is no steady state error for a step input.

Integral action can also be viewed as a method for generating the feedforward term u_{ff} in the proportional controller (10.3) automatically. One way to do this is shown in Figure 10.3a, where the controller output is low-pass filtered and fed back with positive gain. This implementation, called *automatic reset*, was one of the early inventions of integral control. The transfer function of the system in Figure 10.3a is obtained by block diagram algebra; we have

$$G_{ue} = k_p \frac{1 + sT_i}{sT_i} = k_p + \frac{k_p}{sT_i},$$

which is the transfer function for a PI controller.

The properties of integral action are illustrated in Figure 10.2b for a step input. The proportional gain is constant, $k_p = 1$, and the integral gains are $k_i = 0, 0.2, 0.5$ and 1 . The case $k_i = 0$ corresponds to pure proportional control, with a steady state error of 50%. The steady state error is eliminated when integral gain action is used. The response creeps slowly towards the reference for small values of k_i and goes faster for larger integral gains, but the system also becomes more oscillatory.

Integral gain k_i is a useful measure for attenuation of load disturbances. Consider a closed loop system under PID control and assume that the system is stable and initially at rest with all signals being zero. Apply a unit step disturbance at the process input. After a transient the process output goes to zero and the controller output settles at a value that compensates for the disturbance. It follows from (10.1) that

$$u(\infty) = k_i \int_0^{\infty} e(t) dt.$$

The integrated error is thus inversely proportional to integral gain k_i . The integral gain is thus a measure of the effectiveness of disturbance attenuation. A large gain k_i attenuates disturbances effectively but too large a gain gives oscillatory behavior, poor robustness and possibly instability.

We now return to the general PID controller and consider the effect of the derivative term, k_d . Recall that the original motivation for derivative feedback was

to provide predictive action. Notice that the combination of the proportional and the derivative terms can be written as

$$u = k_p e + k_d \frac{de}{dt} = k_p \left(e + T_d \frac{de}{dt} \right) = k_p e_p,$$

where $e_p(t)$ can be interpreted as a prediction of the error at time $t + T_d$ by linear extrapolation. The prediction time $T_d = k_d/k_p$ is the derivative time constant of the controller.

Derivative action can be implemented by taking the difference between the signal and its low-pass filtered version as shown in Figure 10.3b. The transfer function for the system is

$$G_{ue}(s) = k_p \left(1 - \frac{1}{1 + sT_d} \right) = k_p \frac{sT_d}{1 + sT_d}. \quad (10.5)$$

The system thus has the transfer function $G(s) = sT_d/(1 + sT_d)$, which approximates a derivative for low frequencies ($|s| < T_d$).

Figure 10.2c illustrates the effect of derivative action: the system is oscillatory when no derivative action is used and it becomes more damped as derivative gain is increased. Performance deteriorates if derivative gain is too high. When the input is a step the controller output generated by the derivative term will be an impulse. This is clearly visible in Figure 10.2c. The impulse can be avoided by using the controller configuration shown in Figure 10.1b.

Although PID control was developed in the context of engineering applications, it also appears in nature. Disturbance attenuation by feedback in biological systems is often called adaptation. A typical example is the pupillary reflex discussed in Example 8.11 where it is said that the eye adapts to changing light intensity. Analogously, feedback with integral action is called perfect adaptation [196]. In biological systems proportional, integral and derivative action is generated by combining subsystems with dynamical behavior similar to what is done in engineering systems. For example, PI action can be generated by the interaction of several hormones [65].

Example 10.1 PD action in the retina

The response of cone photo receptors in the retina is an example where proportional and derivative action is generated by a combination of cones and horizontal cells. The cones are the primary receptors stimulated by light, the cones in turn stimulate the horizontal cells and the horizontal cells give inhibitory (negative) feedback to the cones. A schematic diagram of the system is shown in Figure 10.4a. The system can be modeled by ordinary differential equations by representing neuron signals by continuous variables representing the average pulse rate. In [194] it is shown that the system can be represented by the differential equations

$$\frac{dx_1}{dt} = \frac{1}{T_c}(-x_1 - kx_2 + u), \quad \frac{dx_2}{dt} = \frac{1}{T_h}(x_1 - x_2),$$

where u is the light intensity and x_1 and x_2 are the average pulse rates from the cones and the horizontal cells. A block diagram of the system is shown in Fig-

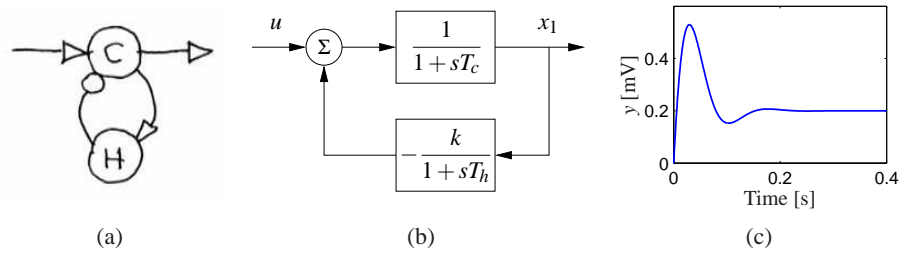


Figure 10.4: Schematic diagram of cone photo receptors (C) and horizontal cells (H) in the retina. Excitatory feedback is indicated by arrows and inhibitory feedback by circles in the schematic diagram in (a). A block diagram is shown in (b) and the step response in (c).

ure 10.4b. The step response of the system shown in Figure 10.4c shows that the system has a large initial response followed by a lower constant steady state response typical of proportional and derivative action. The parameters used in the simulation are $k = 4$, $T_c = 0.025$ and $T_h = 0.08$. ▽

10.2 SIMPLE CONTROLLERS FOR COMPLEX SYSTEMS

Many of the design methods discussed in previous chapters have the property that the complexity of the controller is directly reflected by the complexity of the model. When designing controllers by output feedback in Chapter 7 we found for single-input single-output systems that the order of the controller was the same as the order of the model, possibly one order higher if integral action was required. Applying similar design methods for PID control will require that we have low order models of the processes to be able to easily analyze the results.

Low order models can be obtained from first principles. Any stable system can be modeled by a static system if its inputs are sufficiently slow. Similarly a first order model is sufficient if storage of mass, momentum or energy can be captured by only one variable; typical examples are the velocity of a car on a road, angular velocity of a stiff rotational systems, level in a tank and concentration in a volume with good mixing. System dynamics are of second order if storage of mass, energy and momentum can be captured by two state variable; typical examples are position of a car on the road, stabilization of stiff satellites, levels in two connected tanks and two compartment models. A wide range of techniques for model reduction also available. In this chapter we will focus on design techniques where we simplify the models to capture the essential properties that are needed for PID design.

We begin by analyzing the case of integral control. A stable system can be controlled by an integrating controller provided that the requirements on the closed loop system are modest. To design the controller we assume that the transfer function of the process is a constant $K = P(0)$. The loop transfer function under integral control then becomes Kk_i/s and the closed loop characteristic polynomial is sim-

ply $s + Kk_i$. Specifying performance by the desired time constant T_{cl} of the closed loop system we find that the integral gain is given by

$$k_i = 1/(T_{cl}P(0)).$$

The analysis requires that T_{cl} is large enough that the process transfer function can be approximated by a constant.

For systems that are not well-represented by a constant gain, another way to find a suitable value of integral gain is to make a Taylor series expansion of the loop transfer function

$$L(s) = \frac{k_i P(s)}{s} \approx \frac{k_i(P(0) + sP'(0))}{s} = k_i P'(0) + \frac{k_i P(0)}{s}.$$

Choosing $k_i P'(0) = -0.5$ gives a system with good robustness as will be discussed in Section ???. The controller gain is then given by

$$k_i = -\frac{1}{2P'(0)} \quad (10.6)$$

and the expected closed loop time constant is $T_{cl} \approx -2P'(0)/P(0)$. This approach is useful when the process has a pole at the origin, as illustrated in the following example.

Example 10.2 Integrating control of AFM in tapping mode

A simplified model of the dynamics of the vertical motion of an atomic force microscope in tapping mode was discussed in Exercise 9.1. The transfer function for the system dynamics is

$$P(s) = \frac{a(1 - e^{-s\tau})}{s\tau(s + a)},$$

where $a = \zeta \omega_0$, and $\tau = 2\pi n/\omega_0$ and the gain has been normalized to 1. We have $P(0) = 1$ and $P'(0) = -\tau/2 - 1/a$, and it follows from (10.6) that the integral gain is $k_i = a/(2 + a\tau)$. A Nyquist plot and Bode plot for the resulting loop transfer function are shown in Figure 10.5. ∇

A first order system has the transfer function

$$P(s) = \frac{b}{s + a}.$$

With a PI controller the closed loop system has the characteristic polynomial

$$s(s + a) + bk_p s + bk_i s = s^2 + (a + bk_p)s + bk_i.$$

The closed loop poles can thus be assigned arbitrary values by proper choice of the controller gains. Requiring that the closed loop system has the characteristic polynomial

$$s^2 + a_1 s + a_2^2,$$

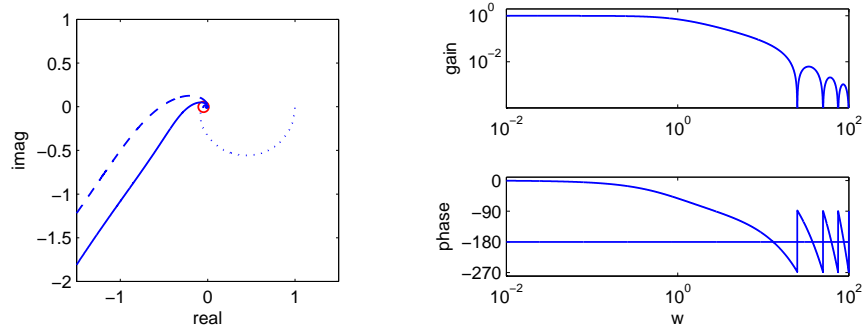


Figure 10.5: Integral control for AFM in tapping mode. An integral controller is designed based on the slope of the process transfer function at 0. The controller gives good robustness properties based on a very simple analysis.

we find that the controller parameters are

$$k_p = \frac{a_1 - a}{b}, \quad k_i = \frac{a_2}{b}. \quad (10.7)$$

If we require a response of the closed loop system that is slower than that of the open loop system, a reasonable choice is $a_1 = a + \alpha$ and $a_2 = \alpha a$. If a response that is faster than the open loop system is required, it is reasonable to choose $a_1 = 2\zeta_0\omega_0$ and $a_2 = \omega_0^2$, where ω_0 and ζ_0 are undamped natural frequency and relative damping of the dominant mode. These choices have significant impact on the robustness of the system and will be discussed in Section 12.4. An upper limit to ω_0 is given by the validity of the model. Large values of ω_0 will require fast control actions and actuators may saturate if the value is too large. A first order model is unlikely to represent the true dynamics for high frequencies. We illustrate the design by an example.

Example 10.3 Cruise control using PI feedback

Consider the problem of maintaining the speed of a car as it goes up a hill. In Example 5.14 we found that there was little difference between the linear and non-linear models when investigating PI control provided that the throttle did not reach the saturation limits. A simple linear model of a car was given in Example 5.11:

$$\frac{d(v - v_e)}{dt} = -a(v - v_e) + b(u - u_e) - g\theta, \quad (10.8)$$

where v is the velocity of the car, u is the input from the engine and θ is the slope of the hill. The parameters were $a = 0.0101$, $b = 1.3203$, $g = 9.8$, $v_e = 20$, and $u_e = 0.1616$. This model will be used to find suitable parameters of a vehicle speed controller. The transfer function from throttle to velocity is thus a first order system. Since the open loop dynamics is so slow it is natural to specify a faster closed loop system by requiring that the closed loop system is of second order with relative damping ζ and undamped natural frequency ω_0 . The controller gains are given by (10.7).

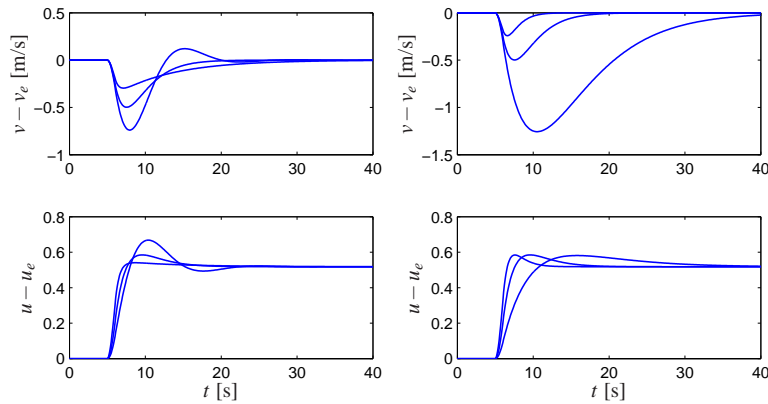


Figure 10.6: Cruise control using PI feedback. The step responses for the error and input illustrate the effect of parameters $\zeta_0 = 1$ and ω_0 on the response of a car with cruise control. A change in road slope from 0° to 4° is applied between $t = 5$ and 6 s. The plot on the left shows the response for $\omega_0 = 0.5$ and $\zeta_0 = 0.5, 1$ and 2 . Choosing $\zeta_0 = 1$ gives no overshoot. The plot on the right shows the response for $\zeta_0 = 1$ and $\omega_0 = 0.2, 0.5$ and 1.0 .

Figure 10.6 shows the velocity and the throttle for a car that initially moves on a horizontal road and encounters a hill with slope 4° at time $t = 6$ sec. To design a PI controller we choose $\zeta_0 = 1$ to obtain a response without overshoot, as shown in Figure 10.6a. The choice of ω_0 is a compromise between response speed and control actions: a large value gives a fast response but it requires fast control action. The trade-off is illustrated in Figure 10.6b. The largest velocity error decreases with increasing ω_0 , but the control signal also changes more rapidly. In the simple model (10.8) it was assumed that the force responds instantaneously to throttle commands. For rapid changes there may be additional dynamics that have to be accounted for. There are also physical limitations to the rate of change of the force, which also restricts the admissible value of ω_0 . A reasonable choice of ω_0 is in the range of 0.5 to 1.0. Notice in Figure 10.6 that even with $\omega_0 = 0.2$ the largest velocity error is only 1 m/s.

▽

A PI controller can also be used for a process with second order dynamics, but there will be restrictions on possible locations of closed loop poles, as shown in Exercise 10.2. Using a PID controller it is possible to control a system of second order in such a way that the closed loop poles have arbitrary locations; see Exercise 10.2.

Instead of finding a low order model and designing controllers for them we can also use a high order model and only attempt to place a few dominant poles. An integrating controller has one parameter and it is possible to position one pole. Consider a process with the transfer function $P(s)$. The loop transfer function with an integrating controller is $L(s) = k_i P(s)/s$. The roots of the closed loop characteristic polynomial are the roots of $s + k_i P(s) = 0$. Requiring that $s = -a$ is

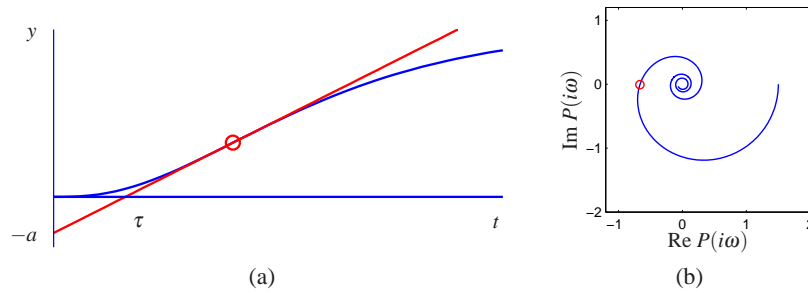


Figure 10.7: Illustration of Ziegler-Nichols step and frequency response experiments. The unit step response in (a) is characterized by the parameters a and T_{del} . The frequency response method characterizes process dynamics by the point of the Nyquist curve of the process transfer function first intersects the negative real axis and the frequency ω_c where this occurs.

a root, we find that the controller gain should be chosen as

$$k_i = \frac{a}{P(-a)}. \quad (10.9)$$

The pole $s = -a$ will be dominant if a is small. A similar approach can be applied to PI and PID controllers.

10.3 PID TUNING

Users of control systems are frequently faced with the task of adjusting the controller parameters to obtain a desired behavior. There are many different ways to do this. One approach is to go through the conventional steps of modeling and control design as described in the previous section. Since the PID controller has so few parameters, a number of special empirical methods have also been developed for direct adjustment of the controller parameters. The first tuning rules were developed by Ziegler and Nichols [199]. Their idea was to make a simple experiment, extract some features of process dynamics from the experiment and determine controller parameters from the features.

Ziegler-Nichols' Tuning

Ziegler and Nichols developed two methods for controller tuning in the 1940s based on simple characterization of process dynamics in the time and frequency domains.

The time domain method is based on a measurement of part of the open loop unit step response of the process, as shown in Figure 10.7a. The step response is measured by applying a unit step input to the process and recording the response. The response is characterized by parameters a and τ , which are the intercepts of the steepest tangent of the step response with the coordinate axes. The parameter τ is an approximation of the time delay of the system and a/τ is the steepest

Table 10.1: Ziegler-Nichols tuning rules. (a) The step response methods give the parameters in terms of the intercept a and the apparent time delay τ . (b) The frequency response method gives controller parameters in terms of critical gain k_c and critical period T_c .

Type	ak_p	T_i/τ	T_d/τ	Type	k_p/k_c	T_i/T_c	T_d/T_c
P	1			P	0.5		
PI	0.9	3		PI	0.4	0.8	
PID	1.2	2	0.5	PID	0.6	0.5	0.125

(a) Step response method (b) Frequency response method

slope of the step response. Notice that it is not necessary to wait until steady state is reached to find the parameters, it suffices to wait until the response has had an inflection point. The controller parameters are given in Table 10.1. The parameters were obtained by extensive simulation of a range of representative processes. A controller was tuned manually for each process and it was then attempted to correlate the controller parameters with a and τ .

In the frequency domain method a controller is connected to the process, the integral and derivative gains are set to zero, and the proportional gain is increased until the system starts to oscillate. The critical value of the proportional gain k_c is observed together with the period of oscillation T_c . It follows from Nyquist's stability criterion that the loop transfer function $L = k_c P(s)$ intersects the critical point for the frequency $\omega_c = 2\pi/T_c$. The experiment thus gives the point on the Nyquist curve of the process transfer function where the phase lag is 180° , as shown in Figure 10.7b.

The Ziegler-Nichols methods had a huge impact when they were introduced in the 1940s. The rules were simple to use and gave initial conditions for manual tuning. The ideas were adopted by manufacturers of controllers for routine use. The Ziegler-Nichols tuning rules have unfortunately two severe drawbacks: too little process information is used and the closed loop systems that are obtained lack robustness.

The step response method can be improved significantly by characterizing the unit step response by parameters K , τ and T in the model

$$P(s) = \frac{K}{1 + sT} e^{-\tau s}. \quad (10.10)$$

The parameters can be obtained by fitting the model to a measured step response. Notice that the experiment takes longer time than the experiment in Figure 10.7a because to determine K it is necessary to wait until the steady state has been reached. Also notice that the intercept a in the Ziegler-Nichols rule is given by $a = K\tau/T$.

The frequency response method can be improved by measuring more points on the Nyquist curve, for example the zero frequency gain K or the point where the process has 90° phase lag. This latter point can be obtained by connecting an integrating controller and increasing its gain until the system reaches the stability

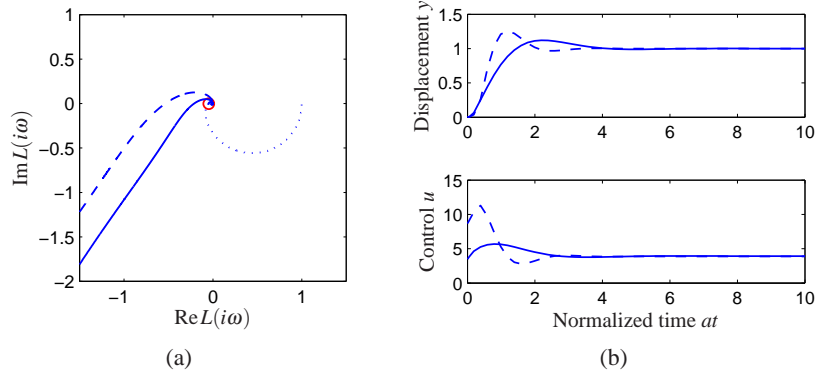


Figure 10.8: PI control of an AFM in tapping mode. Nyquist plots (a) and step responses (b) for PI control of the vertical motion of an atomic force microscope in tapping mode. The averaging parameter is $n = 20$. Results with Ziegler-Nichols tuning are shown in dashed lines, and modified Ziegler-Nichols tuning is shown in full lines. The Nyquist plot of the process transfer function is shown in dotted lines.

limit. The experiment can also be automated by using relay feedback, as will be discussed later in this section.

There are many versions of improved tuning rules. As an illustration we give the following rules for PI control based on [17]:

$$\begin{aligned}
 k_p &= \frac{0.15\tau + 0.35T}{K\tau} \quad \left(\frac{0.9T}{K\tau} \right), & k_i &= \frac{0.46\tau + 0.02T}{K\tau^2} \quad \left(\frac{0.3}{K\tau^2} \right) \\
 k_p &= 0.22k_c - \frac{0.07}{K} \quad \left(0.4k_c \right), & k_i &= \frac{0.07k_c}{T_c} + \frac{0.8}{KT_c} \quad \left(\frac{0.5k_c}{T_c} \right)
 \end{aligned} \tag{10.11}$$

The values for the Ziegler-Nichols rule are given in parentheses. Notice that the improved formulas typically give lower controller gains than the Ziegler-Nichols method. The integral gain is higher for systems whose dynamics are delay dominated, $\tau \gg T$.

Example 10.4 PI control of AFM in tapping mode

A simplified model of the dynamics of the vertical motion of an atomic force microscope in tapping mode was discussed in Example 10.2. The transfer function is normalized by choosing $1/a$ as the time unit. The normalized transfer function is

$$P(s) = \frac{1 - e^{-sT_n}}{sT_n(s+1)}.$$

where $T_n = 2n\pi a/\omega_0 = 2n\pi\zeta$. The Nyquist plot of the transfer function is shown in Figure 10.8a for $z = 0.002$ and $n = 20$. The leftmost intersection of the Nyquist curve with the real axis occurs at $\text{Re } s = -0.0461$ for $\omega = 13.1$. The critical gain is thus $k_c = 21.7$ the critical period is $T_c = 0.48$. Using Ziegler-Nichols tuning rule we find the parameters $k_p = 8.87$ and $k_i = 22.6$ ($T_i = 0.384$) for a PI controller. With this controller the stability margin is $s_m = 0.31$, which is quite small. The

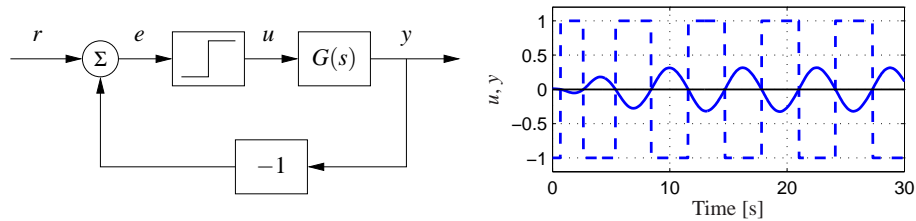


Figure 10.9: Block diagram of a process with relay feedback (left) and typical signals (right). The process output y is solid and the relay output u is dashed. Notice that the signals u and y have opposite phase.

step response of the controller is shown in Figure 10.8. Notice in particular that there is a large overshoot in the control signal.

The modified Ziegler-Nichols rule (10.11) gives the controller parameters $k = 3.47$ and $k_i = 8.73$ ($T_i = 0.459$) and the stability margin becomes $s_m = 0.61$. The step response with this controller is shown in Figure 10.8. A comparison of the responses obtained with the original Ziegler Nichols rule shows that the overshoot has been reduced. Notice that the control signal reaches its steady state value almost instantaneously. It follows from Example 10.2 that a pure integrating controller has the normalized gain $k_i = 1/(2 + T_n) = 0.44$. Comparing this with the gains of a PI controller we can conclude that a PI controller gives much better performance than a pure integrating controller. ∇

Relay Feedback

The Ziegler-Nichols frequency response method increases the gain of a proportional controller until oscillation to determine the critical gain k_c and the corresponding period T_c or equivalently the point where the Nyquist curve intersects the negative real axis. One way to obtain this information automatically is to connect the process in a feedback loop with a nonlinear element having a relay function as shown in Figure 10.9a. For many systems there will then be an oscillation, as shown in Figure 10.9b, where the relay output u is a square wave and the process output y is close to a sinusoid. Moreover the input and the output are out of phase, which means that the system oscillates with the critical period T_c , where the process has a phase lag of 180° . Notice that an oscillation with constant period is established quickly.

The critical period is simply the period of the oscillation. To determine the critical gain we expand the square wave relay output in a Fourier series. Notice in the figure that the process output is practically sinusoidal because the process attenuates higher harmonics effectively. It is then sufficient to consider only the first harmonic component of the input. Letting d be the relay amplitude, the first harmonic of the square wave input has amplitude $4d/\pi$. If a is the amplitude of the process output, the process gain at the critical frequency $\omega_c = 2\pi/T_c$ is

$|P(i\omega_c)| = \frac{\pi a}{4d}$ and the critical gain is

$$K_c = \frac{4d}{a\pi}. \quad (10.12)$$

Having obtained the critical gain K_c and the critical period T_c the controller parameters can then be determined using the Ziegler-Nichols rules. Improved tuning can be obtained by fitting a model to the data obtained from the relay experiment.

The relay experiment can be automated. Since the amplitude of the oscillation is proportional to the relay output, it is easy to control it by adjusting the relay output. Automatic tuning based on relay feedback is used in many commercial PID controllers. Tuning is accomplished simply by pushing a button that activates relay feedback. The relay amplitude is automatically adjusted to keep the oscillations sufficiently small and the relay feedback is switched to a PID controller as soon as the tuning is finished.

10.4 INTEGRATOR WINDUP

Many aspects of a control system can be understood from linear models. There are, however, some nonlinear phenomena that must be taken into account. These are typically limitations in the actuators: a motor has limited speed, a valve cannot be more than fully opened or fully closed, etc. For a system that operates over a wide range of conditions, it may happen that the control variable reaches the actuator limits. When this happens the feedback loop is broken and the system runs in open loop because the actuator will remain at its limit independently of the process output as long as the actuator remains saturated. The integral term will also build up since the error is typically nonzero. The integral term and the controller output may then become very large. The control signal will then remain saturated even when the error changes and it may take a long time before the integrator and the controller output come inside the saturation range. The consequence is that there are large transients. This situation is referred to as *integrator windup*, illustrated in the following example.

Example 10.5 Cruise control

The windup effect is illustrated in Figure 10.10, which shows what happens when a car encounters a hill that is so steep (6°) that the throttle saturates when the cruise controller attempts to maintain speed. When encountering the slope at time $t = 5$ the velocity decreases and the throttle increases to generate more torque. However, the torque required is so large that the throttle saturates. The error decreases slowly because the torque generated by the engine is just a little larger than the torque required to compensate for the gravity. The error is large and the integral continues to build up until the error reaches zero at time 30, but the controller output is still larger than the saturation limit and the actuator remains saturated. The integral term starts to decrease and at time 45 and the velocity settles quickly to the desired value. Notice that it takes considerable time before the controller output comes

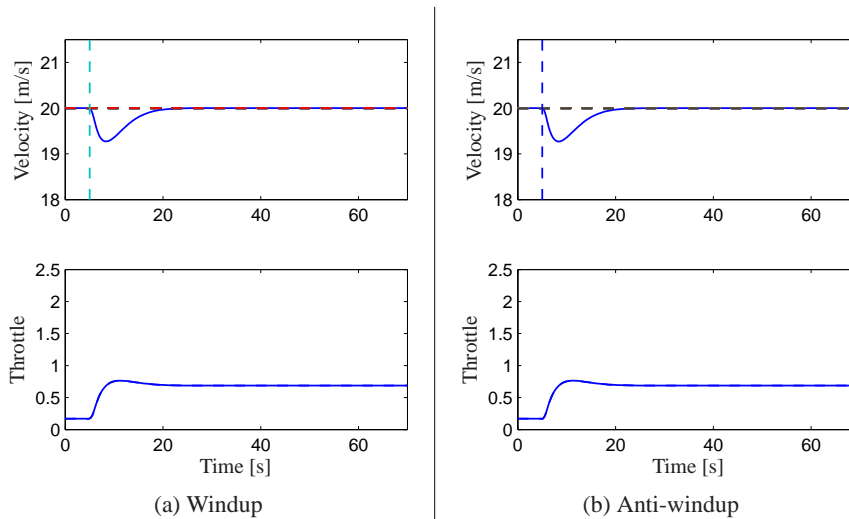


Figure 10.10: Simulation of PI cruise control with windup (left) and anti-windup (right). The figure shows the speed v and the throttle u for a car that encounters a slope that is so steep that the throttle saturates. The controller output is dashed. The controller parameters are $k_p = 0.5$ and $k_i = 0.1$.

into the range where it does not saturate, resulting in a large overshoot. ∇

There are many ways to avoid windup. One method is illustrated in Figure 10.11: the system has an extra feedback path that is generated by measuring the actual actuator output, or the output of a mathematical model of the saturating actuator, and forming an error signal e_s as the difference between the output of the controller v and the actuator output u . The signal e_s is fed to the input of the integrator through gain k_t . The signal e_s is zero when there is no saturation and the extra feedback loop has no effect on the system. When the actuator saturates, the signal e_s is fed back to the integrator in such a way that e_s goes towards zero. This implies that controller output is kept close to the saturation limit. The controller output will then change as soon as the error changes sign and integral windup is avoided.

The rate at which the controller output is reset is governed by the feedback gain, k_t ; a large value of k_t gives a short reset time. The parameter k_t cannot be too large because measurement error can then cause an undesirable reset. A reasonable choice is to choose k_t as a fraction of $1/T_i$. We illustrate how integral windup can be avoided by investigating the cruise control system.

Example 10.6 Cruise control

Figure 10.10b shows what happens when a controller with anti-windup is applied to the system simulated in Figure 10.10a. Because of the feedback from the actuator model, the output of the integrator is quickly reset to a value such that the controller output is at the saturation limit. The behavior is drastically different from that in Figure 10.10a and the large overshoot is avoided. The tracking gain is

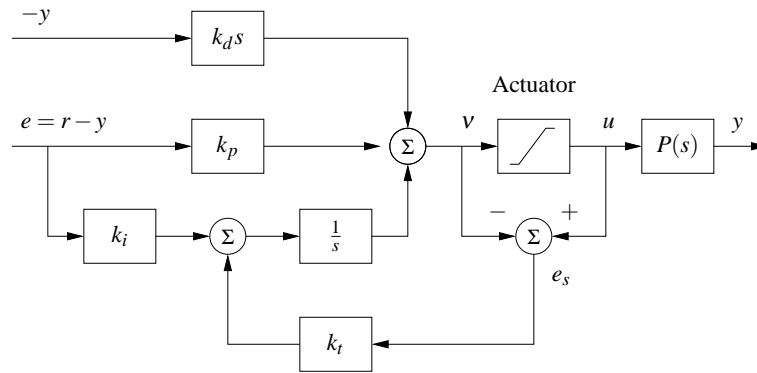


Figure 10.11: PID controller with filtered derivative and anti-windup. The input to the integrator ($1/s$) consists of the error term plus a “reset” based on input saturation. If the actuator is not saturated then $e_s = u - v$, otherwise e_s will decrease the integrator input to prevent windup.

$k_t = 2$ in the simulation.

▽

10.5 IMPLEMENTATION

There are many practical issues that have to be considered when implementing PID controllers. They have been developed over time based on practical experiences. In this section we consider some of the most common. Similar considerations also apply to other types of controllers.

Filtering the Derivative

A drawback with derivative action is that an ideal derivative has high gain for high frequency signals. This means that high frequency measurement noise will generate large variations of the control signal. The effect of measurement noise may be reduced by replacing the term $k_d s$ by $k_d s / (1 + sT_f)$, which can be interpreted as an ideal derivative of a low-pass filtered signal. For small s the transfer function is approximately $k_d s$ and for large s it is equal to k_d / T_f . The approximation acts as a derivative for low-frequency signals and as a constant gain for the high frequency signals. The filtering time is chosen as $T_f = (k_d/k)/N$, with N in the range of 2 to 20. Filtering is obtained automatically if the derivative is implemented by taking the difference between the signal and its filtered version as shown in Figure 10.3b (see equation (10.5)). Instead of filtering just the derivative it is also possible to use an ideal controller and filter the measured signal. The transfer function of such a controller with a filter is then

$$C(s) = k_p \left(1 + \frac{1}{sT_i} + sT_d \right) \frac{1}{1 + sT_f + (sT_f)^2/2}. \quad (10.13)$$

where a second order filter is used.

Setpoint Weighting

Figure 10.1 on page 292 shows two configurations of a PID controller. The system in Figure 10.1a shows a controller with *error feedback* where proportional, integral and derivative action acts on the error. In the simulation of PID controllers in Figure 10.2 there is a large initial peak of the control signal, which is caused by the derivative of the reference signal. The peak can be avoided by using the controller in Figure 10.1b where proportional and derivative action acts only on the process output. An intermediate form is given by

$$u = k_p(\beta r - y) + k_i \int_0^\infty (r(\tau) - y(\tau)) d\tau + k_d \left(\gamma \frac{dr}{dt} - \frac{dy}{dt} \right), \quad (10.14)$$

where the proportional and derivative actions act on fractions β and γ of the reference. Integral action has to act on the error to make sure that the error goes to zero in steady state. The closed loop systems obtained for different values of β and γ respond to load disturbances and measurement noise in the same way. The response to reference signals is different because it depends on the values of β and γ , which are called *reference weights* or *setpoint weights*. We illustrate the effect of setpoint weighting by an example.

Example 10.7 Cruise control

Consider the PI controller for the cruise control system derived in Example 10.3. Figure 10.12 shows the effect of setpoint weighting on the response of the system to a reference signal. With $\beta = 1$ (error feedback) there is an overshoot in velocity and the control signal (throttle) is initially close to the saturation limit. There is no overshoot with $\beta = 0$ and the control signal is much smaller, clearly a much better drive comfort. The frequency responses gives another view of the same effect. The parameter β is typically in the range of 0 to 1 and γ is normally zero to avoid large transients in the control signal when the reference is changed. ∇

The controller given by equation (10.14) is a special case of controller with two degrees of freedom, which will be discussed in more detail in Section 11.2.

Implementation Based on Operational Amplifiers

PID controllers have been implemented in different technologies. Figure 10.13 shows how PI and PID controllers can be implemented by feedback around operational amplifiers.

To show that the circuit in Figure 10.13b is a PID controller we will use the the approximate relation between the input voltage e and the output voltage u of an operational amplifier derived in Example 8.3,

$$u = -\frac{Z_1}{Z_0}e.$$

In this equation Z_0 is the impedance between the negative input of the amplifier and the input voltage e , and Z_1 is the impedance between the zero input of the

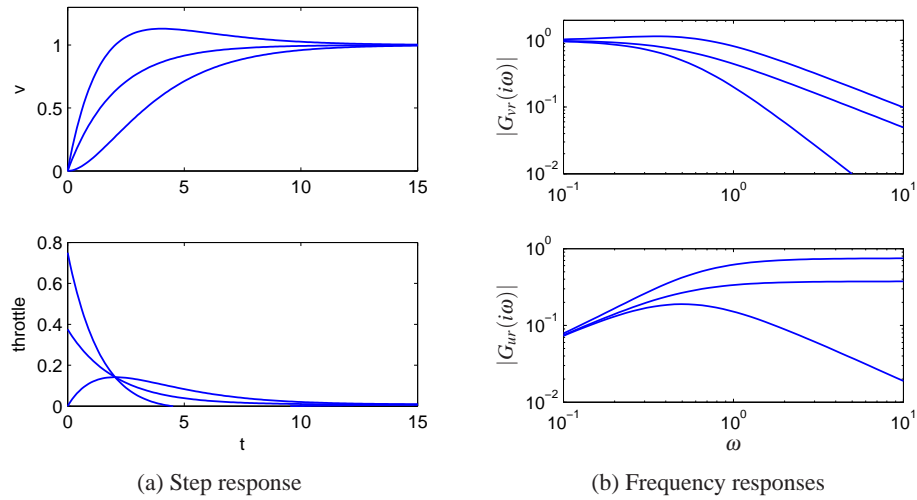


Figure 10.12: Time and frequency responses for PI cruise control with setpoint weighting. Step responses are shown in (a) and the gain curves of the frequency responses in (b). The controller gains are $k_p = 0.74$ and $k_i = 0.19$. The setpoint weights are $\beta = 0, 0.5$ and 1 and $\gamma = 0$.

amplifier and the output voltage u . The impedances are given by

$$Z_0(s) = \frac{R_0}{1 + R_0 C_0 s} \quad Z_1(s) = R_1 + \frac{1}{C_1 s},$$

and we find the following relation between the input voltage e and the output voltage u :

$$u = -\frac{Z_1}{Z_0} e = -\frac{R_1 (1 + R_0 C_0 s)(1 + R_1 C_1 s)}{R_0 R_1 C_1 s} e.$$

This is the input-output relation for a PID controller of the form (10.1) with parameters

$$k_p = \frac{R_1}{R_0} \quad T_i = R_1 C_1 \quad T_d = R_0 C_0.$$

The corresponding results for a PI controller is obtained by setting $C_0 = 0$ (remov-

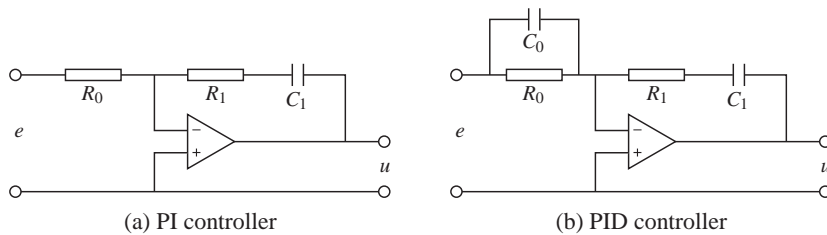


Figure 10.13: Schematic diagrams for PI and PID controllers using op amps. The circuit on the left uses a capacitor in the feedback path to store the integral of the error. The circuit on the right adds a filter on the input to provide derivative action.

ing the capacitor).

Computer Implementation

In this section we briefly describe how a PID controller may be implemented using a computer. The computer typically operates periodically, with signals from the sensors sampled and converted to digital form by the A/D converter, the control signal computed and then converted to analog form for the actuators. The sequence of operation is as follows:

1. Wait for clock interrupt
2. Read input from sensor
3. Compute control signal
4. Send output to the actuator
5. Update controller variables
6. Repeat

Notice that an output is sent to the actuators as soon as it is available. The time delay is minimized by making the calculations in Step 3 as short as possible and performing all updates after the output is commanded. This simple way of reducing the latency is, unfortunately, seldom used in commercial systems.

As an illustration we consider the PID controller in Figure 10.11, which has a filtered derivative, setpoint weighting and protection against integral windup. The controller is a continuous time dynamical system. To implement it using a computer, the continuous time system has to be approximated by a discrete time system.

A block diagram of a PID controller with anti-windup is shown in Figure 10.11. The signal v is the sum of the proportional, integral and derivative terms, and the controller output is $u = \text{sat}(v)$ where sat is the saturation function that models the actuator. The proportional term $k_p(\beta r - y)$ is implemented simply by replacing the continuous variables with their sampled versions. Hence

$$P(t_k) = k_p(\beta r(t_k) - y(t_k)), \quad (10.15)$$

where $\{t_k\}$ denotes the sampling instants, i.e., the times when the computer reads its input. We let h represent the sampling time, so that $t_{k+1} = t_k + h$. The integral term is obtained by approximating the integral with a sum

$$I(t_{k+1}) = I(t_k) + k_i h e(t_k) + \frac{h}{T_i} (\text{sat}(v) - v), \quad (10.16)$$

where $T_i = h/k_i$ represents the anti-windup term. The filtered derivative term D is given by the differential equation

$$T_f \frac{dD}{dt} + D = -k_d y.$$

Approximating the derivative with a backward difference gives

$$T_f \frac{D(t_k) - D(t_{k-1})}{h} + D(t_k) = -k_d \frac{y(t_k) - y(t_{k-1})}{h},$$

which can be rewritten as

$$D(t_k) = \frac{T_f}{T_f + h} D(t_{k-1}) - \frac{k_d}{T_f + h} (y(t_k) - y(t_{k-1})). \quad (10.17)$$

The advantage of using a backward difference is that the parameter $T_f/(T_f + h)$ is non-negative and less than one for all $h > 0$, which guarantees that the difference equation is stable. Reorganizing equations (10.15)–(10.17), the PID controller can be described by the following pseudo code:

```

% Precompute controller coefficients
bi=ki*h
ad=Tf/(Tf+h)
bd=kd/(Tf+h)
br=h/Tt

% Control algorithm - main loop
while (running) {
    r=adin(ch1)           % read setpoint from ch1
    y=adin(ch2)           % read process variable from ch2
    P=kp*(b*r-y)          % compute proportional part
    D=ad*D-bd*(y-yold)    % update derivative part
    v=P+I+D               % compute temporary output
    u=sat(v,ulow,uhigh)   % simulate actuator saturation
    daout(ch1)            % set analog output ch1
    I=I+bi*(r-y)+br*(u-v) % update integral
    yold=y                % update old process output
    sleep(h)              % wait until next update interval
}

```

Precomputation of the coefficients bi , ad , bd and br saves computer time in the main loop. These calculations have to be done only when controller parameters are changed. The main loop is executed once every sampling period. The program has three states: $yold$, I , and D . One state variable can be eliminated at the cost of less readable code. The latency between reading the analog input and setting the analog output consists of 4 multiplications, 4 additions and evaluation of the `sat` function. All computations can be done using fixed point calculations if necessary. Notice that the code computes the filtered derivative of the process output, and that it has set-point weighting and anti-windup protection.

10.6 FURTHER READING

The history of PID control is very rich and stretches back to the beginning of the foundation of control theory. A very readable treatment is given by Bennett [27, 28] and Mindel [143]. The Ziegler-Nichols rules for tuning PID controllers, first presented in 1942 [199], were developed based on extensive experiments with pneumatic simulators and Vannevar Bush's differential analyzer at MIT. An interview with Nichols gives an interesting view of the development of the Ziegler-Nichols rules is given in an interview with Ziegler [39]. An industrial

perspective on PID control is given in [33], [171] and [195] and in the paper [54] cited in the beginning of this chapter. A comprehensive presentation of PID control is given in [16] and [17]. Interactive learning tools for PID control can be downloaded from <http://www.calerga.com/contrib>.

EXERCISES

10.1 Consider the systems represented by the block diagrams in Figure 10.1. Assume that the process has the transfer function $P(s) = b/(s + a)$ show that the transfer functions from r to y are

$$(a) G_{yr}(s) = \frac{bk_d s^2 + bk_p s + bk_i}{(1 + bk_d)s^2 + (a + bk_d)s + bk_i}$$

$$(b) G_{yr}(s) = \frac{bk_i}{(1 + bk_d)s^2 + (a + bk_d)s + bk_i}$$

10.2 Consider a second order process with transfer function

$$P(s) = \frac{b}{s^2 + a_1 s + a_2}.$$

The closed loop system with a PI controller is a third order system. Show that it is possible to position the closed loop poles as long as the sum of the poles is $-a_1$. Give equations for the parameters that give the closed loop characteristic polynomial

$$(s + \alpha_0)(s^2 + 2\zeta_0 \omega_0 s + \omega_0^2).$$

10.3 Consider a system with the transfer function $P(s) = (s + 1)^{-2}$. Find an integrating controller that gives a closed loop pole at $s = -a$ and determine the value of a that maximizes integral gain. Determine the other poles of the system and judge if the pole can be considered to be dominant. Compare with the value of the integral gain given by (10.6).

10.4 Compartment models and many systems encountered in industry have the property that their impulse responses are positive or equivalently that their step responses are monotone. Consider such a system with the transfer function $P(s)$. Show that the impulse response $h_n(t)$ of the normalized system $P(s)/P(0)$ has the properties $h_n(t) \geq 0$ and $\int_0^\infty h_n(t) dt = 1$. The function $h_n(t)$ can be interpreted as a probability density function - the probability that a particle entering the system at time 0 will exit at time t . Let

$$T_{ar} = \int_0^\infty t h_n(t) dt$$

be the average residence time. Show that $T_{ar} = -P'(0)/P(0)$ and that the tuning formula (10.6) can be written as $k_i = 1/(T_{ar}P(0))$.

10.5 Consider a system with the transfer function $P(s) = e^{-s}/s$. Determine parameters of P,PI and PID controllers using Ziegler-Nichols step- and frequency

response methods. Compare the parameter values obtained by the different rules and discuss the results.

10.6 (Vehicle steering) Design a proportional-integral controller for the vehicle steering system that gives closed loop characteristic equation

$$s^3 + 2\omega_0 s^2 + 2\omega_0 s + \omega_0^3.$$

10.7 (Congestion control) A simplified flow model for TCP transmission is derived in [129, 96]. The linearized dynamics are modeled by the transfer function

$$G_{qp}(s) = \frac{b}{(s + a_1)(s + a_2)} e^{-s\tau^*}.$$

which describes the dynamics relating expected queue length q to expected packet drop p . The parameters are given by where $a_1 = 2N^2/(c\tau^{*2})$, $a_2 = 1/\tau^*$ and $b = c^2/(2N)$. The parameter c is the bottleneck capacity, N the number sources feeding the link and τ^* is the round trip delay time. Use the parameter values $N = 75$ sources, $C = 1250$ packets/s and $\tau^* = 0.15$ and find parameters of a PI controller using one of the Ziegler-Nichols rules and the corresponding improved rule. Simulate the responses of the closed loop systems obtained with the PI controllers.

10.8 (Motor drive) Consider the model of the motor drive in Exercise 2.12. Develop an approximative second order model of the system and use it to design an ideal PD controller which gives a closed loop system with eigenvalues in $\zeta_0\omega_d \pm i\omega_d\sqrt{1 - \zeta_0^2}$, add low-pass filtering as shown in Equation 10.13 and explore how large ω_d can be made while maintaining a good stability margin. Simulate the closed loop system with the chosen controller. Compare the results with the controller based on state feedback in Exercise 6.11.

10.9 (Derivative filter) Consider the system in Exercise 6.11 investigate what happens if the second order filtering of the derivative is replaced by a first order filter.

10.10 (Tuning rules) Apply the Ziegler-Nichols and the modified tuning rules to design PI controllers for systems with the transfer functions

$$P_1 = \frac{e^{-s}}{s}, \quad P_2 = \frac{e^{-s}}{s+1}, \quad P_s = e^{-s}.$$

Also compute the stability margins. Analyze the results and explore if you can see some patterns.

Chapter Eleven

Frequency Domain Design

Sensitivity improvements in one frequency range must be paid for with sensitivity deteriorations in another frequency range, and the price is higher if the plant is open-loop unstable. This applies to every controller, no matter how it was designed.

Gunter Stein in the inaugural IEEE Bode Lecture in 1989 [176].

In this chapter we continue to explore the use of frequency domain techniques with a focus on design of feedback systems. We begin with a more thorough description of the performance specifications for control systems, and then introduce the concept of “loop shaping” as a mechanism for designing controllers in the frequency domain. We also introduce some fundamental limitations to performance for systems with right half plane poles and zeros.

11.1 SENSITIVITY FUNCTIONS

In the previous chapter, we considered the use of PID feedback as a mechanism for designing a feedback controller for a given process. In this chapter we will expand our approach to include a richer repertoire of tools for shaping the frequency response of the closed loop system.

One of the key ideas in this chapter is that we can design the behavior of the closed loop system by focusing on the open loop transfer function. This same approach was used in studying stability using the Nyquist criterion: we plotted the Nyquist plot for the *open* loop transfer function to determine the stability of the *closed* loop system. From a design perspective, the use of loop analysis tools is very powerful: since the loop transfer function is $L = PC$, if we can specify the desired performance in terms of properties of L , we can directly see the impact of changes in the controller C . This is much easier, for example, than trying to reason directly about the tracking response of the closed loop system, whose transfer function is given by $G_{yr} = PC/(1 + PC)$.

We will start by investigating some key properties of the feedback loop. A block diagram of a basic feedback loop is shown in Figure 11.1. The system loop is composed of two components, the process and the controller. The controller has two blocks: the feedback block C and the feedforward block F . There are two disturbances acting on the process, the load disturbance d , and the measurement noise n . The load disturbance represents disturbances that drive the process away from its desired behavior, while the measurement noise represents the disturbances that corrupt the information about the process given by the sensors. In the figure,

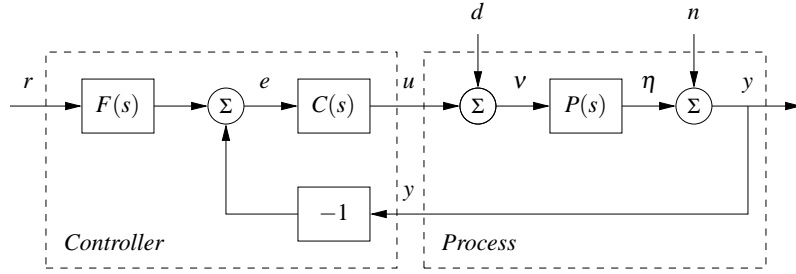


Figure 11.1: Block diagram of a basic feedback loop with two degrees of freedom. The controller has a feedback block C and a feedforward block F . The external signals are the command signal r , the load disturbance d and the measurement noise n . The process output is y and the control signal is u .

the load disturbance is assumed to act on the process input. This is a simplification, since disturbances often enter the process in many different ways, but it allows us to streamline the presentation without significant loss of generality.

The process output η is the real variable that we want to control. Control is based on the measured signal y , where the measurements are corrupted by measurement noise n . The process is influenced by the controller via the control variable u . The process is thus a system with three inputs—the control variable u , the load disturbance d and the measurement noise n —and one output—the measured signal y . The controller is a system with two inputs and one output. The inputs are the measured signal y and the reference signal r and the output is the control signal u . Note that the control signal u is an input to the process and the output of the controller, and that the measured signal y is the output of the process and an input to the controller.

The feedback loop in Figure 11.1 is influenced by three external signals, the reference r , the load disturbance d and the measurement noise n . Any of the remaining signals can be of interest in controller design, depending on the particular application. Since the system is linear, the relations between the inputs and the interesting signals can be expressed in terms of the transfer functions. The following relations are obtained from the block diagram in Figure 11.1:

$$\begin{pmatrix} y \\ \eta \\ v \\ u \\ e \end{pmatrix} = \begin{pmatrix} \frac{PCF}{1+PC} & \frac{P}{1+PC} & \frac{1}{1+PC} \\ \frac{PCF}{1+PC} & \frac{P}{1+PC} & \frac{-PC}{1+PC} \\ \frac{CF}{1+PC} & \frac{1}{1+PC} & \frac{-C}{1+PC} \\ \frac{CF}{1+PC} & \frac{-PC}{1+PC} & \frac{-C}{1+PC} \\ \frac{F}{1+PC} & \frac{-P}{1+PC} & \frac{-1}{1+PC} \end{pmatrix} \begin{pmatrix} r \\ d \\ n \end{pmatrix}. \quad (11.1)$$

In addition, we can write the transfer function for the error between the reference

r and the output η (not an explicit signal in the diagram), which satisfies

$$\varepsilon = r - \eta = \left(1 - \frac{PCF}{1+PC}\right)r + \frac{-P}{1+PC}d + \frac{PC}{1+PC}n.$$

There are several interesting conclusions we can draw from these equations. First we can observe that several transfer functions are the same and that all of the important relations are given by the following set of six transfer functions, which we call the *Gang of Six*:

$$\begin{array}{ccc} \frac{PCF}{1+PC} & \frac{PC}{1+PC} & \frac{P}{1+PC} \\ \frac{CF}{1+PC} & \frac{C}{1+PC} & \frac{1}{1+PC} \end{array} \quad (11.2)$$

The transfer functions in the first column give the response of the process output and control signal to the setpoint. The second column contains the response of the control variable to load disturbance and noise and the final column gives the response of the process output to those two inputs. Notice that only four transfer functions are required to describe how the system reacts to load disturbances and the measurement noise, and that two additional transfer functions are required to describe how the system responds to setpoint changes.

The linear behavior of the system is determined by the six transfer functions in equation (11.2) and specifications can be expressed in terms of these transfer functions. The special case when $F = 1$ is called a system with (pure) error feedback. In this case all control actions are based on feedback from the error only and the system is completely characterized by four transfer functions, namely the four rightmost transfer functions in equation (11.2), which have specific names:

$$\begin{array}{ll} S = \frac{1}{1+PC} & \text{sensitivity function} \\ T = \frac{PC}{1+PC} & \text{complementary sensitivity function} \\ PS = \frac{P}{1+PC} & \text{load sensitivity function} \\ CS = \frac{C}{1+PC} & \text{noise sensitivity function} \end{array} \quad (11.3)$$

These transfer functions and their equivalent systems are called the *Gang of Four*. The load disturbance sensitivity function is sometimes called the input sensitivity function and the noise sensitivity function is sometimes called the output sensitivity function. These transfer functions have many interesting properties that will be discussed in detail in the rest of the chapter. Good insight into these properties is essential for understanding the performance of feedback systems both for the purpose of use and design.

Analyzing the Gang of Six we find that the feedback controller C influences the

the effects of load disturbances and measurement noise. Notice that measurement noise enters the process via the feedback. In Section 12.2 it will be shown that the controller influences the sensitivity of the closed loop to process variations. The feedforward part F of the controller only influences the response to command signals.

In Chapter 9 we focused on the loop transfer function and we found that its properties gave useful insight into the properties of a system. To make a proper assessment of a feedback system it is necessary to consider the properties of all transfer functions (11.2) in the Gang of Six or Gang of Four for error feedback, as illustrated in the following example.

Example 11.1 The loop transfer function only gives limited insight

Consider a process with the transfer function $P(s) = 1/(s - a)$ controlled by a PI controller with error feedback having the transfer function $C(s) = k(s - a)/s$. The loop transfer function is $L = k/s$, and the sensitivity functions are

$$\begin{aligned} T &= \frac{PC}{1+PC} = \frac{k}{s+k} & PS &= \frac{P}{1+PC} = \frac{s}{(s-a)(s+k)} \\ CS &= \frac{C}{1+PC} = \frac{k(s-a)}{s+k} & S &= \frac{1}{1+PC} = \frac{s}{s+k}. \end{aligned}$$

Notice that the factor $s - a$ is canceled when computing the loop transfer function and that this factor also does not appear in the sensitivity function or complementary sensitivity function. However, cancellation of the factor is very serious if $a > 0$ since the transfer function PS relating load disturbances to process output is then unstable. In particular, a small disturbance d can lead to an unbounded output, which is clearly not desirable. ∇

The system in Figure 11.1 represents a special case because it is assumed that the load disturbance enters at the process input and that the measured output is the sum of the process variable and measurement noise. Disturbances can enter in many different ways and the sensors may have dynamics. A more abstract way to capture the general case is shown in Figure 11.2, which only has two blocks representing the process (\mathcal{P}) and the controller (\mathcal{C}). The process has two inputs, the control signal u and a vector of disturbances w , and two outputs, the measured signal y and a vector of signals z that is used to specify performance. The system in Figure 11.1 can be captured by choosing $w = (d, n)$ and $z = (\eta, v, e, \varepsilon)$. The process transfer function \mathcal{P} is a 2×2 block matrix and the controller transfer function \mathcal{C} is a 1×2 block matrix; see Exercise 11.3. Processes with multiple inputs and outputs can also be considered by regarding u and y as vectors. Representations at these higher levels of abstraction are useful for the development of theory because they make it possible to focus on fundamentals and to solve general problems with a wide range of applications. However, care must be exercised to maintain the coupling to the real world control problems we intend to solve.

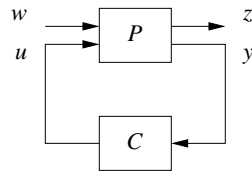


Figure 11.2: A more general representation of a feedback system. The process input u represents the control signal, which can be manipulated, and the process input w represents other signals that influence the process. The process output y is the measured variables and z are other interesting signals of interest.

11.2 FEEDFORWARD DESIGN

Most of our analysis and design tools up to this point have focused on the role of feedback and its effect on the dynamics of the system. Feedforward is a simple and powerful technique that complements feedback. It can be used both to improve the response to reference signals and to reduce the effect of measurable disturbances. Feedforward compensation admits perfect elimination of disturbances but it is much more sensitive than feedback. A general scheme for feedforward was discussed in Section 7.5 on page 219 using Figure 7.10. A simple form of feedforward for PID controllers was discussed in Section 10.5. The controller in Figure 11.1 also has a feedforward block to improve response to reference signals. An alternative version of feedforward is shown in Figure 11.3, which we will use in this section to understand some of the tradeoffs between feedforward and feedback.

Systems with two degrees of freedom (feedforward and feedback) have the advantage that the response to reference signals can be designed independently of the design for disturbance attenuation and robustness. We will first consider the response to reference signals and we will therefore initially assume that the load disturbance d is zero. Let F_m represent the ideal response of the system to reference signals. The feedforward compensator is characterized by the transfer functions F_u and F_m . When the set point is changed the transfer function F_u generates the signal

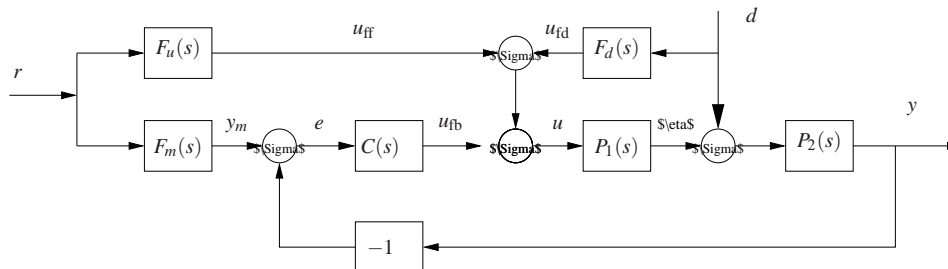


Figure 11.3: Block diagram of a system with feedforward compensation for improved response to reference signals and measured disturbances. Three feedforward elements are present: $F_m(s)$ sets the desired output value, $F_u(s)$ generates the feedforward command u_{ff} and $F_d(s)$ attempts to cancel disturbances.

u_{ff} , which is chosen to give the desired output when applied as input to the process. Under ideal conditions the output y is then equal to y_m , the error signal is zero and there will be no feedback action. If there are disturbances or modeling errors, the signal y_m and y will differ. The feedback then attempts to bring the error to zero.

To make a formal analysis we compute the transfer function from reference to process output

$$G_{yr}(s) = \frac{P(CF_m + F_u)}{1 + PC} = F_m + \frac{PF_u - F_m}{1 + PC}, \quad (11.4)$$

where $P = P_2P_1$. The first term represents the desired transfer function. The second term can be made small in two ways. Feedforward compensation can be used to make $PF_u - F_m$ small or feedback compensation can be used to make $1 + PC$ large. Perfect feedforward compensation is obtained by choosing

$$F_m = PF_u. \quad (11.5)$$

Notice the different character of feedback and feedforward. With feedforward we attempt to match two transfer functions, and with feedback we attempt to make the error small by dividing it by a large number. For a controller having integral action, the loop gain is large for small frequencies and it is thus sufficient to make sure that the condition for ideal feedforward holds at higher frequencies. This is easier than trying to satisfy the condition (11.5) for all frequencies.

We will now consider reduction of effects of the load disturbance d in Figure 11.3. We consider the case where we are able to measure the disturbance signal and assume that the disturbance enters the process dynamics in a known way (captured by P_1 and P_2). The effect of the disturbance can be reduced by feeding the measured signal through a dynamical system with the transfer function F_d . Assuming that the reference r is zero, we can use block diagram algebra to find that the transfer function from disturbance to process output is

$$G_{yd} = \frac{P_2(1 + F_dP_1)}{1 + PC}, \quad (11.6)$$

where $P = P_1P_2$. The effect of the disturbance can be reduced by making $1 - F_dP_1$ small (feedforward) or by making $1 + PC$ large (feedback). Perfect compensation is obtained by choosing

$$F_d = -P_1^{-1}. \quad (11.7)$$

Notice that the feedforward disturbance compensator is the inverse of the transfer function P_1 , requiring precise knowledge of the process dynamics.

As in the case of reference tracking, disturbance rejection can be accomplished by combining Feedback and feedforward controllers. Since low frequency disturbances can be effectively eliminated by feedback we only require the use of feedforward for high frequency disturbances, and the transfer function F_d in equation (11.7) can then be computed using an approximation of P_1 for high frequencies.

Equations (11.5) and (11.7) give analytic expressions for the feedforward compensator. To obtain a transfer function that can be implemented without difficulties

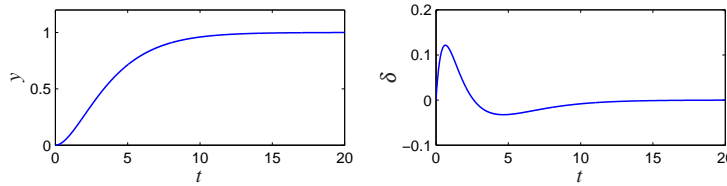


Figure 11.4: Feedforward control for vehicle steering. Lateral deviation y and steering angle δ for smooth lane change control using feedforward.

we require that the feedforward compensator is stable and that it does not require differentiation. Therefore there may be constraints on possible choices of the desired response F_m and approximations are needed if the process has zeros in the right half plane.

Example 11.2 Vehicle steering

A linearized model for vehicle steering was given in Example 6.4. The normalized transfer function from steering angle to lateral deviation is

$$P(s) = \frac{\gamma s + 1}{s^2}.$$

For a lane transfer system we would like to have a nice response without overshoot and we therefore choose the desired response as

$$F_m = \frac{a^2}{(s + a)^2},$$

where the response speed or aggressiveness of the steering is governed by the parameter a . Equation (11.5) gives

$$F_u = \frac{F_m}{P} = \frac{a^2 s^2}{(\gamma s + 1)(s + a)^2},$$

which is a stable transfer function as long as $\gamma > 0$. Figure 11.4 shows the responses of the system for $a = 1.5$. The figure shows that a lane change is accomplished in about 10 vehicle lengths with smooth steering angles. The largest steering angle is a little bit more than 0.1 rad (6 deg). Using the scaled variables the curve showing lateral deviations can also be interpreted as the vehicle path with vehicle length as the length unit. ∇

A major advantage of controllers with two degrees of freedom that combine feedback and feedforward is that the control design problem can be split in two parts. The feedback controller C can be designed to give good robustness and effective disturbance attenuation and the feedforward part can be designed independently to give the desired response to command signals.

11.3 PERFORMANCE SPECIFICATIONS

A key element of the control design process is how we specify the desired performance of the system. It is also important for users to understand performance specifications so that they know what to ask for and how to test a system. Specifications are often given in terms of robustness to process variations and responses to reference signals and disturbances. They can be given both in terms of time and frequency responses. Specifications on the step response to reference signals was given in Figure 5.9 in Section 5.3 and in Section 6.3. Robustness specifications based on the loop transfer function and the sensitivity functions were discussed in Section 9.3 and will be discussed more in Chapter 12. The specifications discussed previously were based on the loop transfer function. Since we found in Section 11.1 that a single transfer functions did not always characterize the properties of the closed loop completely we will give a more complete discussion of specifications in this section, based on the full Gang of Six.

The transfer function gives a good characterization of the linear behavior of a system. To give specifications is desirable to capture the characteristic properties of a system with a few parameters. Common features for time responses are overshoot, rise time and settling time, as shown in Figure 5.9 on page 151. Common features of frequency responses are resonance peak, peak frequency, crossover frequency and bandwidth. The crossover frequency is defined as the frequency where the gain is equal to the low frequency gain for low-pass systems or the high frequency gain for high-pass systems. The bandwidth is defined as the frequencies where the gain is $1/\sqrt{2}$ of the low frequency (low-pass), mid frequency (band-pass) or high frequency gain (high-pass). There are interesting relations between specifications in the time and frequency domain. Roughly speaking, the behavior of time responses for short times is related to behavior of frequency responses at high frequencies and vice versa. The precise relations are not trivial to derive.

Response to Reference Signals

Consider the basic feedback loop in Figure 11.1. The response to reference signals is described by the transfer functions $G_{yr} = PCF/(1 + PC)$ and $G_{ur} = CF/(1 + PC)$ ($F = 1$ for systems with error feedback). Notice that it is useful to consider both the response of the output and that of the control signal. In particular, the control signal response allows us to judge the magnitude and rate of the control signal required to obtain the output response.

The time response of process output can be characterized by rise time T_r , overshoot M_p and settling time T_s . The response of the control signal can be characterized by the largest value of the control signal or the overshoot. The frequency response G_{yr} can be characterized by the resonance peak M_r , the largest value of the frequency response; the peak frequency ω_{mr} , the frequency where the maximum occurs; and the bandwidth ω_b , the frequency where the gain has decreased to $1/\sqrt{2}$. The transfer function G_{ur} can be characterized by the largest value of $|G_{ur}(i\omega)|$.

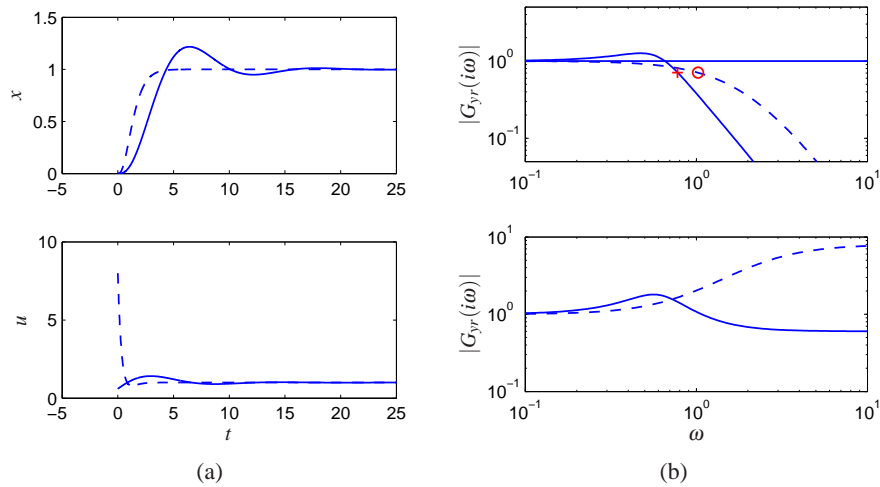


Figure 11.5: Reference signal responses. The responses in process output y and control signal u to a unit step in the reference signal r is shown in (a) and the gain curves of G_{yr} and G_{ur} are shown in (b). Results with PI control with error feedback are shown in full lines, the dashed lines show results for a controller with a feedforward compensator.

Example 11.3 Response to reference signals

Consider a process with the transfer function $P(s) = (s + 1)^{-3}$ and a PI controller with error feedback having the gains $k_p = 0.6$ and $k_i = 0.5$. The responses are illustrated in Figure 11.5. The full lines show results for a PI controller with error feedback. The dashed lines show results for a controller with feedforward designed to give the transfer function $G_{yr} = (0.5s + 1)^{-3}$. Looking at the time responses we find that the controller with feedforward gives a faster response with no overshoot. However, much larger control signals are required to obtain the fast response. The largest value of the control signal is 8 compared to 1.2 for the regular PI controller. The controller with feedforward has a larger bandwidth (marked with \circ) and no resonance peak. The transfer function G_{ur} also has higher gain at high frequencies.

▽

Response to Load Disturbances and Measurement Noise

A simple criterion for disturbance attenuation is to compare the output of the closed loop system in Figure 11.1 with the output of the corresponding open loop system obtained by setting $C = 0$. If we let the disturbances for the open and closed loop systems be identical, the output of the closed loop system is then obtained simply by passing the open loop output through a system with the transfer function S . The sensitivity function tells how the variations in the output are influenced by feedback (Exercise 11.6). Disturbances with frequencies such that $|S(i\omega)| < 1$ are attenuated but disturbances with frequencies such that $|S(i\omega)| > 1$ are amplified by feedback. The maximum sensitivity M_s , which occurs at the sensitivity crossover frequency ω_{sc} , is thus a measure of the largest amplification of

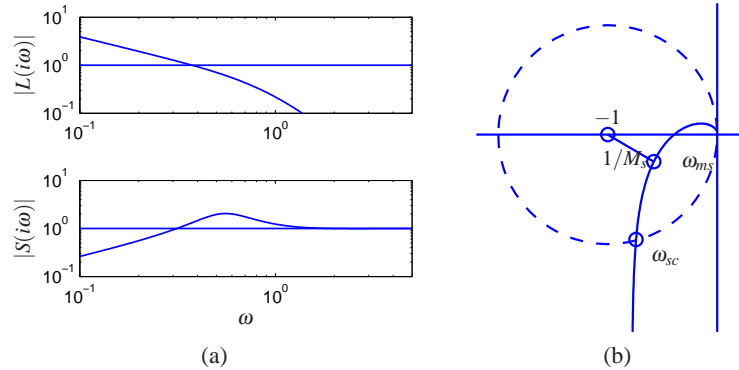


Figure 11.6: Graphical interpretation of the sensitivity function. Gain curves of the loop transfer function and the sensitivity function on the right (a) can be used to calculate the properties of the sensitivity function through the relation $S = 1/(1 + L)$. The sensitivity crossover frequency ω_{sc} and the frequency ω_{ms} where the sensitivity has its largest value are indicated in the figure. All points inside the dashed circle have sensitivities greater than 1.

the disturbances. The maximum magnitude of $1/(1 + L)$ is also the minimum of $|1 + L|$, which is precisely the stability margin s_m defined in Section 9.3, so that $M_s = 1/s_m$. The maximum sensitivity is therefore also a robustness measure.

If the sensitivity function is known, the potential improvements by feedback can be evaluated simply by recording a typical output and filtering it through the sensitivity function. A plot of the gain curve of the sensitivity function is a good way to make an assessment of disturbance attenuation. Since the sensitivity function only depends on the loop transfer function its properties can also be visualized graphically using the Nyquist plot of the loop transfer function. This is illustrated in Figure 11.6. The complex number $1 + L(i\omega)$ can be represented as the vector from the point -1 to the point $L(i\omega)$ on the Nyquist curve. The sensitivity is thus less than one for all points outside a circle with radius 1 and center at -1 . Disturbances with frequencies in this range are attenuated by the feedback.

The transfer function G_{yd} from load disturbance d to process output y for the system in Figure 11.1 is

$$G_{yd} = \frac{P}{1 + PC} = PS = \frac{T}{C}. \quad (11.8)$$

Since load disturbances typically have low frequencies, it is natural to focus on the behavior of the transfer function at low frequencies. For a system with $P(0) \neq 0$ and a controller with integral action, the controller gain goes to infinity for small frequencies and we have the following approximation for small s :

$$G_{yd} = \frac{T}{C} \approx \frac{1}{C} \approx \frac{s}{k_i}, \quad (11.9)$$

where k_i is the integral gain. Since the sensitivity function S goes to 1 for large s we have the approximation $G_{yd} \approx P$ for high frequencies.

Measurement noise, which typically has high frequencies, generates rapid vari-

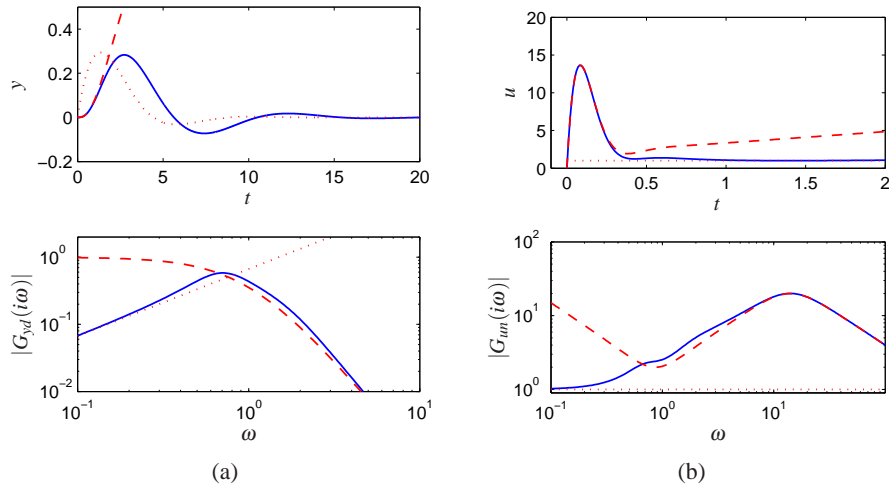


Figure 11.7: Disturbance responses. Time and frequency responses of process output y to load disturbance d are shown in (a) and responses of the control signal u to measurement noise d are shown in (b). The low frequency approximation is shown with dotted lines and the high frequency approximations by dashed lines.

ations in the control variable that are detrimental because they cause wear in many actuators and can even saturate an actuator. It is thus important to keep the variations in the control signal due to measurement noise at reasonable levels—a typical requirement is that the variations are only a fraction of the span of the control signal. The variations can be influenced by filtering and by proper design of the high frequency properties of the controller.

The effects of measurement noise are captured by the transfer function from measurement noise to the control signal,

$$-G_{un} = \frac{C}{1 + PC} = CS = \frac{T}{P}. \quad (11.10)$$

For low frequencies the complementary sensitivity function equals 1 and G_{un} can be approximated by $1/P$. For high frequencies PC is small and G_{un} can be approximated as $G_{un} \approx C$.

Example 11.4 Response to disturbances

Consider a process with the transfer function $P(s) = (s + 1)^{-3}$ and a PID controller with gains $k_p = 0.6$, $k_i = 0.5$ and $k_d = 2.0$. We augment the controller with a second order noise filter with $T_f = 0.1$ so that its transfer function is

$$C(s) = \frac{k_d s^2 + k_s s + k_i}{s(s^2 T_f^2 / 2 + s T_f + 1)}.$$

The system responses are illustrated in Figure 11.7. The response to a step in the load disturbance in the top part of Figure 11.7a has a peak of 0.28 at time $t = 2.73$, and the initial part of the response is well captured by the high frequency approx-

imation $G_{yd} \approx P$ (dashed). The magnitude of the peak is also well approximated by the low frequency approximation $G_{yd} \approx 1/C$ (dotted), but the peak time is not. The frequency response in Figure 11.7a shows that the gain has a maximum 0.58 at $\omega = 0.7$. The figure shows that the gain curve is well captured by the approximations.

The response of the control signal to a step in measurement noise is shown in Figure 11.7b. The high frequency roll-off of the transfer function $G_{un}(i\omega)$ is due to filtering; without that the gain curve in Figure 11.7b would continue to rise after 20 rad/s. The step response has a peak of 13 at $t = 0.08$ which is well captured by the high frequency approximation (dashed). The frequency response has its peak 20 at $\omega = 14$, which is also well captured by the high frequency approximation (dashed). Notice that the peak occurs far above the peak of the response to load disturbances and far above the gain crossover frequency $\omega_{gc} = 0.78$. An approximation derived in Exercise 11.9 gives $\max |CS(i\omega)| \approx k_d/T_f = 20$ which occurs at $\omega = \sqrt{2}/T_d = 14.1$. ∇

11.4 FEEDBACK DESIGN VIA LOOP SHAPING

One advantage of the Nyquist stability theorem is that it is based on the loop transfer function, which is related to the controller transfer function through $L = PC$. It is thus easy to see how the controller influences the loop transfer function. To make an unstable system stable we simply have to bend the Nyquist curve away from the critical point.

This simple idea is the basis of several different design methods, collectively called *loop shaping*. The methods are based on choosing a compensator that gives a loop transfer function with a desired shape. One possibility is to determine a loop transfer function that gives a closed loop system with the desired properties and to compute the controller as $C = L/P$. Another is to start with the process transfer function change its gain and then add poles and zeros until the desired shape is obtained. In this section we will explore different loop shaping methods for control law design.

Design Considerations

We will first discuss a suitable shape of the loop transfer function that gives good performance and good stability margins. Figure 11.8 shows a typical loop transfer function. Good robustness requires good stability margins (or good gain and phase margins) which imposes requirements on the loop transfer function around the crossover frequencies ω_{pc} and ω_{gc} . The gain of L at low frequencies must be large in order to have good tracking of command signals and good rejection of low frequency disturbances. Since $S = 1/(1+L)$ it follows that for frequencies where $|L| > 100$ disturbances will be attenuated by a factor of 100 and the tracking error is less than 1%. It is therefore desirable to have a large crossover frequency and

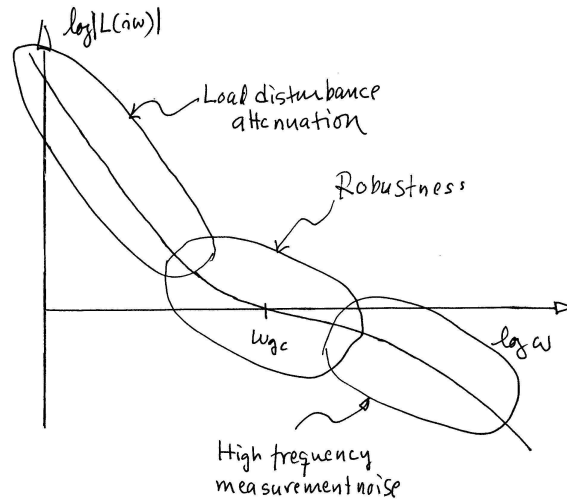


Figure 11.8: Gain curve of the Bode plot for a typical loop transfer function. The gain crossover frequency ω_{gc} and the slope n_{gc} of the gain curve at crossover are important parameters that determine the robustness of the closed loop systems. At low frequency, a large magnitude for L provides good load disturbance rejection and reference tracking, while at high frequency a small loop gain is used to avoid amplifying measurement noise.

a steep (negative) slope of the gain curve. The gain at low frequencies can be increased by a controller with integral action which is also called *lag compensation*. To avoid injecting too much measurement noise into the system it is desirable that the loop transfer function have a low gain at frequencies high frequencies *high frequency roll-off*. The choice of gain crossover frequency is a compromise between attenuation of load disturbances, injection of measurement noise and robustness.

Bode's relations (see Section 9.4) impose restrictions on the shape of the loop transfer function. Equation (9.8) implies that the slope of the gain curve at gain crossover cannot be too steep. If the gain curve is constant slope, we have the following relation between slope n_{gc} and phase margin ϕ_m :

$$n_{gc} = -2 + \frac{2\phi_m}{\pi} [\text{rad}] = -180^\circ + \phi_m [\text{deg}]. \quad (11.11)$$

This formula is a reasonable approximation when the gain curve does not deviate too much from a straight line. It follows from equation (11.11) that the phase margins 30° , 45° and 60° correspond to the slopes $-5/3$, $-3/2$ and $-4/3$.

Loop shaping is a trial and error procedure. We typically start with a Bode plot of the process transfer function. We then attempt to shape the loop transfer function by changing controller gain and adding poles and zeros of the controller. Different performance specifications are evaluated for each controller as we attempt to balance many different requirements by adjusting controller parameters and complexity. Loop shaping is straightforward to apply to single-input, single output systems. It can also be applied to systems with one input and many outputs by closing the loops one at a time starting with the innermost loop. The only

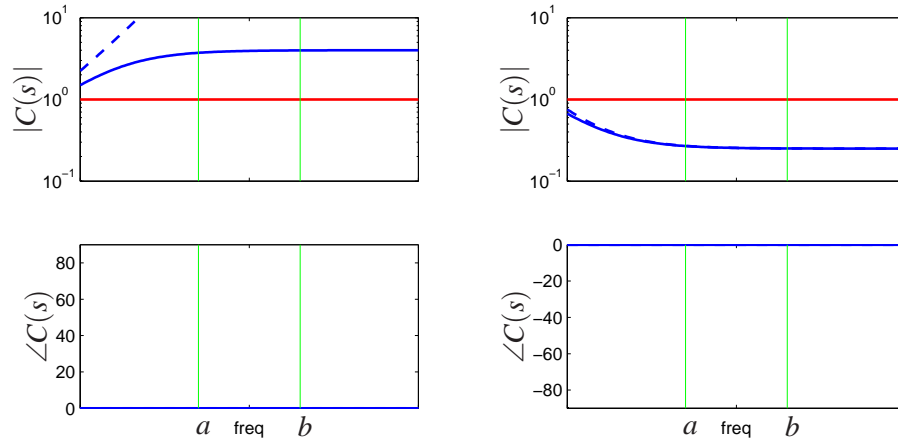


Figure 11.9: Frequency response for lead and lag compensators, $C(s) = k(s+a)/(s+b)$. Lead compensation occurs when $a < b$ (left) and provides phase lead between $\omega = a$ and $\omega = b$. Lag compensation corresponds to $a > b$ and provides low frequency gain. PI control is a special case of lag compensation and PD control is a special case of lead compensations. PI/PD frequency responses are shown in dashed curves.

limitation for minimum phase systems is that large phase leads and high controller gains may be required to obtain closed loop systems with fast response. Many specific procedures are available: they all require experience but they also give a good insight into the conflicting requirements. There are fundamental limitations to what can be achieved for systems that are not minimum phase; they will be discussed in the next section.

Lead and Lag Compensation

A simple way to do loop shaping is to start with the transfer function of the process and to add simple compensators with the transfer function

$$C(s) = k \frac{s+a}{s+b}. \quad (11.12)$$

The compensator is called a lead compensator if $a < b$ and a lag compensator if $a > b$. The PI controller is a special case of lag compensator with $b = 0$ and the ideal PD controller is a special case of a lead compensator with $a = 0$. Bode plots of lead and lag compensators are shown in Figure 11.9. Lag compensation increases the gain at low frequencies. It is typically used to improve tracking performance and disturbance attenuation at low frequencies. The following example gives an illustration.

Example 11.5 Atomic force microscope in tapping mode

A simple model of the dynamics of the vertical motion of an atomic force microscope in tapping mode was given in Exercise 9.1. The transfer function for the

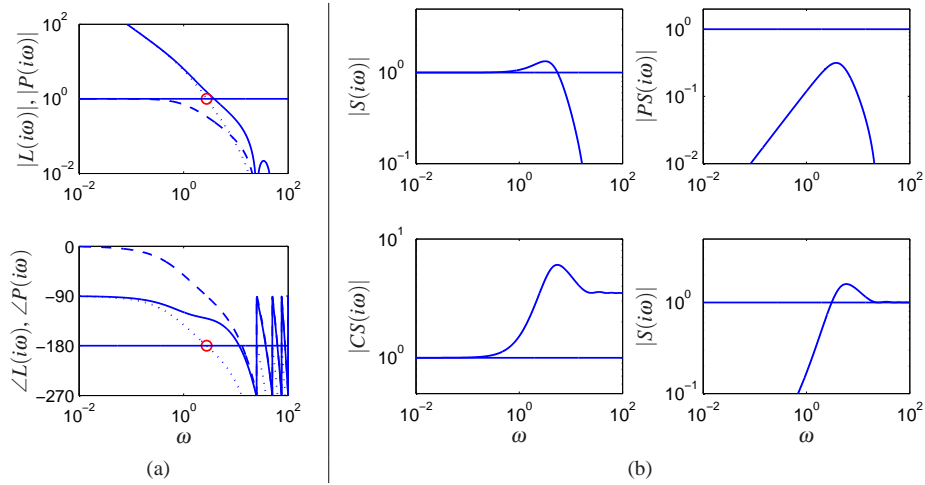


Figure 11.10: Loop shaping design of a controller for an atomic force microscope in tapping mode. Figure 11.5 shows Bode plots of the process (dashed), the loop transfer function with an integral controller with critical gain (dotted) and a PI controller adjusted to give reasonable robustness. Figure 11.5 shows the gain curves for the Gang of Four for the system.

system dynamics is

$$P(s) = \frac{a(1 - e^{-s\tau})}{s\tau(s + a)}.$$

where $a = \zeta\omega_0$, and $\tau = 2\pi n/\omega_0$ and the gain has been normalized to 1. A Bode plot of this transfer function for the parameters $a = 1$ and is shown in dashed curves in Figure 11.5. To improve attenuation of load disturbances we increase the low frequency gain by introducing an integrating controller. The loop transfer function then becomes $L = k_i P(s)/s$ and we adjust the gain so that the phase margin is zero, giving $k_i = 8.3$. Notice the increase of the gain at low frequencies. The Bode plot is shown by the dotted line in Figure 11.5 where the critical point is indicated by \circ . To improve the phase margin we introduce proportional action and we increase the proportional gain k_p gradually until reasonable values of the sensitivities are obtained. The value $k_p = 3.5$ gives $M_s = 1.6$ and $M_t = 1.3$. The loop transfer function is shown in full lines in Figure 11.5. Notice the significant increase of the phase margin compared with the purely integrating controller (dotted line).

To evaluate the design we also compute the gain curves of the transfer functions in the Gang of Four. They are shown in Figure 11.5. The peak of the sensitivity curves are reasonable and the plot of PS shows that the largest value of PS is 0.3 which implies that load disturbances are well attenuated. The plot of CS shows that the largest controller gain is 6. The controller has a gain of 3.5 at high frequencies and hence we may consider adding high frequency roll-off. ∇

A common problem in design of feedback systems is that the phase lag of the system at the desired crossover frequency is not high enough to allow either

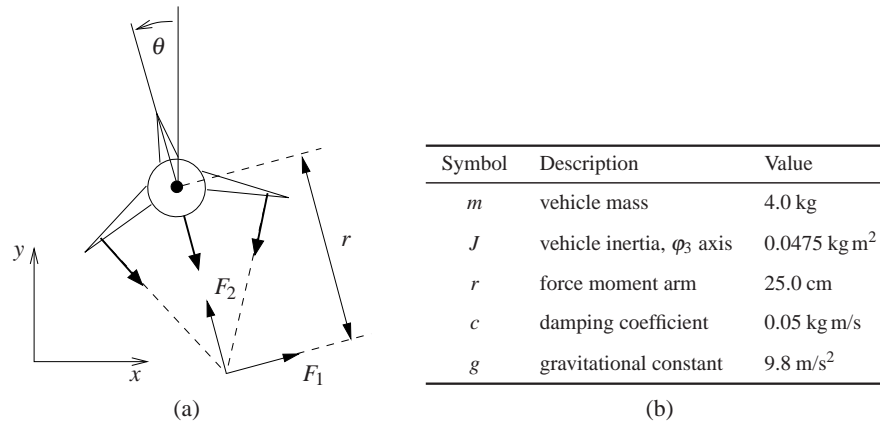


Figure 11.11: Roll control of a vectored thrust aircraft. The roll angle θ is controlled by applying maneuvering thrusters, resulting in a moment generated by F_2 . The table to the right lists the parameter values for a laboratory version of the system.

proportional or integral feedback to be used effectively. Instead, one may have a situation where you need to add phase *lead* to the system, so that the crossover frequency can be increased.

A standard way to accomplish this is to use a *lead compensator*, which has the form

$$C(s) = k \frac{s+a}{s+b} \quad a < b. \quad (11.13)$$

A key feature of the lead compensator is that it adds phase *lead* in the frequency range between the pole/zero pair (and extending approximately 10X in frequency in each direction). By appropriately choosing the location of this phase lead, we can provide additional phase margin at the gain crossover frequency.

Because the phase of a transfer function is related to the slope of the magnitude, increasing the phase requires increasing the gain of the loop transfer function over the frequency range in which the lead compensation is applied. Hence we can also think of the lead compensator as changing the slope of the transfer function and thus shaping the loop transfer function in the crossover region (although it can be applied elsewhere as well).

Example 11.6 Roll control for a vectored thrust aircraft

Consider the control of the roll of a vectored thrust aircraft, such as the one illustrated in Figure 11.11. Following Exercise 8.9, we model the system with a second order transfer function of the form

$$P(s) = \frac{r}{Js^2 + cs},$$

with the parameters given in Figure 11.11b. We take as our performance specification that we would like less than 1% error in steady state and less than 10% tracking error up to 10 rad/sec.

The open loop transfer function is shown in Figure 11.12a. To achieve our

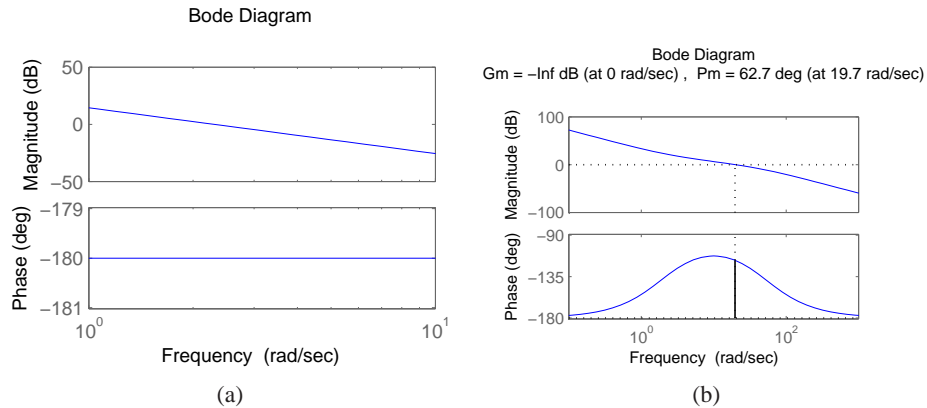


Figure 11.12: Control design for a vectored thrust aircraft using lead compensation. The Bode plot for the open loop process P is shown on the left and the loop transfer function $L = PC$ using a lead compensator on the right. Note the phase lead in the crossover region near $\omega = 100$ rad/s.

performance specification, we would like to have a gain of at least 10 at a frequency of 10 rad/sec, requiring the gain crossover frequency to be at a higher frequency. We see from the loop shape that in order to achieve the desired performance we cannot simply increase the gain, since this would give a very low phase margin. Instead, we must increase the phase at the desired crossover frequency.

To accomplish this, we use a lead compensator (11.13) with $a = 2$ and $b = 50$. We then set the gain of the system to provide a large loop gain up to the desired bandwidth, as shown in Figure 11.12b. We see that this system has a gain of greater than 10 at all frequencies up to 10 rad/sec and that it has over 60° degrees of phase margin. ∇

The action of a lead compensator is essentially the same as that of the derivative portion of a PID controller. As described in Section 10.5, we often use a filter for the derivative action of a PID controller to limit the high frequency gain. This same effect is present in a lead compensator through the pole at $s = b$.

Equation (11.13) is a first order lead compensator and can provide up to 90° of phase lead. Higher levels of phase lead can be provided by using a second order lead compensator:

$$C(s) = k \frac{(s+a)^2}{(s+b)^2} \quad a < b.$$

11.5 FUNDAMENTAL LIMITATIONS

Although loop shaping gives us a great deal of flexibility in designing the closed loop response of a system, there are certain fundamental limits on what can be achieved. We consider here some of the primary performance limitations that can occur due to difficult dynamics; additional limitations having to do with robustness

are considered in the next chapter.

Right Half Plane Poles and Zeros and Time Delays

There are linear systems that are inherently difficult to control. The limitations are related to poles and zeros in the right half plane and time delays. To explore the limitations caused by poles and zeros in the right half plane we factor the process transfer function as

$$P(s) = P_{mp}(s)P_{ap}(s), \quad (11.14)$$

where P_{mp} is the minimum phase part and P_{ap} is the non-minimum phase part. The factorization is normalized so that $|P_{ap}(i\omega)| = 1$ and the sign is chosen so that P_{ap} has negative phase. The transfer function P_{ap} is called an *all-pass system* because it has unit gain for all frequencies. Requiring that the phase margin is φ_m we get

$$\arg L(i\omega_{gc}) = \arg P_{ap}(i\omega_{gc}) + \arg P_{mp}(i\omega_{gc}) + \arg C(i\omega_{gc}) \geq -\pi + \varphi_m, \quad (11.15)$$

where C is the controller transfer function. Let n_{gc} be the slope of the gain curve at the crossover frequency. Since $|P_{ap}(i\omega)| = 1$ it follows that

$$n_{gc} = \left. \frac{d \log |L(i\omega)|}{d \log \omega} \right|_{\omega=\omega_{gc}} = \left. \frac{d \log |P_{mp}(i\omega)C(i\omega)|}{d \log \omega} \right|_{\omega=\omega_{gc}}.$$

Assuming that the slope n_{gc} is negative it has to be larger than -2 for the system to be stable. It follows from Bode's relations, equation (9.8), that

$$\arg P_{mp}(i\omega) + \arg C(i\omega) \approx n_{gc} \frac{\pi}{2}.$$

Combining this with equation (11.15) gives the following inequality for the allowable phase lag

$$-\arg P_{ap}(i\omega_{gc}) \leq \pi - \varphi_m + n_{gc} \frac{\pi}{2} =: \varphi_l. \quad (11.16)$$

This condition, which we call the *crossover frequency inequality*, shows that the gain crossover frequency must be chosen so that the phase lag of the non-minimum phase component is not too large. For systems with high robustness requirements we may choose a phase margin of 60° ($\varphi_m = \pi/3$) and a slope $n_{gc} = -1$, which gives an admissible phase lag $\varphi_l = \pi/6 = 0.52$ rad (30°). For systems where we can accept a lower robustness we may choose a phase margin of 45° ($\varphi_m = \pi/4$) and the slope $n_{gc} = -1/2$, which gives an admissible phase lag $\varphi_l = \pi/2 = 1.57$ rad (90°).

The crossover frequency inequality shows that non-minimum phase components impose severe restrictions on possible crossover frequencies. It also means that there are systems that cannot be controlled with sufficient stability margins. The conditions are more stringent if the process has an uncertainty $\Delta P(i\omega_{gc})$, as we shall see in the next chapter. We illustrate the limitations in a number of commonly encountered situations.

Example 11.7 Zero in the right half plane

The non-minimum phase part of the process transfer function for a system with a right half plane zero is

$$P_{ap}(s) = \frac{z-s}{z+s},$$

where $z > 0$. The phase lag of the non-minimum phase part is

$$-\arg P_{ap}(i\omega) = 2 \arctan \frac{\omega}{z}.$$

Since the phase of P_{ap} decreases with frequency, the inequality (11.16) gives the following bound on the crossover frequency:

$$\omega_{gc} < z \tan(\varphi_l/2). \quad (11.17)$$

With $\varphi_l = \pi/3$ we get $\omega_{gc} < 0.6a$. Slow zeros (z small) therefore give stricter restrictions on possible gain crossover frequencies than fast zeros. ∇

Time delays also impose limitations similar to those given by zeros in the right half plane. We can understand this intuitively from the approximation

$$e^{-s\tau} \approx \frac{1-s\tau}{1+s\tau}.$$

Example 11.8 Pole in the right half plane

The non-minimum phase part of the transfer function for a system with a pole in the right half plane is

$$P_{ap}(s) = \frac{s+p}{s-p},$$

where $p > 0$. The phase lag of the non-minimum phase part is

$$\varphi_l = -\arg P_{ap}(i\omega) = 2 \arctan \frac{p}{\omega}$$

and the crossover frequency inequality becomes

$$\omega_{gc} > \frac{p}{\tan(\varphi_l/2)}. \quad (11.18)$$

Right half plane poles thus require that the closed loop system have sufficiently high bandwidth. With $\varphi_l = \pi/3$ we get $\omega_{gc} > 1.7p$. Fast right half plane poles (p large) therefore gives stricter restrictions on possible gain crossover frequencies than slow poles. Control of unstable systems imposes requirements for process actuators and sensors. ∇

Since a zero in the right half plane gives an upper limit to the achievable gain crossover frequency it follows that zeros far to the right give small limitations but that zeros close to the origin imposes severe limitations. The situation with right half plane poles is different because a pole imposes a lower limit to the gain crossover frequency and poles far to the right require systems with a high gain

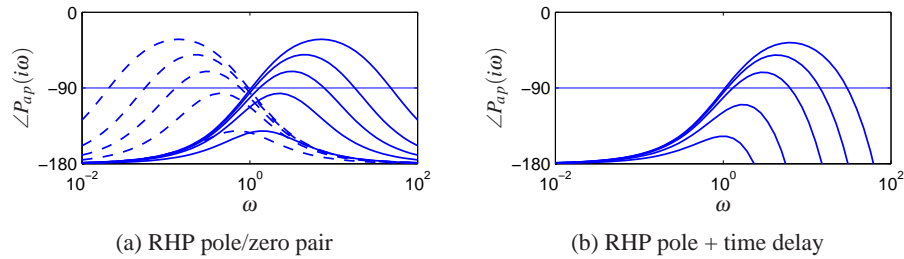


Figure 11.13: Example limitations due to the crossover frequency inequality. The figure illustrates limitations by showing the phase of the minimum phase factor P_{ap} of transfer functions. All systems have a right half plane pole at $s = 1$. The system in (a) has zeros at $s = 2, 5, 10, 20$ and 50 (full lines) and at $s = 0.5, 0.02, 0.1, 0.05$ and 0.02 (dashed lines). The system in (b) has time delays $\tau = 0.05, 0.1, 0.2, 0.5$ and 1 .

crossover frequency. It can thus be expected that systems with poles and zeros cannot be controlled robustly if the poles and zeros are too close.

A straightforward way to use the crossover frequency inequality is to plot the phase of the non-minimum phase factor P_{ap} of the process transfer function. Such a plot will immediately show the permissible gain crossover frequencies. An illustration is given in Figure 11.13 which shows the phase of P_{ap} for systems with a right half plane pole-zero pair and systems with a right half plane pole and a time delay. If we require that the phase lag φ_l of the nonminimum phase factor should be less than 90 deg we must require that the ratio z/p is larger than 6 or smaller than $1/6$ for system with right half plane poles and zeros and that the product $p\tau$ is less than 0.15 for systems with a time delay and a right half plane pole. Notice the symmetry in the problem for $z > p$ and $z < p$: in either case the zeros and the poles must be sufficiently far apart (Exercise 11.11). Also notice that possible values of the gain crossover frequency ω_{gc} are quite limited.

As the examples above show, right half plane poles and zeros significantly limit the achievable performance of a system, hence one would like to avoid these whenever possible. The poles of a system depend on the intrinsic dynamics of the system and are given by the eigenvalues of the dynamics matrix A of a linear system. Sensors and actuators have no effect on the poles; the only way to change poles is to redesign the system. Notice that this does not imply that unstable systems should be avoided. Unstable system may actually have advantages; one example is high performance supersonic aircraft.

The zeros of a system depend on the how sensors and actuators are coupled to the states. The zeros depend on all the matrices A, B, C and D in a linear system. The zeros can thus be influenced by moving sensors and actuators or by adding sensors and actuators. Notice that a fully actuated system $B = I$ does not have any zeros.

Example 11.9 Balance system

As an example of a system with both right half plane poles and zeros, consider the

balance system with zero damping, whose dynamics are given by

$$H_{\theta F} = \frac{ml}{-(M_t J_t - m^2 l^2) s^2 + mgl M_t}$$

$$H_{pF} = \frac{-J_t s^2 + mgl}{s^2 (-(M_t J_t - m^2 l^2) s^2 + mgl M_t)}.$$

Assume that we want to stabilize the pendulum by using the cart position as the measured signal. The transfer function from the input force F to the cart position p has poles $\{0, 0, \pm \sqrt{mgl M_t / (M_t J_t - m^2 l^2)}\}$ and zeros $\{\pm \sqrt{mgl / J_t}\}$. Using the parameters in Example 6.7, the right half plane pole is at $p = 2.68$ and the zero is at $z = 2.09$. The pole is so close to the zero that the system cannot be controlled robustly. Using Figure 11.13, we see that the amount of achievable phase margin for the system is very small if we desire a bandwidth in the range of 2–4 rad/s.

The right half plane zero of the system can be eliminated by changing the output of the system. For example, if we choose the output to correspond to a position at a distance r along the pendulum, we have $y = p - r \sin \theta$ and the transfer function for the linearized output becomes

$$H_{y,F} = H_{pF} - r H_{\theta F} = \frac{(mlr - J_t) s^2 + mgl}{s^2 (-(M_t J_t - m^2 l^2) s^2 + mgl M_t)}.$$

If we choose r sufficiently large then $mlr - J_t > 0$ and we eliminate the right half plane zero, obtaining instead two pure imaginary zeros. Note that $J_t = J + ml^2$ and so if the inertia of the pendulum J is nonzero then $mlr - J_t > 0$ requires $r > l$, indicating that our output must correspond to a point above the center of mass of the pendulum.

If we choose r such that $mlr - J_t > 0$ then the gain crossover frequency inequality is based just on the right half plane pole (Example 11.8). If our desired phase lag is $\varphi_l = 45^\circ$ then our gain crossover must satisfy

$$\omega_{gc} > \frac{p}{\tan \varphi_l / 2} = 2.68.$$

Assuming that our actuators have sufficiently high bandwidth, say a factor of 10 above ω_{gc} or roughly 4 Hz, then we can provide robust tracking up to this frequency.

▽

Bode's Integral Formula

In addition to providing adequate phase margin for robust stability, a typical control design will have to satisfy performance conditions on the sensitivity functions (Gang of Four). In particular the sensitivity function $S = 1/(1 + PC)$ represents disturbance attenuation and also relates the tracking error e to the reference signal: we usually want the sensitivity to be small over the range of frequencies where we want small tracking error and good disturbance attenuation. A basic problem is to

investigate if S can be made small over a large frequency range. We will start by investigating an example.

Example 11.10 System that admits small sensitivities

Consider a closed loop system consisting of a first order process and a proportional controller. Let the loop transfer function be

$$L(s) = PC = \frac{k}{s+1},$$

where parameter k is the controller gain. The sensitivity function is

$$S(s) = \frac{s+1}{s+1+k}$$

and we have

$$|S(i\omega)| = \sqrt{\frac{1+\omega^2}{1+2k+k^2+\omega^2}}.$$

This implies that $|S(i\omega)| < 1$ for all finite frequencies and that the sensitivity can be made arbitrary small for any finite frequency by making k sufficiently large. ∇

The system in Example 11.10 is unfortunately an exception. The key feature of the system is that the Nyquist curve of the process is completely contained in the right half plane. Such systems are called *positive real*. For these systems the Nyquist curve never enters the unit disk centered at -1 (the region is shown in Figure 11.6) where the sensitivity is greater than one.

For typical control systems there are unfortunately severe constraints on the sensitivity function. The following theorem, due to Bode, provides insights into the limits of performance under feedback.

Theorem 11.1 (Bode's integral formula). *Let $S(s)$ be the sensitivity function for a feedback system and assume that it goes to zero faster than $1/s$ for large s . If the loop transfer function has poles p_k in the right half plane then the sensitivity function satisfies the following integral:*

$$\int_0^\infty \log |S(i\omega)| d\omega = \int_0^\infty \log \frac{1}{|1+L(i\omega)|} d\omega = \pi \sum p_k. \quad (11.19)$$

Equation (11.19) implies that there are fundamental limitations to what can be achieved by control and that control design can be viewed as a redistribution of disturbance attenuation over different frequencies. In particular, this equation shows that if the sensitivity function is made smaller for some frequencies it must increase at other frequencies so that the integral of $\log |S(i\omega)|$ remains constant. This means that if disturbance attenuation is improved in one frequency range it will be worse in another, a property sometime referred to as the *waterbed effect*. It also follows that systems with open loop poles in the right half plane have larger overall sensitivity than stable systems.

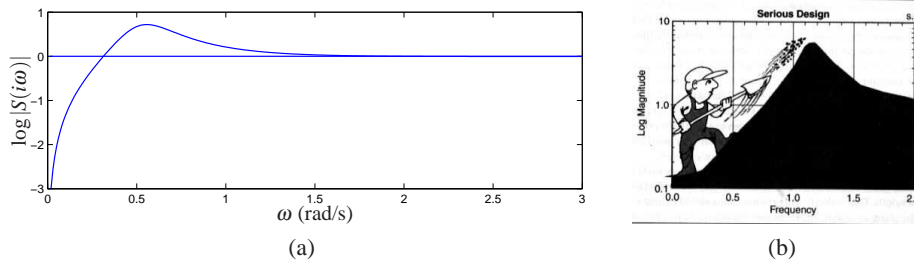


Figure 11.14: Interpretation of the *waterbed effect*. The function $\log |S(i\omega)|$ is plotted versus ω in linear scales in (a). According to Bode's integral formula (11.19) the area of $\log |S(i\omega)|$ above zero must be equal to the area below zero. Gunter Stein's interpretation of design as a trade-off of sensitivities at different frequencies is shown in (b) (from [176]).

Equation (11.19) can be regarded as a *conservation law*: if the loop transfer function has no poles in the right half plane the equation simplifies to

$$\int_0^{\infty} \log |S(i\omega)| d\omega = 0.$$

This formula can be given a nice geometric interpretation as illustrated in Figure 11.14, which shows $\log |S(i\omega)|$ as a function of ω . The area over the horizontal axis must be equal to the area under the axis when frequency is plotted on a *linear* scale. Thus if we wish to make the sensitivity smaller up to some frequency ω_{sc} we must balance this by increased sensitivity above ω_{sc} . Control system design can be viewed as trading the disturbance attenuation at some frequencies for disturbance amplification at other frequencies.

There is an analogous result for the complementary sensitivity function which tells that

$$\int_0^{\infty} \frac{\log |T(i\omega)|}{\omega^2} d\omega = \pi \sum \frac{1}{z_i}, \quad (11.20)$$

where the summation is over all right half plane zeros. Notice that slow right half plane zeros are worse than fast ones and that fast right half plane poles are worse than slow ones.

Example 11.11 X29 aircraft

As an example of the application of Bode's integral formula, we present an analysis of the control system for the X-29 aircraft (see Figure 11.15), which has an unusual configuration of aerodynamic surfaces that are designed to enhance its maneuverability. This analysis was originally carried out by Gunter Stein in his article "Respect the Unstable" [176], which is also the source of the quote at the beginning of this chapter.

To analyze this system, we make use of a small set of parameters that describe the key properties of the system. The X-29 has longitudinal dynamics that are very similar to the inverted pendulum dynamics (Exercise 8.4) and, in particular, have a pair of poles at approximately $p = \pm 6$ and a zero at $z = 26$. The actuators that stabilize the pitch have a bandwidth of $\omega_a = 40$ rad/s and the desired bandwidth of

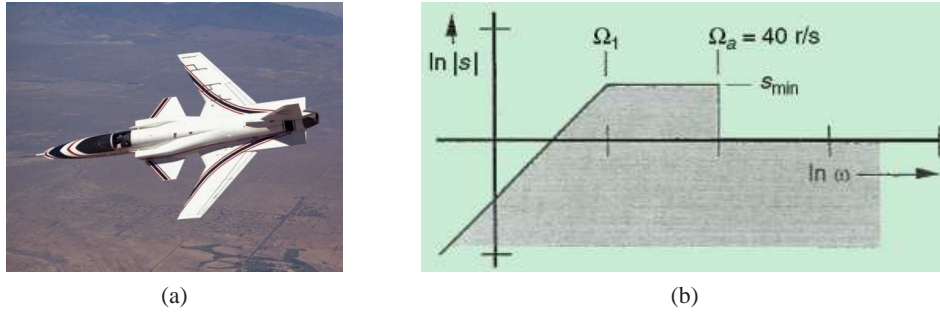


Figure 11.15: X-29 flight control system. The aircraft makes use of forward swept wings and a set of canards on the fuselage to achieve high maneuverability. The figure on the right shows the desired sensitivity for the closed loop system. We seek to use our control authority to shape the sensitivity curve so that we have low sensitivity (good performance) up to frequency ω_1 by creating higher sensitivity up to our actuator bandwidth ω_a .

the pitch control loop is $\omega_1 = 3$ rad/s. Since the ratio of the zero to the pole is only 4.3 we may expect that it may be difficult to achieve the specifications.

To evaluate the achievable performance, we seek to choose the control law such that the sensitivity function is small up to the desired bandwidth and has a value of no greater than M_s beyond that value. Because of the Bode integral formula, we know that M_s must be greater than 1 to balance the small sensitivity at low frequency. We thus ask whether or not we can find a controller that has the shape shown in Figure 11.15b and seek to find the smallest value of M_s that achieves this. Note that the sensitivity above the frequency ω_a is not specified since we have no actuator authority at that frequency. However, assuming that the process dynamics fall off at high frequency, the sensitivity at high frequency will approach 1. Thus, we desire to design a closed loop system that has low sensitivity at frequencies below ω_1 and sensitivity that is not too large between ω_1 and ω_a .

From Bode's integral formula, we know that whatever controller we choose, equation (11.19) must hold. We will assume that the sensitivity function is given by

$$|S(i\omega)| = \begin{cases} \frac{\omega M_s}{\omega_1} & \omega \leq \omega_1 \\ M_s & \omega_1 \leq \omega \leq \omega_a, \end{cases}$$

corresponding Figure 11.15b. If we further assume that $|L(s)| < \delta/\omega^2$ for frequencies larger than the actuator bandwidth, Bode's integral becomes

$$\begin{aligned} \int_0^{\infty} \log |S(i\omega)| d\omega &= \int_0^{\omega_a} \log |S(i\omega)| d\omega + \delta \\ &= \int_0^{\omega_1} \log \frac{\omega M_s}{\omega_1} d\omega + (\omega_a - \omega_1) \log M_s + \delta = \pi p. \end{aligned}$$

If we ignore the small contribution from δ , we can solve for M_s in terms of the remaining parameters of the system,

$$M_s = e^{(\pi p + \omega_1)/\omega_a}.$$

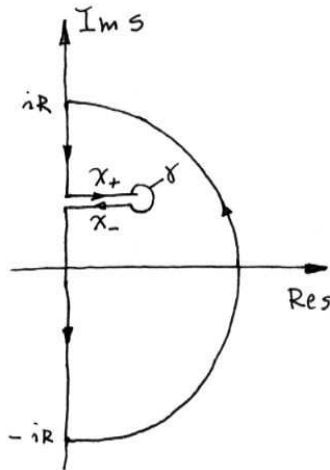


Figure 11.16: Contour used to prove Bode's theorem. For each right half plane pole we create a path from the imaginary axis that encircles the pole as shown in the figure. To avoid clutter we have shown only one of the paths that enclose one right half plane.

This formula tells us what the achievable value of M_s will be for the given control specifications. In particular, using $p = 6$, $\omega_1 = 3$ and $\omega_a = 40$ rad/s we get that $M_s = 1.75$, which means that in the range of frequencies between ω_1 and ω_a , disturbances at the input to the process dynamics (such as wind) will be amplified by a factor of 1.75 in terms of their effect on the aircraft.

Another way to view these results is to compute the phase margin that corresponds to the given level of sensitivity. Since the peak sensitivity normally occurs at or near the crossover frequency, we can compute the phase margin corresponding to $M_s = 1.75$. As shown in Exercise 11.15 the maximum achievable phase margin for this system is approximately 35° , which is below the usual design limit in aerospace systems of 45° . Hence for this system it is not possible to obtain high performance and robustness at the same time, unless more actuator authority is available.

▽

Derivation of Bode's Formula



This is a technical section which requires some knowledge of the theory of complex variables, in particular contour integration. Assume that the loop transfer function has distinct poles at $s = p_k$ in the right half plane and that $L(s)$ goes to zero faster than $1/s$ for large values of s .

Consider the integral of the logarithm of the sensitivity function $S(s) = 1/(1 + L(s))$ over the contour shown in Figure 11.16. The contour encloses the right half plane except the points $s = p_k$ where the loop transfer function $L(s) = P(s)C(s)$ has poles and the sensitivity function $S(s)$ has zeros. The direction of the contour

is counter-clockwise.

The integral of the log of the sensitivity function around this contour is given by

$$\begin{aligned}\int_{\Gamma} \log(S(s)) ds &= \int_{iR}^{-iR} \log(S(s)) ds + \int_R \log(S(s)) ds + \sum_k \int_{\gamma} \log(S(s)) ds \\ &= I_1 + I_2 + I_3 = 0,\end{aligned}$$

where R is a large semicircle on the right and γ_k is the contour starting on the imaginary axis at $s = \text{Im } p_k$ and a small circle enclosing the pole p_k . The integral is zero because the function $\log S(s)$ is regular inside the contour. We have

$$I_1 = -i \int_{-iR}^{iR} \log(S(i\omega)) d\omega = -2i \int_0^{iR} \log(|S(i\omega)|) d\omega$$

because the real part of $\log S(i\omega)$ is an even function and the imaginary part is an odd function. Furthermore we have

$$I_2 = \int_R \log(S(s)) ds = \int_R \log(1 + L(s)) ds \approx \int_R L(s) ds.$$

Since $L(s)$ goes to zero faster than $1/s$ for large s the integral goes to zero when the radius of the circle goes to infinity.

Next we consider the integral I_3 . For this purpose we split the contour into three parts X_+ , γ and X_- as indicated in Figure 11.16. We can then write the integral as

$$I_3 = \int_{X_+} \log S(s) ds + \int_{\gamma} \log S(s) ds + \int_{X_-} \log S(s) ds.$$

The contour γ is a small circle with radius r around the pole p_k . The magnitude of the integrand is of the order $\log r$ and the length of the path is $2\pi r$. The integral thus goes to zero as the radius r goes to zero. Furthermore, making use of the fact that X_- is oriented oppositely from X_+ , we have

$$\int_{X_+} \log S(s) ds + \int_{X_-} \log S(s) ds = \int_{X_+} (\log S(s) - \log S(s - 2\pi i)) ds = 2\pi p_k.$$

Since $|S(s)| = |S(s - 2\pi i)|$ we have

$$\log S(s) - \log S(s - 2\pi i) = \arg S(s) - \arg S(s - 2\pi i) = 2\pi$$

and we find that

$$I_3 = 2\pi \sum p_k$$

Letting the small circles go to zero and the large circle go to infinity and adding the contributions from all right half plane poles p_k gives

$$I_1 + I_2 + I_3 = -2i \int_0^R \log |S(i\omega)| d\omega + \sum_k 2\pi p_k = 0.$$

which is Bode's formula (11.19).

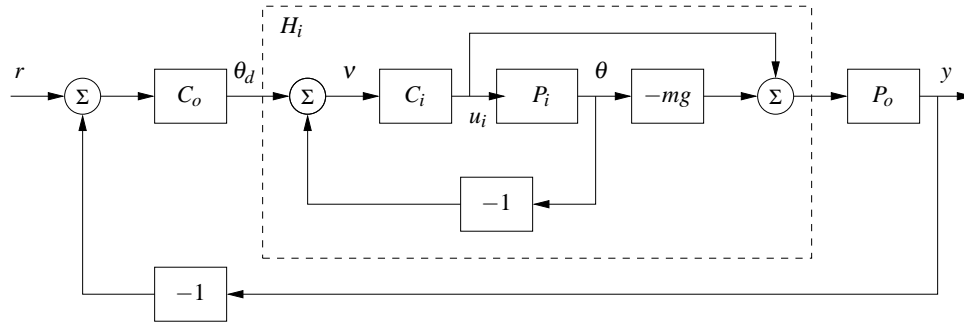


Figure 11.17: Inner/outer control design for a vectored thrust aircraft. The inner loop H_i controls the roll angle of the aircraft using the vectored thrust. The outer loop controller C_o commands the roll angle to regulate the lateral position. The process dynamics are decomposed into inner loop (P_i) and outer loop (P_o) dynamics, which combine to form the full dynamics for the aircraft.

11.6 DESIGN EXAMPLE

In this section we carry out a detailed design example that illustrates the main techniques in this chapter.

Example 11.12 Lateral control of a vectored thrust aircraft

The problem of controlling the motion of a vertical take off and landing (VTOL) aircraft was introduced in Example 2.9 and in Example 11.6, where we designed a controller for the roll dynamics. We now wish to control the position of the aircraft, a problem that requires stabilization of both the attitude and position. To control the lateral dynamics of the vectored thrust aircraft, we make use of a “inner/outer” loop design methodology, as illustrated in Figure 11.17. This diagram shows the process dynamics and controller divided into two components: an “inner loop” consisting of the roll dynamics and control and an “outer loop” consisting of the lateral position dynamics and controller. This decomposition follows the block diagram representation of the dynamics given in Exercise 8.9.

The approach that we take is to design a controller C_i for the inner loop so that the resulting closed loop system H_i provides fast and accurate control of the roll angle for the aircraft. We then design a controller for the lateral position that uses the approximation that we can directly control the roll angle as an input to the dynamics controlling the position. Under the assumption that the dynamics of the roll controller are fast relative to the desired bandwidth of the lateral position control, we can then combine the inner and outer loop controllers to get a single controller for the entire system. As a performance specification for the entire system, we would like to have zero steady state error in the lateral position, a bandwidth of approximately 1 rad/s and a phase margin of 45° .

For the inner loop, we choose our design specification to provide the outer loop

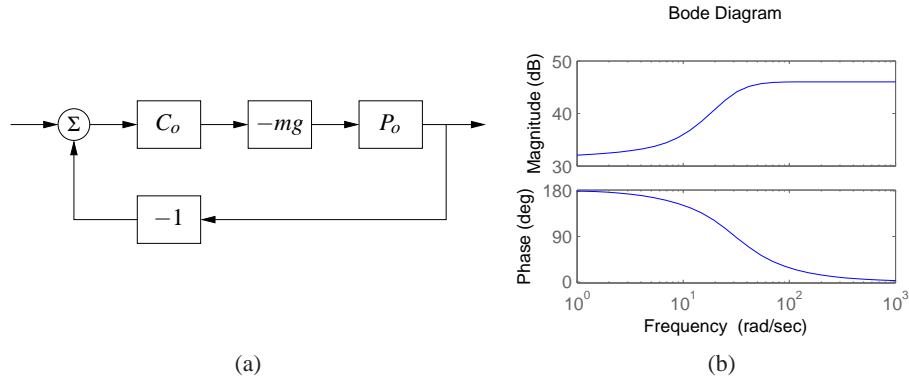


Figure 11.18: Outer loop control design for a vectored thrust aircraft. The outer loop approximates the roll dynamics as a state gain $-mg$. The Bode plot for the roll dynamics are shown on the right, indicating that this approximation is accurate up to approximately 10 rad/s.

with accurate and fast control of the roll. The inner loop dynamics are given by

$$P_i = H_{\theta u_1} = \frac{r}{Js^2 + cs}.$$

We choose the desired bandwidth to be 10 rad/s (10 times the outer loop) and the low frequency error to be no more than 5%. This specification is satisfied using the lead compensator of Example 11.6 designed previously, so we choose

$$C_i(s) = k \frac{s+a}{s+b} \quad a = 2, \quad b = 25, \quad k = 1.$$

The closed loop dynamics for the system satisfy

$$H_i = \frac{C_i}{1 + C_i P_i} - mg \frac{C_i P_i}{1 + C_i P_i} = \frac{C_i(1 - mg P_i)}{1 + C_i P_i}.$$

A plot of the magnitude of this transfer function is shown in Figure 11.18 and we see that it is a good approximation up to 10 rad/s.

To design the outer loop controller, we assume the inner loop roll control is perfect, so that we can take θ_d as the input to our lateral dynamics. Following the diagram shown in Exercise 8.9, the outer loop dynamics can be written as

$$P(s) = H_i(0)P_o(s) = \frac{H_i(0)}{ms^2},$$

where we replace $H_i(s)$ with $H_i(0)$ to reflect our approximation that the inner loop will eventually track our commanded input. Of course, this approximation may not be valid and so we must verify this when we complete our design.

Our control goal is now to design a controller that gives zero steady state error in x and has a bandwidth of 1 rad/s. The outer loop process dynamics are given by a second order integrator and we can again use a simple lead compensator to satisfy the specifications. We also choose the design such that the loop transfer

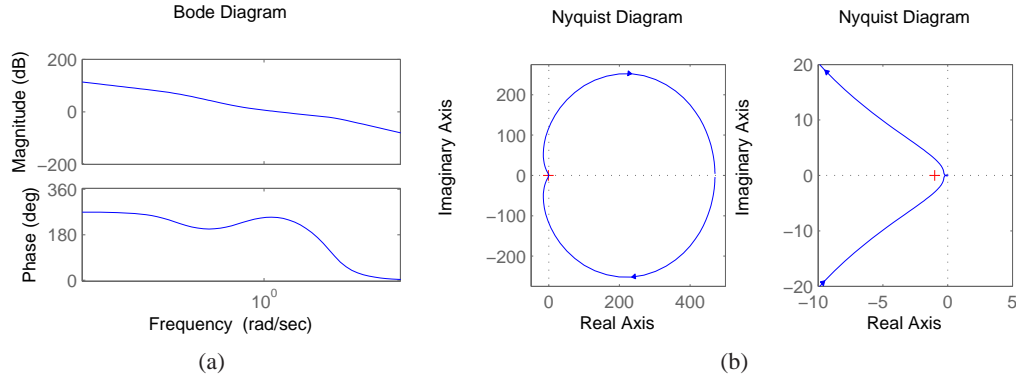


Figure 11.19: Inner/outer loop controller for a vectored thrust aircraft. The Bode and Nyquist plots for the transfer function for the combined inner and outer loop transfer functions are shown. The system has a phase margin of 68° and a gain margin of 6.2.

function for the outer loop has $|L_o| < 0.1$ for $\omega > 10$ rad/s so that the H_i dynamics can be neglected. We choose the controller to be of the form

$$C_o(s) = -k_o \frac{s + a_o}{s + b_o},$$

with the negative sign to cancel the negative sign in the process dynamics. To find the location of the poles, we note that the phase lead flattens out at approximately $b_o/10$. We desire phase lead at crossover and we desire the crossover at $\omega_{gc} = 1$ rad/s, so this gives $b_o = 10$. To insure that we have adequate phase lead, we must choose a_o such that $b_o/10 < 10a_o < b_o$, which implies that a_o should be between 0.1 and 1. We choose $a_o = 0.3$. Finally, we need to set the gain of the system such that at crossover the loop gain has magnitude one. A simple calculation shows that $k_o = 0.8$ satisfies this objective. Thus, the final outer loop controller becomes

$$C_o(s) = 0.8 \frac{s + 0.3}{s + 10}.$$

Finally, we can combine the inner and outer loop controllers and verify that the system has the desired closed loop performance. The Bode and Nyquist plots corresponding to Figure 11.17 with the inner and outer loop controllers are shown in Figure 11.19 and we see the specifications are satisfied. In addition, we show the Gang of Four in Figure 11.20 and we see that the transfer functions between all inputs and outputs are reasonable.

The approach of splitting the dynamics into an inner and outer loop is common in many control applications and can lead to simpler designs for complex systems. Indeed, for the aircraft dynamics studied in this example, it is very challenging to directly design a controller from the lateral position x to the input u_1 . The use of the additional measurement of θ greatly simplifies the system requirements and allows the design to be broken up into simpler pieces.

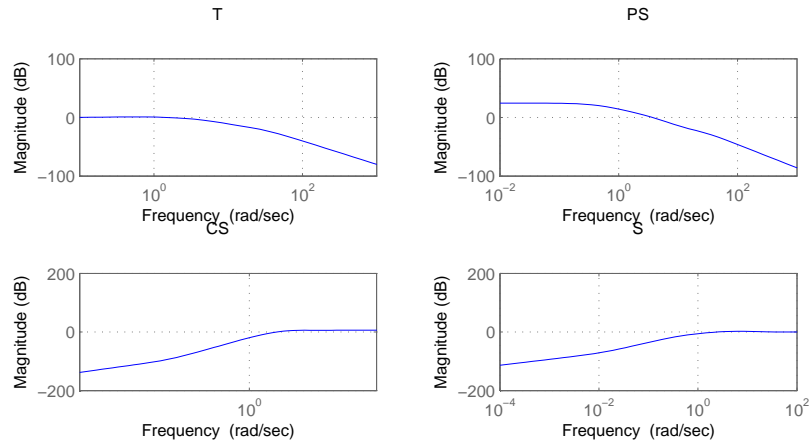


Figure 11.20: Gang of Four for vector thrust aircraft system.

▽


11.7 FURTHER READING

Design by loop shaping was a key element of the early development of control and systematic design methods were developed, see James, Nichols and Philips [103], Chestnut and Mayer [49], Truxal [185], and Thaler [182]. Loop shaping is also treated in standard textbooks such as Franklin, Powell and Emami-Naeini [76], Dorf and Bishop [56], Kuo and Golnaraghi [125] and Ogata [153]. Systems with two degrees of freedom were developed by Horowitz [97], who also discussed limitations of poles and zeros in the right half plane. Fundamental results on limitations are given in Bode [40]; more recent presentations are found in Goodwin, Graebe and Salgado [84]. The treatment in Section 11.5 is based on [15]. Much of the early work was based on the loop transfer function; the importance of the sensitivity functions appeared in connection with the development in the 1980s which resulted in the so called H_∞ design methods. A compact presentation is given in the text by Doyle, Francis and Tannenbaum [59] and Zhou, Doyle and Glover [198]. Loop shaping was integrated with the robust control theory in MacFarlane and Glover [132] and Vinnicombe [187]. Comprehensive treatments of control system design are given in Maciejowski [133] and Goodwin, Graebe and Salgado [84].

EXERCISES

11.1 Consider the system in Figure 11.1 give all signal pairs which are related by the transfer functions $1/(1+PC)$, $P/(1+PC)$, $C/(1+PC)$ and $PC/(1+PC)$.

11.2 (Cancellation of unstable process pole) Consider the system in Example 11.1. Choose the parameters $a = -1$ compute time and frequency responses for all transfer functions in the Gang of Four for controllers with $k = 0.2$ and $k = 5$.

11.3 (Equivalence of Figure 11.1 and 11.2) Show that the system in Figure 11.1 can be represented by 11.2 by proper choice of the matrices \mathcal{P} and \mathcal{C} . 

11.4 (Sensitivity of feedback and feedforward) Consider the system in Figure 11.1, let G_{yr} be the transfer function relating measured signal y to reference r . Compute the sensitivities of G_{yr} with respect to the feedforward and feedback transfer functions F and C ($\partial G_{yr}/\partial F$ and $\partial G_{yr}/\partial C$).


11.5 (Equivalence of controllers with two degrees of freedom) Show that the systems in Figure 11.1 and Figure 11.3 give the same responses to command signals if $F_m C + F_u = CF$.

11.6 Consider the feedback system shown in Figure 11.1. Assume that the reference signal is constant. Let y_{ol} be the measured output when there is no feedback and y_{cl} be the output with feedback. Show that

$$Y_{cl}(s) = S(s)Y_{ol}(s)$$

where S is the sensitivity function.

11.7 (Time delay) Using the gain crossover frequency inequality, show that for a pure time delay we must have $\omega_{gc} \leq \frac{\phi_l}{T}$.

11.8 Let $F(s)$ be the Laplace transform of a signal $f(t)$. Show that the Taylor series expansion for $f(t)$ and its Laplace transform are related by 

$$F(s) = \frac{1}{s}f(0) + \frac{1}{s^2}f'(0) + \frac{1}{2s^3}f''(0) + \dots$$

Then use the result to show that the behavior of a time function for small t is related to the Laplace transform for large s . Derive a similar result for large values of t .

11.9 (Approximate expression for noise sensitivity) Show that the effect of noise on the control signal for the system in Exercise 11.4 can be approximated by

$$CS \approx C \approx \frac{k_d s}{(sT_d)^2/2 + sT_d + 1}$$

Show that using this approximation the largest value of $|CS(i\omega)|$ is k_d/T_f and that it occurs for $\omega = \sqrt{2}/T_f$.

11.10 Show that the nonminimum phase part of the transfer function $P = e^{-sT}$ for a time delay has the phase lag ωT which implies that the gain crossover frequency must be chosen so that $\omega_{gc} T < \phi_l$. Also use the approximation $e^{-sT} \approx \frac{1-sT/2}{1+sT/2}$ so show that a time delay is similar to a system with a right half plane zero at $s = 2/T$. A slow zero thus corresponds to a long time delay.

11.11 (The pole zero ratio) Consider a process with the transfer function

$$P(s) = k \frac{a-s}{s-b}$$

with positive a and b . Show that the the closed loop system with unit feedback is either $b/a < k < 1$ or $1 < k < b/a$.

11.12 (Pole in the right half plane and time delay) The non-minimum phase part of the transfer function for a system with one pole in the right half plane and a time delay T is

$$P_{nmp}(s) = \frac{s+p}{s-p} e^{-sT}. \quad (11.21)$$

Using the gain crossover frequency inequality, compute the limits on the achievable bandwidth of the system.

11.13 (Limitations on achievable phase lag) Derive analytical formulas corresponding to the plots in Figure 11.13.



11.14 (Integral formula for complementary sensitivity) Prove the formula (11.20) for the complementary sensitivity.

11.15 (Phase margin formulas) Show that if the relationship between the phase margin and the magnitude of the sensitivity function at crossover is given by

$$S_{\min} = \frac{1}{2 \sin(\varphi_m/2)}$$

11.16 (Stabilization of inverted pendulum with visual feedback) Consider stabilization of an inverted pendulum based on visual feedback using a video camera with 50 Hz frame rate. Let the effective pendulum length be l . Use the gain crossover frequency inequality to determine the minimum length of the pendulum that can be stabilized if we desire a phase lag φ_l of no more than 90° .



11.17 (Bode's integral) Bode's integral formula in Theorem 11.1 assumes that the loop transfer function has the property $\lim_{s \rightarrow \infty} sL(s) = 0$. Assume instead that the limit is not zero and prove that the corresponding formula becomes

$$\int_0^\infty \log |S(i\omega)| d\omega = \int_0^\infty \log \frac{1}{|1+L(i\omega)|} d\omega = \pi \sum p_k - \frac{\pi}{2} \lim_{s \rightarrow \infty} sL(s).$$

11.18 (Cancellation of unstable process zero) Consider a system with the block diagram in Figure 11.1 where the reference signal r is zero. Let $a > 0$ and let the transfer functions of process and controller be

$$P(s) = \frac{s-a}{s^2}, \quad C(s) = \frac{s+1}{s-a}$$

Compute the Gang of Four and discuss the behavior of the closed loop system when there are load disturbances and measurement noise. Simulate the system and verify your conclusions.

Chapter Twelve

Robust Performance

However, by building an amplifier whose gain is deliberately made, say 40 decibels higher than necessary (10000 fold excess on energy basis), and then feeding the output back on the input in such a way as to throw away that excess gain, it has been found possible to effect extraordinary improvement in constancy of amplification and freedom from non-linearity.

Harold S. Black, “Stabilized Feedback Amplifiers”, 1934 [35].

This chapter focuses on the analysis of robustness of feedback systems, a large topic for which we provide only an introduction to some of the key concepts. We consider the stability and performance of systems whose process dynamics are uncertain and derive fundamental limits for robust stability and performance. To do this we develop ways to describe uncertainty, both in the form of parameter variations and in the form of neglected dynamics. We also briefly mention some methods for designing controllers to achieve robust performance.

12.1 MODELING UNCERTAINTY

Harold Black’s quote above illustrates that one the key uses of feedback is to provide robustness to uncertainty (“consistency of amplification”). It is one of the most useful properties of feedback and is what makes it possible to design feedback systems based on strongly simplified models.

One form of uncertainty in dynamical systems is that the parameters describing the system are unknown, or *parametric uncertainty*. A typical example is the variation of the mass of a car, which changes with the number of passengers and the weight of the baggage. When linearizing a nonlinear system, the parameters of the linearized model also depend on the operating condition. It is straightforward to investigate effects of parametric uncertainty simply by evaluating the performance criteria for a range of parameters. Such a calculation will directly reveal the consequences of parameter variations. We illustrate by a simple example.

Example 12.1 Cruise control

The cruise control problem was described in Section 3.1 and a PI controller was designed in Example 10.3. To investigate the effect of parameter variations we will choose a controller designed for a nominal operating condition corresponding to mass $m = 1600$, fourth gear ($\alpha = 12$) and speed $v_e = 25$ m/s; the controller gains are $k = 0.72$ and $k_i = 0.18$. Figure 12.1a shows the velocity v and the throttle u when encountering a hill with a 3° slope with masses in the range $1600 < m < 2000$, gear ratios 3 to 5 ($\alpha = 10, 12$ and 16) and velocity $10 \leq v \leq 40$

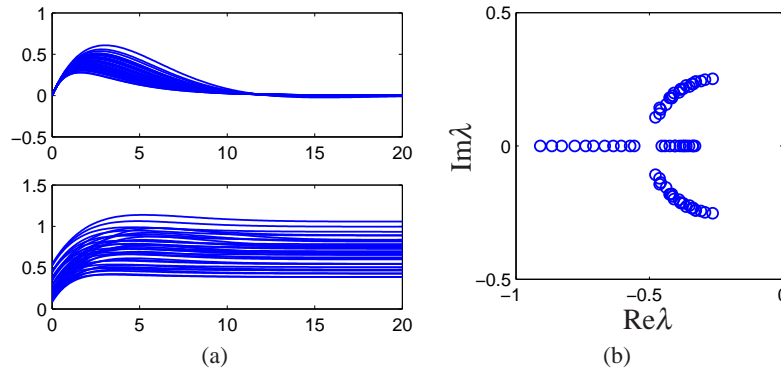


Figure 12.1: Responses of the cruise control system to a slope increase of 3° (left) and the eigenvalues of the closed loop system (right). Model parameters are swept over a wide range.

m/s. The simulations were done using models that were linearized around the different operating conditions. The figure shows that there are variations in the response but that they are quite reasonable. The largest velocity error is in the range of 0.2 to 0.6 m/s, and the settling time is about 15 s. The control signal is marginally larger than 1 in some cases which implies that the throttle is fully open. A full nonlinear simulation using a controller with windup protection is required if we want to explore these cases in more detail. Figure 12.1b shows the eigenvalues of the closed loop system for the different operating conditions. The figure shows that the closed loop system is well damped in all cases. ∇

This example indicates that at least as far as parametric variations are concerned, the design based on a simple nominal model will give satisfactory control. The example also indicates that a controller with fixed parameters can be used in all cases. Notice however that we have not considered operating conditions in low gear and at low speed but cruise controllers are not used in these cases.

Unmodeled Dynamics

It is generally easy to investigate the effects of parametric variations. However, there are other uncertainties that also are important, as discussed at the end of Section 2.3. The simple model of the cruise control system only captures the dynamics of the forward motion of the vehicle and the torque characteristics of the engine and transmission. It does not, for example, include a detailed model of the engine dynamics (whose combustion processes are extremely complex) nor the slight delays that can occur in modern electronically-controlled engines (due to the processing time of the embedded computers). These neglected mechanisms are called *unmodeled dynamics*.

Unmodeled dynamics can be accounted for by developing a more complex model. Such models are commonly used for controller development but substan-

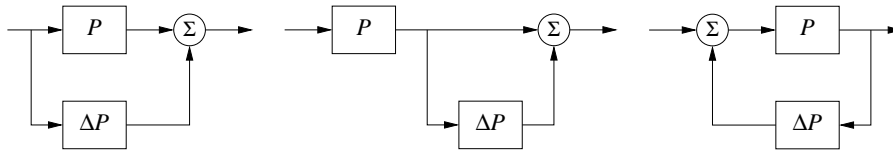


Figure 12.2: Unmodeled dynamics in linear systems. Uncertainty can be represented using additive perturbations (left), multiplicative perturbations (middle) or feedback perturbations (right). The nominal system is P and ΔP represents the unmodeled dynamics.

tial effort is required to develop the models. An alternative is to investigate if the closed loop system is sensitive to generic forms of unmodeled dynamics. The basic idea is to describe the “unmodeled” dynamics by including a transfer function in the system description whose frequency response is bounded, but otherwise unspecified. For example, we might model the engine dynamics in the cruise control example as a system that quickly provides the torque that is requested through the throttle, giving a small deviation from the simplified model, which assumed the torque response was instantaneous. This technique can also be used in many instances to model parameter variations, allowing a quite general approach to uncertainty management.

In particular we wish to explore if additional linear dynamics may cause difficulties. A simple way is to assume that the transfer function of the process is $P(s) + \Delta P(s)$ where $P(s)$ is the nominal simplified transfer function and $\Delta P(s)$ represents the unmodeled dynamics. This case is called *additive uncertainty*. Figure 12.2 shows some other cases to represent uncertainties in a linear system.

When are Two Systems Similar?



A fundamental issue in describing robustness is to determine when two systems are close. Given such a characterization, we can then attempt to describe robustness according to how close the actual system must be to the model in order to still achieve the desired levels of performance. This seemingly innocent problem is not as simple as it may appear. A naive idea is to say that two systems are close if their open loop responses are close. Even if this appears natural, there are complications, as illustrated by the following examples.

Example 12.2 Similar in open loop but large differences in closed loop

The systems with the transfer functions

$$P_1(s) = \frac{100}{s+1}, \quad P_2(s) = \frac{100}{(s+1)(sT+1)^2}$$

have very similar open loop responses for small values of T , as illustrated in the top left corner of Figure 12.3a, where $T = 0.025$. The differences between the step responses are barely noticeable in the figure. The step responses with unit gain error feedback are shown in the bottom left figure. Notice that one closed loop system is stable and the other one is unstable. ∇

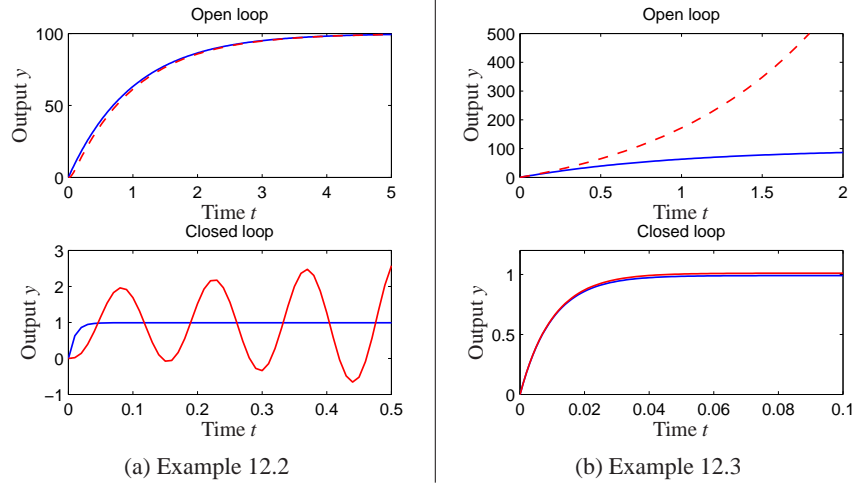


Figure 12.3: Determining when two systems are close. The plots on the left show the open and closed loop responses for two processes that have nearly identical step responses in open loop, but are very different in closed loop. The system on the right shows the opposite: the systems are different in open loop, but similar in closed loop.

Example 12.3 Different in open loop but similar in closed loop

Consider the systems

$$P_1(s) = \frac{100}{s+1}, \quad P_2(s) = \frac{100}{s-1}.$$

The open loop responses are very different because P_1 is stable and P_2 is unstable, as shown in the top right plot in Figure 12.3. Closing a feedback loop with unit gain around the systems we find that the closed loop transfer functions are

$$T_1(s) = \frac{100}{s+101} \quad T_2(s) = \frac{100}{s+99}$$

which are very close as is also shown in Figure 12.3b. ∇

These examples show that if our goal is to close a feedback loop it may be misleading to compare the open loop responses of the system. Inspired by these examples we will introduce a distance measure that is more appropriate for closed loop operation. Consider two systems with the rational transfer functions

$$P_1(s) = \frac{n_1(s)}{d_1(s)} \quad \text{and} \quad P_2(s) = \frac{n_2(s)}{d_2(s)},$$

where $n_1(s)$, $n_2(s)$, $d_1(s)$ and $d_2(s)$ are polynomials. Let

$$p(s) = d_1(s)n_2(-s) - n_1(s)d_2(-s)$$

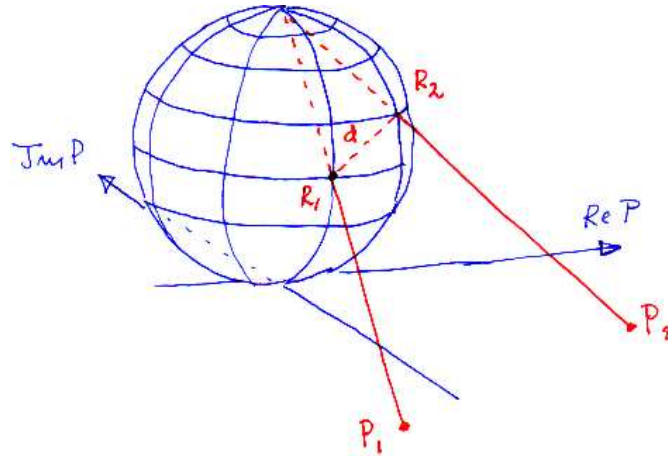


Figure 12.4: Geometric interpretation of the distance $d(P_1, P_2)$ between two transfer functions. At each frequency, the points on the Nyquist curve for P_1 and P_2 are projected onto a unit sphere of radius 1 sitting at the origin of the complex plane. The distance between the two systems is defined as the maximum distance between the points R_1 and R_2 over all frequencies.

and define the *chordal distance* between the transfer functions as

$$d_v(P_1, P_2) = \begin{cases} \sup_{\omega} \frac{|P_1(i\omega) - P_2(i\omega)|}{\sqrt{(1 + |P_1(i\omega)|^2)(1 + |P_2(i\omega)|^2)}} & \text{if } p(s) \text{ has no RHP zeros} \\ 1 & \text{otherwise.} \end{cases} \quad (12.1)$$

The distance has a nice geometric interpretation, as shown in Figure 12.4, where the Nyquist plots of P_1 and P_2 are projected on the Riemann sphere. The Riemann sphere is located above the complex plane. It has diameter 1 and its south pole is at the origin of the complex plane. Points in the complex plane are projected onto the sphere by a line through the point and the north pole (Figure 12.4). The distance $d_v(P_1, P_2)$ is simply the shortest chordal distance between the projections of the Nyquist curves. The distance $d_v(P_1, P_2)$ is similar to $|P_1 - P_2|$ when the transfer functions are small, but very different when $|P_1|$ and $|P_2|$ are large. It is also related to the behavior of the systems under unit feedback as will be discussed in Section 12.5. Since the diameter of the Riemann sphere is 1, it follows that the distance is never larger than 1.

The *Vinnicombe metric* or the *v-gap metric* (12.1) was introduced in [187] and is a natural tool to compare the behavior of two systems under closed loop feedback. Vinnicombe also gave strong robustness results based on the metric. We illustrate by computing the metric for the systems in the previous examples.

Example 12.4 Vinnicombe metric for Examples 12.2 and 12.3

For the systems in Example 12.2 we have

$$n_1(s) = n_2(s) = 100, \quad d_1(s) = s + 1, \quad d_2(s) = (s + 1)(sT + 1)^2$$

and hence

$$p(s) = d_1(s)n_2(-s) - n_1(s)d_2(-s) = 100s(sT^2 + T + 2).$$

This polynomial has no roots in the open right half plane and we can proceed to compute the norm (12.1) numerically, which for $T = 0.025$ gives $d(P_1, P_2) = 0.98$, a quite large value. To have a reasonable robustness the Vinnicombe recommended values less than $1/3$.

For the system in Example 12.3 we have

$$n_1(s) = n_2(s) = 100, \quad d_1(s) = s + 1, \quad d_2(s) = s - 1$$

and

$$p(s) = d_1(s)n_2(-s) - n_1(s)d_2(-s) = 100(s + 1 - (-s + 1)) = 200s.$$

This polynomial has no roots in the open right half plane and we can proceed to compute the norm (12.1) numerically, giving $d(P_1, P_2) = 0.02$, which is a very small value. This explains why both systems can be controlled well by the same controller. ∇

12.2 STABILITY IN THE PRESENCE OF UNCERTAINTY

Having discussed how to describe robustness, we now consider the problem of robust stability: when can we show that the stability of a system is robust with respect to process variations? This is an important question since the potential for instability is one of the main drawbacks of feedback. Hence we want to ensure that even if we have small inaccuracies in our model, we can still guarantee stability and performance.

Robust Stability Using Nyquist's Criterion

The Nyquist criterion provides a powerful and elegant way to study the effects of uncertainty for linear systems. A simple criterion is that the Nyquist curve is sufficiently far from the critical point -1 . Recall that the shortest distance from the Nyquist curve to the critical point is $s_m = 1/M_s$ where M_s is the maximum of the sensitivity function and s_m the stability margin introduced in Section 9.3. The maximum sensitivity M_s or the stability margin s_m is thus a good robustness measure, as illustrated in Figure 12.5a.

We will now derive explicit conditions for permissible process uncertainties. Consider a stable feedback system with a process P and a controller C . If the process is changed from P to $P + \Delta P$, the loop transfer function changes from PC to $PC + C\Delta P$, as illustrated in Figure 12.5b. If we have a bound on the size of ΔP (represented by the dashed circle in the figure), then the system remains stable as long as the process variations never overlap the -1 point, since this leaves the number of encirclements of -1 unchanged.

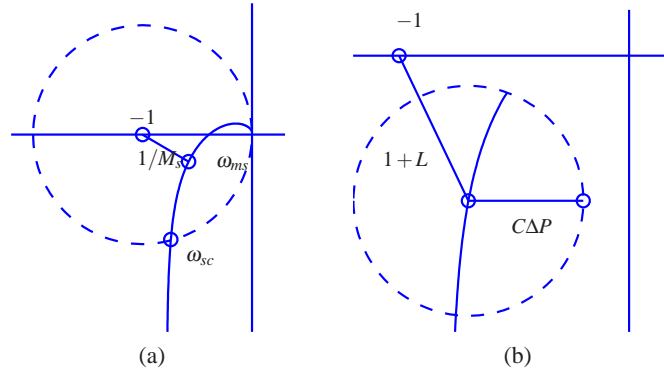


Figure 12.5: Robust stability using the Nyquist criterion. The left figure shows that the distance to the critical point $1/M_s$ is a robustness measure. The right figure shows the Nyquist curve of a nominal loop transfer function and its uncertainty caused by additive process variations ΔP .

Some additional assumptions are required for the analysis to hold. Most importantly, we require that the process perturbations ΔP be stable so that we do not introduce any new right half plane poles that would require additional encirclements in the Nyquist criterion. Also, we note that this condition is conservative: it allows for any perturbation that satisfies the given bounds, while in practice we may have more information about possible perturbations.

We now compute an analytical bound on the allowable process disturbances. The distance from the critical point -1 to the loop transfer function L is $|1 + L|$. This means that the perturbed Nyquist curve will not reach the critical point -1 provided that

$$|C\Delta P| < |1 + L|,$$

which implies

$$|\Delta P| < \left| \frac{1 + PC}{C} \right| \quad \text{or} \quad \left| \frac{\Delta P}{P} \right| < \frac{1}{|T|}. \quad (12.2)$$

This condition must be valid for all points on the Nyquist curve, i.e pointwise for all frequencies. The condition for robust stability can thus be written as

$$\left| \frac{\Delta P(i\omega)}{P(i\omega)} \right| < \frac{1}{|T(i\omega)|} \quad \text{for all } \omega \geq 0. \quad (12.3)$$

This condition allows us to reason about uncertainty without exact knowledge of the process perturbations. Namely, we can verify stability for *any* uncertainty ΔP that satisfies the given bound. From an analysis perspective, this gives us a measure of the robustness for a given design. Conversely, if we require robustness of a given level, we can attempt to choose our controller C such that the desired level of robustness is available (by asking T to be small) in the appropriate frequency bands.

The formula given by equation (12.3) is one of the reasons why feedback systems work so well in practice. The mathematical models used to design control

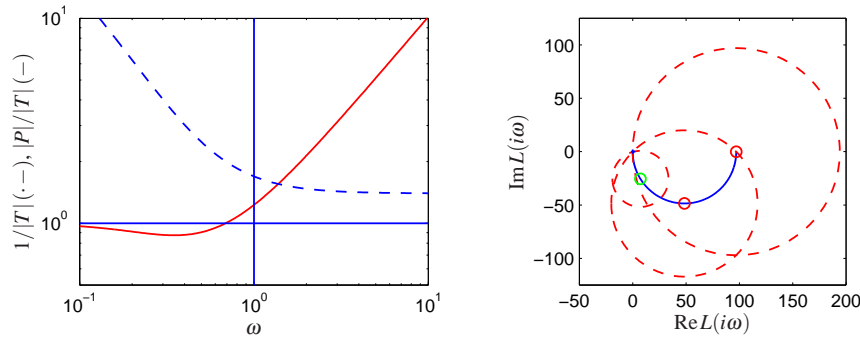


Figure 12.6: Robustness for a cruise controller. The left figure shows the maximum relative error ($1/|T|$, dot-dashed) and absolute error ($|P|/|T|$, solid) for the process uncertainty ΔP . The Nyquist curve is shown in the right figure, as a solid line. The dashed circles show permissible perturbations in the process dynamics, $|\Delta P| = |P|/|T|$, at the frequencies $\omega = 0$, 0.0142 and 0.05.

system are often strongly simplified. There may be model errors and the properties of a process may change during operation. Equation (12.3) implies that the closed loop system will at least be stable for substantial variations in the process dynamics.

It follows from equation (12.3) that the variations can be large for those frequencies where T is small and that smaller variations are allowed for frequencies where T is large. A conservative estimate of permissible process variations that will not cause instability is given by

$$\left| \frac{\Delta P(i\omega)}{P(i\omega)} \right| < \frac{1}{M_t},$$

where M_t is the largest value of the complementary sensitivity

$$M_t = \sup_{\omega} |T(i\omega)| = \left\| \frac{PC}{1+PC} \right\|_{\infty}. \quad (12.4)$$

The value of M_t is influenced by the design of the controller. For example, it is shown in Exercise 12.1 that if $M_t = 2$ then pure gain variations of 50% or pure phase variations of 30° are permitted without making the closed loop system unstable.

Example 12.5 Cruise control

Consider the cruise control system discussed in Section 3.1. The model of the car in fourth gear at speed 25 m/s is

$$P(s) = \frac{1.38}{s + 0.0142},$$

and the controller is a PI controller with gains $k = 0.72$ and $k_i = 0.18$. Figure 12.6 plots the allowable size of the process uncertainty using the bound in equation (12.3). At low frequencies, $T(0) = 1$ and so the perturbations can be

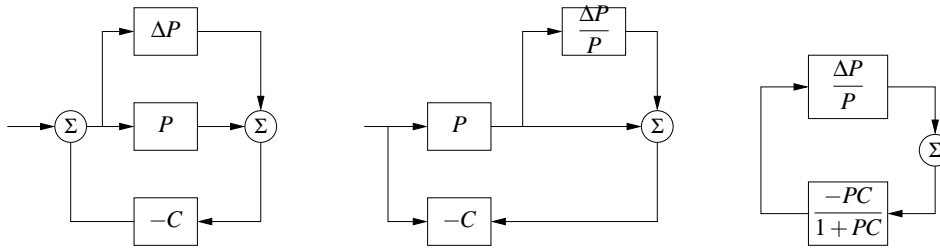


Figure 12.7: Illustration of robustness to process perturbations. A system with additive uncertainty (left) can be manipulated via block diagram algebra (center) to isolate the uncertainty in a manner that allows application of the small gain theorem (right)

as large as the original process ($|\Delta P/P| < 1$). The complementary sensitivity has its maximum $M_t = 1.14$ at $\omega_{mt} = 0.35$ and hence this gives the minimum allowable process uncertainty, with $|\Delta P/P| < 0.87$ or $|\Delta P| < 3.47$. Finally, at high frequencies $T \rightarrow 0$ and hence the relative error can get very large. For example, at $\omega = 5$ we have $|T(i\omega)| = 0.195$ which means that the stability requirement is $|\Delta P/P| < 5.1$. The analysis clearly indicates that the system has good robustness and that the high frequency properties of the transmission system are not important for the design of the cruise controller.

Another illustration of the robustness of the system is given in the right diagram of Figure 12.6, which shows the Nyquist curve of the transfer function of the process and the uncertainty bounds $\Delta P = |P|/|T|$ for a few frequencies. Note that the controller can tolerate large amounts of uncertainty and still maintain stability of the closed loop. ∇

The situation illustrated in the previous example is typical of many processes: moderately small uncertainties are only required around the gain crossover frequencies, but large uncertainties can be permitted at higher and lower frequencies. A consequence of this is that a simple model that describes the process dynamics well around the crossover frequency is often sufficient for design. Systems with many resonance peaks are an exception to this rule because the process transfer function for such systems may have large gains also for higher frequencies, as shown for instance in Example 9.9.

Notice that the results we have given can be conservative. Referring to Figure 12.5, the critical perturbations, which were the basis for our analysis, are in the direction towards the critical point. It is possible to have much larger perturbations in the opposite direction.

The robustness result given by equation (12.3) can be given another interpretation by using the small gain theorem, Theorem 9.4 on page 284. To apply the theorem we start with block diagrams of a closed loop system with a perturbed process and we make a sequence of transformations of the block diagram which isolates the block which represents the uncertainty, as shown in Figure 12.7. The result is the two-block interconnection shown in Figure 12.7c which has the loop

Table 12.1: Conditions for robust stability for different types of uncertainty.

Process	Type	Robust Stability
$P + \Delta P$	Additive	$\ CS\Delta P\ _\infty < 1$
$P(1 + \Delta P)$	Multiplicative	$\ S\Delta P\ _\infty < 1$
$P/(1 + \Delta P \cdot P)$	Feedback	$\ PS\Delta P\ _\infty < 1$

transfer function

$$L = \frac{PC}{1+PC} \frac{\Delta P}{P} = T \frac{\Delta P}{P}.$$

Equation (12.3) implies that the largest loop gain is less than one and hence the systems is stable via the small gain theorem.

The small gain theorem can be used to check robust stability for uncertainty in a variety of other situations. Table 12.1 summarizes a few of the common cases; the proofs (all via the small gain theorem) are left as exercises.

The following example illustrates that it is possible to design systems that are robust to parameter variations.

Example 12.6 Bode's loop transfer function

A major problem in design of electronic amplifiers was to obtain a closed loop system that was insensitive to changes in the gain of the electronic components. Bode found that the loop transfer function $L(s) = ks^n$, with $-5/3 \leq n \leq -1$ was an ideal loop transfer function. Figure 12.8a shows that the Bode and Nyquist plots of the loop transfer function. Notice that the gain curve is a straight line with slope n and that the phase is constant $\angle L(i\omega) = n\pi/2$. The phase margin is thus constant $\varphi_m = -\sin^{-1}(n\pi/2)$ for all values of controller gain k . The Nyquist curve is a straight line from the origin. The transfer function cannot be realized with

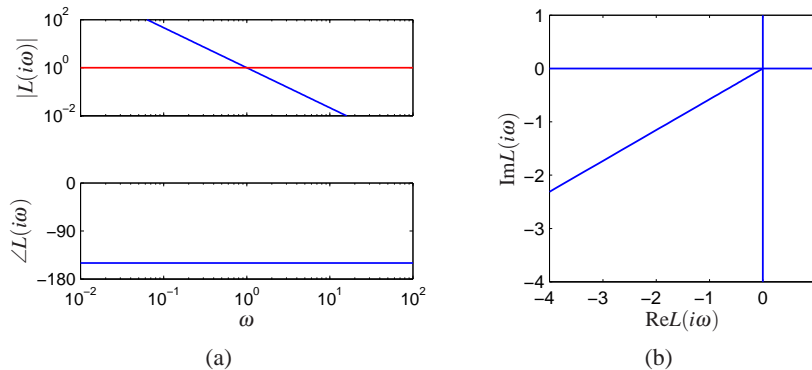


Figure 12.8: Bode's ideal loop transfer function. Bode and Nyquist plots are shown for Bode's ideal loop transfer function $L(s) = ks^n$, for $k = 1$ and $n = 5/3$.

physical components, but it can be approximated over a given frequency range with a rational function that can be implemented. An operational amplifier circuit that has the approximate transfer function $G(s) = k/(s + a)$ is a realization of Bode's ideal transfer function with $n = 1$, as described in Example 8.3. Designers of operational amplifiers make great effort to make the approximation valid over a wide frequency range. ∇

Youla Parameterization



Since stability is such an essential property it is useful to characterize all controllers that will stabilize a given process. Consider a stable process with a rational transfer function P . A system with the complementary sensitivity function T can be obtained by feedforward control with the stable transfer function Q if

$$T = PQ \quad (12.5)$$

Notice that T must have the same right half plane zeros as P since Q is stable. Now assume that we want to obtain the complementary transfer function T by using unit feedback with the controller C . Since $T = PC/(1 + PC) = PQ$ we find that the controller transfer function is

$$C = \frac{Q}{1 - QP}. \quad (12.6)$$

A straightforward calculation gives

$$\frac{1}{1 + PC} = 1 - T, \quad \frac{P}{1 + PC} = P - PT, \quad \frac{C}{1 + PC} = Q, \quad \frac{PC}{1 + PC} = T$$

which are all stable. It can be shown that all stabilizing controllers for a stable process $P(s)$ are given by equation (12.6) for some stable $Q(s)$. Equation (12.6) is called a *Youla parameterization*: it characterizes all controllers that stabilize a stable process. The parameterization is illustrated by the block diagrams in Figure 12.9a.

A similar characterization can be obtained for unstable systems. Consider a process with a rational transfer function $P(s) = a(s)/b(s)$ where $a(s)$ and $b(s)$ are polynomials. By introducing a stable polynomial $c(s)$ we can write

$$P(s) = \frac{a(s)}{b(s)} = \frac{A(s)}{B(s)},$$

where $A(s) = a(s)/c(s)$ and $B(s) = b(s)/c(s)$ are stable rational functions. We have

$$\begin{aligned} \frac{1}{1 + PC_0} &= \frac{AF_0}{AF_0 + BG_0} = S_0 & \frac{P}{1 + PC_0} &= \frac{BF_0}{AF_0 + BG_0} = PS_0 \\ \frac{C_0}{1 + PC_0} &= \frac{AG_0}{AF_0 + BG_0} = CS_0 & \frac{PC_0}{1 + PC_0} &= \frac{BG_0}{AF_0 + BG_0} = T_0 \end{aligned}$$

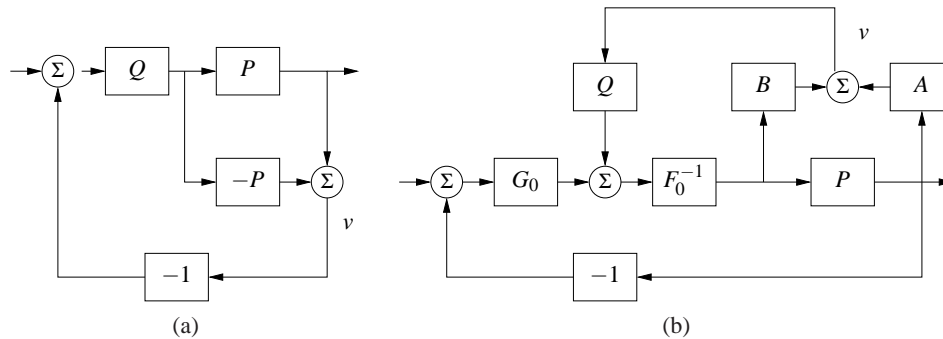


Figure 12.9: Youla parameterization. Block diagrams of Youla parameterizations for a stable system (left) and an unstable system (right). Notice that the signal v is zero in steady state.

Since C is a stabilizing controller the function $AF_0 + BG_0$ must have all its zeros in the left half plane. All stabilizing controllers are now given by

$$C = \frac{G_0 + QA}{F_0 - QB} \quad (12.7)$$

and we have

$$\begin{aligned} \frac{1}{1+PC} &= \frac{A(F_0 - QG)}{AF_0 + BG_0} & \frac{P}{1+PC} &= \frac{BF_0 - QB^2}{AF_0 + BG_0} \\ \frac{C}{1+PC} &= \frac{AG_0 + QA^2}{AF_0 + BG_0} & \frac{PC}{1+PC} &= \frac{AF_0 + BG_0}{AF_0 + BG_0}. \end{aligned}$$

Equation (12.7) reduces to equation (12.6) for $F_0 = 1$ and $G_0 = 0$. A block diagram is shown in Figure 12.9b. Notice that the transfer function Q appears affinely in the expressions for the Gang of Four, which is very useful if we want to determine the transfer function Q to obtain specific properties.

12.3 PERFORMANCE IN THE PRESENCE OF UNCERTAINTY

So far we have investigated the risk for instability and robustness to process uncertainty. We will now explore how responses to load disturbances, measurement noise and command signal following are influenced by process variations. To do this we will analyze the system in Figure 12.10, which is identical to the basic feedback loop analyzed in Chapter 11.

Disturbance Attenuation

The sensitivity function S gives a rough characterization of the effect of feedback on disturbances as was discussed in Section 11.1. A more detailed characterization

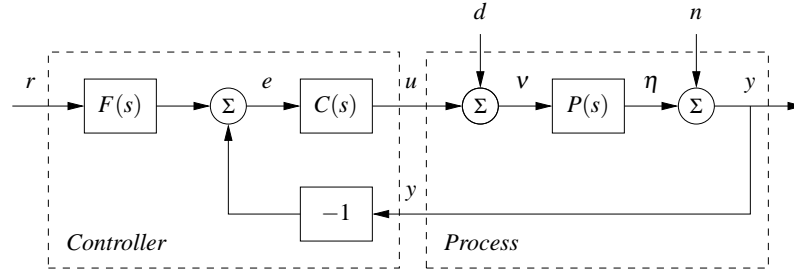


Figure 12.10: Block diagram of a basic feedback loop. The external signals are the command signal r , the load disturbance d and the measurement noise n . The process output is y and the control signal is u . The process P may include unmodeled dynamics, such as additive perturbations.

is given by the transfer function from load disturbances to process output:

$$G_{yd} = \frac{P}{1 + PC} = PS. \quad (12.8)$$

Load disturbances typically have low frequencies and it is therefore important that the transfer function is small for low frequencies. For processes with constant low frequency gain and a controller with integral action we have $G_{yd} \approx s/k_i$. Integral gain k_i is thus a simple measure of attenuation of load disturbances.

To find how the transfer function G_{yd} is influenced by small variations in the process transfer function we write P as $P + \Delta P$ and try to find the corresponding ΔG_{yd} . If the perturbations are sufficiently small, we can show that

$$\begin{aligned} G_{yd} + \Delta G_{yd} &\approx \frac{P + \Delta P}{1 + (P + \Delta P)C} \approx \frac{P}{1 + PC} + \frac{\Delta P}{1 + PC} \\ &= PS + S\Delta P = G_{yd} + \frac{G_{yd}}{P}\Delta P, \end{aligned}$$

where we have ignored terms that are quadratic and higher in ΔP . It follows that

$$\frac{dG_{yd}}{G_{yd}} = S \frac{dP}{P}, \quad (12.9)$$

where we write dG and dP as a reminder that this expression holds for small variations. The response to load disturbances is thus insensitive to process variations for frequencies where $|S(i\omega)|$ is small, i.e. for those frequencies where load disturbances are important.

A drawback with feedback is that the controller feeds measurement noise into the system. In addition to the load disturbance rejection, it is thus also important that the control actions generated by measurement noise are not too large. It follows from Figure 12.10 that the transfer function G_{un} from measurement noise to controller output is given by

$$G_{un} = -\frac{C}{1 + PC} = -\frac{T}{P}. \quad (12.10)$$

Since measurement noise typically has high frequencies, the transfer function G_{um} should not be too large for high frequencies. The loop transfer function PC is typically small for high frequencies, which implies that $G_{um} \approx C$ for large s . To avoid injecting too much measurement noise it is therefore important that $C(s)$ is small for large s . This property is called high frequency roll-off. An example is filtering of the measured signal in a PID controller to reduce injection of measurement noise; see Section 10.5.

To find how the transfer function G_{um} is influenced by small variations in the process transfer function we expand equation (12.10) and obtain the first order variations, which gives

$$\frac{dG_{um}}{G_{um}} = T \frac{dP}{P}. \quad (12.11)$$

Note that this same expression can be also be obtained by differentiation of equation (12.10):

$$\frac{dG_{um}}{dP} = \frac{d}{dP} \left(-\frac{C}{1+PC} \right) = \frac{C}{(1+PC)^2} C = T \frac{G_{um}}{P}.$$

Measurement noise typically has high frequencies. Since the complementary sensitivity function is also small for high frequencies, we find that process uncertainty has little influence on the transfer function G_{um} for frequencies where measurements are important.

Command Signal Following

The transfer function from reference to output is given by

$$G_{yr} = \frac{PCF}{1+PC} = TF, \quad (12.12)$$

which contains the complementary sensitivity function. To see how variations in P affect the performance of the system, we differentiate equation (12.12) with respect to the process transfer function:

$$\frac{dG_{yr}}{dP} = \frac{CF}{1+PC} - \frac{PCFC}{(1+PC)^2} = \frac{CF}{(1+PC)^2} = S \frac{G_{yr}}{P}.$$

and it follows that

$$\frac{dG_{yr}}{G_{yr}} = S \frac{dP}{P}. \quad (12.13)$$

The relative error in the closed loop transfer function thus equals the product of the sensitivity function and the relative error in the process. In particular, it follows from equation (12.13) that the relative error in the closed loop transfer function is small when the sensitivity is small. This is one of the useful properties of feedback.

As in the last section, there are some mathematical assumptions that are required in order for the analysis presented here to hold. As already stated, we require that the perturbations ΔP be small (as indicated by writing dP). Secondly, we require that the perturbations be stable, so that we do not introduce any new

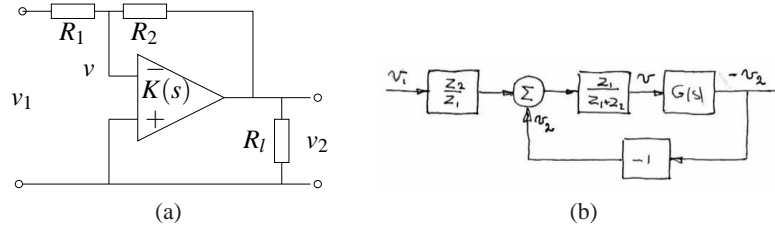


Figure 12.11: Op amp with uncertain dynamics. The op amp circuit (right) is modeled using $G(s)$ to capture its dynamic properties and includes a load at the output. The block diagram (right) shows the input/output relationships. The load is represented as a disturbance d applied at the output of $G(s)$.

right half plane poles that would require additional encirclements in the Nyquist criterion. Also, as before this condition is conservative: it allows for any perturbation that satisfies the given bounds, while in practice the perturbations may be more restricted.

Example 12.7 Op amp

To illustrate the use of these tools, consider the performance of an op amp based amplifier, as shown in Figure 12.11. We wish to analyze the performance of the amplifier in the presence of uncertainty in the dynamic response of the op amp and changes in the loading on the output. We model the system using the block diagram in Figure 12.11b, which is based on the derivation in Example 9.1.

Consider first the effect of unknown dynamics for the operational amplifier. If we model the dynamics of the op amp as

$$v_{\text{out}} = G(s)(v_+ - v_-)$$

then transfer function for the overall circuit is given by

$$H_{v_2 v_1} = -\frac{R_2}{R_1} \frac{G(s)}{G(s) + R_2/R_1 + 1}.$$

We see that if $G(s)$ is large over the desired frequency range, then the closed loop system is very close to the ideal response R_2/R_1 . We can make this more explicit by assuming that $G(s)$ has the form

$$G(s) = \frac{b}{s + a}, \quad \frac{a - a_{\text{nom}}}{a_{\text{nom}}} < \delta, \quad b_{\text{min}} \leq b \leq b_{\text{max}}.$$

The term a is the bandwidth of the amplifier and b is the bandwidth product for the amplifier as discussed in Example 8.3.

The sensitivity function and complementary sensitivity function for the nominal dynamics are given by

$$S = \frac{s + a}{s + a + \alpha b} \quad T = \frac{\alpha b}{s + a + \alpha b},$$

where $\alpha = R_2/R_1$. The sensitivity function around the nominal values tell us how

the tracking response response varies as a function of process perturbations:

$$\frac{dG_{yr}}{G_{yr}} = S \frac{dP}{P}$$

We see that for low frequencies, where S is small, variations in the bandwidth or the gain-bandwidth product will have relatively little effect on the performance of the amplifier (under the assumption that b is sufficiently large).

To model the effects of unknown load, we consider the addition of a disturbance at the output of the system, as shown in Figure 12.11b. This disturbance represents changes in the output voltage to due loading effects. The transfer function $G_{yd} = S$ gives the response of the output to the load disturbance and we see that if S is small then we are able to reject such disturbances. The sensitivity of G_{yd} to perturbations in the process dynamics can be computed by taking the derivative of G_{yd} with respect to P :

$$\frac{dG_{yd}}{dP} = \frac{-C}{(1+PC)^2} = \frac{T}{P} G_{yd} \quad \implies \quad \frac{dG_{yd}}{G_{yd}} = T \frac{dP}{P}.$$

Thus we see that the relative changes in the disturbance rejection are roughly the same as the process perturbations at low frequency (when T is approximately 1) and drop off at higher frequencies. However, it is important to remember that G_{yd} itself is small at low frequency, and so these variations in relative performance may not be an issue in many applications. ∇

12.4 ROBUST POLE PLACEMENT

In Chapters 6 and 7 we saw how to design controllers by setting the locations of the eigenvalues of the closed loop system. If we analyze the resulting system in the frequency domain, the closed loop eigenvalues correspond to the poles of the closed loop transfer function and hence these methods are often referred to as design by “pole placement”.

The design methods we used in the state space, as with many methods developed for control system design, did not explicitly take robustness into account. In such cases it is essential to always investigate the robustness because there are seemingly reasonable designs that give controllers with poor robustness. We illustrate this by analyzing controllers designed by state feedback and observers. The closed loop poles can be assigned to arbitrary locations if the system is observable and reachable. However if we want to have a robust closed loop system, the poles and zeros of the process impose severe restrictions on the location of the closed loop poles. Some examples are first given; based on analysis of these examples we then describe design rules for robust pole placement.

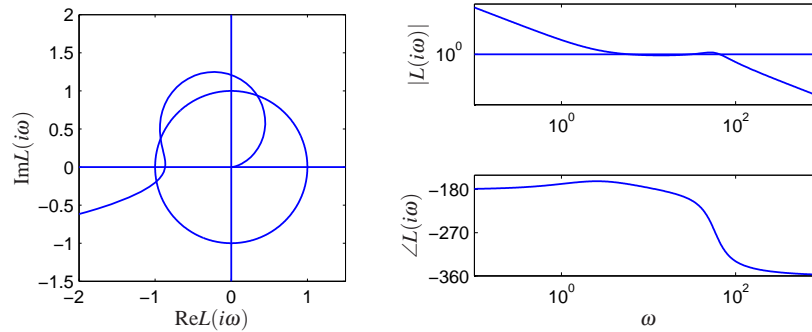


Figure 12.12: Observer-based control of steering. The Nyquist plot (left) and Bode plot (right) of the loop transfer function for vehicle steering with a controller based on state feedback and an observer. The controller provides stable operation, but with very low gain and phase margin.

Slow Stable Zeros

We will first explore the effects of slow stable zeros, and we begin with a simple example.

Example 12.8 Vehicle steering

Consider the linearized model for vehicle steering in Example 8.6, which has the transfer function

$$P(s) = \frac{0.5s + 1}{s^2}.$$

A controller based on an observer and state feedback with the closed loop poles given by $\omega_c = 1$, $\zeta_c = 0.707$, $\omega_o = 2$ and $\zeta_o = 0.707$ was designed in Example 7.3. Assume that we want a faster closed loop system and choose $\omega_c = 10$, $\zeta_c = 0.707$, $\omega_o = 20$ and $\zeta_o = 2$. A pole placement design gives state feedback gain $k_1 = 100$ and $k_2 = -35.86$ and observer gains $l_1 = 28.28$ and $l_2 = 400$. The controller transfer function is

$$C(s) = \frac{-11516s + 40000}{s^2 + 42.4s + 6657.9}.$$

Figure 12.12 shows Nyquist and Bode plots of the loop transfer function. The Nyquist plot indicates that the robustness is poor since the loop transfer function is very close to the critical point -1 . The phase margin is only 7° . This also shows up in the Bode plot where the gain curve hovers around the value 1 and the phase curve is close to 180° for a wide frequency range.

More insight is obtained by analyzing the sensitivity functions, shown by full lines in Figure 12.13. The maximum sensitivities are $M_s = 13$ and $M_t = 12$, indicating that the system has poor robustness.

At first sight it is surprising that a controller where the nominal system has well damped poles and zeros is so sensitive to process variations. We have an indication that something is unusual because the controller has a zero $s = 3.9$ in the right half plane. To understand what happens we will investigate the reason for the peaks of

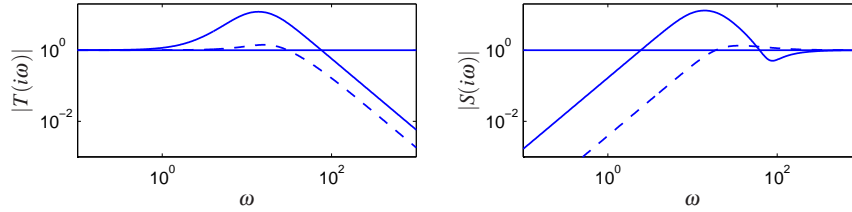


Figure 12.13: Sensitivity functions for observer-based control of vehicle steering. The complementary sensitivity function (left) and sensitivity function (right) for the original controller with $\omega_c = 10$, $\zeta_c = 0.707$, $\omega_o = 20$, $\zeta_o = 0.707$ (solid) and the improved controller with $\omega_c = 10$, $\zeta_c = 2.6$ (dashed).

the sensitivity functions.

Let the transfer functions of the process and the controller be

$$P(s) = \frac{n_p(s)}{d_p(s)} \quad C(s) = \frac{n_c(s)}{d_c(s)},$$

where $n_p(s)$, $n_c(s)$, $d_p(s)$ and $d_c(s)$ are the numerator and denominator polynomials. The complementary sensitivity function is

$$T(s) = \frac{PC}{1+PC} = \frac{n_p(s)n_c(s)}{d_p(s)d_c(s) + n_p(s)n_p(s)}.$$

$T(s)$ is 1 for low frequency and starts to increase at its first zero, which is the process zero at $s = 2$. It increases further at the controller zero at $s = 3.9$ and it does not start to decrease until the closed loop poles appear at $\omega_c = 10$ and $\omega_o = 20$. We can thus conclude that there will be a peak in the complementary sensitivity function. The magnitude of the peak depends on the ratio of the zeros and the poles of the transfer function.

The peak of the complementary sensitivity function can be avoided by assigning a closed loop zero close to the slow process zero. We can achieve this by choosing $\omega_c = 10$ and $\zeta_c = 2.6$ which gives the closed loop poles at $s = -2$ and $s = -50$. The controller transfer function then becomes

$$C(s) = \frac{3628s + 40000}{s^2 + 80.28s + 156.56} = 3628 \frac{s + 11.02}{(s + 2)(s + 78.28)}$$

The sensitivity functions are shown in dashed lines in Figure 12.13. The controller gives the maximum sensitivities $M_s = 1.34$ and $M_t = 1.41$, which gives much better robustness. Notice that the controller has a pole at $s = -2$ that cancels the slow process zero. The design can also be done simply by canceling the slow, stable process zero and designing the system for the simplified system. ∇

One lesson from the example is that it is necessary to choose closed loop poles that are equal to or close to slow, stable process zeros. Another lesson is that slow, unstable process zeros impose limitations on the achievable bandwidth, as was already noted in Section 11.5.

Fast Stable Process Poles

The next example shows the effect of fast stable poles.

Example 12.9 Fast system poles

Consider a PI controller for a first order system, where the process and the controller have the transfer functions

$$P(s) = \frac{b}{s+a} \quad C(s) = k + \frac{k_i}{s}.$$

The loop transfer function is

$$L(s) = \frac{b(ks + k_i)}{s(s+a)}$$

and the closed loop characteristic polynomial is

$$s(s+a) + b(ks + k_i) = s^2 + (a+bk)s + k_i.$$

If we let the desired closed loop characteristic polynomial be

$$(s+p_1)(s+p_2),$$

we find that the controller parameters are given by

$$k = \frac{p_1 + p_2 - a}{b} \quad k_i = \frac{p_1 p_2}{b}.$$

The sensitivity functions are then

$$S(s) = \frac{s(s+a)}{(s+p_1)(s+p_2)} \quad T(s) = \frac{(p_1 + p_2 - a)s + p_1 p_2}{(s+p_1)(s+p_2)}.$$

Assume that the process pole a is much larger than the closed loop poles p_1 and p_2 , say $p_1 < p_2 < a$. Notice that the proportional gain is negative and that the controller has a zero in the right half plane if $a > p_1 + p_2$, an indication that the system has bad properties.

Next consider the sensitivity function, which is 1 for high frequencies. Moving from high to low frequencies we find that the sensitivity increases at the process pole $s = a$. The sensitivity does not decrease until the closed loop poles are reached, resulting in a large sensitivity peak that is approximately a/p_2 . The magnitude of the sensitivity function is shown in Figure 12.14 for $a = b = 1$, $p_1 = 0.05$, $p_2 = 0.2$. Notice the high sensitivity peak. For comparison we have also shown the gain curve for the case when the closed loop poles are faster than the process pole ($p_1 = 5$, $p_2 = 20$). The problem with the poor robustness can be avoided by choosing one closed loop pole equal to the process pole, i.e. $p_2 = a$. The controller gains then become

$$k = \frac{p_1}{b} \quad k_i = \frac{ap_1}{b},$$

which means that the fast process pole is canceled by a controller zero. The loop

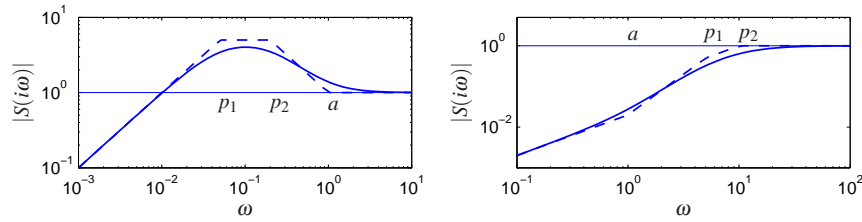


Figure 12.14: Gain curves for Bode plots of the sensitivity function S for designs with $p_1 < p_2 < a$ (left) and $a < p_1 < p_2$ (right). The full lines are the true sensitivities and the dashed lines are the asymptotes

transfer function and the sensitivity functions are

$$L(s) = \frac{bk}{s} \quad S(s) = \frac{s}{s + bk} \quad T(s) = \frac{bk}{s + bk}.$$

The maximum sensitivities are less than 1 for all frequencies. Notice that this is possible because the process transfer function goes to zero as s^{-1} . ∇

Design Rules for Pole-Placement

Based on the insight gained from the examples it is now possible to obtain design rules that give designs with good robustness. Consider the expression (12.8) for the complementary sensitivity function, repeated here:

$$M_t = \sup_{\omega} |T(i\omega)| = \left\| \frac{PC}{1 + PC} \right\|_{\infty}.$$

Let ω_{gc} be the desired gain crossover frequency. Assume that the process has zeros that are slower than ω_{gc} . The complementary sensitivity function is 1 for low frequencies and it increases for frequencies close to the process zeros unless there is a closed loop pole in the neighborhood. To avoid large values of the complementary sensitivity function we find that the closed loop system should have poles close to or equal to the slow stable zeros. This means that slow stable zeros should be canceled by controller poles. Since unstable zeros cannot be canceled, the presence of slow unstable zeros means that achievable gain crossover frequency must be smaller than the slowest unstable process zero.

Now consider process poles that are faster than the desired gain crossover frequency. Consider the expression for the maximum of the sensitivity function.

$$M_s = \sup_{\omega} |S(i\omega)| = \left\| \frac{1}{1 + PC} \right\|_{\infty}.$$

The sensitivity function is 1 for high frequencies. Moving from high to low frequencies the sensitivity function increases at the fast process poles. Large peaks can result unless there are closed loop poles close to the fast process poles. To avoid large peaks in the sensitivity the closed loop system should have poles that match the fast process poles. This means that the controller should cancel the fast

process poles by controller zeros. Since unstable modes cannot be canceled, the presence of a fast unstable pole implies that the gain crossover frequency must be sufficiently large.

To summarize, we obtain the following simple design rule: slow stable process zeros should be matched slow closed loop poles and fast stable process poles should be matched by fast process poles. Slow unstable process zeros and fast unstable process poles impose severe limitations.

Example 12.10 Nanopositioner

A simple nanopositioner was explored in Example 9.9 where it was shown that the system could be controlled using an integrating controller. The performance of the closed loop was poor, because the gain crossover frequency was limited to $2\zeta_0\omega_0(1-s_m)$. In Exercise ?? it was also shown that little could be gained by adding proportional action. To obtain improved performance we will therefore use a PID controller. For modest increases we will use the design rule derived in Example 12.9 that fast stable process poles should be canceled by controller zeros. The controller transfer function should thus be chosen as

$$C(s) = \frac{k_d s^2 + k_p s + k_i}{s} = \frac{k_i}{s} \frac{s^2 + 2\zeta s + a^2}{a^2} \quad (12.14)$$

which gives $k_p = 2\zeta k_i/a$ and $k_d = k_i/a^2$.

Figure 12.15 shows the gain curves for the Gang of Four for a system designed with $k_i = 0.5$. A comparison with Figure 9.12 on page 279 shows that the bandwidth is increased significantly from $\omega_{gc} = 0.01$ to $\omega_{gc} = k_i = 0.5$. Since the process pole is canceled the system will however still be very sensitive to load disturbances with frequencies close to the resonant frequency. The gain curve of $CS(s)$ has a dip or a notch at the resonance frequency, which implies that the controller gain is very low for frequencies around the resonance. The gain curve also shows that the system is very sensitive to high frequency noise. The system will likely be unusable because the gain goes to infinity for high frequencies.

This can easily be remedied by modifying the controller to

$$C(s) = \frac{k_i}{s} \frac{s^2 + 2\zeta s + a^2}{a^2(1 + sT_f + (sT_f)^2/2)}, \quad (12.15)$$

which has high-frequency roll-off. Selection of the constant T_f of the filter is a compromise between attenuation of high frequency measurement noise and robustness. A large value of T_f reduces effects of sensor noise significantly but it also reduces the stability margin. A bit of experimentation using the Gang of Four gives $T_f = 0.75$ as a good compromise and the curves shown in full lines in Figure 12.15. The curves for $CS(s)$ shown that the effect of high-frequency roll-off due to filtering is quite dramatic. Notice that the poor attenuation of disturbances with frequencies close to the resonance are not visible in the sensitivity function because of the cancellation of poles and zeros.

The designs thus far have the drawback that load disturbances with frequencies close to the resonance are not attenuated. We will now consider a design that

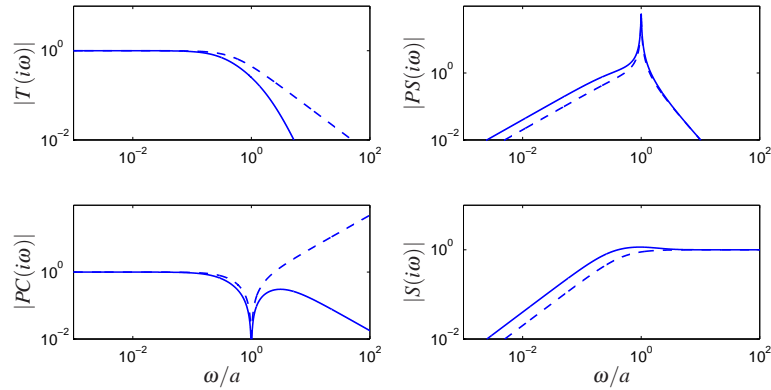


Figure 12.15: Nanopositioner control via cancellation of the fast process pole. Gain curves for the Gang of Four for PID control with second order filtering (12.15) are shown in full and the dashed lines show results for an ideal PID controller without filtering (12.14).

that actively attenuates the poorly damped modes. We will start with an ideal PID controller where the design can be done analytically and we will add high frequency roll-off. The loop transfer function obtained with this controller is

$$L(s) = \frac{k_d s^2 + k_p s + k_i}{s(s^2 + 2\zeta a s + a^2)}. \quad (12.16)$$

The closed loop system is of third order and its characteristic polynomial is

$$s^3 + (k_d a^2 + 2\zeta a)s^2 + (k_p + 1)a^2 s + k_i a^2. \quad (12.17)$$

A general third order polynomial can be parameterized as

$$(s + \alpha_0 \omega_0)(s^2 + 2\zeta_0 \omega_0 s + \omega_0^2) = s^3 + (\alpha_0 + 2\zeta_0)\omega_0 s^2 + (1 + 2\alpha_0 \zeta_0)\omega_0^2 s + \alpha_0 \omega_0^3. \quad (12.18)$$

Parameters α_0 and ζ_0 give the configuration of the poles and parameter ω_0 their magnitudes and therefore also the bandwidth of the system.

Identification of coefficients of equal powers of s in equations (12.17) and (12.18) gives the following equations for the controller parameters

$$\begin{aligned} k_d a^2 + 2\zeta a &= (\alpha_0 + 2\zeta_0)\omega_0 \\ a^2(k_p + 1) &= (1 + 2\alpha_0 \zeta_0)\omega_0^2 \\ a^2 k_i &= \alpha_0 \omega_0^3. \end{aligned} \quad (12.19)$$

To obtain a design with active damping it is necessary that the closed loop bandwidth is at least as fast as the oscillatory modes. Adding high frequency roll-off the controller becomes

$$C(s) = \frac{k_d s^2 + k_p s + k}{s(1 + sT_f + (sT_f)^2/2)}. \quad (12.20)$$

The value $T_f = T_d/10 = k_d/(10k)$ is a good value of the filtering time constant.

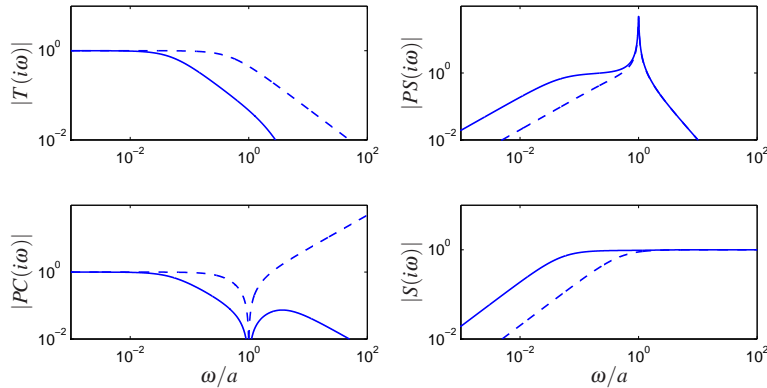


Figure 12.16: Nanopositioner control using active damping. Gain curves for the Gang of Four for PID control using the controller (12.16). The controller has high frequency roll-off and has been designed to give active damping of the oscillatory mode. The different curves correspond to different choices of magnitudes of the poles, parameterized by ω_0 in equation (12.16).

In Figure 12.16 we show the gain curves of the Gang of Four for designs with $\zeta = 0.707$, $\alpha_0 = 2$ and $\omega_0 = a, 2a$ and $4a$. The figure shows that the largest values of the sensitivity function and the complementary sensitivity function are small. The gain curve for $PS(s)$ shows that load disturbances are now well attenuated over the whole frequency range. The gain curve for CS shows that large control signals are required to provide active damping. The high values of $CS(i\omega)$ for high frequencies also show that low noise sensors and actuators with a wide range are required. The largest gains for $CS(s)$ are 60, 262 and 1074 for $\omega_0 = a, 2a$ and $4a$ respectively. The high frequency gain of the controller thus increases dramatically with the value of ω_0 . A comparison of Figures 12.15 and 12.16 illustrates the trade-offs between control action and disturbance attenuation for the designs with cancellation of the fast process pole and active damping. ∇

12.5 DESIGN FOR ROBUST PERFORMANCE



Control design is a rich problem where many factors have to be taken into account. Typical requirements are that load disturbances should be attenuated, the controller should only inject a moderate amount of measurement noise, the output should follow variations in the command signal well and the closed loop system should be insensitive to process variations. For the system in Figure 12.10 these requirements can be captured by specifications on the sensitivity functions S and T and the transfer functions G_{yd} , G_{un} , G_{yr} and G_{ur} . Notice that it is necessary to consider at least six transfer functions, as discussed Section 11.1. The requirements are mutually conflicting and it is necessary to make tradeoffs. Attenuation of load disturbances will be improved if the bandwidth is increased but so will the noise injection.

It is highly desirable to have design methods that can guarantee robust performance. Such design methods did not appear until the late 1980s. Many of these design methods result in controllers having the same structure as the controller based on state feedback and an observer. In this section we provide a brief review of some of the techniques as a preview for those interested in more specialized study.

Linear Quadratic Control (LQG)

One way to make the trade-off between attenuation of load disturbances and injection of measurement noise is to design a controller that minimizes the loss function

$$J = \frac{1}{T} \int_0^T (y^2(t) + \rho u^2(t)) dt,$$

where ρ is a weighting parameter as discussed in Section 6.3. This loss function gives a compromise between load disturbance attenuation and disturbance injection because it balances control actions against deviations in the output. If all state variables are measured, the controller is a state feedback

$$u = -Kx$$

The controller has the same form as the controller obtained by eigenvalue assignment (pole placement) in Section 6.2. However, the controller gain is obtained by solving an optimization problem. It has been shown that this controller is very robust. It has a phase margin of at least 60° and an infinite gain margin. The controller is called a *linear quadratic control* or *LQ control* because the process model is linear and the criterion is quadratic.

When all state variables are not measured, the state can be reconstructed using an observer, as discussed in Section 7.3. It is also possible to introduce process disturbances and measurement noise explicitly in the model and to reconstruct the states using a Kalman filter as discussed briefly in Section 7.4. The Kalman filter has the same structure as the observer designed by pole assignment in Section 7.3, but the observer gains L are now obtained by solving an optimization problem. The control law obtained by combining linear quadratic control with a Kalman filter is called *linear quadratic Gaussian control* or *LQG Control*. The Kalman filter is optimal when the models for load disturbances and measurement noise are Gaussian.

It is interesting that the solution to the optimization problem leads to a controller having the structure of a state feedback and an observer. The state feedback gains depend on the parameter ρ and the filter gains depend on the parameters in the model that characterize process noise and measurement noise (see Section 7.4). There are efficient programs to compute these feedback and observer gains.

The nice robustness properties of state feedback are unfortunately lost when the observer is added. It is possible to choose parameters that give closed loop systems with poor robustness, similar to Example 12.8. We can thus conclude that there

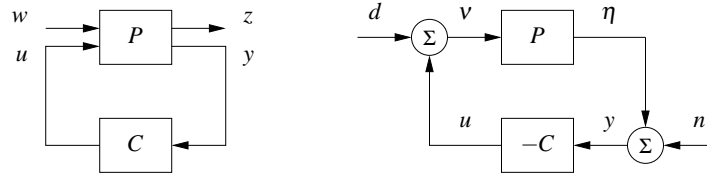


Figure 12.17: H_∞ robust control formulation. The left figure shows a general representation of a control problem used in robust control. The input u represents the control signal, the input w represents the external influences on the system, the output z is the generalized error and the output y is the measured signal. The right figure shows the special case of the basic feedback loop in Figure 12.10 where the reference signal is zero. In this case we have $w = (-n, d)$ and $z = (\eta, v)$.

is a fundamental difference between using sensors for all states and reconstructing the states using an observer.

H_∞ Control



Robust control design is often called H_∞ control for reasons that will be explained shortly. The basic ideas are simple but the details are complicated and we will therefore just give the flavor of the results. A key idea is illustrated in Figure 12.17 where the closed loop system is represented by two blocks, the process P and the controller C as discussed in Section 11.1. The process P has two inputs, the control signal u which can be manipulated by the controller, and the generalized disturbance w , which represents all external influences, for example command signals and disturbances. The process has two outputs, the generalized error z which is a vector of error signals representing the deviation of signals from their desired values and the measured signal y which can be used by the controller to compute u . For a linear system and a linear controller the closed loop system can be represented by the linear system

$$z = H(P(s), C(s))w \quad (12.21)$$

which tells how the generalized error w depends on the generalized disturbances w . The control design problem is to find a controller C such that the gain of the transfer function H is small even when the process has uncertainties. There are many different ways to specify uncertainty and gain, giving rise to different designs. The names H_2 and H_∞ control correspond to the norms $\|H\|_2$ and $\|H\|_\infty$.

To illustrate the ideas we will consider a regulation problem for a system where the reference signal is assumed to be zero and the external signals are the load disturbance d and the measurement noise n , as shown in Figure 12.17b. The generalized input is $w = (-n, d)$. (The negative sign of n is not essential, but is chosen to get somewhat nicer equations.) The generalized error is chosen as $z = (\eta, v)$, where η is the process output, and v is the part of the load disturbance that is not

compensated by the controller. The closed loop system is thus modeled by

$$z = \begin{pmatrix} \eta \\ v \end{pmatrix} = H(P, C) \begin{pmatrix} -n \\ d \end{pmatrix} = \begin{pmatrix} \frac{1}{1+PC} & \frac{P}{1+PC} \\ C & PC \\ \frac{1}{1+PC} & \frac{PC}{1+PC} \end{pmatrix} \begin{pmatrix} -n \\ d \end{pmatrix}, \quad (12.22)$$

which is the same as equation (12.21). A straightforward calculation shows that

$$\|H(P, C)\|_\infty = \sup_{\omega} \frac{\sqrt{(1+|P(i\omega)|^2)(1+|C(i\omega)|^2)}}{|1+P(i\omega)C(i\omega)|}. \quad (12.23)$$

There are efficient numerical methods to find a controller such that $\|H(P, C)\|_\infty < \gamma$, if such a controller exists. The best controller can then be found by iterating on γ . The calculations can be made by solving *algebraic Riccati* equations, for example by using the command `hinfsyn` in MATLAB. The controller has the same order as the process and the same structure as the controller based on state feedback and an observer; see Figure 7.7 and equation (7.18) on page 214.

Notice that if we minimize $\|H(P, C)\|_\infty$ we make sure that the transfer functions $G_{yd} = P/(1+PC)$, representing transmission of load disturbances to the output, and $G_{un} = -C/(1+PC)$, representing how measurement noise is transmitted to the control signal, are small. Since the sensitivity and the complementary sensitivity functions are also elements of $H(P, C)$ we have also guaranteed that the sensitivities are also less than γ . The design methods thus balance performance and robustness.

There are strong robustness results associated with the H_∞ controller. We can understand this intuitively by comparing equations (12.1) and (12.23). We can then conclude that

$$\|H(P, C)\|_\infty = \frac{1}{d_v(P, -1/C)}. \quad (12.24)$$

The inverse of $\|H(P, C)\|_\infty$ is thus equal to chordal distance between P and $1/C$. If we find a controller C with $\|H(P, C)\|_\infty < \gamma$ this controller will then stabilize any process P_* such that $d_v(P, P_*) < \gamma$.

Disturbance Weighting

Minimizing the gain $\|H(P, C)\|_\infty$ means that gains of all individual signal transmissions from disturbances to outputs are less than γ for all frequencies of the input signals. The assumption that the disturbances are equally important and that all frequencies are also equally important is not very realistic, recall that load disturbances typically have low frequencies and measurement noise is typically dominated by high frequencies. It is straightforward to modify the problem so that disturbances of different frequencies are given different emphasis, by introducing a weighting filter on the load disturbance as shown in Figure 12.17. For example low frequency load disturbances will be enhanced by choosing W_d as a low pass filter because the actual load disturbance is $W_d \bar{d}$.

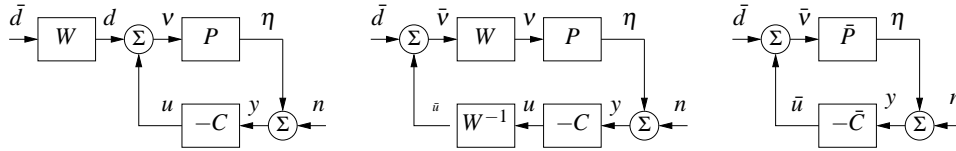


Figure 12.18: Block diagrams of a system with disturbance weighting. The left figure provides a frequency weight on processes disturbances. Through block diagram manipulation, this can be converted to the standard problem on the right.

By using block diagram manipulation as shown in Figure 12.18 we find that the system with frequency weighting is equivalent to the system with no frequency weighting in Figure 12.18 and the signals are related through

$$z_w = \begin{pmatrix} \eta \\ \bar{v} \end{pmatrix} \begin{pmatrix} \frac{1}{1 + P_w C_w} & \frac{P_w}{1 + P_w C_w} \\ \frac{C_w}{1 + P_w C_w} & \frac{P_w C_w}{1 + P_w C_w} \end{pmatrix} \begin{pmatrix} -n \\ \bar{d} \end{pmatrix} = H(P_w, C_w) w_w, \quad (12.25)$$

where $P_w = PW_d$ and $C_w = W_d^{-1}C$. The problem of finding a controller C_w that minimizes the gain of $H(P_w, C_w)$ is thus equivalent to the problem without disturbance weighting; having obtained C_w , the controller for the original system is then $C = W_d C_w$. Notice that if we introduce the frequency weighting $W_d = k/s$ we will automatically get a controller with integral action.

Limits of Robust Design

There is a limit to what can be achieved by robust design. In spite of the nice properties of feedback, there are situations where the process variations are so large that it is not possible to find a linear controller that gives a robust system with good performance. It is then necessary to use other types of controllers. In some cases it is possible to measure a variable that is well correlated with the process variations. Controllers for different parameter values can then be designed and the corresponding controller can be chosen based on the measured signal. This type of control design is called *gain scheduling*. The cruise controller is a typical example where the measured signal could be gear position and velocity. Gain scheduling is the common solution for high performance aircraft where scheduling is done based on Mach number and dynamic pressure. When using gain scheduling it is important to make sure that switches between the controllers do not create undesirable transients (often referred to as *bumpless transfer*).

If it is not possible to measure variables related to the parameters, it is possible to use *automatic tuning* and *adaptive control*. In automatic tuning the process dynamics are measured by perturbing the system and a controller is then designed automatically. Automatic tuning requires that parameters remain constant and it has been widely applied for PID control. It is a reasonable guess that in the fu-

ture many controllers will have features for automatic tuning. If parameters are changing it is possible to use adaptive methods where process dynamics are measured on-line.

12.6 FURTHER READING

The topic of robust control is a large one, with many articles and textbooks devoted to the subject. Robustness was a central issue in classical control as described in Bode's classical book [40]. Robustness was deemphasized in the euphoria of the development of design methods based on optimization. The strong robustness of controllers based on state feedback shown by Anderson and Moore [7] contributed to the optimism. The poor robustness of output feedback was pointed out by Rosenbrock [160], Horowitz [98] and Doyle [58] and resulted in a renewed interest in robustness. A major step forward was the development of design methods where robustness was explicitly taken into account, such as the seminal work by Zames [197]. Robust control was originally developed using powerful results from the theory of complex variables, which unfortunately gave controllers of high order. A major breakthrough was given by Doyle, Glover, Khargonekar, and Francis [60], who showed that the solution to the problem could be obtained using Riccati equations and that a controller of low order could be found. This paper led to an extensive treatment of the so-called H_∞ control, including books by Francis [75], McFarlane and Glover [132], Doyle, Francis and Tannenbaum [59], Green and Limebeer [86], Zhou, Doyle and Glover [198], Skogestad and Postlethwaite [172], and Vinnicombe [187]. A major advantage of the theory is that it combines much of the intuition from servomechanism theory with sound numerical algorithms based on numerical linear algebra and optimization. The results have been extended to nonlinear systems by treating the design problem as a game where the disturbances are generated by an adversary, as described in the book by Basare and Beernhard [23].

EXERCISES

12.1 Consider a feedback loop with a process and a controller having transfer functions P and C . Assume that the maximum sensitivity is $M_t = 2$. Show that the phase margin is at least 30° and that the closed loop system will be stable if the gain is changed by 50%.

12.2 Show that a stable additive perturbation ΔP_{add} can create right half plane zeros, but not right half plane poles, and that a stable feedback perturbation ΔP_{fbk} can create right half plane poles but not right half plane zeros. Give constructive examples of each.

12.3 Compute the μ -gap metric between the systems

$$P_1(s) = \frac{k}{s+1} \quad \text{and} \quad P_2(s) = \frac{k}{s-11}$$

for $k = 1, 2$ and 5 .

12.4 The distance measure is closely related to closed loop systems with unit feedback. Show how the measure can be modified to apply to an arbitrary feedback.

12.5 Consider the transfer functions in Examples 12.2 and 12.3. Compute the distance measure $d_v(P_1, P_2)$ in both cases. Repeat the calculations when the controller is $C = 0.1$.

12.6 Consider the Nyquist curve in Figure 12.12. Explain why part of the curve is approximately a circle. Derive a formula for the center and the radius and compare with the actual Nyquist curve.

12.7 (Ideal delay compensator) Consider a process whose dynamics are a pure time delay with transfer function $P(s) = e^{-s}$. The ideal delay compensator is a controller with the transfer function $C(s) = 1/(1 - e^{-s})$. Show that the sensitivity functions are $T(s) = e^{-s}$ and $S(s) = 1 - e^{-s}$ and that the closed loop system will be unstable for arbitrarily small changes in the delay.

12.8 Let P and C be matrices whose entries are complex numbers. Show that the singular values of the matrix

$$H(P, C) = \begin{pmatrix} \frac{1}{1+PC} & \frac{P}{1+PC} \\ \frac{C}{1+PC} & \frac{1}{1+PC} \end{pmatrix}$$

are

$$\sigma_1 = 0 \quad \sigma_2 = \sup_{\omega} \frac{\sqrt{(1+|P(i\omega)|^2)(1+|C(i\omega)|^2)}}{|1+P(i\omega)C(i\omega)|}.$$

12.9 Show that

$$\sup_{\omega} \frac{|1+P(i\omega)C(i\omega)|}{\sqrt{(1+|P(i\omega)|^2)(1+|C(i\omega)|^2)}} = d(P, -1/C).$$

12.10 (Bode's ideal loop transfer function) When designing electronic amplifiers Bode proposed that the loop transfer function should have the form $L(s) = ks^{-n}$ with $0 < n < 2$. Show that such a loop transfer function has constant stability margin $s_m = \arcsin \pi(1 - n/2)$. Plot the Nyquist curve of the system and determine phase and gain margins.

12.11 Consider the system

$$\begin{aligned} \frac{dx}{dt} &= Ax + Bu = \begin{pmatrix} -1 & 0 \\ 1 & 0 \end{pmatrix} x + \begin{pmatrix} a-1 \\ 1 \end{pmatrix} u \\ y &= Cx = \begin{pmatrix} 0 & 1 \end{pmatrix} x. \end{aligned} \quad (12.26)$$

The system has the transfer function

$$G_P(s) = C[sI - A]^{-1}B = \frac{s + a}{s(s + 1)} \quad (12.27)$$

12.12 Rewrite the solution below as an exercise.

12.13 (Disk drive tracking) Insert from CDS 110a, using sensitivity. Noise \rightarrow sensitivity spec \rightarrow design \rightarrow robustness check.

Bibliography

- [1] M. A. Abkowitz. *Stability and Motion Control of Ocean Vehicles*. MIT Press, Cambridge, MA, 1969.
- [2] R. H. Abraham and C. D. Shaw. *Dynamics—The Geometry of Behavior; Part 1: Periodic Behavior*. Aerial Press, Inc., 1982.
- [3] J. Ackermann. Der entwurf lineare regelungssysteme im zustandsraum. *Regelungstechnik und Prozessdatenverarbeitung*, 7:297–300, 1972.
- [4] J. Ackermann. *Sampled-Data Control Systems*. Springer, Berlin, 1985.
- [5] C. E. Agnew. Dynamic modeling and control of congestion-prone systems. *Operations Research*, 24(3):400–419, 1976.
- [6] L. V. Ahlfors. *Complex Analysis*. McGraw-Hill, New York, NY, 1966.
- [7] B. D. O. Anderson and J. B. Moore. *Optimal Control Linear Quadratic Methods*. Prentice Hall, Englewood Cliffs, NJ, 1990. Republished by Dover Publications, 2007.
- [8] A. A. Andronov, A. A. Vitt, and S. E. Khaikin. *Theory of Oscillators*. Dover, New York, 1987.
- [9] T. M. Apostol. *Calculus, Volume II: Multi-Variable Calculus and Linear Algebra with Applications*. Wiley, 1967.
- [10] T. M. Apostol. *Calculus, Volume I: One-Variable Calculus with an Introduction to Linear Algebra*. Wiley, 1969.
- [11] R. Aris. *Mathematical Modeling Techniques*. Dover, New York, 1994. Originally published by Pitman in 1978.
- [12] V. I. Arnold. *Mathematical Methods in Classical Mechanics*. Springer, New York, 1978.
- [13] V. I. Arnold. *Ordinary Differential Equations*. MIT Press, Cambridge, MA, 1987. 10th printing 1998.
- [14] K. J. Åström. *Introduction to Stochastic Control Theory*. Academic Press, 1970. Republished by Dover Publications, 2006.
- [15] K. J. Åström. Limitations on control system performance. *European Journal on Control*, 6(1):2–20, 2000.
- [16] K. J. Åström and T. Hägglund. *PID Controllers: Theory, Design and Tuning*. Instrument Society of American, 1995.
- [17] K. J. Åström and T. Hägglund. *Advanced PID Control*. ISA - The Instrumentation, Systems, and Automation Society, Research Triangle Park, NC 27709, 2005.
- [18] K. J. Åström, R. E. Klein, and A. Lennartsson. Bicycle dynamics and control. *IEEE Control Systems Magazine*, 25(4):26–47, 2005.
- [19] K. J. Åström and B. Wittenmark. *Computer-Control Systems: Theory and Design*. Prentice Hall, 1990.
- [20] D. P. Atherton. *Nonlinear Control Engineering*. Van Nostrand, New York, NY, 1975.

- [21] M. Atkinson, M. Savageau, J. Myers, and A. Ninfa. Development of genetic circuitry exhibiting toggle switch or oscillatory behavior in *Escherichia coli*. *Cell*, 113(5):597–607, 2003.
- [22] M. B. Barron and W. F. Powers. The role of electronic controls for future automotive mechatronic systems. *IEEE Transactions on Mechatronics*, 1(1):80–89, 1996.
- [23] T. Basar and P. Bernhard. *H[∞]-Optimal Control and Related Minimax Design Problems: A Dynamic Game Approach*. Birkhauser, Boston, 1991.
- [24] J. Bechhoefer. Feedback for physicists: A tutorial essay on control. *Reviews of Modern Physics*, 77:783–836, 2005.
- [25] R. Bellman and K. J. Åström. On structural identifiability. *Mathematical Biosciences*, 7:329–339, 1970.
- [26] R. E. Bellman and R. Kalaba. *Selected Papers on Mathematical Trends in Control Theory*. Dover, New York, NY, 1964.
- [27] S. Bennett. *A History of Control Engineering: 1800–1930*. Peter Peregrinus, 1986.
- [28] S. Bennett. *A History of Control Engineering: 1930–1955*. Peter Peregrinus, 1986.
- [29] L. L. Beranek. *Acoustics*. McGraw-Hill, New York, NY, 1954.
- [30] R. N. Bergman. Toward physiological understanding of glucose tolerance: minimal model approach. *Diabetes*, 38:1512–1527, 1989.
- [31] R. N. Bergman. The minimal model of glucose regulation: a biography. In J. Novotny, M. Green, and R. Boston, editors, *Mathematical Modeling in Nutrition and Health*. Kluwer Academic/Plenum, New York, 2001.
- [32] D. Bertsekas and R. Gallager. *Data Networks*. Prentice Hall, Englewood Cliffs, 1987.
- [33] B. Bialkowski. Process control sample problems. In N. J. Sell, editor, *Process Control Fundamentals for the Pulp & Paper Industry*. Tappi Press, 1995.
- [34] G. Binnig and H. Rohrer. Scanning tunneling microscopy. *IBM Journal of Research and Development*, 30(4):355–369, 1986.
- [35] H. S. Black. Stabilized feedback amplifiers. *Bell System Technical Journal*, 13:1–2, 1934.
- [36] H. S. Black. Inventing the negative feedback amplifier. *IEEE Spectrum*, pages 55–60, 1977.
- [37] J. F. Blackburn, G. Reethof, and J. L. Shearer. *Fluid Power Control*. MIT Press, Cambridge, MA, 1960.
- [38] J. H. Blakelock. *Automatic Control of Aircraft and Missiles*. Addison-Wesley, Cambridge, MA, second edition, 1991.
- [39] G. Blickley. Modern control started with ziegler-nichols tuning. *Control Engineering*, 37:72–75, 1990.
- [40] H. W. Bode. *Network Analysis and Feedback Amplifier Design*. Van Nostrand, 1945.
- [41] H. W. Bode. Feedback—The History of an Idea. In *Symposium on Active Networks and Feedback Systems*. Polytechnic Institute of Brooklyn, 1960. Reprinted in [26].
- [42] W. E. Boyce and R. C. DiPrima. *Elementary Differential Equations*. Wiley, 2004.
- [43] R. Brockett. *Finite Dimensional Linear Systems*. Wiley, New York, NY, 1970.
- [44] R. W. Brockett. New issues in the mathematics of control. In B. Engquist and W. Schmid, editors, *Mathematics Unlimited—2001 and Beyond*, pages 189–220. Springer Verlag, 2000.
- [45] G. S. Brown and D.P. Campbell. *Principles of Servomechanisms*. Wiley, New York, NY, 1948.
- [46] F. M. Callier and C. A. Desoer. *Linear System Theory*. Springer-Verlag, 1991.
- [47] R. H. Cannon. *Dynamics of Physical Systems*. Dover, 2003. Originally published by Mc-Graw Hill, 1967.

- [48] H. S. Carslaw and J. C. Jaeger. *Conduction of Heat in Solids*. Carendon Press, Oxford, second edition, 1959.
- [49] H. Chestnut and R. W. Mayer. *Servomechanisms and Regulating System Design Vol 1*. Wiley, New York, NY, 1951.
- [50] C. Cobelli and G. Toffolo. A model of glucose kinetics and their control by insulin, compartmental and non-compartmental approaches. *Math. Biosciences*, 72:291–235?, 1984.
- [51] R. F. Coughlin and F. F. Driscoll. *Operational Amplifiers and Linear Integrated Circuits. 6th Edition*. Prentice Hall, Englewood Cliffs, NJ, 1975.
- [52] L. B. Cremean, T. B. Foote, J. H. Gillula, G. H. Hines, D. Kogan, K. L. Kriechbaum, J. C. Lamb, J. Leibs, L. Lindzey, C. E. Rasmussen, A. D. Stewart, J. W. Burdick, and R. M. Murray. Alice: An information-rich autonomous vehicle for high-speed desert navigation. *Journal of Field Robotics*, 23(9):777–810, 2006.
- [53] H. de Jong. Modeling and simulation of genetic regulatory systems: A literature review. *Journal of Computational Biology*, 9:67–103, 2002.
- [54] L. Desborough and R. Miller. Increasing customer value of industrial control performance monitoring—Honeywell’s experience. In *Sixth International Conference on Chemical Process Control*. AIChE Symposium Series Number 326 (Volume 98), 2002.
- [55] Y. Diao, N. Gandhi, J. L. Hellerstein, S. Parekh, and D. M. Tilbury. Using mimo feedback control to enforce policies for interrelated metrics with application to the apache web server. In *Proceedings of the IEEE/IFIP Network Operations and Management Symposium*, pages 219–234, 2002.
- [56] R. C. Dorf and R. H. Bishop. *Modern Control Systems*. Prentice Hall, tenth edition, 2004.
- [57] F. H. Dost. *Grundlagen der Pharmakokinetik*. Thieme Verlag, Stuttgart, 1968.
- [58] J. C. Doyle. Guaranteed margins for lqg regulators. *IEEE Transactions on Automatic Control*, 23(4):756–757, 1978.
- [59] J. C. Doyle, B. A. Francis, and A. R. Tannenbaum. *Feedback Control Theory*. Macmillan Publishing Company, 1992.
- [60] J. C. Doyle, K. Glover, P. P. Khargonekar, and B. A. Francis. State-space solutions to standard H_2 and H_∞ control problems. *IEEE Transactions on Automatic Control*, 34(8):831–847, 1989.
- [61] L. E. Dubins. On curves of minimal length with a constraint on average curvature, and with prescribed initial and terminal positions and tangents. *American Journal of Mathematics*, 79:497–516, 1957.
- [62] F. Dyson. A meeting with Enrico Fermi. *Nature*, 247(6972):297, 2004.
- [63] R. Oldenburger (editor). *Frequency Response*. MacMillan, New York, NY, 1956.
- [64] T. Basar (editor). *Control Theory Twenty-five Seminal Papers (1932-1981)*. IEEE Press, New York, NY, 2001.
- [65] H. El-Samad, J. P. Goff, and M. Khammash. Calcium homeostasis and parturient hypocalcemia an integral feedback perspective. *J. theor. Biol.*, 214:17–29, 2002.
- [66] J. R. Ellis. *Vehicle Handling Dynamics*. Mechanical Engineering Publications, London, 1994.
- [67] S. P. Ellner and J. Guckenheimer. *Dynamic Models in Biology*. Princeton University Press, 2005.
- [68] M. B. Elowitz and S. Leibler. A synthetic oscillatory network of transcriptional regulators. *Nature*, 403(6767):335–338, 2000.
- [69] P. G. Fabietti, V. Canonico, M. O. Federici, M. Benedetti, and E. Sarti. Control oriented model of insulin an glucose dynamics in type 1 diabetes. *Med. Biol. Eng. Comput.*, 44:66–78, 2006.

- [70] M. Fliess, J. Levine, P. Martin, and P. Rouchon. On differentially flat nonlinear systems. *Comptes Rendus des Séances de l'Académie des Sciences*, 315:619–624, 1992. Serie I.
- [71] M. Fliess, J. Levine, P. Martin, and P. Rouchon. Flatness and defect of non-linear systems: Introductory theory and examples. *International Journal of Control*, 61(6):1327–1361, 1995.
- [72] J. W. Forrester. *Industrial Dynamics*. MIT Press, Cambridge, MA, 1961.
- [73] J. B. J. Fourier. *On the Propagation of Heat in Solid Bodies*. 1807.
- [74] A. Fradkov. *Cybernetical Physics: From Control of Chaos to Quantum Control*. Springer, 2007.
- [75] B. A. Francis. *A Course in \mathcal{H}_∞ Control*. Springer-Verlag, Berlin, 1987.
- [76] G. F. Franklin, J. D. Powell, and A. Emami-Naeini. *Feedback Control of Dynamic Systems*. Addison Wesley Longman, fifth edition, 2005.
- [77] B. Friedland. *Control System Design: An Introduction to State Space Methods*. Dover, 2004.
- [78] M. A. Gardner and J. L. Barnes. *Transients in Linear Systems*. John Wiley, New York, 1942.
- [79] E. Gilbert. Controllability and observability in multivariable control systems. *SIAM J. Control*, 1(1):128–151, 1963.
- [80] M. Giobaldi and D. Perrier. *Pharmacokinetics*. Marcel Dekker, New York, second edition, 1982.
- [81] K. Godfrey. *Compartment models and their application*. Academic Press, New York, NY, 1983.
- [82] H. Goldstein. *Classical Mechanics*. Addison-Wesley, Cambridge, MA, 1953.
- [83] S. W. Golomb. Mathematical models—uses and limitations. *Simulation*, 4(14):197–198, 1970.
- [84] G. C. Goodwin, S. F. Graebe, and M. E. Salgado. *Control System Design*. Prentice Hall, Upper Saddle River, NJ, 2001.
- [85] D. Graham and D. McRuer. *Analysis of Nonlinear Control Systems*. Wiley, New York, NY, 1961.
- [86] Michael Green and D. J. N. Limebeer. *Linear Robust Control*. Prentice Hall, Englewood Cliffs, N.J., 1995.
- [87] J. Guckenheimer and P. Holmes. *Nonlinear Oscillations, Dynamical Systems, and Bifurcations of Vector Fields*. Springer Verlag, 1983.
- [88] E. A. Guillemin. *Theory of Linear Physical Systems*. MIT Press, Cambridge, MA, 1963.
- [89] L. Gunkel and G. F. Franklin. A general solution for linear sampled data systems. *IEEE Transactions on Automatic Control*, AC-16:767–775, 1971.
- [90] W. Hahn. *Stability of Motion*. Springer, Berlin, 1967.
- [91] D. Hanahan and R. A. Weinberg. The hallmarks of cancer. *Cell*, 100:57–70, 2000.
- [92] J. L. Hellerstein, Y. Diao, S. Parekh, and D. M. Tilbury. *Feedback Control of Computing Systems*. John Wiley, New York, 2004.
- [93] David V. Herlihy. *Bicycle—The History*. Yale University Press, Yale, NH, 2004.
- [94] M. B. Hoagland and B. Dodson. *The Way Life Works*. Times Books, 1995.
- [95] A. L. Hodgkin and A. F. Huxley. A quantitative description of membrane current and its application to conduction and excitation in nerve. *Journal of Physiology*, 117(500–544), 1952.
- [96] C. V. Hollot, V. Misra, D. Towsley, and W-B. Gong. A control theoretic analysis of red. *Proc IEEE INFOCOM*, 2000.

- [97] I. M. Horowitz. *Synthesis of Feedback Systems*. Academic Press, New York, NY, 1963.
- [98] I. M. Horowitz. Superiority of transfer function over state-variable methods in linear, time-invariant feedback system design. *IEEE Transactions on Automatic Control*, AC-20(1):84–97, 1975.
- [99] T. P. Hughes. *Elmer Sperry Inventor and Engineer*. John Hopkins Press, Baltimore, MD, 1993.
- [100] A. Isidori. *Nonlinear Control Systems*. Springer-Verlag, 2nd edition, 1989.
- [101] V. Jacobson. Congestion avoidance and control. *ACM SIGCOMM Computer Communication Review*, 25:157–173, 1995.
- [102] J. A. Jacquez. *Compartment analysis in biology and medicine*. Elsevier, Amsterdam, 1972.
- [103] H. James, N. Nichols, and R. Philips. *Theory of Servomechanisms*. McGraw-Hill, 1947.
- [104] P. D. Joseph and J. T. Tou. On linear control theory. *Transactions of AIEE*, 80(18), 1961.
- [105] W. G. (editor) Jung, editor. *Op Amp Applications*. Analog Devices, Norwood, MA, 2002.
- [106] R. E. Kalman. Contributions to the theory of optimal control. *Boletín de la Sociedad Matemática Mexicana*, 5:102–119, 1960.
- [107] R. E. Kalman. New methods and results in linear prediction and filtering theory. Technical Report 61-1, Research Institute for Advanced Studies (RIAS), February 1961.
- [108] R. E. Kalman. On the general theory of control systems. In *Proceedings First IFAC Congress on Automatic Control, Moscow, 1960*, volume 1, pages 481–492, London, 1961. Butterworths.
- [109] R. E. Kalman and R. S. Bucy. New results in linear filtering and prediction theory. *Trans ASME (J. Basic Engineering)*, 83 D:95–108, 1961.
- [110] R. E. Kalman, P. L. Falb, and M. A. Arbib. *Topics in Mathematical System Theory*. McGraw-Hill, 1969.
- [111] R. E. Kalman, Y. Ho, and K. S. Narendra. *Controllability of Linear Dynamical Systems*, volume 1 of *Contributions to Differential Equations*. John Wiley & Sons, Inc., New York, 1963.
- [112] J. Keener and J. Sneyd. *Mathematical Physiology*. Springer, New York, 2001.
- [113] F. P. Kelley. Stochastic models of computer communication. *J. Royal Statistical Society*, B47(3):379–395, 1985.
- [114] K. Kelly. *Out of Control*. Addison-Wesley, 1994. Available at <http://www.kk.org/outofcontrol>.
- [115] J. M. Keynes. *The General Theory of Employment, Interest and Money*. Cambridge University Press, Cambridge, UK, 1936.
- [116] H. K. Khalil. *Nonlinear Systems*. Macmillan Publishing Company, 3rd edition, 2001.
- [117] U. Kiencke and L. Nielsen. *Automotive Control Systems: For Engine, Driveline, and Vehicle*. Springer, Berlin, 2000.
- [118] C. Kittel. *Introduction to Solid State Physics*. John Wiley, New York, 1995.
- [119] L. R. Klein and A. S. Goldberger. *An Econometric Model of the United States 1929-1952*. North Holland, Amsterdam, 1955.
- [120] L. Kleinrock. *Queuing Systems Vol I and II*. Wiley-Interscience, New York, 1975. 2nd edition.
- [121] N. N. Krasovskii. *Stability of Motion*. Stanford University Press, Stanford, CA, 1963.
- [122] M. Krstić, I. Kanellakopoulos, and P. Kokotović. *Nonlinear and Adaptive Control Design*. Wiley, 1995.

- [123] P. R. Kumar. New technological vistas for systems and control: The example of wireless networks. *Control Systems Magazine*, 21(1):24–37, 2001.
- [124] P. R. Kumar and P. Varaiya. *Stochastic Systems: Estimation, Identification, and Adaptive Control*. Prentice Hall, Inc., 1986.
- [125] B. C. Kuo and F. Golnaraghi. *Automatic Control Systems*. Wiley, eighth edition, 2002.
- [126] M. Kurth and E. Welfonder. Oscillation behavior of the enlarged european power system under deregulated energy market conditions. *Control Engineering Practice*, 13:1525–1536, 2005.
- [127] J. P. LaSalle. Some extensions of lyapunov’s second method. *IRE Trans. Circuit Theory*, CT-7(4):520–527, 1960.
- [128] A. D. Lewis. A mathematical approach to classical control. Technical report, Queens University, 2003.
- [129] S. H. Low, F. Paganini, and J. C. Doyle. Internet congestion control. *IEEE Control Systems Magazine*, pages 28–43, February 2002.
- [130] K. H. Lundberg. History of analog computing. *IEEE Control Systems Magazine*, 25(3):22–28, 2005.
- [131] L.A. MacColl. *Fundamental Theory of Servomechanisms*. Van Nostrand, Princeton, NJ, 1945. Dover reprint 1968.
- [132] D. C. MacFarlane and K. Glover. *Robust controller design using normalized coprime factor plant descriptions*. Springer, New York, 1990.
- [133] J. M. Maciejowski. *Multivariable Feedback Design*. Addison Wesley, Reading, MA, 1989.
- [134] D. A. MacLulich. *Fluctuations in the numbers of the varying hare (Lepus americanus)*. University of Toronto Press, 1937.
- [135] A. Makroglou, J. Li, and Y. Kuang. Mathematical models and software tools for the glucose-insulin regulatory system and diabetes: an overview. *Applied Numerical Mathematics*, 56:559–573, 2006.
- [136] J. G. Malkin. *Theorie der Stabilität einer Bewegung*. Oldenbourg, München, 1959.
- [137] R. Mancini. *Op Amps for Everyone*. Texas Instruments, Houston. TX, 2002.
- [138] J. E. Marsden and M. J. Hoffmann. *Basic Complex Analysis*. Springer, 1999.
- [139] J. E. Marsden and T. S. Ratiu. *Introduction to Mechanics and Symmetry*. Springer Verlag, 1994.
- [140] O. Mayr. *The Origins of Feedback Control*. MIT Press, 1970.
- [141] M. W. McFarland, editor. *The Papers of Wilbur and Orville Wright*. McGraw Hill, 1953.
- [142] H. T. Milhorn. *The Application of Control Theory to Physiological Systems*. Saunders, 1966.
- [143] D. A. Mindel. *Between Human and Machine: Feedback, Control, and Computing Before Cybernetics*. Johns Hopkins University Press, 2002.
- [144] D. Möhl, G. Petrucci, L. Thorndahl, and S. van der Meer. Physics and technique of stochastic cooling. *Physics Reports*, 58(2):73–102, 1980.
- [145] L. Moore and D. Smith. Predator-prey models, 1993. <http://www.math.duke.edu/education/ccp>.
- [146] J. D. Murray. *Mathematical Biology*, volume I and II. Springer, third edition, 2004.
- [147] R. M. Murray, editor. *Control in an Information Rich World: Report of the Panel on Future Directions in Control, Dynamics and Systems*. SIAM, 2003. Available at <http://www.cds.caltech.edu/~murray/cdspanel>.

- [148] P. J. Nahin. *Oliver Heaviside: Sage in Solitude: The Life, Work and Times of an Electrical Genius of the Victorian Age*. IEEE Press, New York, NY, 1988.
- [149] A. O. Nier. Evidence for the existence of an isotope of potassium of mass 40. *Physical Review*, 48:283–284, 1935.
- [150] H. Nijmeijer and J. M. Schumacher. Four decades of mathematical system theory. In J. W. Polderman and H. L. Trentelman, editors, *The Mathematics of Systems and Control: From Intelligent Control to Behavioral Systems*, pages 73–83. Univ. of Groningen, 1999.
- [151] H. Nyquist. Regeneration theory. *Bell System Technical Journal*, 11:126–147, 1932.
- [152] H. Nyquist. The regeneration theory. In R. Oldenburger, editor, *Frequency Response*, page 3, New York, 1956. MacMillan.
- [153] K. Ogata. *Modern Control Engineering*. Prentice-Hall, fourth edition, 2001.
- [154] R. Olfati-Saber, J. A. Fax, and R. M. Murray. Consensus and cooperation in networked multi-agent systems. *Proceedings of the IEEE*, 95(1):215–233, 2007.
- [155] G. Pacini and R. N. Bergman. A computer program to calculate insulin sensitivity and pancreatic responsiveness from the frequently sampled intravenous glucose tolerance test. *Computer Methods and Programs in Biomedicine*, 23:113–122, 1986.
- [156] G. A. Philbrick. Designing industrial controllers by analog. *Electronics*, 21(6):108–111, 1948.
- [157] W. F. Powers and P. R. Nicastrì. Automotive vehicle control challenges in the 21st century. *Control Engineering Practice*, 8:605–618, 2000.
- [158] S. Prajna, A. Papachristodoulou, and P. A. Parrilo. SOSTOOLS: Sum of squares optimization toolbox for MATLAB, 2002. Available from <http://www.cds.caltech.edu/sostools>.
- [159] D. S. Riggs. *The Mathematical Approach to Physiological Problems*. MIT Press, Cambridge, MA, 1963.
- [160] H. H. Rosenbrock and P. D. Moran. Good, bad or optimal? *IEEE Transactions on Automatic Control*, AC-16(6):552–554, 1971.
- [161] F. Rowsone Jr. What it’s like to drive an auto-pilot car. *Popular Science Monthly*, April 1958. Available at <http://www.imperialclub.com/ImFormativeArticles/1958AutoPilot>.
- [162] W. J. Rugh. *Linear System Theory*. Prentice Hall, Englewood Cliffs, NJ, 2nd edition, 1995.
- [163] E. B. Saff and A. D. Snider. *Fundamentals of Complex Analysis with Applications to Engineering, Science and Mathematics*. Prentice Hall, 2002.
- [164] D. Sarid. *Atomic Force Microscopy*. Oxford University Press, Oxford, 1991.
- [165] S. Sastry. *Nonlinear Systems*. Springer, New York, NY, 1999.
- [166] G. Schitter. High performance feedback for fast scanning atomic force microscopes. *Review of Scientific Instruments*, 72(8):3320–3327, 2001.
- [167] G. Schitter, K. J. Åström, B. DeMartini, P. J. Thurner, K. L. Turner, and P. K. Hansma. Design and modeling of a high-speed afm-scanner. *IEEE CST*, 2007.
- [168] M. Schwartz. *Telecommunication Networks*. Addison Wesley, Reading MA, 1987.
- [169] D. E. Seborg, T. F. Edgar, and D. A. Mellichamp. *Process Dynamics and Control*. Wiley, 2003.
- [170] S. D. Senturia. *Microsystem Design*. Kluwer, Boston, MA, 2001.
- [171] F. G. Shinskey. *Process-Control Systems. Application, Design, and Tuning*. McGraw-Hill, New York, 4 edition, 1996.

- [172] S. Skogestad and I Postlethwaite. *Multivariable Feedback Control*. Wiley, Hoboken, NJ, 2nd edition, 2005.
- [173] E. P. Sontag. *Mathematical Control Theory: Deterministic Finite Dimensional Systems*. Springer, New York, NY, 2nd edition, 1998.
- [174] L. Stark. Oscillations and noise in the human pupil servomechanism. *Proceedings of the Institute of Radio Engineers*, IRE-47:1925–1939, 1959.
- [175] L. Stark. *Neurological Control Systems - Studies in Bioengineering*. Plenum Press, New York, N. Y., 1968.
- [176] G. Stein. Respect the unstable. *Control Systems Magazine*, 23(4):12–25, 2003.
- [177] J. Stewart. *Calculus: Early Transcendentals*. Brooks Cole, 2002.
- [178] G. Strang. *Linear Algebra and its Applications*. Harcourt Brace Jovanovich, San Diego, third edition, 1988.
- [179] S. H. Strogatz. *Nonlinear Dynamics and Chaos, with Applications to Physics, Biology, Chemistry, and Engineering*. Addison-Wesley, 1994.
- [180] A. S. Tannenbaum. *Computer Networks*. Prentice Hall, Upper Saddle River, NJ, 3rd edition, 1996.
- [181] T. Teorell. Kinetics of distribution of substances administered to the body I and II. *Archives Internationales de Pharmacodynamie et de Therapie*, 57:205–240, 1937.
- [182] G. T. Thaler. *Automatic Control Systems*. West Publishing Company, St. Paul, MN, 1989.
- [183] M. Tiller. *Introduction to Physical Modeling with Modelica*. Springer, 20001.
- [184] D. Tipper and M. K. Sundareshan. Numerical methods for modeling computer networks under nonstationary conditions. *IEEE J. Selected Areas in Communications*, 8(9):1682–1695, 1990.
- [185] J. G. Truxal. *Automatic Feedback Control System Synthesis*. McGraw-Hill, New York, NY, 1955.
- [186] H. S. Tsien. *Engineering Cybernetics*. McGraw-Hill, 1954.
- [187] G. Vinnicombe. *Uncertainty and Feedback: \mathcal{H}_∞ loop-shaping and the v -gap metric*. Imperial College Press, London, 2001.
- [188] F. J. W. Whipple. The stability of the motion of a bicycle. *Quarterly Journal of Pure and Applied Math.*, 30:312–348, 1899.
- [189] D. V. Widder. *Laplace Transforms*. Princeton University Press, Princeton, NJ, 1941.
- [190] E. P. M. Widmark and J. Tandberg. Über die bedingungen fr die akkumulation indifferenten narkotika. *Biochemische Zeitung*, 148:358–389, 1924.
- [191] N. Wiener. *Cybernetics: Or Control and Communication in the Animal and the Machine*. John Wiley, 1948.
- [192] S. Wiggins. *Introduction to Applied Nonlinear Dynamical Systems and Chaos*. Springer-Verlag, 1990.
- [193] D. G. Wilson. *Bicycling Science*. MIT Press, Cambridge, MA, third edition, 2004. With contributions by Jim Papadopoulos.
- [194] H. R. Wilson. *Spikes, Decisions, and Actions: The Dynamical Foundations of Neuroscience*. Oxford University Press, 1999.
- [195] S. Yamamoto and I. Hashimoto. Present status and future needs: The view from Japanese industry. In Yaman Arkun and W. Harmon Ray, editors, *Chemical Process Control—CPCIV*, 1991. Proceedings of the Fourth International Conference on Chemical Process Control, Texas.

- [196] T-M. Yi, Y. Huang, M. I. Simon, and J. Doyle. Robust perfect adaptation in bacterial chemotaxis through integral feedback control. *PNAS*, 97:4649–4653, 2000.
- [197] G. Zames. Feedback and optimal sensitivity: Model reference transformations, multiplicative seminorms, and approximative inverse. *IEEE Transactions on Automatic Control*, AC-26(2):301–320, 1981.
- [198] J. C. Zhou, J. C. Doyle, and K. Glover. *Robust and Optimal Control*. Prentice Hall, New Jersey, 1996.
- [199] J. G. Ziegler and N. B. Nichols. Optimum settings for automatic controllers. *Trans. ASME*, 64:759–768, 1942.

Index

- Q*-value, 63
- v-gap metric, 349

- 6, 237, 238

- A/D converters, *see*
 - analog-to-digital converters
- active filter, 154
- actuation, 4
- adaptation, 295
- adaptive control, 371
- additive uncertainty, 347
- admission control, 54, 78, 79, 272
 - in queueing systems, 63
- aerospace systems, 8
- AFM:state feedback, 200
- airspace management, 9
- algebraic loop, 211, 249
- all-pass system, 330
- alternating current (AC), 7
- analog-to-digital converters, 4, 225, 309
- analytic function, 236
- anti-resonance, 156
- anti-windup, 305
- argument, of a complex number, 250
- asymptotic stability, 103
- atomic force microscope, 81–84, 156, 257, 279, 297, 302, 326, 365
 - with preloading, 93
- attractor, 104
- automatic reset, 294
- automatic tuning, 371
- automobiles, 6, 22, 51, 56, 69
 - zz*, *see also* cruise control, vehicle steering
- autonomous system, 29, 202
 - zz*, *see also* time-invariant systems

- autonomous vehicles, 20–21
- autopilot, 19

- balance system, 35, 189, 241, 332
 - exercises, 26, 61
 - normalized coordinates, 49, 63
 - reachability, 170
- band pass filter, 155, 255
- bandwidth, 156, 320
- Bell Labs, 18, 287
- bicycle dynamics, 69–71, 123, 227
 - state space form, 92
- bicycle model
 - Whipple model, 71
- bicycle model, for vehicle steering, 52
- bicycle:state feedback, 200
- bifurcation, 121
- bifurcation diagram, 122
- biological circuits, 58, 115, 256
 - genetic switch, 64
 - positive feedback, 129
 - repressilator, 59–60
- biological engineering, 4
- biological systems, 1
 - zz*, *see also* biological circuits, drug administration, population dynamics
- bistability, 23
- Black, H. S., 18, 20, 71, 73, 131, 345
- block diagonal system, 129
- block diagrams, 44
- Bode plot, 250
 - interpreting, 250
 - sketching, 250
- Bode's integral formula, 334

- Bode's loop transfer function, 354
- Bode's relations, 280
- breakpoint, 252
- Brockett, R. W., x, 1
- bumpless transfer, 371

- calibration, 180
- carrying capacity, 90
- center, 104
- centrifugal governor, 2, 6
- chain of integrators, 61
- chemical industry, 9
- chordal distance, 349
- circular reasoning, 70
- closed loop, 2, 4, 6, 162, 265
 - versus open loop, 2, 267, 285, 313
- command and control, 9
- command signal, 291
- command signals, 5
- compartment model, 107, 152, 186, 203, 208
- compartment models, 85
 - state variables, 94
- complementary sensitivity function, 315, 358
- complexity
 - of control systems, 21
- component failures, robustness to, 4
- computation, 4
- computed torque, 163
- computer science
 - relationship to control, 5
- computer system, 158
- computer systems, 13, 39
- computing systems, 12, 54
- conditional stability, 273
- Congestion control, 289
- congestion control, 12, 77–80, 104, 128, 271, 312

- router dynamics, 93
- consensus, 56
- conservation law, 335
- consumer electronics, 3
- control, 3–5
 - early examples, 5
 - modeling, 31–32
 - successes of, 25
 - system, 4
- control error, 23
- control law, 5, 23, 176
- control Lyapunov function, 124
- control matrix, 34, 38
- controllability, 198
- controlled differential equation, 29
- convolution equation, 145, 146
- coupled spring-mass system, 149
- critical point, 269
- critically damped, 184
- crossover frequency, 320
- crossover frequency inequality, 330
- cruise control, 6, 65–69, 126, 158, 162, 196, 248, 298, 304, 305, 307, 345, 352
 - exercises, 26, 91
- cybernetics, 11

- d, 200
- D/A converters, *see* digital-to-analog converters
- damped frequency, 184
- damped oscillator, 96
- damping factor, 184
- DARPA Grand Challenge, 20
- DC gain, *see* zero frequency gain
- delay margin, 278
- delta function, *see* impulse
- derivative action, 294
- derivative gain, 292
- derivative time (constant), 292
- describing functions, 285
- design of dynamics, 18
- design rule, 365
- diagonal system, 138
- diagonalizable system, 129
- difference equations, 37–40
- differential algebraic equations, 33
- differential equations, 28, 95–98
 - finite escape time, 97
 - non-unique solutions, 98
 - solution, 96, 137
- differential flatness, 221
- digital-to-analog converters, 4
- dimension free variables, 49
- direct term, 34, 38, 249
- discrete time systems, 38, 61
 - Keynes' model, 62
- disturbance rejection, 4, 5
- disturbances, 5, 32
- Dodson, B., 1
- dominant pair, 188
- double integrator, 137, 168
- Doyle, J. C., x, 372
- drug administration, 85–89, 186
 - alcohol metabolism, 94
- drugadministration
 - zz, *see also* compartment models
- dual, 204
- duality, 207
- dynamic compensator, 196
- dynamic inversion, 163
- dynamical system, 27
- dynamics, 4, 6
- dynamics matrix, 34, 38, 105, 142

- economic systems, 22
- economics, 14–15
- ecosystems, 3, 17
- eigenvalue assignment, 180, 208, 212
- eigenvalues, 105, 114
- electrical circuits, 236
- electrical engineering, 29–31
- electronic amplifiers, 3
- email server, 39
- emissions control, 6
- entertainment robots, 12
- environmental science, 3, 9, 17
- equilibrium
 - discrete time, 61
- equilibrium point, 90, 100
 - stability, 102
- error feedback, 292, 307, 315

- exponential signals, 231
- extended Kalman filter, 220
- external disturbances, 4
- Eye motion, 26

- feedback, 1–3, 5, 6, 18
 - as technology enabler, 3
 - drawbacks, 21
 - in biological systems, 1, 2, 16
 - zz, *see also* biological circuits
 - in ecological systems, 16–17
 - in engineered systems, *see* control
 - in financial systems, 3
 - in nature, 15–17
 - loop, 4
 - positive, *see* positive feedback
 - versus control, 3
- feedback linearizable, 162
- feedback loop, 4
- feedforward, 22
 - design, 317
- finite escape time, 97
- first order system, 296
- flight control, 19, *see also* vectored thrust aircraft X-29, 335
- flow, 29
- flow model, 55
- flyball governor, *see* centrifugal governor
- force feedback, 10
- frequency domain modeling, 230
- frequency response, 30, 43, 152
- fully actuated, 240
- fundamental limitations, 334

- gain, 43, 153, 283–285
 - zero frequency, *see* zero frequency gain
- gain crossover frequency, 276
- gain margin, 276, 278
- gain scheduling, 220, 371
- Gang of Four, 315
- Gang of Six, 315
- gene regulation, 16
- genetic switch, 115

- global climate, *see*
 environmental science
 glucose regulation, 2
- Harrier AV-8B aircraft, 53
 heat propagation, 60, 238, 288
 Heaviside, 164
 high frequency roll-off, 325, 358
 high pass filter, 255
 higher levels of decision
 making, 9, 20
 Hoagland, M. B., 1
 Hodgkin-Huxley equations, 60
 homeostasis, *see* biological systems
 homogeneous solution, 133, 239
 Honeywell, 6
 hysteresis, 286
- IBM Lotus server, 39, 158
 ideal PID controller, 291
 impedance, 236
 impulse, 146
 impulse response, 135, 146, 147
 infinity norm, 284
 information science, 4
 information systems, 12
 initial value problem, 96
 input, 29
 input sensitivity function, 315
 input/output models, 5
 instability, 21
 instrumentation, 10
 insulin, *see* glucose regulation
 insulin-glucose
 minimal model, 88
 integral action, 6, 26, 180, 293
 integral control, 24
 integral gain, 292, 357
 integral time (constant), 292
 integrator windup, 226, 304–306
 intelligent machines, *see* robotics
 interconnection, 5
 internal model principle, 214, 221
 Internet, 3, 12
 Internet Protocol (IP), 78
- invariant set, 118
 inverse response, 290
 inverted pendulum, 37, 100, 119, 121, 264, 274
 linear approximation, 108
 swing up control, 128
- Jacobian linearization, 160
 Jordan decomposition, 139
 Jordan form, 139
- Kalman decomposition, 224, 262
 Kalman, R. E., 167
 Kelly, K., 25
 Keynes' model, 62
 Krasovskii-Lasalle principle, 118
- LabVIEW, viii, 123
 lag compensation, 325
 Laplace transform, 259–261
 Laplace transforms, ix
 Laplacian matrix, 57
 Lasalle's invariance principle, *see* Krasovskii-Lasalle principle
 latency, 309
 lead compensator, 326, 328
 limit cycle, 91, 101, 109
 linear, 34
 linear and time-invariant, 34
 linear input/output system, 132
 linear quadratic control, 368
 linear system, 34
 linear systems, 30
 linearization, 158–163
 Lipschitz continuity, 98
 load disturbance, 313
 load sensitivity function, 315
 logistic growth model, 90
 logistic model, 94
 loop analysis, 265
 loop shaping, 268, 324
 loop transfer function, 266
 lotus notes server, 158
 low pass filter, 255
 LQ control, 368
 LTI, *see* linear and time-invariant
 LTI systems, 134
 Lyapunov equation, 114, 128
- Lyapunov function, 111, 112
 Lyapunov functions, 127
 Lyapunov stability theorem, 112
- Mars Exploratory Rovers, 12
 materials science, 9
 Mathematica, 41, 123
 MATLAB, viii, 26, 41, 123, 140, 160, 181, 190, 192, 211, 216, 370
 matrix exponential, 136–139
 Mayr, O., 25
 measurement noise, 313
 mechanical systems, 163
 mechanics, 28–29
 Mindell, D., 25
 minimal model
 (insulin-glucose), 88
 minimum phase, 280
 modal, 145
 modal form, 129, 149
 mode, 142–144, 239
 mode shape, 143
 model, 27
 model reduction, 5
 model uncertainty, 50, 352, 354
 Modelica, 33
 modeling, 5
 modeling from experiments, 47
 motor drive, 64, 199, 312
- nanopositioning, 280, 367
 negative definite, 112
 negative feedback, 18
 networks, 12
 neural systems, 295
 neuroscience, 60
 neutrally stable, 102
 Nobel Prize, 10, 11, 14, 60, 81
 noise, 214
 noise cancellation, 124
 noise sensitivity function, 315
 non-minimum phase, 280
 non-unique solutions, 98
 nonopositioning system, 365
 normalization, 49, 161
 Nyquist criterion, 269, 273
 Nyquist plot, 268

- observability, 32, 202
 - rank condition, 203
- Observable Canonical Form, 205
- observable canonical form, 204
- observer, 201
- observers, 201
- ODEs, *see* differential equations
- on-off control, 23, 24
- op amp, 154, 266, 359
 - circuits, 92
 - oscillator, 92
- open loop, 2, 168
- operational amplifier, 71–75, 237
 - oscillator, 128
- operational amplifier (op amp), 71
- order, 34
- order of a system, 35
- ordinary differential equation
 - controlled, 29
- ordinary differential equations, *see* differential equations, 34–37
- oscillator, 233
- oscillator dynamics, 138
 - normal form, 62
- output sensitivity function, 315
- overdamped, 184
- overshoot, 151, 320

- parametric stability diagram, 122
- parametric uncertainty, 345
- particular solution, 133
- passive systems, 285
- passivity theorem, 285
- patch clamp, 10
- peak frequency, 156, 320
- pendulum dynamics, 113
- seeinverted pendulum, 113
- perfect adaptation, 295
- performance limits
 - right half plane poles, 281
 - right half plane zeros, 281
- pharmacodynamics, 85
- pharmacokinetics, *see* drug administration
- phase, 43, 153
 - minimum vs. nonminimum, 280
- phase crossover frequency, 276
- phase margin, 276, 278
- phase portrait, 99
- physics
 - relationship to control, 5
- PI control, first order systems, 296
- PID control, 25
- PID controller, 329
- pitchfork bifurcation, 130
- pole, 239
 - right half plane, 331, 344
- pole placement, *see* eigenvalue placement 177
- pole zero diagram, 240
- pole/zero cancellation
 - cruise control, 249
- pole/zero cancellations, 247
- pollution, 6
- population dynamics, 89–91
- positive definite, 111, 114
- positive feedback, 22
- positive real, 334
- positive semidefinite, 112
- power grid, 63, 127
- power network, 7
- power systems, 6–8
- predator-prey system, 38, 90, 121, 181
- prediction, ability of
 - controllers, 25
- principle of the variation of the argument, 275
- process control, 9, 22
- proportional control, 24
 - zz, *see also* PID control
- proportional gain, 291
- proportional, integral,
 - derivative control, *see* PID control
- protocols, 3, 78
- pupil response, 258
- pure error feedback, 315
- pure exponential response, 232

- Q value, 186
- Q-value, 253
- queueing systems
 - admission control, 63
- queuing systems, 54

- reachability, 32, 167, 198
 - rank condition, 170
- reachability matrix, 169
- reachable canonical form, 35, 172, 174, 175, 179
- real-time systems, 5
- reference value, 291
- reference weighting, 307
- reference weights, 307
- region of attraction, 120
- regulation, 1
- relay feedback, 303
- repressilator, 59–60
- reset, 293
- resonance peak, 156, 320
- retina, 295
- Riccati equation, 192, 370
- rise time, 151, 320
- robotics, 4, 11–12
- robustness, 17–18
- root locus plots, 122
- rush-hour effect, 55, 64

- saddle, 104
- sampling, 157
- saturation function, 72
- scaling, 49
- second order system, 28
- second order systems, 183
- self-repression, 166, 256
- sensing, 4
- sensitivity function, 315
 - disturbance attenuation, 321
- sensor fusion, 202
- sensor matrix, 34, 38
- sensors, 10
- separation principle, 201, 213
- setpoint, 291, 307
- setpoint weights, 307
- settling time, 151, 320
- simple models, 353
- simulation, 40
- SIMULINK, 161
- sink, 104
- small gain theorem, 284–285, 353–354
- software tools for control, viii
- Sony AIBO, 12
- source, 104
- spectrum analyzer, 257
- Sperry autopilot, 19
- spring mass system, 40

- spring-mass system, 127, 149
 - normalization, 49
 - system identification, 47
- stability, 4, 5, 19, 42, 102–119
 - limit cycle, 109
 - of a solution, 102
 - linear system, 107
 - local versus global, 103, 120, 121
 - of a system, 105
 - solutions, 102
- stability by linearization, 118
- stability margin, 277, 278
- Stability margins, 289
- stability margins, 276
- stable
 - transfer function, 240
- state, 28, 34
- state estimators, *see* observers201
- state feedback: AFM, 200
- state feedback: bicycle, 200
- state space, 28, 34–43
- state space model, 34
- state vector, 34
- steady state, 26
 - value, 151
- steady state gain, *see* zero frequency gain
- steady state response, 42, 150
- steam engine, 2
- steering dynamics
 - tanker, 130
- Stein, G., x, 1
- step input, 150
- step response, 30, 135, 147, 150
- subcritical pitchfork
 - bifurcation, 130
- supercritical pitchfork
 - bifurcation, 130
- superposition, 133
- supremum (sup), 284
- system identification
 - least squares, 62
- tank model, 126
- temperature control, 1, 5
- thermostat, 5, 6
- three term controllers, 291
- thrust vectored aircraft, 141
- time constant, 165
- time delay, 6, 13, 235, 280, 343, 344
- time invariance, 126, 134
- time shift, *see* time invariance
- time-invariant system, 34
- time-invariant systems, 30
- traffic management, 9
- trail, 70
- transcriptional regulation, 58, 256
- transfer function, 229, 233, 235
 - differentiator, 235
 - integrator, 235
- transient, 168
- transient response, 150
- Transmission Control Protocol (TCP), 78
- transportation systems, 8
- Tsien, H. S., 11
- tuning rules, 312
- two degrees of freedom, 220, 317
- two-degree-of-freedom, 292
- uncertainty, 4, 17–18, 32, 345–350
 - component or parameter variation, 5
 - unmodeled dynamics, 5, 346
- uncertainty lemon, 50, 51
- undamped oscillator, 138
- underdamped, 97, 184
- unit step, 150
- unmodeled dynamics, 346
- unobservable systems, 204
- unreachable system, 199
- unstable, 103
- unstable pole/zero cancellation, 248
- vector field, 29
- vectored thrust aircraft, 53, 192, 217, 227, 289, 339
 - pitch control, 328
- seeflight control, 335
- vehicle steering, 51, 161, 177, 209, 214, 221, 245, 281
 - feedforward, 319
 - lack of robustness, 361
- seecoupled spring-mass system, 149
- vertical takeoff and landing, *see* vectored thrust aircraft
- Vinnicombe metric, 349
- voltage clamp, 10, 11
- waterbed effect, 334, 335
- Watt governor, *see* centrifugal governor
- web server, 194
- web server control, 75–77
- web site, viii
- Wiener, N., 11
- winding number, 269, 275
- windup, *see* integrator windup
- Wright brothers, 19
- Youla parameterization, 355
- zero, 239
- zero frequency gain, 155, 177, 180, 239
- zeros
 - effect of sensor location, 282
- zeros, signal blocking property, 239
- Ziegler-Nichols methods, 300
- Ziegler-Nichols tuning rules, 302
- Ziegler-Nichols, 312

